ORGANIZED BY:

NATIONAL RESEARCH & DEVELOPMENT
INSTITUTE FOR TEXTILES
AND LEATHER (INCDTP) - DIVISION
LEATHER AND FOOTWEAR
RESEARCH INSTITUTE (ICPI)

ICAMS 2022

ADVANCED MATERIALS AND SYSTEMS

Proceedings of the 9th International Conference

October 26th - 28th, 2022

Bucharest, ROMANIA

Laurenția ALEXANDRESCU
Gheorghe COARĂ

EDITORS

Proceedings of

THE 9th INTERNATIONAL CONFERENCE ON ADVANCED MATERIALS AND SYSTEMS

Bucharest, ROMANIA
26-28 October, 2022

INCDTP-ICPI
ROMANIA

Disclaimer

Editura CERTEX
certex@ns.certex.ro
Bucureşti, str. Lucreţiu Patrascanu nr. 16, sector 3
Tel/ fax: 021 3405515

Descrierea CIP a Bibliotecii Naţionale a României
Laurenția ALEXANDRESCU
Gheorghe COARĂ
The 9th International Conference on Advanced Materials and Systems
Laurenția ALEXANDRESCU, Gheorghe COARĂ
Bucureşti: CERTEX, 2022
ISSN: 2068 – 0783

Şef redacţie:
Emilia Visileanu

Coordonator & Coperta: Dana Gurău
Procesare text: Dana Gurău, Elena Ninciuleanu, Ciprian Chelaru, Mihai Georgescu, Dan Vicovan

SCIENTIFIC COMMITTEE

Arife Candas ADIGUZEL ZENGIN, Ege University, Izmir, TR
Mădălina Georgiana ALBU KAYA, INCDTP-ICPI, RO
Laurenția ALEXANDRESCU, INCDTP-ICPI, RO
Carmen ARIAS CASTELLANO, General Secretary, CEC, BE
Anna BACARDIT, University of Lleida, ES
Elena BADEA, University of Craiova and INCDTP-ICPI, RO
Bahri BASARAN, Ege University, Izmir, TR
Behzat Oral BITLISLI, Ege University, Izmir, TR
Cristina CARȘOTE, National Museum of Romanian History, RO
Gheorghe COARĂ, INCDTP-ICPI, RO
Nizami DURAN, Mustafa Kemal University, Antakya, TR
Alexandra Gabriela ENE, INCDTP, RO
Maria José FERREIRA, CTCP, PT
Anton FICAI, "Politehnica" University Bucharest, RO
Margareta FLORESCU, Bucharest Academy of Economic Studies, RO
Carmen GAIDĂU, INCDTP-ICPI, RO
Mihaela GHICA, "Carol Davila" Univ. of Medicine&Pharmacy, RO
Gustavo GONZALEZ-QUIJANO, Secretary General, COTANCE, BE
Gurbuz GULUMSER, Ege University, Izmir, TR
Huseyin Ata KARAVANA, Ege University, Izmir, TR
Alpaslan KAYA, Mustafa Kemal University, Antakya, TR
Karel KOLOMAZNIK, Tomas Bata University, Zlin, CZ
Jeannette LUCEJKO, University of Pisa, IT
Jianzhong MA, Shaanxi University of Science and Technology, CN
Stelian MAIER, "Gheorghe Asachi" Technical Univ. of Iasi, RO
Minodora MARIN, INCDTP-ICPI, RO
Alcino MARTINHO, CTIC, PT
Aura MIHAI, "Gheorghe Asachi" Technical Univ. of Iasi, RO
Lucreția MIU, INCDTP-ICPI, RO
Olena MOKROUSOVA, Kyiv National University of Technologies and Design, UA
Enrique MONTIEL PARREÑO, Vesica Piscis Footwear, ES
Mehmet Mete MUTLU, Ege University, Izmir, TR
Georgios PANAGIARIS, Technological Education Institute, GR
Mirela PANTAZI-BĂJENARU, INCDTP-ICPI, RO
Dimosthenis PAPAKONSTANTINOU, CRE.THI.DEV, GR
Vera PINTO, CTCP, PT
Victoriya PLAVAN, Kiev Nat. Univ. of Techn&Design, UA
Alina POPESCU, INCDTP, RO
Maria SÖNMEZ, INCDTP-ICPI, RO
Paul STĂNESCU, "Politehnica" University Bucharest, RO
Keyong TANG, Zhengzhou University, CN
Irina TITORENCU, "N. Simionescu" I.C.B.P., RO
Jin ZHOU, Sichuan University, CN

ORGANIZING COMMITTEE

Laurentia ALEXANDRESCU, Chair, Director, INCDTP - ICPI, RO
Gheorghe COARA, Co-Chair, INCDTP - Leather and Footwear Research Institute Division (ICPI), RO
Alexandra Gabriela ENE, Co-Chair, General Director, National Research and Development Institute for Textile and Leather, RO
Dana GURAU, INCDTP - ICPI, RO
Ioana PIVNICERU, INCDTP - ICPI, RO
Ciprian CHELARU, INCDTP - ICPI, RO
Mihai GEORGESCU, INCDTP - ICPI, RO
Elena NINCIULEANU, INCDTP - ICPI, RO
Dan VICOVAN, INCDTP - ICPI, RO
Durmuș Alpaslan KAYA, Mustafa Kemal University, Antalya, TR
Roxana CONSTANTINESCU, INCDTP-ICPI, RO

ORGANIZED BY:

NATIONAL RESEARCH & DEVELOPMENT INSTITUTE FOR TEXTILE AND LEATHER (INCDTP), BUCHAREST, ROMANIA

DIVISION LEATHER & FOOTWEAR RESEARCH INSTITUTE (ICPI) BUCHAREST, ROMANIA

PARTNERS:

LEATHER ENGINEERING DEPARTMENT
EGE UNIVERSITY, TURKEY

MUSTAFA KEMAL UNIVERSITY, ANTAKYA-HATAY, TURKEY

CHINA LEATHER & FOOTWEAR RESEARCH INSTITUTE Co. Ltd., CHINA

"POLITEHNICA" UNIVERSITY BUCHAREST, ROMANIA

"GH. ASACHI" TECHNICAL UNIVERSITY OF IASI, ROMANIA

BUCHAREST ACADEMY OF ECONOMIC STUDIES, ROMANIA

CONFEDERATION OF NATIONAL ASSOCIATIONS OF TANNERS AND DRESSERS OF THE EUROPEAN COMMUNITY

"ITA TEXCONF" ROMANIAN ENTITY WITHIN INNOVATION & LEATHER TECHNOLOGICAL TRANSFER

SFERA FACTOR
THE ROMANIAN LEATHER MANUFACTURERS ORGANIZATION

FOREWORD

ICAMS 2022 is offering the framework for presenting the latest results in research, focusing on the field of Materials Science and Innovative Technologies, which records an impressive dynamic and is recognized as a current national and European priority.

The ICAMS 2022 international event, organised by the National Institute for Research and Development for Textiles and Leather - Division Leather and Footwear Institute (INCDTP-ICPI), took place online on 26-28 October 2022. ICAMS 2022 brought together different stakeholders and provided a platform for a better understanding of the European innovation ecosystem while raising awareness of the actions needed to enable synergies and drawing lessons for future actions.

The conference provided the opportunity for exchanging ideas and experience with researchers, scientists and experts at international level, and for developing new scientific contributions.

Participants virtually attended the event from several academic and research institutions, public and private sectors. Participants presented their experience on research, innovation, policies and the creation of synergies. All these inputs offered insightful elements for discussion in the different participatory sessions throughout the event.

The conference topics include, but are not limited to:

1. **Advanced Materials and Nanomaterials**
2. **Biomaterials and Biotechnologies**
3. **Innovative Systems, Technologies and Quality Management**
4. **Ecological Processes for Circular and Neutral Economy**
5. **Creative Industries and Cultural Heritage**
6. **Education and Digitalization**

We would like to thank all the participants, the International Scientific Committee, and partners that made this scientific event possible. ICAMS Conference has already become a tradition, contributing to the advancement of Materials Science in research, academic, social and business environments worldwide.

EDITORS,

Dr. Laurenția ALEXANDRESCU
Director, INCDTP – Division: Leather and Footwear Research Institute (ICPI), RO

Dr. Gheorghe COARĂ
INCDTP – Division: Leather and Footwear Research Institute (ICPI), RO

CONTENTS

TOPIC 3: INNOVATIVE SYSTEMS, TECHNOLOGIES AND QUALITY MANAGEMENT

TOPIC 4: ECOLOGICAL PROCESSES FOR CIRCULAR AND NEUTRAL ECONOMY

TOPIC 5: CREATIVE INDUSTRIES AND CULTURAL HERITAGE

TOPIC 6: EDUCATION AND DIGITALIZATION

WORKSHOP: MUSEION *IoT*-Based System for Understanding and Controlling the Environmental Quality in Museums

INVITED LECTURES

Giuseppe LAZZARA, Giuseppe CAVALLARO, Lorenzo LISUZZO, Maria Rita CARUSO, Martina CALVINO
Preparation of Wax Microparticles Stabilized by Halloysite Nanotubes: A Versatile Material for Restoration of Cultural Heritage

Maria G. KATSIKOGIANNI
Development of Sub-micron Patterned Polymeric Surfaces that Enhance Cell Adhesion for Orthopaedic Applications

Ana Francisca BETTENCOURT
Multifunctional Advanced Drug Delivery Systems: From Nano to Macro

Viorica ROSCULEȚ, Laurenția ALEXANDRESCU
Quality Management in Leather and Footwear Research Institute (ICPI)


Enrica VESCE, Rosalia Stella EVOLA, Carlo INGRAO
Assessment and Life Cycle Costing as Decision-Making Tools for a Suitable Leather Industry

Cristina CARSOTE, Elena BADEA, Noemi PROIETTI, Valeria Di TULLIO, Sebestyen ZOLTAN, Zsuzanna CZEGENY
Leather and Parchment Making and Their Preservation over Millennia – Enhanced Data by Analytical Methods Coupling

I.

ADVANCED MATERIALS AND NANOMATERIALS

PREDICTIVE ANALYSIS OF THE ELECTROMAGNETIC SHIELDS EFFECTIVENESS

RALUCA MARIA AILENI[1], ELENA CRISTINA STROE[1], CRISTIAN MORARI[2]

[1]*The National Research & Development Institute for Textiles and Leather, Lucretiu Patrascanu 16, Bucharest, raluca.aileni@incdtp.ro, cristina.stroe@incdtp.ro*

[2]*INCDIE ICPE-CA, Splaiul Unirii 313, Bucharest 030138*

This paper presents a predictive analysis of the electromagnetic attenuation effectiveness for conductive textile materials obtained by coating with polypyrrole, conductive paste-based aluminum, nickel, copper, silver, and graphene oxide. The predictive analysis was provided by the multiple regression modeling of the effectiveness of electromagnetic attenuation at 5 MHz, respective 700 MHz frequency depending on independent variables such as mass (M [g/m^2]) and thickness (δ [mm]) of the fabric coated with the conductive paste by screen printing. Usually, flexible electromagnetic shields, based on textile materials, are necessary for shielding electric fields, representing a potential reference for cables and filters and ensuring the return path of parasitic currents. Protection against the harmful action of electromagnetic fields can be achieved using textile screens based on conductive coatings that ensure the reflection of the waves when they meet the surface, respectively, the absorption of the waves. In general, the wave representing the incident electromagnetic field propagates in the direction of the screen, undergoing a reflection at contact with the screen, then repeated internal reflections inside it, part of the wave being transmitted into the protected space.

Keywords: textile, electromagnetic shielding. predictive

INTRODUCTION

The disruptive presence of electromagnetic fields is the cause of numerous malfunctions of equipment used in various fields of activity (Deruelle, 2020). In addition, electromagnetic waves can generate harmful activity (Moon, 2020) in living organisms (Saunders, 2003; Stuchly, 2003; Ahlbom *et al*., 2008; Seitz *et al*., 2005; Matthes *et al*., 2003; Perrin and Souque, 2012), materializing cellular anomalies (e.g., cancers (Hendee and Boteler, 1994)). Currently, the share of electromagnetic fields is in the range of tens and hundreds of MHz, where a wide variety of radio-electronic equipment works by emitting and receiving electromagnetic radiation.

International bodies recommend measures to reduce the negative impact of electromagnetic fields (Aldrich and Easterly, 1987; Vecchia *et al*., 2009; Modenese and Gobba, 2021) generated by the great diversity of equipment and their inclusion in electromagnetic compatibility requirements.

The electromagnetic field is the consequence of the electric and magnetic fields generated around a conductor traversed by a variable (electric) current (in time). Electromagnetic waves represent (periodic) variations in the time and space of the electromagnetic field. They are generated around the emission antennas, representing open oscillating systems and propagating in space at the speed of light. They are characterized by a series of parameters such as intensity, polarization, wavelength, etc.

In their propagation, electromagnetic waves are subject to reflection, refraction, diffraction, change of polarization plane, etc. The particularities of the propagation depend primarily on the frequency.

Some researchers identified a harmful effect of exposure to the electromagnetic field at 300 Hz - 10 MHz depending on the dosimetry limits (Vecchia *et al*., 2009; Litvak *et*

https://doi.org/10.24264/icams-2022.I.1

al., 2002). Generally, some concerns are related to exposure to electromagnetic fields from mobile phones (Röösli, 2010; Frank, 2021; Seitz *et al*., 2005).

EXPERIMENTAL PART

The experimental model based textile support and having conductive properties were developed (Table 1) by applying different pastes/dispersions based on polymeric matrices (polyvinyl alcohol (PVA – samples 1-3, 7-9), polypyrrole (PPY – samples 3 and 6), polyvinylpyrrolidone (PVP – samples 4 and 5)), microparticles of copper (Cu) having the size of microparticles < 25 μm, nickel (Ni) having the size < 150 μm, aluminum (Al), silver (Ag) and graphene oxide (GO). Using deposition technologies such as immersion, rinsing and ultrasound, followed by free drying at 20...22°C for 24h, and crosslinking for 3-5 minutes at 140...160°C for samples functionalized by rinsing, respectively drying at 100...105°C, for 5-6 minutes for samples functionalized by ultrasound. The experimental models of functionalized fabrics (9) were evaluated in order to determine the effectiveness of electromagnetic shielding (SE_{dB}) according to the ASTM ES7-83 standard, using specific equipment (from the INCDIE ICPE-CA endowment): coaxial cell model TEM 2000. The measurements were performed for the frequency f [MHz] between 0.1 MHz – 1000 MHz. Table 1 shows the physical, mechanical and electrical characteristics and the effectiveness of electromagnetic shielding (SE_{dB}) for the maximum areas recorded at 5 MHz and 700 MHz, respectively.

Table 1. Physico-mechanical and electrical properties of the samples developed using polymer pastes containing metal microparticle

Sample No.	PPY	Ni	Cu	Al	Ag	GO	Etanol	Distilled water	Rs [Ω]	M [g/m^2]	δ [mm]	SEdB, f=5MHz	SEdB, f=700 MHz
1	-	x	x	-	-	-	-	x	10^7	623.2	1.424	0.5	1.2
2	-	-	x	-	-	-	-	x	10^{11}	623.6	1.42	0	0.1
3	x	-	-	-	-	-	-	x	10^8	513.6	1.472	0	0
4	-	-	-	-		x	-	x	10^{10}	671	1.51	0	0.7
5	-					x	x	-	10^{10}	518.8	1.37	0	0.6
6	x	-	-	-	-	-	-	-	10^5	513.6	1.472	0.2	0
7	-	x	-	-	-	-		x	10^3	834	1.71	22.9	14.6
8	-	-	-	-	x	-		x	10^8	608	2.096	0.1	0
9	-	x	-	x	-	-		x	10^3	769.6	3.878	18.1	20.8

PREDICTIVE ANALYSIS

To develop the mathematical models for predictive analyses the multiple regression modeling was used, studying the correlations between the independent variables (mass (M [g/m^2]), thickness (δ [mm]) and dependent variable electromagnetic attenuation effectiveness SE_{dB} [dB] having frecquency of 5MHz, respective 700MHz.

$$Y=a_1+b_1*X_1+b_2*X_2+b_3*X_3+....+b_kX_k \quad (1)$$

https://doi.org/10.24264/icams-2022.I.1

where:
Y is the estimated value for the dependent variable;
$X_1,X_2,X_3,....X_k$ are the values of the k predictor variables;
a_1 is the point of origin;
$b_1,b_2,b_3,...b_k$ are the coefficients for the k predictor variables.

For the prediction of electromagnetic shielding effectiveness (SE_{dB}) values, the following mathematical models were developed:

- The mathematical model 1 (2) for predicting the values of the effectiveness of electromagnetic attenuation (SE_{dB} [dB]) depending on the electrical surface resistance (Rs [Ω]) and the thickness of the functionalized material (δ [mm]):

$$z_1 = 3.313 + 6.837*x + 0.059*y \quad (2)$$

where:
z= $SedB_{700\ MHz}$;
x = δ;
y=Rs.

- The mathematical model 2 (3) and 3 (4) for predicting the values of the effectiveness of electromagnetic attenuation (SE_{dB}5MHz [dB], respectively SE_{dB}700MHz [dB]) depending on the electrical surface resistance (Rs [Ω]) and the mass of the functionalized material (M [g /m^2]).

$$z_2 = -0.506 - 4.132*x + 0.675*y + 1.489*x^2 - 7.079*x*y + 2.108*y^2 \quad (3)$$

where:
z= $SedB_{700MHz}$;
x=Rs;
y=M.

$$z_3 = -2.093 – 6.473*x + 1.659*y+2.566*x^2 -8.348*x*y + 3.992*y^2 \quad (4)$$

where:
z= $SedB_{5MHz}$;
x=Rs;
y=M.

- The mathematical model M4 (5) and M5 (6) for the prediction of the electromagnetic attenuation effectiveness values (SEdB5MHz [dB], respectively SEdB700MHz [dB]) depending on the mass (M [g/m^2]) and the thickness of the functionalized material (δ [mm]). Figure 1 shows the effectiveness of electromagnetic attenuation (Se_{dB}) as a function of mass (m[g/m^2]) and thickness (δ[mm]).

$$z_4 = 0.642 +0.803*x +4.029*y +3.065*x*y + 2.351*y^2 \quad (5)$$

where:

https://doi.org/10.24264/icams-2022.I.1

z= $SedB_{700MHz}$;
x=δ;
y= M.

$$z_5 = 0.619 + 0.815x + 4.801*y + 0.1887*x^2 + 0.5648*x*y + 4.32*y^2 \quad (6)$$

where:
z= $SedB_{5MHz}$;
x=δ;
y= M.

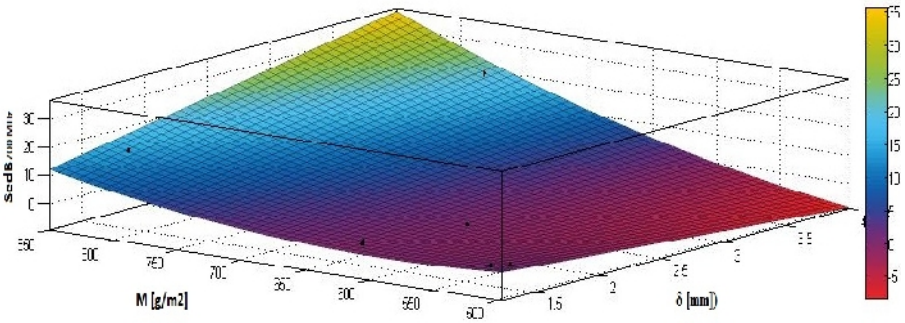

Figure 1. 3D graphical representation of electromagnetic shielding effectiveness depending on the thickness (δ[mm]) and mass (M [g/m^2])

Table 2 presents the elements that define the predictive power of mathematical models, such as the determination coefficient which is the square of the multiple correlation coefficient R^2 (Pal and Bharati, 2019), the square root of the root mean square error (RMSE) and the adjusted coefficient of determination (adjusted R^2). In the case of model no. 1, the RMSE value is 3.789 (Table 2). In the case of model no. 2, the RMSE value is 4.893, respectively in the case of model no. 3 it is 2.025, it can be concluded that these models do not have the necessary accuracy because they generate multiple residual variables. Since the RMSE value is 0.7583 (Table 2) for model no. 4, this model shows good accuracy.

$$RMSE = \sqrt{\frac{1}{T}\sum_{i=1}^{T}(E_1^2(X))} \quad (7)$$

$$E(X) = X^{Prognosis} - X^{Effective} \quad (8)$$

Table 2. Elements that define the predictive power of mathematical models

Model	R^2	Adjusted R^2	RMSE*
1	0.8234	0.7645	3.789
2	0.8527	0.6073	4.893
3	0.9813	0.9502	2.025
4	0.9953	0.9906	0.7583
5	0.9939	0.9836	1.161

https://doi.org/10.24264/icams-2022.I.1

CONCLUSIONS

In conclusion, analyzing the values of the adjusted coefficient of determination (adjusted R^2), it is observed that the predictive power of model no. 3-5 is good. In addition, we observed that the values of the coefficient of determination (R^2) are close to 1 for mathematical model no. 3-5, but the best prediction is provided by model no. 3-5. In contrast, analyzing the square root values of the root mean square error (RMSE), it is observed that the small values, which do not lead to multiple residuals, are found for model no. 4.

Acknowledgement

This scientific paper has been funded by the Ministry of Research, Innovation and Digitalization, project 3D Electrotex, PN 19 17 01 01.

REFERENCES

Ahlbom, A., Bridges, J., De Seze, R., Hillert, L., Juutilainen, J., Mattsson, M.O., Neubauer, G., Schüz, J., Simko, M. and Bromen, K. (2008), "Possible Effects of Electromagnetic Fields (EMF) on Human Health – Opinion of the Scientific Committee on Emerging and Newly Identified Health Risks (SCENIHR)", *Toxicology*, 246(2-3), 248-50, https://doi.org/10.1016/j.tox.2008.02.004.

Aldrich, T.E. and Easterly, C.E. (1987), "Electromagnetic Fields and Public Health", *Environmental Health Perspectives*, 75, 159-171, https://doi.org/10.1289/ehp.8775159.

Deruelle, F. (2020), "The Different Sources of Electromagnetic Fields: Dangers Are Not Limited to Physical Health", *Electromagnetic Biology and Medicine*, 39(2), 166-175, https://doi.org/10.1080/15368378.2020.1737811.

Frank, J.W. (2021), "Electromagnetic Fields, 5G and Health: What about the Precautionary Principle?", *Journal of Epidemiology and Community Health*, 75(6), 562-566, https://doi.org/10.1136/jech-2019-213595.

Hendee, W.R. and Boteler, J.C. (1994), "The Question of Health Effects from Exposure to Electromagnetic Fields", *Health Physics*, 66(2), 127-136, https://doi.org/10.1097/00004032-199402000-00001.

Lin, J.C. (2012), *Electromagnetic Fields in Biological Systems*, Taylor & Francis, p. 458.

Litvak, E., Foster, K.R. and Repacholi, M.H. (2002), "Health and Safety Implications of Exposure to Electromagnetic Fields in the Frequency Range 300 Hz to 10 MHz", *Bioelectromagnetics*, 23(1), 68-82, https://doi.org/10.1002/bem.99.

Matthes, R., McKinlay, A.F., Bernhardt, J.H., Vecchia, P. and Veyret, B. (2003), *Exposure to Static and Low Frequency Electromagnetic Fields, Biological Effects and Health Consequences (0-100 kHz). Review of the scientific evidence on dosimetry, biological effects, epidemiological observations, and health consequences concerning exposure to static and low frequency electromagnetic fields (0-100 kHz)*, report no. ICNIRP-13-2003.

Modenese, A. and Gobba, F. (2021), "Occupational Exposure to Electromagnetic Fields and Health Surveillance According to the European Directive 2013/35/EU", *International Journal of Environmental Research and Public Health*, 18(4), p. 1730, https://doi.org/10.3390/ijerph18041730.

Moon, J.H. (2020), "Health Effects of Electromagnetic Fields on Children", *Clinical and Experimental Pediatrics*, 63(11), p. 422, https://doi.org/10.3345/cep.2019.01494.

Pal, M. and Bharati, P. (2019), "Introduction to Correlation and Linear Regression Analysis", in: *Applications of Regression Techniques*, 1-18, Springer, Singapore, https://doi.org/10.1007/978-981-13-9314-3_1.

Perrin, A. and Souques, M. (2012), *Electromagnetic Fields, Environment and Health*, Paris, France: Springer, 11-24, https://doi.org/10.1007/978-2-8178-0363-0_2.

Röösli, M. (2013), "Health Effects of Electromagnetic Fields", *Therapeutische Umschau*, 70(12), 733-738, https://doi.org/10.1024/0040-5930/a000472.

Röösli, M., Frei, P., Mohler, E. and Hug, K. (2010), "Systematic Review on the Health Effects of Exposure to Radiofrequency Electromagnetic Fields from Mobile Phone Base Stations", *Bulletin of the World Health Organization*, 88, 887-896, https://doi.org/10.2471/BLT.09.071852.

Saunders, T. (2003), "Health Hazards and Electromagnetic Fields", *Complementary Therapies in Nursing and Midwifery*, 9(4), 191-197, https://doi.org/10.1016/S1353-6117(03)00086-6.

Seitz, H., Stinner, D., Eikmann, T., Herr, C. and Röösli, M. (2005), "Electromagnetic Hypersensitivity (EHS) and Subjective Health Complaints Associated with Electromagnetic Fields of Mobile Phone

Communication—A Literature Review Published between 2000 and 2004", *Science of the Total Environment*, 349(1-3), 45-55, https://doi.org/10.1016/j.scitotenv.2005.05.009.

Stuchly, M.A. (1993), "Electromagnetic Fields and Health", *IEEE Potentials*, 12(2), 34-39, https://doi.org/10.1109/45.283813.

Vecchia, P., Matthes, R., Ziegelberger, G., Lin, J., Saunders, R. and Swerdlow, A. (2009), *Exposure to High Frequency Electromagnetic Fields, Biological Effects and Health Consequences (100 kHz-300 GHz)*, International Commission on Non-Ionizing Radiation Protection, 378.

World Health Organization (2000), "Electromagnetic Fields and Public Health: Cautionary Policies", *WHO Backgrounder*.

*** (2008), "EMF-NET MT-2 D49 Final Technical Report on Occupational EMF Exposure", Project Title: "Effects of the Exposure to Electromagnetic Fields: From Science to Public Health and Safer Workplace (EMF-NET)", available at: https://www.ciop.pl/CIOPPortalWAR/file/74478/EMFNET_MT2_D49_Final_technical_report.pdf

https://doi.org/10.24264/icams-2022.I.1

POLYAMIDE/POLYETHYLENE/CARBON FIBRE POLYMER NANOCOMPOSITES

LAURENTIA ALEXANDRESCU[1], MIHAI GEORGESCU[1], MARIA SÖNMEZ[1], ANTON FICAI[2], ROXANA TRUSCA[2], IOANA LAVINIA ARDELEAN[2]

[1]*The National Research & Development Institute for Textiles and Leather - Leather and Footwear Research Institute Division, 93 Ion Minulescu St., district 3, Bucharest, Romania, laurentia.alexandrescu@icpi.ro, laura_alexandrescu@yahoo.com*

[2]*Faculty of Applied Chemistry and Materials Science, University Politehnica of Bucharest, 1 Polizu St., 011061, Bucharest, Romania*

Polyamide and polyethylene are well known as engineering thermoplastic materials that are widely used in industrial applications for their good mechanical and thermal properties. The paper presents the study of the new nanostructured polymer composites based on polyamide/ compatibilizers/polyethylene/carbon fibres nanoparticles-PA/PE-g-MA/PE/CF in order to obtain, by injection, centre pivot liner, centre plates, and other components for the railway industry, with impact resistance higher than 5-8 kJ/m², abrasion resistance below 100 mm^3, resistance to temperatures of -40 - 240°C, resistance to impact and to outdoor applications, with temperatures ranging from -40 to +60°C, in rain, snow or sunshine. The influence of carbon fibres nanoparticles (CF) on the rheological and physico-mechanical properties of the polyamide was studied. The nanocomposites based on polyamide/ compatibilizers/ polyethylene/carbon fibres nanoparticles were characterized by scanning electron microscopy (SEM) and Fourier transformation infrared spectrum (FT-IR) and in terms of physico-mechanical properties. The studied nanocomposites have higher values compared to the blank samples, and the requirements of the railway of impact strength of 5 KJ/m^2. Carbon fiber concentrations greater than 1.5% result in decreases in impact strength values, similar to traction resistance values, but not lower than standard values. This leads to the conclusion that the percentages of carbon fibers in the range of 0.1-1.5% achieve maximum values of physical-mechanical parameters.

Keywords: nanocomposites, polyamide, carbon fibres, impact resistance

INTRODUCTION

The disadvantage is that the polymers are usually not compatible and the preparation of compounds with suitable (mainly processing and physico-mechanical) properties is not performant. Polyamide (PA) is a thermoplastic material, widely used in the industry, with varied applications (e.g. fibres, films, textiles, and various casting products) due to its mechanical and thermal properties. However, it has some limitations, such as: humidity absorption, sensitivity to shock, relatively low impact resistance and a weak dimensional stability. As a result, it is necessary to modify PA to improve physical-mechanical properties favourable for the industrial environment (Bhattacharya, 2016). Polyamide-based polymer composites are currently used to obtain components in the field of transport equipment. This equipment is used in working environments with varying temperatures (-40–200°C), subject to shocks and are equipped with elastomeric components, which deteriorate due to the environment, are purchased from abroad and are made of expensive materials and through lengthy technical processes (Dintcheva *et al*., 2017). Polyethylene is a thermoplastic polymer obtained by polymerizing ethylene at low, medium or high pressures, with the use of oxygen as initiator. It is presented in translucent solid form (granules or powders) for molding or viscous liquid for lubrication. High-density polyethylene (HDPE) is obtained at low pressure 8-10 at and has the following applications: - various foils and packaging; - rigid packaging such as bottles, cans, crates, barrels and auxiliaries such as caps; - printed foils in the form of

https://doi.org/10.24264/icams-2022.I.2

rolls for processing on packaging machines; - synthetic foam materials in the form of foils used as shock absorbers; - as coating material for other supports (e.g. glass). The compatibilisation of binary polymer compounds can be achieved by the addition of graft copolymer, segments of which have physical or chemical affinity with two immiscible homopolymers. In this case, polyethylene grafted with maleic anhydride (PE-g-MA) was used (Mistretta *et al*., 2015; Périé *et al*, 2012). Nano reinforcement materials are therefore components of composite materials designed to improve their mechanical properties. They are presented in different forms and orientations, according to which, the following aspects are pursued: 1. Increasing mechanical features; 2. Improving thermal resistance; 3. Compatibility with the composite matrix; 4. Good adaptation to processing; 5. lightness; 6. low price (Bose *et al*., 2011). Carbon fibers have remarkable properties, resulting from the preferential orientation of the crystals parallel to the fiber axis, and refer to very high stiffness and strength in the longitudinal direction, associated with a very low coefficient of linear dilatation in the same direction. The electrical and thermal conductivity of the carbon fiber composite depends on the degree of graphitization and the degree of anisotropy. Carbon fibers are obtained by pyrolysis of organic fibers. Two groups of fibers are distinguished: high tenacity fibers (Rm = 2500 ... 3100 MPa, and E = 200000Mpa); high modulus fibers (Rm = 2000 ... 2500 Mpa, and E = 400000Mpa). The thermal decomposition of an organic matter in a non-oxidizing atmosphere produces a carbon residue, which has a structure consisting of hexagonal carbon atoms arranged on parallel planes, offset so that a carbon atom projects into the center of a hexagon from the adjacent plan (Xu *et al*., 2016; Alexandrescu *et al*., 2018).

The paper presents the study of the new nanostructured polymer composites from PA/PE-g-MA/PE/CF nanoparticles to manufacture, by injection, bearing seals, contact plates, and other components for the railway industry, with impact resistance higher than 5-8 kJ/m², resistance to temperatures of -40 - 240°C and to outdoor applications, with temperatures ranging from -40 to +60°C, in rain, snow or sunshine.

EXPERIMENTAL SECTION

Materials

All composites contain the same two components in variable proportions: the polyamide (PA) elastomer PA6 (POLIMID B AV NATURALE – Poliblend Engineering Polymers Italy), with the following characteristics: specific weight, 1.40g/cm^3; impact resistance, 1.4 KJ/m^2; melt flow index (230°C /2.16 kg), 14g/10 min; melt temperature, 215-230°C and high density polyethylene (HDPE -TIPELIN 1108J - for impact and injection molding – MOL Petrochemicals Group) with the following characteristics: impact resistance – 3 KJ/m^2, flex module -1.5 Mpa, M.F.I (190°C/2.16 kg) – 8g/10 min, specific weight – 0.96 g/cm^3 and melting point 170-180°C. Other components: compatibilizers – polyethylene grafted with maleic anhydride PE-g-MA and carbon nanofibres (CF), black pellets with dimensions DxL-10x20-50 nm, all two products from Sigma Aldrich.

Preparation of Polyamide/Polyethylene/Carbon Fibre Polymer Nanocomposites

Polyamide (PA), polyethylene (HDPE), PE-g-MA and oxidized carbon fibres were mechanically mixed in a Brabender Plasti-Corder PLE-360 at 10-120 rotations/min, for

https://doi.org/10.24264/icams-2022.I.2

2 min. at 230°C to melt the plastomer, mixed for 3 min. at 240°C, and 2 min. at 200°C for homogenisation. The total time was 7 minutes. Table 1 shows tested formulations. The Brabender mixing diagrams, figures 1 and 2, show that the temperature in the chamber drops from 220 to 213°C for higher percentages of carbon fiber (starts at 213°C, decreases to about 200°C with a peak of 220°C at the end, in the case of the 0.15 CF percentage, and a lower at 213°C in the case of 5% CF percentage), and there are minor time variations in achieving maximum mixing forces. The maximum force is achieved at 30s in the case of 0.1% CFO percentage and 1.5 min. in the case of maximum percentage of 5% and its value exceeds 400Nm.

Table 1. Control and PA/HDPE/CFO polymer nanocomposite formulations with varying CF amounts (CFPE1-0.1%; CFPE2-0.3%; CFPE3-1%; CFPE4-2.5%; CFPE5-5%)

Compound	CFPE1	CFPE2	CFPE3	CFPE4	CFPE5
Polyamide – sebamid	270	270	270	270	270
Polyethylene	30	30	30	30	30
Carbon fibres	0.3	1.5	3	6	9
PE-g-MA	9	9	9	9	9
Total	309.3	310.5	312	315	318

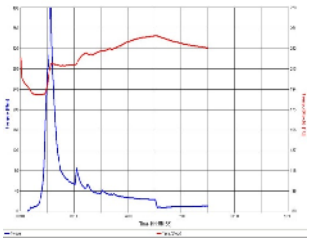

Figure 1. Brabender mixing diagram for PA

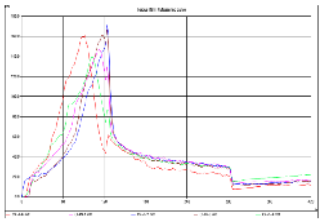

Figure 2. Brabender mixing diagram for composite CFPE 1-5

The compounds were then compression-molded (using an electrically heated laboratory press) to achieve a sheet of about 2 mm thick. Press parameters: preheating 3 min.; pressing 4 min.; cooling 13 min.; pressure 300 kN.; temperature 230°C. The sheet was then cooled down to room temperature under the same pressure. The specimens were die-cut from the compression molded sheet and used for testing after 24 hours of storage at room temperature.

RESULTS AND DISCUSSION

The polymer structures obtained, in initial state and after accelerated ageing were characterized in terms of their physical-mechanical properties, and results are presented in table 2. Analyzing the values of physical-mechanical tests reveals the following:

Hardness of PA/PE-g-MA/HDPE/CF polymer nanocomposites reinforced with carbon fibers varies within the range of 78-83 °Sh D, proportional to the amount of carbon fibers in the composites (0.1-3% mass percentages compared to the mass of polymers).

https://doi.org/10.24264/icams-2022.I.2

Table 2. Physico-mechanical characteristics for PA / HDPE composites - Oxidized carbon fibers

Mixtures	PA	CFPE1	CFPE2	CFPE3	CFPE4	CFPE5
Normal state						
Hardness °Sh D SR ISO 7619-1:2011	78	80	81	81	82	83
Tensile strength, N /mm^2 SR ISO 37:2012	30.5	65.3	68.5	73.8	69.4	55.9
Density, g /cm^3 SR ISO 2781:2010	1.14	1.14	1.14	1.14	1.15	1.16
Izod test, [KJ/m^2] STAS 7310-87	2.5	3.58	5.01	6.40	4.60	3.99
Melt flow index - 230°C force of 5 Kg, g/10min	160	169	180	159	139	126
Accelerated ageing 200°C x 168 h SR ISO 188 : 2007						
Hardness °Sh D SR ISO 7619-1:2011	77	77	77	77	78	79
Tensile strength, N /mm^2 SR ISO 37:2012	26.8	28.5	30.0	37.7	49.2	51.6

The value of the ***tensile strength*** of the nanocomposites increases compared to the concentration of carbon fibers (PA sample – 30.5 N/mm^2), the highest value is that of the CFPE3 sample – 73.8 N/mm^2 (1% CF). The percentage of carbon fibers of 2 and 3% added to the composite leads to an increase in the tensile strength values, compared to the control sample (69.4 and 55.9 N/mm^2, respectively).

The ***density*** values increase by two units, compared to the control sample (1.14 g/cm^3, proportionally with amount of carbon fibers added to the composites.

In order to test resistance to high temperature, ***accelerated ageing tests*** were conducted on the samples conditioned at 200°C for 168h. The analysis of the resulting values shows that they have changed within normal limits; samples are not deteriorated.

In order to estimate the resistance of brittleness of polymer nanocomposites, they were tested by ***Izod test*** method. This determination is the most important one due to the fact that one of the requirements of polymer nanocomposites is optimized impact resistance, for use in heavy impact conditions. PA value is 2.5 KJ/m^2. All nanocomposites tested have increased values compared to the control sample (PA), ranging between 3.58 to 6.40 KJ/m^2. Increased values were obtained for samples CFPE3 (PA/PE/1% CF) – 6.40 KJ/m^2 and CFPE2 (PA/PE/-0.5% CF) – 5.01 KJ/m^2. CF concentrations higher than 1% led to decreases in impact resistance values similarly to tensile strength values, but not lower than the reference value of 2.5 KJ/m^2.

In order to establish the technological parameters for processing CFPE1-CFPE5 polymeric structures in finished products, tests were carried out to determine the ***melt flow index*** at temperatures of 230°C and a pressure of 5 kg. The analysis of the obtained values (Table 2) shows an increased flow compared to PA (160g/10min) for the samples: CFPE1 (0.1% CF) – 169 g/10min, CFPE2 (0.5% CF) 180 g/10 min, CFPE3 (1% CF) 159 g/10 min, CFPE4 (2% CF) 139 g/10 min. and CFPE5 (3% CF) 126 g/10 min. The presented data indicate that carbon fibers decrease flow, which leads to modified technological parameters compared to the reference material, PA. Thus, product processing parameters are the following: temperature of 230-235°C, injection machine equipped with piston screw, pressure of 150-200 atm.

https://doi.org/10.24264/icams-2022.I.2

SEM image of the cross section of the fracture obtained from polyamide elastomer (PA), presented in Figure 3, emphasize a lamellar structure. The SEM images of cross sections of the fracture obtained from the other three samples (CFPE1, CFPE3 and CFPE5), shown in the Figures 4-6, in which the nanocomposites with rates differ from CF, have completely different aspects: they show a biphasic type morphology consisting in spheroid particles of PE distributed within a matrix of PA with evident lamellar morphology. The number of particles increases directly with the amount of CF of the nanocompound.

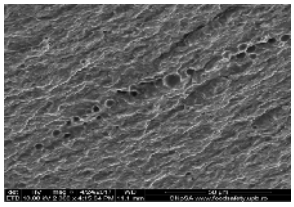

Figure 3. SEM Images from sample PA

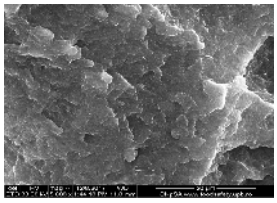

Figure 4. SEM Images from sample CFPE1-10

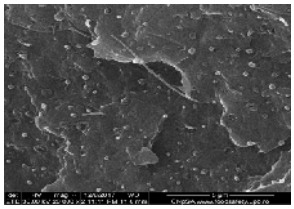

Figure 5. SEM Images from sample CFPE3

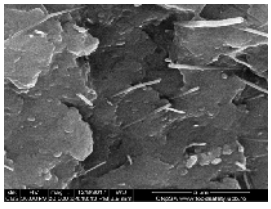

Figure 6. SEM Images from sample CFPE5

TG/DSC – To highlight thermal changes of the studied composites, the samples CFPE0-control sample (polymeric composite based on PA, PE and compatibilizer) and CFPE4 (polymeric composite based on PA, PE, compatibilizer and 1.5% carbon fibers) were compared.

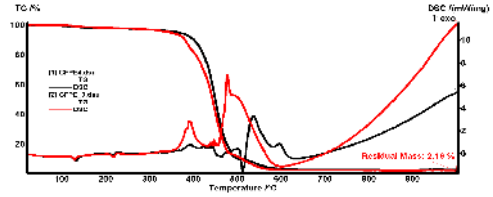

Figure 7. TG/DSG Images from sample CFPE0 and CFPE4

Between 335 and 500°C, the main degradation process of the sample takes place, which is accompanied by a multitude of slightly exothermic effects. The jagged appearance of the DSC curve indicates the multitude of overlapping and chained processes taking place. Between 335 and 480°C, the main stage of degradation takes place, with a mass loss of 81.44%. The process is a complex one, consisting of several overlapping and chained reactions, as can be seen from the shape of the DSC curve.

https://doi.org/10.24264/icams-2022.I.2

Between 480-600°C, the burning of the carbon mass left after the degradation of the polymer takes place, the process being accompanied by a strong exothermic effect, with a maximum at 497°C. The residual mass is 2.19%. Because the residual mass at 1000°C is higher in the case of the CFPE4 sample compared to the control sample CFPE0, it also indicates the fact that the carbon material additionally stabilizes the composite.

CONCLUSIONS

The paper presents the study of the new nanostructured polymer composites based on polyamide/polyethylene/PE-G-MA/carbon fibres in order to obtain, by injection, centre pivot liners, centre plates, and other components for the railway industry, with impact resistance higher than 5-8 kJ/m², abrasion resistance below 100 mm^3, resistance to impact and to outdoor applications, with temperatures ranging from -40 to +60°C, in rain, snow or sunshine. Polyamide, polyethylene, PE-g-MA and carbon fibres were mechanically mixed in a Brabender Plasti-Corder PLE-360 at 10-120 rotations/min, for 2 min. at 230°C to melt the plastomer, mixed for 3 min. at 240°C and 2 min. at 200°C for homogenisation. The nanocomposites polyamide/polyethylene/PE-g-MA/carbon fibres were characterized by scanning electron microscopy (SEM), TG/DSC and physico-mechanical tests. Carbon fibres concentrations higher than 1% lead to decreases in impact resistance values and tensile strength values. This leads to the conclusion that percentages in the 0.1-1% range lead to maximum values of physical-mechanical parameters.

Acknowledgements

This research was financed through PN-III-P2-2.1-PTE-2016, project: "New nanostructured polymeric composites for centre pivot liners, centre plate and other components for the railway industry - RONERANANOSTRUCT" supported by UEFISCDI Romania.

REFERENCES

Alexandrescu, L., Sonmez, M., Ficai, A., Trusca, R. and Tudoroiu, L. (2018), "Polymer Nanocomposites Polyamide/Polyethylene/Functionalized Carbon Fibres", *Conference Proceedings Volume 18: The 18th International Multidisciplinary Scientific GeoConference SGEM 2018*, Nano, Bio, Green and Space – Technologies for a Sustenable Future, Issue 61, Section: Micro and Nano Techn., 401-408, https://doi.org/10.5593/sgem2018/6.1/S24.054.

Bhattacharya, M. (2016), "Polymer Nanocomposites – A Comparison between Carbon Nanotubes, Graphene, and Clay as Nanofillers", *Materials*, 9, 262, https://doi.org/10.3390/ma9040262.

Bose, S., Bhattacharyya, A.R., Khare, R.A., Kamath, S.S. and Kulkarni, A.R. (2011), "The Role of Specific Interaction and Selective Localization of Carbon Fibres on the Electrical Conductivity and Phase Morphology of Multicomponent Polymer Blends", *Polymer Engineering and Science*, 51, https://doi.org/10.1002/pen.21998.

Dintcheva, N.Tz., Filippone, G., Arrigo, R. and LaMantia, F.P. (2017), "Low-Density Polyethylene/Polyamide/Clay Blend Nanocomposites: Effect of Morphology of Clay on Their Photooxidation Resistance", *Journal of Nanomaterials*, 1-9, https://doi.org/10.1155/2017/3549475.

Mistretta, M.C., Fontana, P., Ceraulo, M., Morreale, M. and La Mantia, F.P. (2015), "Effect of Compatibilization on the Photooxidation Behaviour of Polyethylene/Polyamide 6 Blends and Their Nanocomposites", *Polymer Degradation and Stability*, 112, 192–197, https://doi.org/10.1016/j.polymdegradstab.2015.01.002.

Périé, T., Brosse, A.-C., Tencé-Girault, S. and Leibler, L. (2012), "Co-continuous Nanostructured Nanocomposites by Reactive Blending of Carbon Nanotube Masterbatches", *Polymer*, 53, 984–992, https://doi.org/10.1016/j.polymer.2012.01.007.

Xu, Z., Yang, T., Nakamura, M., Yang, Y. and Hamada, H. (2016), "Effect of Carbon Powder Surface Treatment on Carbon Fiber Reinforced PA Composites", *Energy Procedia*, 89, 15-23, https://doi.org/10.1016/j.egypro.2016.05.003.

INVESTIGATIONS AND ANALYSIS OF EARTH MATERIALS TOWARDS THE DEVELOPMENTS IN SOME ADVANCED CHEMICAL AND CATALYTIC USES

SURESH ALUVIHARA[1]*, C.S. KALPAGE[1], P.W.S.K. BANDARANAYAKE[2], W.M.A.T. BANDARA[3], CIPRIAN CHELARU [4]

[1]*University of Peradeniya, Chemical and Process Engineering Department, Peradeniya, Sri Lanka, sureshaluvihare@gmail.com, +94758578194*

[2]*University of Peradeniya, Physics Department, Peradeniya, Sri Lanka*

[3]*University of Peradeniya, Chemistry Department, Peradeniya, Sri Lanka*

[4]*The National Research & Development for Textiles and Leather - Leather and Footwear Research Institute Division, Bucharest, Romania, cchelaru_cciprian@yahoo.com, +40722405053*

Earth materials are some sort of valuable resources with some multiples uses in some of industrial purposes and they are obtaining some economical values based upon the demand and the abundance. According to the most of research and experiments that relevant with the characteristics of solid earth materials, mainly there were obtained and disclosed some various outstanding physic-chemical characteristics of a large number of earth materials including the applications of material processing, nano-materials, composite materials and hard materials. In the existing research there were expected to characterize some selected clay varieties, a dolomite variety and a feldspar variety which are available in Sri Lanka towards the developments especially in some advanced chemical and catalytic applications. The X-ray fluorescence (XRF) spectroscopic analysis and Scanning electron microscopic (SEM) analysis were done for all of selected materials. The X-ray diffraction (XRD) analysis was done for three different selected clays and the Fourier transforms infrared (FT-IR) spectroscopic analysis was done for three different clay types and for a dolomite variety. According to the obtained results for the research, there were found the presence of at least 75% of Fe as the major element in each of clay with some other trace metallic elements such as K, Ti, Ca, Ba and Zr in such clays, kaolinite, montmorillonite and some of Fe minerals namely as muscovite and glauconite in such clays with quartz as a non-clayey mineral. There were found some higher amount of calcite in the selected dolomite with a trace amount of K and also there were found some higher K and Ca amounts presence in the selected feldspar rocks. When comparing the obtained results with past research out comes and modifications of materials, it seems that these materials will be much useful in the industrial applications such as the catalytic activities, waste water treatment applications in the removal of heavy metals due to the adsorption capacity, ion exchanging materials to remove unnecessary ions from waste water and in the removal of hardness from waste water due to the adsorption capacity of dolomite.

Keywords: earth materials, chemical analysis, chemical characteristics, essential applications

INTRODUCTION

Earth materials are natural resources in different phases such as gas, liquid and solid materials. Among all phases of earth materials, the solid earth materials are being considered under different categories such as the rocks, minerals, soil and organic materials. In the consideration of their physic-chemical and mechanical characteristics of such materials, there can be found some variations and applicability in various tasks even in their raw forms or they can be utilized for some advanced industrial applications in alteration. According to the categorizations of solid earth materials, soil types and mineral resources are considered as industrially demanded materials because of the variations in physic-chemical and mechanical characteristics of such earth resources which are focused on a vast range of industrial requirements and to solve a series of industrial problems (Ahmaruzzaman, 2011). When considering the important characteristics of most of solid earth materials, the variations in mineralogy, chemical contents, physical characteristics and mechanical strength of such materials are highlighted. In the short listing of the existing industrial applications of such earth materials, the following important applications and there can be found most of research works are being progressed that

https://doi.org/10.24264/icams-2022.I.3

associated with earth materials and their important characteristics for the sake of industrial applications as mentioned in Table 1 (Al-Anber, 2015).

Table 1. Earth resources/ materials and their applications

Earth Material	Applications/ Utilization
Clay, dolomite, feldspar	Water treatment applications/ adsorbents
Clay, dolomite	Catalytic applications/ catalytic materials
Dolomite, feldspar, charcoal	Recovery materials
Dolomite, clay	Refractory materials

When considering the distribution of some outstanding earth materials throughout the world, mostly there can be found uneven distributions at around some particular locations around the world based upon the geological incidents happened with the time. Sri Lanka is rich in mineral and earth resources as some of them are already being utilized in various industrial purposes such as tile manufacturing, brick manufacturing, composite materials and some of advanced chemical applications. It is an essential concern to discover some unexposed earth materials in the industrial applications based upon the requirements in the solving of environmental issues. In the existing research there were expected to analyze a few of selected earth materials for the sake of introducing a series of new and advanced applications that associated with the outstanding characteristics of such earth resources.

MATERIALS AND METHODOLOGY

According to the availability and expectations of the existing research, there were selected three different types of clay, a selected type of dolomite and a selected type of feldspar available at around different regions in Sri Lanka.

Three different types of clay samples were collected from three particular locations in Sri Lanka as mentioned in the Table 2.

Table 2. A brief description about the selected clays

Clay Type	Location	Current Applications
Anthill Clay	Matale, Sri Lanka	-
Brick Clay	Maduragoda, Sri Lanka	Manufacturing of bricks
Roof Tile Clay	Dankotuwa, Sri Lanka	Manufacturing of roof tiles

A few of representative clay samples are shown in the following figures.

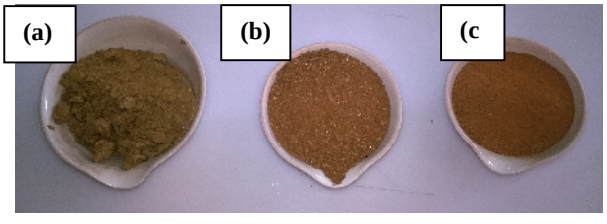

Figure 1. (a) Roof tile clay, (b) brick clay and (c) anthill clay

Apart from the clays, two different types of earth materials were selected. Those are dolomite and feldspar as described in the Table 3.

https://doi.org/10.24264/icams-2022.I.3

Table 3. A brief description about the selected dolomite and feldspar

Earth Material	Location	Current Applications
Dolomite	Matale, Sri Lanka	Lime productions
Feldspar	Owala-Kaikawala, Sri Lanka	Ceramic and porcelain purposes

A few of dolomite and feldspar samples were shown in the following figures.

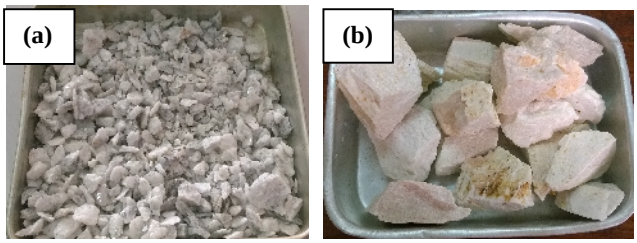

Figure 2. (a) Dolomite and (b) feldspar samples

In the preparation of the final representative samples for the experimentation, the following methodology was followed.

- Drying of each row sample and removal of the moisture content
- Pulverizing or the comminuting of each sample to prepare a powdered samples as <0.075mm of particle size.

Each powdered raw material sample was characterized using X-ray fluorescence (XRF) spectrometer, Scanning electron microscope (SEM), Fourier transform infrared (FT-IR) spectrometer and X-ray diffraction (XRD) spectrometer.

RESULTS AND DISCUSSION

The X-ray fluorescence (XRF) spectroscopic results regarding the selected earth materials are shown in the Table 4.

Table 4. Elemental compositions of earth materials

Element (%)	Fe	Ti	Ba	K	Ca	Zr	Zn
Anthill Clay	82.08	4.84	0.79	12.28	-	-	-
Brick Clay	84.38	5.92	2.14	-	7.56	-	-
Roof Tile Clay	75.72	2.95	5.30	12.67	-	3.36	-
Dolomite	-	-	-	0.54	99.46	-	-
Feldspar	5.14	-	-	52.98	41.43	-	0.45

According to the elemental chemical compositions of the selected clays there were obtained at least 75% of Fe in each clay type with the trace amounts of Ti, Ba, K, Ca and Zr in some of clays. It was not detected any toxic element even in any of earth material apart from the basic metallic elements. Based upon the non toxicities of clays, it is possible to recommend these clays for the applications of waste water treatments only considering the phenomenon of filtration. However, the adsorption capacities of such clays can be further discussed with the mineralogy of such clays furthermore (Ashutosh *et al*., 2018).

When considering the chemical composition of dolomite, it seems that the content is much closer to the chemical content of calcite rather than the chemical content of dolomite because of the lack of Mg which is an essential element for dolomite and the

https://doi.org/10.24264/icams-2022.I.3

relatively higher content of Ca in such dolomite. Also it was observed some significant percentage of Ca in feldspar and it is possible to recommend both materials for the applications as the strong refractory materials as CaO is a strong refractory agent.

The Fourier transform infrared (FT-IR) spectra and Scanning electron micrographs (SEM) of clays and other earth materials are shown in the following figures.

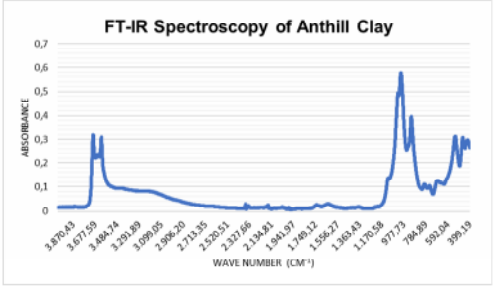

Figure 3. FT-IR spectroscopy of anthill clay

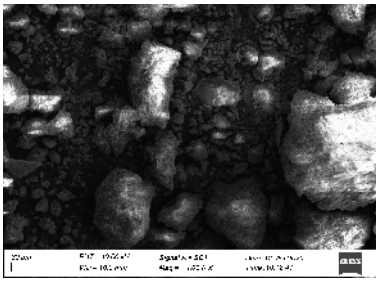

Figure 4. SEM micrographs of anthill clay

The above spectroscopes and micrographs showed the presence of kaolinite which is known as a leading clay mineral and a strong adsorbent for heavy metals, pathogens, particulate matter and some organic matter presence in waste water and polluted air.

In the consideration of FT-IR spectroscopy of this clay type especially there were identified some peaks at the wave numbers of ~3700 cm^{-1}, ~3650 cm^{-1}, ~1100 cm^{-1}, ~900 cm^{-1}, ~700 cm^{-1} and ~550 cm^{-1} that relevant with the compound kaolinite.

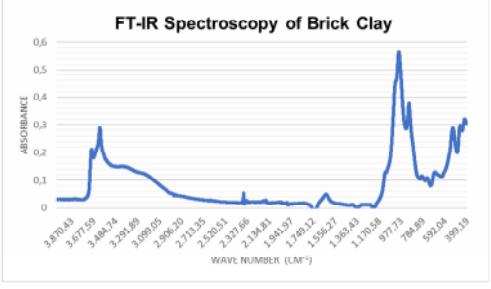

Figure 5. FT-IR spectroscopy of brick clay

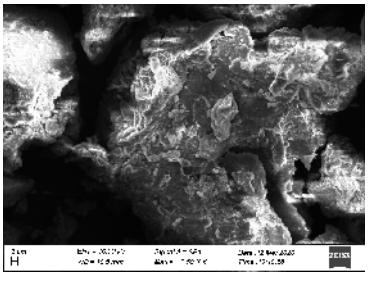

Figure 6. SEM micrographs of brick clay

Apart from the leading clay mineral kaolinite, there can be identified a few of various clay minerals and non clayey minerals with respect to the peaks at ~1100 cm^{-1}, ~800 cm^{-1} and ~450 cm^{-1} for quartz and ~1000 cm^{-1} for muscovite.

Muscovite is known as a clay mineral which is having the property of electrical conductivity. Therefore, it is possible to expect some electrical conductivity from such clay types based upon the content of such mineral (Parker *et al*., 1969).

https://doi.org/10.24264/icams-2022.I.3

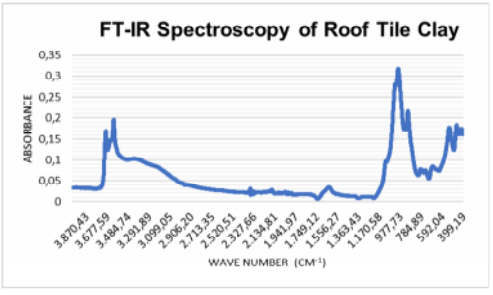

Figure 7. FT-IR spectroscopy of roof tile clay

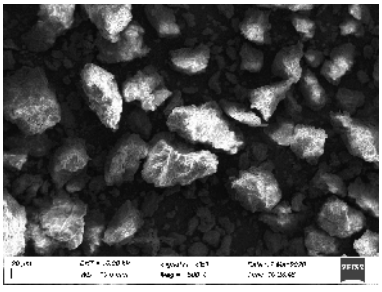

Figure 8. SEM micrographs of roof tile clay

As the overall analysis of the above results, there can be observed the presence of kaolinite in each as every clay type in different contents and it is possible to these clay types for the sake of following applications (Srinivasan, 2011).

- Waste water treatments such as the removals of particulate matter, heavy metals, organic pollutants and pathogens.
- Catalytic applications that associated with the advanced chemical processes

The analytical results of dolomites and feldspar are shown in the following graphs and figures.

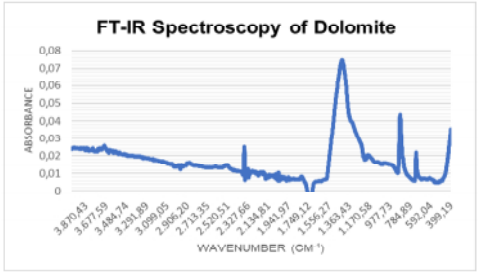

Figure 9. FT-IR spectroscopy of dolomite

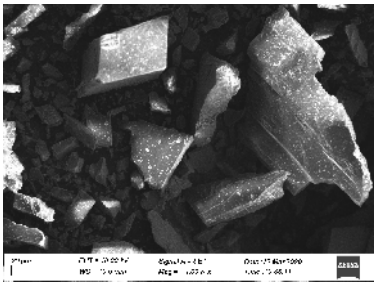

Figure 10. SEM micrographs of dolomite

According to the above results of the dolomites, especially it is bit difficult to distinguish the FT-IR spectroscopy of dolomite from the same spectroscopy of calcite. Therefore, some specific advanced analytical method would be an essential step for the further analysis. The SEM micrographs interpreted the tabular and massive crystals which are much similar with the crystal systems of dolomite.

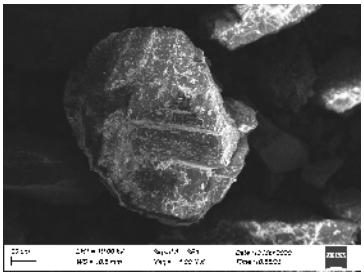

Figure 11. SEM micrographs of feldspar

https://doi.org/10.24264/icams-2022.I.3

The SEM micrograph of feldspar shows the massive crystals with cracked surfaces and some advanced microscopic or elemental chemical compositional analysis will be needed in further analysis.

When considering the obtained results for both feldspar and dolomite and comparing them with the past research outcomes and literature concepts, it is possible to recommend the following industrial applications.

- Water treatment applications such as the removal of hardness from water due to the adsorption capacities;
- Recovery material due to the adsorption;
- Refractory material due to the heat resistant capacity.

CONCLUSION AND FURTHER RECOMMENDATIONS

The characterization results of the earth materials interpret the non toxicity in clays, dolomites and feldspar and there were observed the presence of kaolinite, muscovite and quartz as the minerals, relatively higher content of calcite in the selected dolomite variation and relatively higher amount of Ca in the selected feldspar. Therefore, these earth materials can be further developed towards the applications in waste water treatments based upon the adsorption capacities of them including the clay and dolomite, refractory materials, catalysis applications and some particular advanced chemical applications.

It is possible to recommend the following advanced analysis for the above materials based upon the advanced industrial application purposes of such materials.

- Advanced microscopic analysis, advanced compositional analysis and performing of nano-technological uses.

Acknowledgement

We wish to acknowledge the technical staff at the Department of Chemistry, Department of Physics, Department of Zoology, Department of Chemical and Process Engineering and Department of Civil Engineering, University of Peradeniya, Sri Lanka and voluntary material providers on behalf of their great assistance in our research works.

REFERENCES

Ahmaruzzaman, M. (2011), "Industrial Wastes as Low-cost Potential Adsorbents for the Treatment of Wastewater Laden with Heavy Metals", *Advanced Colloid Interface*, 166(1-2), 36–59, https://doi.org/10.1016/j.cis.2011.04.005.

Al-Anber, M.A. (2015), "Adsorption of Ferric Ions onto Natural Feldspar: Kinetic Modeling and Adsorption Isotherm", *International Journal of Environmental Science and Technology*, 12, 139–150. https://doi.org/10.1007/s13762-013-0410-1.

Ashutosh, M., Lav, K. and Munish, K.M. (2018), "Analysis of Heavy Metal in Soil through Atomic Absorption Spectroscopy for Forensic Consideration", *International Journal for Research in Applied Science & Engineering Technology*, 6(6), 1188-1192, https://doi.org/10.22214/ijraset.2018.6173.

Parker, T.W. (1969), "A Classification of Kaolinites by Infrared Spectroscopy", *Clay Minerals*, 8, 135-141, https://doi.org/10.1180/claymin.1969.008.2.02.

Srinivasan, R. (2011), "Advances in Application of Natural Clay and Its Composites in Removal of Biological, Organic, and Inorganic Contaminants from Drinking Water", *Advances in Materials Science and Engineering*, 872531, 1-17, https://doi.org/10.1155/2011/872531.

Yu, C. and Han, X. (2015), "Adsorbent Material Used in Water Treatment – A Review", *2nd International Workshop on Materials Engineering and Computer Sciences*, 290-293, https://doi.org/10.2991/iwmecs-15.2015.55.

NANOPIGMENTS FOR LEATHER FINISHING COATINGS

ANNA BONDARYEVA[1], MARYNA ZHALDAK[1], OLENA MOKROUSOVA[1,2], OLENA OKHMAT[2]

[1]*State University of Trade and Economics, Ukraine*

[2]*Kyiv National University of Technologies and Design, Ukraine, olenamokrousova@gmail.com*

The work is focused on obtaining nanopigments by adsorption of anionic dyes on positively charged montmorillonite. The effect of sequential modification of aqueous dispersions of montmorillonite with cationic and anionic compounds on the structural and charge characteristics of mineral dispersions was studied. The effect of chemical dispersion of agglomerates of aqueous montmorillonite dispersions after adding carbonate solutions was shown. The treatment of dispersions of original montmorillonite with sodium carbonate provides maximum dispersion of mineral aggregates by penetrating into the interstructural space of aluminosilicate packets, moving them apart and separating them. It was found that the modification of montmorillonite dispersed by sodium carbonate by adding basic chromium sulfate is accompanied by a change in the surface chemistry of the mineral and structural transformations. Structural changes are manifested by the formation of a developed structure of cationic montmorillonite. The cationic surface charge of montmorillonite and high specific surface of montmorillonite are important factors for ensuring effective adsorption of anionic dyes on the surface of the mineral. The efficiency of adsorption of anionic dyes on cationic montmorillonite is investigated. It was shown that the adsorption of dyes depended on the pH of the medium. The scheme of obtaining nanopigments, which were characterized by good covering power, saturated and intense colour was proposed.

Keywords: montmorillonite, pigment, leather finishing coating

INTRODUCTION

Traditional leather finishing involves applying a covering composition to the surface of leather. The finishing coating provides protection of leather from external atmospheric and mechanical impacts (Covington, 2009).

The type of leather coating depends on the content of pigments and can be (Covington, 2017; Zhuravsky *et al*., 1996; Kasyan, 2019): aniline – a transparent coating without the use of pigments; semi-aniline – characterized by a small content of pigments to provide, mainly, a shade of color; and pigmented – with a significant content of pigments for complete coverage of the surface of leather with a colored covering layer.

Pigments provide color and covering power to the finishing coating (Winter *et al*., 2017). Organic or inorganic pigments are used in the finishing coating of leathers. Covering compositions with organic pigments provide leather with shine, bright and intense color, but have low light fastness and heat resistance. Inorganic pigments create a high-quality coating with good light fastness and water resistance, but are characterized by a high tendency to sedimentation and are limited in color and brightness (Winter *et al*., 2017; Osgood, 1990).

The ability of the coating to form a uniform coating stable composition with required thickness depends on the properties of the pigment, the origin of their surface, and the size of the particles.

The use of nanopigments provide improved physical and mechanical indexes of the leather finishing coating (Bondaryeva and Mokrousova, 2020; Bondaryeva *et al*., 2021).

The aim of the work was to describe the scientific basis of patterns of anionic dyes adsorption on positively charged montmorillonite to obtain nanopigments for leather finishing coatings.

https://doi.org/10.24264/icams-2022.I.4

EXPERIMENTAL

Materials

Bentonite clay from the Cherkassky deposit (Ukraine), after thorough purification and washing was used as a basis for obtaining nanopigments. The main mineral was montmorillonite, the content was 85±3 %. The value of the exchange capacity was 72 mg-eq/100 g of clay. Humidity – 27 ± 3 %.

The sodium carbonate, basic chromium sulfate (Ш) and anionic dyes were used to modify dispersions of montmorillonite.

Methods

The nanopigments were obtained by sequential treatment of aqueous montmorillonite dispersions (100 g/l) with sodium carbonate, basic chromium sulfate and anionic dyes.

Firstly, 6,0% of sodium carbonate from weight of dry montmorillonite was used, and then the cationic form of montmorillonite was obtained by modifying the dispersion of Na^+-montmorillonite with chromium compound. For this purpose, the basic chromium sulfate was used – $Cr_2(SO_4)_n(OH)_{6-2n}$, chromium oxide (III) content was 25.6 %. A solution of basic chromium sulfate in the amount of 10.0% Cr_2O_3 (by weight of the montmorillonite) was added to the dispersion of Na^+-montmorillonite (MMT–Na^+). Mixing was continued until a homogeneous mass of gray colour was obtained. The pH value of the modified dispersion of cationic montmorillonite (MMT-Cr^{3+}) was 4.5-5.2.

The nanopigments were prepared by gradually mixing the cationic form of montmorillonite with the anionic dyes. Mixing was performed using a mechanical mixer (30–40 min, 40–45°C) to obtain time-stable dispersions in the form of nanopigments of saturated deep colour. The consumption of anionic dyes in a ratio of 1:1 according to the mineral component. The nanopigments were obtained as the colored modified dispersions of montmorillonite.

A laser-correlation spectrometer “ZetaSizer–3” (Malvern Instrument, USA) with a Multi Computing Correlator type 7032 CE was used to study the dispersion of mineral systems.

The adsorption of dyes from aqueous solutions on the cationic form of montmorillonite was determined by measuring the light transmittance of dye solutions of different concentrations.

The electrokinetic potential was determined by microelectrophoresis.

RESULTS AND DISCUSSION

In montmorillonite modification, molecules of polar liquids (for example, sodium carbonate) can freely penetrate into the interpackets space of montmorillonite, push them apart and increase the distance between packets. As a result, montmorillonite particles disperse spontaneously in water, their number per unit volume increases significantly, and the number of direct contacts for further interactions increases.

It is shown that treatment of dispersions of native montmorillonite with sodium carbonate provides maximum dispersion of mineral aggregates by penetrating into the interstructural space of aluminosilicate packets, moving them apart and separating them.

https://doi.org/10.24264/icams-2022.I.4

Aqueous dispersion of original montmorillonite with a concentration of 100 g/l (Fig. 1a) is characterized by a monomodal distribution of mineral aggregates in terms of size, intensity, and volume. In the dispersion of native montmorillonite, there are mainly aggregates with sizes of 1678 nm, 2265.8 nm, and 3059.5 nm. The volume of the dispersed medium is 40% filled with aggregates with a size of 2265.8 nm, and the number of particles in this volume is 60% of the total number in the dispersion. In the aqueous dispersion of montmorillonite, there are aggregates of 1242.7 nm (the smallest size) and 4131.3 nm (the largest size).

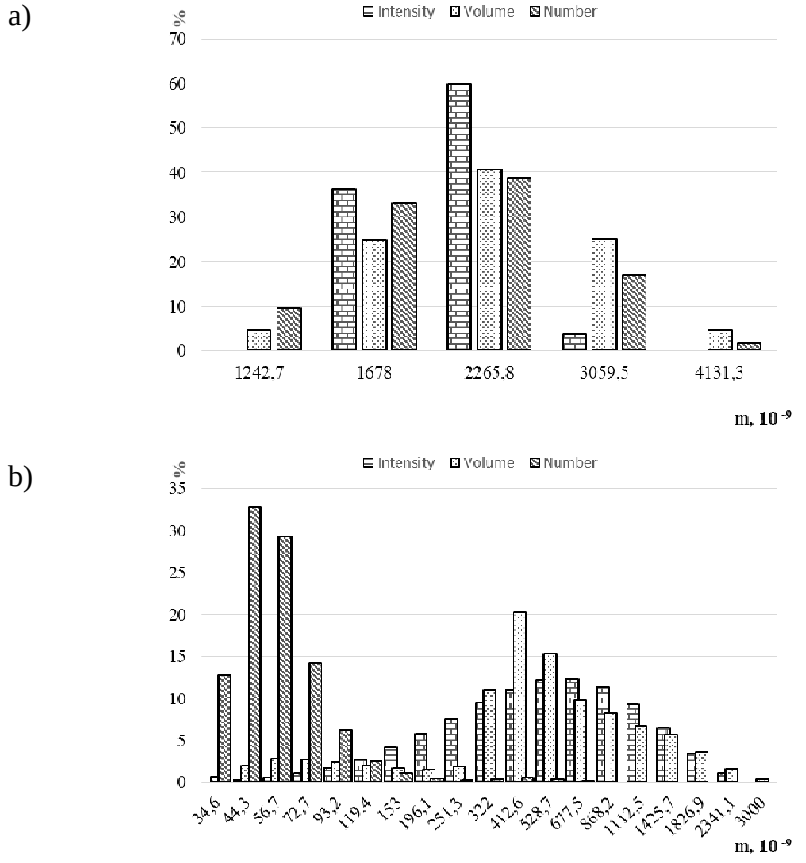

Figure 1. Distribution of montmorillonite particles in aqueous dispersion

After processing montmorillonite (Fig. 1b) with sodium carbonate, the largest number of mineral particles with sizes of 34.6-93.2 nm was found. This indicates the dispersion of montmorillonite aggregates. It was also found that the amount of mineral particles with sizes of 153.0-1826.9 nm increases in the volume, which indicates the polymodal nature of the montmorillonite dispersion after treatment with sodium carbonate.

https://doi.org/10.24264/icams-2022.I.4

That is, the dispersion of MMT–Na^+ contains nano-sized particles with a significant number of contacts for further effective modification with chromium compounds and obtaining the cationic form of montmorillonite.

It was found that the replacement of exchangeable cations Ca^{2+} and Mg^{2+} of native montmorillonite with Na^+ cations in modified montmorillonite leads to a shift of the basal reflex to larger 2θ° angles and a decrease in d_{001} to 12.8 Å (Table 1). The transformation of MMT–Na^+ into the form of MMT–Cr^{3+} is accompanied by a shift of the basal reflex toward smaller 2θ° angles and a subsequent increase in the value of d_{001} to 14.4 Å (Table 1). The change in the diffraction pattern is due to the different orientation of chromium complexes in the interlayer space of montmorillonite.

Table 1. The structural changes of montmorillonite

Indicator	Montmorillonite		
	native	MMT–Na^+	MMT–Cr^{3+}
The basal spacing (d_{001}) values MMT, Å	14.8	12.8	14.4
The specific surface area, m^2/g	60	160	280

The specified effect was confirmed by the results of an increase in the specific surface of montmorillonite (Table 1) from 60 to 280 m^2/g.

It was also shown that the surface of the mineral particles acquires the maximum positive charge in the pH range of 4.6-6.2 (Fig. 2).

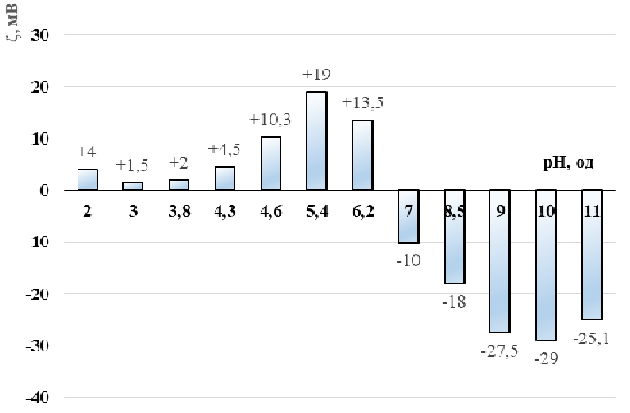

Figure 2. Effect of pH on the level of ζ-potential of modified MMT–Cr^{3+}

The cationic surface charge of montmorillonite and high exchange capacity are important factors for ensuring effective adsorption of anionic dyes on the surface of the mineral.

Adsorption of anionic dyes on the surface of modified montmorillonite is based on energy unsaturation, which after cationization of montmorillonite with Cr^{3+} compounds causes intense attraction of molecules of the dispersion medium and the formation of a monomolecular layer with the help of hydrogen bonds.

https://doi.org/10.24264/icams-2022.I.4

A high level of adsorption of anionic blue and anionic dark green dyes was shown. Adsorption isotherms of these dyes on the surface of modified montmorillonite are presented in Fig. 3.

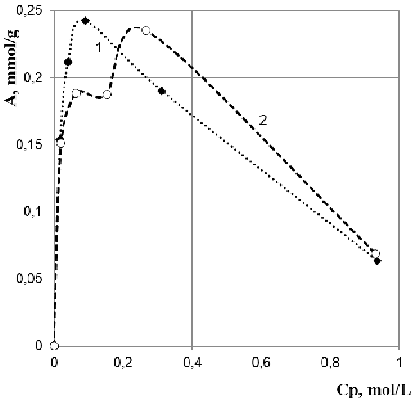

Figure 3. The adsorption isotherms of anionic dyes of montmorillonite after dye treatment: anionic dark green (1), anionic blue (2)

Colored modified montmorillonite dispersions of blue and dark green colors were characterized by color saturation and intensity. Color stability was also established in the range of pH 5.0–6.5, which indicates the possibility of using colored dispersions of montmorillonite as nanopigments for finishing coating leather.

The mechanism of obtaining nanopigments for leather decoration by sequential modification of montmorillonite with sodium carbonate, basic chromium sulfate, and anionic dyes is presented in the scheme (Fig. 4).

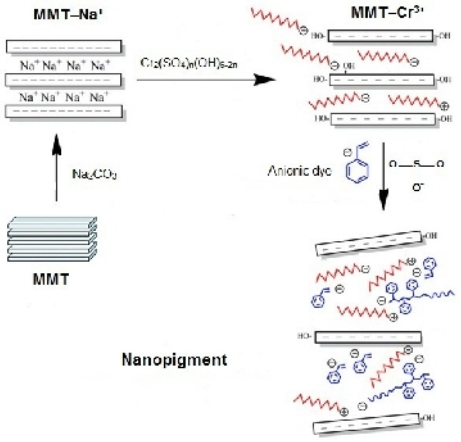

Figure 4. The mechanism of obtaining nanopigments

Nanopigments of dark green and dark blue were obtained according to the presented scheme. The properties of the nanopigments obtained are presented in Table 2.

https://doi.org/10.24264/icams-2022.I.4

Table 2. The properties of nanopigments

Indicator	Nanopigment / color	
	Dark green	Blue
The dry residue, %	21.1	23.7
Sedimentation, %	0	0
Covering power, g/m^2	14.0	16.0
Resistance to stratification, days	more than 240	

In general, the results of studies of structural and electrosurface changes of montmorillonite indicate the expediency of mineral modifications by sequential processing with multifunctional substances to obtain nanopigments for covering compositions and leather finishing.

CONCLUSIONS

The effect of sequential modification of aqueous dispersions of montmorillonite with cationic and anionic compounds on the structural and charge characteristics of mineral dispersions was studied. The effect of chemical dispersion of agglomerates of aqueous montmorillonite dispersions after adding carbonate solutions and obtaining a polymodal distribution of montmorillonite dispersion particles was shown. It was found that the modification of montmorillonite dispersed by sodium carbonate by adding basic chromium sulfate is accompanied by a change in the surface chemistry of the mineral and structural transformations. Structural changes are manifested by the formation of a developed micro- and mesoporous structure of cationic montmorillonite. The intensive attraction of molecules of the dispersion medium of anionic dyes on the surface of the cationic form of montmorillonite was studied. It has been proven that anionic dark green and anionic blue dyes were capable to adsorb on the cationic surface of montmorillonite at a ratio 1:1. The maximum level of adsorption of anionic dark green and blue dyes on the cationic surface of montmorillonite occurs in the range of pH 5–6.5. The nanopigments were characterized by deep intense colour; they were stable over time and had good covering power.

REFERENCES

Bondaryeva, A., Mokrousova, O. and Okhmat, O. (2021), "Hybrid Pigments Based on Montmorillonite and Anionic Dyes for Leather Finishing", *Solid State Phenomena*, 320, 198-203, https://doi.org/10.4028/www.scientific.net/SSP.320.198.

Bondaryeva, A. and Mokrousova, O. (2020), "The Acrylic/Montmorillonite Nanocomposites for Leather Finishing", *Proceedings of the 8th International conference on Advanced Materials and Systems – ICAMS 2020*, Bucharest, 43-48, https://doi.org/10.24264/icams-2020.I.3.

Covington, T. (2009), *Tanning Chemistry: The Science of Leather*, RSC Publishing, Cambridge, 315 p.

Kasyan, E.E. (2019), *Physico-Chemistry of Polymer Film Formers for Leather Finishing*, Education of Ukraine, Kyiv, 178 p. (in Ukrainian).

Osgood, M.J. (1990), "Pigments in Modern Leather Finishing", *Journal of the Society of Leather Technologists and Chemists*, 74(1), 1-6.

Winter, C., Agustini C.B., Elizabeth, M., Schultz, R. and Gutterres, M. (2017), "Influence of Pigment Addition on the Properties of Polymer Films for Leather Finishing", *Journal of the Society of Leather Technologists and Chemists*, 101(2), 78-85.

Zhuravsky, V.A., Kasyan, E.E. and Danylkovych, A.G. (1996), *Technology of Leather and Fur*, KDUTD, Kyiv, 744 p. (in Ukrainian).

https://doi.org/10.24264/icams-2022.I.4

INFLUENCE OF OLIVE MATURITY ON SOME PHYSICO-CHEMICAL PROPERTIES AND FATTY ACID COMPOSITION OF MONOVARIETAL OLIVE OIL EXTRACTED FROM HALHALI CULTIVAR

DILSAT BOZDOGAN KONUSKAN

Mustafa Kemal University, Faculty of Agriculture, Food Engineering Department, dilsat@mku.edu.tr

This study was carried out to determine influence of olive maturity on some physicochemical properties and fatty acid compositions of olive oils extracted from the Halhalı cultivar which harvested from Hatay in the Eastern Mediterranean region of Turkey. For this purpose, olive oils were obtained by mechanical method from olives collected from Halhalı cultivar in 3 different olive maturity of the 2021 production season. Ripening index and oil yield analysis of the olives and free fatty acids, peroxide value, fatty acid compositions were carried out in Halhalı olive oil. Free fatty acids and peroxide values of olive oils were found in the range of 0.39-0.73 (%oleic acid) and 5.14-9.43 meq O_2/kg respectively. The amount of free fatty acids increased with maturity. It was determined that the oleic acid in the range of 67.59%-70.26%, palmitic acid in the range of 13.56-15.82%, linoleic acid in the range of 9.52-13.65%, stearic acid in the range of 3.34-4.13%, palmitoleic acid 0.96%-1.29%, linolenic acid 0.86-0.98% and arachidic acid 0.42-0.53. It was determined that decrease in oleic acid and palmitic acid contents and an increase in linoleic acid content with maturity. It has been determined that Halhalı monovarietal olive oil is within the limits specified in the Turkish Food Codex on Olive Oil and Pirina Olive Oil in terms of the examined properties.

Keywords: Olive oil, ripening, fatty acids

INTRODUCTION

Virgin olive oil (VOO) has nutritional and functional characteristics that make it unique among other vegetable oils (Baieno *et al*., 2015). Virgin olive oil is mainly composed of two different fractions: the saponifiable fraction and the unsaponifiable fraction. The saponifiable fraction represents nearly 98% of the total composition, including the fatty acids and triacylglycerols (Visioli and Galli 2002; Ranalli *et al*., 2004). The main components in the unsaponifiable fraction are sterols, alcohols, vitamin E, hydrocarbons, carotenoids, volatile compounds and phenolic compounds, representing only 2% of the total (Antonini *et al*., 2015). Olive oil has a source of monounsaturated fatty acids, especially oleic acid (60–80%), which is less susceptible to oxidation, having an important role in terms of contributing to the high stability and long shelf life of olive oil (Anastasopoulos *et al*., 2012). Several factors such as variety, ripening degree, climate and geographic conditions, extraction methods, and preservation conditions significantly influence the chemical composition and quality of VOO (Salvador *et al*., 2013; Tura *et al*., 2007; Konuskan and Mungan, 2016). Quality properties and fatty acid composition are significantly affected by olive fruit maturity. Maximum oil content is reported to occur between 60th to 75th days after the start of the ripening process (Aloiwaiesh *et al*., 2018). The objective of this study was to evaluate the influence of olive maturity and on Halhalı monovarietal olive oil quality and fatty acid compositions.

https://doi.org/10.24264/icams-2022.I.5

EXPERIMENTAL

Olive Sampling

This study was conducted during the crop season of 2021. Halhalı olive variety obtained from three single trees of a given variety were collected from in Hatay (Fig. 1). Only undamaged fruits which were considered healthy were hand-picked from each younger tree. Three harvesting dates (from October to December with 20 days intervals) corresponding to three different ripening stages (green–spotted–ripe) was selected. At the end of each harvest, the samples were labelled and immediately transported to the laboratory. They were extracted to olive oil within 24 h.

Figure 1. Halhalı variety tree in Hatay

A representative 3 kg olive sample was extracted to obtain the oil by a laboratory scale mechanical mill (Hakkı Usta, Turkey) with a crusher, a vertical malaxer and a two-phase centrifuge. Malaxation and centrifuge processes was performed at 28 °C for 45 min and at 3000 rpm, respectively. The oil was separated by decanting and put into dark glass bottles. Oil samples were stored in darkness at 4 °C until chemical analysis which were triplicated.

Ripening Index

The ripening index (RI) was determined from one hundred olive fruits randomly drawn from each olive variety. This parameter, which is based on evaluating the color of both skin and pulp of olives, was determined according to International Olive Council (IOOC 2001).

Oil Content (%)

Oil content was determined according to the method described in American Oil Chemists' Society (AOCS) Official Methods Am 2–93 (AOCS, 2003) by Soxhlet extraction method using n-hexane at 80°C for 6 h.

https://doi.org/10.24264/icams-2022.I.5

Olive Oil Extraction

Three kg of olive samples selected from Halhalı variety were eliminated from unhealthy and decay fruits. Olive oil extraction (Figure 2) was performed using a laboratory scale mechanical extractor. It is equipped with a crusher, a malaxer and a decanter. In fact, olives were crushed and then slowly kneaded for 40 min at 28°C. Next, the obtained paste was centrifuged at 3000 rpm for 2 min with the decanter. The oil was put into dark glass bottles under a nitrogen atmosphere of 100 ml without headspace. The oil obtained was kept at 4°C in the dark area until analyses which were duplicated.

Figure 2. Olive oil extraction

Fatty Acid Composition

Fatty acid composition of Halhalı olive oils was determined according to the analytical method described in by the International Olive Oil Council, COI/T.20/Doc.No.24 (IOOC, 2004). Methyl-esters were prepared by vigorous shaking of a solution of oil in n-heptane (0.1 g in 2 mL) with 0.2 ml of 2 N methanolic potassium hydroxide and analyzed by Agilent gas chromatography system (Agilent 6850, USA) equipped with a hydrogen flame ionization detector (FID) and a capillary column DB-23 of 60 m length × 0.25 mm i.d. and 0.25 µm of film thickness. The carrier gas was helium at 1.0 ml/min ratio. Injector, oven and detector temperatures were 250, 230 and 280 °C, respectively. The injection volume was 1 µL. The results were expressed as a relative area percentage of total fatty acid methyl esters. Fatty acids were determined by comparing their retention times with those of reference compounds.

https://doi.org/10.24264/icams-2022.I.5

RESULTS AND DISCUSSION

Ripening Index

Table 1 reports the ripening index (RI) and oil content of Halhalı variety. The RI values was determined in the range of 0.75 (green) – 4.56 (ripe). RI values were increased with the ripening degree. RI analysis are very important for determining the harvesting time during the fruit ripening process (Yang *et al*., 2021).

Oil Content (%)

As can be seen in Table 1, the oil content of Halhalı olives varied between 27.03 (green) and 34.19% (ripe). The oil content of Halhalı olives increased remarkably from green to ripe maturation stage. In similar studies, this value was found to be 16.19-33.93% by Yorulmaz and Bozdogan Konuskan (2017) and 24.69-41.70% by Emmanouilidou *et al*. (2021).

Table 1. Physicochemical properties of Halhalı monovarietal olive oil

Physicochemical properties	Green	Spotted	Ripe
Ripening Index	0.75±0.06	2.58±0.03	4.56±0.06
Oil content (%)	27.03±1.24	30.16±1.36	34.19±2.17
Free fatty acids (%Oleic)	0.39±0.07	0.58±0.16	0.73±0.22
Peroxide value (meqO_2/kg)	5.14±0.61	8.02±0.52	9.43±0.18

Free Faty Acids (% Oleic)

As can be seen in Table 1, free fatty acids of olive oils ranged between %0.39 (green)–%0.73 (ripe). Moreover, the free fatty acid content of oils was below the limit of 0.8% established by Turkish Food Codex and Regulation EC/ 1989/2003 (European Union Commission, 2003; Turkish Food Codex, 2014). The free fatty acids of olive oils increased with the olive maturity. Moreover, the free fatty acid percentages of our olive oil samples were higher than those of the values reported by Emmanouilidou *et al*. (2021). De Mendoza *et al*. (2013) reported that the related the highest acidity value of olive oils during olive maturation to the progressive action of the lipolytic activity.

Peroxide Value

Peroxide values varied between 5.14 (green) and 9.43 (ripe) meqO_2/kg oil and the peroxide values of olive oils were below 20 meq/O_2 kg which is accepted as the legal limit for extra virgin olive oils by Turkish Food Codex and Regulation EC/1989/2003 (European Union Commission, 2003; Turkish Food Codex, 2014). The peroxide values increased with significantly throughout maturation. These results were in accordance with those of Polari *et al*. (2020).

Fatty Acid Composition

The fatty acids composition of Halhalı olive oils are shown in Table 2. As shown in Table 2. major fatty acids that were found in olive oils were palmitic (C16:0), oleic (C18:1), linoleic (C18:2) acid. The minor fatty acids were palmitoleic (C16:1), stearic (C18:0), linolenic (C18:3), arachidic (C20:0), gadoleic (C20:1), behenic (C22:0) acids. Olive oil characterized by a high level of oleic acid. The main fatty acid in Halhalı olive oil

https://doi.org/10.24264/icams-2022.I.5

was oleic acid, ranging from 67.59 % (ripe) to 70.26 % (green) and it was determined that there was a decrease in oleic acid content with olive maturation. Our results showed similarity with those of the results obtained by Navajas Porras *et al*. (2020). Palmitic acid, which was the second most abundant fatty acid, ranged from 13.56 (ripe) to 15.82% (green). It was determined that the palmitic acid values of the Halhalı olive oils decreased with the olive ripening. Linoleic acid content ranged between 9.52 % (green) and 13.65 % (ripe). Linoleic acid content increased during maturation, confirming the results reported by Konuskan and Mungan (2016). Palmitoleic, linolenic, arachidic, gadoleic and behenic acids were between 0.96–1.29, 0.86–0.98, 0.42–0.53, 0.19–0.27 and 0.09-0.14 %, respectively. The fatty acid compositions of oils from Halhalı monovarietal olive oils were within the legal limits established by Turkish Food Codex and Regulation EC/ 1989/2003 (European Union Commission, 2003; Turkish Food Codex, 2014). The fatty acid composition of olive oil is significantly influenced by the cultivar, olive maturation, growing region (Salvador *et al*., 2003; Yorulmaz and Bozdogan Konuskan, 2017; Alowaiesh, 2018).

Table 2. Fatty acid compositions (%) of Halhalı monovarietal olive oil

Fatty acids (%)	Green	Spotted	Ripe
Palmitic acid (16:0)	15.82±0.46	14.09±0.88	13.56±0.79
Palmitoleic acid (16:1)	1.29±0.27	1.02±0.44	0.96±0.08
Stearic acid (18:0)	3.34±0.12	3.92±0.67	4.13±0.53
Oleic acid (18:1)	70.26±1.25	68.81±0.94	67.59±0.88
Linoleic acid (18:2)	9.52±0.32	11.23±0.24	13.65±0.69
Linolenic acid (18:3)	0.86±0.03	0.91±0.22	0.98±0.02
Arachidic (C20:0)	0.42±0.01	0.48±0.03	0.53±0.08
Gadoleic (C20:1)	0.27±0.07	0.21±0.06	0.19±0.05
Behenic (C22:0)	0.14±0.01	0.09±0.04	0.11±0.03

CONCLUSIONS

As a result, it has been determined that the changes in physicochemical properties and fatty acid compositions of monovarietal of olive oil extracted from Halhalı cultivar depending on different olive maturation. As maturation progressed, a series of changes occurred in olive oil samples and with an influence especially on some parameters such as oil content, free fatty acids and fatty acid composition. The results of this study showed that olive maturation had an important role on the physicochemical properties and fatty acid compositions of olive oils.

REFERENCES

Alowaiesh, B., Singh, Z., Fang, Z. and Kailis, S.G. (2018), "Harvest Time Impacts the Fatty Acid Compositions, Phenolic Compounds and Sensory Attributes of Frantoio and Manzanilla Olive Oil", *Scientia Horticulturae*, 234, 74-80(2018), https://doi.org/10.1016/j.scienta.2018.02.017.

Anastasopoulos, E., Kalogeropoulos, N., Kaliora, A.C., Falirea, A., Kamvissis, V.N. and Andrikopoulos, N.K. (2012), "Quality Characteristics and Antioxidants of Mavrolia cv. Virgin Olive Oil", *Journal of the American Oil Chemists' Society*, 89, 253–259, https://doi.org/10.1007/s11746-011-1991-9.

Antonini, E., Farina, A., Leone, A., Mazzara, E., Urbani, S., Selvaggini, R., Servili, M. and Ninfali P. (2015), "Phenolic Compounds and Quality Parameters of Family Farming Versus Protected Designation of Origin (PDO) Extra-Virgin Olive Oils", *Journal of Food Composition and Analysis*, 43, 75–81, https://doi.org/10.1016/j.jfca.2015.04.015.

AOCS (2003), "Official Methods and Recommended Practices of the American Oil Chemists' Society", AOCS Press, Champaign.

https://doi.org/10.24264/icams-2022.I.5

Baieno, A., Terracone, C., Viggiani, I. and Del Nobile, M.A. (2013), "Effects of Cultivars and Location on Quality, Phenolic Content and Antioxidant Activity of Extra-Virgin Olive Oils", *Journal of the American Oil Chemists' Society*, 90, 103–111, https://doi.org/10.1007/s11746-012-2141-8.

De Mendoza, M.F., Gordillo, C.D.M., Expoxito, JM. Casas, J.S., Cano, M.M., Vertedor, D.M. and Baltasar, M.N.F. (2013), "Chemical Composition of Virgin Olive Oils According to Ripening", *Food Chemistry*, 141, 2575-2581(2013), https://doi.org/10.1016/j.foodchem.2013.05.074.

Emmanouilidou, M.G., Koukourikou-Petridou, M., Gerasopoulos, D., Marios, C.K. (2021), "Oxidative Stability, Fatty-Acid and Phenolic Composition of Cypriot Monovarietal Virgin Olive Oils with Progressive Fruit Maturity", *Journal of Food Composition and Analysis*, 104, 104191, https://doi.org/10.1016/j.jfca.2021.104191.

European Union Commission (1989/2003), "Regulation characteristics of olive oil and pomace oils and their analytical methods", *The Official Journal of the European Union*, L295, 57–66.

IOOC (2001), "Guide for the Determination of the Characteristics of Oil Olives", International Olive Oil Council COI/OH/Doc. No 1.

IOOC (2004), "Preparation of the Fatty Acid Methyl Esters from Olive Oil and Olive Pomace Oil", COI/T.20/Doc.No.24/Rev.1, 2001.

Konuskan, D.B. and Mungan, B. (2016), "Effects of Variety, Maturation and Growing Region on Chemical Properties, Fatty Acid and Sterol Compositions of Virgin Olive Oils", *Journal of the American Oil Chemists' Society*, 93, 1499-1508(2016), https://doi.org/10.1007/s11746-016-2904-8.

Navajas-Porras, B., Perez-Burillo, S., Morales-Perez, J., Rufian-Henares, J.A. and Pastoriza, S. (2020), "Relationship of Quality Parameters, Antioxidant Capacity and Total Phenolic Content of EVOO with Ripening State and Olive Variety", *Food Chemistry*, 325, 126926, https://doi.org/10.1016/j.foodchem.2020.126926.

Polari, J.J., Mori, M. and Wang, S.C. (2020), "Virgin Olive Oils from Super-High-Density Orchards in California: Impact of Cultivar, Harvest Time, and Crop Season on Quality and Chemical Composition", *European Journal of Lipid Science and Technology*, 123, 2000180, 2021, https://doi.org/10.1002/ejlt.202000180.

Ranalli, A., Lucera, L., Contento, S., Simone, N. and Del Re, P. (2004), "Bioactive Constituents, Flavors and Aromas of Virgin Oils Obtained by Processing Olives with a Naturel Enzyme Extract", *European Journal of Lipid Science and Technology*, 106, 187–197, https://doi.org/10.1002/ejlt.200300863.

Salvador, M.D., Aranda, F., Gomez-Alonso, S. and Fregapane, G. (2003), "Influence of Extraction Systems, Production Year and Area on Cornicabra Virgin Olive Oil. A Study of Five Crop Seasons", *Food Chemistry*, 80, 359-366(2003), https://doi.org/10.1016/S0308-8146(02)00273-X.

Tura, D., Gigliotti, C., Pedo, S., Failla, O., Bassi, D. and Serraiocco, A. (2006), "Influence of Cultivar and Site of Cultivation on Levels of Lipophilic and Hydrophilic Antioxidants in Virgin Olive Oils (*Olea europea* L.) and Correlations with Oxidative Stability", *Scientia Horticulturae*, 112, 108-119(2007), https://doi.org/10.1016/j.scienta.2006.12.036.

Turkish Food Codex (2014), "Communique on Olive Oil and Pomace Oil", The Official Gazette of Republic of Turkey, Number 27665, Ankara.

Visioli, F., Poli, A. and Galli, C. (2002), "Antioxidant and Other Biological Activities of Phenols from Olives and Olive Oil", *Medicinal Research Reviews*, 22(1), 65–75, https://doi.org/10.1002/med.1028.

Yang, L., Ma, J., Yan, H., Lü, X., Guo, J., Kong, W. and Deng, Y. (2020), "Changes in Quality and Antioxidant Properties of Virgin Olive Oil of 'Cornicabra' According to Fruit Maturation in Longnan, China", *Journal of Oleo Science*, 70(12), 1731-1740(2021), https://doi.org/10.5650/jos.ess20289.

Yorulmaz, O. and Bozdogan Konuskan, D. (2017), "Antioxidant Activity, Sterol and Fatty Acid Compositions of Turkish Olive Oils as an Indicator of Variety and Ripening Degree", *Journal of Food Science and Technology*, (November 2017) 54(12), 4067–4077, https://doi.org/10.1007/s13197-017-2879-y.

https://doi.org/10.24264/icams-2022.I.5

STAINLESS STEEL AND COPPER MAGNETRON PLASMA COATING OF FABRICS WITH METALLIC YARNS FOR ELECTROMAGNETIC SHIELDING APPLICATIONS

ION RAZVAN RADULESCU[1], EMILIA VISILEANU[1], RAZVAN SCARLAT[1], CRISTIAN MORARI[2], CRISTIAN STANCU[3], BOGDANA MITU[3]

[1]*The National Research & Development Institute for Textiles and Leather, 16 Lucretiu Patrascanu St., 030508 Bucharest, sector 3, razvan.radulescu@incdtp.ro, e.visileanu@incdtp.ro, razvan.scarlat@incdtp.ro*

[2]*ICPE-CA, 313 Splaiul Unirii, 030138 Bucharest, sector 3, cristian.morari@icpe-ca.ro*

[3]*INFLPR, 409 Atomistilor St., 077125 Magurele, Bucharest, cristian.stancu@inflpr.ro, mitu.bogdana@inflpr.ro*

Electromagnetic shielding is needed to protect human beings from undesired non-ionizing radiation and to protect electronic equipment from EM interferences. Shielding solution of Electromagnetic Compatibility domain is tackled nowadays by modern manufacturing methods of flexible textile fabrics with electrically conductive properties. Our research focuses on the additional electromagnetic shielding effectiveness (EMSE) rendered by plasma coating of flexible woven fabrics with inserted conductive yarns. EMSE was computed for an experimental plan formed of plasma coating with Copper and Stainless steel with thicknesses of 400 nm and 1200 nm on both sides of woven fabrics with inserted conductive yarns of stainless steel and silver. An additional EMSE of 5-20 dB on the frequency range of 0.1-1000 MHz was achieved by plasma coating. This proves the enhancement of the shielding properties by magnetron plasma coating, without altering the bulk properties of textile fabrics, such as flexibility and mechanical resistance. The paper presents EMSE results in relation to fabric structure, raw metallic materials and frequency of the incident electromagnetic field.

Keywords: magnetron plasma, fabrics, electromagnetic shielding effectiveness

INTRODUCTION

Electromagnetic shielding is useful nowadays in various applications, such as avoiding interference of electronic equipment and ensuring wellbeing of humans, against hazards caused by non-ionizing radiation. Electromagnetic shielding' theoretical background is related to the larger field of Electromagnetic Compatibility (EMC) (Schwab and Kuerner, 2012). Two mathematical models describe the electromagnetic shielding effectiveness in relation to the geometric and electric parameters of the shielding material: the impedance method and the circuit method (Kaden, 1959). The progress of textile technology in manufacturing metallic yarns, leaded to the development of textile based electrically conductive structures with flexible properties. The main required property of textile shields is their electric conductivity. Two main technologies of imparting electrical conductivity may be distinguished within the scientific literature: inserting metallic yarns into the fabric structure and coating with metallic layers (Ziaja and Jaroszewski, 2011). The present paper is a contribution to new manufacturing methods of textile shields and combines these two main technologies: woven fabrics with metallic yarns (of steel and silver) within their structure are coated with thin metallic layers (of copper and steel) by magnetron sputtering. Recent developments encompass additional properties rendered to textile shields: hydrophobic character (Dai *et al*., 2020), good air permeability (Liu *et al*., 2021), wash-ability (Xu *et al*., 2020), good mechanical resistance (Pakdel *et al*., 2020) and self-cleaning (Kardarian *et al*., 2014). Aspects such as the cover factor (Surdu *et al*., 2020) and yarn's density (Radulescu *et al*., 2020) on the shielding effectiveness of the

https://doi.org/10.24264/icams-2022.I.6

mentioned structures were studied too, as well as a model related to the main electric and geometric parameters (Radulescu *et al*., 2021).

EXPERIMENTAL

Two manufacturing stages were accomplished in order to produce textile shields with inserted metallic yarns and plasma metallic coating:

1. Manufacturing of woven fabrics with inserted metallic yarns of steel and silver;
2. Coating of these woven fabrics by magnetron sputtering with thin layers of copper and steel.

The design and the physical-mechanical parameters of the woven fabrics produced at stage one is presented in Table 1.

Table 1. Design and physical-mechanical properties woven fabrics with inserted conductive yarns

Fabric design and physical-mechanical properties	F1 – woven fabric with inserted stainless-steel yarns	F2 – woven fabric with inserted silver yarns
Linear density of yarns [dtex]	400	220
Float repeat warp	6:2	no yarns
Float repeat weft	6:2	6:1
[Cotton yarns: Metallic yarns]		
Yarn density warp [yarns/10 cm]	180	650
Yarns density weft [yarns/10 cm]	170	340
Distance conductive yarns [mm]	4	4
Specific mass [g/m^2]	143	114
Thickness [mm]	0.55	0.33

The experimental plan of plasma coating of the raw fabrics F1 and F2 at stage two is presented in Figure 1. The two fabrics were coated with copper and steel on both sides with thicknesses of 400 nm and 1200 nm.

Figure 1. Experimental plan of plasma coating on fabrics

https://doi.org/10.24264/icams-2022.I.6

The coating technology of fabrics with thin layers was based on magnetron sputtering from copper and stainless-steel targets, respectively. The coatings were achieved at INFLPR into a dedicated stainless steel spherical vacuum chamber (K.J. Lesker, UK), pumped out by an assembly of a fore pump and turbomolecular pump (Pfeiffer, DE), which allowed the obtaining of a base pressure down to $3 \times 10{-}5$ mbar. A constant argon flow (purity 6.0) of 50 sccm was continuously introduced into the chamber by means of a Bronkhorst mass flow controller, which allowed establishing the processing pressure around $5 \times 10{-}3$ mbar. The chamber is provisioned with a 2" magnetron sputtering gun from K.J. Lesker, accommodating the target. The magnetron discharge was running at 100 W by means of a radio frequency generator (13.56 MHz) provisioned with an automatic matching box for adapting the impedance, and the deposition time was set to ensure coating thicknesses of 400 nm and 1200 nm on each side of the textile fabrics. Enhanced deposition uniformity was achieved by rotating the samples during the deposition process (200 rotations/ min).

Electromagnetic shielding effectiveness (EMSE) was measured at ICPE-CA according to the standard ASTM ES-07, via a TEM cell and the related signal generator, power amplifier and spectrum analyzer.

RESULTS AND DISCUSSION

The physical-mechanical properties of the achieved samples F3-F10 are presented in Table 2.

Table 2. Physical-mechanical properties of plasma coated samples

	Mass [g/m^2]	Thickness [mm]	Yarns density [yarns / 10 cm]	
			Warp	Weft
F3	149	0.55	180	170
F4	125	0.39	660	330
F5	158	0.523	180	170
F6	131	0.38	660	330
F7	155	0.58	180	170
F8	119	0.48	650	340
F9	164	0.52	180	180
F10	133	0.38	660	330

An increase of the shields' mass by an increased thickness of metallic layer may be deducted from the physical-mechanical properties. The thickness of the shield, although measured with a precision of 1 µm, shows relevant increase too. The plasma coating has less influence on the fabric's yarn density.

The EMSE was measured in the frequency domain of 0.1-1000 MHz at various key frequencies and represented on a logarithmic scale (Figures 2-5).

https://doi.org/10.24264/icams-2022.I.6

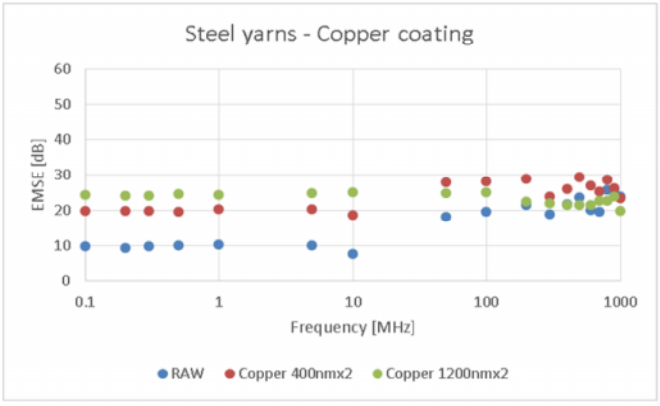

Figure 2. EMSE results of fabrics with steel yarns and copper coating

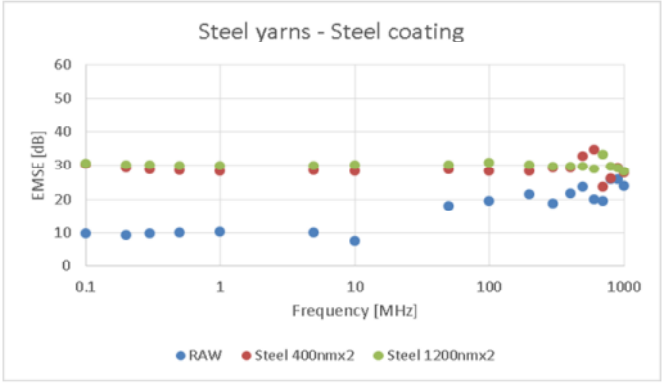

Figure 3. EMSE results of fabrics with steel yarns and steel coating

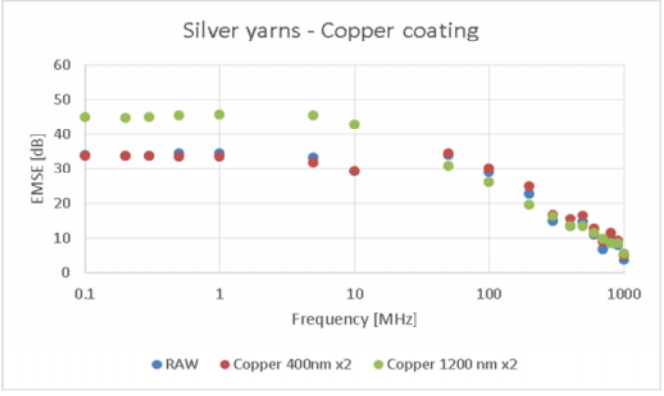

Figure 4. EMSE results of fabrics with silver yarns and copper coating

https://doi.org/10.24264/icams-2022.I.6

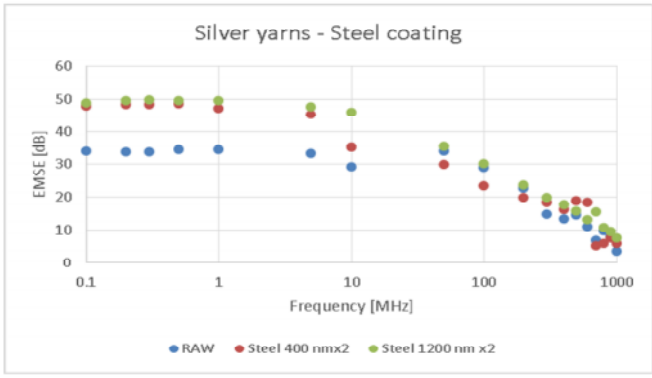

Figure 5. EMSE results of fabrics with silver yarns and steel coating

Plasma coating of the woven fabrics improves EMSE with 5-20 dB on the frequency domain 0.1-100 MHz, which represents a significant result. The steel coating has better results on steel yarns (an increase of 20 dB), a fact to be explained by the homogeneity of the metallic material (Figure 3). A significant difference between the 400 nm layer and the 1200 nm layer is shown in case of the copper coating of the woven fabric with silver yarns (an increase of 10 dB – Figure 4) and steel yarns (an increase of 5 dB – Figure 2). This fact may be explained by the superior conductivity properties of copper and the relevance of the coating thickness. The woven fabrics with silver yarns and steel coating (Figure 5) have best EMSE properties in the frequency range of 0.1-10 MHz with values reaching 50 dB.

For the frequency range of 100-1000 MHz a decrease of EMSE is shown in Figures 2-5. According to the accepted shielding theory (White, 1980), for homogenous conductive materials EMSE shows an almost exponential increase at high frequencies, where the material becomes electrically thick. In practice, it is difficult to have the same conditions assumed in the theoretical model and the measurements often offer results that don't follow the theoretical prediction due to the leakages that can appear. Thus, two factors could explain the decrease shown in Figures 2-5. The first, relates to the fact that perforations could exists in the metallic coated layer through which EM field is likely to leak thus altering the shielding capability of the samples at high frequencies. The second factor, refers to the leakages that appear at the contact between the material sample and the sample holder (in this case the TEM cell) and that increase with frequency.

CONCLUSION

A new manufacturing method of flexible EM shields is proposed by plasma metallic coating of woven fabrics with inserted metallic yarns. A comprehensive experimental plan of coating two woven fabrics with steel and silver yarns by magnetron plasma of copper and steel on both sides of the fabric with thicknesses of 400 nm and 1200 nm was accomplished. EMSE results show variations related to the applied metallic raw materials. The magnetron plasma coating preserves the flexibility of the textile shield and improves EMSE with 5-20 dB on the frequency range of 0.1-100 MHz. Best EMSE

https://doi.org/10.24264/icams-2022.I.6

results is achieved by steel coating of woven fabric with silver yarns with 50 dB on the frequency range of 0.1-10 MHz. These types of flexible EM shields may find different application fields, such as curtains and panels for EM shielding in Buildtech domain, medical clothes for radiation shielding in Medtech domain, or special RF suits for working in antenna proximity environment in Clotech domain.

Acknowledgement

Research work for this study has been performed within ERA-NET Manunet project Contract no. 28/2018 TexEMFiRe – "Manufacturing textiles with electromagnetic shielding and fire-retardant properties by plasma based methods". The publication of the scientific paper is funded by the Ministry of Research, Innovation and Digitization within Program 1 – Development of the national R&D system, Subprogram 1.2 – Institutional Performance – RDI excellence funding projects, Contract no. 4 PFE/2021.

REFERENCES

Dai, M., Zhai, Y. and Zhang, Y. (2020), "A Green Approach to Preparing Hydrophobic, Electrically Conductive Textiles Based on Waterborne Polyurethane for Electromagnetic Interference Shielding with Low Reflectivity", *Chemical Engineering Journal*, 421, part 2, https://doi.org/10.1016/j.cej.2020.127749.

Kaden, H. (1959), *Wirbelstroeme und Schirmung in der Nachrichtentechnik*, Springer, Germany, https://doi.org/10.1007/978-3-540-32570-3.

Kardarian, K., Busani, T., Osório, I., Domingos, H., Igreja, R., Fraco, R. and Cortez, J. (2014), "Sintering of Nanoscale Silver Coated Textiles, a New Approach to Attain Conductive Fabrics for Electromagnetic Shielding", *Materials Chemistry and Physics*, 147, 815e822, https://doi.org/10.1016/j.matchemphys.2014.06.025.

Liu, Q., Yi, C., Chen, J., Xia, M., Lu, Y., Wang, Y., Liu, X., Li, M., Liu, K. and Wang, D. (2021), "Flexible, Breathable, and Highly Environmental-stable Ni/PPy/PET Conductive Fabrics for Efficient Electromagnetic Interference Shielding and Wearable Textile Antennas", *Composites Part B*, 215, 108752, https://doi.org/10.1016/j.compositesb.2021.108752.

Pakdel, E., Wang, J., Kashi, S., Sun, L. and Wang, X. (2020), "Advances in Photocatalytic Self-cleaning, Superhydrophobic and Electromagnetic Interference Shielding Textile Treatments", *Advances in Colloid and Interface Science*, 277, 102116, https://doi.org/10.1016/j.cis.2020.102116.

Radulescu, I.R., Surdu, L., Scarlat, R., Constantin, C., Mitu, B., Morari, C. and Costea, M. (2021), "Modelling the Woven Structures with Inserted Conductive Yarns Coated with Magnetron Plasma and Testing Their Shielding Effectiveness", *MDPI Textiles*, 1(1), pp. 4–20, https://doi.org/10.3390/textiles1010002.

Radulescu, I.R., Surdu, L., Visileanu, E., Scarlat, R., Constantin, C., Morari, C. and Mitu, B. (2020), "Influence of Plasma Coated Woven Fabrics Yarn's Density on Electromagnetic Shielding Effectiveness", *Annals of the University of Oradea Fascicle of Textiles, Leatherwork*, 21(1), ISSN 1843 – 813X.

Schwab, A. and Kuerner, W. (2012), *Electromagnetic Compatibility* (in Romanian), AGIR Publishing, Bucharest.

Surdu, L., Radulescu, I.R., Visileanu, E., Stancu, C., Ardeleanu, A., Sandulache, I., Mitran, C. and Mitu, B. (2020), "Research Regarding the Cover Factor of Magnetron Sputtering Plasma Coated Fabrics", *Industria Textila*, 70(2), pp. 154-162, https://doi.org/10.35530/IT.070.02.1618.

White, D.R.J. (1980), *A Handbook on Electromagnetic Shielding Materials and Performance*, Don White Consultants Inc.

Xu, C., Zhao, J., Chao, Z., Wang, J., Wang, W., Zhang, X. and Li, Q. (2020), "Developing Thermal Regulating and Electromagnetic Shielding Textiles Using Ultra-thin Carbon Nanotube Films", *Composites Communications*, 21, 100409, https://doi.org/10.1016/j.coco.2020.100409.

Ziaja, J. and Jaroszewski, M. (2011), "EMI Shielding using Composite Materials with Plasma Layers", in V. Zhurbenko (ed.), *Electromagnetic Waves*, IntechOpen, https://doi.org/10.5772/16553.

SMART TEXTILES BASED ON CONDUCTIVE WOVEN STRUCTURES

TEODOR SARBU

The National Research & Development Institute for Textiles and Leather, Bucharest, Romania, teodor.sarbu@incdtp.ro

We live in a knowledge-based society, which is facing an increasing impact of science and technology on all aspects of life through products, services and consumer needs. The field of functional textiles is an interdisciplinary field that incorporates science, technology and design, and its future lies in the potential to combine different technologies. Functional textiles will serve to improve the quality of life by increasing the well-being of society and could lead to significant savings for health and budget. The uniqueness and challenge of technical textiles lies in the need to understand and apply the principles of textiles science and engineering to provide the right solutions for the growing and varied demands of their applications in areas such as protective clothing, automotive textiles, geotextiles, agricultural textiles, medical textiles, textiles used for construction, specialized textiles for defense and military applications, etc. Woven fabrics of copper and stainless steel wires, because of their structural order and ability to bend and conform to the most desirable forms, offers a great opportunity to develop a new generation of multifunctional and interactive textiles. The term "Smart Textiles" refers to a wide range of studies and products that extend the functionality and usefulness of common fabrics.
Keywords: smart textiles, functionality, conductivity

INTRODUCTION

Smart textiles are defined as textiles such as fibers and filaments, yarns along with woven, knitted or nonwoven structures that can interact with the environment / user.

The convergence of textiles and electronics (e-textiles) may be relevant to the development of smart materials that are able to perform a wide range of functions, encountered in rigid and inflexible electronic products today (Perumalraj *et al*., 2010).

Active functionality could include power generation or storage, human interface elements, radio frequency (RF) functionality, or assistive technology. All electronic devices require energy, and this is a significant design challenge for smart textiles. Energy generation can be achieved by piezoelectric elements that collect energy from motion or photovoltaic elements. Human interfaces to active systems can be grouped into approximately two categories: input devices and announcement or display devices. Input devices may include capacitive portions that function as buttons or fabrics that are sensitive to shape, which can record movement or bending, pressure, and stretching or compression. Advertising and display devices may include material speakers, electroluminescent wires, or wires that are processed to contain organic light emitting diode (OLED) networks. Fabrics can also include elements that provide bio-feedback or simply vibrate. Fabric-based antennas are a relatively simple application of smart textiles. Simple fabric antennas are only conductive yarns of specific lengths that can be sewn or woven into non-conductive fabrics (Stoppa and Chiolerio, 2014).

Smart textiles will serve as a means of increasing social welfare and could lead to significant savings in the welfare budget. They integrate a high level of intelligence and can be divided into three subgroups:

- Passive smart textiles: only able to feel the environment / user, based on sensors;
- Smart active textiles: detection reactive to environmental stimuli, integrating an actuating function and a detection device;

https://doi.org/10.24264/icams-2022.I.7

• Very intelligent textiles: able to feel, react and adapt their behavior to the given circumstances (Stoppa and Chiolerio, 2014).

Smart textiles are a challenge in many areas, such as the medical, sports and arts, military and aerospace communities.

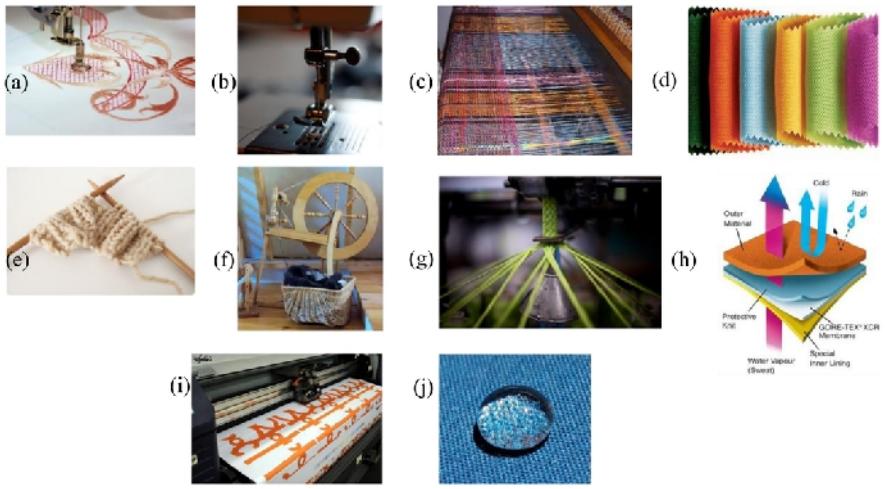

Figure 1. Different types of manufacture and treatment of textiles / fabrics. (a) embroidery; (b) sewing; (c) tissue; (d) nonwovens; (e) knitting; (f) spinning; (g) bread; (h) coating / rolling; (i) printing and (j) chemical treatment (Stoppa and Chiolerio, 2014)

Countless combinations of these source materials result in a whole range of textiles, but sometimes commercial production is represented by garments containing conventional conductors, miniaturized electronic components and special connectors.

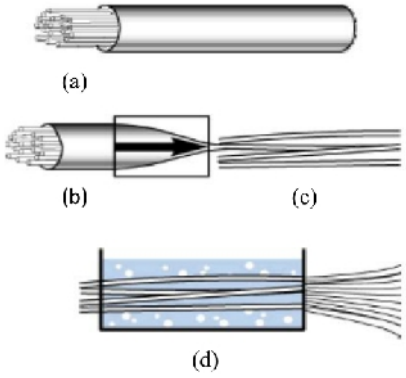

Figure. 2. (a) Metal coated wire combined in an iron tube; (b) Several reductions in tube diameter; (c) Pipe fitting; (d) Leaching, fiber making (Stoppa and Chiolerio, 2014)

https://doi.org/10.24264/icams-2022.I.7

The firing die, used to pull the fiber, consists of a steel frame with a ceramic, carbide or diamond core. The initial diameter of the wire varies depending on the material. For copper, for example, it is usually 8 mm, while for iron it is 5 mm. After drawing, the wire is annealed at temperatures between 600 and 900°C. Subsequently, they are extinguished. The fine metal wire is then wound on a rotating wire drawing cylinder (Stoppa and Chiolerio, 2014).

Table 1. Electrical properties of metal monofilament fibers

Element	Electrical properties				
	Conductivity [S·m/mm^2]	Resistivity [Ω·mm^2/m]	Heat resistance coefficient [10^{-6} K^{-1}]		
			Min	Typ	Max
Cu	58.5	0.0171	3900	3930	4000
Cu/Ag	58.5	0.0171	3900	4100	4300
Ag 99%	62.5	0.0160	3800	3950	4100
Ms * 70	16.0	0.0625	1400	1500	1600
Ms/Ag	16.0	0.0625	1400	1500	1600
AgCu	57.5	0.0174	3800	3950	4100
Bronze	7.5	0.1333	600	650	700
Steel 304	1.4	0.7300	-	1020	-
Steel 316L	1.3	0.7500	-	1020	-

CONDUCTIVITY OF TEXTILES

There is a growing interest in conductive textiles in the scientific and industrial community. Textile structures that have conductivity or serve an electronic or computational function are called electrotextiles (Šafářová and Grégr, 2010).

Due to the attributes of textiles (softness and flexibility), electrical properties are increasingly required in technical applications to perform functions such as heating, shielding from electromagnetic interference, transporting electrical data or signal detection. With the growing interest in smart textiles, the demand for highly conductive textiles has also increased.

In general, textile structures are electrically inactive and can be transformed into electrically active materials by various methods (Aileni *et al*., 2017).

https://doi.org/10.24264/icams-2022.I.7

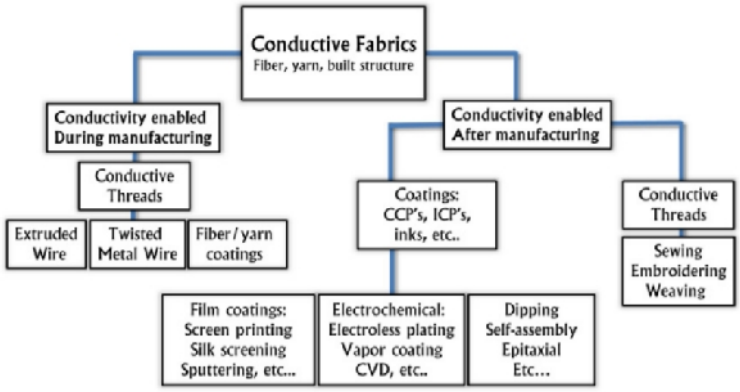

Figure 3. Techniques for introducing electrical conductivity into textiles (Castano and Flatau, 2014)

Thus, conductivity can be introduced at different levels in a textile material (Kirstein, 2013):

- at the level of fibers, yarns or fabrics;
- during production;
- or applied as post-treatments.

The electrical conductivity of flat textiles results from the electrical conductivity of their components, fibers and yarns. It is obvious that the electrical conductivity depends on the structure of the textile material (Tokarska, 2019).

Production of a network of conductive yarns in a textile structure can be obtained through textile manufacturing techniques (weaving, knitting) and fabric manufacturing techniques (sewing, embroidery). Fabrics are used as electrically conductive anisotropic substrates with conductive yarns in the direction of the weft or warp or as electrically conductive isotropic substrates with woven conductors in the direction of the warp and weft (Aileni *et al*., 2017).

The choice of conductive yarns for a smart textile application is the basis of some essential requirements that must be taken into account for the development of the application (Raji *et al*., 2017):

- necessary conductivity level,
- durability of the conductive component,
- yarn content,
- method used in manufacturing,
- degree of fit for the wearer and comfort.

There are several methods for making electric wires:

- the easiest way is to incorporate filaments / metal fibers into yarns;
- another approach is the production of all-metal wires, such as stainless steel wires;
- the use of wet spinning or spinning processes with intrinsically conductive polymers or conventional polymers with conductive additives such as carbon nanotubes or carbon black particles;

https://doi.org/10.24264/icams-2022.I.7

- electrospinning is another useful process for obtaining electroconductive fibers / wires, either by using conductive polymers or by using electroconductive additives homogeneously dispersed in polymer matrices, thus obtaining micro- and nano-composite materials with good mechanical and electrical properties;
- coating non-conductive yarns/ fibers with electro-conductive materials such as metallic powder, carbon black, carbon nanotubes (CNT) or intrinsically conductive polymers (Latifi *et al*., 2010).

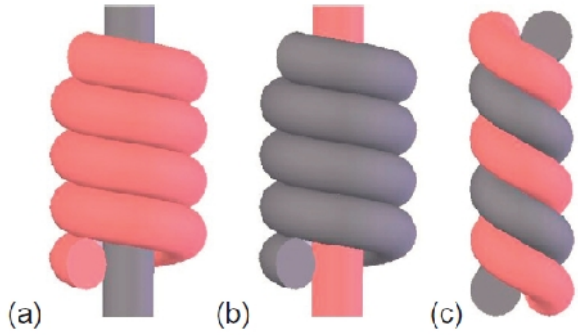

Figure 4. Three typical structures for polymer-metal hybrid yarns: (a) metal-core yarns, (b) metal-threaded polymeric yarn cores, and (c) polymer-metal braided yarns. (Polymeric fibers are displayed in red, while metallic fibers are displayed in gray) (Dias, 2015)

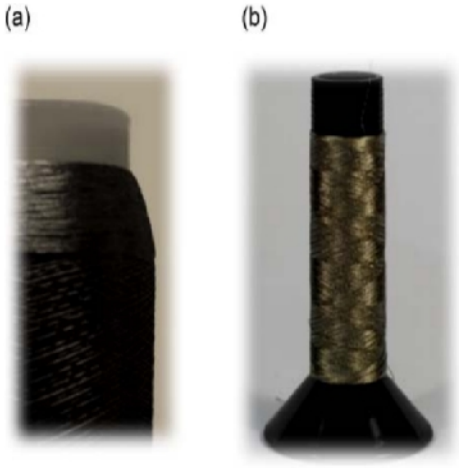

Figure 5. Electrically conductive wires of: a) stainless steel (Bekaert); b) silver coated nylon (Statex) (Koncar, 2019)

https://doi.org/10.24264/icams-2022.I.7

CONCLUSIONS

Fabric testing plays a crucial role in evaluating product quality, ensuring compliance with regulations, and evaluating the performance of textiles.

The critical factors that control the properties of the fabric are the properties of the yarns, the thickness of the fabrics and their design. The handling of these elements and the way they interact produce fabrics with different physical and mechanical properties.

For the realization of advanced textile materials, the research methodology includes innovative techniques for functionalizing the materials by:

- High-tech yarn processing, with functionalizations at nano and micro level through classic, flexible, ecological technologies;
- Incorporation of passive and / or active interactive elements in textile structures;
- Eco-technologies such as electrospinning or 3D printing;
- Closing the value chain through eco-innovative waste processing technologies.

Acknowledgements

This work is funded by the Ministry of Research, Innovation and Digitization, Romania, through the National Project "Macro-mezo-micro advanced materials meant for health and improvement of life quality (AkSuTex)" [Project Number PN 19 17 03 03].

REFERENCES

Aileni, R.M., Valderrama, A.C. and Strungaru, R. (2017), "Chapter 10 – Wearable Electronics for Elderly Health Monitoring and Active Living", in C. Dobre, C. Mavromoustakis, N. Garcia, R. Goleva, G. Mastorakis (eds.), *Ambient Assisted Living and Enhanced Living Environments*, 247-269, ISBN 9780128051955, https://doi.org/10.1016/B978-0-12-805195-5.00010-7.

Castano, L.M. and Flatau, A.B. (2014), "Smart Fabric Sensors and e-textile Technologies: A Review", *Smart Materials and Structures*, 23, 053001, https://doi.org/10.1088/0964-1726/23/5/053001.

Dias, T. (2015), *Electronic Textiles*, *Smart Fabrics and Wearable Technology*, Woodhead Publishing Limited, ISBN 978-0-08-100201-8 (print);

Kirstein, T. (2013), *Multidisciplinary Know-how for Smart-Textiles Developers*, Woodhead Publishing Limited, ISBN 978-0-85709-342-4 (print), https://doi.org/10.1533/9780857093530.

Koncar, V. (2019), *Smart Textiles for In Situ Monitoring of Composites*, Woodhead Publishing Limited, ISBN (Print): 978-0-08-102308-2.

Latifi, M., Payvandy, P. and Yousefzadeh-Chimeh, M. (2010), "10 – Electro-conductive Textile Yarns", in R. Alagirusamy and A. Das (eds.), *Technical Textile Yarns*, 298–328, https://doi.org/10.1533/9781845699475.2.298.

Perumalraj, R., Dasaradhan, B.S. and Nalankilli, G. (2010), "Copper, Stainless Steel, Glass Core Yarn, and Ply Yarn Woven Fabric Composite Materials Properties", *Journal of Reinforced Plastics and Composites*, 29(20), https://doi.org/10.1177/0731684410365007.

Raji, R.K., Miao, X. and Boakye, A. (2017), "Electrical Conductivity in Textile Fibers and Yarns—Review", *AATCC Journal of Research*, 4(3), 8–21, https://doi.org/10.14504/ajr.4.3.2.

Šafářová, V. and Grégr, J. (2010), "Electrical Conductivity Measurement of Fibers and Yarns", *7th International Conference - TEXSCI 2010*, Czech Republic.

Stoppa, M. and Chiolerio, A. (2014), "Wearable Electronics and Smart Textiles: A Critical Review", *Sensors (Basel)*, 14(7), 11957-92, https://doi.org/10.3390/s140711957.

Tokarska, M. (2019), "Characterization of Electro-Conductive Textile Materials by Its Biaxial Anisotropy Coefficient and Resistivity", *Journal of Materials Science: Materials in Electronics*, 30(4), 4093–4103, https://doi.org/10.1007/s10854-019-00699-1.

REVIEW OF GREEN METHODS OF SYNTHESIS OF SILVER NANOPARTICLES

OLGA SHYDLOVSKA[1], YEVHEN KHARCHENKO[1,2]

[1]*Kyiv National University of Technology and Design, Kyiv, Ukraine*
[2]*JSC "Farmak", Kyiv, Ukraine*

Green synthesis of metal nanoparticles is a very promising area of research. Silver nanoparticles are the most interesting type of nanoparticle in nanotechnology because they have varied properties, such as antibacterial, antioxidant, and antibiofilm forming properties. This review aims to establish which of the most common approaches for the biological synthesis of nanoparticles is the best. In this work, the methods of synthesis of silver nanoparticles using plant extracts, bacteria, and yeast are considered. Each of these methods has its advantages and disadvantages. The most common method of synthesis of silver nanoparticles is the method using plant extracts, however, stabilizing substances from plant extracts have their own direct biological activity, which can be both enhanced and suppressed by silver nanoparticles. Green synthesis of nanoparticles thanks to microorganisms makes it possible to use a wide range of bacterial strains, but it is important to remember of the pathogenicity of the strains and their danger to humans. From this perspective, the use of yeast for the synthesis of silver nanoparticles is the most promising method, as it allows obtaining a large amount of nanomaterial. The synthesis, thanks to yeast method, allows us to control the size and shape of the nanoparticles. Nanoparticles obtained from yeast lysates have effective antibacterial and antifilm-forming activity.

Keywords: silver nanoparticles, green synthesis, biotechnology

INTRODUCTION

At the nanoscale, there are significant differences in many material properties that are not usually observed in the same materials at the macroscale. Physical and chemical methods of nanoparticle synthesis have certain disadvantages due to their environmental hazards and high-energy costs. The biological method of synthesis is an environmentally friendly technology that involves the use of biological materials, such as actinomycete algae, bacteria, fungi, viruses, yeasts and plants, to create nanoparticles through transformations in a number of biochemical and biophysical processes. Biological synthesis using nanobiotechnological processes has significant potential to increase the production of nanoparticles without the use of aggressive, toxic and expensive chemicals as mentioned by Shah *et al*. (2015). Among nanoparticles, special attention is paid to silver nanoparticles due to their antimicrobial activity, the possibility of use as drug delivery agents, use as a nanocoating for medical equipment, etc. (Velusamy *et al*., 2016).

Numerous biological materials are used for the intracellular and extracellular biosynthesis of nanoparticles: bacteria, fungi, yeast, algae, actinomycetes, and plant extracts. Green synthesis makes it possible to obtain nanoparticles of variable size, shape, and degree of stability, which have defined mechanical, optical, magnetic and chemical properties related to their shape, size, surface charge and surface area (Salem and Fouda, 2021).

In this review, the authors conduct a brief analysis of the spectrum of materials used for the green synthesis of silver nanoparticles.

https://doi.org/10.24264/icams-2022.I.8

SYNTHESIS OF SILVER NANOPARTICLES USING PLANT EXTRACTS

Jagtap and Bapat (2013), Arokiyaraj *et al*. (2015), Mittal *et al*. (2013) and Kazlagić *et al*. (2020) report the synthesis of Ag nanoparticles using plants, in particular, using extracts of *Artocarpus heterophyllus*, *Chrysanthemum indicum*, *Polyalthia longifolia*, *Cinnamomum camphora*, *Ficus benghalensis*, *Pelargonium graveolens*, *Datura metel*, *Eclipta prostrata*, *Piper longum*, *Malus domestica*. Furthermore, the authors report on the antifungal and antibacterial properties of nanoparticles obtained from plant extracts, in particular against *Candida albicans*, *Escherichia coli*, *Salmonella* spp., *Bacillus cereus*, *Bacillus subtilis*, *Staphyloccocus aureus*, *Pseudomonas aeruginosa*. To analyze the characteristics of nanoparticles obtained thanks to plant extracts, generally accepted methods of analysis are used. Thus, for nanoparticles obtained by synthesis using a plant extract from the leaves of *Mentha arvensis*, the absorption peaks of reduced silver at 1650 cm^{-1} were shown using IR-Fourier transform spectroscopy, and the absorption peak in the region of 340 nm was determined using UV spectroscopy. The obtained nanoparticles demonstrate a maximum activity of 40% observed at a concentration of 600 μg/ml (SivaKumar *et al*., 2015).

The main mechanism for the formation of Ag nanoparticles is based on reactions involving phytochemicals such as terpenoids, flavonoids, ketones, aldehydes, amines, and carboxylic acids. Flavones, organic acids and quinones participate in the immediate reduction of Ag^{+} ions (Abou El-Nour *et al*., 2010).

Plant extracts are a good material for the synthesis of silver nanoparticles. However, the stabilizing substances in the extracts themselves have biological properties. Nanoparticles stabilized by substances from plant extracts can either enhance the effect of flavonoids, amines, aldehydes, etc., or reduce it. Moreover, certain substances can be toxic to normal cells of the human body.

MICROORGANISMS FOR THE SYNTHESIS OF SILVER NANOPARTICLES

Bacteria synthesize nanoparticles both intracellularly and extracellularly. An example of intracellular production of nanoparticles is the synthesis of Ag nanoparticles thanks to bacteria *Rhodococcus* sp. — the accumulation of nanoparticles occurs in the cytoplasm (Otari *et al*., 2015). Moreover, *Vibrio alginolyticus* is used, which synthesizes Ag nanoparticles by reducing silver nitrate (Rajeshkumar *et al*., 2012), and the bacterium *Pseudomonas stutzeri* AG 259, isolated from silver mines, produces nanoparticles inside the periplasmic space of the bacterium (Prabhu and Poulose, 2012). Seetharaman *et al*. (2018) used *Phomopsis liquidambaris* to synthesize Ag nanoparticles. They obtained nanoparticles with a spherical shape and an average size of 18.7 nm, which had antimicrobial and anti-mosquito activity.

The exact mechanism of nanoparticle production by bacteria has not yet been elucidated. However, it is known that during the synthesis of metal nanoparticles intracellularly or extracellularly, it is necessary to consider important physicochemical parameters such as pH, contact time, temperature, the number of bacteria and the concentration of metal salts (Beveridge and Murray, 1980). An interesting fact is that the accumulation of metal ions in the cell is one of the mechanisms of resistance to silver in microorganisms. It is possible that the phenomenon of biosynthesis of silver-based single crystals is based on this. Thus, thanks to *Pseudomonas stutzeri* AG259, nanoparticles with a well-defined shape, such as equilateral triangles and hexagons up to 200 nm in size, are

https://doi.org/10.24264/icams-2022.I.8

synthesized at the cell poles. These Ag-containing crystals are embedded in the organic matrix of the bacteria (Klaus, 1999).

The use of bacteria as material for the synthesis of silver nanoparticles is limited by the direct antibacterial effect of silver. Furthermore, the safety of using silver nanoparticles synthesized by bacteria is limited to pathogenic strains. This method has prospects under the condition of using bacteria useful for the human body, for example, lactic acid and probiotic strains.

YEAST AS AN OBJECT OF THE SYNTHESIS OF SILVER NANOPARTICLES

Yeasts are potentially the best biological agents for the synthesis of nanoparticles due to the use of simple and controlled environments, rapid biomass growth (Sasidharan and Joseph, 2014).

There are various approaches to the synthesis of nanoparticles using yeast as biomatrices. In particular, lyophilized yeast and live cultures can be used for synthesis. Thus, when using *Saccharomyces cerevisiae*, it was found that when using freshly cultivated cells, the yield of nanoparticles is greater than when using a lyophilized preparation. The resulting Ag nanoparticles are spherical with a diameter of 2-20 nm. In yeast cells, nanoparticles accumulate inside the cell membrane, or are attached to the cell membrane during exocytosis. A certain number of nanoparticles is synthesized extracellularly (Korbekandi *et al*., 2016).

For the synthesis of Ag nanoparticles, it is possible to use supernatants of yeast cultures, in particular, such as *Cryptococcus laurentii* and *Rhodotorula glutinis*. These nitrate-reducing yeasts made it possible to obtain dispersed and stable nanoparticles that had differences in size, zeta potential, concentration, and stabilizing compounds depending on the type of yeast (Fernández *et al*., 2016).

Furthermore, for the synthesis of Ag nanoparticles, yeast extract can be used as a source of reducing and capping agents. Ag nanoparticles thus synthesized have a uniform spherical shape with an average size of 13.8 nm. A significant role in the formation of such Ag nanoparticles is played by biomolecules of reducing amino acids, alpha-linolenic acid and carbohydrates found in the yeast extract (Shu *et al*., 2020).

Synthesis of nanoparticles using yeast is the safest method. In addition, the size and shape of silver nanoparticles can be adjusted with this method.

CONCLUSIONS

Silver nanoparticles obtained by green synthesis have various biological properties, namely antioxidant, antibacterial and antifungal properties. The variety of approaches to "green" synthesis using yeast provides significant potential for regulating the shape, size, and composition of reducing and capping agents, which in turn determines the biological properties of synthesized silver nanoparticles.

REFERENCES

Abou El-Nour, K.M., Eftaiha, A.A., Al-Warthan, A. and Ammar, R.A. (2010), "Synthesis and Applications of Silver Nanoparticles", *Arabian Journal of Chemistry*, 3(3), 135-140, https://doi.org/10.1016/j.arabjc.2010.04.008.

Arokiyaraj, S., Kumar, V.D., Elakya, V., Kamala, T., Park, S.K., Ragam, M. and Vincent, S. (2015), "Biosynthesized Silver Nanoparticles Using Floral Extract of *Chrysanthemum indicum* L.—Potential for

Malaria Vector Control", *Environmental Science and Pollution Research*, 22(13), 9759-9765, https://doi.org/10.1007/s11356-015-4148-9.

Beveridge, T.J., and Murray, R.G. (1980), "Sites of Metal Deposition in the Cell Wall of *Bacillus subtilis*", *Journal of Bacteriology*, 141(2), 876-887, https://doi.org/10.1128/jb.141.2.876-887.1980.

Fernández, J.G., Fernández-Baldo, M.A., Berni, E., Camí, G., Durán, N., Raba, J. and Sanz, M.I. (2016), "Production of Silver Nanoparticles Using Yeasts and Evaluation of Their Antifungal Activity against Phytopathogenic Fungi", *Process Biochemistry*, 51(9), 1306-1313, https://doi.org/10.1016/j.procbio.2016.05.021.

Jagtap, U.B. and Bapat, V.A. (2013), "Green Synthesis of Silver Nanoparticles Using *Artocarpus heterophyllus* Lam. Seed Extract and Its Antibacterial Activity", *Industrial Crops and Products*, 46, 132-137, https://doi.org/10.1016/j.indcrop.2013.01.019.

Kazlagić, A., Abud, O.A., Ćibo, M., Hamidović, S., Borovac, B. and Omanović-Mikličanin, E. (2020), "Green Synthesis of Silver Nanoparticles Using Apple Extract and Its Antimicrobial Properties", *Health and Technology*, 10(1), 147-150, https://doi.org/10.1007/s12553-019-00378-5.

Klaus, T., Joerger, R., Olsson, E. and Granqvist, C.G. (1999), "Silver-based Crystalline Nanoparticles, Microbially Fabricated", *Proceedings of the National Academy of Sciences*, 96(24), 13611-13614, https://doi.org/10.1073/pnas.96.24.13611.

Korbekandi, H., Mohseni, S., Mardani Jouneghani, R., Pourhossein, M. and Iravani, S. (2016), "Biosynthesis of Silver Nanoparticles Using *Saccharomyces cerevisiae*", *Artificial Cells, Nanomedicine, and Biotechnology*, 44(1), 235-239, https://doi.org/10.3109/21691401.2014.937870.

Mittal, A.K., Chisti, Y. and Banerjee, U.C. (2013), "Synthesis of Metallic Nanoparticles Using Plant Extracts", *Biotechnology Advances*, 31(2), 346-356, https://doi.org/10.1016/j.biotechadv.2013.01.003.

Otari, S.V., Patil, R.M., Ghosh, S.J., Thorat, N.D. and Pawar, S.H. (2015), "Intracellular Synthesis of Silver Nanoparticle by Actinobacteria and Its Antimicrobial Activity", *Spectrochimica Acta Part A: Molecular and Biomolecular Spectroscopy*, 136, 1175-1180, https://doi.org/10.1016/j.saa.2014.10.003.

Prabhu, S., and Poulose, E.K. (2012), "Silver Nanoparticles: Mechanism of Antimicrobial Action, Synthesis, Medical Applications, and Toxicity Effects", *International Nano Letters*, 2(1), 1-10, https://doi.org/10.1186/2228-5326-2-32.

Rajeshkumar, S., Kannan, C. and Annadurai, G. (2012), "Green Synthesis of Silver Nanoparticles Using Marine Brown Algae *Turbinaria conoides* and Its Antibacterial Activity", *International Journal of Pharma and Bio Sciences*, 3(4), 502-510, https://doi.org/10.1186/2193-8865-3-44.

Salem, S.S. and Fouda, A. (2021), "Green Synthesis of Metallic Nanoparticles and Their Prospective Biotechnological Applications: An Overview", *Biological Trace Element Research*, 199(1), 344-370, https://doi.org/10.1007/s12011-020-02138-3.

Sasidharan, S. and Joseph, P. (2014), "Formulation and Evaluation of Fairness Serum Using Polyherbal Extracts", *International Journal Pharmaceuticals*, 4(3), 105-12.

Seetharaman, P.K., Chandrasekaran, R., Gnanasekar, S., Chandrakasan, G., Gupta, M., Manikandan, D.B. and Sivaperumal, S. (2018), "Antimicrobial and Larvicidal Activity of Eco-friendly Silver Nanoparticles Synthesized from Endophytic Fungi *Phomopsis liquidambaris*", *Biocatalysis and Agricultural Biotechnology*, 16, 22-30, https://doi.org/10.1016/j.bcab.2018.07.006.

Shah, M., Fawcett, D., Sharma, S., Tripathy, S.K. and Poinern, G.E.J. (2015), "Green Synthesis of Metallic Nanoparticles via Biological Entities", *Materials*, 8(11), 7278-7308, https://doi.org/10.3390/ma8115377.

Shu, M., He, F., Li, Z., Zhu, X., Ma, Y., Zhou, Z. and Zeng, M. (2020), "Biosynthesis and Antibacterial Activity of Silver Nanoparticles Using Yeast Extract as Reducing and Capping Agents", *Nanoscale Research Letters*, 15(1), 1-9, https://doi.org/10.1186/s11671-019-3244-z.

SivaKumar, T., Rathimeena, T., Thangapandian, V. and Shankar, T. (2015), "Silver Nanoparticles Synthesis of *Mentha arvensis* Extracts and Evaluation of Antioxidant Properties", *Journal of Bioscience and Bioengineering*, 1, 22-28.

Velusamy, P., Kumar, G.V., Jeyanthi, V., Das, J. and Pachaiappan, R. (2016), "Bio-inspired Green Nanoparticles: Synthesis, Mechanism, and Antibacterial Application", *Toxicological Research*, 32(2), 95-102, https://doi.org/10.5487/TR.2016.32.2.095.

MODELING THE ENCAPSULATION OF TURMERIC IN NANOEMULSIONS

DEMETRA SIMION*, CARMEN GAIDAU, MARIANA DANIELA BERECHET, MARIA STANCA, RODICA ROXANA CONSTANTINESCU

The National Research & Development Institute for Textiles and Leather - Leather and Footwear Research Institute Division, 93 Street Ion Minulescu, 031215, Bucharest, Romania, demetra.simion@yahoo.com

The interaction of turmeric powder with five surfactants (isopropyl oleate, diester of sucrose, polymethylene-α, ω-bis (N, N-dialkyl-N-deoxy-d-glucitolammonium iodides, bis [2-butyl (sodium bis-thioacetate) sodium dicarboxylate 1,10 decanediyl] ester, demecarium bromide) and obtaining nanoemulsions, has been investigated by spectroscopy, dynamic light scattering, optical microscopy and microbiological tests. The modeling encapsulation of turmeric powder in nanoemulsions was carried out taking into account the following parameters: the concentration and type of surfactants, the ratio between turmeric and surfactant, micellar critical concentration, speed and time of stirring, temperature, pH, average diameter of particles, zeta potential, conductivity. The known antibacterial and anti-inflammatory properties of turmeric can be improved by dispersing it in nanoemulsions resulting in better functional efficacy. The specific factors in designing nanoemulsion systems that affect the chemical stability of the encapsulated turmeric are discussed. In order to enhance turmeric effectiveness and improve bioavailability, surfactant assemblies as the colloidal carriers with desired properties have been largely used. The interaction takes place above the critical concentrations of the surfactants, when the encapsulation/ solubilization of turmeric in the micelles occurs. In our research we have elaborated a method for including turmeric in surfactants, following the preparation parameters modeling with the final aim of developing enhanced antibacterial properties.

Keywords: encapsulation, nanoemulsions, modelling the interaction of turmeric with surfactants

INTRODUCTION

Turmeric gets its health benefits primarily because of curcumin, a bioactive component. Curcumin (1,7-bis(4-hydroxy-3-methoxyphenyl)-1,6-heptadien-3,5-dione called as diferuloylmethane) is a bioactive constituent of turmeric, the Indian spice, obtained from the "*Curcuma longa*" rhizome and has been known for centuries as a household remedy to many ailments. Modern scientific research works (Das *et al*., 2022; Hughes *et al*., 2021; Nuraje *et al*., 2013; Varasteanu, 2014; Bungay and Smolders, 1986) are just beginning to study the positive impact of turmeric for leather. Clinical development of turmeric is mainly hindered due to its low aqueous solubility (20 μg/mL) which can be improved by increasing the pH of the solution. Surfactant micelles are largely used as colloidal carriers by encapsulation of the drugs (like turmeric) in order to ensure the transport to specific sites of action, to minimize drug degradation and loss. Therefore, the study of drug (like turmeric)–surfactant interactions has received an increased attention lately. In this research the interactions of 5 surfactants (gemini, bola and classical) with turmeric compared to a control sample (turmeric in water) at pH=6, was studied by: UV/VIS spectroscopic technique, dynamic light scattering, optical microscopy, microbiological tests and proposed the mechanisms of turmeric-surfactants interactions at low, intermediate, and high surfactant concentration region, which is relating to interaction forces, surfactant aggregations, as well as structural alterations of turmeric. DLS investigations showed a favourable thermodynamic stability of turmeric in the five micellar systems used. The surfactant-turmeric molecular interaction was determined on the basis of shift in absorption UV/VIS spectra of the turmeric when going from an aqueous to a more hydrophobic environment at various concentrations of surfactant. The mechanism of surfactant-turmeric interaction has been proposed at pre-micelles, intermediate, and post-micellar surfactant concentrations regime, which relate to various attractive and repulsive forces

https://doi.org/10.24264/icams-2022.I.9

arising, structure and aggregations of surfactant, as well as structural alterations of turmeric. The mechanism proposed for surfactant-turmeric interaction may be used as model for several systems when gemini or bola tensides and turmeric were utilized.

EXPERIMENTAL

Materials and Methods

In order to obtain nanoemulsions with turmeric encapsulated (Fig. 1), the following materials have been used: turmeric powder (*Curcuma longa*) from Sigma-Aldrich; isopropyl oleate – classical surfactant from Sigma-Aldrich; diester of sucrose-gemini 1 from SERVA Feinbiochemica GmbH & Co; sugar-based gemini surfactant (polymethylene-α,ω-bis(N,N-dialkyl-N-deoxy-d-glucitolammonium iodides) – gemini 2 from SERVA Feinbiochemica GmbH & Co; bis [2-butyl (sodium bis-thioacetate) sodium dicarboxylate 1,10 decanediyl] ester-BOLA 1, obtained in an original method at ICECHIM in an PhD Thesis (Varasteanu, 2014); demecarium bromide – bola 2 from Sigma-Aldrich; ethanol is of AnalaR grade. Phosphate buffer solution (PBS) of pH 6 is prepared in the laboratory by dissolving of potassium dihydrogen phosphate in water adjusting the pH with 1.0 M potassium hydroxide and diluting to 1.0 L with water. Triple distilled deionized water for sample preparation and all-PyrexTM glass apparatus was always used. The experimental techniques used consist in: UV/VIS spectrophotometer (V-550, JASCO) for UV/VIS spectroscopy; BS-2082 Research Biological Microscope, Magnification:40x-1000x for optical microscopy; "MALVERN" zetasizer-nano equipment, with measuring range between 0.3 nm – 60.0 microns and zeta potential determination with an accuracy of +/-2%. A number of 5 samples of: turmeric powder/surfactant (gemini, bola and classical)/ ethanol/water compared with a control sample (turmeric in water) – sample 6, were prepared in the working conditions: water-ethanol solvents at 1:1 ratio, temperature=75°C for 60 minutes with turmeric powder-c=0.1%; surfactant concentration-c=0.3%, at pH=6 adjusting with a phosphate buffer solution (PBS), speed at 200 rot/min, HLB from 7 to 10, Fig. 1. The samples in this research are: sample 1 – turmeric powder/ isopropyl oleate-classical tenside/ethanol/water; sample 2 – turmeric powder/sucrose diester- Gemini 1/ethanol/water; sample 3 – turmeric powder/ polymethylene-α,ω-bis(N,N-dialkyl-N-deoxy-d-glucitolammonium iodides-Gemini 2/ ethanol/water; sample 4 – turmeric powder/ bis [2-butyl (sodium bis-thioacetate) sodium dicarboxylate 1,10 decanediyl] ester-Bola 1/ ethanol/water; sample 5 – turmeric powder/ demecarium bromide – Bola 2/ethanol/water; sample 6 – control sample with turmeric powder/water.

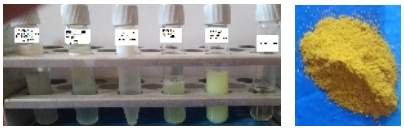

a) 1 2 3 4 5 6 b)

Figure 1. a) Photographic image of 6 samples; b) Image of turmeric powder

RESULTS AND DISCUSSIONS

Obtaining Emulsions with Turmeric Encapsulated

The encapsulated of turmeric in emulsions is a two-step emulsification process. The result are multiple emulsions with turmeric encapsulated due to the properties of the

https://doi.org/10.24264/icams-2022.I.9

five surfactants (gemini, bola and classical) used, to orient and form emulsions at the nano and micro levels. Multiple emulsions are complex systems, also called 'emulsions of emulsions', in which the dispersed phase droplets contain a continuous phase with other dispersed droplets. The main types of multiple emulsions are water-oil-water and oil-water-oil. In the first step (I) introduction in water/ethanol at 1:1 ratio, the surfactant (c=0.3%) with HLB from 7 to 10, by homogenized and stirring at 75°C for 60 minutes, speed at 200 rpm, to obtain a water-oil emulsion. In second step (II) turmeric powder is added at c=0.1%, pH=6 adjusting with a phosphate buffer solution (PBS), to create water-oil emulsion, and homogenized by stirring at 75°C, for 60 minutes, speed at 200 rpm obtaining a multiple water-oil-water emulsion (W/O/W) with turmeric encapsulated. Multiple emulsions are fragile systems, so the choice of emulsification methods is of particular importance in the success of obtaining the dispersed-turmeric in emulsions with the desired properties.

Characteristics of Emulsions with Turmeric Encapsulated

Dynamic Light Scattering (DLS)

A number of five samples of: turmeric powder/surfactant (gemini, bola and classical)/ ethanol/water compared with a control sample (turmeric in water) – sample 6, were characterized by dynamic light scattering. Dynamic light scattering tests showed that all five emulsions with turmeric are nano and microstructured. The size, percentage of the particles and Zeta potential were determined (indicating their stability). From the five selected surfactants, it was found that the best dispersion of turmeric in emulsions created was achieved in the following descending order for: polymethylene-α,ω-bis(N,N-dialkyl-N-deoxy-d-glucitolammonium iodides – Gemini 2 (particle diameter=0.72 nm)>isopropyl oleate-classical tenside (particle diameter=52.4 nm)>diester of sucrose – Gemini 1 (particle diameter=81.3 nm)> demecarium bromide – Bola 2 (particle diameter=98.2 nm) > bis [2-butyl (sodium bis-thioacetate) sodium dicarboxylate 1,10 decanediyl] ester – Bola 1 (particle diameter=98.6 nm). Zeta potential without dilution and stirring for 5 minutes showing a tendency to agglomerate. The influence of surfactants facilitates obtaining stable emulsions with turmeric encapsulated.

Optical Microscopy Tests

The optical microscopy images from Fig. 2, showed the five emulsions with turmeric encapsulated, samples compared with control sample 6. All five emulsions presented in Fig. 2 had a good turmeric encapsulation process. Fig. 2 shows oriented and agglomerated structures. The results are in agreement with literature data (Das *et al*., 2022; Hughes *et al*., 2021; Nuraje *et al*., 2013; Varasteanu, 2014) related to the formation of structures in multiple water-oil-water emulsions.

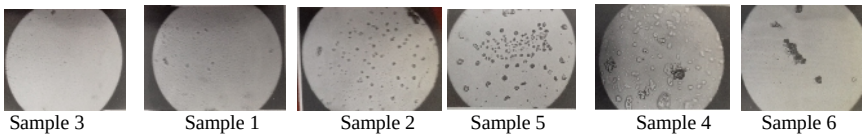

Figure 2. Optical microscopy images (1000x) for samples 1-6

The best dispersion for turmeric was in sample 3 with polymethylene-α, ω-bis (N, N-dialkyl-N-deoxy-d-glucitolammonium iodides-Gemini 2. Fig. 2 shows, in descending order, turmeric dispersion samples and sample 6 (control) is turmeric agglomerated in solvents.

https://doi.org/10.24264/icams-2022.I.9

UV-VIS Spectroscopy Tests

An UV/VIS spectrophotometer (V-550, JASCO) was used for tests. All the analyzed emulsions: 1-5 (Fig. 3) have a rightward displacement of the absorption maxima due to the presence of surfactants (bola, classical and gemini).

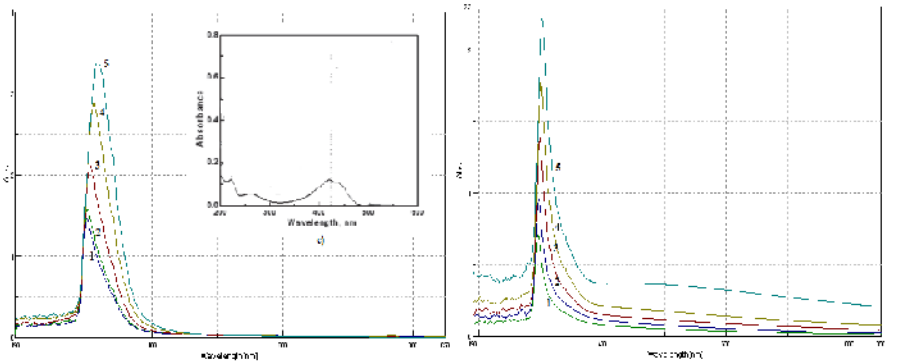

a) *b)*

Figure 3. Overlapping UV-VIS spectra in pre-micellar regions a) and post-micellar b) of samples: 1-5; c) UV/VIS fingerprint spectra of turmeric in ethanol/water at 420 nm

Absorption spectra of turmeric (at fixed 10µm concentration) were in the range of 200 to 600 nm. Blank turmeric calibration curves were developed by dissolving a given amount of turmeric in ethanol followed by the required dilution by water. The presence of ethanol did not alter either the extinction co-efficient or the specific wavelength at which the maximum in UV absorbance appeared. The UV-VIS absorbance fingerprint spectra of turmeric (without surfactant), in water/ethanol are shown in Figure 3-c. Turmeric has the absorption peak at 420 nm, which indicates an increase in intensities with turmeric concentrations. Calibration with dilute solutions of the turmeric in water/ethanol gave satisfactory Beer–Lambert plot with $R^2 = 0.98161$.

Microbiological Tests

The 6 samples were also microbiologically analysed, to determine behaviour to bacterial attack of *Staphylococcus aureus* and *Escherichia coli*, carrying out analysis three days from inoculations. The best results were obtained both for *Staphylococcus aureus* and *Escherichia coli* for samples 3>1>2.

The Mechanism Proposed for Interaction of Surfactant with Turmeric

The interaction of turmeric with five surfactants (gemini, bola and classical) was investigated using UV-VIS absorption spectroscopy, DLS and optical microscopy. The results have outlined three distinct processes depending on the surfactant concentration. In the pre-micellar range, the variation of the absorbance and peak was assigned to attraction of initially positive head group towards the b-diketone group of turmeric. At surfactant concentration in intermediate/micellar region including CMC, a second type of interaction is observed, corresponding to the attachment of alkyl chains of surfactant to aryl groups of turmeric and displacement of head group from b-diketone group of the turmeric. Finally at surfactant concentration higher than the CMC, in the postmicellar region, a type of interaction is observed, which corresponds to the encapsulation/ solubilization of the turmeric into micelles, predominantly in monomeric form (Fig. 4).

https://doi.org/10.24264/icams-2022.I.9

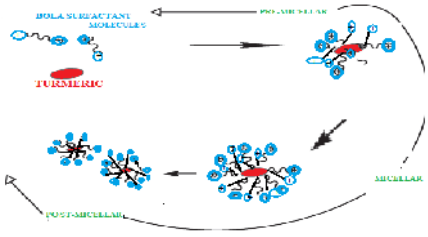

Figure 4. Schematic presentation of a mechanism proposed, of interaction between turmeric and Bola surfactant molecules (with positive charge)

Modeling the Encapsulation Process of Turmeric in Emulsions

Modeling encapsulation of turmeric in emulsions was carried out taking into account all the parameters: the concentration and type of surfactants, the ratio between turmeric and surfactant, micellar critical concentration, speed and time of stirring, temperature, pH, average diameter of particles, zeta potential, conductivity (Fig. 5).

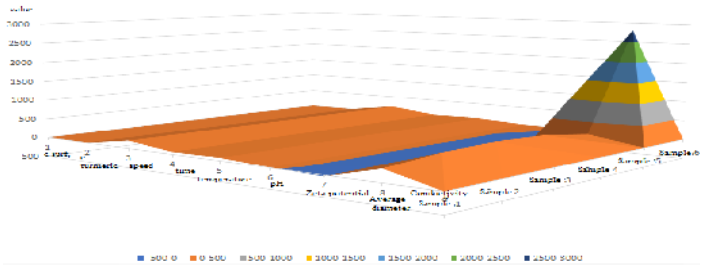

Figure 5. Schematic representation of modelling process, proposed, with all parameters for the six samples obtained

In this research the speed yield of turmeric in water (which is encapsulated in emulsions) was modeled for the best results of samples: 3 and 1. The dependence of absorbance to the encapsulated turmeric from samples 3 and 1, yielded in water, on the time (at λ= 420 nm), was also analysed. The calculation modeling program created is in VBA with the Excel Worksheet interface. For sample 1, the speed yield in water of turmeric encapsulated in emulsions, according to the modeling program is: v= 0.0000023214 units of Abs/min (0.23214 $.10^{-5}$ units of Abs/min). For sample 3, the speed yield in water of turmeric encapsulated in emulsions, is v= 0.0036596821 units of Abs/min. Program modeling indicates that speed yield of turmeric in water encapsulated in emulsions is different depending on the type of surfactant used and its interaction with turmeric. The modeling of release speed in water, of turmeric encapsulated in emulsions, can be done based on (Bungay and Smolders, 1986). In Table 1 the theoretical results of three models on a data set (for sample 3) are presented comparatively, and in Figure 6, the comparative graphic representation.

Table 1. Comparison of failure profiles (Bungay and Smolders, 1986)

	$S.10^5$	a	σa	b	σb	c	σc
Zero order	4.4	0.496645	5.39E-05	-0.00015	1.97E-05		
Order one	2.41	0.49589	0.000156	0.000956	8.46E-05	0.407194	0.173009
Radical order	2.32	0.496968	4.93E-05	-0.00045	3.12E-05		

https://doi.org/10.24264/icams-2022.I.9

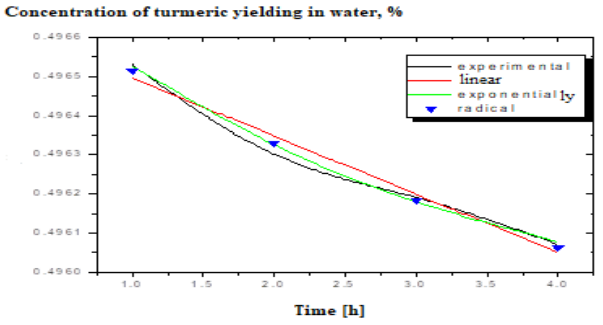

Figure 6. Comparison of yield profiles

The first order failure profile was chosen because there are 2 values of the absorbance (initial and final), and the failure of speeds yield of turmeric in water is very low. The modeling of release speed in water of turmeric encapsulated in emulsions can be done based on the first-order profile.

CONCLUSIONS

Turmeric powder has low aqueous solubility and the solution of this research is to encapsulate it in nanoemulsions with surfactants. Turmeric encapsulated in nanoemulsions applied to leather may revive it by bringing out its natural glow, luster and enhance its antibacterial properties due to the antioxidans and antiinflammatory components. The mechanism of interaction for surfactant-turmeric was created. Also, the encapsulation of turmeric powder in nanoemulsions was modeled taking into account all the parameters.

Acknowledgements

The present work was supported by the Romanian Ministry of Research, Innovation and Digitalization, Nucleus Program, project PN 19 17 01 02/ 2022, contract 4N/2019; project E!12610, project number PN-III-P3-3.5-EUK-2017-D-0098, FERTI-MAIZE, contract 127/2020, within PNCDI III; project number PN-III-P3-3.5-EUK-2019-0237 within PNCDI III (NonActivPans), Contract 219/23.12.2020; and project 4 PFE/2022.

REFERENCES

Bungay, R.W. and Smolders, L.M. (1986), "Controlled Release Delivery Systems", in P.M. Bungay, H.K. Lonsdale and M.N. de Pinho (eds.), *Synthetic Membranes: Science, Engineering and Applications*, NATO ASI series, Series C, 181, D. Reidel Publishing Company.

Das, P., Mandal, P., Shit, D. and Pramanik, S. (2022), "Unraveling the Effect of Surfactant Chain Length on the Binding Interaction of Curcumin with Cationic and Non-ionic Micelles", *Journal of Surfactants and Detergents*, 25(5), 655-664, https://doi.org/10.1002/jsde.12592.

Hughes, J.R., Miller, A.S., Wallace, C.E, Vemuri, G.N. and Iovine, P.M. (2021), "Biomedically Relevant Applications of Bolaamphiphiles and Bolaamphiphile-Containing Materials", Frontiers in Chemistry, 8, 604151-604155, https://doi.org/10.3389/fchem.2020.604151.

Nuraje, N., Baib, H. and Su, K. (2013), "Bolaamphiphilic Molecules: Assembly and Applications, Progress", *Polymer Science*, 38, 302–343, https://doi.org/10.1016/j.progpolymsci.2012.09.003.

Varasteanu, D.S. (2014), "Surfactants Based on Proteins – Obtaining and Applications", PhD Thesis, "Politehnica" University of Bucharest.

THE INFLUENCE OF NBR WASTE MODIFIED WITH SiO_2/NOT MODIFIED ON PROCESSABILITY, PHYSICAL-MECHANICAL AND STRUCTURAL PROPERTIES OF PVC

MARIA SÖNMEZ, MIHAELA NITUICA (VILSAN), MIHAI GEORGESCU,
MARIA DANIELA STELESCU, LAURENTIA ALEXANDRESCU,
DENIS-ANDREI DRUSAN, ANA-MARIA CIOBANU, DANA GURAU, CIPRIAN CHELARU

The National Research & Development Institute for Textiles and Leather - Leather and Footwear Research Institute Division, Ion Minulescu St. 93, Bucharest, Romania, maria.sonmez@icpi.ro

The finished products made of PVC and NBR after the end of the life (waste) are considered harmful, because they do not degrade and thus remain for a long time in the environment. Therefore, there is intense research in order to recycle such materials and reintroduce them into the productive cycle in a new form, without compromising very much their mechanical properties. In the case of rubber recycling, there are currently several methods, from reducing the dimensions to expensive devulcanization processes in order to use them in different thermoplastic matrices. However, the simple reduction of the size of the vulcanized rubber and the mixing with PVC, leads to weak mechanical properties, due to the incompatibility and immiscibility between the phases. Such a composite material was obtained using recycled vulcanized NBR rubber particles (0.35 mm) unmodified/ modified with 10% PDMS, in virgin PVC matrix and waste PVC (50:50) and in the presence of the genioplast additive by the homogeneous mixing technique in the Brabender mixer. The materials experimented were analyzed structurally – FTIR, rheological (torque versus time), from the point of view of processability (flow index) but also mechanically. The analysis of the physico-mechanical values shows that the addition of 10% NBR in the PVC matrix reduces the tensile strength, the 100 and 300% modulus, the elongation at the break, the tear due to their agglomeration, reduce processability (based on the MFR obtained values) but improve the abrasion resistance, an important property of the materials used especially in the footwear industry. However, these types of materials can be used in other applications (automotive, agriculture, etc.) where very high resistances are not required.

Keywords: NBR waste, PVC, genioplast, recycling.

INTRODUCTION

The accentuated trend of widespread use of plastics and elastomers in a wide range of applications (automotive industry, packaging, toys, etc.) has led to the need to develop efficient and fast solutions / methods for their recycling (Fazli and Rodrigue, 2020). It is known that the decomposition of polymers is a long-term process causing harmful effects on the environment and health. Currently 1.5 billion tons of tires/year are decommissioned worldwide and discarded, with a content of up to 90% vulcanized rubber that is not easy to be reprocessed (recycled) due to its highly cross-linked structure (Medina *et al*., 2018; Przydatek *et al*., 2022). Other products that generate rubber waste are represented by discarded rubber pipes, shoe soles, belts, etc. Numerous studies have focused on rubber recycling, using different methods (size reduction, devulcanization, irradiation, etc.) to improve compatibility with other polymers (Dobrotă *et al.*, 2020; Fazli and Rodrigue, 2020; Rad *et al*., 2019; Stelescu, 2013). The objective of this study was to bring added value to waste from different industries and especially PVC and NBR by making new composites, able to re-enter the productive circuit, without significant alteration of the properties of interest.

EXPERIMENTAL

Materials

Plasticized PVC granules (GST type) – Cardinal SRL, Romania; PVC technological waste from the processing of the soles injection; NBR powder obtained by cryogenic grinding (≤ 0.35 mm) of the materials left over from plate stamping to obtain the specimens

https://doi.org/10.24264/icams-2022.I.10

used in the mechanical tests; Genioplast®Pellet P Plus from Wacker-Germany; Poly (dimethylsiloxane) (PDMS), grade: analytical standard, density: 0.82 g/mL, molecular weight: 236.53 wt.%-Sigma Aldrich; Ethanol (96%) from Chemreactiv S.R.L., Romania.

Method

Surface Modification of the NBR Waste

The NBR waste was modified with PDMS by the hydrolysis-condensation method. In the first stage, 150g of NBR waste was weighed in a plastic Berzelius glass over which 600 mL of ethyl alcohol (96%) was added and stirred mechanically for 2 h. Afterwards, 15.4 mL of PDMS (10% relative to the amount of waste) was introduced in the form of fine drops and continued shaking for another 1h. In order for the hydrolysis of the silane to take place, 150 mL of distilled water was added and stirred for another 2h. The obtained powder was filtered, washed with abundant ethanol to remove the unreacted PDMS, and dried in the hot air oven at 70°C, 24 h.

Obtaining Mixtures Based on PVC and/ or NBR Waste

All variants of tested composites (presented in Table 1) were obtained by melt mixing technique using the Brabender plasticorder. During the experiments, the following parameters were recorded: the actual temperature of the mixture during processing and the torque versus time, in the form of a diagram called the plastogram (Figure 4).

Table 1. Composition of tested materials

Sample symbol/Raw material	Raw PVC	PVC waste	P0	P1A	5	6
Virgin PVC, g	350	-	175	175	175	175
PVC waste, g	-	350	175	175	175	175
Genioplast, g	-	-	-	3.5	3.5	3.5
NBR waste not functionalized, g	-	-	-	-	35	-
NBR waste / 10% PDMS, g	-	-	-	-	-	35
Total, g	350	350	350	353.5	388.5	388.5

All of the mixtures in Table 1 were processed under similar conditions in Brabender at 160°C, 30 rpm (2 minutes) and 100 rpm (5 minutes), respectively. After processing, the mixtures were removed from the chamber and used to obtain sheets (15x15 cm, and 2 mm thick, respectively 6 mm thick sheets – to determine the abrasion resistance) in a Fontijne electric press with the following parameters: electric heated plates – 170°C; preheating – 2 minutes; pressing – 5 minutes; cooling – 10 minutes; Force pressure – 300 kN. From the obtained sheets, after conditioning 24 h at room temperature, test specimens (dumbbell, trousers, and cylindrical shapes) are stamped to perform physico-mechanical tests.

RESULTS AND DISCUSSION

Primary Identification Process (FTIR Analysis)

The spectra obtained on the NBR and NBR waste/10% PDMS in relation to the virgin NBR rubber (Figure 1), highlight specific groups, namely: the bands from 2918, 2849 and 1450 cm^{-1} (stretching and deformation vibration of the -C-H bond), the band from 2238 cm^{-1} (stretching vibration of the -CN bond), the band from 1539 cm^{-1} (the stretching vibration of the -CN bond, from the additives added into the rubber). The band from 967 cm^{-1} comes from the -C=C- double bond (1.4 trans) (Liu *et al.*, 2020; Samantarai *et al.*,

https://doi.org/10.24264/icams-2022.I.10

2019). Additionally in the spectrum of NBR waste (not modified) intense bands at 1078 cm^{-1} originated from the Si-O-Si group (silicon dioxide) can be observed. The spectra obtained on the NBR/10%PDMS waste, highlights the groups originated from PDMS at 1260 cm^{-1} (symmetrical bending of the CH_3 bonds from the Si-CH_3 group), and the band from 800 cm^{-1} (rocking CH_3 bond from Si-CH_3 group) (Shi *et al*., 2016). Spectra obtained on raw PVC, PVC waste and P0 (Figure 2), highlight groups originated from PVC, plasticizer (dibutyl phthalate) and $CaCO_3$ (filler ingredient).

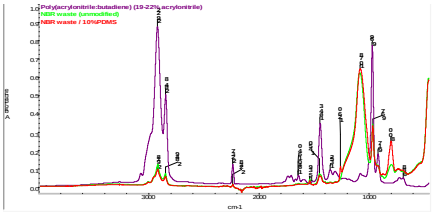

Figure 1. FTIR spectrum of waste: NBR unchanged and NBR / 10%PDMS

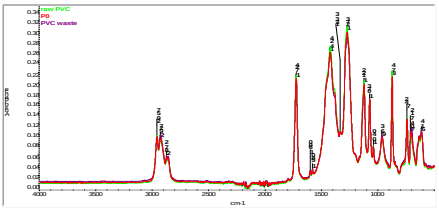

Figure 2. FTIR spectra of: raw PVC, PVC waste and P0 (50:50 raw PVC: PVC waste)

Thus, PVC bands can be observed at 2872 and 2927 cm^{-1} (stretch vibration of the -CH bond); The band from 1424 cm^{-1} (wagging of CH_2), 1333 cm^{-1} (deformation of CH_2 bond from CH-Cl group), the band from 1273 and 1073 cm^{-1} (the stretching vibration of the C-H bonds from the -CH-Cl group) and the one at 963 cm^{-1} (rocking of CH_2). The band at 614.27 cm^{-1} is associated with the C-Cl bond (Hashmi *et al*., 2022). The bands coming from dibutyl phthalate can be identified at 1724 cm^{-1} (the stretching vibration of the C=O ester group), at 1600 and 1580 cm^{-1} (stretching vibration of the aromatic ring structure) and those of 1122 and 1073 cm^{-1} are attributed to C-O stretching vibration (Kumari and Kaur, 2022). The bands at 874 and 712 cm^{-1} correspond to asymmetrical and symmetrical CO_3^{2-} bonds from $CaCO_3$. The $CaCO_3$ band from ~ 1413 cm^{-1} cannot be detected because it overlaps with the plasticizer bands (Bwatanglang *et al*., 2021). The FTIR spectrum of genioplast (Figure 3) highlights specific silicone rubber bands: 2958 cm^{-1} – stretching vibration of the CH_3 bonds; the bands from 1258 cm^{-1} (bending vibration of the Si-CH_3 bond) and those from 1080 and 1011 cm^{-1} (stretching vibration of the Si-O-Si bonds). The peak from 792 cm^{-1} is attributed to the coupling of the stretching vibration of Si-C bonds and the balance vibration of the -CH_3 bond (Salih *et al*., 2018). The band from 461 cm^{-1} is attributed to the presence of ultrafine silica (Li *et al*., 2014). In the case of samples 5 and 6, the presence of NBR waste can be clearly detected at ~ 800 cm^{-1}, with the highest intensity in sample 6 (besides Genioplast it also contains PDMS).

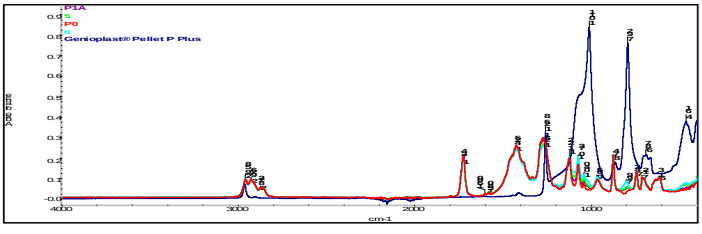

Figure 3. FTIR spectra of the obtained composites

Rheological Analysis

The torque-time recording shows the change in dynamics that took place in virgin PVC, waste PVC, polymer mixtures (samples P0, P1A) but also in the PVC/NBR waste

https://doi.org/10.24264/icams-2022.I.10

composites, processed according to the so-called gelation process. In Figure 4 (A-F diagrams), a sudden torque increase in point A (the effect of loading the material, followed by a decrease in temperature inside the chamber) is observed in all mixtures. Then the torque dropped to a minimum at point B, exceeded the inflection point G and reached its maximum at point X. Such a curve at this stage indicated the coalescence of the particles. At the same time, the temperature of the mixtures increased slowly until reaching the set values, increasing even more near the G-X points. After passing the X-point, the torque decreased slightly then stabilized (point E), indicating the homogeneity of the mixture. The temperature of the material still increased slightly between X and E and the recording continued until the value of the torque stabilized. The following values were read from plastograms and compared in Table 2: the torque at the gelation point (Mx), the temperature at the gelation point (Tx), the torque (ME) and the temperature of the mixture (TE) at the end point and the gelling speed (Mirowski *et al*., 2021), respectively. The results (Table 2) show that the addition of 1% Genioplast (Sample P1A) and 10% NBR waste (Samples 5 and 6), respectively, increases the value of Mx and ME, as the filling is added, but also of Tx and TE. PVC gelling depends on the applied shear force (speed), temperature and composition. The action of shear tensions induces the disintegration of granules into smaller elements (agglomerated by primary particles). Subsequently, the heating determines the progressive plasticization and melting of these elements. These thermo-mechanical changes of the morphological structure of PVC grains involve the smallest elements, the so-called primary crystallites. It is assumed that the addition of a filler promotes the release of more heat, as a result of the friction between filler particles, against PVC grains, filler particles or PVC granules against chamber walls. Moreover, for the same weight of the batch, the volume of the mixture containing NBR waste is higher than that of PVC, which results in a higher shear effort. Due to these effects, the gelling of mixtures containing PVC/NBR waste functionalized/ unfunctionalized is faster than that of PVC (Bendjaouahdou and Aidaoui, 2021; Jubsilp *et al*., 2022; Mirowski *et al*., 2021).

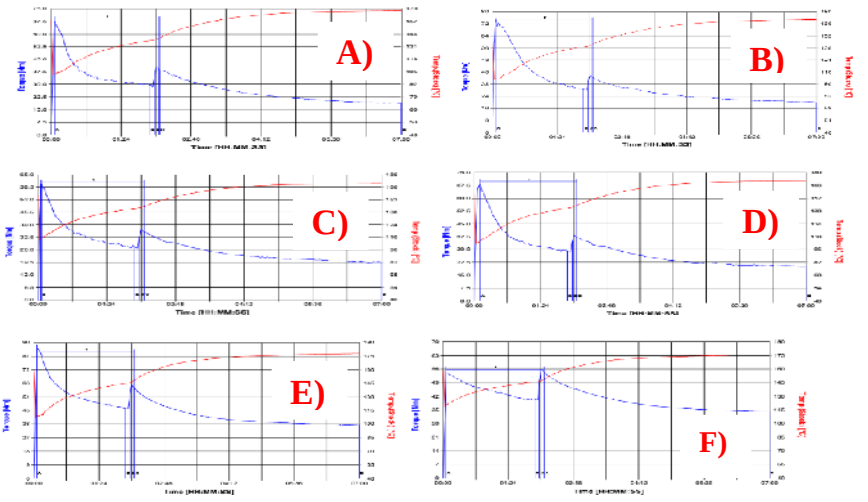

Figure 4. The plastograms obtained on virgin PVC (A), waste PVC (B), P0(C), P1A (D), Sample 5 (E) and 6 (F) with characteristic values related to the gelling process

https://doi.org/10.24264/icams-2022.I.10

Table 2. Analysis of values in plastograms

Features / Samples	M_x, Nm	T_x, °C	M_E, Nm	T_E, °C	Gelling rate, Nm
Virgin PVC	38.7	140	19.1	168	219.5
PVC waste	36.7	142	20.2	171	183.3
P0	35.3	145	19.5	170	181.2
P1A	37.1	144	20.4	171	165.5
5	59.9	149	35.1	178	273.8
6	54.4	149	34.1	176	233.6

Physico-Mechanical and Melt Flow Index Analysis

The properties were determined according to their standards: hardness (SR ISO 7619-1), modulus -100, 300%, elongation and tensile strength (SR ISO 37), tear strength (SR ISO 12771), MFR (SR ISO1133). Analyzing the values in Figure 5, it can be seen that PVC waste has tensile strength, modulus at 100 and 300%, elongation at break, and tear strength superior compared to raw PVC. This was also observed by Roman and Zattera (2014), that repeated reprocessing improve mechanical properties (especially due to the presence of $CaCO_3$ from PVC). In the case of samples 5 and 6, it can be observed the decrease of the tensile strength, modulus, elongation at break, and tear strength, due to the agglomerations and the reduced compatibility between phases (Stelescu, 2013; Subramanian *et al*., 2021). It has been found that recycled rubber particles (i.e. the cross-linked gel part) act as pressure concentration points, so that increasing the concentration of rubber (gel content) of mixtures increases the cross-linking density, lead to a lower tensile strength, elongation at break, and melt flow indices (MFR) (Fazli and Rodrigue, 2020). In the case of P1A mixture (50:50 PVC raw/PVC waste and 1% Genioplast) the highest values of tensile strength, modulus, and abrasion resistance (only 208.56 mm^3) are obtained, of all mixtures, but also good tear strength, elongation, and processability (MFR). These results prove that there is a very good compatibility between PVC and silicone rubber, respectively the ultrafine silica existing in Genioplast (Dobrotă *et al*., 2020).

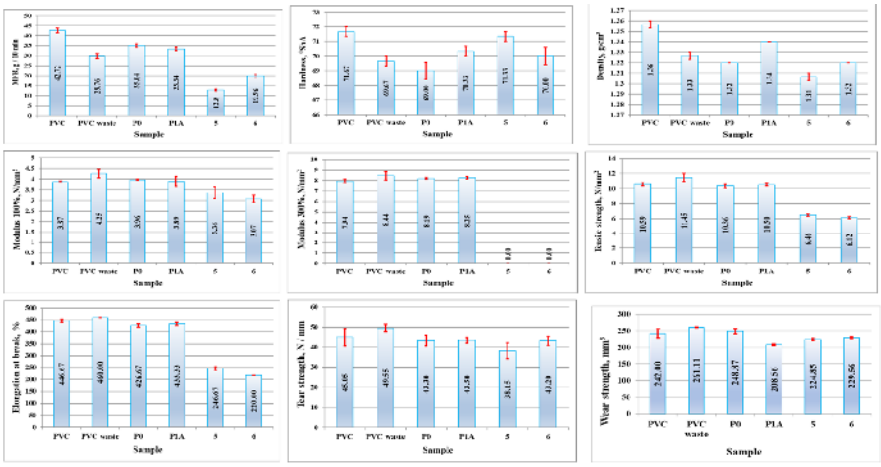

Figure 5. Values of the physico-mechanical characteristics and of the melt flow indices (MFR, g/10min)

https://doi.org/10.24264/icams-2022.I.10

CONCLUSIONS

The results obtained prove that the use of NBR waste in PVC matrix is possible, with the mention that the particle size must be more diminished.

Acknowledgment

This research was financed by MCI through PN 19 17 01 03/2019 project.

REFERENCES

Bendjaouahdou, C. and Aidaoui, K. (2021), "Synthesis and Characterization of Polyvinyl Chloride/Wood Flour/Organoclay Ternary Composites", *Polymers and Polymer Composites*, 29, 949-958, https://doi.org/10.1177/09673911211031139.

Bwatanglang, I.B., Magili, S.T. and Kaigamma, I. (2021), "Adsorption of Phenol over Bio-based Silica/Calcium Carbonate (CS-SiO_2/$CaCO_3$) Nanocomposite Synthesized from Waste Eggshells and Rice Husks", *PeerJ Physical Chemistry*, 3, 1-20, https://doi.org/10.7717/peerj-pchem.17.

Dobrotta, D., Petrescu, V., Dimulescu, C.S. and Oleksik, M. (2020), "Preparation and Characterization of Composites Materials with Rubber Matrix and with Polyvinyl Chloride Addition (PVC)", *Polymers*, 12(9), 1-27, https://doi.org/10.3390/polym12091978.

Fazli, A. and Rodrigue, D. (2020), "Waste Rubber Recycling: A Review on the Evolution and Properties of Thermoplastic Elastomers", *Materials (Basel)*, 13(3), 1-31, https://doi.org/10.3390/ma13030782.

Hashmi, S.U.M., Iqbal, M.A., Malik, M., Qamar, M.T., Khan, M., Zahid, A., Islam, M.R., Al-Bahrani, M., Morsy, K. and Lai, W.-C. (2022), "Synthesis and Characterization of Polyvinyl Chloride Matrix Composites with Modified Scrap Iron for Advanced Electronic", *Photonic and Optical Systems*, 12(18), 1-15, https://doi.org/10.3390/nano12183147.

Jubsilp, C., Asawakosinchai, A., Mora, P., Saramas, D. and Rimdusit, S. (2022), "Effects of Organic Based Heat Stabilizer on Properties of Polyvinyl Chloride for Pipe Applications: A Comparative Study with Pb and CaZn Systems", *Polymers*, 14(1), 1-16, https://doi.org/10.3390/polym14010133.

Kumari, A. and Kaur, R. (2022), "Uptake of a Plasticizer (di-n-butyl phthalate) Impacts the Biochemical and Physiological Responses of Barley", *PeerJ*, 10, 1-28, https://doi.org/10.7717/peerj.12859.

Li, K., Jiang, J.G., Tian, S.C., Chen, X.J. and Yan, F. (2014), "Influence of Silica Types on Synthesis and Performance of Amine-Silica Hybrid Materials Used for CO_2 Capture", *The Journal of Physical Chemistry C*, 118(5), 2454-2462, https://doi.org/10.1021/jp408354r.

Liu, J., Sun, J., Zhang, Z., Yang, H. and Nie, X. (2020), "One-step Synthesis of End-Functionalized Hydrogenated Nitrile-Butadiene Rubber by Combining the Functional Metathesis with Hydrogenation", *ChemistryOpen*, 9, 374-380, https://doi.org/10.1002/open.201900369.

Medina, N.F., Garcia, R., Hajirasouliha, I., Pilakoutas, K., Guadagnini, M. and Raffoul, S. (2018), "Composites with Recycled Rubber Aggregates: Properties and Opportunities in Construction", *Construction and Building Materials*, 188, 884–897, https://doi.org/10.1016/j.conbuildmat.2018.08.069.

Mirowski, J., Oliwa, R., Oleksy, M., Tomaszewska, J., Ryszkowska, J. and Budzik, G. (2021), "Poly(vinyl chloride) Composites with Raspberry Pomace Filler", *Polymers*, 13(7), 1-19, https://doi.org/10.3390/polym13071079.

Przydatek, G., Budzik, G. and Janik, M. (2022), "Effectiveness of Selected Issues Related to Used Tyre Management in Poland", *Environmental Science Pollution Research International*, 29(21), 31467-31475, https://doi.org/10.1007/s11356-022-18494-7.

Rad, A.S., Aali, E., Hallajian, S., Zangeneh, D., Tavakoli, M., Ayub, K. and Peyravi, M. (2019), "Enhancement in the Mechanical Property of NBR/PVC Nanocomposite by Using Sulfur and Electron Beam Curing in the Presence of Cloisite 30B Nanoclay", *Journal of Macromolecular Science, Part A*, 57, 1-8, https://doi.org/10.1080/10601325.2019.1673663.

Roman, C. and Zattera, A.J. (2014), "Study on the Recycling of Waste PVC Compounds from Electrical Wires", *AIP Conference Proceedings*, 52, 52-55, https://doi.org/10.1063/1.4873732.

Salih, S.I., Oleiwi, J.K. and Ali, H.M. (2018), "Study the Mechanical Properties of Polymeric Blends (SR/PMMA) Using for Maxillofacial Prosthesis Application", *IOP Conference Series: Materials Science and Engineering*, 454, 1-10, https://doi.org/10.1088/1757-899X/454/1/012086.

Samantarai, S., Nag, A., Singh, N., Dash, D., Basak, A., Nando, G.B. and Das, N.C. (2019), "Chemical Modification of Nitrile Rubber in the Latex Stage by Functionalizing Phosphorylated Cardanol Prepolymer: A Bio-based Plasticizer and a Renewable Resource", *Journal of Elastomers & Plastics*, 51(2), 99-129, https://doi.org/10.1177/0095244318768644.

Shi, D., Li, P. and Cao, B. (2016), "Preparation of PDMS/PVDF Composite Pervaporation Membrane Modified with Hydrophobic TiO_2 Nanoparticles for Separating Formaldehyde Solution", *Polymer Sciences*, 2(1), 1-7, https://doi.org/10.4172/2471-9935.100012.

Stelescu, M.D. (2013), "Polymer Composites Based on Plasticized PVC and Vulcanized Nitrile Rubber Waste Powder for Irrigation Pipes", *ISRN Materials Science*, 2013, 726121, 1-5, https://doi.org/10.1155/2013/726121.

Subramanian, N., Senthilvel, K. and Prabu, B. (2021), "Studies on the Morphology and Physico-Mechanical Properties of NBR/PVC Hybrid Nanocomposites", *Materials Today: Proceedings*, 38, Part 5, 2810-2816, https://doi.org/10.1016/j.matpr.2020.08.739.

UNMANNED AERIAL VEHICLES – CLASSIFICATION, TYPES OF COMPOSITE MATERIALS USED IN THEIR STRUCTURE AND APPLICATIONS

MARIA SÖNMEZ[1], CRISTINA-ELISABETA PELIN[2], MIHAI GEORGESCU[1], GEORGE PELIN[2], MARIA DANIELA STELESCU[1], MIHAELA NITUICA (VILSAN)[1], GEORGE STOIAN[2], LAURENTIA ALEXANDRESCU[1], DANA GURAU[1]

[1]*The National Research & Development Institute for Textiles and Leather - Leather and Footwear Research Institute Division, 93 Ion Minulescu St., district 3, Bucharest, Romania, maria.sonmez@icpi.ro*

[2]*INCAS – National Institute for Aerospace Research "Elie Carafoli", Iuliu Maniu Blvd.220, Bucharest 061136, Romania, pelin.cristina@incas.ro*

Unmanned aerial vehicles (UAV) or drones, due to their versatility can be used in a wide range of applications, from army missions to industrial ones. With all these capabilities, the widespread use of drones in smart cities is limited, due to problems and concerns related to safety (their crash for technical reasons, collision in the air with other planes, extreme natural weather), confidentiality (hackers can use malicious applications to exploit and obtain personal data / profiles of people using the wireless location method) and security (thanks to the technology inside the drone-GPS, Wi-Fi that could be hacked/destroyed by attackers). Currently there are many types of drones classified by size, weight, altitude, endurance, landing method (VTOL, HTOL), etc. However, these parameters vary depending on the application of the drone. The performance of drones is focused on the type of built-in electronics but also on the material used to make it. All modern drones are equipped with a series of sensors and other communication systems, increasing inevitably the total weight and reducing the flight time. Therefore, weight reduction is a vital parameter to build the drone's body/structure (generally using thermosetting fibers and resins) without compromising their resistance. Thus, high strength-to-weight ratio, facilitates maneuverability, reduces energy consumption, increases the ability to carry more payload, flight time, etc. The use of composites compared to aluminum reduces weight by 15-45%, increases corrosion, fatigue, impact resistance, reduces noise and vibrations. The composites most used for manufacturing the structure of UAVs (fuselage, wing, landing gear) are: polymers reinforced with carbon fibers (CFRP), polymers reinforced with fiberglass (GFRP), boron and aramid fibers.

Keywords: UAV, composite, application.

INTRODUCTION

Unmanned aerial vehicles (UAVs), known as drones are defined as "dynamic remote controlled navigation equipment", capable of performing critical operations without risking human safety. Drones can fly in the air, over large areas but also areas difficult to reach by humans (Sivakumar and Naga Malleswari, 2021). An UAV can be operated remotely by pilots or programmed to operate without human assistance (autonomously) using autopilot and various IMUs (Inertial Measurement Unit) and GPS (Ochoa-de-Eribe-Landaberea *et al.*, 2022). UAVs are also equipped with radars, image enhancers, infra-red imaging technology (Shakhatreh *et al.*, 2019). Fixed-wing and multi-rotor UAVs are the most commonly used mainly in military and civilian applications. Drones with multiple rotors tend to be more popular, because they can vertical take-off and land (VTOL), no special tracks are required, they can fly at a fixed point, they are fast (agile) which makes them suitable for applications that require more precise maneuverability. However, they require more mechanical and electronic complexity which leads to higher maintenance costs, less payload capacity and higher power requirements (Townsend *et al.*, 2020). Fixed-wing drones have the advantage of a simpler structure, reduced

https://doi.org/10.24264/icams-2022.I.11

maintenance costs, longer flight time, can carry a larger payload over longer distances using less energy. However, fixed-wing drones must accelerate horizontally along a track to take off or land (Horizontal take-off and landing – HTOL UAVs), cannot fly at a fixed point and tend to be much bulkier compared to multi-rotor ones (Cevher, 2019; Elmeseiry *et al*., 2021). There is also a unique type of drone that combines the fixed wings with the rotating ones (hybrid), offering the stability and maneuverability of a drone with a rotating wing but also the long flight range of a drone with a fixed wing, without the need for additional runways for take-off (Saeed *et al.*, 2018). The performance of drones is focused on the type of built-in electronics, on the material used to make it (frame, wing, etc.) but also on the energy source (battery, electric motor, combustion engine, solar / photovoltaic panels, hydrogen fuel cell, etc.) (Elmeseiry *et al*., 2021; Townsend *et al*., 2020). A crucial parameter that reduces flight time is weight (Shria and Mishra, 2022; Wang *et al.*, 2019). Weight reduction is a vital parameter to build the drone's body without compromising its resistance. Thus, high strength-to-weight ratio facilitates maneuverability, reduces energy consumption, improving flight time, etc. Currently most UAVs are made of carbon fiber reinforced polymers (CFRP), but there are studies that show that they can partially disrupt/attenuate RC signals (Ramadhoni *et al.*, 2020; Verma *et al.*, 2018). Composite materials are promising to reduce weight, but some of the manufacturing processes require both shape/size limitations and non-alignment of the fibers during processing (Geiger *et al.*, 2019).

The purpose of this review was to provide an overview of the types of existing UAVs, their applications as well as the progress made in the development of composite materials and the technologies used in their structure.

Drone Classification – Size, Weight and Use

This section presents a short classification of UAVs according to their size, weight and usefulness (consumer, commercial, and military drones respectively). Tables 1 and 2 show some representative examples of drones, each with its own technical characteristics.

Table 1. Consumer and Commercial UAV classification based on size and weight (Boeing, 2019; https://www.thecoronawire.com/drone-sizes-explained-consumer-commercial-and-military-drone-sizes/)

Size	Weight	Length	Diameter Propeller	Short description
Very small or "nano" drones	200g	≤150 Mm	51 mm	One of the smallest drones in the world is **the Cheerson CX-10**, with a length of 41mm, weight - 12g, *used for recreational purposes for children*
Small *"Mini"*	200-1000g	Up to 300mm	76-152 mm	Example: **DJI Mini 2**, 249g, length – 159mm, propeller diameter – 119 mm, *used for shooting*
Medium	1-20kg	300-1200mm	150-640mm	**DJI Mavic 2 Entreprise advanced**, 1.1 kg, length-322mm, propeller diameter – 22cm, *used for search /rescue operations being equipped with thermal cameras, inspection of high power lines.*
Large	20 kg or more	120 cm or more	64 cm or more	Currently one of the largest drones in the world, is the cargo drone from Boeing called **Cargo AirVehicle** (currently experimental), weighing 498.95 kg and a length of 533cm.

https://doi.org/10.24264/icams-2022.I.11

Table 2. Millitary drone classification based on size, weight, endurance

Class	Category	Description and examples
	Tactics Espionage, Disaster Applications (earthquakes, hurricanes, terrorist attacks)	**Black Hornet PRS** (personal reconnaissance system) developed by Teledyne FLIR, (classified as nano or mini drone) finds applications in the defense sector. It is equipped with optical and thermal cameras, and transmits video images from distances up to 2 km. It has an endurance of up to 25 minutes, a length of 168 mm, rotor diameter – 123 mm, weight – under 33 grams. Due to its small size, this drone can enter narrow spaces, thus being useful in determining the number of victims, their location (FlyMotion, 2021).
Class I – nano, mini, small drones, (≤ 150 kg)	Tactics Intelligence-Surveillance-Reconnaissance (ISR)	**Fulmar-X** is a mini UAV developed by Thales Group to support surveillance missions for military and civilian operators. The main missions of Fulmar X include: border surveillance, intelligence, target acquisition, emergency and natural disasters response, monitoring of illegal traffic and critical infrastructure security. Fulmar X has a fixed wing structure made of carbon fiber composites, a length of 1.2 m, height – 0.5 m, wingspan – 3 m, maximum take-off weight – 19 kg. The aircraft can be equipped with a wide range of sensors such as a multispectral camera and a LIDAR (light detection and ranging) system. The payload carrying capacity of the Fulmar X is 8 kg. The UAV also has a combined electro-optical / infrared sensor for night operations and offers a real-time video transmission range of up to 90 km. Fulmar X has an endurance maximum of up to 12 h and can reach a maximum range of 800 km without refueling. The maximum altitude is 3000 m (https://www.militaryfactory.com/aircraft/detail.php?aircraft_id=1756).
Class II, medium drones, (150-600kg)	Tactics, used for medium range surveillance	**MQ-1B Predator** developed by General Atomics – is an armed aircraft, multi-mission, medium-altitude long-endurance (MALE) having the following characteristics: length – 8.22 m, height – 2.1 m, weight – 512 kg, maximum takeoff weight – 1020 kg, payload – 204 kg, maximum altitude – 7620 m, autonomy – 1240 km. Armament – 2 AGM-114 Hellfire laser-guided missiles (https://www.af.mil/About-Us/Fact-Sheets/Display/Article/104469/mq-1b-predator/).
Class III, large drone (≥600 kg)	Strategic	**WZ-7 Soar Dragon** was designed by Chengdu Aircraft Industry Group and built by Guizhou Aircraft Industry Corporation. It is a High-Altitude Long Endurance (HALE) drone was deployed for the first time by the Chinese armed forces to conduct live combat training. It features a unique design using a tandem wing with one in the middle of the fuselage and one at the rear. The WZ-7 will be used by the Chinese military to conduct reconnaissance missions and can provide data for ballistic missile launcher units such as the DF-21D. It is equipped with advanced communication and jamming equipment. The drone can reach a speed of 750 km/ h, autonomy of maximum 7000 km, length – 14.33m, wingspan – 24.86m, flight of endurance – 10 h, payload capacity – 650 kg (Babashov, 2021).

Composite Materials Used in the Structure of UAVs

The use of UAVs in almost all fields has engaged scientists to conduct extensive research and development, from body design, components, control methods to improving energy efficiency. In the design and manufacture of drones are used different materials and technologies (e.g., additive manufacturing so-called 3D printing, fused deposition modelling-FDM or fused filament fabrication-FFF, etc.). Research has shown that weight reduction is an essential parameter in the design of the frame or component parts (Palinkas *et al.*, 2022; Piljek *et al.*, 2022). All modern drones are equipped with a series of sensors, communication systems, localization that increase weight and reduce flight time. Thus, weight reduction is essential to build the body/structure of the drone (in general, thermoreactive fibers and resins are used) without compromising their resistance. The use

https://doi.org/10.24264/icams-2022.I.11

of composites compared to aluminum reduces weight by 15-45%, noise and vibrations and improves resistance to corrosion, impact (in the case of collision with birds or other objects). The composites most used for the manufacture of UAVs (fuselage, wing, landing gear) are: polymers reinforced with carbon fibers (CFRP), polymers reinforced with fiberglass (GFRP), boron and aramid fibers (Shria and Mishra, 2022). In Figure 1, a 3D model made by INCAS is presented, highlighting the shape of the case having the role of protecting the electronic components (which are expensive).

Figure 1. UAV (drone) owned by INCAS: (a) model without encapsulation of the electronics, (b), (c) different form of the proposed encapsulation of the electronics

Table 3. Types of composite materials used in the UAVs structure

Matrix	Fiber	Technology	UAV component
Epoxy resin	plain weave glass fiber (E-glass) fabric and plain weave carbon fiber fabric	vacuum resin infusion	alternative materials for the airframe (Poopakdee and Thammawichai, 2021)
PLA GF20 PP GF30 PET CF15 PAHT CF15 CFRP*	Short carbon fiber (CF) and fiberglass (GF) (chopped)	fused filament fabrication process	landing gear (Lancea *et al*., 2022)
-	-	method of 4D printing of composites	manufacturing of adaptive compliant trailing edge (ACTE) morphing wing. The wing is a sandwich structure made of composite materials, with a flat upper/ lower sheet and a corrugated core. The corrugated core was made using 4D technique. The wing prototype has been tested and it has been shown that the wing can support the load for a medium-sized UAV (Hoa *et al*., 2022).
Epoxy	E-glass S-glass Aramid fibers	vacuum infusion	UAV frame (Ramadhoni *et al*. 2020)
ABS	carbon fibre reinforced polymer (CFRP) layer	3D fusion deposition modeling (FDM) method	Fuselage parts of Quadcopter unmanned aerial vehicle (Galatas *et al*., 2018)
Continuous carbon fiber and two matrix materials – thermoset resulting in a unidirectional composite		layer-by-layer CFRC 3D printing	frame structure of small UAV, the mass of the frame is 75 g (Azarov *et al*., 2019)
Low temperature pre-preg – combined with careful processing methods and carbon fibre-reinforced CNC direct mould tools		9m x 5m composite curing oven	manufacture of all primary composite structures for a solar-powered UAV (wing, frame, etc.) (Richardson, 2018)

*PLA – polylactic acid; PP – polypropylene; PET – polyethylene terephthalate; PA – polyamide; CFRP – High-quality carbon-fiber-reinforced polymer

https://doi.org/10.24264/icams-2022.I.11

Drone Applications

For years, UAVs have played an important role in national security operations, in the military field, including in the prevention of terrorist threats and humanitarian assistance and disaster relief, due to their superior functionality to the people. Many countries and government agencies have invested huge sums/billions to improve their performance (Poopakdee and Thammawichai, 2021). Drones are definitely the most important technology that can be used in anti-terrorism operations being equipped with electro-optical cameras that can track both stationary / moving targets. Some drones are used exclusively for surveillance operations, but there are also drones designed for critical operations such as ammunition transport. Drones are also used to collect data about ongoing and life-threatening military missions with the help of their real-time intelligence, surveillance and reconnaissance (ISR) capabilities. Drones are increasingly finding applications in the civilian and military sectors (Nawaz *et al.*, 2019; Singhal *et al.*, 2018). The integration of commercial UAVs in smart cities is very difficult due to safety problems and concerns (their crash for technical reasons, collision in the air with other objects, extreme natural elements), confidentiality (hackers can use malicious applications to exploit and obtain personal data or profiles of people, using the wireless location method) and security (thanks to the technology inside the drone-GPS, Wi-Fi that could be hacked or destroyed by attackers). The rapidly growing number of drones can bring new challenges to the aviation industry, especially in air traffic control (Nguyen and Nguyen, 2021).

CONCLUSIONS

Although UAVs have been used for many years in military applications, their use for commercial purposes (package delivery) is still limited due to safety, security and privacy issues. The improvement of current technologies regarding the detection and avoidance of obstacles will create the future premises for drones to operate autonomously and safely in urban areas. Moreover, finding more cost-effective manufacturing materials and technologies with high productivity to achieve their lightweight and durable structures of UAV parts is still a challenge. Moreover, finding more cost-effective manufacturing materials and technologies with high productivity to achieve their lightweight and durable structures of UAV parts is still a challenge.

Acknowledgement

This work was supported by a grant of the Ministry of Research, Innovation and Digitization, CNCS/CCCDI – UEFISCDI, project no. 601PED/26.07.2022, within PNCDI III.

REFERENCES

Azarov, A.V., Antonov, F.K., Golubev, M.V., Khaziev, A.R. and Ushanov, S.A. (2019), "Composite 3D Printing for the Small Size Unmanned Aerial Vehicle Structure", *Composites Part B: Engineering*, 169, 157-163, https://doi.org/10.1016/j.compositesb.2019.03.073.

Babashov, Z. (2021), "New Largest Chinese-made HALE Combat Drone WZ-7 Soar Dragon Enters into Service", *Polygon Military Magazine.*

Boeing (2019), "Watch: Cargo Air Vehicle Completes First Outdoor Flight", *Technology, Innovation.*

Boon, M.A. Drijfhout, A.P. and Tesfamichael, S. (2017), "Comparison of a Fixed-wing and Multi-rotor UAV for Environmental Mapping Applications: A Case Study", *The International Archives of the Photogrammetry, Remote Sensing and Spatial Information Sciences*, XLII-2/W6, 47-54, https://doi.org/10.5194/isprs-archives-XLII-2-W6-47-2017.

Cevher, L. (2019), "Control System Design and Implementation of a Tilt Rotor UAV", Thesis, *Middle East Technical University*, Ankara, Turkey.

https://doi.org/10.24264/icams-2022.I.11

Elmeseiry, N., Alshaer, N. and Ismail, T. (2021), "A Detailed Survey and Future Directions of Unmanned Aerial Vehicles (UAVs) with Potential Applications", *Aerospace*, 8(12), 1-29, https://doi.org/10.3390/aerospace8120363.

FlyMotion (2021), "FLIR's Black Hornet is the World's Smallest Military Drone", *News*.

Galatas, A., Hassanin, H., Zweiri, Y. and Seneviratne, L. (2018), "Additive Manufactured Sandwich Composite/ABS Parts for Unmanned Aerial Vehicle Applications'', *Polymers*, 10(11), 1-17, https://doi.org/10.3390/polym10111262.

Geiger, R., de Sousa, A.R. and Hannan, Y.A. (2019), "Advanced Composite Drone Manufacturing", *8th Annual World Congress of Advanced Materials*, Osaka, Japan.

Hoa, S., Abdali, M., Jasmin, A., Radeschi, D., Prats, V., Faour, H. and Kobaissi, B. (2022), "Development of a New Flexible Wing Concept for Unmanned Aerial Vehicle Using Corrugated Core Made by 4D Printing of Composites'', *Composite Structures*, 290, https://doi.org/10.1016/j.compstruct.2022.115444.

Lancea, C., Chicos, L.-A., Zaharia, S.-M., Pop, M.-A., Pascariu, I.S., Buican, G.-R. and Stamate, V.-M. (2022), "Simulation, Fabrication and Testing of UAV Composite Landing Gear", *Applied Science*, 12(17), 1-16, https://doi.org/10.3390/app12178598.

Nawaz, H., Ali, H.M., and Massan, S. (2019), "Applications of Unmanned Aerial Vehicles: A Review", *3C Tecnología*(Special Issue), 85-105, https://doi.org/10.17993/3ctecno.2019.specialissue3.85-105.

Nguyen, D.H.D.P. and Nguyen, D.D. (2021), "Drone Application in Smart Cities: The General Overview of Security Vulnerabilities and Countermeasures for Data Communication", *Springer*, 185-210, https://doi.org/10.1007/978-3-030-63339-4_7.

Ochoa-de-Eribe-Landaberea, A., Zamora-Cadenas, L., Peñagaricano-Muñoa, O. and Velez, I. (2022), "UWB and IMU-Based UAV's Assistance System for Autonomous Landing on a Platform", *Sensors*, 22(6), 1-24, https://doi.org/10.3390/s22062347.

Palinkas, I., Pekez, J., Desnica, E., Rajic, A. and Nedelcu, D. (2022), "Analysis and Optimization of UAV Frame Design for Manufacturing from Thermoplastic Materials on FDM 3D Printer", *Materiale Plastice*, 58(4), 238-249, https://doi.org/10.37358/MP.21.4.5549.

Piljek, P., Krznar, N., Krznar, M. and Kotarski, D. (2022), "Framework for Design and Additive Manufacturing of Specialised Multirotor UAV Parts. Trends and Opportunities of Rapid Prototyping Technologies", *IntechOpen*, 1-16, https://doi.org/10.5772/intechopen.102781.

Poopakdee, N. and Thammawichai, W. (2021), "Improvement on Cost-Performance Ratio of Fiberglass/Carbon Fiber Hybrid Composite", *Journal of Metals, Materials and Minerals*, 31(1), 35-43, https://doi.org/10.55713/jmmm.v31i1.985.

Ramadhoni, B.F., Rizkyta, A.G., Bintoro, A. and Nugroho, A. (2020), "Effect of Glass Fibers and Aramid Fiber on Mechanical Properties of Composite Based Unmanned Aerial Vehicle (UAV) Skin", *iMEC-APCOMS 2019 – Lecture Notes in Mechanical Engineering*, Springer, 435-440, https://doi.org/10.1007/978-981-15-0950-6_66.

Richardson, M. (2018), "On the Silent Wings of Freedom", *Composites in Manufacturing*.

Saeed, A.S., Younes, A.B., Cai, C. and Cai, G. (2018), "A Survey of Hybrid Unmanned Aerial Vehicles", *Progress in Aerospace Sciences*, 98, 1-54, https://doi.org/10.1016/j.paerosci.2018.03.007.

Shakhatreh, H., Sawalmeh, A.H., Al-Fuqaha, A., Dou, Z., Almaita, E., Khalil, I., Othman, N.S., Khreishah, A. and Guizani, M. (2019), "Unmanned Aerial Vehicles (UAVs): A Survey on Civil Applications and Key Research Challenges", *IEEE Acces*, 7, 48572-48634, https://doi.org/10.1109/ACCESS.2019.2909530.

Shria, A. and Mishra, A.K. (2022), "High-performance materials used for UAV manufacturing: Classified Review", *International Journal of All Research Education and Scientific Methods*, 10(7), 2811-2819.

Singhal, G., Bansod, B. and Mathew, L. (2018), "Unmanned Aerial Vehicle Classification, Applications and Challenges A Review", *Preprints*,1-20, https://doi.org/10.20944/preprints201811.0601.v1.

Sivakumar, M. and Naga Malleswari, T.Y.J. (2021), "A Literature Survey of Unmanned Aerial Vehicle Usage for Civil Applications", *Journal of Aerospace Technology and Management*, 13, 1-23, https://doi.org/10.1590/jatm.v13.1233.

Townsend, A., Jiya, I.N., Martinson, C., Bessarabov, D. and Gouws, R. (2020), "A Comprehensive Review of Energy Sources for Unmanned Aerial Vehicles, their Shortfalls and Opportunities for Improvements", *Heliyon*, 6(11), 1-9, https://doi.org/10.1016/j.heliyon.2020.e05285.

Verma, A.K., Pradhan, N.K., Nehra, R. and Prateek (2018), "Challenge and Advantage of Materials in Design and Fabrication of Composite UAV", *IOP Conference Series: Materials Science and Engineering*, 455(1), 1-10, https://doi.org/10.1088/1757-899X/455/1/012005.

Wang, X., Huang, Z., Sui, G. and Lian, H. (2019), "Analysis on the Development Trend of Future UAV Equipment Technology", *Academic Journal of Engineering and Technology Science*, 2(1), 114-121, https://doi.org/10.25236/AJETS.020022.

*** (2020), "Thales Fulmar X Mini-Unmanned Aerial Vehicle (UAV)", available at https://www.militaryfactory.com/aircraft/detail.php?aircraft_id=1756.

*** https://www.af.mil/About-Us/Fact-Sheets/Display/Article/104469/mq-1b-predator/.

*** https://www.thecoronawire.com/drone-sizes-explained-consumer-commercial-and-military-drone-sizes/

THE INFLUENCE OF ADDITIVE MANUFACTURING IN THE TEXTILE INDUSTRY

CRISTINA ELENA STROE, RALUCA MARIA AILENI

The National Research & Development Institute for Textiles and Leather, Lucretiu Patrascanu 16, Bucharest, Romania, e-mail: cristina.stroe@incdtp.ro

Currently, the textile industry represents a big threat to the environment and human health, through the large resource consumption, through the harmful chemicals eliminated in the environment, and through the enormous amounts of waste resulted from both the pre-consumption and post-consumption phases. Moreover, it is a continuous need to bring digitalization in this industry to promote sustainability and resource efficiency. Additive manufacturing or 3D Printing is proposed lately as a solution to all these issues created by the textile industry, thus an emphasis has been placed on this technology to replace traditional textile production technologies. Although it has not yet had considerable success in practice, manufacturing of textiles via 3D printing is still a promising effort, due to the benefits it brings, and thus the research continues. This technology has the ability to build remarkable structures with limitless shapes and size, it can functionally optimize the products right from the start, and most important, the production steps can be skipped, thus allowing to reduce the production time and to bring digitisation closer to this sector. Furthermore, the resource consumption can be reduced, the transport routes can be eliminated as well as the textile waste generated during production. In conclusion, this technology is a totally different way to design which diminishes the effort and can conduct to a strong change in the industry. This paper discusses the advantages of the 3D Printing process for the textile field, the encountered difficulties, and recent developments in terms of materials, technologies, and applications.

Keywords: 3D printing, sustainability, advanced materials

INTRODUCTION

The process of Additive Manufacturing (AM) or in other words 3D Printing (3DP) or Rapid Prototyping enables to use different kinds of materials to create unique 3D structures with controlled shapes and sizes by depositing material layer-by-layer, instead of subtracting material or redistributing material as in the classical technologies of manufacturing (forging, milling, drilling, casting, plastic deformation, etc.). A special printing machine is used to convert the virtually created geometry of an object (a 3-dimensional computer-aided-design (CAD) model), which is sliced in discrete layers, into the physical object (Lussenburg *et al*., 2014).

The first AM process was invented by Charles Hull in 1986, namely, stereolithography, currently existing various other additive manufacturing processes differentiated by the specific method of forming the layers and materials used. The diversity of materials that can be used confirms the continuous evolution of the AM field (metals, polymers, photopolymers, ceramics, sand, paper, food and even organic tissues).

In the field of 3D printed textiles, Selective Laser Sintering (SLS) (Beecroft, 2019) and Fused Deposition Modelling (FDM) (Takahashi and Kim, 2019; Partsch *et al*., 2015) are two commonly used processes. Also, Polyjet technology was introduced recently to the list of technologies that can be used to print directly to textiles and create clothing items that unlock a limitless colour palette, limitless creativity and unparalleled flexibility through a wide range of rigid and flexible materials (Molitch-Hou, 2022). Table 1 describes these three different types of additive manufacturing technologies.

https://doi.org/10.24264/icams-2022.I.12

Table 1. Description of some of the existing AM technologies (DelVecchio, 2021)

	Resin-based	Powder-based	Filament
Method	Material Jetting	Powder Bed Fusion	Material Extrusion
Alternative name	Polyjet	Selective laser sintering (SLS)	Fused Deposition Modelling (FDM)
Key Materials	Photopolymers, polymers, waxes	Plastic, metal, and ceramic powders, sand	Thermoplastic filaments, liquids, and slurries (syringe types)
Bonding principle	Cured with UV light	Fused with laser	Fused with heat
Strengths	Low surface roughness; Enables multiple materials in a single part; High level of accuracy; Full-colour printing.	Medium surface roughness; High mechanical properties; Powder acts as material support.	Low build cost; Good mechanical properties; Allows for multiple colour printing.
Weaknesses	Limited material options; Overexposure to outdoor UV light can weaken parts; Costly and time-consuming.	High build cost; Cool-down time of 50% of print time, leading to longer production time.	High surface roughness; Slow build speed.

Some frequently used materials for 3D printing with FDM technology (Table 2), for example, are filaments of polylactic acid (PLA), the most commonly used material, acrylonitrile butadiene styrene (ABS), Nylon, thermoplastic polyurethane (TPU), polycarbonate (PC), blends of PC and ABS and others, and also composites made of plastic filaments that contain a certain fraction of fibres or particles (e.g., wood fibres, ceramic particles, brass particles, short carbon fibres, electrically conductive carbon black) which can give special properties to the printed structure (e.g., electrical conductivity).

Table 2. Properties of the most common used materials in FDM technology (Bates-Green and Howie, 2017)

PLA	A biodegradable polymer, it creates no toxic gases while melting (no ventilation system needed), low glass transition temperature ~60-65°C (PLA parts can often be printed in unheated atmosphere with no build plate heat and no special adhesives), flows and is extruded around 215°C, is susceptible to water degradation.
ABS	Has good rheological properties which make relatively smooth surfaces, it has stiffness, resistance to heat and environmental degradation, needs a well-ventilated space when printed, extruded around 220°C needs an elevated build plate temperature and/or atmospheric temperature and use of chemical adhesives on the build plate because of high glass transition temperature (~ 105°C).
Nylon	Has high toughness, flexibility in bending and stiffness in tension, resistance to fatigue, heat and wear resistance, and strong adhesion between layers, absorbs water from the atmosphere quickly (needs to be desiccated), more expensive than other materials, extruded at temperatures from 240°C to 270°C, which can harm some printers.
TPU	An elastomeric, rubbery material with very good flexibility, melts at easy FDM temperatures around 230°C, resistant to abrasion and solvents like petroleum chemicals.
PC	Has high strength, high layer adhesion, high impact resistance and toughness, ability to plastically deform greatly before it breaks, high-temperature stability, a smooth printed texture and optical clarity, extruded at 315°C, a temperature that many printers can't reach with difficulty adhering it to the build plate, and it's easily scratched.

https://doi.org/10.24264/icams-2022.I.12

THE POSITIVE IMPACT OF 3DP ON THE TEXTILE SECTOR

- Sustainable process of manufacturing - the additive process reduces material waste during production, reduces the use of materials that are intensive water consuming such as cotton, as well as the need for extensive human labour.
- Offers an easier recycling potential for the 3DP apparel than current materials, thus helping reduce the amount of clothing thrown into landfills.
- Production can be local and on-demand -this means that there is no need for stock products, and no overproduction occurs.
- At-home printers can help reduce the impact of large factories.
- Faster manufacturing cycles - allowing the manufacturers to speed up the market and supply chain.
- High accuracy and efficiency.
- In fashion it is important to introduce new design forms that keep up with consumer requirements, thus 3D printing allows designers to innovate faster and can contribute to design freedom and personalization (customized design).
- 3D models for fashion accessories, such as buttons, cufflinks, and bag clips, can also be printed.
- Prototyping, or getting a sample made, is also cheap and time-efficient with 3D printing (Flynt, 2019).

DIFFICULTIES ENCOUNTERED BY 3DP TECHNOLOGY

The use of 3D printers in the production of textiles is still extremely complex. When 3D printed fabrics are used to create wearable garments, strength, flexibility and comfort are the main requirements. But this technology still struggles to achieve them.

Moreover, 3DP is still an expensive technology in most cases or the quality of objects is not high enough, to which is added limited expertise and limited materials choice, so the development of the technology approach in different fields is hampered by these aspects (Everett, 2021).

With the increasing introduction of digitalization in the industrial sectors, people are not yet very open to embrace this concept, because it is associated with the loss of manufacturing jobs, but still, it seems like they are beginning to understand the practical aspects of 3D printing.

Also, with the download-and-print-yourself option, controlling the originality of products produced as well as their quality can become a problem if people print their personal items (Flynt, 2019).

To overcome the problem of flexibility and strength multiple approaches, based on shape complexity and material behaviour, were addressed by researchers and manufacturers to create products with appropriate properties, as follows:

a. printing fibre-shaped structures ultra-long and flexible that can be woven/knitted into fabrics - mostly developed to be used in the sector of energy storage, as batteries or supercapacitors, that can be further utilized in wearable and smart products (Praveen *et al*., 2021);
b. printing of flexible structures based on rigid materials (Čuk *et al*., 2020), but with discrete bodies that make up multiple assemblies (the so-called “chain-mail-like structure”);
c. printing using materials that are capable to be flexible (e.g., TPU) and creating common textile structures like knit or woven, or other complex geometries (Čuk *et al*., 2020);
d. printing rigid plastic on top of the existing traditional fabric (direct-to-textile 3DP), which is the most used process at the moment (Čuk *et al*., 2020).

Figure 1 exemplifies some types of the mentioned structures.

https://doi.org/10.24264/icams-2022.I.12

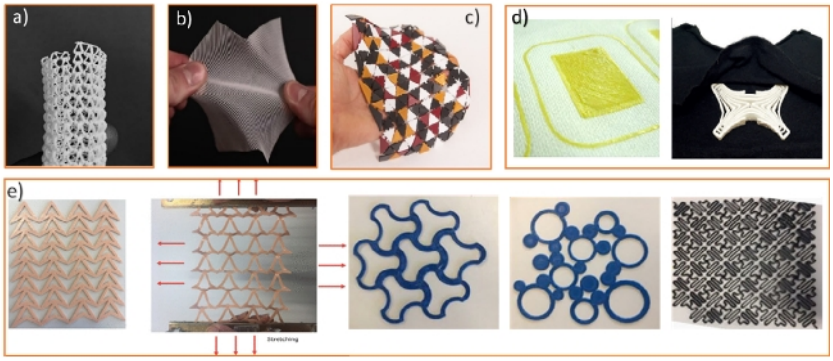

Figure 1. Types of textile structures created by 3D Printing: a) tubular weft-knit (Beecroft, 2019); b) quasi-woven fabric ("DefeXtiles") (Forman *et al*., 2020); c) chain-mail-like model (Mings, 2017); d) direct to-textile printing (Martens and Ehrmann, 2017; Korger *et al*., 2020); e) other flexible structures (Spahiu *et al*., 2020)

In addition to the performance of the material itself and the design, also the printing technology of the fabric has a critical impact. It is necessary to be used flexible-material specialized 3D printers, like for example, the INTAMSYS FLEX 510 printer and Raise3D E2 printer, two printers developed recently by INTAMSYS, Raise 3D, Covestro and Polymaker, which are highly adapted for printing flexible materials which match the characteristics required for a 3D printed fabric (Stevenson, 2020).

APPLICATIONS

Fashion Sector

The fashion industry is now turning to 3D technologies to create innovative products such as 3D printed shoes, garments, accessories, ties and bags designed by many prominent brands and designers (Čuk *et al*., 2020).

Most of the 3D printed clothing is printed using the selective laser sintering process. This method of 3D printing offers the ability to make intricate designs and achieve a high level of detail which is a requirement in fashion and clothing (Flynt, 2019).

Recently created by a Dutch designer, a 3D printed impressive dress made entirely from a vegan organic material based on cocoa bean shells brought together nature, fashion, and technology. Also, Kornit Digital, a sustainable fashion brand adopted additive manufacturing (direct-to-yarn printing technology) to produce knit-like garments that can contribute to sustainable and waste-reducing fashion (Alexandrea, 2022).

Homemade clothes represent an alternative to the expensive designer creations and can also sustain the friendliness with the environment. People are now able to print personal items with an at-home printer. However, the quality control aspect remains a challenge.

Besides the haute couture creations, 3D printing is now useful to create smart clothes that can respond to stimuli and offer new functionalities, in addition to beautification and comfort. For example, some high-tech 3D printed dresses with interesting sensing functions were created: releases smoke to alert when someone is invading the personal space of the wearer (the Smoke dress - the first fully-flexible 3D printing material) (Materialise, 2021), tracks the wearer's attention level and alerts other people around the wearer (through lighting) to not disturb the wearer from activities that require a lot of

https://doi.org/10.24264/icams-2022.I.12

attention (the Synapse dress) (Boorman, 2014) or captures the breathing intensity of the wearer and when breathing becomes heavy, some robotic arms attached on the dress extend out like the legs of a spider to "defend" the wearer (the Spider Dress) (Starr, 2014).

Technical Textiles Sector

3D printed textiles were explored lately in different areas of the technical textiles sector. In this field the main focus is on functional properties.

The so-called "DefeXtiles", a technique that can produce thinner and flexible fabric-like structures with a fused deposition modelling (FDM) printer and PLA, TPU, ABS, PA etc. as extrusion materials has demonstrated its efficiency in the creation of different interesting objects, like a lampshade that can be turned on and off by pinching her pleats, tough and deformable badminton shuttlecocks and a fabric-like tendon actuator for a dancing person toy which has the necessary flexibility to curve during actuation (Forman *et al*., 2020).

As wearable devices are gaining more interest from the general population, a group of scientists developed a 3D printed fibre-based sensitive strain sensor that can be used as a skin-attached wearable device for the real-time detection of human activities (Cao *et al*., 2019).

A newly developed chain-mail-like fabric shows good potential for use in many technical applications. This fabric has advanced properties. When encased in a plastic envelope and vacuum-packed, it can become more than twenty-five times as hard as its original state under pressure and can hold up over 50 times its weight, it is lightweight, adaptable to the shape of the body and can retain a fairly flat shape under load. Selective laser sintering printing of nylon material was used to obtain the structure (Wang *et al*., 2021). It can be used for stab- and bullet-proof vests, for wearable exoskeletons and reconfigurable medical supports, or for protective vests for high-contact sports.

A decorative (panel) curtain that aims to improve room acoustics using functional 3D prints is another example of an application of 3DP in the field of technical textiles. The combination of TPU material printed on a PES-weave demonstrated that can suit requirements regarding both material properties like flexibility and feel as well as performance characteristics of adhesion and abrasion (Korger *et al*., 2020).

Scientists in the field of space also integrated 3D Printed fabrics as materials for astronaut spacesuits or as shields and insulation for spacecraft. They used additive manufacturing with metallic materials to create a chain-mail-like fabric that possesses four essential functions: reflectivity, passive heat management, foldability, and tensile strength (Jet Propulsion Laboratory-Caltech, 2017).

CONCLUSIONS

The possibility of using 3DP on a large scale in the textile sector is getting closer. Despite some disadvantages, the technology offers a multitude of advantages that combat the weaknesses. The innovative part of the fashion designers, engineers, and manufacturers of 3D printers will bring us step by step closer to this technology. It is up to us and our openness to accept it as a technology that can change our future in a good way, in order to influence the market of 3D printed products and contribute to the health of the environment and future generations.

Acknowledgements

This work was funded by the Ministry of Research, Innovation and Digitization, Romania, through the National Project "Electroconductive composite textiles based on

3D polymer matrices for sensor systems monitoring and attenuating electromagnetic waves (3D ELECTROTEX)", Grant Agreement PN 19 17 01 01.

REFERENCES

Alexandrea, P. (2022), "3D Printed Fashion: The Top Designs", 3Dnatives, available at https://www.3dnatives.com/en/3d-printing-fashion-designs150620174/#!

Bates-Green, K. and Howie, T. (2017), "Materials for 3D Printing by Fused Deposition", Edmonds Community College, 1-21, available at https://www.materialseducation.org/educators/matedu-modules/docs/Materials_in_FDM.pdf

Beecroft, M. (2019), "Digital Interlooping: 3D Printing of Weft-Knitted Textile-Based Tubular Structures Using Selective Laser Sintering of Nylon Powder", *International Journal of Fashion Design, Technology and Education*, 12(2), 218-224, https://doi.org/10.1080/17543266.2019.1573269.

Boorman, E. (2014), "Wearable Tech Just Got Smarter: Anouk Wipprecht's Intel-Edison-powered, 3D-printed "Synapse Dress" Logs Your Mood", *Materialise*, available at https://www.materialise.com/en/blog/wearable-tech-just-got-smarter-anouk-wipprechts-intel-edison-powered-3d-printed-synapse-dress

Cao, W., Ma, C., Mao, D.S., Zhang, J., Ma, M.G. and Chen, F. (2019), "MXene-Reinforced Cellulose Nanofibril Inks for 3D-Printed Smart Fibres and Textiles", *Advanced Functional Materials*, 29(51), 1905898, https://doi.org/10.1002/adfm.201905898.

Čuk, M., Bizjak, M., Muck, D. and Kočevar, T.N. (2020), "3D Printing and Functionalization of Textiles", *Proceedings - The Tenth International Symposium GRID 2020*, 499-506, https://doi.org/10.24867/grid-2020-p56.

DelVecchio, S. M. (Ed.), (2021), Women in 3D Printing. Women in Engineering and Science, Springer Nature Switzerland AG, https://doi.org/10.1007/978-3-030-70736-1.

Everett, H. (2021), "3D Hubs AM Trends Report Reveals 3d Printing Grew 21% Despite Covid-19", *3D Printing Industry*, available at https://3dprintingindustry.com/news/3d-hubs-am-trends-report-reveals-3d-printing-grew-21-despite-covid-19-189087/

Flynt, J. (2019), "3D Printing Fashion: Advantages, Disadvantages, and Future", *3D Insider*, available at https://3dinsider.com/3d-printing-fashion/

Forman, J., Dogan, M.D., Forsythe, H. and Ishii, H. (2020), "DefeXtiles: 3D Printing Quasi-Woven Fabric via Under-Extrusion", *Proceedings of the 33rd Annual ACM Symposium on User Interface Software and Technology*, 1222-1233, https://doi.org/10.1145/3379337.3415876.

Jet Propulsion Laboratory-Caltech (2017), "'Space Fabric' Links Fashion and Engineering", available at https://www.jpl.nasa.gov/news/space-fabric-links-fashion-and-engineering.

Korger, M., Glogowsky, A., Sanduloff, S., Steinem, C., Huysman, S., Horn, B., Ernst, M. and Rabe, M. (2020), "Testing thermoplastic elastomers selected as flexible three-dimensional printing materials for functional garment and technical textile applications", *Journal of Engineered Fibers and Fabrics*, 15, 155892502092459, https://doi.org/10.1177/1558925020924599.

Lussenburg, K., van der Velden, N., Doubrovski, Z., Geraedts, J. and Karana, E. (2014), "Designing with 3D Printed Textiles – A Case Study of Material Driven Design", *Proceedings of 5th International Conference on Additive Technologies*, 74-81, https://doi.org/10.3390/su14137872.

Martens, Y. and Ehrmann, A. (2017), "Composites of 3D-Printed Polymers and Textile Fabrics", *IOP Conference Series: Materials Science and Engineering*, 225, 012292, https://doi.org/10.1088/1757-899x/225/1/012292.

Materialise (2021), "'Smoke Dress' Hits the Volkswagen Catwalk", available at https://www.materialise.com/en/cases/smoke-dress-hits-volkswagen-catwalk.

Mings, J. (2017), "Model of the Week: 3D Printed Triangular Mesh Fabric [100X Better Than Polyester!]", SolidSmack, available at https://www.solidsmack.com/cad/model-week-3d-printed-triangular-mesh-fabric-100x-better-polyester/

Molitch-Hou, M. (2022), "Fashion 3D Printing Targeted by Stratasys with New Textile 3D Printer", available at https://3dprint.com/290932/fashion-3d-printing-targeted-by-stratasys-with-new-textile-3d-printer/

Partsch, L., Vassiliadis, S. and Papageorgas, P. (2015), "3D Printed Textile Fabrics Structures", *5th International Istanbul Textile Congress 2015: Innovative Technologies "Inspire to Innovate"*, Istanbul.

Praveen, S., Sim, G.S., Ho, C.W. and Lee, C.W. (2021), "3D-Printed Twisted Yarn-Type Li-Ion Battery towards Smart Fabrics", *Energy Storage Materials*, 41, 748-757, https://doi.org/10.1016/j.ensm.2021.07.024.

Spahiu, T., Canaj, E. and Shehi, E. (2020), "3D Printing for Clothing Production", *Journal of Engineered Fibers and Fabrics*, 15, 155892502094821, https://doi.org/10.1177/1558925020948216.

Starr, M. (2014), "Robotic Spider Dress Defends Your Personal Space", *CNET*, available at https://www.cnet.com/culture/robotic-spider-dress-defends-your-personal-space/

Stevenson, K. (2020), "Major Development in 3D Printed Fabric", *Fabbaloo*, available at https://www.fabbaloo.com/2020/07/major-development-in-3d-printed-fabric.

Takahashi, H., and Kim, J. (2019), "3D Printed Fabric: Techniques for Design and 3D Weaving Programmable Textiles", *Proceedings of the 32nd Annual ACM Symposium on User Interface Software and Technology*, https://doi.org/10.1145/3332165.3347896.

Wang, Y., Li, L., Hofmann, D., Andrade, J.E. and Daraio, C. (2021), "Structured Fabrics with Tunable Mechanical Properties", *Nature*, 596(7871), 238-243, https://doi.org/10.1038/s41586-021-03698-7.

https://doi.org/10.24264/icams-2022.I.12

II.

BIOMATERIALS AND BIO-TECHNOLOGIES

THE IMPACT OF ENVIRONMENTAL KNOWLEDGE ON RECYCLING INTENTION: THE MEDIATING ROLE OF PERCEIVED BEHAVIOURAL CONTROL

AHMED HUSSEIN ALI, HABIBA SHERIF EL ROUBY,
MAHMOUD RAMADAN BARAKAT

Arab Academy for Science, Technology and Maritime Transport, College of International Transport and Logistics, 9 Abou Qear, Abu Qir Al Gharbeyah, Montaza 2, Alexandria, ahmed.husseincitl@aast.edu, mahmoud.barakat@aast.edu, habiba.roubi@aast.edu

Currently, sustainability goals are the prior aim to be achieved by any organization as the united nation called to apply sustainability practices to be achieved by 2030. Recycling is one of the main extracted strategies from SDG 12 that countries try to increase and rely on landfills. Therefore, this study aims to measure the impact of environmental knowledge (EK) on recycling intention (RI); in addition, it tries to explore the mediation role of Internal perceived behavioural control (IPBC) and External perceived behavioural control (EPBC)). The research used a quantitative approach through distributing an online questionnaire to people in Egypt in order to examine the research variables. Number of 416 valid responses were analyzed using SPSS through conducting Bootstrapping method to analyzed the mediation role. The findings showed that environmental knowledge has a direct impact on recycling intention; moreover, the mediation role of Internal perceived behavioural control and External perceived behavioural control is rejected. This proves that increasing the environmental knowledge will enhance the behaviours of the societies. Furthermore, will grab the societies' attention to apply the sustainability practices in the future. Future studies need to consider recycling activities, especially in developing countries, and to improve the awareness and behaviour levels.

Keywords: sustainability, recycling, quantitative study

INTRODUCTION

Solid waste is one of the most difficult problems in developing countries because of the increase in urbanization, population growth, and economic expansion. These reasons have led to an increase in the amount of solid waste in Egypt. According to Ibrahim, Abo El-Ata, and El-Hattab (2020), the different sectors in Egypt are generating around 95 million tons of solid waste, and the waste generated per capita increased from 0.2 kg to 0.6. Therefore, Egypt developed eight sustainable goals Based on the UN SDGs to be achieved by 2030 (https://mped.gov.eg/EgyptVision?lang=en). Based on these goals, especially goal 7 which is related to decreasing the pressure on the environment and saving the biological environment and series of habitats from the effect of human activities, the study will try to increase the awareness of recycling in society.

Egypt is seeking to spread sustainability awareness and knowledge within the community (Ali *et al*., 2022; Ali *et al*., 2021). As Ibrahim *et al*. (2020) mentioned that the awareness is the main key to achieving better sustainable performance.

LITERATURE REVIEW AND HYPOTHESES DEVELOPMENT

Environmental Knowledge (EK)

Environmental knowledge issues have begun to grow in developing countries, especially after launching sustainability goals from the Egyptian government. EK has been defined from different perspectives; according to Fryxell and Lo (2003), EK is described as a broad understanding of facts, ideas, and relationships related to the natural environment and its primary ecosystems. EK includes three main dimensions:

https://doi.org/10.24264/icams-2022.II.1

system, action-related, and effectiveness knowledge (Frick *et al*., 2004). Chan *et al*. (2014) mentioned that the person or customer will not buy or engage into specific activity or product if the knowledge steer behaviour in that context is insufficient. In addition, Boo and Park (2013) stated that when a customer or person believes that they have enough knowledge about something specific when they see themselves doing better than others. Some researchers highlighted that EK can be reflected on the person's behaviours (Vicente-Molina *et al*., 2013).

Recycling Intention (RI) and Perceived Behavioural Control (PBC)

Recycling is an effort to reduce human impacts on the environment and to achieve environmental sustainability (Ali *et al*., 2019). In 1991, Ajzen proposed the Theory of Planned Behaviour (TPB), which is related to studying the RI; this theory is extended already from Theory of Reasoned Action (TRA) (Ajzen and Fishbein, 1975). TPB proposed that the person's intention to perform an action comes originally from "positive evaluation of the behaviour (attitude), social pressure encouraging the behaviour (subjective norm) and perceived ease of performing such behaviour (perceived behavioural control)" (Wan *et al*., 2017). These three dimensions had confirmed to be the indicators for RI such as (Aboelmaged, 2021; Passafaro *et al*., 2019; Wan *et al*., 2017). Perceived Behavioural Control (PBC) as one of RI indicators is characterised as a self-perception of the person to complete the behaviour (Valle *et al*., 2005). Manstead and Van Eekelen (1998) explored the operationalized weaknesses of PBC and suggested that PBC should have two dimensions (Internal and External). In addition, the behaviour for the individual could be affected through either internal or external factors.

Environmental Knowledge refers to the awareness of the person for something specific or specific issues, This knowledge is based on the real information or behavioural knowledge (Jaiswal and Kant, 2018). Vicente-Molina *et al*. (2013) used EK variable to measure its impact on behaviour. Moreover, Liefländer and Bogner (2018) measured the relationship between EK and attitudes and behaviour. In addition, (Maurer and Bogner, 2020) modelled the relationship between EK and behaviour. The TPB has been confirmed in numerous research studies on RIs and behaviour (Aboelmaged, 2021; Davis *et al*., 2006; Smith and McSweeney, 2007). Based on the above discussion, the following hypotheses have been shaped:

- H_1: Environmental knowledge has a positive impact on IPBC.
- H_2: Environmental knowledge has a positive impact on EPBC.
- H_3: IPBC is mediating the relationship between Ek and RI.
- H_4: EPBC is mediating the relationship between Ek and RI.
- H_5: Environmental knowledge has a positive impact on Recycle Intention.

Based on the discussion above, a conceptual framework is formulated in Figure 1.

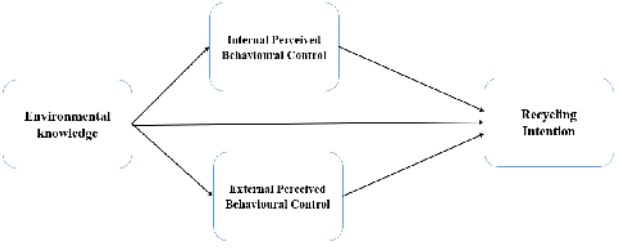

Figure 1. The conceptual framework

https://doi.org/10.24264/icams-2022.II.1

RESEARCH METHODOLOGY AND INSTRUMENTIN THIS STUDY

The quantitative approach was used in order to collect data, and to achieve the study's main goal. Online 416 respondents were collected and five-point Likert scale was used to measure items of the proposed model. The research items have developed from previous literature.

DESCRIPTIVE ANALYSIS

This study set three descriptive questions; the first one was related to the educational level of the respondents, the majority of whom were Bachelor degree holders with 67.3%, and 2.98 % were PhD holders. For gender, 61.5 % were male and 38.5 female. Finally, for income, the majority of income level of the respondents was between 1000 to 5000, with 58.7 %.

RELIABILITY AND VALIDITY TEST

Validity and reliability are used for data testing to verify that the data collected are suitable enough for testing the research hypotheses. To test validity, the average variance extracted (AVE) and factor loading (FL) are tested. The Cronbach's alpha value is tested to measure the reliability. Table1 illustrates the validity and reliability tests, all outputs have met the threshold, except RI4 with FL score .397.

Table 1. Validity and reliability for study variables

Variables						
Environmental knowledge	EK1	EK2	EK3	EK4	EK5	EK6
FL	.774	.709	.815	.776	.806	.830
Cronbach's alpha			0.875			
AVE			61.786			
Internal perceived behavioural control	IPBC1	IPBC2	IPBC3	IPBC4		
FL	.908	.821	.811	.811		
Cronbach's alpha			0.855			
AVE			70.385			
External perceived behavioural control	EPBC1	EPBC2	EPBC3	EPBC4		
FL	.868	.818	.841	.862		
Cronbach's alpha			0.868			
AVE			71.803			
Recycling intention	RI1	RI2	RI3	RI4		
FL	.761	.799	.842	Delete		
Cronbach's alpha			0.625			
AVE			52.120			

HYPOTHESES TESTING

- *H_1: Environmental knowledge has a positive impact on IPBC*

The regression test has been conducted, it could be observed that there is a positive significant effect of EK on IPBC, as P-value is 0.000 (which is less than 0.05, indicating a significant relationship), and the estimate value is 0. 526 (which is greater than zero, indicating a positive relationship). furthermore, the R Square (Coefficient of

https://doi.org/10.24264/icams-2022.II.1

determinations) is 0.27, which means that 27% of the variation in IPBC is explained by the independent variable EK. Accordingly, the first hypothesis testing is supported.

- *H2: Environmental knowledge has a positive impact on EPBC*

The regression test has been conducted; it could be observed that there is a positive significant effect of EK on EPBC, as P-value is 0.000 and the estimate value is 0.592. Furthermore, the R Square is 0.35, which means that 35% of the variation in EPBC is explained by the independent variable EK. Accordingly, the second hypothesis testing is supported.

- *H_3: IPBC is mediating the relationship between Ek and RI.*
- *H_4: EPBC is mediating the relationship between Ek and RI.*

Bootstrapping method with bias-correlated confidence estimates is used in order to measure the mediation role of (IPBC and EPBC) between EK and RI (Preacher and Hayes, 2004). The study used 95% confidence interval with 5000 bootstrapping resamples (Preacher and Hayes, 2008). The results showed, as in Table 4, that the mediation role of IPBC between the EK and RI is supported as (B= 0.0423, CI = 0.16 to 0.32), In contrast, the results showed that the mediation role of EPBC between the EK and RI is rejected as (B= 0.0331, CI =-0.0028 to 0.1266).

- *H5: Environmental knowledge has a positive impact on Recycle Intention.*

The regression test has been conducted; it could be observed that there is a positive significant effect of EK on RI, as P-value is 0.000, and the estimate value is 0.65. Furthermore, the R Square (Coefficient of determinations) is 0.42, which means that 42% of the variation in RI is explained by the independent variable EK.

Based on the discussion above, EK is positively affected by IPBC and EPBC; this finding is in line with many studies, like (Foroughi *et al*., 2022; Jaiswal and Kant, 2018; Kumar *et al*., 2017). It means that increasing the EK will enhance the behaviours of the societies; in addition, Mostafa (2007) who applied his study in Egypt confirmed that increasing the awareness about environmental problems is an important aspect toward the behaviour and attitude.

Finally, as for the mediating role of IPBC and EPBC, the study found that the IPBC, which is the skills and resources gained from practicing, has a positive impact on the RI. The result is supported by Shabbir *et al*. (2016). In contrast, the external perceived behaviour control is not affecting the RI as the external behaviour comes originally from the societies around the person, and it could affect him positively or negativity.

CONCLUSION

This study aims to measure the impact of EK on (RI), in addition to exploring the mediation role of (IPBC and EPBC) The implications of this study are in two sections: firstly, the theoretical implications are related to using the Theory of Planned Behaviour in the field of recycling intention, as the theory explains that the person' intention to take an action depends on many factors whether internal or external. This study expanded the use of TPB through testing the impact of EK, IPBC, and EPBC on RI. Secondly, the practical implications are related to the role of the government and relevant bodies to increase the consciousness about the benefits of recycling as a part of the sustainability development goals, in addition to creating training programs related to preserving the environment and spreading the sustainability culture.

https://doi.org/10.24264/icams-2022.II.1

REFERENCES

Aboelmaged, M. (2021), "E-waste Recycling Behaviour: An Integration of Recycling Habits into the Theory of Planned Behaviour", *Journal of Cleaner Production*, 278, 124182, https://doi.org/10.1016/j.jclepro.2020.124182.

Ajzen, I. (1991), "The Theory of Planned Behavior", *Organizational Behavior and Human Decision Processes*, 50(2), 179-211, https://doi.org/10.1016/0749-5978(91)90020-T.

Ajzen, I. and Fishbein, M. (1975), "A Bayesian Analysis of Attribution Processes", *Psychological Bulletin*, 82(2), 261, https://doi.org/10.1037/h0076477.

Ali, A., Chauhan, K., Barakat, M. and Eid, A. (2019), "The Role of Sustainability for Enhancing Third-Party Logistics Management Performance", *Journal of Management and Sustainability*, 9, 14, https://doi.org/10.5539/jms.v9n1p14.

Ali, A.H., Gruchmann, T. and Melkonyan, A. (2022), "Assessing the Impact of Sustainable Logistics Service Quality on Relationship Quality: Survey-based Evidence in Egypt", *Cleaner Logistics and Supply Chain*, 4, 100036, https://doi.org/10.1016/j.clscn.2022.100036.

Ali, A.H., Melkonyan, A., Noche, B. and Gruchmann, T. (2021), "Developing a Sustainable Logistics Service Quality Scale for Logistics Service Providers in Egypt", *Logistics*, 5(2), 21, https://doi.org/10.3390/logistics5020021.

Boo, S. and Park, E. (2013), "An Examination of Green Intention: The Effect of Environmental Knowledge and Educational Experiences on Meeting Planners' Implementation of Green Meeting Practices", *Journal of Sustainable Tourism*, 21(8), 1129-1147, https://doi.org/10.1080/09669582.2012.750327.

Chan, E.S., Hon, A.H., Chan, W. and Okumus, F. (2014), "What Drives Employees' Intentions to Implement Green Practices in Hotels? The Role of Knowledge, Awareness, Concern and Ecological Behaviour", *International Journal of Hospitality Management*, 40, 20-28, https://doi.org/10.1016/j.ijhm.2014.03.001.

Davis, G., Phillips, P.S., Read, A.D. and Iida, Y. (2006), "Demonstrating the Need for the Development of Internal Research Capacity: Understanding Recycling Participation Using the Theory of Planned Behaviour in West Oxfordshire, UK", *Resources, Conservation and Recycling*, 46(2), 115-127, https://doi.org/10.1016/j.resconrec.2005.07.001.

Foroughi, B., Arjuna, N., Iranmanesh, M., Kumar, K.M., Tseng, M.-L. and Leung, N. (2022), " Determinants of Hotel Guests' Pro-Environmental Behaviour: Past Behaviour as Moderator", *International Journal of Hospitality Management*, 102, 103167, https://doi.org/10.1016/j.ijhm.2022.103167.

Frick, J., Kaiser, F.G. and Wilson, M. (2004), "Environmental Knowledge and Conservation Behavior: Exploring Prevalence and Structure in a Representative Sample", *Personality and Individual differences*, 37(8), 1597-1613, https://doi.org/10.1016/j.paid.2004.02.015.

Fryxell, G.E. and Lo, C.W. (2003), "The Influence of Environmental Knowledge and Values on Managerial Behaviours on Behalf of the Environment: An Empirical Examination of Managers in China", *Journal of Business Ethics*, 46(1), 45-69, https://doi.org/10.1023/A:1024773012398.

Ibrahim, N., Abo El-Ata, G. and El-Hattab, M. (2020), "Status, Problems and Challenges for Municipal Solid Waste Management in Assiut Governate", *Journal of Environmental Studies and Researches*, 10(2), 362-384, https://doi.org/10.21608/jesr.2020.136575.

Jaiswal, D. and Kant, R. (2018), "Green Purchasing Behaviour: A Conceptual Framework and Empirical Investigation of Indian Consumers", *Journal of Retailing and Consumer Services*, 41, 60-69, https://doi.org/10.1016/j.jretconser.2017.11.008.

Kumar, B., Manrai, A.K. and Manrai, L.A. (2017), "Purchasing Behaviour for Environmentally Sustainable Products: A Conceptual Framework and Empirical study", *Journal of Retailing and Consumer Services*, 34, 1-9, https://doi.org/10.1016/j.jretconser.2016.09.004.

Liefländer, A. and Bogner, F.X. (2018), "Educational Impact on the Relationship of Environmental Knowledge and Attitudes", *Environmental Education Research*, 24(4), 611-624, https://doi.org/10.1080/13504622.2016.1188265.

Manstead, A.S. and Van Eekelen, S.A. (1998), "Distinguishing between Perceived Behavioral Control and Self-Efficacy in the Domain of Academic Achievement Intentions and Behaviors", *Journal of Applied Social Psychology*, 28(15), 1375-1392, https://doi.org/10.1111/j.1559-1816.1998.tb01682.x.

Maurer, M. and Bogner, F.X. (2020), "Modelling Environmental Literacy with Environmental Knowledge, Values and (Reported) Behaviour", *Studies in Educational Evaluation*, 65, 100863, https://doi.org/10.1016/j.stueduc.2020.100863.

Mostafa, M.M. (2007), "A Hierarchical Analysis of the Green Consciousness of the Egyptian Consumer", *Psychology & Marketing*, 24(5), 445-473, https://doi.org/10.1002/mar.20168.

Passafaro, P., Livi, S. and Kosic, A. (2019), "Local Norms and the Theory of Planned Behavior: Understanding the Effects of Spatial Proximity on Recycling Intentions and Self-Reported Behavior", *Frontiers in Psychology*, 10, 744, https://doi.org/10.3389/fpsyg.2019.00744.

Preacher, K. and Hayes, A. (2004), "SPSS and SAS Macros for Bootstrapping Indirect Effects in Multiple Mediator Models", Retrieved August, 17, 2006.

Preacher, K.J. and Hayes, A.F. (2008), "Asymptotic and Resampling Strategies for Assessing and Comparing Indirect Effects in Multiple Mediator Models", *Behavior Research Methods*, 40(3), 879-891, https://doi.org/10.3758/BRM.40.3.879.

Shabbir, M.S., Shariff, M.N.M. and Shahzad, A. (2016), "Mediating Role of Perceived Behavioral Control and Stakeholders' Support System on the Relationship between Entrepreneurial Personal Skills and Entrepreneurial Intentions of IT Employees in Pakistan", *International Business Management*, 10(9), 1745-1755.

Smith, J.R. and McSweeney, A. (2007), "Charitable Giving: The Effectiveness of a Revised Theory of Planned Behaviour Model in Predicting Donating Intentions and Behaviour", *Journal of Community & Applied Social Psychology*, 17(5), 363-386, https://doi.org/10.1002/casp.906.

Valle, P.O.D., Rebelo, E., Reis, E. and Menezes, J. (2005), "Combining Behavioral Theories to Predict Recycling Involvement", *Environment and Behavior*, 37(3), 364-396, https://doi.org/10.1177/0013916504272563.

Vicente-Molina, M.A., Fernández-Sáinz, A. and Izagirre-Olaizola, J. (2013), "Environmental Knowledge and Other Variables Affecting Pro-Environmental Behaviour: Comparison of University Students from Emerging and Advanced Countries", *Journal of Cleaner Production*, 61, 130-138, https://doi.org/10.1016/j.jclepro.2013.05.015.

Wan, C., Shen, G.Q. and Choi, S. (2017), "Experiential and Instrumental Attitudes: Interaction Effect of Attitude and Subjective Norm on Recycling Intention", *Journal of Environmental Psychology*, 50, 69-79, https://doi.org/10.1016/j.jenvp.2017.02.006.

HAIR MASKS BASED ON KERATIN AND COLLAGEN

MĂDĂLINA GEORGIANA ALBU-KAYA[1], MIHAELA-VIOLETA GHICA[2*], CRISTINA-ELENA DINU-PÎRVU[2], LĂCRĂMIOARA POPA[2], ELENA DĂNILĂ[2], CIPRIAN CHELARU[1], VALENTINA ANUȚA[2], DURMUȘ ALPASLAN KAYA[3], MARINA-THEODORA TALIANU[2], ANA-MARIA STAVRI[2]

[1]*The National Research & Development Institute for Textiles and Leather - Leather and Footwear Research Institute Division, 93 Ion Minulescu Str., 031215, Bucharest, Romania*

[2]*"Carol Davila" University of Medicine and Pharmacy, Faculty of Pharmacy, Physical and Colloidal Chemistry Department, 6 Traian Vuia Str., 020956, Bucharest, Romania, *mihaelaghica@yahoo.com*

[3]*Mustafa Kemal University, Agriculture Faculty, Field Crops Department, 31034, Antakya-Hatay Metropolitan Municipality, 31034, Antakya-Hatay, Turkey*

The study aimed to develop and characterize some O/W emulsions, designed as nourishing hair masks. The cosmetic formulations based on collagen hydrolysate, keratin, and natural ingredients (essential and vegetable oils) were organoleptically evaluated. The pH, morphological, superficial, and rheological properties were assessed as a physicochemical background. The rheological measurements were performed at 23 and 32°C, and the shear stress versus shear rate ascending and descending rheograms were built, together with the flow profiles of viscosity as a function of shear rate. The cosmetic emulsions were stable at temperature variation and the pH values were considered physiologically acceptable for the skin, indicating that formulations can be safely applied for cosmetic purposes. Results from the optical microscopy analysis showed that all emulsions presented a creamy and non-greasy appearance. The superficial profiles, quantified through contact angle at solid/liquid interface, were specific for hydrophilic formulations. The emulsions showed pseudoplastic and thixotropic behavior, facilitating the formulations' flow and the topical application. The Power law model was used to quantify the flow properties, and the thixotropic analysis was conducted using particular descriptors, namely thixotropic area, and thixotropic index. The designed emulsions presented appropriate physicochemical properties for cosmetic applications in hair care.

Keywords: collagen/keratin-based emulsions, hair masks, physicochemical characteristics

INTRODUCTION

Hair represents an essential component in terms of a person's physical appearance, with a high social impact on both women and men. For this reason, to make it as visually pleasing as possible, the hair is often subjected to thermal or chemical treatments affecting its structure (Tinoco *et al*., 2018).

Keratin is a protein found in the structure of the hair and is directly involved in maintaining its resistance, flexibility, and durability by ensuring a proper degree of hydration and a shiny appearance (Basit *et al*., 2018, Tinoco *et al*., 2018). Collagen, as essential protein for the human body, is also found in the connective tissue surrounding hair follicle. It contributes to the process of hair growth and regeneration by facilitating the formation of stem cells, giving birth to new hair follicles (Natsuga *et al*., 2019).

Emulsions are soft coarse dispersions intensively selected in cosmetic applications and body care (Talianu *et al*., 2019). To incorporate proteins with role in hair regeneration (keratin, collagen) into an emulsion component, they must be soluble in water and have a reduced ability to aggregate the peptides in its structure (Dănilă *et al*., 2019b). Thus, the use of protein hydrolysates in the formulation of cosmetic products is indicated due to their ability to prevent damage to the hair strand or to repair the already damaged one (Tinoco *et al*., 2018, Dănilă *et al*., 2020).

The purpose of this study consisted in the research of new hair care products in the

https://doi.org/10.24264/icams-2022.II.2

form of O/W emulsions that can be used as hair masks based on keratin and collagen, but also other natural ingredients such as panthenol, vegetable oils, and essential oils.

MATERIALS AND METHODS

Materials

Vegetable oils (avocado oil, argan oil), emulsifiers (Varisoft emulsifier: cetearyl alcohol, behentrimonium methosulfate), floral water, panthenol, and essential oils and keratin were purchased from a local pharmacy. Type I collagen hydrolysate was obtained by acidic hydrolysis (Dănilă *et al*., 2019b).

Preparation of the O/W Emulsions

According to Table 1, the ingredients of phase A (oils and emulsifier) and phase B (floral water, distilled water, keratin, collagen hydrolysate) were heated in a water bath in two heat-resistant Berzelius beakers, under homogenisation. When both phases reached a temperature of about 75°C, they were removed from the water bath. The content of phase A was slowly added over phase B under continuous stirring. The mixing continued for a few minutes, avoiding the aeration of the emulsions. Over the obtained composition, C phase ingredients were added and mixed for about one minute. The beaker was placed in a cold-water bath under continuous stirring for 3 minutes. In the cooled composition, the ingredients of phase D were gradually added and mixed after each one. The obtained emulsions, coded as Emulsions 1-3, were transferred through sterile containers.

Table 1. Composition of the O/W hair balm emulsions

Phase	Ingredients (%)	Emulsion 1	Emulsion 2	Emulsion 3
A	avocado oil (mL)	5	10	15
A	argan oil (mL)	5	10	15
A	emulsifier* (g)	5	8	10
B	floral water (mL)	40	30	20
B	distilled water (mL)	41	38	36
B	collagen hydrolisate (g)	1	1	1
B	keratin (mL)	1	1	1
C	panthenol (mL)	1	1	1
D	Cosgard preservative (mL)	0.5	0.5	0.5
D	essential oils (mL)**	0.5	0.5	0.5

* Varisoft emulsifier: cetearyl alcohol, behentrimonium methosulfate; **essential oils: Eucalyptus, pine, rosemary, oregano

pH Determination

The pH of dermatocosmetic emulsions was evaluated using an inoLab pH meter.

Optical Microscopy Analysis

The morphology of the designed emulsions was carried out using a LEICA optical microscope model S8AP0, with the increased power of 20-160x.

Goniometric Evaluation

The superficial properties were performed with CAM 101 (KSV Instruments), using the *contact angle method*: liquid drop (water) was spread on a solid surface (emulsion-coated slide test), analyzing the modifications of liquid drop shape on this surface.

https://doi.org/10.24264/icams-2022.II.2

Rheological Analysis

The flow properties of the emulsions were performed using a rotational viscometer Multi-Visc Rheometer (Fungilab), equipped with TR 9 standard spindle, and a ThermoHaake P5 Ultrathermostat to ensure a constant temperature (23±0.1°C and 32±0.1°C). The operational conditions were previously reported (Ghica *et al*., 2016).

RESULTS AND DISCUSSION

All emulsions were homogeneous, stable, with no phase separation, and a sweet scent, well defined by the selected ingredients. The O/W emulsions presented a pH of 5.5, compatible with the skin pH. Optical microscopy was used to study the morphology of the emulsions. The images of the samples are presented in Figure 1.

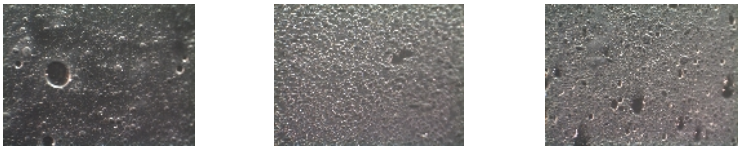

Emulsion 1 Emulsion 2 Emulsion 3

Figure 1. Optical microscopy images of O/W cosmetic hair balm emulsions

It can be noticed that all emulsions had a white aspect, with non-greasy structure. Emulsion 1 was characterized by a foam-like appearance, while the other two emulsions had creamy appearance. Differences between the microscopic images were attributed to various vegetable oils with different content in fatty acids, used as oil phases.

Contact angle values (CA°) represent a benchmark to quantify the superficial properties of the emulsions. Drops dynamic was monitored with a digital camera and the contact angle was mathematically depicted for each emulsion, as previously (Popa *et al*., 2013).

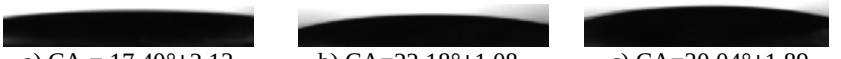

a) CA = 17.40°±2.13 b) CA=22.18°±1.08 c) CA=30.04°±1.89

Figure 2. Images of the drop shape for the W/O dermatocosmetic emulsions: a) Emulsion 1; b) Emulsion 2; c) Emulsion 3

It can be observed that CA values increased proportionally with the oil content. For Emulsions 3 it was found the maximum value of contact angle of 30.04° which was 1.72 fold higher than Emulsion 1. Globally, the recorded CA values indicated a marked hydrophilicity of the emulsions, an important quality in their design, with direct implications for skin hydration and hair nourishing potential.

The rheograms – viscosity as a function of shear rate – were built (Figure 3) and the Power law model was used to quantify the flow behavior of the formulations:

$$\eta = m \cdot \dot{\gamma}^{-n} \quad (1)$$

where m parameter represents the viscosity obtained for the shear rate value of $1 \cdot s^{-1}$, and n is the flow behaviour index (Dănilă *et al*., 2019a), and determined through the linearization of equation (1) by double logarithmic method (Figure 4).

https://doi.org/10.24264/icams-2022.II.2

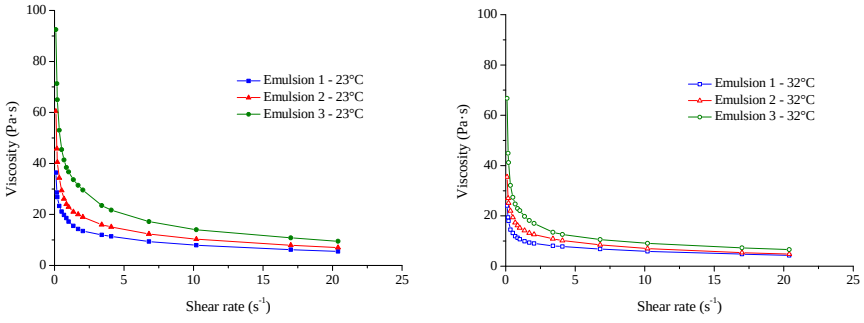

a) b)

Figure 3. Plots of viscosity versus shear rate for the Emulsions 1-3, evaluated at: a) 23°C; b) 32°C

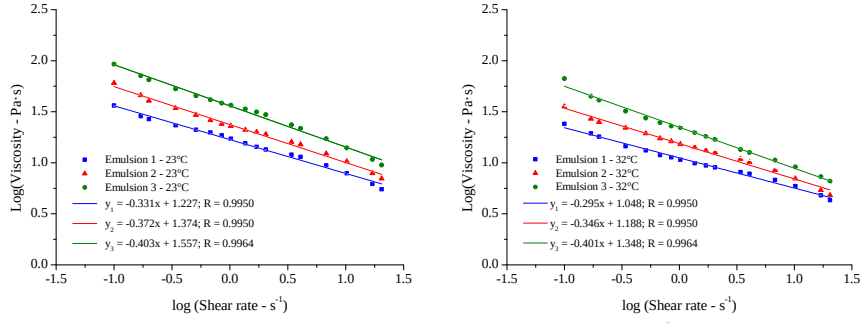

a) b)

Figure 4. Log-log plots of viscosity versus shear rate, for the Emulsions 1-3 evaluated at: a) 23°C; b) 32°C

Analyzing Figure 3a-b, the emulsions viscosity decreased at shear rate increase, showing a pseudoplastic behavior at both working temperatures, aspect which was well defined through the log-log plots presented in Figure 4a-b. The pseudoplastic behavior is a requirement for the dermatocosmetic emulsions, both conditioning aspect and spreading as a continuous film on the hair surface. The parameters n and m, specific to the Power law model, are listed in Tables 2 and 3 for both working temperatures.

Table 2. Values for the determination coefficient and parameter specific to the Power law model, and the thixotropic descriptors determined at 23°C

Formulation	R	m	n	S_{asc} (Pa·s^{-1})	S_{thix} (Pa·s^{-1})	$T_{hyst\%}$ (%)
Emulsion 1	0.9950	16.869	0.331	1507.694	127.699	8.47
Emulsion 2	0.9960	23.664	0.372	1951.959	201.807	10.34
Emulsion 3	0.9960	36.107	0.403	2697.663	317.649	11.77

https://doi.org/10.24264/icams-2022.II.2

Table 3. Values for the determination coefficient and parameter specific to the Power law model, and the thixotropic descriptors determined at 32°C

Formulation	R	m	n	S_{asc} (Pa·s^{-1})	S_{thix} (Pa·s^{-1})	$T_{hyst\%}$ (%)
Emulsion 1	0.9950	11.168	0.295	1129.760	88.713	7.85
Emulsion 2	0.9950	15.417	0.346	1332.160	126.726	9.51
Emulsion 3	0.9964	22.284	0.401	1756.404	188.342	10.31

The experimental data well fitted the Power law model, and correlation coefficients had high values, up to 0.9960 at 23°C and 0.9964 at 32°C. The most fluid system was Emulsion 1, the m parameter having the lowest value. In the case of Emulsion 2, it was recorded an intermediate value of the m parameter, being correlated with a medium viscosity. The maximum values for the m parameter were recorded for Emulsion 3. The forward and backward rheograms – shear stress as a function of shear rate – were also recorded (Figure 5) and the thixotropic behavior was quantified through the thixotropy area (S_{thix}) and thixotropy index ($T_{hyst\%}$). Thixotropic systems are those with $T_{hyst\%}$ values greater than 5% (Dănilă *et al.*, 2019b), and can be depicted from Table 2 and Table 3, where S_{asc}, S_{thix}, and $T_{hyst\%}$ were presented for both working temperatures alike.

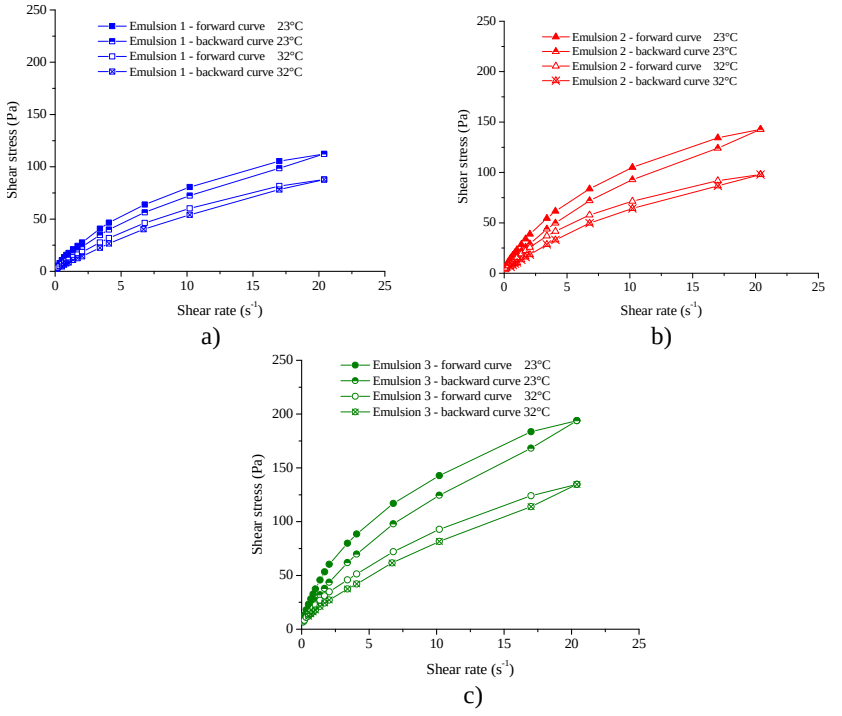

Figure 5. Forward and backward rheograms, shear stress versus shear rate, evaluated at 23˚C and 32˚C, for: a) Emulsion 1; b) Emulsion 2; c) Emulsion 3

Figure 4a-c indicates that the backward curve is positioned under the forward curve. Thus, for the same shear rate, the shear stress for the backward curve is smaller. The thixotropic character is defined by the thixotropy index higher than 5% for both

https://doi.org/10.24264/icams-2022.II.2

temperatures. The thixotropic behavior is also a quality requirement targeted in emulsions design, allowing the transition of a viscous product into a more fluid one, easy to spread. Another influencing factor is related to the temperature. Thus, for temperature increase, it can be noticed that m parameter decreases for all emulsions, about 1.5-1.6 times, and a decrease of thixotropic parameters by about 1.4-1.68 times.

CONCLUSIONS

All emulsions obtained were stable and the pH values corresponded to the skin physiological one, indicating that hair masks can be safely applied to the skin and hair. The optical microscopy analysis shows that all emulsions presented a creamy and foamy appearance with a non-greasy structure. The superficial profiles, quantified through contact angle, indicated a high degree of hydrophilicity. The emulsions showed a pseudoplastic and thixotropic behavior, facilitating the formulations flow and the application as hair balms. It can be appreciated that the designed emulsions presented adequate physicochemical properties for a cosmetic purpose, being considered suitable hair balm formulations for hair care.

Acknowledgement

This research was financially supported by "Carol Davila" University of Medicine and Pharmacy Bucharest, Romania, through Contract no. CNFIS-FDI-2022-0253, funded by the Romanian Ministry of Education.

REFERENCES

Basit, A., Asghar, F., Sadaf, S. and Akhtar, M.W. (2018), "Health Improvement of Human Hair and Their Reshaping Using Recombinant Keratin K31", *Biotechnology Reports*, 20, https://doi.org/10.1016/j.btre.2018.e00288.

Dănilă, E., Kaya, D.A., Ghica, M.V., Albu Kaya, M.G., Negrea, C., Popa, L. and Nitipir, C. (2019a), "Rheological Properties and Stability of Dermatocosmetic Emulsions with Collagen and Natural Ingredients Used as Color Correcting Cream and Cream Foundation", *Revista de Chimie*, 70(6), 1928-1933, https://doi.org/10.37358/RC.19.6.7249.

Dănilă, E., Moldovan Z., Albu Kaya, M.G. and Ghica, M.V. (2019b), "Formulation and Characterization of Some Oil in Water Cosmetic Emulsions Based on Collagen Hydrolysate and Vegetable Oils Mixtures", *Pure and Applied Chemistry*, 91(9), 1493-1507, https://doi.org/10.1515/pac-2018-0911.

Dănilă, E., Albu Kaya, M.G., Ghica, M.V., Bunea, A.M., Popa, L., Kaya, D.A., Öztürk, Ş., Marin, M.M., Dinu-Pîrvu, C.-E. and Anuța, V. (2020), "Formulation and Characterization of Anti-Aging Cosmetic Emulsions Based on Collagen Hydrolysate and Caffeine", *Proceedings of the 8th International Conference on Advanced Materials and Systems (ICAMS)*, Bucharest, 1-3 October 2020, 139-144, https://doi.org/10.24264/icams-2020.II.6.

Ghica, M.V., Hîrjău, M., Lupuleasa, D. and Dinu-Pîrvu, C.-E. (2016), "Flow and Thixotropic Parameters for Rheological Characterization of Hydrogels", *Molecules*, 21(6), E 786, https://doi.org/10.3390/molecules21060786.

Natsuga, K., Watanabe, M., Nishie, W. and Shimizu, H. (2019), "Life Before and Beyond Blistering: The Role of Collagen XVII in Epidermal Physiology", *Experimental Dermatology*, 28, 1135-1141, https://doi.org/10.1111/exd.13550.

Popa, L., Ghica, M.V., Albu, M.G., Ortan, A. and Dinu-Pirvu, C.-E. (2013), "Hysteresis of Contact Angle. Dynamic Wettability Studies of Collagen and Doxycycline Porous Matrices Crosslinked with Tannic Acid", *Digest Journal of Nanomaterials and Biostructures*, 8(3), 937-943.

Talianu, M.-T., Dinu-Pîrvu, C.-E., Ghica, M.V., Anuța, V., Jinga, V. and Popa, L. (2019), "Foray into Concepts of Design and Evaluation of Microemulsions as a Modern Approach for Topical Applications in Acne Pathology", *Nanomaterials*, 10(11), 1-43, https://doi.org/10.3390/nano10112292.

Tinoco, A., Gonçalves, J., Silva, C., Loureiro, A., Gomes, A.C., Cavaco-Paulo, A. and Ribeiro A. (2018), "Keratin-Based Particles for Protection and Restoration of Hair Properties", *International Journal of Cosmetic Sciences*, 40(4), 408-419, https://doi.org/10.1111/ics.12483.

ACTIVE PRINCIPLES IN BASIL ESSENTIAL OIL – *Ocimum basilicum* L. COTTON LININGS WITH ANTIBACTERIAL PROPERTIES

MARIANA DANIELA BERECHET, DEMETRA SIMION, RODICA ROXANA CONSTANTINESCU, MARIA STANCA, COSMIN ANDREI ALEXE

The National Research & Development Institute for Textiles and Leather - Leather and Footwear Research Institute Division, Bucharest, 031215, Romania, marianadanielaberechet@yahoo.co.uk, demetra.simion@yahoo.com, rodica.roxana@yahoo.com, maria.stanca@icpi.ro; cosminandrei.alexe@yahoo.com

*Ocimum basilicu*m L. is an aromatic plant in the family *Lamiaceae* with bioactive properties used since ancient times in traditional medicine. The active ingredients of basil essential oil can be used in perfumes, pharmaceuticals, medicine, cosmetics or spices. In this study, the essential oil of basil was obtained by hydrodistillation in the Clevenger continuous extractor. It was characterized by GC-MS and 53 constituent compounds were identified. The majority compounds were highlighted: linalool, 64,569%, p-allyl anisol, 5,163%, Eucalyptol, 3,745%, α-Cadinene, 3,510%. Kovats indices were calculated and FT-IR analysis was performed to confirm the specific constituent compounds. The essential oil of basil was microbiologically analyzed against *Escherichia coli* (ATCC 10536) Gram-negative bacteria and against *Staphylococcus aureus* (ATCC 6538) Gram-positive bacteria by diffusometric working method. Antibacterial activity was determined by measuring the diameter of the inhibition zone around the samples. Samples of filter paper and cotton fabric were used to simulate shoe lining and bandages. Basil essential oil has resistance against the tested strains, observing the increase of the inhibition zone with the increase of the amount of essential oil used in treatments (20 µL, 30 µL, 50 µL). The results showed that *Ocimum basilicum* L. may be a good candidate as a plant-derived antibacterial agent for medical footwear, wound dressings and other medical applications.

Keywords: *Ocimum basilicum* L., bioactive compounds, antibacterial activity

INTRODUCTION

Natural products obtained from medicinal and aromatic plants have been widely consumed for centuries due to their therapeutic properties and aromaticity (Alsaraf *et al*., 2020). The need for medicinal and aromatic plants is in a growing demand for the active component principles that can be used in perfumes, pharmaceuticals, medicine, cosmetics or spices (Tursun, 2022). Basil (*Ocimum basilicum* L.) is considered one of the common aromatic plants with pharmacological properties such as antioxidant, chemo-preventive, anti-inflammatory, antimicrobial, immunomodulatory activity (Shalaby *et al*., 2020; Tursun, 2022, El-Nekeety *et al*., 2021), sedative and digestive due to the presence of specific compounds in the essential oil. It is also used as a toxin eliminator, to treat cough, colds, in the treatment of insomnia and constipation (Shalaby *et al*., 2020). Basil has effects on dermal pathology and in wound healing, including acne, eczema, boils, psoriasis and rashes (Tursun, 2022).

This work aims to highlight the composition of basil essential oil and the use of active principles in obtaining cotton linings with antibacterial properties.

EXPERIMENTAL

Materials

Cotton fabric has been used for impregnation with different concentrations of basil essential oil to simulate the lining of shoes or bandages. In the microbiological analyses, the filter paper was also used. Other chemical reagents were of analytical grade.

https://doi.org/10.24264/icams-2022.II.3

Extraction of Volatile Oil

The essential oil of basil was extracted from 100g of the shredded dried plant, in a balloon with a round bottom of 2L, in the ratio of 1:10 m / V (plant: distilled water), by continuous hydrodistillation in the Clevenger extractor, for 240 min. (Ilić *et al*., 2022). Approximately 0.7 mL of essential oil was obtained which was dried on sodium anhydrous sulphate to remove traces of water (Ilić *et al*., 2022).

ATR-FTIR Spectroscopy

ATR-FTIR analysis was performed with a FT-IR/ATR spectrometer-Jasco 4200 operating in the range of 4000 to 600cm^{-1}, with a spectral resolution of 0.5 cm^{-1}.

GC-MS Analysis

An Agilent 6890 N gas chromatograph was used to identify the compounds in the volatile oil. An Agilent 5958 C mass spectrometer was used as a detector to obtain the molecular weights of the compounds separated in the chromatograph. The Kovats retention indices have been calculated to confirm the identification of the constituent compounds in the essential oil of basil. For the calculation of kovats retention indices was used the standard mixture of alkanes - C8-C20 and the calculation formula (1):

$$K = 100 \bullet \left[n + \frac{(\log t_{Rx} - \log t_{Rn})}{(\log t_{Rn+1} - \log t_{Rn})} \right] \quad (1)$$

T_{Rx} = retention time of the compound to be analyzed;
T_{Rn} = the retention time of the alkane with n C atoms in the molecule of which the bit is placed to the left of the peak to be analyzed;
T_{Rn+1} = retention time of the alkane with n+1 carbon atoms placed to the right of the peak to be analyzed from the chromatogram.

Microbiological Analysis

The samples were tested on ATCC strains from the ICPI biotechnology laboratory collection, namely, on *Escherichia coli* (ATCC 10536) Gram-negative bacteria and *Staphylococcus aureus* (ATCC 6538) Gram-positive bacteria. The working method was diffusimetric. Antibacterial activity was determined by measuring the diameter of the zone of inhibition around the disc. Sample discs of filter paper and cotton (diameter 15mm) were treated with different amounts of basil essential oil: 20 µL, 30 µL and 50 µL, labeled as HFB20, HFB30, HFB50 and as BBCB20, BBCB30, BBCB50. Samples of filter paper and cotton without essential oil was used as a blank.

RESULTS AND DISCUSSIONS

Basil essential oil was obtained by hydrodistillation in Clevenger continuous extractor (El-Nekeety *et al*., 2021). Large variations in the content of essential oils in basil could be attributed to a number of factors, such as varied agroclimatic conditions, harvesting region, diversity of genotypes and basil population, harvest time, methods of drying and storage of basil after harvest (Ilić *et al*., 2022).

The ATR-FTIR spectrum showed in Figure 1 reveals the spectral bands at: 3410 cm^{-1} (O-H in alcohols), 2966 cm^{-1}, 2925 cm^{-1} (aliphatic C-H), 1708 cm^{-1}, 1639 cm^{-1}, 1511 cm^{-1}, 1451 cm^{-1}, 1411 cm^{-1} (C=C stretching vibration), 1375 cm^{-1} (isopropyl methyl group

https://doi.org/10.24264/icams-2022.II.3

symmetric bending vibration), 1246 cm^{-1} (C–O–C stretching), 1174 cm^{-1}, 1112 cm^{-1}, (CH_3 deformations), 1037 cm^{-1}, 994 cm^{-1} (para-substituted phenyl), 887 cm^{-1}, 834 cm^{-1} (C-H bend pattern), 767 cm^{-1}, (aromatic C-H out-of-plane bend) (Valderrama and Rojas De, 2017).

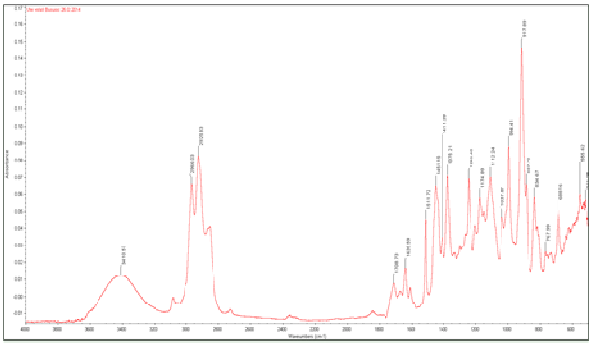

Figure 1. ATR-FTIR spectrum of *Ocimum basilicum* essential oil

By GC-MS analysis of basil essential oil, 53 different volatile organic compounds were identified (Table 1).

Table 1. Compounds identified in basil volatile oil

No.	Retention time, minutes	Name	Formula	Percentage of area, %	Kovats indices, K x10^3
1	7.251	Bicyclo[3.1.1]hept-2-ene, 2,6,6-trimethyl-,	$C_{10}H_{16}$	0.118	0.656
2	8.968	α-pinene	$C_{10}H_{16}$	0.222	0.698
3	9.877	Geranyl bromide	$C_{10}H_{17}Br$	0.190	0.718
4	11.379	Sylvestrene	$C_{10}H_{16}$	0.205	1.06
5	11.441	Eucalyptol	$C_{10}H_{18}O$	3.745	1.062
6	12.507	Ocimene	$C_{10}H_{16}$	0.214	1.086
7	13.537	Methyl 6-nonynoate	$C_{10}H_{16}O_2$	0.111	1.107
8	14.986	Linalol	$C_{10}H_{18}O$	64.569	1.134
9	15.144	3,7-Octadiene-2,6-diol, 2,6-dimethyl	$C_{10}H_{18}O_2$	1.442	1.504
10	16,697	Camphor	$C_{10}H_{16}O$	0.537	1.542
11	17.714	Isobornyl thiocyanoacetate	$C_{13}H_{19}NO_2S$	0.161	1.565
12	17.854	2-(4-Methylcyclohexylidene)-1-propanol	$C_{10}H_{18}O$	0.133	1.568
13	18.105	Carane	$C_{10}H_{18}$	0.130	1.574
14	18.239	5-Isopropyl-2-methylbicyclo[3.1.0]hexan-2-ol	$C_{10}H_{18}O$	0.171	1.576
15	18.815	α-Terpineol	$C_{10}H_{18}O$	1.112	1.589
16	19.165	Anisole, p-allyl	$C_{10}H_{12}O$	5.163	1,596
17	20.367	m-Toluic acid, 4-methylpentyl ester	$C_{14}H_{20}O_2$	0.151	1.968
18	21.331	Nerol	$C_{10}H_{18}O$	1.521	1.996
19	22.252	1,5,5-Trimethyl-6-methylene-1-cyclohexene	$C_{10}H_{16}$	0.412	2.022
20	24.487	Eugenol	$C_{10}H_{12}O_2$	0.689	2.34

https://doi.org/10.24264/icams-2022.II.3

No.	Retention time, minutes	Name	Formula	Percentage of area, %	Kovats indices, K x10^3
21	24.570	p-Cresol, 2-amino-6-tert-butyl-	$C_{11}H_{17}NO$	0.045	2.343
22	24.960	Copaene	$C_{15}H_{24}$	0.067	2.356
23	25.205	Methyl cinnamate	$C_{10}H_{10}O_2$	0.546	2.364
24	25.257	Caryophyllene oxide	$C_{15}H_{24}O$	0.229	2.366
25	25.364	Lanceol, cis	$C_{15}H_{24}O$	0.282	2.561
26	25.466	β-Elemene	$C_{15}H_{24}$	1.541	2.565
27	26.166	Alloaromadendren	$C_{15}H_{24}$	0.594	2.593
28	26.695	Bergamotene	$C_{15}H_{24}$	1.176	2.613[3]
29	27.102	α-Bisabolene	$C_{15}H_{24}$	0.483	2.629
30	27.365	bicyclosesquiphellandrene	$C_{15}H_{24}$	0.193	2.638
31	27.853	β-Cubebene	$C_{15}H_{24}$	0.697	2.656
32	27.971	α-Selinene	$C_{15}H_{24}$	0.432	2.661
33	28.262	δ-Elemene	$C_{15}H_{24}$	0.474	2.837
34	28.476	Alloaromadendrene oxide-(2)	$C_{15}H_{24}O$	0.245	2.846
35	28.524	δ-Guaiene	$C_{15}H_{24}$	0.890	2.848
36	28.727	τ-Cadinene	$C_{15}H_{24}$	0.719	2.856
37	28.989	δ-Cadinene	$C_{15}H_{24}$	0.301	2.867
38	30.019	Varidiflorene	$C_{15}H_{24}$	0.724	3.909
39	30.286	Spathulenol	$C_{15}H_{24}O$	0.911	2.92
40	30.413	τ -Himachalene	$C_{15}H_{24}$	0.460	2.925
41	31.048	3,7,11-Trimethyl-oxa-cyclotrideca-7,11-diene-2,4-dione	$C_{15}H_{22}O_3$	0.130	3.097
42	31.138	Cedren-13-ol, 8-	$C_{15}H_{24}O$	0.123	3.101
43	31.205	Cubenol	$C_{15}H_{26}O$	0.523	3.104
44	31.817	α-Cadinene	$C_{15}H_{24}$	3.510	3.131
45	31.941	Farnesyl bromide	$C_{15}H_{25}Br$	0.188	3.136
46	32.009	Phen-1,4-diol, 2,3-dimethyl-5-trifluoromethyl	$C_9H_9F_3O_2$	0.443	3.139
47	32.123	α-Guaiene	$C_{15}H_{24}$	0.763	3.144
48	32.331	7-Tetracyclo[6.2.1.0(3.8)0(3.9)]undecanol, 4,4,11,11-tetramethyl-	$C_{15}H_{24}O$	0.180	3.153
49	32.537	Spathulenol	$C_{15}H_{24}O$	0.311	3.162
50	33.358	6-Isopropenyl-4,8a-dimethyl-1,2,3,5,6,7,8,8a-octahydro-naphthalen-2-ol	$C_{15}H_{24}O$	0.175	3.328
51	33.547	α-Vatirenene	$C_{15}H_{22}$	0.143	3.337
52	33.638	Ledene oxide-(II)	$C_{15}H_{24}O$	0.336	3. 341
53	38.459	n-Hexadecanoic acid	$C_{16}H_{32}O_2$	0.089	3. 804

The majority compounds in the analyzed basil essential oil are linalool, 64.569%, p-allyl anisol, 5.163%, Eucalyptol, 3.745 and α-Cadinene, 3.510%. The essential oils from basil collected from different regions and in different periods have different compositions in percentages of majority compounds and identified compounds that give different

https://doi.org/10.24264/icams-2022.II.3

qualitative and quantitative bioproprieties. The main components of Serbian sweet basil essential oil were linalool (35.1 %), eugenol (20.7 %) and 1.8-cineol (9.9 %) (Ilić *et al*., 2022). Both essential oils had the main compound linalool that gives antimicrobial characteristics (Hussain *et al*., 2008) and insect-repellent properties, anti-inflammatory activity, antihyperlipidemic, antidepressant, neuroprotective and anticancer properties (Alsaraf *et al*., 2020), antiviral, antifungal (Tursun, 2022). Basil essential oils from European countries contain methyl chavicol and linalool. Methyl cinnamate is the main constituent of tropical basil, while Indian basil essential oil is characterized by a high percentage of methyl eugenol (Ilić *et al*., 2022). Microbiological analyses were done on filter paper and cotton fabric. In order to interpret the measurements, a classification of the samples was chosen, according to a scale used in similar studies, starting from the diameter of the inhibition zone.

$$H = \frac{D-d}{2} \quad (2)$$

H = the zone of inhibition, in millimeters;
D = total diameter of the disc and the inhibition zone, in millimeters;
d = disc diameter, in millimeters.

Table 2. Resistance against *Escherichia coli* of filter paper samples treated with *Ocimum basilicum* L. essential oil

Sample	Control	HFB20	HFB30	HFB50
Images		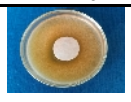	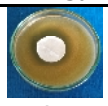	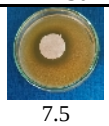
Inhibition zone (mm)	Contaminated	2.5	6.5	7.5

Table 3. Resistance against *Staphylococcus aureus* of filter paper samples treated with *Ocimum basilicum* L. essential oil

Sample	Control	HFB20	HFB30	HFB50
Images	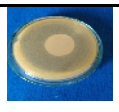	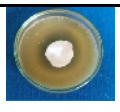	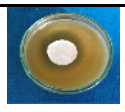	
Inhibition zone (mm)	Contaminated	6.5	11.5	12.5

Table 4. Resistance against *Escherichia coli* of cotton samples treated with *Ocimum basilicum* L. essential oil

Sample	Control	BBCB20	BBCB30	BBCB50
Images		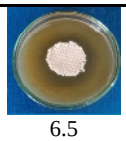	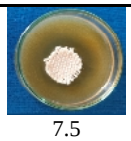	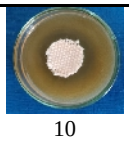
Inhibition zone (mm)	Contaminated	6.5	7.5	10

https://doi.org/10.24264/icams-2022.II.3

Table 5. Resistance against *Staphylococcus aureus* of cotton samples treated with *Ocimum basilicum* L. essential oil

Sample	Control	BBCB20	BBCB30	BBCB50
Images	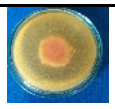	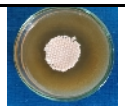	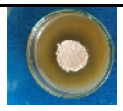	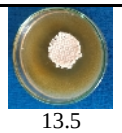
Inhibition zone (mm)	Contaminated	6.5	9.5	13.5

From the microbiological results obtained (Tables 2-5) it is observed that the zone of inhibition increases with the increase of the concentration of basil essential oil used in the treatment of samples. The inhibition zone obtained against *Staphylococcus aureus* samples is higher than in the case of samples against *Escherichia coli*.

CONCLUSION

Basil essential oil was obtained by hydrodistillation in continuous Clevenger extractor. By GC-MS analysis, 53 constituent compounds were identified and the Kovats indices were calculated. The majority compounds of linalool (64,569%), p-allyl anisol (5,163%), eucalyptol (3,745%), α-Cadinene (3,510%) were highlighted. Microbiological analysis showed that basil essential oil has resistance against *Escherichia coli* and against *Staphylococcus aureus* developing a higher inhibition zone with increased concentration of essential oil. The results obtained showed that *Ocimum basilicum* can be a good candidate as a plant-derived antibacterial agent for medical shoes, wound dressings and other medical applications. Basil essential oil has been used in traditional medicine and spices in various dishes since ancient times. Nowadays it is widely used in medical products, pharmaceuticals, cosmetics, perfumes.

Acknowledgements

The research was carried out under project PN 19 17 01 02/2022, CREATIV_PIEL, and 4PFE project, funded by Romanian Ministry of Education and Research.

REFERENCES

Alsaraf, S., Hadi, Z., Al-Lawati, W.M., Al Lawati, A.A. and Khan, S.A. (2020), "Chemical Composition, *in vitro* Antibacterial and Antioxidant Potential of Omani Thyme Essential Oil along with *in silico* Studies of Its Major Constituent", *Journal of King Saud University – Science*, 32(1), 1021–1028, https://doi.org/10.1016/j.jksus.2019.09.006.

El-Nekeety, A.A., Hassan, M.E., Hassan, R.R., Elshafey, O.I., Hamza, Z.K., Abdel-Aziem, S.H., Hassan, N.S. and Abdel-Wahhab, M.A. (2021), "Nanoencapsulation of Basil Essential Oil Alleviates the Oxidative Stress, Genotoxicity and DNA Damage in Rats Exposed to Biosynthesized Iron Nanoparticles", *Heliyon*, 7(7), e07537, https://doi.org/10.1016/j.heliyon.2021.e07537.

Hussain, A.I., Anwar, F., Sherazi, S.T.H. and Przybylski, R. (2008), "Chemical Composition, Antioxidant and Antimicrobial Activities of Basil (*Ocimum basilicum*) Essential Oils Depends on Seasonal Variations", *Food Chemistry*, 108(3), 986–995, https://doi.org/10.1016/j.foodchem.2007.12.010.

Ilić, Z.S., Milenković, L., Tmušić, N., Stanojević, L., Stanojević, J. and Cvetkovićb, D. (2022), "Essential Oils Content, Composition and Antioxidant Activity of Lemon Balm, Mint and Sweet Basil from Serbia", *LWT - Food Science and Technology*, 153, 1-12, 112210, https://doi.org/10.1016/j.lwt.2021.112210.

Shalaby, S.M., Darwesh, M., Ghoname, M.S., Salah, Sh.El., Nehela, Y. and Fetouh, M.I. (2020), "The Effect of Drying Sweet Basil in an Indirect Solar Dryer Integrated with Phase Change Material on Essential Oil Valuable Components", *Energy Reports*, 6(S9), 43–50, https://doi.org/10.1016/j.egyr.2020.10.035.

Tursun, A.O. (2022), "Impact of Soil Types on Chemical Composition of Essential Oil of Purple Basil", *Saudi Journal of Biological Sciences*, 29(7), 103314, https://doi.org/10.1016/j.sjbs.2022.103314.

Valderrama, A. and Rojas De, G. (2017), "Traceability of Active Compounds of Essential Oils in Antimicrobial Food Packaging Using a Chemometric Method by ATR-FTIR", *American Journal of Analytical Chemistry*, 8(11), 726-741, https://doi.org/10.4236/ajac.2017.811053.

THERMOSTABILITY STUDY OF NATURAL POLYMER MICROCAPSULES

CIPRIAN CHELARU, MARIA MINODORA MARIN, MĂDĂLINA IGNAT

The National Research & Development Institute for Textiles and Leather - Leather and Footwear Research Institute Division, Minulescu *Ion 93, Bucharest, Romania,*
cchelaru_cciprian@yahoo.com

Microcapsules represent a stand-alone system that has applicability in a multitude of fields. The raw materials for microcapsules are very varied and with different properties. In this paper, biodegradable raw materials from natural sources were used to create/develop microcapsules. The chemical-structural stability of microcapsules under working conditions is a factor that must be considered. The aims were to obtain microcapsules from the previously specified raw materials, to perform a microscopic characterization, to establish their dimensional profile as well as their thermal stability over a range of 25-100°C, in aqueous solution. The study of the thermal stability of microcapsules can provide information regarding the temperature of the environment in which they can be used, specifically, whether they can withstand in medical products, which are subjected to high thermal treatments (up to 100°C), at the same time being susceptible to degradation by chemical action, gradually releasing the active components they may contain.

Keywords: microcapsules, thermal stability, thermal treatments

INTRODUCTION

Microencapsulation is the technique by which a solid, liquid, or gaseous component is retained by a second compound to protect the active component from environmental actions (Gharsallaoui *et al*., 2007). The materials used to make the microcapsules are called coatings/membranes/walls. These materials can be part of a wide range of compounds such as polymers, sugars, proteins. Components contained in microcapsules are called "fillers" or "core". Encapsulation can be performed for pure compounds, mixtures or living organisms (Gharsallaoui *et al*., 2007; Dubey *et al*., 2009; Rowe *et al*., 2009). The microcapsules can have dimensions between 1 µm and 1000 µm, dimensions that depend on the obtaining method (Ghosh, 2006). Microcapsules obtained from natural polymers are in high demand because, due to the very nature of the raw materials, which are biodegradable, their decomposition does not produce toxic products. The structure of a microcapsule depends on the physico-chemical properties of the core, the composition of the wall and the technique used for microencapsulation. In this sense, the obtained particles can have a shape as close as possible to a sphere or with an irregular shape, with a single or multi-layer coating. At the same time, they can have multiple cores, which can be found either in the center of the microcapsule or in the shell. At the same time, a matrix structure of the microcapsule can be obtained, in which case the active substance is uniformly distributed in the structure of the microcapsule. The microcapsule aspect can be seen in Figure 1 (Bakry *et al*., 2016).

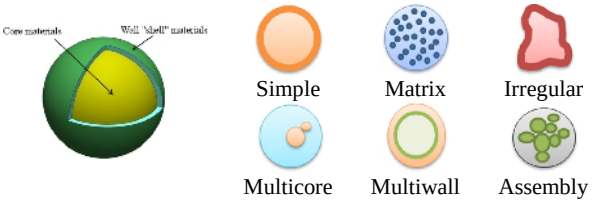

Figure 1. Microcapsule types

https://doi.org/10.24264/icams-2022.II.4

EXPERIMENTAL

Materials

Collagen hydrolysate (powder) – obtained by atomizing the collagen hydrolysate solution, obtained from bovine skin, within the Collagen department of The National Research & Development for Textiles and Leather – Leather and Footwear Research Institute Division.

Chitosan – purchased from Sigma-Aldrich, Germany. Chitosan is obtained from chitin by applying chemical or enzymatic treatments to the exoskeleton of crustaceans.

Sodium alginate – purchased from Sigma-Aldrich, Germany.

Acetic acid – purchased from Merck-Millipore, Germany.

Glutaraldehyde (25% aqueous solution) – purchased from Merk-Millipore, Germany, and was used as a crosslinking agent.

Equipment

Magnetic Stirrers with Hot Plates – with 50-300°C temperature interval.

Stereomicroscope – S8AP0 (Leica). Magnification is from 10x to 160x, it has incident and transmitted light and possibility to observe the samples with polarized light.

Micro-hot table (Caloris) – device that has the possibility to heat with a preset speed, allowing to visualize the sample behavior, from the upper part of the equipment, with the help of a stereomicroscope.

Zetasizer Micro ZS (Malvern) – particle size determination.

Hot plate

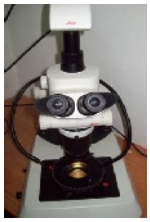

Optical stereomicroscope

Micro-hot table

Zetasizer Micro ZS

Figure 2. Equipment

https://doi.org/10.24264/icams-2022.II.4

RESULTS AND DISCUSSIONS

Because the raw materials used are part of the group of natural polymers, although they are soluble in water, for this study, 2% solutions were made for each individual polymer. The recipe for microcapsule is displayed in the Table 1.

Table 1. Microcapsule recipe

No.	Sample code	Collagen hydrolysate	Sodium alginate	Chitosan
1	MC-1	Yes	Yes	-
2	MC-2	Yes	-	Yes

In order to obtain the microcapsules, the following operations were performed:

- collagen hydrolysate solution was heated to temperature interval of 40-60°C and mixed at 1000 rpm;
- addition of the secondary polymer, while maintaining the mixing speed and temperature;
- decrease medium temperature below 10°C, followed by the pH correction, in the sense of establishing an acid environment;
- gradual addition of the crosslinking agent, with permanent monitoring of the reaction temperature;
- completing the crosslinking by keeping the mixing speed at a lower speed then initial, for 3 hours.
- increasing medium temperature up to 40-60°C interval with permanent mixing for 2 hours;
- washing the obtained microcapsules with water, to remove unreacted materials.

Based on the Table 1 recipe, a number of two liquid suspensions were obtained, based on the raw materials used – Figure 3.

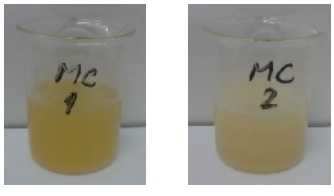

a) MC-1 b) MC-2

Figure 3. Obtained microcapsules

Optical microscopy test reveals the microcapsule spherical aspect for MC-1 (a) and MC-2 (b) – Figure 4.

https://doi.org/10.24264/icams-2022.II.4

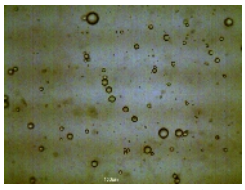
a) MC-1 (100x)

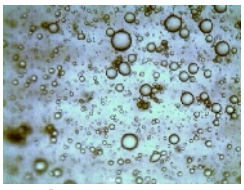
b) MC-2 (100x)

Figure 4. Optical microscopy for obtained microcapsules

Microcapsule size determination for MC-1 shows that the microcapsules have sizes between 0.6 and 63 µm diameter, the majority been of them having 20 µm diameter. Microcapsule size determination for MC-2 shows that the microcapsules have sizes between 0.6 and 1000 µm diameter, the majority been of them having 40 µm diameter. The microcapsules size shift can be explained due to variable mixing speed throughout the synthesis, a larger microcapsule size being the result of lower stirring speed. The microcapsule size profile can be seen in Figure 5.

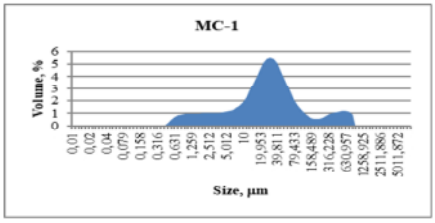

a) MC-1 Microcapsule

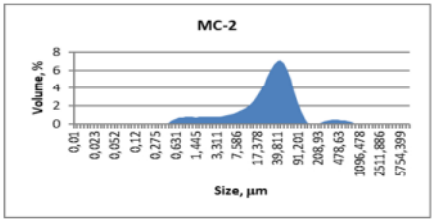

b) MC-2 Microcapsule

Figure 5. Microcapsule size profile

Thermostability of the microcapsules was performed with an equipment combination of micro-hot table and stereomicroscope. The set temperature range was 25°C-95°C with 2°C/min heating rate and 20x magnification.

The behavior of MC-1 and MC-2 microcapsules was observed in aqueous environment, at regular temperature intervals. Sequential images of MC-1 microcapsules during the analysis demonstrate that microcapsules do not undergo structural changes for the entire temperature interval – Figure 6, which indicates good stability at high temperatures. The sequential images for MC-2 microcapsules taken during the analysis demonstrate the fact that they undergo structural changes at a temperature of 40°C, which indicates that their stability is maintained only up to this temperature.

https://doi.org/10.24264/icams-2022.II.4

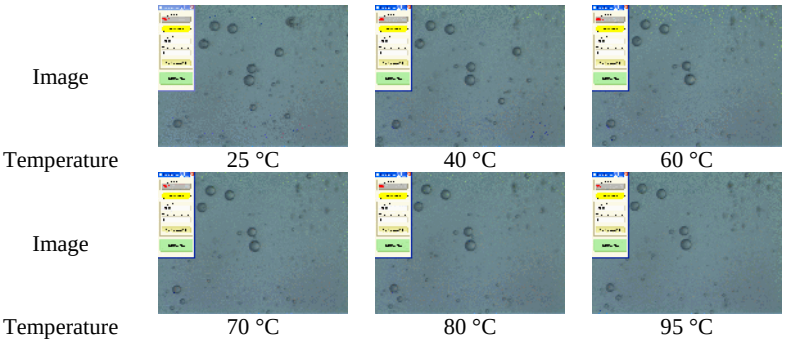

Figure 6. MC-1 microcapsules under thermal treatment, in aqueous medium

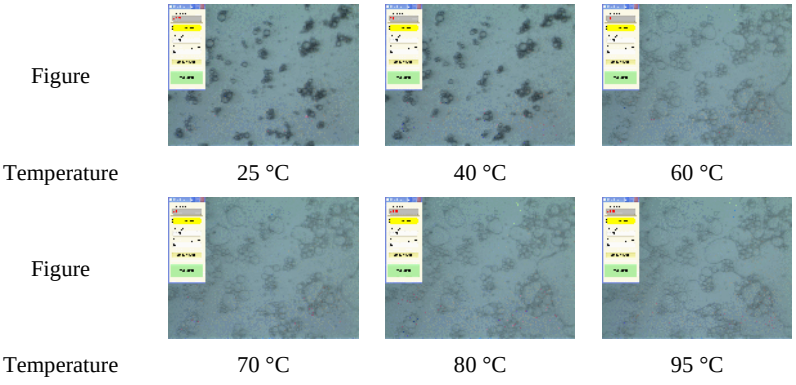

Figure 7. MC-2 microcapsules under thermal treatment, in aqueous medium

CONCLUSION

The optical microscopy for the obtained emulsions identified the presence of microcapsules. The size of the microcapsules is quite varied, also confirmed by the dimensional analysis graphs. Based on the profiles of the dimensional distribution of the microcapsules, it can be said that the obtained microcapsules are divided into two major areas, namely microcapsules with dimensions of 20 μm and 40 μm, respectively. At the same time, it is possible to identify the existence of microcapsules with dimensions between 0.5 and 10 μm as well as in the interval 40-90 μm and a small group around 200-1000 μm, due to the fluctuating stirring speed.

The thermal stability of the microcapsules up to 100°C (MC-1) indicates the possibility of using them in a wearable materials matrix that can be subjected to washing.

The thermal stability of the microcapsules up to 40°C (MC-2) can imply the use for controlled release of substances that they may contain.

https://doi.org/10.24264/icams-2022.II.4

Acknowledgements

This study was funded by the Ministry of Research and Innovation through the Program 1 - Development of the National R&D System, Subprogram 1.2 - Institutional Performance - RDI excellence funding projects, Contract no. 4PFE/30.12.2021: "INCDTP in the vanguard of excellence research" – TEX&PEL FOR FUTURE.

REFERENCES

Bakry, A.M., Abbas, S., Ali, B., Majeed, H., Abouelwafa, M.Y., Mousa, A. and Liang, L. (2016), "Microencapsulation of Oils: A Comprehensive Review of Benefits, Techniques, and Applications", *Comprehensive Reviews in Food Science and Food Safety*, 15(1), 143-182, https://doi.org/10.1111/1541-4337.12179.

Dubey, R., Shami, T.C. and Bhasker Rao, K.U. (2009), "Microencapsulation Technology and Applications", *Defence Science Journal*, 59(1), 82-95.

Gharsallaoui, A., Roudaut, G., Chambin, O., Voilley, A. and Saurel, R. (2007), "Applications of Spray-Drying in Microencapsulation of Food Ingredients: An Overview", *Food Research International*, 40(9), 1107–1121, https://doi.org/10.1016/j.foodres.2007.07.004.

Ghosh, S.K. (2006), *Functional Coatings: By Polymer Microencapsulation*, WILEY-VCH Verlag GmbH &Co. KGaA, Weinheim.

Rowe, R.C., Sheskey, P.J. and Quinn, M.E. (2009), *Handbook of Pharmaceutical Excipients*, 6th Edition, Pharmaceutical Pr, 11–12.

https://doi.org/10.24264/icams-2022.II.4

ECO-FRIENDLY BIODEGRADATION OF SKINS AND HIDES BY KERATINOLYTIC FUNGUS *Cladosporium* SP.

MARIANA CONSTANTIN[1], ROXANA RODICA CONSTANTINESCU [2]*, MIHAELA GANCIAROV[1], RALUCA SUICA-BUNGHEZ[1], ANA-MARIA GURBAN[1], CRISTINA FIRINCA[1], GELU VASILESCU[1], LUIZA JECU[1], IULIANA RAUT[1]*, MADALINA IGNAT[2]

[1]*National Institute for Research & Development in Chemistry and Petrochemistry (ICECHIM), Spl. Independentei 202, 060021 Bucharest, Romania iulia_rt@yahoo.com*

[2]*The National Research & Development for Textiles and Leather - Leather and Footwear Research Institute Division, 93 Ion Minulescu Str., 031215, Bucharest, Romania rodica.roxana@yahoo.com*

As a result of population growth and changes in lifestyles, livestock and meat production is increasing throughout the world. Therefore, a large amount of keratinaceous waste is generated annually from food and leather industry. The conventional method of hair removal in the leather industry through all the chemical processes used creates a great concern for the environment, being a major contributor to the production of waste water. The enzymatic process through microorganism is an eco-friendly option to reduce the oxygen demands in leather processing. In biodegradation and bioremediation processes, waste or polluting products found in different waste substrate can be transformed or converted into unpolluted end products. Our experiments are related to the biodegradative potential of fungi in reducing and reusing waste from the leather industry. The aim of the present study was to evidence the biodegradative ability of the fungal strain *Cladosporium* sp. on keratin wastes.

Keywords: biodegradation, keratinolytic fungi, leather industry

INTRODUCTION

Leather industry is one of the most polluting industries, harmful to the environment due to different dangerous chemicals that are used during the process (Awulachew, 2021; Silva, 2021). The produces high amount of dissolved and suspended organic and inorganic solids that are giving rise to high oxygen requirement. The presence of sulphide, ammonia and other volatile compounds are toxic to environment. At the same time, it also results in solid waste, including animal skin trims, animal hairs, flesh wastes, and keratin wastes, whose protein content is responsible for dangerous pollution problems to environment (Jaouadi *et al*., 2018; Călin *et al*., 2017). There are many countries where leather industry brings social and economic benefits in daily lives, but on the other hand, the industry has a negative impact on environment (Kanagaraj *et al*., 2015; Elhoul *et al*., 2020; Wu *et al.*, 2017). Accordingly, restricted environmental regulations have focused to develop an economic, social, and environmentally sustainable system, to manage, to minimize and finally to eliminate the hazardous chemicals.

Significant efforts were been made to develop sustainable alternatives, like, partially replacement of chemicals by biological and enzyme-based process, or combined technologies. Application of biotechnological methods has showed a reduction of environmental negative impact.

Our experiments represent an attempt to apply biotechnological methods in leather manufacture, and therefore, the present experimental study was dedicated to highlighting the biodegradative ability of the fungal strain *Cladosporium* sp. expressed against keratin wastes.

https://doi.org/10.24264/icams-2022.II.5

MATERIALS AND METHODS

Fungal Strain

The geophylic fungal strain *Cladosporium* sp. belonging to Microbial Collection of Microbiology Laboratory from INCDCP-ICECHIM was used in the experimental study. Prior to use the stock culture, *Cladosporium* sp. isolate was maintained at 4°C on potato-dextrose-agar medium (PDA, Scharlau) having the following composition (g/L): 4, peptone; 20, glucose; 15, agar; final pH = 5.6.

Keratin Substrates

Keratinous substrates used in the experiment were sheepskins and sheep leather, from the INCDTP - National Research & Development Institute for Textiles and Leather, Bucharest. All the samples of keratin substrate were sterilized, three times, at 121°C, 15 min.

Fungal Cultivation in Liquid Culture Media for Substrate Biodegradation

Cultivation in liquid culture medium was performed in Erlenmeyer flask, in mineral basal medium with the following composition (g/L): 0.1, CaCl2; 0.1, KH2PO4; 0.1, FeSO4 × 7H2O; 0.005, ZnSO4 × 7H2O; pH=7.5. The medium was autoclaved at 121°C, for 15 min. For the biodegradation ability test, an animal skin fragment (5x5 cm) was placed in culture medium. The flasks were incubated on rotary incubator Heidolph Unimax 1010, at 100 rpm and 28°C for 3 weeks. Control flasks used in tests were as follows: i) basal mineral medium with fungal strain; ii) basal mineral medium with keratin substrate and without fungal strain. After 3 weeks, the sheepskins and sheep leather were collected, dried in an oven at a temperature of 75°C for 48 hours, and examined. The degree of substrate biodegradation was evaluated with several methods, as follows: microscopic observations at light microscopy on Olympus BX51 and Scanning Electron Microscopy (SEM) on a FEI-QUANTA 200 microscope; FTIR (Fourier transform infrared spectroscopy) spectra recorded by using the FTIR Spectrum GX (Perkin Elmer), by ATR tehnique, 600 to 4000 cm^{-1}, with 32 scans.

RESULTS AND DISCUSSIONS

Following the contact between the keratin substrate and the fungal strain, several structural changes of the substrate were observed compared to the control specimens, like (Figure 1): loss of protein material, formation of mycelium networks around the substrate, exfoliation and partial destruction of the substrate (Figures 2-3).

https://doi.org/10.24264/icams-2022.II.5

Control – sheep skin sample

Sheep skin sample after incubation with *Cladosporium* sp.

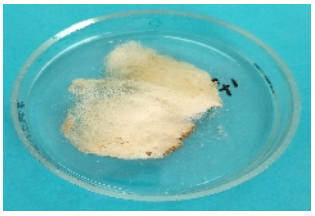

Control – sheep fur sample

Sheep fur sample after incubation with *Cladosporium* sp.

Figure 1. Samples after incubation in liquid culture medium with (right) or without fungal strains (left)

Microscopic images of the substrates incubated with the fungal strain are presented in Figure 2. It can be observed the formation of hyphae networks of *Cladosporium* sp. on the substrate surface, intertwining among the hair strands of sheep skin sample.

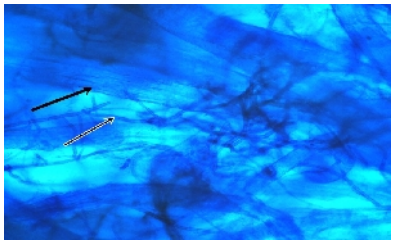

Sheep skin sample after incubation with *Cladosporium* sp. Formation of hyphae networks of *Cladosporium* sp. (white arrow) on the substrate surface (black arrow) (10x)

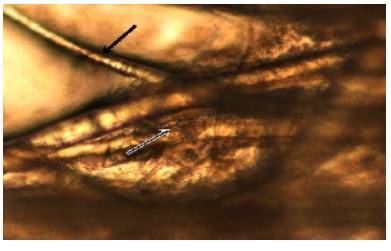

Sheep fur sample after incubation with *Cladosporium* sp. Hyphae (white arrow) intertwining among the hair strands of sheep skin sample (black arrow) (10x)

Figure 2. Microscopic images (SEM) of the substrates incubated with the fungal strain (lactophenol blue cotton staining)

The SEM analysis highlighted some structural changes in samples incubated with fungal strain as compared to control samples (Figure 2). A dense network of hyphae tightly adhered to the surface of the hair strand from the substrate, producing exfoliation and even destruction of the substrate.

https://doi.org/10.24264/icams-2022.II.5

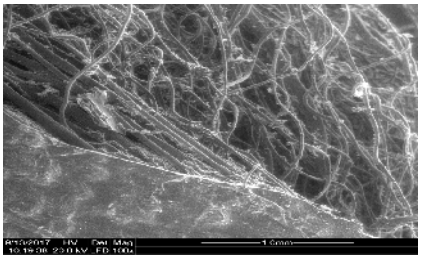

Control – sheep skin sample

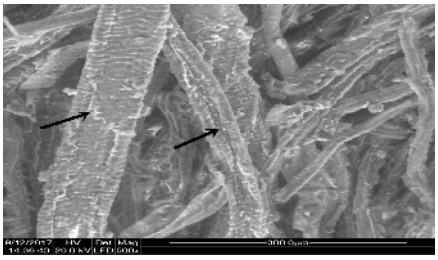

Sheep skin sample after incubation with *Cladosporium* sp. (hair strands and exfoliation breakage under the degradative action)

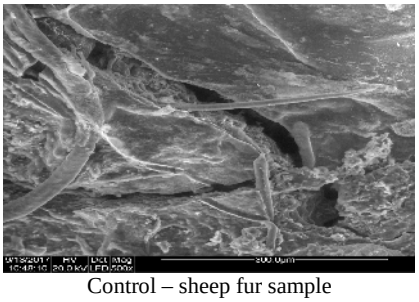

Control – sheep fur sample

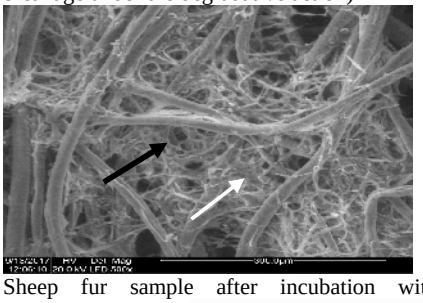

Sheep fur sample after incubation with *Cladosporium* sp. (dense network of hyphae (white arrow) tightly adhered to the surface of the hair strands from the substrate (black arrow)

Figure 3. SEM micrographs of the animal skins sample after incubation with *Cladosporium* sp.

FTIR results for sheep skin sample incubated with *Cladosporium* sp. strain are presented in Figure 4.

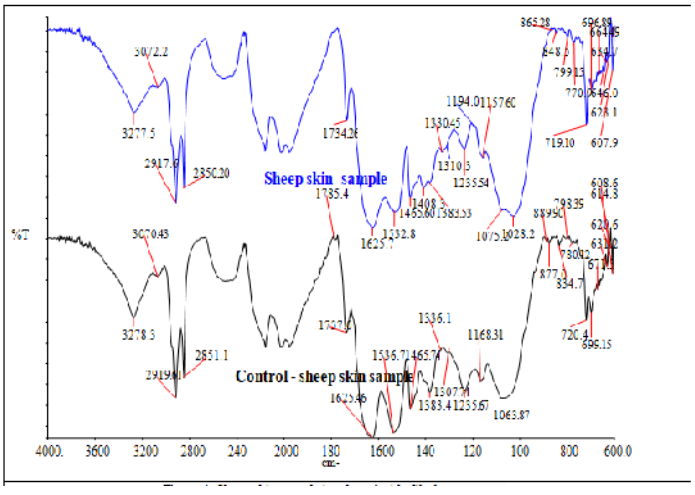

Figure 4. Sheep skin sample incubated with *Cladosporium* sp.

https://doi.org/10.24264/icams-2022.II.5

In FTIR spectra it can be observed the absorption bands at 3276 cm^{-1} and 3072 cm^{-1} which are assigned to the stretching vibrations of O-H and N-H. The strong absorption bands at 1626 and 1533 cm^{-1} are derived from the C=O stretching, N-H bending, and C-H stretching, respectively. The band at 1236 cm^{-1} resulted from the combination of C-N stretching and N-H in plane bending as well as some contribution from C-C stretching and C=O bending vibration (Ma *et al*., 2017).

During the degradation process, the C-S and S–S bonds were affected by the biodegradative activity of microorganism. The bands assigned to sulfide bonds S–S occured in the range 635–600 cm^{-1} and the bands assigned to C-S bonds occured in the range 670-646 cm^{-1}. As signs of degradation initiation can be considered the appearance of the bands at 1075–1028 cm^{-1} assigned to the sulfoxide bond (S-O), resulted form the breaking of disulfide S–S bonds. The presence of the oxide forms of sulfur is important for the oxidative process occurring as monoxide-to-dioxide, then proceeding to full oxidation with the formation of cysteic acid.

Figure 5 depicted FTIR results for sheep fur sample incubated with *Cladosporium* sp. strain.

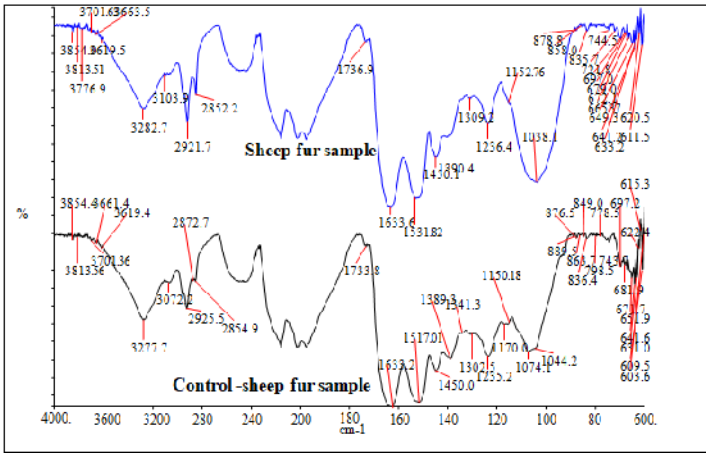

Figure 5. Sheep fur sample incubated with *Cladosporium* sp.

For the sheep fur sample, FTIR analysis shows significant change in amide region. The characteristic amide A band occurred at 3280–3270 cm^{-1}. Thus, amide I is related to C–O stretching and occurs at 1700–1600 cm^{-1}, while amide II is related to N-H bending and C–H stretching vibration and falls in 1540–1520 cm^{-1}. Amide III is related to a combination of C–N stretching and C–O bending vibration and occurs in the range 1300–1220 cm^{-1}. For the Ot2 sample, the amide I, II, and III bands were visible at 1634 cm^{-1}, 1532 cm^{-1}, and 1236 cm^{-1}, respectively in accordance with other reports on horsehair biodegradation.

In the sulphoxide region at 1074 cm^{-1}, the band corresponding to S-O bond was observed of medium intensity for undegraded sample (Ot, martor, reference), while for degraded sample (Ot2), this band disappeared and appeared as a large band and much intensive at 1038 cm^{-1}, corresponding also to S-O, due to S–S bond breaking (Kumar *et al.*, 2020).

https://doi.org/10.24264/icams-2022.II.5

In conclusion, FTIR spectra of samples incubated with fungal strain showed that C-S and S–S bonds were affected by fungal strain enzymes, indicating the progress of the degradative process.

CONCLUSIONS

Incubation of keratinolytic fungal strain with keratin substrates allowed to evidence significant aspects. Thus, microscopic examinations showed several changes, like, dense network of hyphae tightly adhered to the surface of the hair strand from the substrate, hair breakage under the degradative action, and the exfoliation and even substrate destruction. FTIR spectra showed the presence of bands assigned to the sulfoxide bond, resulted from the breaking of disulfide S–S bonds from keratin. The corroboration of microscopic observations with FTIR results proved that *Cladosporium* sp. had the ability to exert a biodegradative activity on keratin substrates and may play an important role in leather manufacture for removing hair from animal skins.

Acknowledgments

The authors thank the Ministry of Research, Innovation and Digitization of Romania through Program 1 - Development of the national research and development system, Subprogram 1.2 -Institutional performance- Projects to finance excellence in RDI, Contract no. 15PFE / 2021.

REFERENCES

Awulachew, M. (2021), "A Review of Pollution Prevention Technology in Leather Industry", *Environment Pollution and Climate Change*, 5(10), 244-250, https://doi.org/10.4172/2573-458X.1000244.

Călin, M., Constantinescu-Aruxandei, D., Alexandrescu, A., Răut, I., Doni, M.B., Arsene, M.L., Oancea, F., Jecu, L. and Lazăr, V. (2017), "Degradation of Keratin Substrates by Keratinolytic Fungi", *Electronic Journal of Biotechnology*, 28, 101–112, https://doi.org/10.1016/j.ejbt.2017.05.007.

Ben Elhoul, M., Jaouadi, N.Z., Bouacem, K., Allala, F., Rekik, H., Mechri, S., Ezzine, K.H., Miled, M. and Jaouadi, B. (2020), "Heterologous Expression and Purification of Keratinase from *Actinomadura viridilutea* DZ50: Feather Biodegradation and Animal Hide Dehairing Bioprocesses", *Environmental Science and Pollution Research*, 28, 9921–9934, https://doi.org/10.1007/s11356-020-11371-1.

Jaouadi, N.Z., Rekik, H., Badis, A., Trabelsi, S., Belhoul, M., Hila, C.G., Irmani, A., Kemir, H., Toumi, A., Bejar, S. and Jaouadi, B. (2018), "The Promising Keratin-Biodegradation and Hide-Dehairing Activities of the Keratinase KERUS from Brevibacillus Brevis Strain US575" in: Kallel, A., Ksibi, M., Ben Dhia, H., Khélifi, N. (eds.), *Recent Advances in Environmental Science from the Euro-Mediterranean and Surrounding Regions*, Advances in Science, Technology & Innovation Series, Springer, Cham., 133-135, https://doi.org/10.1007/978-3-319-70548-4_45.

Kanagaraj, J., Senthilvelan, T., Panda, R.C. and Kavitha, S. (2015), "Eco-friendly Waste Management Strategies for Greener Environment towards Sustainable Development in Leather Industry: A Comprehensive Review", *Journal of Cleaner Production*, 89, 1-17, https://doi.org/10.1016/j.jclepro.2014.11.013.

Kumar, J. and Yadav, R. (2020), "Keratinolysis of Chicken Feather and Human Hair by Nondermatophytic Keratinophilic Fungi Isolated from Soil", *Journal of Applied and Natural Sciences*, 12(4), 568–574, https://doi.org/10.31018/jans.v12i4.2398.

Ma, B., Sun, Q., Yang, J., Wizi, J., Hou, X. and Yang, Y. (2017), "Degradation and Regeneration of Feather Keratin in NMMO Solution", *Environmental Science* and *Pollution Research*, 24, 17711–17718, https://doi.org/10.1007/s11356-017-9410-x.

Silva, V.S.F.M. (2021), "Overview of the Leather Industry and Pollution Impact", *University of Porto Journal of Engineering*, 7(4), 1-15, https://doi.org/10.24840/2183-6493_007.004_0001.

Wu, J., Zhao L., Liu, X., Chen, W. and Gu, H. (2017), "Recent Progress in Cleaner Preservation of Hides and Skins", *Journal of Cleaner Production*, 148, 158-173, https://doi.org/10.1016/j.jclepro.2017.01.113.

ISOLATION AND CHARACTERIZATION OF BACTERIAL PROTEASE ENZYME OF LEATHER WASTE

RODICA ROXANA CONSTANTINESCU[1], MARIANA FERDES[2], MADALINA IGNAT[1], CIPRIAN CHELARU[1], ANA-MARIA CIOBANU[1], DENIS-ANDREI DRUSAN[1]

[1]*The National Research & Development Institute for Textiles and Leather - Leather and Footwear Research Institute Division, 93 Ion Minulescu Str., 031215, Bucharest, Romania, rodica.roxana@yahoo.com*

[2]*University Politehnica Bucharest, Romania, marianaferdes@yahoo.com*

The objectives of this study were to isolate and characterize bacteria which produced protease enzyme from tannery solid waste. A solid leather waste sample was used for bacterial isolation, taken from different waste warehouses (solid waste in unhairing phase). Several bacterial strains were isolated from the cultures in Petri dishes, after the growth of the colonies. These strains were characterized in terms of the production of proteolytic enzymes, by a method of screening on the media with casein, which allows the determination of proteolytic indices of microorganisms, the colony diameter, diameter of clear zone, proteolytic index, and enzymatic activities characterization on difference of pH and temperature.

Keywords: leather waste, enzymes, proteolytic bacteria

INTRODUCTION

The versatility and abundance of proteases are unmatchable and hence have drawn the attention of many researchers for use in various industrial processes (Naveed *et al*., 2021). The leather industry has started using proteases in various processes to combat pollution-related issues. Protease enzyme can be produced from animals, plants and microorganism products. When the enzyme derived from plant and animal products is used, it may have drawbacks (Thanikaivelan *et al*., 2004). This is because the plant tissues contain hazardous materials such as phenolic compounds. Protease enzymes used in the industry are generally produced from microorganisms (Baehaki *et al*., 2011). The use of microorganisms to produce the protease enzyme has several advantages. It can be easily produced on a large scale, it has relatively short production time, and it can be produced in a sustainable manner with a relatively low cost (Noble *et al*., 2009, Kanagaraj *et al*., 2015, Fernandez *et al*., 2019).

For a time, numerous natural enzymes have been attempted to investigate in leather processing to replace chemicals, although complete chemical substitution by enzymes has yet to be done (Calin *et al*., 2019). Degradation of unwanted protein by a simple eco-friendly and inexpensive method is one of the central requirements in several industries, especially the leather industry. Enzymes are employed as an auxiliary during liming to speed up the processing stages.

Proteases are fundamental industrial enzymes having wide applications in biochemical and chemical processes because they can break peptide bonds present in proteins. The major advantages of using proteases are specificity, biodegradability, the opportunity of producing natural products and activity under mild reaction conditions (Hamza *et al*., 2017).

Proteases are the most important extensively utilized enzymes for dehairing hides and skins. Some researchers have utilized them in rehydration, pickling, soaking, and chrome tanning (Nyakundi *et al*., 2021). Proteases differ in terms of substrate selectivity, working pH, catalytic activity, working temperature, active site specificity,

https://doi.org/10.24264/icams-2022.II.6

stability profiles, and other characteristics (Kumar *et al*., 1999). There are 259 different families of proteolytic enzymes that have been indexed in the MEROPS peptidase database so far, grouped according to amino acid sequence similarity. It is known that proteases from microbial sources account for around 40–60% of the total global enzyme sales (Kumar *et al*., 2020).

Recently, several proteolytic bacteria of the genus *Bacillus* have been tested for waste treatment in the leather industry, due to their properties for the synthesis of hydrolytic enzymes, especially collagenases and keratinases, as well as resistance to environmental factors (Li *et al*., 2021; Ferdes *et al*., 2020)

The objectives of this study were to isolate and characterise the bacteria producing protease enzyme from solid waste of tannery.

The protease is characterized for enzymatic activities. Results of this study are proposed as an alternate source of protease enzyme contributing to the tanning industry, especially in the unhairing phase (Zouboulis *et al*., 2004; Ferdes *et al*., 2020).

MATERIALS AND METHODS

The studied samples were mainly protein waste from different phases of leather processing in tanneries. In order to determine the pH value of the samples, fragments of 1 cm^2 were taken from each protein waste, which were suspended in Erlenmeyer flasks with 25 ml physiological serum. Also, sample specimens with the same surface area were suspended in Erlenmeyer flasks with 25 ml nutrient broth and incubated at 28°C for 72 hours. The resulting culture liquids were used to make serial decimal dilutions. These were seeded by embedding in Petri plates with nutrient agar, in three repetitions, in order to obtain isolated colonies and determine the number of viable cells. The plates were incubated for 24 hours in a bacteriological thermostat, at 28°C and then the number of isolated colonies was estimated by calculating the average of the values obtained in the three repetitions performed for each dilution. In order to obtain pure cultures, the isolated colonies were transplanted onto tubes with the solidified nutrient medium, which were incubated for 24 hours. After this interval, the bacterial strains were examined in terms of colonial morphological characteristics, Gram staining, the presence of endospores, the ability to hydrolyze proteins. The study of the morphological characteristics of the isolated microorganisms was carried out by optical microscopy observations on smears stained by the Gram staining method, which were examined under a microscope with a 100x immersion objective.

The proteolytic activity of isolated microorganisms was determined by a semi-quantitative screening method in Petri dishes, on an agar medium containing 0.25% casein as sole carbon source. Due to the hydrolysis of casein (which causes opacification of the agar medium), a transparent area appears around the colonies producing proteolytic enzymes.

After the development of the colonies (3 days for bacteria) the diameters of the colonies and of the hydrolysis zone were measured. The proteolytic index was determined as the ratio between the 2 diameters:

$$I_P = \frac{Diameter\ of\ hydrolysis\ zone}{Diameter\ of\ colony} \quad (1)$$

https://doi.org/10.24264/icams-2022.II.6

RESULTS AND DISCUSSION

The determination of the pH value highlighted the pH change of the physiological serum after the immersion of the leather samples, from pH 6.4 to values between 6.6-8.6.

The calculation of the number of viable cells obtained on plates with agar nutrient medium led to values between $2 \cdot 10^7$ in the case of skin samples P_1 and P_2, and $4 \cdot 10^7$ in sample P_3 while, sample P_4 presented a relatively lower number of bacterial cells - $2 \cdot 10^5$ / cm^2 (Table 1).

Table 1. Determining the number of cells obtained on plates with agar nutrient medium

No.	Sample	pH	Number of bacteria / cm^2 sample	Number of isolated strains
1.	P 1	6.82	$2 \cdot 10^7$	12
2.	P 2	6.80	$2 \cdot 10^7$	9
3.	P 3	6.66	$4 \cdot 10^7$	8
4.	P 4	8.69	$2 \cdot 10^5$	11

From the four samples analysed, a total number of 40 bacterial strains were isolated using the method of serial decimal dilutions, which were seeded on nutrient agar. Among the strains, the majority presented white-beige colonies, with a matte, rough surface and irregular edges. In the case of sample P_3, the strains that formed spherical, white colonies on nutrient agar predominated, with a smooth surface and whole edges. Strains $P_{4/10}$ and $P_{4/11}$ were differentiated by the color and appearance of the colonies formed, which were flat, semi-glossy, dark beige, with a smooth surface and whole edges.

Examination by optical microscopy of the smears stained by the Gram method enabled checking the purity of the cultures and highlighted the fact that most of the strains were represented by Gram-positive bacilli, with rounded ends, arranged in short chains of 2-4 cells or in irregular agglomerations.

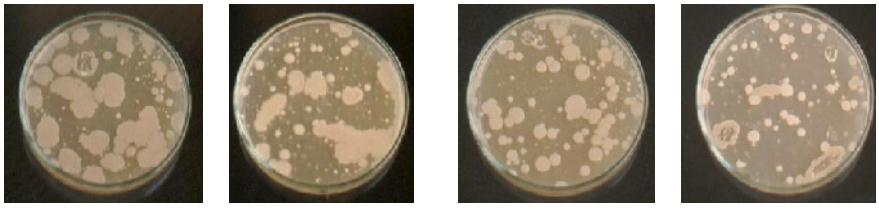

P1 P2 P3 P4

Figure 1. Isolation results of tannery solid samples obtained from tanning industry

https://doi.org/10.24264/icams-2022.II.6

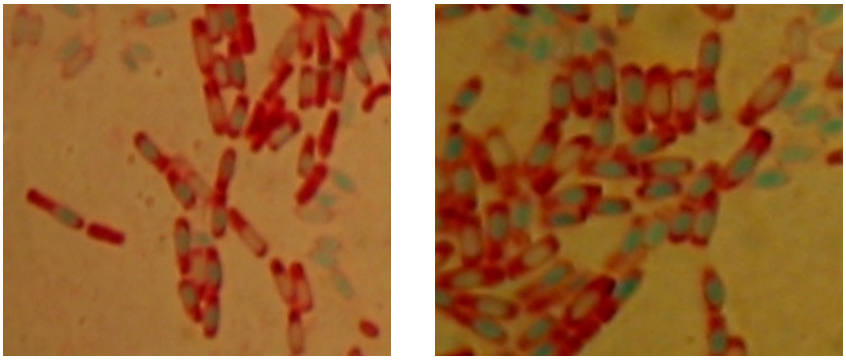

Figure 2. Microscopic highlighting of bacterial endospores in strains P 4/1 (left) and P 4/5 (right). Green spores are observed in the red vegetative cells

Gelatin hydrolysis testing highlighted the fact that out of the 40 isolated strains, 38 determined the complete liquefaction of the culture medium, while two strains P 4/10 and P 4/11 (isolated from sample P 4) did not present the ability to hydrolyze gelatin.

Testing the casein hydrolysis capacity led to similar results in the case of both experimental variants. Thus, all the strains tested determined the hydrolysis of the substrate and the clarification of the culture medium around the areas of bacterial growth. The determination of the hydrolysis zone size led to the observation of some differences between the tested microorganisms so that, in 17 strains (42%) the diameter of the hydrolysis zone was between 6-12 mm, while 23 strains (58%) showed superior activity of casein hydrolysis, the diameter of the clear zone exceeding 12 mm (Fig. 3).

Figure 3. Testing the ability of the isolated strains to hydrolyze the casein present in the sample plate (left) compared to the control plate (right)

CONCLUSION

The microbiological analysis of leather waste samples revealed the presence of bacteria and the density of bacteria developed on the leather samples was estimated at $2 \cdot 10^7$ cells/cm^2 in the case of samples P 1 – P 3 and $2 \cdot 10^5$ cells/cm^2 in the case of P 4.

https://doi.org/10.24264/icams-2022.II.6

The vast majority of isolated colonies have a morphology characteristic of *Bacillus* species, with irregular, flat "R"-type shapes. This suggests specific colonization and restricted species diversity. Microscopic observations revealed the presence of bacillary, sporulated, Gram-positive cell forms.

Following the isolation work in pure cultures, 40 strains of bacteria were obtained which constitute a first collection of bacteria that contaminate the skin samples. The proteolytic capacity of the tested strains was highlighted by the gelatine and casein hydrolysis test.

Acknowledgement

This study was funded by the Ministry of Research and Innovation through the Program 1 - Development of the National R&D System, Subprogram 1.2 - Institutional Performance - RDI excellence funding projects, Contract no. 4PFE/30.12.2021: "INCDTP in the Vanguard of Excellence Research" – TEX&PEL FOR FUTURE.

REFERENCES

Baehaki, A., Rinto, D. and Budiman, A. (2011), "Isolation and Characterization of Proteases from Indralaya Soil Swamp Bacteria, Soulth", *Sumatera Journal Teknolgi dan Industri Pangan*, 22, 10-16.

Calin, M., Raut, I., Doni, M., Alexandrescu, E., Macovescu, G., Arsene, M.L., Gurban, A.M., Vasilescu, G. and Jecu, L. (2019), "The Potential of Keratinolytic Fungi for Biotechnological Applications in Leather Manufacture", *Revista de Chimie*, 70(9), 3152-3157, https://doi.org/10.37358/RC.19.9.7506.

Fernandez, M., Pereira, P.P., Agostini, E. and González, P.S. (2019), "How the Bacterial Community of a Tannery Effluent Responds to Bioaugmentation with the Consortium SFC 500-1. Impact of Environmental Variables", *Journal of Environmental Management*, 247, 46–56, https://doi.org/10.1016/j.jenvman.2019.06.055.

Ferdeş, M., Dincă, M.N., Moiceanu, G., Zabava, B.S. and Paraschiv, G. (2020), "Microorganisms and Enzymes Used in the Biological Pretreatment of the Substrate to Enhance Biogas Production: A Review", *Sustainability (Switzerland)*, 12(17), 7205-7230, https://doi.org/10.3390/su12177205.

Ferdeş, M. and Constantinescu, R.R. (2020), "Isolation and Characterization of Fungal and Bacterial Proteolytic Strains from Chrome Shavings", *Proceedings of the 8th International Conference on Advanced Materials and Systems*, Certex, Bucharest, 57-162, https://doi.org/10.24264/icams-2020.II.9.

Hamza, T.A. (2017), "Bacterial Protease Enzyme: Safe and Good Alternative for Industrial and Commercial Use", *International Journal of Chemical and Biomolecular Science*, 3(1), 1-10.

Kanagaraj, J., Senthilvelan, T., Panda, R.C. and Kavitha, S. (2015), "Eco-friendly Waste Management Strategies for Greener Environment Towards Sustainable Development in Leather Industry: A Comprehensive Review", *Journal of Cleaner Production*, 89, 1-17, https://doi.org/10.1016/j.jclepro.2014.11.013.

Kumar, M. (2020), "Industrial Applications of Protease: A Review", *Journal of Natural Remedies*, 20(4), 1-6

Kumar, D. and Takagi, H. (1999), "Microbial Alkaline Proteases: from a Bioindustrial Viewpoint", *Biotechnology Advances*, 17, 561-594, https://doi.org/10.1016/S0734-9750(99)00027-0.

Li, X., Zhang, Q., Gan, L., Jiang, G., Tian, Y. and Shi, B. (2021), "Exoproduction and Biochemical Characterization of a Novel Thermophilic Serine Protease from *Ornithinibacillus caprae* L9T with Hide-Dehairing Activity", https://doi.org/10.21203/rs.3.rs-573853/v1.

Naveed, M., Nadeem, F., Mehmod, T., Bilal, M., Anwar, Z. and Amjad, F. (2021), "Protease—A Versatile and Ecofriendly Biocatalyst with Multi-Industrial Applications: An Updated Review", *Catalysis Letters*, 151, 307-323, https://doi.org/10.1007/s10562-020-03316-7.

Nyakundi, J.O., Ombui, J.N. and Mulaa, F.J. (2021), "Evaluation of the *Bacillus cereus* Strain 1-p Protease for the Unhairing of Goatskins During Leather Production", *Textile & Leather Review*, 4(1), 38–54, https://doi.org/10.31881/TLR.2020.18.

Noble, J.E. and. Bailey, M.J.A. (2009), "Quantitation of Protein", *Methods Enzymology*, 463, 73-95, https://doi.org/10.1016/s0076-6879(09)63008-1.

Maitig, A.M.A., Alhoot, M.A. and Tiwari, K. (2018), "Isolation and Screening of Extracellular Protease Enzyme from Fungal Isolates of Soil". *Journal of Pure and Applied Microbiology*, 12(4), 2059–2067, https://doi.org/10.22207/JPAM.12.4.42.

Thanikaivelan, P., Rao, J.R., Nair, B.U. and Ramasami, T. (2004), "Progress and Recent Trends in Biotechnological Methods for Leather Processing", *Trends in Biotechnology*, 22(4), 181–188, https://doi.org/10.1016/j.tibtech.2004.02.008.

Zouboulis, A.I., Loukidou, M.X. and Matis, K.A. (2004), "Biosorption of Toxic Metals from Aqueous Solutions by Bacteria Strains Isolated from Metal-Polluted Soils", *Process Biochemistry*, 39(8), 909–916, https://doi.org/10.1016/S0032-9592(03)00200-0.

https://doi.org/10.24264/icams-2022.II.6

COMPARISON OF AERIAL PARTS ESSENTIAL OILS OF PURPLE AND WHITE FLOWERED *Vitex agnus-castus* (LAMIACEAE) POPULATIONS

YELDA GÜZEL[1], DURMUŞ ALPASLAN KAYA[2]*, MUSA TÜRKMEN[2]

[1]*Mustafa Kemal University, Faculty of Arts and Sciences, Biology Department, Hatay, 31034, Türkiye, email: yeldaguzel@gmail.com*

[2]*Mustafa Kemal University, Agriculture Faculty, Field Crops Department, 31034, Hatay, Türkiye, e-mail: dkaya@mku.edu.tr; musaturkmen@mku.edu.tr.*

Essential oils obtained by hydrodistillation of purple and white flowered *Vitex agnus-castus* (Lamiaceae) from Hatay (Türkiye), were analyzed by GC/MS. The total ratio of 53 components in *Vitex agnus-castus* volatile components with purple flowers is 99.87%. This ratio is seen as 43 components and 98.86% in white-flowered *Vitex agnus-castus*. Eucalyptol, sabinene, α-pinene, α-terpinyl acetate and trans-caryophyllene were identified as the main components of the essential oils of *Vitex agnus-castus* with purple and white flowers. In the essential oils of purple flowering *Vitex agnus-castus*, the highest component was determined as eucalyptol with a rate of 15.41%, followed by nerolidol with 12.76%, caryophyllene oxide with 12.43% and sabinene with 9.4%. When the essential oils of white-flowered *Vitex agnus-castus* were examined, the rate of eucalyptol was determined as 21.62%. Sabinene ratio was determined as 17.6%, followed by 10.76% α-pinene and 5.69% α-terpinyl acetate, respectively.

Keywords: essential oil, GC-MS, *Vitex agnus-castus*

INTRODUCTION

Vitex agnus-castus, the fruits of which are used for gynecological disorders such as menstrual pain, irregularity and premenstrual symptoms (pms), especially proven pharmacological activity against premenstrual mastalgia (mastodynia) (Jarry *et al.*, 1991; Wuttke *et al*., 1997; Jarry *et al*., 1999) is a widely used medicinal plant. While it was in the Verbenaceae family in the past, it has been included in the Lamiaceae family as a result of molecular analyzes in recent years (Güner *et al*., 2012).

There are purple-flowered (fig. 1) or white-flowered populations of the plant. White-flowered populations have occasionally been evaluated as varieties or forms, in separate taxonomic categories, such as: *Vitex agnus-castus* var. *alba* Weston, *Vitex agnus-castus* f. *albiflora* Moldenke (IPNI, 2022; WFO, 2022). Today, these populations are considered as intraspecific variation and do not need to be evaluated in a separate taxonomic category (WFO, 2022). However, there are studies showing that populations with different flower colors have different compositions of fruit essential oils, and populations with white flowers have higher monoterpene content (Sanatore *et al.*, 2003). 1,8-cineole and sabinene are the main monoterpene compounds and beta-caryophyllene is the main sesquiterpene compound of the fruit essential oils and sabinene, 1,8-cineole, trans-beta-farnesene, α-pinene, trans-β-caryophyllene and limonene are the main compounds of the leave essential oils of *Vitex agnus-castus* (Sanatore *et al.*, 2003; Stojković *et al.*, 2011; Khalilzadeh *et al.*, 2015). Studies on the essential oils of the plant are generally about fruit essential oils, as its fruits are used more for medicinal purposes. However, aerial parts in and around Hatay are also widely used for medicinal purposes such as menstrual pains, depilatory-weakening the hair, and care is taken for flower color in these uses, and it is stated that purple-flowered plants are more effective (Guzel *et al.*, 2015). Although there is a study comparing fruit essential oils of populations with different colors, there is no study comparing aerial parts.

https://doi.org/10.24264/icams-2022.II.7

Therefore, the aim of this study was to determine and compare the essential oil compositions of *Vitex agnus-castus* populations with white and purple flowers.

Figure 1. Aerial parts of the *Vitex agnus-castus*

EXPERIMENTAL

Plant Material

The plant materials were collected from their natural habitats and identified by Yelda Güzel. Purple flowering plants from Serinyol-Yıldırım Valley-Hatay-Türkiye, white-flowered plants from Harbiye-Döver Valey-Hatay-Türkiye. Vouchers from the plants numbered Y. Güzel-3137 and Y. Güzel-3138 were stored in the herbarium of the Hatay Mustafa Kemal University, Biology Department.

Essential Oil Isolation

The essential oil was obtained from dried leaves. A total of 50 g of the ground plant samples was used for hydrodistillation experiment. A sample weight was individually and carefully placed into a 2000 mL flask. Distilled water was added until it covered the sample completely. Essential oils were obtained by hydrodistillation method which was carried out in an all-glass Clevenger-type distillation. The essential oil ratio was calculated according to dry weight of plant materials and amount of essential oils obtained. The obtained essential oil samples were dried over anhydrous sodium sulfate and stored in amber vials at +4 .

https://doi.org/10.24264/icams-2022.II.7

GC-MS Analysis of the Essential Oils

Analysis of the essential oil was carried out using a Thermo Scientific Focus gas chromatograph equipped with MS, auto sampler, and TR-5MS (5% phenyl polysilphenylene-siloxane, 0.25 mm i.d. x 60 m length, film thickness 0.25 µm). The carrier gas was helium (99.9%) at a flow rate of 1 mL/min; ionization energy 70 eV. Mass range m/z 50–650 amu. Data acquired at scan mode. MS transfer line temperature 250°C; MS ionization source temperature 220°C, injection port temperature 220°C. The samples were injected with a 250 split ratio. The injection volume was 1 µL. Oven temperature was programmed from 50°C to 220°C at 3°C/min. The structure of each compound was identified by comparison of their mass spectrum with the Wiley Registry, 9th edition. Data acquisition used the Xcalibur software program.

RESULTS AND DISCUSSION

When the essential oil contents obtained from the purple flowering *Vitex agnus* plant were examined, the main components were determined as eucalyptol, nerolidol, caryophyllene oxide and sabinene, respectively. The highest component was determined as eucalyptol with a rate of 15.41%, followed by nerolidol with 12.76%, caryophyllene oxide with 12.43% and sabinene with 9.4%. In the essential oil components of *Vitex agnus-castus* with white flowers, the main components were determined as eucalyptol, sabinene, α-pinene and α-terpinyl acetate. When the components were examined, the rate of eucalyptol was determined as 21.62%. Sabinene ratio was determined as 17.6%, followed by 10.76% α-pinene and 5.69% α-terpinyl acetate, respectively. In previous study, showing that populations with different flower colors have different compositions of fruit essential oils, and populations with white flowers have higher monoterpene content (Sanatore *et al*., 2003). 1,8-cineole and sabinene are the main monoterpene compounds and β-caryophyllene is the main sesquiterpene compound of the fruit essential oils and sabinene, 1,8-cineole, trans-β-farnesene, α-pinene, trans-β-caryophyllene and limonene are the main compounds of the leave essential oils of *Vitex agnus-castus* (Sanatore *et al.,* 2003; Stojković *et al.,* 2011; Khalilzadeh *et al.,* 2015).

https://doi.org/10.24264/icams-2022.II.7

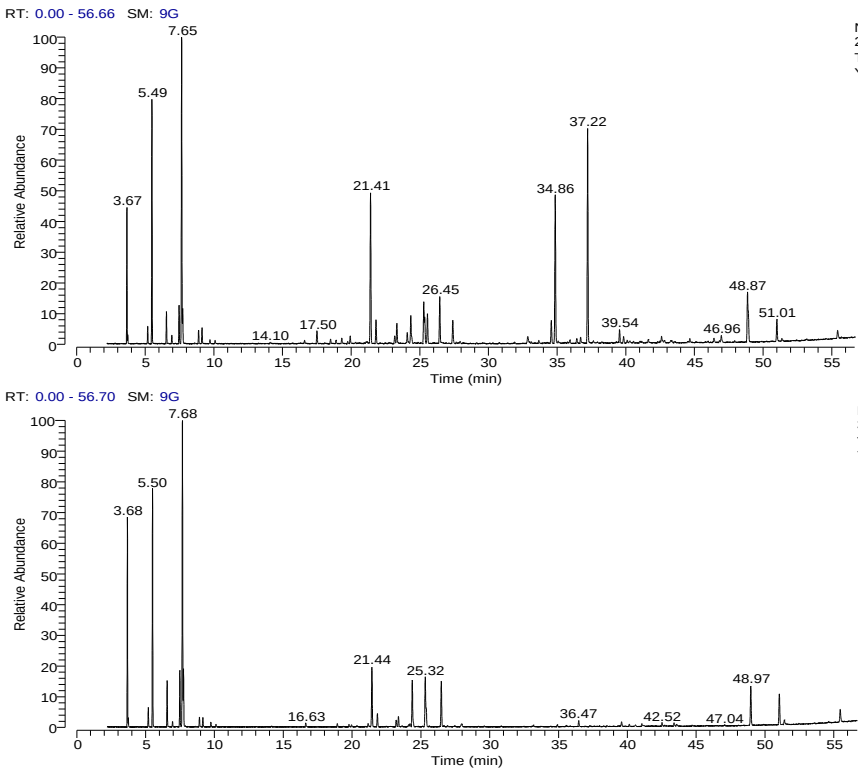

Figure 2. Essential oil chromatograms obtained from purple (above) and white (below) flowered *Vitex agnus-castus*

Table 1. Comparison of essential oil components of purple and white flowered *Vitex agnus-castus*

RT	Compound Name	Purple	White
3.67	α-pinene	4.58	10.76
5.18	β-pinene	0.71	1.19
5.49	Sabinene	9.4	17.6
6.55	Myrcene	1.37	2.95
6.94	2-carene	0.38	0.38
7.47	Limonene	1.71	3.87
7.65	Eucalyptol	15.41	21.62
8.89	γ-terpinene	0.64	0.74
9.14	trans-β-Ocimene	0.73	0.69
9.72	m-cymene	0.23	0.38
10.09	α-terpinolene	0.2	0.23
16.61	cis-sabinene hydrate	0.21	0.48
18.5	β-bourbonene	0.28	nd
18.89	α-Gurjunene	0.22	0.3

https://doi.org/10.24264/icams-2022.II.7

RT	Compound Name	Purple	White
19.75	trans-sabinene hydrate	0.15	0.23
19.93	Linalool	0.45	0.22
21.16	α-bergamotene	nd	0.34
21.41	trans-caryophyllene	9.28	5.62
21.81	Terpinen-4-ol	1.43	1.22
23.17	Alloaromadendrene	0.48	0.66
23.33	Pulegone	1.26	0.94
24.08	Humulene	0.68	0.18
24.21	Citronellyl acetate		0.25
24.34	trans-β-farnesene	1.83	4.34
25.29	α-terpinyl acetate	2.39	5.69
25.35	α-terpineol	1.28	nd
25.56	Germacrene D	2.21	nd
26.45	Bicyclogermacrene	2.88	4.32
27.4	σ-Cadinene	1.54	nd
27.43	α-Copaene	nd	0.12
27.94	Citronellol	0.19	nd
27.95	β-famesene	nd	0.39
33.17	Palustrol	nd	0.18
33.66	Veridiflorol	0.21	nd
34.86	Caryophyllene oxide	12.43	0.46
35.07	exo-2-Hydroxycineole acetate;	0.13	nd
36.43	Ledol	0.35	0.81
36.71	1,2-dimethylcyclooctene	0.38	nd
37.22	Nerolidol	12.76	nd
37.64	Cubenol	0.14	nd
39.33	Tetrahydro-Ionone	nd	0.11
39.54	Spathulenol	0.87	0.6
39.84	Nerolidol-epoxyacetate	0.46	nd
40.11	Lanceol	0.19	nd
40.31	Ledene oxide	0.17	nd
41.01	α-cadinol	0.15	0.34
41.16	Alloaromadendrenoxide	0.14	nd
41.2	Ethyl linoleate	nd	0.15
41.64	Cedrenol	0.28	nd
42.61	Carvacrol	0.46	nd
42.82	Globulol	0.15	0.47
48.97	β-methylionone	4.68	3.85
51	Sclareol	1.47	3.58
55.43	Thunbergol	0.6	1.36

nd: not detected

CONCLUSIONS

In this study, it is seen that the essential oil components of purple and white flowered *Vitex agnus castus* are similar. However, although the components are similar, there are

https://doi.org/10.24264/icams-2022.II.7

great differences in the ratios of the components. This study is a pioneer in terms of breeding *Vitex agnus-castus* for producers, whichever component is needed.

REFERENCES

Güner, A., Aslan, S., Ekim, T., Vural, M. and Babaç, M.T. (2012), "Türkiye Bitkileri Listesi (Damarlı Bitkiler)", *Nezahat Gökyiğit Botanik Bahçesi ve Flora Araştırmaları Derneği Yayını*, İstanbul.

Güzel, Y., Güzelşemme, M. and Miski, M. (2015), "Ethnobotany of Medicinal Plants Used in Antakya: A Multicultural District in Hatay Province of Turkey", *Journal of Ethnopharmacology*, 174, 118-152, https://doi.org/10.1016/j.jep.2015.07.042.

Jarry, H., Leonhardt, S., Wuttke, W., Behr, B. and Gorkow, C. (1991), "*Agnus Castus* als Dopaminerges Wirkprinzip in Mastodynon N", *Zeitschrift für Phytotherapie*, 12, 77–82.

Jarry, H., Leonhardt, S., Wuttke, W., Spengler, B. and Christoffel, V. (1999), "Auf der Suche Nach Dopaminergen Substanzen in Agni-casti-fructus-Präparaten: Warum eigentlich" *Zeitschrift für Phytotherapie*, 20, 150–152.

Khalilzadeh, E., Saiah, G.V., Hasannejad, H., Ghaderi, A., Ghaderi, S., Hamidian, G. and Zangisheh, M. (2015), "Antinociceptive Effects, Acute Toxicity and Chemical Composition of *Vitex Agnus-Castus* Essential Oil", *Avicenna Journal of Phytomedicine*, 5(3), 218-230.

Senatore, F., Napolitano, F. and Dung, M.O. (2003), "Chemical Composition and Antibacterial Activity of Essential Oil from Fruits of *Vitex Agnus-Castus* L. (Verbenaceae) Growing in Turkey", *Journal of Essential Oil Bearing Plants*, 6(3), 185-190, https://doi.org/10.1080/0972-060X.2003.10643349.

Stojković, D., Soković, M., Glamočlija, J., Džamić, A., Ćirić, A., Ristić, M. and Grubišić, D. (2011), "Chemical Composition and Antimicrobial Activity of *Vitex Agnus-Castus* L. Fruits and Leaves Essential Oils", *Food Chemistry*, 128(4), 1017–1022, https://doi.org/10.1016/j.foodchem.2011.04.007.

Wuttke, W., Splitt, G., Gorkow, C. and Sieder, C. (1997), "Behandlung Zyklusabhängiger Brustschmerzen mit einem Agnus Castus-Haltigen Arzneimittel–Ergebnisse einer Randomisierten, Plazebokontrollierten Doppelblindstudie", *Geburtsh u Frauenheilk*, 57, 569–574, https://doi.org/10.1055/s-2007-1023139.

*** (2022), "*Vitex* L.", The World Flora Online (WFO), available at: http://www.worldfloraonline.org/taxon/wfo-4000040364, accessed on: 28 Sep 2022.

*** (2022), International Plant Names Index (IPNI), available at: http://www.ipni.org, The Royal Botanic Gardens, Kew, Harvard University Herbaria & Libraries and Australian National Botanic Gardens, accessed 22 September 2022.

https://doi.org/10.24264/icams-2022.II.7

ESSENTIAL OIL COMPOSITION OF *Teucrium montbretii* SUBSP. *montbretii* BENTH. (LAMIACEAE)

YELDA GÜZEL[1], DURMUŞ ALPASLAN KAYA[2], MUSA TÜRKMEN[2]

[1] *Mustafa Kemal University, Faculty of Arts and Sciences, Biology Department, Hatay, 31034, Türkiye, email: yeldaguzel@gmail.com*

[2] *Mustafa Kemal University, Agriculture Faculty, Field Crops Department, 31034, Hatay, Türkiye, e-mail: dkaya@mku.edu.tr; musaturkmen@mku.edu.tr*

Essential oils obtained by hydrodistillation of *Teucrium montbretii* subsp. *montbretii* Benth. (Lamiaceae) from Hatay (Turkey), were analyzed by GC/MS. Forty-four volatile components were identified in the oils, representing 98.12 % of the total oils. The sample was yielded 0.24% of yellowish oil (w/w), with a pleasant smell. The main essential oil compounds of the plant were trans-caryophyllene, germacrene-D and caryophyllene oxide, representing 66.7%. Trans-caryophyllene, which has the highest ratio (36.78%), also known as β-caryophyllene, is a component that is the main constituent of many plants included in the sesquiterpene chemical class. Second main component germacrene-D (19.87%) is also sesquiterpene and detected in the essential oil of many plants. α-Copaene, humulene, aromadendrene and globulol were the other components detected at ratio of 5.45%, 4.29%, 3.99% and 3.35%, representing 17.08%, respectively.

Keywords: essential oil, GC-MS, *Teucrium montbretii* subsp. *montbretii* Benth.

INTRODUCTION

Teucrium montbretii Benth. (Lamiaceae) with its 6 subspecies, is an Eastern Mediterranean species naturally distributed in Lebanon, Western Syria, Palestine, Türkiye's Mediterranean region and South Aegean Islands (Navarro, 2020; POWO, 2022). Its subspecies and distribution areas are as follows: *Teucrium montbretii* subsp. heliotropiifolium (Barbey) P.H. Davis endemic to the Kárpathos Island; *Teucrium montbretii* subsp. judaicum P.H. Davis, endemic to Israel; *Teucrium montbretii* subsp. libanoticum P.H. Davis, endemic to Lebanon; *Teucrium montbretii* subsp. montbretii Benth. have a narrow distribution between South Türkiye and North-West Syria; *Teucrium montbretii* subsp. pamphylicum P.H. Davis, endemic to Türkiye; *Teucrium montbretii* subsp. yildirimlii Dinç & Dogu, endemic to Türkiye.

Although it is not endemic to a country because it is found in both Türkiye and Syria, *Teucrium montbretii* subsp. *montbretii* Benth., is a taxon that can be considered as geographical endemic since it naturally found in a narrow region, around the Türkiye-Syria border, in characteristic, rocky habitats. Of these subspecies, only *Teucrium montbretii* ssp. *heliotropiifolium* (Martino *et al.*, 2010; Menichini *et al.*, 2009) and *T. montbretii* subsp. *pamphylicum* (Küçük *et al.*, 2016), investigated in terms of essential oil composition. There is no literature on essential oil compositions of other subspecies, including *Teucrium montbretii* subsp. *montbretii*. The only two studies on the phytochemical content of *Teucrium montbretii* subsp. *montbretii* is the study in which diterpenoids isolated from acetone extracts of aerial parts by column chromatography and determined by physical and spectroscopic (1H NMR, MS) analyses and by comparisons with authentic samples (mmp, TLC) (Bruno *et al.*, 1992; Aydoğan, 2019). As a result of this studies, neo-derodane diterpenoids such as 2-deoxychamaedroxide, teuflin, 6-ketoteuscordin, montanin C, 6-acetylteucjaponin B,

https://doi.org/10.24264/icams-2022.II.8

teucrin H2, 6β-hydroxyteuscordin, 2β-hydroxyteuscordinon, montanin D and teugin were detected in the subspecies.

In addition, Atay and Özdikmen (2022) reported that the first host record of *Chrysolina blanchei* (Fairmaire, 1865) (Chrysomelidae: Chrysomelinae) was made on *Teucrium montbretii* subsp *montbretii* from Hatay province on Türkiye.

This study will be the first publication on the essential oil content of the subspecies.

EXPERIMENTAL

Plant Material

Plant material (Figure 1) was collected from the natural habitat and identified by Dr. Yelda Güzel. Voucher specimen was deposited in the herbarium of HMKÜ Biology department. Collection details are as follows: *Teucrium montbretii* subsp. *montbretii*: Antakya, Habib-i Neccar Mountain, Demirkapı vicinity, rock crevices of the cliffs, 190 m elevation, 36°12′10″N 36°10′45″E, 29 v 2020, Y. Güzel-3134.

Figure 1. *Teucrium montbretii* subsp. *montbretii*. General appearance

https://doi.org/10.24264/icams-2022.II.8

Figure 1. *Teucrium montbretii* subsp. *montbretii*. detailed appearance

Essential Oil Isolation

The essential oil was obtained from dried leaves. A total of 50 g of the ground plant samples was used for hydrodistillation experiment. A sample weight was individually and carefully placed into a 2000 mL flask. Distilled water was added until it covered the sample completely. Essential oils were obtained by hydrodistillation method which was carried out in an all-glass Clevenger-type distillation. The essential oil ratio was calculated according to dry weight of plant materials and amount of essential oils obtained. The obtained essential oil samples were dried over anhydrous sodium sulfate and stored in amber vials at +4 .

https://doi.org/10.24264/icams-2022.II.8

GC-MS Analysis of the Essential Oils

Analysis of the essential oil was carried out using a Thermo Scientific Focus gas chromatograph equipped with MS, auto sampler, and TR-5MS (5% phenyl polysilphenylene-siloxane, 0.25 mm i.d. x 60 m length, film thickness 0.25 µm). The carrier gas was helium (99.9%) at a flow rate of 1 mL/min; ionization energy 70 eV. Mass range m/z 50–650 amu. Data acquired at scan mode. MS transfer line temperature 250°C; MS ionization source temperature 220°C, injection port temperature 220°C. The samples were injected with a 250 split ratio. The injection volume was 1 µL. Oven temperature was programmed from 50°C to 220°C at 3°C/min. The structure of each compound was identified by comparison of their mass spectrum with the Wiley Registry, 9th edition. Data acquisition used the Xcalibur software program. The retention indices (RIs) were calculated for all volatile constituents using a homologous series of n-alkane standard solutions C8–C20 (Fluka, product No. 04070) and C21–C40 (Fluka, product No. 04071).

RESULTS AND DISCUSSION

The sample was yielded 0.24% of yellowish oil (w/w), with a pleasant smell. A total of 44 essential oil components were identified from dried leaves of *Teucrium montbretii* subsp. *montbretii* Benth (Table 1). The main essential oil compounds of the plant were trans-caryophyllene, germacrene-D and caryophyllene oxide, representing 66.7%. Similar to the present study, in studies on essential oil components of some Teucrium species, trans-caryophyllene and germacrene-D were main components (Gagliano Candela *et al*., 2021; Hayta *et al*., 2017; Baser and Demirçakmak, 1997) and also addition to these components, caryophyllene oxide in the study of Çakir *et al.* (1998). Trans-caryophyllene, which has the highest ratio (36.78%), also known as β-caryophyllene, is a component that is the main constituent of many plants included in the sesquiterpene chemical class. It was reported that trans-caryophyllene has anti-inflammatory effects in many different models of inflammation (Fernandes *et al.*, 2007). In the same as trans-caryophyllene, second main component germacrene-D (19.87%) is also sesquiterpene and detected in the essential oil of many plants. Noge and Becerra (2009) determined that germacrene-D have inhibition effects to herbivores and act as repellent against aphids, ticks and mosquitoes. The third major constituent caryophyllene oxide, which belongs to sesquiterpene class of terpenoids was identified at a ratio of 10.07% as in Table 1. This component has a significant role in plant defense and serves as insecticidal and antifungal (Bettarini *et al.*, 1993). α-Copaene, humulene, aromadendrene and globulol were the other components detected at ratio of 5.45%, 4.29%, 3.99% and 3.35%, representing 17.08%, respectively. It should be noted that this is the first report on the essential oil composition of *Teucrium montbretii* subsp. *montbretii* Benth.

https://doi.org/10.24264/icams-2022.II.8

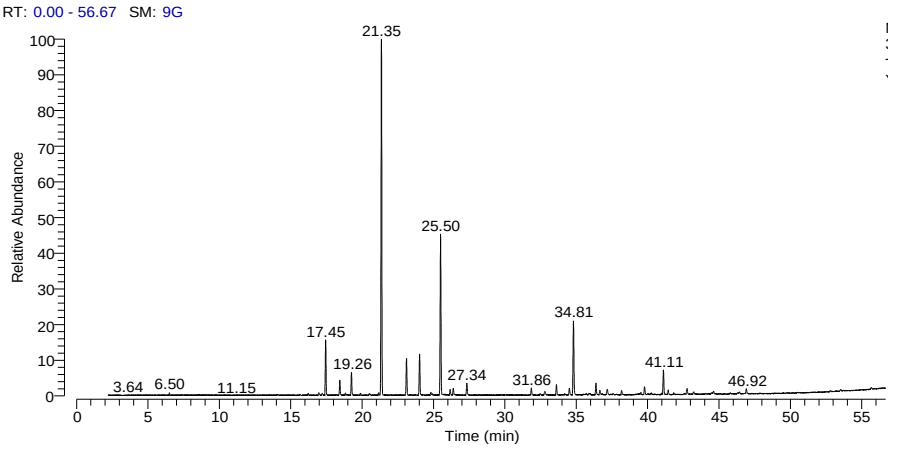

Figure 2. Essential oil chromatograms obtained from *Teucrium montbretii subsp. montbretii*

Table 1. Essential oil composition of *Teucrium montbretii* subsp. *montbretii* Benth.

RI	Compound Name	Area %
1170	Sabinene	0.19
1440	2-methyldecane	0.13
1456	α-Cubebene	0.20
1474	Cyclosativene	0.27
1480	α-amorphene	0.19
1486	α-copaene	5.45
1511	β-bourbonene	1.74
1522	α-gurjunene	0.27
1551	Linalool	0.20
1588	*trans*-caryophyllene	36.78
1635	Aromadendrene	3.99
1660	Humulene	4.29
1680	Alloaromadendrene	0.37
1698	Germacrene D	19.87
1717	α-muurolene	0.59
1723	Bicyclogermacrene	0.71
1750	σ-cadinene	1.32
1930	Cubenol	1.81
1967	Caryophyllene oxide	10.07
2014	Ledol	1.25
2024	1,2-dimethylcyclooctene	0.57
2047	α-funebrene	0.10
2073	Veridiflorol	0.49
2122	Spathulenol	0.18
2136	Hexahydrofarnesyl acetone	0.87
2158	8-dimethylamino-1-naphthalenecarboxylic acid	0.21
2200	Globulol	3.35
2219	α-cadinol	0.32
2243	τ-muurolol	1.22
2286	2H-pyran, 2-(7-heptadecynyloxy)tetrahydro-	0.22

https://doi.org/10.24264/icams-2022.II.8

RI	Compound Name	Area %
2350	Hexadecatrienoic acid, methyl ester	0.39
2611	Triethylene glycol monododecyl ether	0.22
2689	Decaoxabicyclo[15.13.0]triacontane	0.29

CONCLUSIONS

In our study, trans-caryophyllene, germacrene-D, α-copaene, humulene, aromadendrene and globulol were found to be the most abundant essential oil components. Similar to the present study, in studies on essential oil components of some *Teucrium* species, trans-caryophyllene and germacrene-D were main components (Gagliano Candela *et al.*, 2021; Hayta *et al.*, 2017; Baser and Demirçakmak, 1997).

REFERENCES

Atay, E. and Özdikmen, H. (2022), "The First Observation on Host Plant of *Chrysolina Blanchei* (Fairmaire, 1865) (Chrysomelidae: Chrysomelinae)", *Munis Entomology and Zoology Journal*, 17(2), 1502-1505.

Aydoğan, F. (2019), "Phytochemical and Bioactivity Studies on Some *Teucrium* L. Species Growing in Turkey", Doctoral dissertation, *Ege University*, 413 p.

Baser, K.H.C. and Demirçakmak, B. (1997), "Composition of the Essential Oils of Three Teucrium Species from Turkey", *Journal of Essential Oil Research*, 9(5), 545-549, https://doi.org/10.1080/10412905.1997.9700774.

Bettarini, F., Borgonovi, G.E., Fiorani, T., Gagliardi, I., Caprioli, V., Massardo, P., Ogoche, J.I.J., Hassanali, A., Nyandat, E. and Chapya, A. (1993), "Antiparasitic Compounds from East African Plants: Isolation and Biological Activity of Anonaine, Matricarianol, Canthin-6-One, and Caryophyllene Oxide", *International Journal of Tropical Insect Science*, 14(1), 93-99, https://doi.org/10.1017/S174275840001345X.

Bruno, M., Piozzi, F., Rodríguez, B., Savona, G., María, C. and Servettaz, O. (1992), "Neo-clerodane Diterpenes from Teucrium Species", *Phytochemistry*, 31(12), 4366-4367, https://doi.org/10.1016/0031-9422(92)80480-3.

Çakir, A., Emin Duru, M. and Harmandar, M. (1998), "Volatile Constituents of *Teucrium polium* L. from Turkey", *Journal of Essential Oil Research*, 10(1), 113-115, https://doi.org/10.1080/10412905.1998.9700855.

Fernandes, E.S., Passos, G.F., Medeiros, R., da Cunha, F.M., Ferreira, J., Campos, M.M., Pianowski, L.F. and Calixto, J.F. (2007), "Anti-Inflammatory Effects of Compounds Alpha-humulene and (−)-trans-caryophyllene Isolated from the Essential Oil of *Cordia verbenacea*", *European Journal of Pharmacology*, 569(3), 228-236, https://doi.org/10.1016/j.ejphar.2007.04.059.

Gagliano Candela, R., Ilardi, V., Badalamenti, N., Bruno, M., Rosselli, S. and Maggi, F. (2021), "Essential Oil Compositions of *Teucrium fruticans*, *T. scordium* subsp. Scordioides and *T. siculum* Growing in Sicily and Malta", *Natural Product Research*, 35(20), 3460-3469, https://doi.org/10.1080/14786419.2019.1709193.

Hayta, Ş., Yazgın, A. and Bağcı, E. (2017), "Constituents of the Volatile Oils of Two Teucrium Species from Turkey", *Bitlis Eren University Journal of Science and Technology*, 7(2), 140-144, https://doi.org/10.17678/beuscitech.348447.

Küçük, S., Köse, Y.B., Demirci, B. and Baser, K.H.C. (2016), "*Teucrium montbretii* and *Teucrium odontites* Lamiaceae'nin Karşılaştırmalı Sistematik, Morfolojik, tüy ve Fitokimyasal Özellikleri" *Biyolojik Çeşitlilik ve Koruma*, 9(2), 15-23.

Martino, L.D., Formisano, C., Mancini, E., Feo, V.D., Piozzi, F., Rigano, D. and Senatore, F. (2010), "Chemical Composition and Phytotoxic Effects of Essential Oils from Four Teucrium Species" *Natural Product Communications*, 5(12), 1969-1976, https://doi.org/10.1177/1934578X1000501230.

Menichini, F., Conforti, F., Rigano, D., Formisano, C., Piozzi, F. and Senatore, F. (2009), "Phytochemical Composition, Anti-Inflammatory and Antitumour Activities of Four Teucrium Essential Oils from Greece", *Food Chemistry*, 115(2), 679-686, https://doi.org/10.1016/j.foodchem.2008.12.067.

Navarro, T. (2020), "Systematics and Biogeography of the Genus Teucrium (Lamiaceae)" *In Teucrium Species: Biology and Applications*, 1-38, Springer, Cham, https://doi.org/10.1007/978-3-030-52159-2_1.

Noge, K. and Becerra, J.X. (2009), "Germacrene D, A Common Sesquiterpene in the Genus Bursera (Burseraceae)", *Molecules*, 14(12), https://doi.org/10.3390/molecules14125289.

*** (2022), Plants of the World Online (POWO), Facilitated by the Royal Botanic Gardens, Kew, available at: http://www.plantsoftheworldonline.org/, retrieved 18 May 2022.

https://doi.org/10.24264/icams-2022.II.8

REDUCTION OF RESIDUAL TANNINS CONCENTRATION USING *Cerioporus squamosus* BIO-AUGMENTED POLYMERIC CARRIERS

OVIDIU IORDACHE[1], IOANA-CORINA MOGA[2], ELENA-CORNELIA TĂNĂSESCU[1], ELENA PERDUM[1], LUCIA SECĂREANU[1], MIHAELA-CRISTINA LITE[1], IRINA-MARIANA SĂNDULACHE[1], ELENA-LAURA TROANCĂ[2]

[1]*The National Research & Development Institute for Textiles and Leather, Lucrețiu Pătrășcanu Street, no. 16, Bucharest, Romania, iordacheovidiu.g@gmail.com*

[2]*DFR Systems, Drumul Taberei 46, Bucharest, Romania*

The oldest use of polyphenols in the leather industry is based on their ability to stabilize collagen in the skin against rotting. Leather tanning processes are among the most polluting industrial sources in terms of undesirable and toxic parameters (COD, BOD, content of tannic acids, fats, sulphureous residues, chloride, chromium, suspended solids etc.). Tannic acid is a naturally occurring phenolic compound and is widely used in the tanning processes, being one of the main pollutants in leather industry derived wastewaters. Current paper explored the ability of HDPE carrier, functionalized with *Cerioporus squamosus* microbial strain, to reduce the residual concentration of five natural tannins, widely used in the tanning processes in leather industry: Quebracho, Chestnut, Mimosa, Myrobalan and Gambier, in concentration of 1% in the tested solution. Bio-augmentation experiment of the HDPE structures were carried out in an experimental laboratory installation, and treatment of each aqueous solution, was carried out for 7 straight days, and percentage reduction of residual tannins was calculated at 3 and 7 days. Results highlighted varying degrees of reduction of the residual tannin concentration in the solutions, depending on the tannin tested, the best efficiency being achieved against Myrobalan tannin, with a maximum percentage reduction in residual concentration of 41% after 7 days, followed by Mimosa tannin (34%-7 days), Quebracho (28%-7 days), Chestnut (22%-7 days) and Gambier (9.30%-7 days).

Keywords: Wastewater, tannins, MBBR.

INTRODUCTION

Environmental protection issues have become an essential component of the last thirty years. Determining the origin and quality characteristics of wastewater requires knowledge of the industrial technological process for the proper design of treatment technologies, along with knowledge of the source of the main tributaries and their characteristics is necessary to define the treatment methods (Yusuf and Sonibare, 2004). As far as the leather industry is concerned, the leather tanning process consists of converting raw leather, into leather, a stable material that can be used to manufacture a wide range of products. The whole process involves a complex sequence of chemical and physical operations. Following these operations, the finished product will have excellent properties such as stability, appearance, water resistance, temperature resistance, elasticity, air permeability, etc. This process is a major producer of waste water, air and soil pollutants (Zao and Chen, 2019). Environmental impacts come from liquid, solid and gaseous waste streams and the consumption of raw materials such as raw hides and skins, energy, chemicals and water. The main pollutants in the wastewaters come from wet processing and post tanning operations.

The process of disposing of leather wastes or residues from the tanning process represents an important niche for the protection of both the human health and the environment. Tannins, or tanning substances, are a class of organic compounds with a heterogeneous polyphenolic structure. Compounds in this class are mainly used in the leather industry, having the property of transforming raw leather into tanned leather.

https://doi.org/10.24264/icams-2022.II.9

There are two subclasses of tannins, based on structural criteria and chemical properties: gallo tannins (hydrolysable tannins) and catechin tannins (condensed tannins) (Neamțu, 2011).

MATERIALS AND METHODS

Microbial Strain and Treatment Installation

For the reduction of tannins experiments, *Cerioporus squamosus* (a basidiomycete bracket fungus) strain was used, which was started as fresh culture, on Sabouraud-Dextrose-Agar media (SAB) (Fig. 1). *Cerioporus squamosus* is a bracket fungus species in the *Polyporaceae* family, and it is most commonly known by the names of "Dryad's Saddle" and "Pheasant's Back Mushroom".

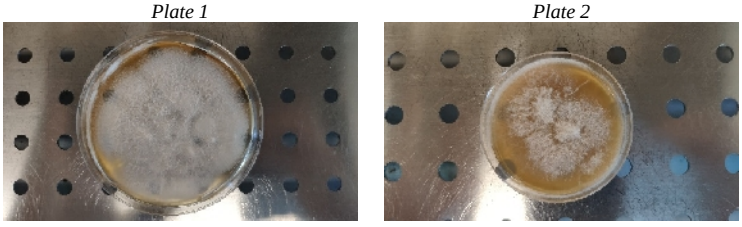

Figure 1. *Cerioporus squamosus* grown on SAB nutritive media

A laboratory treatment installation (Fig. 2-a) was used for the biofunctionalization of the high-density polyethylene (HDPE) structures (Fig. 2-b) with the *C. squamosus* strain. The installation allowed controlled aeration of the media, by infusions of filtered air, which served a dual purpose: providing oxygenation for microbial growth, and bubbling of the media, for a better dispersion of the strain inside the liquid volume.

Laboratory treatment installation | HDPE carriers in treatment installation | HDPE carriers

Figure 2. Bio-augmentation of HDPE structure

The polymeric structures, with composition of 5% talcum, 7% cellulose and 88% HDPE, were bio-augmented in the experimental treatment installation, in a total volume of 12L, with addition of Czapek-Dox nutrient media, for 14 days, at 28°C, and continuous aeration (in a Lovibond thermoreactor). The initial microbial inoculum volume was 100mL of fresh strain, obtained in Czapek-Dox liquid media. The process

https://doi.org/10.24264/icams-2022.II.9

led to obtaining of polymeric structures covered with fungal biomass, which where the active part of the treatment process.

Selected Tannins

Five natural tannins were selected for experiments to reduce the residual concentration in synthetic solutions: Quebracho, Chestnut, Mimosa, Myrobalan and Gambier. The reduction of the residual tannin concentration in the analyzed samples was performed on a UV-VIS T70 spectrophotometer (Oasis Scientific) with 5-point calibration curves for each tested tannin. The ability of the phenolic ring to absorb UV light is exploited to quantify these compounds (Aleixandre-Tudo *et al.*, 2017). The visible UV spectra of a tannin are thus attributed to electronic transitions occurring in the hydroxyl groups of phenolic molecules, with different transitions corresponding to different phenolic subclasses (Sanna *et al*., 2014). Different classes of tannins from different sources show characteristic UV absorption bands (Nakagawa and Sugita, 1999).

After the bio-augmentation period, the entire medium was evacuated from the installation, leaving only the polymeric supports in the reaction vessel. The installation was again charged with 12L of solution of each tannin, at 1% concentration (Quebracho solution=1%; Chestnut solution=1%/; Mimosa solution=1%; Myrobalan solution=1%; Gambier solution=1%), with the process run in five distinct batches for each tannin.

RESULTS AND DISCUSSION

The HDPE carrier's specific composition allowed for both growth and fixation of the microbial strain, especially in the chambers of the carriers. Constituent cellulose was used as C source by the strain, while talcum allowed a better fixation of the biofilm inside the chambers (Fig. 3).

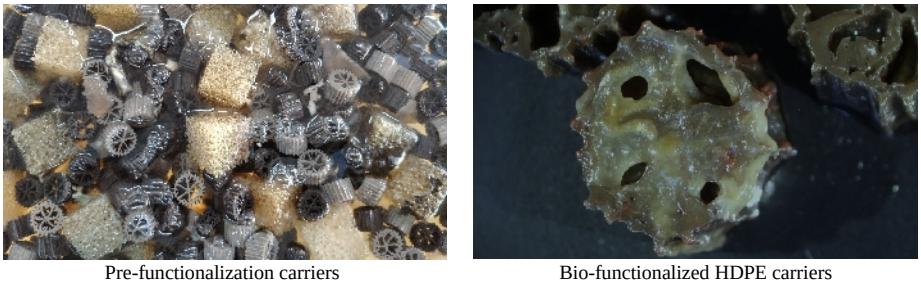

Pre-functionalization carriers Bio-functionalized HDPE carriers

Figure 3. Percentage reduction grades of Quebracho tannin residual concentration

The treatment process was carried out for 7 days, for each tannin, with incubation at 28°C (Lovibond thermoreactor) with continuous aeration. Samples were taken at T3 (3 days of process) and T7 (7 days of process) and the degree of percentage reduction compared to T0 (considered 0% percentage reduction of residual tannin concentration at the beginning of the process) was calculated (Fig. 4-8).

https://doi.org/10.24264/icams-2022.II.9

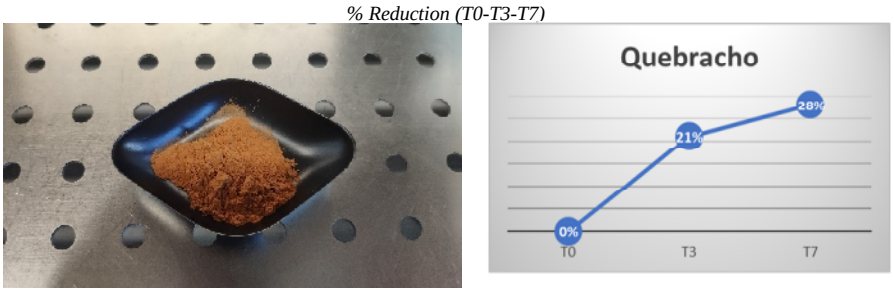

Figure 4. Percentage reduction grades of Quebracho tannin residual concentration

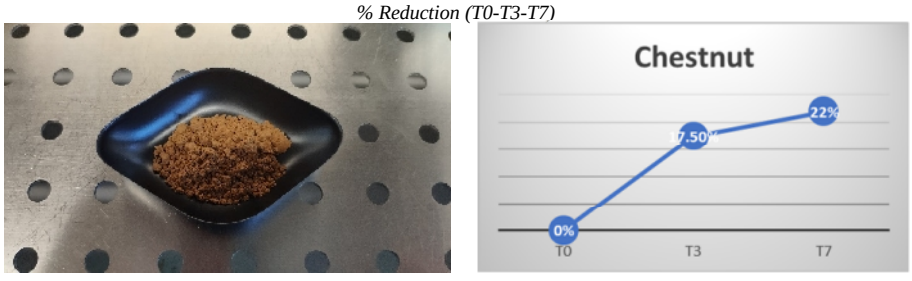

Figure 5. Percentage reduction grades of Chestnut tannin residual concentration

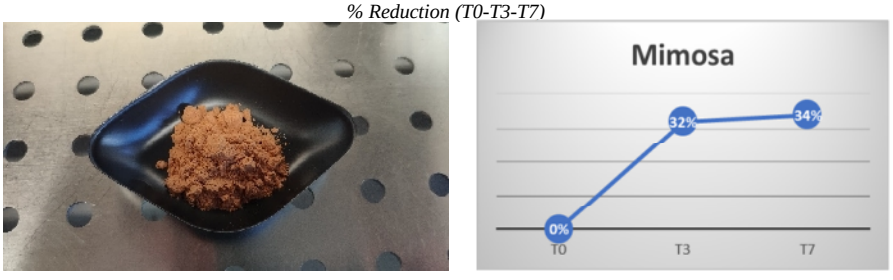

Figure 6. Percentage reduction grades of Mimosa tannin residual concentration

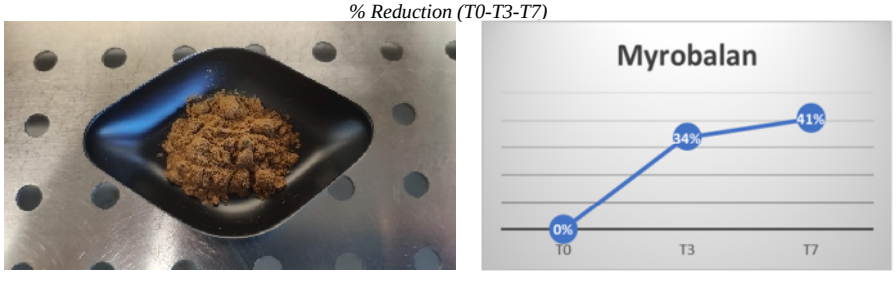

Figure 7. Percentage reduction grades of Myrobalan tannin residual concentration

https://doi.org/10.24264/icams-2022.II.9

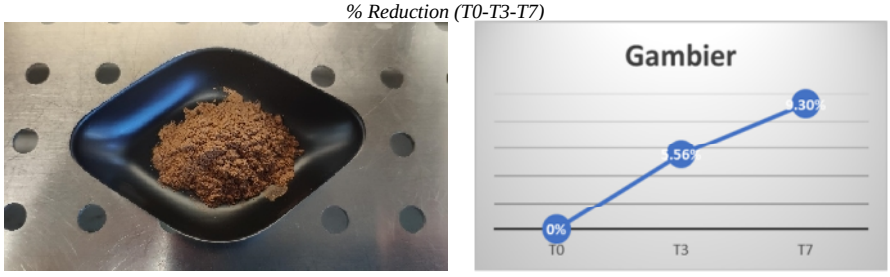

Figure 8. Percentage reduction grades of Gambier tannin residual concentration

The results of the analyses show varying degrees of reduction of the residual tannin concentration in the solutions, depending on the tannin tested. Thus, the best efficiency was shown for the tannin Myrobalan, with a maximum percentage reduction in residual concentration of 41% after 7 days, followed by Mimosa tannin (34%), Quebracho (28%), Chestnut (22%) and Gambier (9.30%). An upward trend could be observed on all samples, with the reduction rates increasing from T3 to T7. Gambier tannin showed the lowest percentage reduction rates of residual concentration in solution, which may be due to a pronounced antimicrobial character that this tannin has, due to the (+) catechin content, thus inhibiting the enzymatic activity of the microbial strain.

The use of MBBR specific technology is not currently emerging as a novel treatment technology, as the treatment efficiency of this technology is already settled throughout the years. However, new demands regarding treatment of industrial wastewater, which also includes leather industry specific wastewaters, dictates the necessity of novelty within the MBBR treatment systems, along with intelligent approaches for the efficient treatment of complex wastewater matrices.

CONCLUSIONS

A large amount of waste, especially organic waste, is inherent in leather manufacturing industry. Both organic waste fractions and other residues can be prevented and reduced to a large extent in process units, by use of non-conventional treatment technologies. Tanning agents such as plant tannins, synthases and aldehydes mainly affect surface water, leading to problems which arise because of their low biodegradability and toxicity to aquatic life. Tannins residual concentration reduction experiments, carried out on *Cerioporus squamosus* bio-functionalized HDPE carriers (specific to MBBR systems), showed promising efficiency for leather industry originated wastewaters, with efficiencies ranging from 5.56% (Gambier tannin) to 34% (Myrobalan tannin), after 3 days of treatment, and between 9.30% (Gambier tannin) to 41% (Myrobalan tannin), after 7 days of treatment. The proposed treatment technology proved more efficient against Myrobalan tannin, which was the most susceptible to microbial degradation, compared to Gambier tannin, which was the most resistant, with catechin constituent, which is proven to have antimicrobial activity.

https://doi.org/10.24264/icams-2022.II.9

Acknowledgment

The publication of the scientific paper is funded by the Ministry of Research, Innovation and Digitization within Program 1 – Development of the national R&D system, Subprogram 1.2 – Institutional Performance – RDI excellence funding projects, Contract no. 4 PFE/2021.

REFERENCES

Aleixandre-Tudo, J.L., Buica, A., Nieuwoudt, H., Aleixandre, J.L. and du Toit, W. (2017), "Spectrophotometric Analysis of Phenolic Compounds in Grapes and Wines", *Journal of Agricultural and Food Chemistry*, 65, pp. 4009-4026, https://doi.org/10.1021/acs.jafc.7b01724.

Nakagawa, K. and Sugita, M. (1999), "Spectroscopic Characterization and Molecular Weight of Vegetable Tannins", *Journal of the Society of Leather Technologies and Chemists*, 83, 261–264.

Neamțu, G. (2001), *Biologically Active Natural Substances – Vol. I. Vitamins* (in Romanian), R.A. Press, Bucharest.

Sanna, R., Piras, C., Marincola, F.C., Lecca, V., Maurichi, S. and Scano, P. (2014), "Multivariate Statistical Analysis of the UV-vis Profiles of Wine Polyphenolic Extracts during Vinification", *The Journal of Agricultural Science*, 6, pp. 152-162, https://doi.org/10.5539/jas.v6n12p152.

Yusuf, R. and Sonibare, J. (2004), "Characterization of Textile Industries Effluents in Kaduna, Nigeria and Pollution Implications", *Global NEST Journal*, 6, pp. 212-221, https://doi.org/10.30955/gnj.000284.

Zao, C. and Chen, W. (2019), "A Review for Tannery Wastewater Treatment: Some Thoughts under Stricter Discharge Requirements", *Environmental Science and Pollution Research*, 26, pp. 26102–26111, https://doi.org/10.1007/s11356-019-05699-6.

ANTIMICROBIAL ACTIVITY OF FIR FUNCTIONALIZED TEXTILE MATERIALS AGAINST PATHOGENIC FUNGI STRAINS

OVIDIU IORDACHE, ELENA-CORNELIA TĂNĂSESCU, ELENA PERDUM, LUCIA SECAREANU, MIHAELA-CRISTINA LITE, IRINA-MARIANA SANDULACHE

The National Research & Development Institute for Textiles and Leather, Lucrețiu Pătrășcanu Street, no. 16, Bucharest, Romania, iordacheovidiu.g@gmail.com

Far infrared (FIR) functional textiles are a new category of functional textiles that have the potential to improve well-being and health. At the molecular level, FIR exerts strong rotational and vibrational effects with potential biological benefits. The majority of textiles with antimicrobial functionalization are based on synthetic products, and there is a need to link current end-user demands with both efficient products and low environmental impact, promoting natural antimicrobial treatments as viable solutions. Two structures of knitwear were obtained, with functional inorganic particles with antimicrobial, anti-UV and IR emission properties: variant 1: 100% BBC gauze ground yarn plated with functionalized polyamide yarn; variant 2: 85% wool/15% cashmere blend ground yarn plated with functionalized polyamide yarn. The antimicrobial efficiency of two types of functionalized materials was tested against six pathogenic microbial strains: *Tricoderma viride* (laboratory strain), *Aspergillus flavus* (laboratory strain), *Candida albicans* (ATCC 90028), *Epidermophyton floccosum* (CCM 8339), *Trichophyton interdigitale* (ATCC 9533) and *Aspergillus niger* (IMI 45551), highlighting various degrees of microbial reduction, depending on both the material and the tested strain, with lowest percentage microbial reduction of 9.67&, against *Aspergillus niger* strain, and highest of 86.65%, against *Candida albicans*.

Keywords: Antimicrobial, fungi, textile materials.

INTRODUCTION

Pyroelectric materials are functional materials that can generate an electrical response following a temperature change (Best *et al*., 2008). Modern solutions often include a combination of polypropylene and special lead-free bio-ceramics to create functional FIR (Far Infrared) garments, which are materialized in commercially available products such as socks, pillows, underwear, knee pads, trousers, bed covers, bed linen, shoulder pads etc. The functionalization materials of FIR functional products consist of a wide range of inorganic bio-ceramic compounds, such as: bamboo charcoal, pearl powder, tourmaline, carbide-based materials (ZrC, SiC), oxide-based materials (magnesium, zirconium, alumina, iron, germanium), photocatalytic compounds (TiO_2), which impart controlled infrared radiation (Wang and Li, 2010).

Currently, the synthetic fibers generating pyroelectric effects are obtained by introducing minerals (e.g., superfine tourmaline powder) into melted polymers before spinning or by dispersing the minerals into the spinning solution (Taekyung *et al*., 2020). Regarding the current state of the art level, regarding FIR functionalized materials, emerging technologies, like PRTM (Personal Radiant Thermal Management), are being widely adopted for manufacturing advance clothing materials, that can promote thermal comfort to the wearer, while reducing energy consumption (Zhu and Feng, 2021).

Processing methods for anionic fibers and functional textiles can be divided into two main categories. In the first category, the anionic additive is integrated into the anionic fibers, and in the second category, the textiles are functionalized with negative ion generating materials during the finishing process. The main method of manufacturing anionic fibers is coating and surface modification, melt spinning and copolymerization.

https://doi.org/10.24264/icams-2022.II.10

MATERIALS AND METHODS

Functionalization Masterbatches

The functionalization masterbatches, used for the development of the textile structures used in the antimicrobial testing, were developed by Clavis Corporation (Korea) by blending functional inorganic particles (Fig. 1) into PET and PA. In order to impart multiple functional properties, inorganic particles with antimicrobial, anti-UV and IR emission properties were used. Extrusion characteristics between PET polymer and inorganic particles were considered, taking into account particle size, specific gravity, color and accounting with other additives.

IR emission Antimicrobial properties Anti-UV

Figure 1. Inorganic particles with dedicated functional properties

Textile Materials

For the antimicrobial testing, two knitted textile structures were executed, with a plated glazed structure: knit 1: 100% BBC gauze ground yarn plated with functionalized polyamide yarn; knit 2: 85% wool/15% cashmere blend ground yarn plated with functionalized polyamide yarn (Fig. 2).

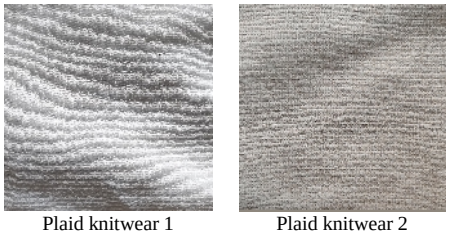

Plaid knitwear 1 Plaid knitwear 2

Figure 2. Knitted textile materials

Testing Method and Microbial Strains

The antimicrobial efficacy testing was done according to ISO 20743:2007, a method applicable to all textile products, including canvas, wadding, yarns and materials for clothing, home furnishings and various products, regardless of the type of antibacterial agent used (organic, inorganic, natural or synthetic) or the method of application (incorporated, post-treatment or grafting). The absorption method was used, in which the microbial suspension is inoculated directly onto the samples, with previous sample sterilization. The samples were inoculated with 50µL of the last dilution performed for each strain tested in the step (in pre-sterilized tubes) and incubated for 24 hours at 28°C for filamentous fungal strains and 37°C for *Candida albicans* strain. After the

https://doi.org/10.24264/icams-2022.II.10

incubation period, each sample was vortexed for approx. 20" in 1mL sterile distilled water and inoculated on specific nutrient medium (Czapek-Dox and Sabouraud-Agar), followed by an incubation period of 2-3 days. To quantify the results, the CFU (Colony Forming Units) counting technique was used on the incubated plates and the strain as a control was used to report the antimicrobial efficacy.

Antimicrobial evaluation was performed on the 2 functionalized materials, compared to a 0 control (single control, from each strain, taken as microbial inoculum), against six microbial strains: *Trichoderma viride* (laboratory strain), *Aspergillus flavus* (laboratory strain), *Candida albicans* (ATCC 90028), *Epidermophyton floccosum* (CCM 8339), *Trichophyton interdigitale* (ATCC 9533) and *Aspergillus niger* (IMI 45551).

RESULTS AND DISCUSSION

Fungi are ubiquitous microorganisms with representative species that have a high pathogenic potential for human hosts, especially for immunocompromised and immunocompetent individuals. Pathogenicity is the ability of an organism to affect a living host by deregulating homeostatic parameters, triggering an immunological response or mechanical action at the tissue level (Siscar-Lewin *et al*., 2022).

Testing against *Aspergillus niger* (Fig. 3) indicates a low efficiency of functionalized materials against the strain, with a maximum of 20% (T1 material), which is more than twice as efficient as T2 material (9.67%). *Aspergillus niger* is a highly resistant strain to the action of certain antimicrobial agents, combined with the high microbial concentration of the inoculum (8.9x103 CFU/mL), leading to low microbial reduction rates.

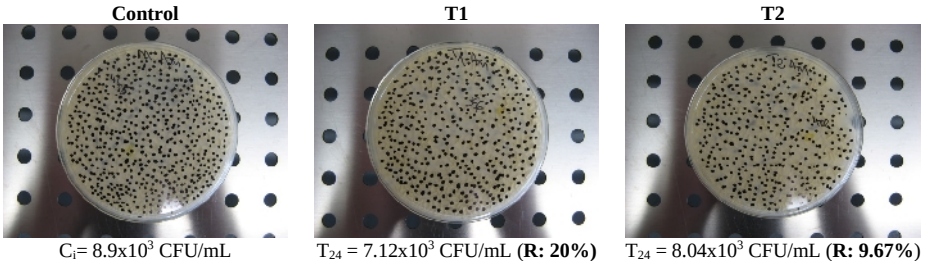

$C_i = 8.9x10^3$ CFU/mL $T_{24} = 7.12x10^3$ CFU/mL (**R: 20%**) $T_{24} = 8.04x10^3$ CFU/mL (**R: 9.67%**)

Figure 3. Antimicrobial activity against *Aspergillus niger* strain

The results of the antimicrobial test against *Candida albicans* (Fig. 4) highlighted better degrees of microbial reduction than against *Aspergillus niger*. The T1 material showed better antimicrobial efficacy (86.65%) compared to the T2 material (65.48%). This may also be due to the higher cotton composition, correlated with a higher mechanical retention, T2 also having polyester in its composition.

https://doi.org/10.24264/icams-2022.II.10

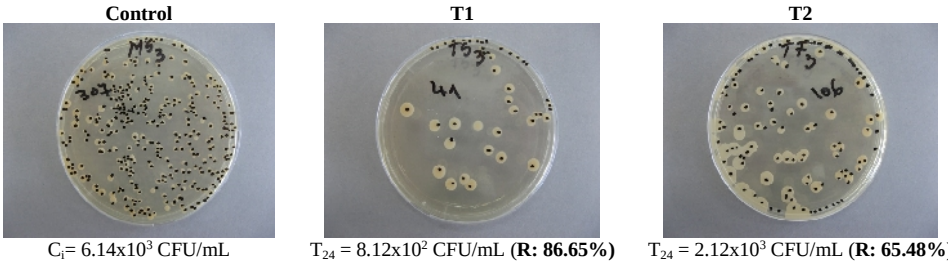

C_i= 6.14x10^3 CFU/mL T_{24} = 8.12x10^2 CFU/mL (**R: 86.65%**) T_{24} = 2.12x10^3 CFU/mL (**R: 65.48%**)

Figure 4. Antimicrobial activity against *Candida albicans* strain

Antimicrobial analysis against *Aspergillus flavus* (Fig. 5) showed good degrees of microbial reduction, with very close values between the two materials (T1 and T2). Even if a slight similarity between inoculum concentration and *Aspergillus niger* is observed, the reduction rates are significantly higher against *A. flavus* strain, showing the difference in susceptibility to treatment of one strain versus another, even between species of the same genus.

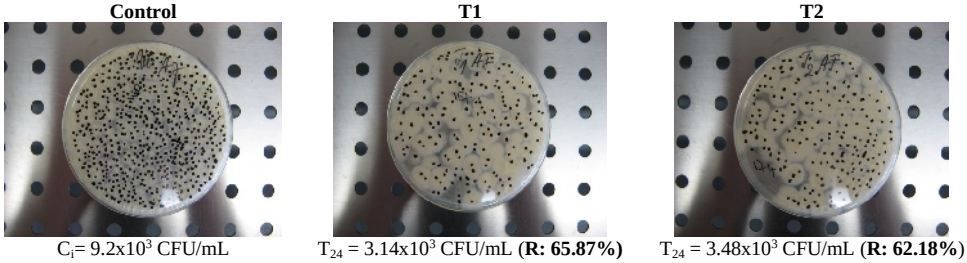

C_i= 9.2x10^3 CFU/mL T_{24} = 3.14x10^3 CFU/mL (**R: 65.87%**) T_{24} = 3.48x10^3 CFU/mL (**R: 62.18%**)

Figure 5. Antimicrobial activity against *Aspergillus flavus* strain

Epidermophyton floccosum is an anthropophilic dermatophyte with a worldwide distribution and one of the most common causes of dermatophytosis in healthy individuals. The strains infect the skin (tinea corporis, tinea cruris, tinea pedis) and nails (onychomycosis). Infection is limited to the horny layers of the epidermis, as the microorganism does not have the ability to penetrate the viable tissues of the immunocompetent host. Antimicrobial testing against *E. floccosum* (Fig. 6) highlighted satisfactory degrees of microbial reduction, with 45.17% for T2 material, and 30.97% for T1.

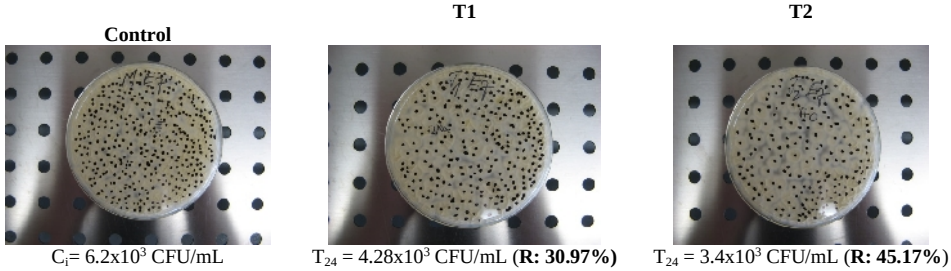

C_i= 6.2x10^3 CFU/mL T_{24} = 4.28x10^3 CFU/mL (**R: 30.97%**) T_{24} = 3.4x10^3 CFU/mL (**R: 45.17%**)

Figure 6. Antimicrobial activity against *Epidermophyton floccosum* strain

https://doi.org/10.24264/icams-2022.II.10

Tests carried out on the second dermatophyte strain, *Trichophyton interdigitale* (Fig. 7), showed sub-medium degrees of microbial reduction, with similar results for both treated materials: T1 = 19.12% and T2 = 21.57%. Compared to the other dermatophyte fungal strain, *Epidermophyton floccosum*, this one was found to be more resistant to the action of the antimicrobial agent.

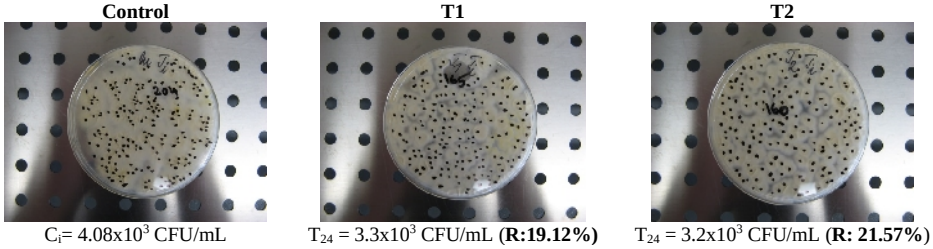

C_i= 4.08x10^3 CFU/mL T_{24} = 3.3x10^3 CFU/mL (**R:19.12%**) T_{24} = 3.2x10^3 CFU/mL (**R: 21.57%**)

Figure 7. Antimicrobial activity against *Tricophyton interdigitale* strain

The results of the analysis against *Trichoderma viride* (Fig. 8) strain indicated a good antimicrobial efficiency of both materials, with very low variation (9.24%), thus promoting this type of functionalization as a biological barrier against *T. viride* strain.

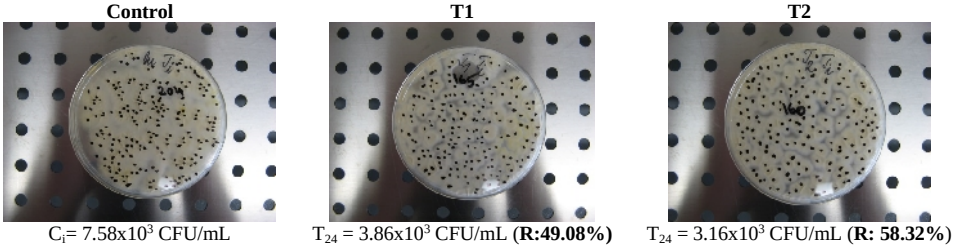

C_i= 7.58x10^3 CFU/mL T_{24} = 3.86x10^3 CFU/mL (**R:49.08%**) T_{24} = 3.16x10^3 CFU/mL (**R: 58.32%**)

Figure 8. Antimicrobial activity against *Trichoderma viride* strain

CONCLUSIONS

Materials functionalized with FIR compounds are based on the principle of absorbing light energy and then radiating this energy back onto the body at specific wavelengths. Textiles are constantly exposed to the action of microorganisms, so their functionalization may prove to be an efficient method of obtaining antimicrobial active barriers, among other special properties. The antimicrobial evaluation performed on the 2 functionalized materials, compared to a 0 control, under static contact conditions (under agitation), against the six microbial strains showed good reduction rates, especially against *C. albicans* (max of 86.65%), *A. flavus* (max of 65.87%), *E. floccosum* (max of 45.17%) and *T. viride* (max of 58.32%), thus validating this type of functionalization treatment for inducing antimicrobial properties, beside FIR specific ones.

https://doi.org/10.24264/icams-2022.II.10

Acknowledgment

The publication of the scientific paper is funded by the Ministry of Research, Innovation and Digitization within Program 1 – Development of the national R&D system, Subprogram 1.2 - Institutional Performance – RDI excellence funding projects, Contract no. 4 PFE/2021.

REFERENCES

Best, S.M., Porter, A.E., Thian, E.S. and Huang, J. (2008), "Bioceramics: Past, Present and for the Future", *Journal of the European Ceramic Society*, 28(7), pp. 1319-1327, https://doi.org/10.1016/j.jeurceramsoc.2007.12.001.

Siscar-Lewin, S., Hube, B. and Brunke, S. (2022), "Emergence and Evolution of Virulence in Human Pathogenic Fungi", *Trends in Microbiology*, 30(7), pp. 693-704, https://doi.org/10.1016/j.tim.2021.12.013.

Taekyung, L., Sang-Mi, J., Keumyoung, S., Jeong, H.P., Yong, K.C. and Sanghyun, J. (2020), "Development of Fiber-based Active Thermal Infrared Camouflage Textile", *Applied Materials Today*, 20, September 2020, 100624, https://doi.org/10.1016/j.apmt.2020.100624.

Wang, L. and Li, Y. (2010), "The Function and Health Care of Negative Ion Fibers and Textiles", in: *Proceedings of the 2010 International Conference on Information Technology and Scientific Management*, Tianjin, China, pp. 20-21.

Zhu, F.L. and Feng, Q.Q. (2021), "Recent Advances in Textile Materials for Personal Radiative Thermal Management in Indoor and Outdoor Environments", *International Journal of Thermal Sciences*, 165, July 2021, 106899, ISSN 1290-0729, https://doi.org/10.1016/j.ijthermalsci.2021.106899.

PLANT GROWTH-PROMOTING CHARACTERISTICS OF ANTARCTIC ENDOPHYTIC BACTERIA

OLGA IUNGIN[1], IEVGENIIA PREKRASNA[2], IHOR BORTYANUY[1], VALERIIA MASLAK[1], SAULIUS MICKEVIČIUS[3]

[1]*Kyiv National University of Technologies and Design, Ukraine, olgaungin@gmail.com*

[2]*State Institution National Antarctic Scientific Center, Ukraine*

[3]*Vytautas Magnus University, Lithuania*

The work is focused on studying bacteria associated with vascular plants in Antarctic region. Climate changes affecting the Antarctic Peninsula favor the successful colonization of ice-free lands by two Antarctic vascular plants (*Deschampsia antarctica* and *Colobanthus quitensis*). Bacteria isolated from *D. antarctica* collected during the 25th Ukrainian Antarctic Expedition (January-April 2020) along the Western part of the Antarctic Peninsula were studied for plant growth-promoting characteristics (nitrogen fixation, phosphate solubilization, cyclic lipopeptide production, exoprotease production, motility and carbohydrate utilization). The heterotrophy of bacterial isolated from *D. antarctica* and the presence of a wide range of saccharolytic enzymes for the utilization of mono- and disaccharides in studied cultures were shown. This may indicate the plasticity of metabolism and the high adaptation potential of microorganisms associated with *D. antarctica*. PGPT of studied bacteria were mostly presented by nitrogen-fixing ability and cyclic lipopeptides synthesis.

Keywords: PGPB, antarctic vascular plants, endophytic bacteria

INTRODUCTION

The arisen interest shown to microorganisms associated with vascular plants of the Antarctic region was not only due to the knowledge about plant-microbial interactions, but also due to the prospects of climate change in the world and the biotechnological potential of these microorganisms. Climate changes affecting the Antarctic Peninsula favor the successful colonization of ice-free lands by two Antarctic vascular plants (*Deschampsia antarctica* and *Colobanthus quitensis*). Bacteria are important for the growth and adaptation of plants to extreme conditions of growth and development.

Antarctic plants have developed adaptation mechanisms that allow them to successfully survive the extreme conditions of the region. Thus, recently it was shown the leading role of micromycetes-endophytes in the tolerance of plants to UV-B and minimizing damage to plant cells (Barrera *et al.*, 2020); stimulation of plant growth by increasing nitrogen mineralization (Oses-Pedraza *et al.*, 2020); improvement of physiological indicators under salt stress due to energy docking and complex formation with Na^+ (Molina-Montenegro *et al.*, 2020). However, there are almost no studies on the development and influence of bacterial endophytes of vascular plants in the Antarctic region.

The understanding of interactions in the "microorganism-plant" system helps to assess the effect of bacteria on the growth and development of plants consisted of its ability to participate in biochemical mechanisms shared with the plant (Compant *et al*., 2021).

The aim of the study was to screen plant growth-promoting traits in endophytic bacteria of antarctic vascular plants.

EXPERIMENTAL

Materials

We have studied 8 bacterial cultures isolated from *D. antarctica* collected during the 25th Ukrainian Antarctic Expedition (January-April 2020) along the Western part of the Antarctic Peninsula.

https://doi.org/10.24264/icams-2022.II.11

Methods

Overnight liquid cultures were obtained on diluted Nutrient Broth medium (HiMedia, Ltd.) in a shaking incubator (26 , 160 rpm).

The ability of bacterial isolates to utilize different carbohydrates was tested with long “Hiss rows” with the use of 9 carbohydrate substrates: glucose, fructose, mannose, galactose, arabinose, xylose, ribose, lactose, sucrose (Gunkova *et al*., 2021).

Nitrogen-fixing activity were checked on Ashby's combined-nitrogen-free medium with sucrose. Bacterial growth was determined by the change of optical density (OD600) and evaluated as + (weak growth), ++ (moderate growth), +++ (abundant growth) (Mohite and Patil, 2022).

Drop collapse assay for cyclic lipopeptides production (CLPs) was performed onto Parafilm. The reduction of the surface tension and the collapse of the droplet (10 µL aliquots of bacterial overnight culture) indicated the presence of surfactants (De Souza *et al.*, 2003).

Motility assay was performed onto 1/5 Nutrient agar (0.3%). 10 µL aliquots of bacterial overnight culture were spot in medium surface. Colony diameter was measured in 24, 48 and 72 h after inoculation on 0.3% 1/5 NA (Ha *et al.*, 2014).

Exoprotease production was tested using skim milk agar (Vazquez *et al.*, 1995). A cleared zone surrounding bacterial growth after incubation for 48 and 72 h at 28°C was the evidence of exoprotease production. Phosphate solubilizing ability was tested on Pikovskaya (PVK) medium (Pikovskaya, 1948) incorporated with $Ca_3(PO_4)_2$.

All experiments were performed in triplicates.

RESULTS AND DISCUSSION

Carbohydrates fermentation ability is both the way to help with bacteria taxonomic identification and to describe possible physiological characteristics of the isolates, predict their range of substrates and enzymes.

Table 1. Saccharolytic enzymes of studied isolates

Isolate	Hexoses					Pentoses		Disaccharides	
№	Glu	Fru	Man	Gal	Ara	Xyl	Ryb	Lac	Suc
10.4	+	-	+	+	-	+	+	-	-
15.6	+	-	-	-	-	+	-	-	-
25.2	+	+	+	+	-	+	+	+	+
26.2	+	-	+	+	-	+	-	-	+-
26.4	+	-	+	+	-	+	-	-	+
26.7	+	+	+	-	-	-	+	+-	+
39.12	+	+	-	-	-	-	+	-	-
40.1	+	+	+	+	+	+	+	+-	+

«+» positive reaction; «+-» doubtful reaction; «-» negative reaction

The most usable substrates were glucose, mannose and xylose. Mannose is an isomer of glucose, a component of many polysaccharides and mixed biopolymers of plant, animal and bacterial origin. Xylose as the main component of polymers in plants is considered one of the most abundant carbohydrates on earth after glucose. Taking into account that the studied isolates are associated with plants, it is quite clear that these carbohydrates could be promising for metabolic use by bacteria. The ability of microorganisms to metabolize a wide range of Carbon and Nitrogen sources, to participate in global cycles of transformation of the main biogenic elements, and to

https://doi.org/10.24264/icams-2022.II.11

function in harsh environments can be the basis of plant adaptation to adverse environmental factors (Singh, 2018).

However, bacteria associated with plants can promote plant growth directly usually by either facilitating resource acquisition (including micronutrients and minerals), or indirectly by decreasing the inhibitory effects of various pathogenic agents on plant growth and development (Glick, 2012). The direct stimulation of plant growth may be a consequence of nitrogen fixation, phosphate solubilization, iron sequestration, synthesis of phytohormones (such as auxins, cytokinins, and gibberellins), or modulation of plant ethylene levels (Gamalero and Glick, 2011) helping plants to overcome stress and support cell metabolism.

That is why the mentioned set of screened plant growth-promoting characteristics was chosen based on the importance of adequate nutrition in low-temperature environment and defence system against numerous of pathogens (Pršić and Ongena, 2020). All studied isolates have shown plant growth-promoting traits (Table 2).

Table 2. PGPT shown by antarctic bacterial isolates

Isolate №	CLPs	N_2-fixing activity**	Motility
10.4	+	+++	-
15.6	-	+	+
24.4	+	+++	+
25.2	+	+++	+
26.2	+	+++	+
26.7	+	++	-
39.12	+	-	+
40.1	+	-	-

* Phosphate solubilizing ability and exoprotease production are not shown because it was not detected;

** + weak growth, ++ moderate growth, +++ abundant growth in Ashby's medium.

The most abundant were nitrogen-fixing activity, cyclic lipopeptides production and motility. These traits play important role in plant colonization and promoting the growth of plants in harsh environments. Nitrogen is known as one of the limiting factors regarding plant growth (Puri *et al*., 2018). Biological nitrogen fixation plays a great role in subsidizing plants with nitrogen in such limiting or low-mobility environments as Antarctic region. Phosphorus is one of the six elements essential for plant growth. The majority of phosphate solubilizing bacteria affiliates with Paenibacillus, Bacillus, Pseudomonas, Lactococcus, Enterobacter and Alcaligenes (Li *et al*., 2021). Although there were Bacillus and Pseudomonas among studied isolates there was no evidences of phosphate solubilizing ability as well as exoproteases synthesis.

The evidences of CLPs were shown by almost all isolates. Despite the fact that CLPs are known as biocontrol molecules, their role is believed more complicated than this (Wan *et al*., 2021). CLPs exhibit interesting biological activities including interactions with biofilms (Balleza *et al*., 2019) which affect not pathogens only but could manage colonization activity and the balance among endophytic community itself.

CONCLUSIONS

The heterotrophy of bacterial isolated from *Deschampsia antarctica* and the presence of a wide range of saccharolytic enzymes for the utilization of mono- and disaccharides in these cultures were shown. This may indicate the plasticity of metabolism and the high adaptation potential of microorganisms associated with *D. antarctica.* PGPT of studied bacteria were mostly presented by nitrogen-fixing ability and cyclic lipopeptides synthesis.

https://doi.org/10.24264/icams-2022.II.11

REFERENCES

Balleza, D., Alessandrini, A., and Beltrán García, M.J. (2019), "Role of Lipid Composition, Physicochemical Interactions, and Membrane Mechanics in the Molecular Actions of Microbial Cyclic Lipopeptides", *The Journal of Membrane Biology*, 252(2), 131-157, https://doi.org/10.1007/s00232-019-00067-4.

Barrera, A., Hereme, R., Ruiz-Lara, S., Larrondo, L.F., Gundel, P.E., Pollmann, S., Barrera, A., Hereme, R., Ruiz-Lara, S., Larrondo, L.F., Gundel, P.E., Pollmann, S., Molina-Montenegro, M.A. and Ramos, P. (2020), "Fungal Endophytes Enhance the Photoprotective Mechanisms and Photochemical Efficiency in The Antarctic Colobanthus Quitensis (Kunth) Bartl. Exposed to UV-B Radiation", *Frontiers in Ecology and Evolution*, 8, 122, 13 pages, https://doi.org/10.3389/fevo.2020.00122.

Compant, S., Cambon, M.C., Vacher, C., Mitter, B., Samad, A., and Sessitsch, A. (2021), "The Plant Endosphere World–Bacterial Life Within Plants", *Environmental Microbiology*, 23(4), 1812-1829, https://doi.org/10.1111/1462-2920.15240.

De Souza, J.T., De Boer, M., De Waard, P., Van Beek, T.A., and Raaijmakers, J.M. (2003), "Biochemical, Genetic, and Zoosporicidal Properties of Cyclic Lipopeptide Surfactants Produced by *Pseudomonas fluorescens*", *Applied and Environmental Microbiology*, 69(12), 7161-7172, https://doi.org/10.1128/AEM.69.12.7161-7172.2003.

Gamalero, E. and Glick, B.R. (2011), "Mechanisms Used by Plant Growth-Promoting Bacteria", in: Maheshwari, D. (ed.), *Bacteria in Agrobiology: Plant Nutrient Management*, Springer, Berlin, Heidelberg, pp. 17-46, https://doi.org/10.1007/978-3-642-21061-7_2.

Glick, B.R. (2012), "Plant Growth-Promoting Bacteria: Mechanisms and Applications", *Scientifica*, 2012, Article ID 963401, 15 pgs, https://doi.org/10.6064/2012/963401.

Gunkova, P.I., Buchilina, A.S., Maksimiuk, N.N., Bazarnova, Y.G. and Girel, K.S. (2021), "Carbohydrate Fermentation Test of Lactic Acid Starter Cultures", in: *IOP Conference Series: Earth and Environmental Science*, 852(1), 012035, IOP Publishing, https://doi.org/10.1088/1755-1315/852/1/012035.

Ha, D.G., Kuchma, S.L. and O'Toole, G.A. (2014), "Plate-Based Assay for Swimming Motility in *Pseudomonas aeruginosa*", in: Filloux, A., Ramos, J.L. (eds), *Pseudomonas Methods and Protocols. Methods in Molecular Biology*, vol 1149, Humana, New York, 59-65, https://doi.org/10.1007/978-1-4939-0473-0_7.

Li, J.T., Lu, J.L., Wang, H.Y., Fang, Z., Wang, X.J., Feng, S.W., Wang, Z., Yuan, T., Zhang, S.C., Ou, S.N., Yang, X.D., Wu, Z.H., Du, X.D., Tang, L.Y., Liao, B., Shu, W.S., Jia, P. and Liang, J.L. (2021), "A Comprehensive Synthesis Unveils the Mysteries of Phosphate‐Solubilizing Microbes", *Biological Reviews of the Cambridge Philosophical Society*, 96(6), 2771-2793, https://doi.org/10.1111/brv.12779.

Mohite, B.V. and Patil, S.V. (2022), "Isolation and Identification of Nonsymbiotic Azotobacter and Symbiotic Azotobacter Paspali–Paspalum notatum", in: Amaresan, N., Patel, P., Amin, D. (eds.), *Practical Handbook on Agricultural Microbiology*, Humana, New York, 25-33, https://doi.org/10.1007/978-1-0716-1724-3_3.

Molina-Montenegro, M.A., Acuña-Rodríguez, I.S., Torres-Díaz, C., Gundel, P.E. and Dreyer, I. (2020), "Antarctic Root Endophytes Improve Physiological Performance and Yield in Crops under Salt Stress by Enhanced Energy Production and Na+ Sequestration", *Scientific Reports*, 10, Article number 5819, 1-10, https://doi.org/10.1038/s41598-020-62544-4.

Oses-Pedraza, R., Torres-Díaz, C., Lavín, P., Retamales-Molina, P., Atala, C., Gallardo-Cerda, J., Acuña-Rodríguez, I.S. and Molina-Montenegro, M.A. (2020), "Root Endophytic Penicillium Promotes Growth of Antarctic Vascular Plants by Enhancing Nitrogen Mineralization", *Extremophiles: Life under Extreme Conditions*, 24(5), 721-732, https://doi.org/10.1007/s00792-020-01189-7.

Pikovskaya, R.I. (1948), "Mobilization of Phosphorus in Soil in Connection with Vital Activity of Some Microbial Species", *Mikrobiologiya*, 17, 362-370.

Pršić, J., and Ongena, M. (2020), "Elicitors of Plant Immunity Triggered by Beneficial Bacteria", *Frontiers in Plant Science*, 11, article 594530, 12 pages, https://doi.org/10.3389/fpls.2020.594530.

Puri, A., Padda, K.P. and Chanway, C.P. (2018), "Nitrogen-Fixation by Endophytic Bacteria in Agricultural Crops: Recent Advances", in: Khan, A. and Fahad, S. (eds.), *Nitrogen in Agriculture*, IntechOpen, London, 73-94, https://doi.org/10.5772/intechopen.71988.

Singh, I. (2018), "Plant Growth Promoting Rhizobacteria (PGPR) and Their Various Mechanisms for Plant Growth Enhancement in Stressful Conditions: A Review", *European Journal of Biological Research*, 8(4), 191-213.

Vazquez, S.C., Rios Merino, L.N., MacCormack, W.P. and Fraile, E.R. (1995), "Protease-Producing Psychrotrophic Bacteria Isolated from Antarctica", *Polar Biology*, 15(2), 131-135, https://doi.org/10.1007/BF00241051.

Wan, C., Fan, X., Lou, Z., Wang, H., Olatunde, A. and Rengasamy, K.R. (2022), "Iturin: Cyclic Lipopeptide with Multifunction Biological Potential", *Critical Reviews in Food Science and Nutrition*, 62(29), 7976-7988, https://doi.org/10.1080/10408398.2021.1922355.

COLLAGEN-BASED GEL WITH ANTIMICROBIAL ACTIVITY FROM LEATHER WASTE

OLGA IUNGIN[1,3], LESIA MAISTRENKO[1], KATERYNA RUDNIEVA[2], OLENA MOSHYNETS[3], VIKTORIIA POTOCHYLOVA[4], OLENA MOKROUSOVA[1]

[1]*Kyiv National University of Technologies and Design, Ukraine, olgaungin@gmail.com*

[2]*Kyiv Regional Clinical Hospital, Ukraine*

[3]*Institute of Molecular Biology and Genetics of the National Academy of Sciences of Ukraine, Ukraine*

[4]*Communal non-profit enterprise "Kyiv Maternity Hospital 2"*

The work is focused on obtaining collagen-based gel from leather waste with antimicrobial activity for further use with biomedical application and as dressings for wounds. Two antibiotics - macrolide azithromycin and phenicol chloramphenicol were tested using both laboratory strain and clinical isolates of Staphylococcus species from patients with wounds in Kyiv region. Collagen matrix was obtained from delimed pelt leather waste by acetic acid extraction. The biofilm assay and MTT assay were applied to study the effect of antimicrobial component in collagen-based gel. The reduced growth rate, cells attachment level and cells metabolic activity were the evidences of strains inhibition and biofilm development prevention.

Keywords: collagen, antimicrobial, wounds

INTRODUCTION

The skin is the largest organ of the body and the main barrier that protects the us from the external environment (Landén *et al.*, 2016). It is characterized by complexity due to the combination of sebaceous glands, blood vessels, sweat glands, sensory cells, nerves, epidermal cells and, finally, hair. The skin consists of two layers - epidermis and dermis (Benson, 2012). Incompletely permeable wounds are formed within the upper part of the dermis (epidermis) and tighten due to the regeneration process. Full-thickness wounds are associated with damage to the epidermis, dermis, and underlying fatty tissue. Such wounds are prolonged due to the processes of granulation, contraction and epithelization (reconstruction of the wound surface) (Dalton *et al.*, 2007). Effective tissue and skin surface repair requires interaction between different types of cells. This process is precisely organized and regulated at several levels - biochemical, molecular, cellular (Reinke and Sorg, 2012).

Collagen, as the main component of the skin, plays an important role in the healing process of wounds, and also affects the course of the inflammatory process. The most promising collagen for the creation of wound surface treatment agents is type I collagen. Further development of agents based on collagen and its derivatives requires solving the problems of improving the structure and maximum therapeutic effect against pathological processes (Velnar *et al.*, 2009). The pathogenesis of many orthopedic infections is associated with the presence of microorganisms in the form of a biofilm. By definition, a biofilm is a growth strategy of microorganisms in which cells attach to a surface or interphase and synthesize a polymer matrix covering intact cells (Flemming and Wingender, 2010). In biofilms, microorganisms function as clusters with structural and functional heterogeneity similar to multicellularity. Microorganisms in the form of a biofilm show less sensitivity to the action of antimicrobial substances. Biofilm tolerance to antibiotics is multifactorial, including physical, physiological, and genetic

https://doi.org/10.24264/icams-2022.II.12

determinants, while antibiotic resistance of biofilm bacteria is mutational and due to repeated exposure to high-concentration antibiotics.

The aim of the work was to develop an antimicrobial component for collagen-based gel for further biomedical application.

EXPERIMENTAL

Materials

Collagen-based acid extracts from leather waste were obtained as it was described previously (Maistrenko *et al.*, 2020). Delimed pelt was used as a source of collagen type I. Two types of antibiotics – phenicol antibiotic chloramphenicol (CAP) and macrolide antibiotic azithromycin (AZM) – in collagen matrix from delimed pelt – against opportunistic pathogens were studied.

Pathogenic opportunistic infectious agents were used as test cultures - laboratory strain *Staphylococcus aureus* ATCC 25923 and two clinical isolates from wounds - *S. aureus* 1536 and *S. epidermidis* 190.

Methods

Isolation, identification and antibiotic resistance estimation were performed in Kyiv Regional Clinical Hospital (Kyiv) according to generally accepted methods and international recommendations of EUCAST with use of VITEK 2 compact 15 (France).

For biofilm studies 96-well microtiter plate assay was used. The overnight cultures (NB, HiMedia Ltd.) of studied strains were inoculated (1:10 ratio) in plates contained collagen matrices with concentration range of CAP and AZM. There was also a positive control for CAP test – 96% ethanol and a negative control - collagen without antibiotics. The strains were cultivated 24 hours at 37°C. The OD600 was measured and the crystal violet assay was applied (Kragh *et al*., 2019).

To estimate metabolic activity of bacterial cells MTT assay was performed as described (Wang *et al.*, 2010)

All measurements were done in 3 parallel replicas with calculation of the mean deviation. For all tests, $p < 0.05$ was considered reliable.

RESULTS AND DISCUSSION

In order to develop collagen-based gel with antimicrobial component there was a need to prepare collagen part (matrix) and the antimicrobial part. Collagen matrix was obtained from delimed pelt waste (1st extraction) by acetic acid extraction protocol. Collagen extract was washed from acetic acid by dialysis against deionized water, 18 МОм·см, pH 7 during 48 hours with changing the water every 12 hours. Strong transparent gel was obtained (Fig.1).

Figure 1. Collagen-based gel obtained from delimed pelt

https://doi.org/10.24264/icams-2022.II.12

As the obtained gel was an aqueous solution the antimicrobial components should be applied as those which are dissolved in water. Both antibiotics - AZM and CAP - could be easily dissolved in water, however CAP should be dissolved in ethanol first.

During the period August 2019 —March 2021, 1560 strains of infectious agents from purulent wounds were isolated and analyzed in the Kyiv region. The most common infectious agents from wounds were representatives of the genera *Staphylococcus.* Though *Escherichia, Klebsiella*, *Pseudomonas,* and *Enterococcus* species might be presented but the number of such cases in skin wounds was much less. The most part of isolates from wound surfaces were presented by *S. epidermidis* and *S. aureus.* Among the gram-negative microflora *Enterobacteriaceae* was dominated and presented by *Klebsiella pneumoniae*, *Escherichia coli* and others. The isolates were mostly resistant to fosfomycins, penicillins, β-lactam inhibitors and monobactams. At the same time, they were highly sensitive to the last line antibiotics - teicoplanin, vancomycin and linezolid.

Monitoring of antibiotic resistance of isolates from wounds allows to assess the future prospects for antibiotic therapy and the current situation in the hospitals. At the same time, the search for promising antibiotics and antimicrobial substances for new treatment strategies and overcoming antibiotic resistance of microorganisms is continued.

Previously it was described that collagen from leather waste could be a fine matrix for bacterial biofilm formation (Iungin *et al*., 2020). Numerous studies have shown that biofilm mode of growth has greater resistance to wide range of antimicrobials compare to planktonic one (Olsen, 2015; Dier-Pereira *et al*., 2021). In the same time the generally accepted methods of antibiotic susceptibility testing are focused on planktonic mode of bacterial growth. As a result, levels of antibiotic concentrations considered to be MIC might be insufficient to suppress the development of biofilm in case of wound infection especially if the wound was already infected for a while. That is why when it comes to develop the antimicrobial component for collagen-based gel we were focused on biofilm studies only.

Within the concentration range of AZM there was definite inhibition of growth rate of all studied strains (Fig. 2).

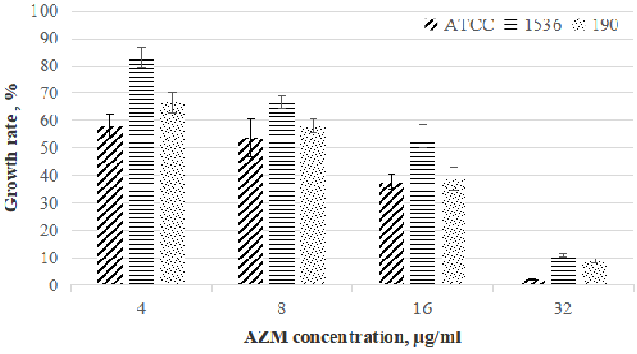

Figure 2. Staphylococcal biomass growth rate (%) in the presence of AZM

https://doi.org/10.24264/icams-2022.II.12

It was shown that AZM in concentrations up to 16 µg/ml reduce the growth rate up to half whereas 32 µg/ml was enough to inhibit totally the laboratory strain. Clinical isolates were suppressed as well and the growth rate reached up 10% only.

At the same time cells attachment level has shown opposite tendency within the mentioned concentration range (Fig. 3).

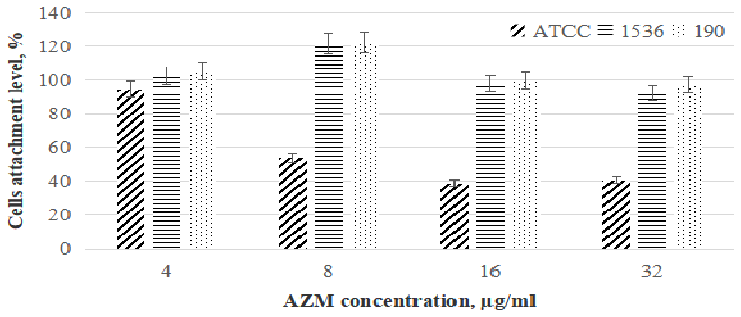

Figure 3. Staphylococcal cells attachment level (%) in the presence of AZM

Thus, the attachment level of clinical isolates was almost the same as in control. However, there was a slight raise at the point of 8 µm/ml. That could be explained by the response mechanisms to the small level stress caused by antibiotic compound. It is known that cells under small stress pressure can increase the attachment level or push planktonic cells to switch into surface-attached biofilm lifestyle (Grinberg *et al*., 2019). There is a difference between these two options. The first one is described as a shield or self-sacrifice function. In this case attached cells could act as a protector from antimicrobial surface preventing the metabolically active cells faced with the toxic molecules. It is still unknown how the part of bacterial population decide what cells should go down. The second could be connected with the presence of toxic molecule as well, however the decision of planktonic cells to attach to the surface and to change its lifestyle could be controlled by different factors including not only environmental but physiological as well (Busscher, 2012).

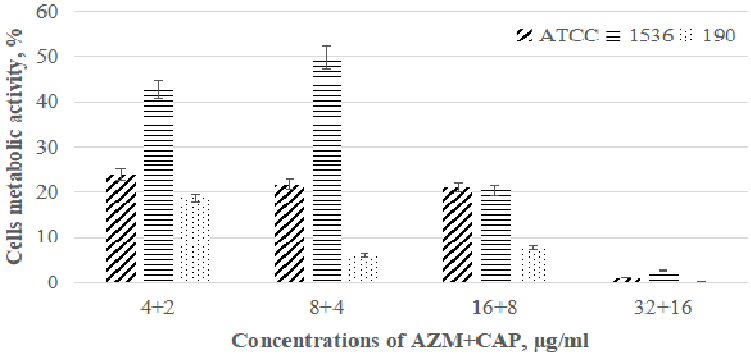

Figure 4. Staphylococcal cells metabolic activity (%) in the presence of AZM+CAP

https://doi.org/10.24264/icams-2022.II.12

It was shown that combination of studied antibiotics incredibly reduces the metabolic activity of bacteria cells. The CAP itself didn't seem to reduce the growth rate, but it definitely reduces the biofilm-forming ability possibly due to the solvent ethanol presence (data is not shown). So, the role of CAP in this combination is still needed to be defined.

In general, the combination of antibiotics was more effective in fighting Staphylococcal biofilms compare to single AZM. The results also depended on the strain origin - laboratory or clinical. Clinical isolates were more adaptive to changing environments and could stand higher concentrations of antibiotics.

CONCLUSIONS

Collagen-based gel with antimicrobial component from leather waste for further biomedical application was developed. The most efficient combination of antibiotics (AZM and CAP) for treating laboratory and clinical strains was shown. However, the role of CAP is still needed to be studied. The reduced growth rate, cells attachment level and cells metabolic activity were the evidences of strains inhibition and biofilm development prevention. The slight increase in attachment level in the presence of AZM in low concentrations could be explained by small stress phenomenon.

REFERENCES

Benson, H.A.E. (2012), "Skin Structure, Function, and Permeation", in: H.A.E. Benson and A.C. Watkinson (eds.), *Topical and Transdermal Drug Delivery*, 1-22, https://doi.org/10.1002/9781118140505.ch1.

Busscher, H.J. and van der Mei, H.C. (2012), "How do Bacteria Know They are on a Surface and Regulate Their Response to an Adhering State?", *PLoS Pathogens*, 8(1), e1002440, https://doi.org/10.1371/journal.ppat.1002440.

Dalton, S.J., Whiting, C.V., Bailey, J.R., Mitchell, D.C. and Tarlton, J.F. (2007), "Mechanisms of Chronic Skin Ulceration Linking Lactate, Transforming Growth Factor-B, Vascular Endothelial Growth Factor, Collagen Remodeling, Collagen Stability, and Defective Angiogenesis", *Journal of Investigative Dermatology*, 127(4), 958-968, https://doi.org/10.1038/sj.jid.5700651.

Dier-Pereira, A.P., Trevizani Thihara, I.R., Duarte, F.C., da Silva, R.S., Santos, J.P., Tavares, E.R., de Oliveira, F.C., Pinge-Filho, P., Kerbauy, G., Perugini, Regina, E.M., Yamauchi, M.L. and Yamada-Ogatta, S.F. (2021), "Methicillin-Resistant *Staphylococcus haemolyticus* Displaying Reduced Susceptibility to Vancomycin and High Biofilm-Forming Ability", *Infectious Disorders-Drug Targets*, 21(7), 63-70, https://doi.org/10.2174/1871526521666210217151807.

Flemming, H.C. and Wingender, J. (2010), "The Biofilm Matrix", *Nature Reviews Microbiology*, 8(9), 623-633, https://doi.org/10.1038/nrmicro2415.

Grinberg, M., Orevi, T. and Kashtan, N. (2019), "Bacterial Surface Colonization, Preferential Attachment and Fitness under Periodic Stress". *PLoS Computational Biology*, 15(3), e1006815, https://doi.org/10.1371/journal.pcbi.1006815.

Iungin, O., Maistrenko, L., Rebrykova, P. and Duka, I. (2020), "Biofilm-Formation Ability of *S. aureus* on Collagen Matrices", *Scientific Works of NUFT*, 26(5), 26-31, (in Ukrainian).

Kragh, K.N., Alhede, M., Kvich, L. and Bjarnsholt, T. (2019), "Into the Well—A Close Look at the Complex Structures of a Microtiter Biofilm and the Crystal Violet Assay", *Biofilm*, 1, 100006, https://doi.org/10.1016/j.bioflm.2019.100006.

Landén, N.X., Li, D. and Ståhle, M. (2016), "Transition from Inflammation to Proliferation: A Critical Step During Wound Healing", *Cellular and Molecular Life Sciences*, 73(20), 3861-3885, https://doi.org/10.1007/s00018-016-2268-0.

Lesia, M., Iungin, O., Savchuk, O. and Okhmat, O. (2020), "Collagen Matrices from Leather Industry Wastes for Biomedical Application", *Proceedings of the 8th International Conference on Advanced Materials and Systems – ICAMS 2020*, Certex, Bucharest, 195-200, https://doi.org/10.24264/icams-2020.II.15.

Olsen, I. (2015), "Biofilm-Specific Antibiotic Tolerance and Resistance", *European Journal of Clinical Microbiology & Infectious Diseases*, 34(5), 877-886, https://doi.org/10.1007/s10096-015-2323-z.

Reinke, J.M. and Sorg, H. (2012), "Wound Repair and Regeneration", *European Surgical Research*, 49(1),

35-43, https://doi.org/10.1159/000339613.

Velnar, T., Bailey, T. and Smrkolj, V. (2009), "The Wound Healing Process: An Overview of The Cellular and Molecular Mechanisms", *Journal of International Medical Research*, 37(5), 1528-1542, https://doi.org/10.1177/147323000903700531.

Wang, H., Cheng, H., Wang, F., Wei, D. and Wang, X. (2010), "An Improved 3-(4, 5-Dimethylthiazol-2-Yl)-2, 5-Diphenyl Tetrazolium Bromide (Mtt) Reduction Assay for Evaluating the Viability of *Escherichia coli* Cells", *Journal of Microbiological Methods*, 82(3), 330-333, https://doi.org/10.1016/j.mimet.2010.06.014.

https://doi.org/10.24264/icams-2022.II.12

DETERMINATION OF ESSENTIAL OIL COMPONENTS OBTAINED FROM LEAVES AND AERIAL PARTS OF *Ferulago syriaca*

DURMUŞ ALPASLAN KAYA[1], YELDA GÜZEL[2], MUSA TÜRKMEN[1]

[1]*Mustafa Kemal University, Agriculture Faculty, Field Crops Department, 31034, Hatay, Turkey, e-mail: dkaya@mku.edu.tr. musaturkmen@mku.edu.tr.*

[2]*Mustafa Kemal University, Faculty of Arts and Sciences, Biology Department, Hatay, 31034, Turkey, email: yeldaguzel@gmail.com*

In this study, the contents of essential oils obtained from the leaves and aerial parts of *Ferulago syriaca* were investigated by GC-MS. *Ferulago syriaca* used in the study was obtained from Hatay flora. 57 components of the essential oils obtained from the leaves of the plant were determined at a rate of 99.99%. When the essential oil components obtained from the aerial-parts were examined, 43 components were determined at a rate of 98.47%. When the essential oil components obtained from *Ferulago syriaca* leaves and aerial parts were examined, the main components were determined as Myrcene, durylaldehyde, α-pinene, β-phellandrene, α-terpinolene, limonene, bornyl acetate, p-cymene in both parts of the plant.

Keywords: essential oil, GC-MS, *Ferulago syriaca*

INTRODUCTION

Ferulago syriaca, whose native range is Southern Turkiye, Syria, Israel and Cyprus, is an aromatic medicinal plant with anti-Alzheimer (Karakaya *et al*., 2018) and aphrodisiac (Öztürk *et al*., 2018) pharmacological activities proven in vitro. The essential oil content of the fruits and roots of the species was investigated (Erdurak *et al*., 2006). The essential oil yield of the fruits was 4.8%, the essential oil content was determined to be 27.8% monoterpene and 10.7% sesquiterpene. The main fruit essential oil compounds were found as myrcene (15.3), terpinolene (12.5) and 4,6-guaiadiene (10.7). The essential oil yield of the roots was found to be 1.1%, and it was determined that it consisted of oxygenated monoterpene (69.4) and monoterpene (12.5) compounds. Major compounds were found as bornyl acetate (69.4), and terpinolene (12.5). The essential oil content of aerial parts (i.e. leaves, branchs and flowers) has not been investigated, this is the first study on aerial part essential oils. In the study, the leaves and other aerial parts (branches and flowers) were studied and compared separately because the plant spends the first few years of its perennial life period above the ground just giving leaves (Figure 1, left). In this process, photosynthesizing leaves enlarge the root by sending storage nutrients to the root, which is in the form of rhizomes. After a development period of several years, the flowering branches of the plant occur (Figure 1, right). By the time it reaches the fruiting stage, the leaves are already dry. Since different stages of the plant's life cycle are represented by different organs, we found it worth examining the essential oil contents of the leaves separately from other aerial parts.

MATERIAL AND METHODS

Plant Material

The study material plant was collected from its natural habitat, Amanos Mountains-Hatay-Turkiye and identified by Yelda Güzel. A plant that has just formed its branches

https://doi.org/10.24264/icams-2022.II.13

and flowers and whose leaves have not yet dried was preferred. Since the plant is 1.5 m tall and large, one plant was sufficient for the study. The essential oil yield of branches and flowers was 1.3%, and the essential oil yield of leaves was 2.9%. A voucher from the plant, numbered Y. Güzel-3135, was stored in the herbarium of the MKU biology department.

Figure 1. *Ferulago syriaca*, with only leaves above ground, during the first years of its life cycle (left), a few years old that has formed stems and flowers from above-ground parts (right)

Essential Oil Isolation

The essential oil was obtained from dried leaves. A total of 50 g of the ground plant samples was used for hydrodistillation experiment. A sample weight was individually and carefully placed into a 2000 ml flask. Distilled water was added until it covered the sample completely. Essential oils were obtained by hydrodistillation method which was carried out in an all-glass Clevenger-type distillation. The essential oil ratio was calculated according to dry weight of plant materials and amount of essential oils obtained. The obtained essential oil samples were dried over anhydrous sodium sulfate and stored in amber vials at +4 .

GC-MS Analysis of the Essential Oils

Analysis of the essential oil was carried out using a Thermo Scientific Focus gas chromatograph equipped with MS, auto sampler, and TR-5MS (5% phenyl polysilphenylene-siloxane, 0.25 mm i.d. x 60 m length, film thickness 0.25 µm). The carrier gas was helium (99.9%) at a flow rate of 1 mL/min; ionization energy 70 eV. Mass range m/z 50–650 amu. Data acquired at scan mode. MS transfer line temperature 250°C; MS ionization source temperature 220°C, injection port temperature 220°C. The samples were injected with a 250 split ratio. The injection volume was 1 µL. Oven temperature was programmed from 50°C to 220°C at 3°C /min. The structure of each

https://doi.org/10.24264/icams-2022.II.13

compound was identified by comparison of their mass spectrum with the Wiley Registry, 9th edition.

RESULTS AND DISCUSSION

When the essential oil components obtained from the leaves and aerial parts of the *Ferulago syriaca* plant were examined, 57 components of the essential oils obtained from the leaves of the plant were determined at a rate of 99.99%. When the essential oil components obtained from the aerial-parts were examined, 43 components were determined at a rate of 98.47%. When the essential oil components obtained from *Ferulago syriaca* leaves and aerial parts were examined, the main components were determined as myrcene, durylaldehyde, α-pinene, β-phellandrene, α-terpinolene, limonene, bornyl acetate, p-cymene in both parts of the plant. The main component in the leaves was myrcene with a rate of 50.27%, followed by durylaldehyde, p-cymene and β-phellandrene components, respectively. Durylaldehyde ratio was determined as 6.55%, while p-cymene and β-phellandrene ratios were determined as 5.32% and 5.13%, respectively. When the essential oil components obtained from the aerial-parts of the plant were examined, the main component was myrcene with a rate of 51.32%. When the other components of the essential oil obtained from the aerial-parts are examined, it is seen that the durylaldehyde ratio is 6.75%. It is seen that this is followed by β-phellandrene with 5.01%, α-terpinolene with 4.6% and bornyl acetate with 4.16%. In previous study, the essential oil content was determined to be 27.8% monoterpene and 10.7% sesquiterpene. The main fruit essential oil compounds were found as myrcene (15.3), terpinolene (12.5) and 4,6-guaiadiene (10.7). The essential oil composition of the roots was found to be 1.1%, and it was determined that it consisted of oxygenated monoterpene (69.4) and monoterpene (12.5) compounds. Major compounds were found as bornyl acetate (69.4), and terpinolene (12.5) (Erdurak *et al*., 2006).

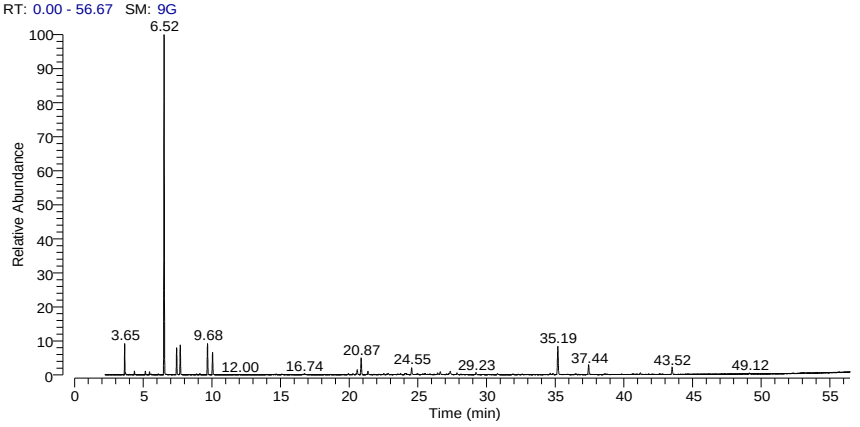

Figure 2. Essential oil chromatograms obtained from *Ferulago syriaca* leaf

https://doi.org/10.24264/icams-2022.II.13

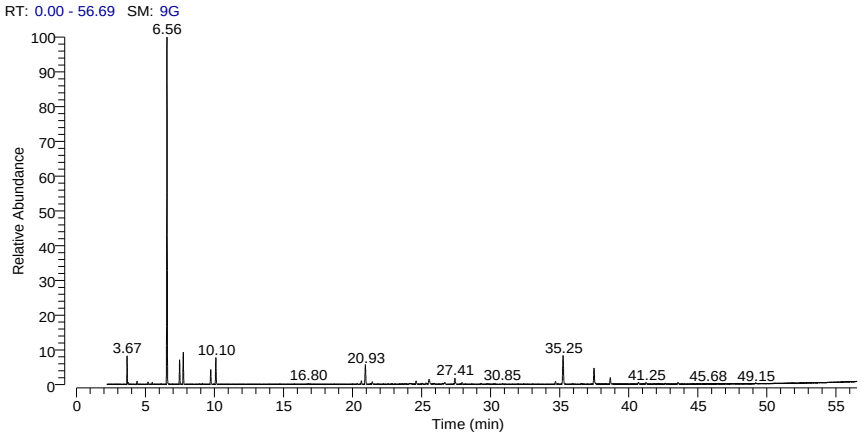

Figure 3. Essential oil chromatograms obtained from *Ferulago syriaca* aerial parts

Table 1. Essential oil components obtained from *Ferulago syriaca* leaf and aerial parts

		Area (%)	
RT	Compound Name	Leaves	Aerial parts
3.65	α-pinene	3.65	3.35
4.36	Camphene	0.49	0.44
5.16	β-pinene	0.48	0.30
6.1	3-carene	0.13	0.13
6.52	Myrcene	50.27	51.32
7.43	Limonene	4.14	3.73
7.7	β-phellandrene	5.13	5.01
8.86	γ-terpinene	0.11	0.12
9.1	α-ocimene	0.18	0.21
9.68	p-cymene	5.32	2.90
10.05	α-terpinolene	3.89	4.6
14.66	β-ocimene epoxide	0.11	nd
19.91	Linalool	0.18	nd
20.27	Cis-sabinene hydrate	0.23	nd
20.48	Safranal	0.12	nd
20.59	Chrysanthenyl acetate	1.01	0.73
20.87	Bornyl acetate	3.57	4.16
21.37	trans-caryophyllene	0.88	0.53
22.5	p-diethylbenzene	0.20	0.13
22.73	1-terpinenol	0.14	0.24

https://doi.org/10.24264/icams-2022.II.13

RT	Compound Name	Area (%) Leaves	Aerial parts
22.84	β-farnesene epoxide	0.31	0.11
23.51	Pinocarvyl acetate	0.12	0.14
23.74	Verbenol	0.27	nd
24.05	Humulene	0.29	0.19
24.13	5-Ethyltricyclo[4.3.1.1(2,5)]undec-3-en-10-one	0.16	nd
24.55	cis-verbenol	1.47	0.92
24.89	α-muurolene	nd	0.1
24.98	1,8-menthadien-4-ol	0.29	0.21
25.35	Bornyl methyl ether	0.09	0.25
25.51	Germacrene D	0.28	0.21
25.55	Isoledene	nd	1.46
25.87	σ-cadinene	0.09	0.09
25.9	γ-gurjunene	nd	0.23
26.44	α-phellandren-8-ol	0.37	0.17
26.64	m-cymene	0.6	0.18
27.07	Piperitol isomer II	0.11	nd
27.26	1,5,7-Octatrien-3-ol, 2,6-dimethyl	0.24	nd
27.36	γ-muurolene	0.81	1.34
27.85	δ-elemene	0.55	0.5
28.11	Phenyl-2-nitropropene	0.11	nd
29.23	α-phellandrene	0.49	0.22
29.7	Perilla alcohol	0.08	0.19
30.8	p-Cymen-8-ol	0.28	0.19
32.58	Sabinyl acetate	0.11	nd
34.7	Cedrol	nd	0.71
34.82	Caryophyllene oxide	0.24	0.11
35.19	Durylaldehyde	6.55	6.75
36.45	10,13-octadecadiynoic acid, methyl ester	0.19	nd
37.44	Cubenol	2.24	3.86
38.61	β-eudesmol	0.17	1.42
41.2	Globulol	0.74	0.42
42.58	Carvacrol	0.17	nd
43.52	Spathulenol	1.62	0.42

Nd: not detected

https://doi.org/10.24264/icams-2022.II.13

CONCLUSIONS

The contents of essential oils obtained from the leaf and aerial parts of *Ferulago syriaca* obtained from Hatay flora were examined by GC-MS and 57 components were determined in the essential oil obtained from the leaves of the plant and 43 components from the above-ground parts. As a result of the studies, the main components of the essential oils obtained from the leaves and aerial parts of *Ferulago syriaca* were determined as Myrcene, durylaldehyde, α-pinene, β-phellandrene, α-terpinolene, limonene, bornyl acetate, p-cymene, both in the leaves and in the aerial parts.

REFERENCES

Erdurak, C.S., Coşkun, M., Demirci, B. and Başer, K.H.C. (2006), "Composition of the Essential Oil of Fruits and Roots of *Ferulago isaurica* Peşmen and *F. syriaca* Boiss. (Umbelliferae) from Turkey", *Flavour and Fragrance Journal*, 21(1), 118-21, https://doi.org/10.1002/ffj.1540.

Karakaya, S., Koca, M., Kılıc, C.S. and Coskun, M. (2018), "Antioxidant and Anticholinesterase Activities of *Ferulago syriaca* Boiss. and *F. isaurica* Peşmen Growing in Turkey", *Medicinal Chemistry Research*, 27, 1843-50, https://doi.org/10.1007/s00044-018-2196-7.

Öztürk, B., Gür, S., Coskun, M., Kosan, M., Erdurak, C., Hafez, G., Ozgunes, O. and Cetinkaya, M. (2004), "Relaxant Effect of *Ferulago syriaca* Root Extract on Human Corpus Cavernosum", *European Urology Supplements*, 3(2), 62, https://doi.org/10.1016/S1569-9056(04)90238-2.

https://doi.org/10.24264/icams-2022.II.13

COMPARING OF EUCALYPTUS (*Eucalyptus camaldulensis* AND *Eucalyptus grandis*) ESSENTIAL OIL COMPOSITIONS GROWING IN HATAY ECOLOGICAL CONDITIONS

DURMUŞ ALPASLAN KAYA, MUSA TÜRKMEN

Mustafa Kemal University, Agriculture Faculty, Field Crops Department, 31034, Hatay, Türkiye, e-mail: dkaya@mku.edu.tr, musaturkmen@mku.edu.tr.

Essential oils obtained by hydrodistillation of *Eucalyptus camaldulensis* and *Eucalyptus grandis* from Hatay (Turkey), were analyzed by GC/MS. The total ratio of twenty-three components in *Eucalyptus camaldulensis* volatile components with 98.15%. This ratio is seen as forty-seven components and 99.66% in *Eucalyptus grandis.* Eucalyptol, limonene and α-pinene were identified as the main components of the essential oils of *Eucalyptus camaldulensis.* Cymene, α-pinene, isoborneol, trans-pinocarveol and eucalyptol were identified as the main components of the essential oils of *Eucalyptus grandis.* When compare the components of *E. camaldulensis* and *E. grandis* essential oils, the main component was determined as eucalyptol with 74.11% and cymene with 31.67% respectively.

Keywords: Essential oil, GC-MS, *Eucalyptus grandis*, *Eucalyptus camaldulensis*

INTRODUCTION

The world forest industry has recently been changing to shift at an increasing rate towards the tropics and subtropics. Especially eucalyptus species play a significant role in this process (Kellison, 2001). Highly productive eucalyptus forests provide high-quality raw materials for pulp, paper, wood and energy from native tropical forests (Grattapaglia, and Kirst 2008). In traditional popular medicine, *Eucalyptus* spp. essential oil traditionally used to treat respiratory disorders (Harkenthal *et al*., 1999; Nicoletti and Quaglio, 2022; Salari *et al.,* 2006). The area afforested with eucalyptus in our country is approximately 20,000. around a hectare. There are eucalyptus afforestation areas belonging to the private and public sector, which develop very well in places where the choice of location and species is well made (Gürses, 1990; Baser *et al*., 2001).

In this study, essential oil contents of *Eucalyptus camaldulensis* and *Eucalyptus grandis* plants were investigated.

EXPERIMENTAL

Plant Material

The plant materials were collected from Kırıkhan-Hatay-Türkiye (*Eucalyptus camaldulensis*) and Dörtyol-Hatay-Türkiye (*Eucalyptus grandis*).

Essential Oil Isolation

The essential oil was obtained from dried leaves. A total of 50 g of the ground plant samples was used for hydrodistillation experiment. A sample weight was individually and carefully placed into a 2000 ml flask. Distilled water was added until it covered the sample completely. Essential oils were obtained by hydrodistillation method which was conducted in an all-glass clevenger-type distillation. The essential oil ratio was calculated according to dry weight of plant materials and amount of essential oils obtained. The obtained essential oil samples were dried over anhydrous sodium sulfate and stored in amber vials at +4 .

https://doi.org/10.24264/icams-2022.II.14

GC-MS Analysis of the Essential Oils

Analysis of the essential oil was carried out using a Thermo Scientific Focus gas chromatograph equipped with MS, auto sampler, and TR-5MS (5% phenyl polysilphenylene-siloxane, 0.25 mm i.d. x 60 m length, film thickness 0.25 µm). The carrier gas was helium (99.9%) at a flow rate of 1 mL/min, ionization energy 70 eV. Mass range m/z 50–650 amu. Data acquired at scan mode. MS transfer line temperature 250°C; MS ionization source temperature 220°C, injection port temperature 220°C. The samples were injected with a 250 split ratio. The injection volume was 1 µL. Oven temperature was programmed from 50°C to 220°C at 3°C /min. The structure of each compound was identified by comparison of their mass spectrum with the Wiley Registry, 9th edition. Data acquisition used the Xcalibur software program.

RESULTS AND DISCUSSION

In *E. camaldulensis* essential oil, twenty-three components were determined at a rate of 98.15%. When the components of *E. camaldulensis* were examined, the main component was determined as eucalyptol with 74.11% (Table 1). This was followed by α-pinene with 6.82% and limonene with 6.55%, respectively (Figure 1). The present study showed differences from those who reported eucalyptol as a main component in *E. camaldulensis* essential oil (Tsiri *et al*., 2003; Su *et al*., 2006; Rasooli *et al*., 2009).

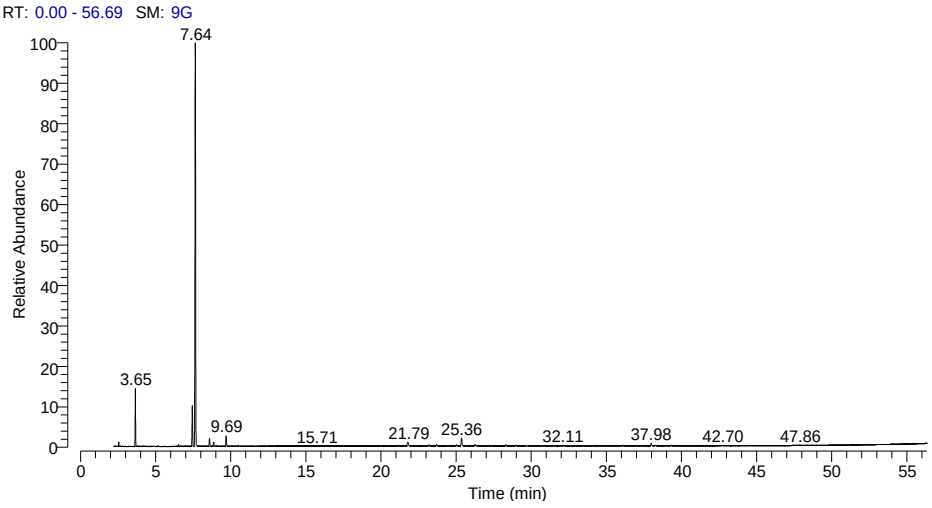

Figure 1. Essential oil chromatograms obtained from *Eucalyptus camaldulensis*

https://doi.org/10.24264/icams-2022.II.14

Table 1. Comparison of essential oil components of *Eucalyptus camaldulensis*

RT	Compound Name	Area (%)
2.54	Methylpentaldehyde	0.45
3.65	α-pinene	6.82
5.16	β-pinene	0.16
6.52	Myrcene	0.33
7.44	Limonene	6.55
7.64	Eucalyptol	74.11
8.58	cis-ocimene	1.30
8.86	γ-terpinene	0.74
9.11	trans-β-ocimene	0.17
9.69	o-cymene	1.92
10.52	Isovaleric acid, isopentyl ester	0.22
19.93	Linalool	0.11
21.79	Nerolidol	1.10
23.18	Alloaromadendrene	0.22
23.69	trans-pinocarveol	0.33
24.42	α-terpineol	0.12
25.01	E-citral	0.24
25.36	α-terpineol	1.81
26.24	Isopiperitone	0.32
28.28	Hotrienol	0.23
28.94	p-mentha-1(7),8-dien-2-ol	0.17
37.98	Veridiflorol	0.62
39.28	Rosifoliol	0.11

When *Eucalyptus grandis* essential oil components are examined, forty-seven components are found at a rate of 99.66%. When the components of *E. grandis* essential oils were examined, the main components were determined as cymene, α-pinene, isoborneol, trans-pinocarveol and eucalyptol (Figure 2). The main component was determined as cymene with 31.67%, followed by α-pinene with 21.96%, isoborneol with 8.41% and trans-pinocarveol with 6.02%, respectively (Table 2). It is seen that the essential oil components determined by Soyingbe *et al*. (2013) in their study on *Eucalyptus grandis* essential oil are similar to this study.

https://doi.org/10.24264/icams-2022.II.14

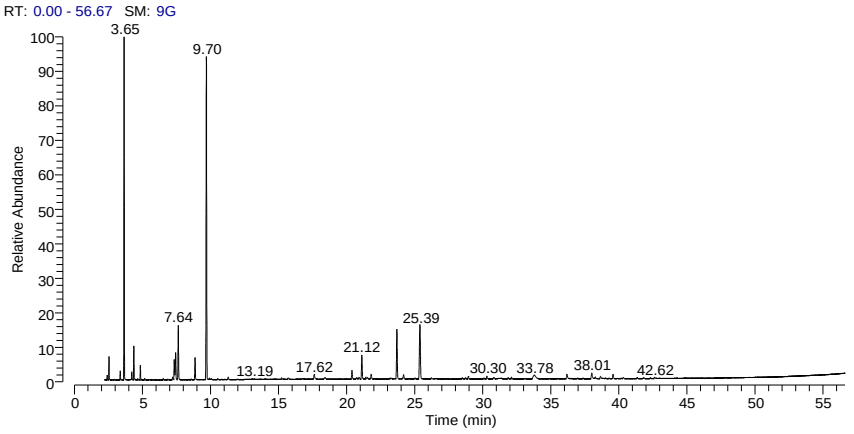

Figure 2. Essential oil chromatograms obtained from *Eucalyptus grandis*

Table 2. Comparison of essential oil components of *Eucalyptus grandis*

RT	Compound Name	Area
2.41	Butanal	0.26
2.54	Methylpentaldehyde	1.25
3.37	3-pentanone, 2,4-dimethyl-	0.64
3.65	α-pinene	21.96
4.22	α-fenchene	0.57
4.37	Camphene	2.46
4.85	2-methylpropyl isobutyrate	1.03
5.16	β-pinene	0.14
6.53	α-phellandrene	0.14
7.22	Amyl propionate	0.3
7.34	1-methylbutyl butyrate	1.74
7.44	Limonene	2.54
7.64	Eucalyptol	5.17
8.87	γ-terpinene	2.06
9.7	Cymene	31.67
9.92	3-methylbutyl 2-methylbutanoate	0.14
10.07	α-terpinene	0.15
10.53	3-methylbutyl pentanoate	0.15
11.3	3-methyl-4-cyclohexene-1,2-dicarboxylic anhydride	0.33
15.22	α-campholene aldehyde	0.21
15.71	2,5-octadecadiynoic acid, methyl ester	0.24
17.62	α-campholene aldehyde	0.61

https://doi.org/10.24264/icams-2022.II.14

RT	Compound Name	Area
18.42	Isopinocamphone	0.28
20.39	Pinocarvone	1.07
20.71	Bornyl formate	0.16
20.91	Fenchyl acetate	0.21
21.12	D-fenchyl alcohol	2.82
21.41	trans-caryophyllene	0.24
21.54	Terpene-4-ol	0.81
23.69	trans-pinocarveol	6.02
24.19	Cryptone	0.56
25.39	Isoborneol	8.41
26.23	Verbenone	0.16
28.72	Myrtenol	0.14
28.94	cis-p-mentha-1(7),8-dien-2-ol	0.32
30.3	trans-carveol	0.39
30.79	1,3-propanediol, 2,2-dibromo-	0.24
31.85	2-Phenylethyl butanoate	0.14
32.11	cis-p-mentha-1(7),8-dien-2-ol	0.24
36.19	1,5-cyclododecanediol, diacetate	0.63
38.01	Octadecanal, 2-bromo-	0.81
38.26	Veridiflorol	0.19
38.65	Isochiapin B	0.34
39.57	Spathulenol	0.57

CONCLUSIONS

In this study, it is seen that the essential oil contents of *Eucalyptus* spp. differ according to the species. According to the results of this study, breeders will be able to decide more easily which type of eucalyptus to grow.

REFERENCES

Başer, K.H.C., Gülbaba, A.G., Azcan, N., Kara, M., Kırımer, N., Kürkçüoğlu, M., Özek, T. and Özkur N. (2001), "Study of the Technology, Yield and Composition of Essential Oils from Some Eucalyptus species Grown in Turkey", *Eastern Mediterranean Forestry Research Institute* Orman Bakanlığı Yayın No: 084.

Grattapaglia, D. and Kirst, M. (2008), "Eucalyptus Applied Genomics: From Gene Sequences to Breeding Tools", *New Phytologist*, 179, 911–929, https://doi.org/10.1111/j.1469-8137.2008.02503.x.

Gürses, M.K. (1990), "Dünya'da ve Türkiye'de Okaliptüs. Türkiye'de Okaliptüs yetiştiriciliğinin son 50. Yılı", *Kavak ve Hızlı Gelişen Yabancı Tür Orman Ağaçları Araştırma Enstitüsü Dergisi*, 1990/1, İzmit.

Harkenthal, M., Reichling, J., Geiss, H.K. and Saller, R. (1999), "Comparative Study on the *In Vitro* Antibacterial Activity of Australian Tea Tree Oil, Cajuput Oil, Niaouli Oil, Manuka Oil, Kanuka Oil, and Eucalyptus Oil, *Pharmazie*, 54, 460–463.

Kellison, RC. (2001), "Present and Future Uses of Eucalyptus Wood in the World", *Proceedings of the IUFRO International Symposium "Developing the eucalypt of the future"*, Valdivia, Chile: INFOR Instituto Forestal (published on CD).

https://doi.org/10.24264/icams-2022.II.14

Nicoletti, P. and Quaglio, P. (2002), "Valutazione preliminare dell'attivita'antimicrobica in vitro di alcuni oli essenziali", *Microbiol Med*, 17, 373–377.

Rasooli, I., Shayegh, S. and Astaneh, S.D.A. (2009), "The Effect of *Mentha spicata* and *Eucalyptus camaldulensis* Essential Oils on Dental Biofilm", *International Journal of Dental Hygiene*, 7(3), 196–203, https://doi.org/10.1111/j.1601-5037.2009.00389.x.

Salari, M.H., Amine, G., Shirazi, M.H., Hafezi, R. and Mohammadypour, M. (2006), "Antibacterial Effects of *Eucalyptus globulus* Leaf Extract on Pathogenic Bacteria Isolated from Specimens of Patients with Respiratory Tract Disorders", *Clinical Microbiology and Infection*, 12(2), 194–196, https://doi.org/10.1111/j.1469-0691.2005.01284.x.

Soyingbe, O., Oyedeji, A., Basson, A. and Opoku, A. (2013), "The Essential Oil of *Eucalyptus grandis* W. Hill ex Maiden Inhibits Microbial Growth by Inducing Membrane Damage" *Chinese Medicine*, 4(1), Article ID: 28560, 7-14, https://doi.org/10.4236/cm.2013.41002.

Su, Y.C., Ho, C.L., Wang, E.I. and Chang, S.T. (2006), "Antifungal Activities and Chemical Compositions of Essential Oils from Leaves of Four Eucalyptus, *Taiwan Journal of Forest Science*, 21(1), 49–61.

Tsiri, D., Kretsi, O., Chinou, I.B. and Spyropoulos, C.G. (2003), "Composition of Fruit Volatiles and Annual Changes in the Volatiles of Leaves of *Eucalyptus camaldulensis* Dehn Growing in Greece", *Flavour and Fragrance Journal*, 18(3), 244–247, https://doi.org/10.1002/ffj.1220.

https://doi.org/10.24264/icams-2022.II.14

THE EFFECT OF DIFFERENT SOWING TIMES ON CORN SILK TEA

ÖMER KONUŞKAN, DURMUŞ ALPASLAN KAYA
Mustafa Kemal University, Agriculture Faculty, Field Crops Department,
okonuskan@mku.edu.tr; dak1976@msn.com

Corn silks, a by-product of corn, are an important herb used traditionally by many countries to treat many diseases. They are also used as traditional medicine in many parts of the world because of corn silks were used as a source of phenolic component and beverages (diuretic and antiseptic) all over the World. This study aim is determination of proper using method the corn silk image and FTIR at different sowing time of corn. The result of this study show that properties of raw, lyophilized products and evaporated materials are not changed at different sowing time. Also probably, to lyophilized products can be use food additive and prepare tea again with adding water.

Keywords: tea, corn silk, sowing time, FTIR.

INTRODUCTION

Corn is one of the warmest climate cereals in the world and one of the most important people, animals and plants used in the industry. It is known that corn was used kernels and plant with animal which is an indispensable feed source for animals due to its high efficiency in the field and industry. Besides, people have used them for various purposes. Especially as a grain cookie, boiled and flour are the most used parts.
Corn silk is made from stigmas, the yellowish thread like strands from the female flower of corn. In addition, the use of corn silk has been in medicine and in the world and in our country for many years. Corn silk, a by-product of corn, is also a medical product used as a beverage because it is a source of phenolic components (Liu *et al.*, 2012; Sarepoua *et al.*, 2015; Zulkadir *et al.*, 2016; Al-Khayri *et al.*, 2022).

The corn tassel consists of 6.26% protein, 10.1% fat, 11.06% ash and 70.26% carbohydrate (Mohsen and Ammar, 2009). For many years corn tufts have been used in diuretics, antilithiatic, uricosurics and antiseptics. It is used in the treatment of edema and urinary incontinence (Ebrahimzadeh *et al.*, 2003; Hasanuddin *et al.*, 2012). It also consists of proteins, vitamins, carbohydrates, calcium, potassium, magnesium and sodium salts, volatiles oils and steroids such as sitosterol and stigmasterol, alkaloids, and saponins (Ebrahimzadeh *et al.*, 2008).

After the corn harvest, many crops remain on the field. Corn tassel is one of these products. The corn tassels are a vast part of the plant, which could be considered as a great source of products. Currently, many studies have focused on agricultural and industrial wastes in the search for natural antioxidants (Zaho *et al.*, 2013).

Preparing commercial preparations, the material obtained as lyophilized can be better preserved and stored for a long time. Fourier transform infrared (FTIR) methods were used for rapid characterization and classification of different materials. FTIR spectroscopy is rapid, easy to handle and provides easy sampling. So, usage of this technique in food analysis increases nowadays (Gordon *et al.*, 2007; Popescu *et al.*, 2009; Rohman and Man, 2010;).

To accomplish this, we determined surface characteristics of corn stalk powder, determined proper using method the corn silk, determination of the state of these substances inside the corn tassel, determination of the remaining substance after the tea water was evaporated. FTIR and XRD in conjunction with physical characterization measurements are used to examine.

https://doi.org/10.24264/icams-2022.II.15

MATERIALS AND METHODS

Corn silks are taken dent corn (*Zea mays* var. *indentata* Sturt). Corn silk were obtained from the farm of the Faculty of Agriculture, Mustafa Kemal University, Hatay, Turkey (Figure 1). This corn investigation was planted second crop seasons.

Figure 1. Corn silk

Sample Preparation

After harvest, corn silks were dried, milled to a size of 1 mm with porcelain mortar, packaged in glass jars and stored at room temperature (25) till use. Then, all samples (P1: 1st June, P2: 15th June and P3: 10th July) with three different fractions; A (original raw materials), B: (lyophilized after prepare tea) and C: (evaporated residue after boiled tea) were analyzed with FTIR.

https://doi.org/10.24264/icams-2022.II.15

SEM Analysis: One of the key equipment present with in the CSSNT-UPB group, namely a Hitachi SU 8230 Scanning Electron Microscope was used to perform sample analysis. For analysis was used 1kV voltage. Secondary electron images were acquired at 300x magnification.

FITR measurement conditions: FTIR analysis was used Spectrum Two IR Spectrometer from PerkinElmer. Mid infrared ray wave (MIR; 400~4000 cm^{-1}); Scan resolution 1 cm^{-1}; Frequency range 450 – 4.000 cm^{-1}; No. of spectrum 10. FTIR analysis was used Spectrum Two IR Spectrometer from PerkinElmer.

RESULTS AND DISCUSSION

A scanning electron microscope (SEM) is a type of electron microscope that produces images of a sample by scanning the surface with a focused beam of electrons. Scanning Electron Microscope (SEM) images are given Figure 2.

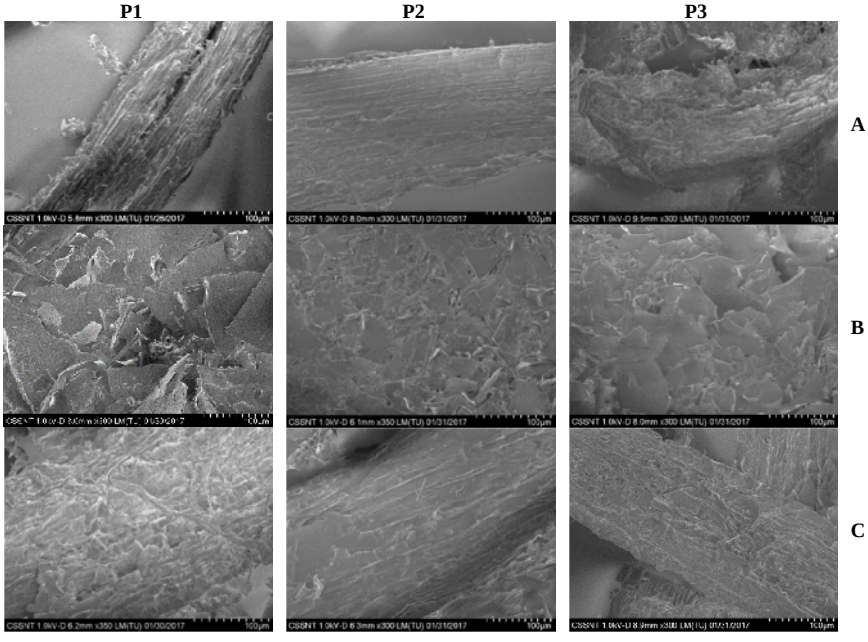

Figure 2. SEM images of corn silks

(P1: 1st June; P2: 15th June; P3: 1st July; A: Original; B: Lyophilized; C: Evaporated)

https://doi.org/10.24264/icams-2022.II.15

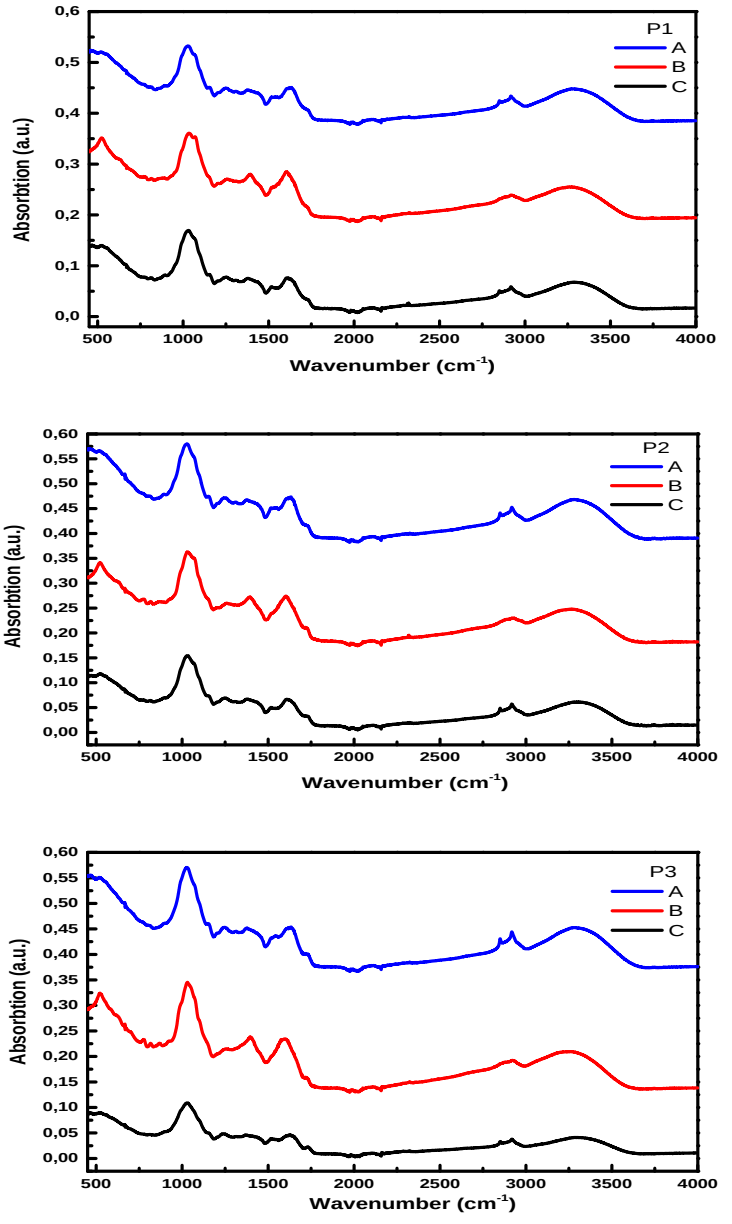

Figure 3. FTIR spectrums of corn silks

(P1: 1st June; P2: 15th June; P3: 1st July; A: Original; B: Lyophilized; C: evaporated)

https://doi.org/10.24264/icams-2022.II.15

It was determined that there was not much change in appearance of SEM images in original and evaporated silk materials of corn silk. But lyophilized materials were seen a looks like small cracks (Figure 2).

The FTIR is used a fingerprint at different materials. The FTIR spectrum 500-4000 cm^{-1} is shown in Figure 3, the result show that no change is produced in the corn silk material. Absorption values were found to be approximately 55, 30 and 10 a.u. in original corn silk, lyophilized and evaporated materials first sowing time.

In all three graphic curves, the images of the active ingredients in corn silk at different wavelengths were determined. It is seen that there is no change in the substances in the corn silks.

FTIR results show that, active ingredients are not affected by sowing times. At the same time, it was clearly seen that depending on the processes performed as A, B, C, the original to lyophilized and evaporation gradually decreased. However, this homogeneously decreasing occurs for all active ingredients without being converted to each other. Hrebicik *et al.* (1995) reported that small molecular changes occurred according to FTIR analysis in their study in rice and oats. Corn varieties and silk developmental stages showed significant variations investigation parameters (Duangpapeng *et al.*, 2018).

CONCLUSIONS

In the results of working, it has been determined that the active substances in the silk can be homogeneously dispersed in water. It has been concluded that all water-soluble substances can be easily stored, used in lyophilized products and food additives, and also corn silks tea can be prepared again by adding hot water with powdered product.

Acknowledgements

This research was supported by CSSNT-UPB through SEM and FTIR analysis. The authors thank to Prof. Marius Enachescu and his team for their support.

REFERENCES

Al-Kyayri, J., Yuksel, A.K., Yuksel, M., Isık, M. and Dikici, E. (2022), "Phenolic Profile and Antioxidant, Anticholinergic, and Antibacterial Properties of Corn Tassel", *Plants*, 11(5), 1899, https://doi.org/10.3390/plants/11151899.

Duangpapeng, P., Ketthaisong, D., Lompthaisong, K., Lertrat, K., Scott, M.P. and Suriharn, B. (2018), "Corn Tassel: A New Source of Phytochemicals and Antioxidant Potential for Value-Added Product Development in the Agro-Industry", *Agronomy*, 8(11), 242, https://doi.org/103390/agronomy8110242.

Ebrahimzadeh, M.A., Pourmorad, F. and Hafe, S. (2008), "Antioxidant Activities of Iranian Corn Silk", *Turkish Journal of Biology*, 32(1), 43–49, https://journals.tubitak.gov.tr/biology/vol32/iss1/7.

Gordon, S.H., Schudy, R.B., Wheeler, B.C., Wicklow, D.T. and Greene. R.W. (1997), "Identification of Fourier Transform Infrared Photoacoustic Spectral Features for Detection of *Aspergillus jlavus* Infection in Corn", *International Journal of Food Microbiology*, 35, 179-186, https://doi.org/10.1016/s0168-1605(96)01217-2.

Hasanuddin, K., Hashim, P. and Mustafa, S. (2012), "Corn Silk (*Stigma Maydis*) in Healthcare: A Phytochemical and Pharmacological Review", *Molecules*, 17, 9697-9715, https://doi.org/10.3390/molecules17089697.

Hrebicik, M., Suchanek, M., Volka, K., Novak, P. and Scooter, C.N.G. (1995), "The Potential of Diffuse Eflectance Spectroscopy in the Examination of Small Changes in Polyethylene and Dry Foods", *Journal of Molecular Structure*, 347,485-494, https://doi.org/10.1016/0022-2860(95)08571-C.

Liu, J., Lin, S., Wang, Z., Wang, C., Wang, E., Zhang, Y. and Liu, J. (2011), "Supercritical Fluid Extraction of Flavonoids from *Maydis stigma* and its Nitrite-Scavenging Ability", *Food and Bioproducts Processing*, 89, 333–339, https://doi.org/10.1016/j.fbp.2010.08.004.

Mohsen, S.A. and Ammar, S.M. (2009), "Total Phenolic Contents and Antioxidant Activity of Corn Tassel Extracts", *Food Chemistry*, 112(3), 595–598, https://doi.org/10.1016/j.foodchem.2008.06.014.

Popescu, C.M., Singurel, G., Popescu, M.C., Vasile, C., Argyropoulas, D.S. and Willför, S. (2009), "Vibrational Spectroscopy and X-Ray Diffraction Methods to Establish the Differences Between Hardwood and Softwood", *Carbohydrate Polymers*, 77(4), 851-857, https://doi.org/10.1016/j.carbpol.2009.03.011.

Rohman, A. and Che Man, Y.B. (2010), "Fourier Transform Infrared (FTIR) Spectroscopy for Analysis of Extra Virgin Olive Oil Adulterated with Palm Oil", *Food Research International*, 43(3), 886-892, https://doi.org/10.1016/j.foodres.2009.12.006.

Sarepoua, E., Tangwongchai, R., Suriharn, B. and Lertrat, K. (2015), "Influence of Variety and Harvest Maturity on Phytochemical Content in Corn Silk", *Food Chemistry*, 169(15), 424–429, https://doi.org/10.1016/j.foodchem.2014.07.136.

Zaho, X., Chen, J., Chen, F., Wang, X., Zhu, Q. and Ao, Q. (2013), "Surface Characterization of Corn Stalk Superfine Powder studied FTIR and XRD", *Colloids and Surfaces B: Biointerfaces*, 104, 207-212, https://doi.org/10.1016/j.colsurfb.2012.12.003

Zulkadir, G., Idikut, L. and Çölkesen, M. (2016), "Determination of Total Antioxidantand Phenolic Amount of Matured and Immature Corn Silk", *International Journal of Agriculture and Wildlife Science*, 2(1), 28-32.

https://doi.org/10.24264/icams-2022.II.15

NEW COSMETICS BASED ON COLLAGEN AND CAFFEINE WITH ANTIMICROBIAL ACTIVITY

MARIA MINODORA MARIN, GEORGETA BUMBENECI, RODICA ROXANA CONSTANTINESCU, CIPRIAN CHELARU, MADALINA GEORGIANA ALBU-KAYA

The National Research & Development Institute for Textiles and Leather - Leather and Footwear Research Institute Division, 93 Ion Minulescu Str., 031215, Bucharest, Romania, icpi@icpi.ro

Cosmetic area has increased worldwide and will continue to expand as long as there are users. At the moment, the interest leads towards cosmetics based on natural ingredients. A common aesthetic problem for majority of the people is represented by dark circles which appear in the infraorbital region. The purpose of this work was to prepare and analyze new cosmetics based on collagen and caffeine with antimicrobial activity that can be used for the treatment of dark circles. The obtained cosmetics are stable at the natural pH of the skin, indicating that new products can be securely used. Images from the optical microscopy evaluation revealed that cosmetics have a soft and foam like appearance. All the obtained cosmetics present excellent stability at 4 and 40°C. The antimicrobial activity against *Staphylococcus aureus* and *Escherichia coli* was also performed showing that the cream with collagen hydrolysate and smallest amount of caffeine is the most efficient Some more analysis need to be performed before notification.

Keywords: collagen hydrolysate, caffeine, cosmetic.

INTRODUCTION

Over the last years, the majority of the people no longer view cosmetics as strange products because everyone uses them, regardless of appearance. Cosmetics are defined by the Food, Drug, and Cosmetics Act (FDCA) as items that are brushed, sprayed on, or applied to the human body in order to clean, enhance, and change one's appearance (Shafie *et al*., 2022). Cosmetics are used to take care of the body's parts, the active compounds they contain helping to improve the healthiness, treatment of acne, and anti-aging of human skin (Joshi *et al*., 2018). Cosmeceuticals are the name given to these active substances (Panico *et al*., 2019; Shafie *et al*., 2022). One of these components, collagen hydrolysate, is known to be used in cosmetic formulations to protect the structure and function of the skin as well as to improve its appearance. In addition to the beauty business, collagen is a naturally occurring biological substance that is used in ophthalmology, dentistry, pharmacy, and biotechnology (Yorgancioglu *et al*., 2013).

Dark circles, which appear in the infraorbital region, are characterized as bilateral, ovoid, homogeneously pigmented macules with a multifactorial etiology. There are a variety of treatments available, such as laser therapy, chemical peels, whitening creams, topical retinoid acid, autologous fat transplantation, injectable fillers, and surgery interventions (Eyraud *et al*., 2021). Therefore, it is not surprising that dark rings are a substantial source of aesthetic concern for certain individuals (Friedmann *et al*., 2015).

The naturally occurring methylxanthine caffeine is found in the cherry beans of *Rubiaceae* plants. Caffeine can be consumed by people through foods, drinks, dietary supplements, drugs and cosmetics (Bury *et al*., 2021). Various animal and human data addressing the pharmacological and toxicological effects of caffeine are available. Caffeine is a well-known compound with a wealth of data (Alexander-White *et al*., 2021). Also, the efficacy and tolerance of a cream based on caffeine and used for the improving of the visible, under-eye dark circles, was evaluated for different clinical studies (Ahmadraji *et al*., 2015). Since the dawn of time, cosmetics have played a significant role in human life. Although they are not required to be sterile microbiologically, they must

https://doi.org/10.24264/icams-2022.II.16

be of a proper quality for consumer health (Halla *et al*., 2018). It has been established that these cosmetics are susceptible to contamination by microorganisms from the production environment or from raw materials, particularly water, and that the contamination can happen either during or after production due to unsanitary storage conditions (Halla *et al*., 2018). The fragrance, color, viscosity, and performance of cosmetic products may alter unintentionally as a result of microbial contamination (Halla *et al*., 2018). Due to the elements in their composition, cosmetics are a good growth media for microorganisms (Lundov *et al*., 2009).

The aim of this research work was to obtain and analyze new cosmetics based on collagen and caffeine with antimicrobial activity that can be used for the treatment of dark circles. The obtained cosmetics are stable at the natural pH of the skin, indicating that new products can be securely used.

MATERIALS AND PREPARATION METHOD

Materials

Type I collagen hydrolysate was obtained by acidic hydrolysis as we previously described (Ficai *et al*., 2013). Ingredients: Stearine, Lanoline, White wax, Paraffin oil and methylxanthine caffeine were purchased from a local pharmacy. Nutrient agar and nutrient broth and *Staphylococcus aureus* (*S. aureus*, ATCC 6538), *Escherichia coli* (*E. coli*, ATCC 10536) and Cetyl alcohol were purchased from Novachim (Bucharest, Romania).

Preparation of the Cosmetics

The composition of cosmetics is given in Table 1. For all the samples, the components of phase A and phase B were heated using a water bath and heating-resistant Berzelius beakers, under intermittently homogenization. When both parts reached a temperature of about 70-75°C, they were removed from the water bath; part B was mixed with part A under constant stirring for 10 minutes. The recipient was put in a cold-water bath with continuous stirring for 3 minutes. In the cooled composition, the ingredients of phase C were introduced and mixed gradually.

Table 1. Composition of the obtained samples

Phase	Ingredients	C1	C2	C3	C4
A	Stearine, %	7.8	7.8	7.8	7.8
A	Lanoline, %	2.6	2.6	2.6	2.6
A	White wax, %	1.6	1.6	1.6	1.6
B	Paraffin oil, %	27	27	27	27
B	Cetyl alcohol, %	1	1	1	1
B	Ultrapure water, %	48.3	48.2	48	47,6
C	Collagen hydrolysate, %	1.6	1.6	1.6	1.6
C	Caffeine, %	0.1	0.2	0.4	0.8
C	Triethanolamine, %	1.6	1.6	1.6	1.6

The obtained cosmetics were transferred to a sterile vessel and analyzed.

https://doi.org/10.24264/icams-2022.II.16

METHODS

pH Determination

The pH of the obtained cosmetics was determined using an inoLab pH meter.

Stability Determination at 4 and 40°C

The stability determination of the obtained cosmetics was evaluated using a thermostat that ensures a constant temperature of 4 and 40°C, respectively. 5g of the sample was placed in a weighting Petri, covered with a lid and kept in a thermostat for 8 hours at a temperature of 4°C. The Petri dish was removed from the thermostat; the sample was examined, covered with the lid and reinserted into the thermostat at a temperature of 40°C for 8 hours. After that the sample was examined again. The sample is considered stable if the phases do not separate. All the experiments were performed in triplicate for all the samples.

Optical Microscopy

The microscopic determinations of the designed cosmetics were carried out using a LEICA optical microscope model S8AP0, with an increase power factor of 20-160x.

Antimicrobial Activity

Microbiologic tests were performed using ISO 16187:2013 standard - Footwear and footwear components.

When the test is considered to be effective, the antibacterial activity ratio is obtained according to the following formula:

$$R = \frac{C_t - T_t}{C_t} X100\% \quad (1)$$

R – is the ratio of the antibacterial activity;

C_t – is the average of the number of bacteria obtained from three control samples after an incubation period of 18 to 24 h;

T_t – is the average number of bacteria obtained on three samples with antimicrobial effect after an incubation period of 18 to 24 h.

RESULTS AND DISCUSSION

All new cosmetics presented a homogeneous, stable, and free of phase separation state. The pH of the obtained cosmetics ranged from 5.5 to 6, which is in line with the skin's pH (Dănilă *et al*., 2020).

The stability determination of the obtained cosmetics was evaluated. Figure 1 shows the samples before and after the evaluation of stability at 4 and 40°C during 8 hours.

In Figure 1 can be seen that after the determination of the stability at 4 and 40°C, all the creams were stable at the tested temperatures during the 8 hours period of treatment.

Figure 2 shows the images that were acquired after optical microscope investigation of the cosmetics morphology.

Figure 2 showed that all creams exhibit a “foam-like” appearance. The different caffeine amounts are what caused the variations in the microscopic images.

https://doi.org/10.24264/icams-2022.II.16

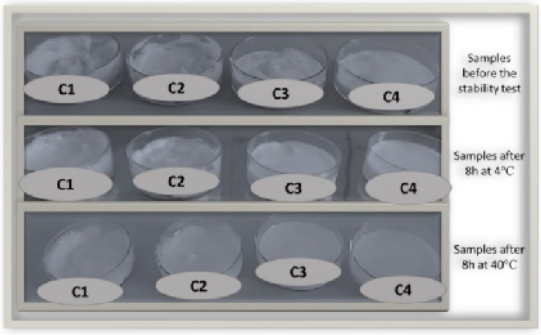

Figure 1. Stability determination at 4 and 40°C of the obtained cosmetics

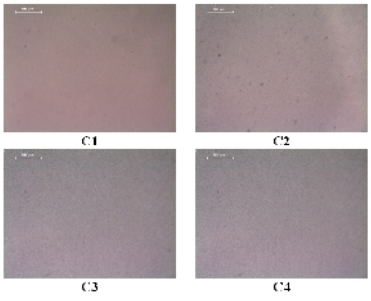

Figure 2. Optical microscopy images of the obtained cosmetics

The most significant feature of cosmetics is to obtain them without developing microbial growth (Dadashi *et al*., 2016). For all obtained cosmetics, the total number of viable aerobic microorganisms was determined. The results can be seen in Table 2.

Table 2. Total number of viable aerobic microorganisms

Microbiological characteristics	Admissibility conditions	Results			
		C1	C2	C3	C4
Total number of aerobic microorganisms (TAMC), CFU/g	Up to 100 CFU/g for topical products Up to 1000 CFU/g for pharmaceutical products	0 CFU	1 CFU	2 CFU	3 CFU
Total number of fungi and filamentous fungi (TYMC) CFU/g	Up to 100 CFU/g for topical products Up to 1000 CFU/g for pharmaceutical products	0 CFU	0 CFU	0 CFU	1 CFU
Staphylococcus aureus	absent	absent	absent	absent	absent
Escherichia coli	absent	absent	absent	absent	absent
Pseudomonas aeruginosa	absent	absent	absent	absent	absent

From the Table 2 can be observed that all tested samples show admissible limits for microbial contamination.

https://doi.org/10.24264/icams-2022.II.16

The antibacterial activity ratio for all new cosmetics is presented in Table 3.

Table 3. Antibacterial activity ratio of the obtained cosmetics (*Staphylococcus aureus ATCC 6538* and *Escherichia coli ATCC 10536*)

Sample	Result (*Staphylococcus aureus ATCC 6538* and *Escherichia coli ATCC 10536*)	R%	Log10 red.
C 1	T0=1,5x105CFU/mL T24= 0 CFU/mL	100%	5,00
C 2	T0=1,5x105 CFU/mL T24=0 CFU/mL	100%	5,00
C 3	T0=1,5x105 CFU/mL T24= 0 CFU/mL	100%	5,00
C 4	T0=1,5x105 CFU/mL T24= 0 CFU/mL	100%	5,00

For all the samples the antibacterial activity ratio was 100 %. Further, in accordance with SR EN ISO 20645/2005—Control of the antibacterial activity, the resulting cosmetics were evaluated by the inhibitory activity. The evaluation of the samples is based on the absence or presence of bacterial proliferation in the contact region between the inoculum and the sample and on the emergence of an inhibition zone surrounding the samples (Figure 3).

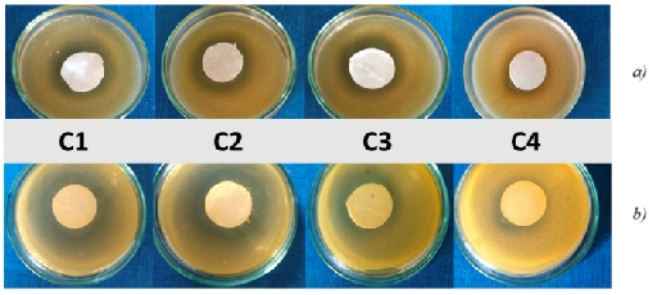

Figure 3. Inhibitory activity against a) *Escherichia coli* and b) *Staphylococcus aureus*

The inhibition areas formed by all the formulations showed diameters varying between 6, and 12.5 mm when tested against *Staphylococcus aureus* and 5.5 and 10 mm against *Escherichia coli* after 24 h of incubation. The samples with the higher concentration of caffeine presented the smallest antimicrobial activity. The best antimicrobial potential against both bacterial strains was obtained for the sample C1 which contain the lowest concentration of caffeine.

CONCLUSIONS

New cosmetics based on collagen and caffeine with antimicrobial activity that can be used for the treatment of dark circles were obtained and evaluated. The obtained cosmetics had a pH that ranged from 5.5 to 6, indicating that the new products can be securely used for skin care. Images from the optical microscopy evaluation revealed that cosmetics have a foam like appearance. All the obtained cosmetics present excellent

https://doi.org/10.24264/icams-2022.II.16

stability at 4 and 40°C. The antimicrobial activity against *Staphylococcus aureus* an *Escherichia coli* was also performed. Further, rheological analyses and clinical tests are necessary for the new obtained cosmetics.

REFERENCES

Ahmadraji, F. and Shatalebi, M.A. (2015), "Evaluation of the Clinical Efficacy and Safety of an Eye Counter Pad Containing Caffeine and Vitamin K in Emulsified Emu Oil Base", *Advanced Biomedical Research*, 6(4), 10, https://doi.org/10.4103/2277-9175.148292.

Alexander-White, C., Mahony, C., Bury, D., Cronin, M., Dent, M., Hack, E., Hewitt, N., Kenna, G., Naciff, J., Ouedraogo, G. and Shepky, A. (2022), "A 10-step Framework for Use of Read-across (RAX) in Next Generation Risk Assessment (NGRA) for Cosmetics Safety Assessment", *Regulatory Toxicology and Pharmacology*, 129, 105094, https://doi.org/10.1016/j.yrtph.2021.105094.

Bury, D., Alexander-White, C., Clewell, H.J., Cronin, M., Desprez, B., Detroyer, A., Efremenko, A., Firman, J., Hack, E., Hewitt, N.J., Kenna, G., Klaric, M., Lester, C., Mahony, C., Ouedraogo, G., Paini, A. and Schepky, A. (2021), "New Framework for a Non-animal Approach Adequately Assures the Safety of Cosmetic Ingredients – A Case Study on Caffeine", *Regulatory Toxicology and Pharmacology*, 123, 104931, https://doi.org/10.1016/j.yrtph.2021.104931.

Dadashi, L. and Dehghanzadeh, R. (2016), "Investigating Incidence of Bacterial and Fungal Contamination in Shared Cosmetic Kits Available in the Women Beauty Salons", *Health Promotion Perspectives*, 10(3), 159-63, https://doi.org/10.15171/hpp.2016.25.

Dănilă, E., Albu Kaya, M.G., Ghica, M.V., Bunea, A.M., Popa, L., Kaya, D.A., Öztürk, Ş., Marin, M.M., Anuța, V. and Dinu Pîrvu, C.E. (2020), "Formulation and Characterization of Anti-aging Cosmetic Emulsions Based on Collagen Hydrolysate and Caffeine", *Proceedings of ICAMS 2020 – 8th International Conference on Advanced Materials and Systems*, 139-144, https://doi.org/10.24264/icams-2020.II.6.

Eyraud, Q., La Padula, S., Pizza, C., Hersant, B. and Meningaud, J.P. (2021), "Carboxytherapy, Subcutaneous Injections of Carbon Dioxide in the Management of Infraorbital Dark Circles: A Reliable and Effective Procedure", *Journal of Cranio-Maxillofacial Surgery*, 49(8), 670-674, https://doi.org/10.1016/j.jcms.2021.01.028.

Ficai, A., Albu, M.G., Birsan, M., Sonmez, M., Ficai, D., Trandafir, V. and Andronescu, E. (2013), "Collagen Hydrolysate Based Collagen/Hydroxyapatite Composite Materials", *Journal of Molecular Structure*, 1037, 154-159, https://doi.org/10.1016/j.molstruc.2012.12.052.

Friedmann, D.P. and Goldman, M.P. (2015), "Dark Circles: Etiology and Management Options", *Clinics in Plastic Surgery*, 42(1), 33-50, https://doi.org/10.1016/j.cps.2014.08.007.

Halla, N., Fernandes, I.P., Heleno, S.A., Costa, P., Boucherit-Otmani, Z., Boucherit, K., Rodrigues, A.E., Ferreira, I.C.F.R. and Barreiro, M.F. (2018), "Cosmetics Preservation: A Review on Present Strategies", *Molecules*, 23(7), 1571, https://doi.org/10.3390/molecules23071571.

Joshi, S., Kumari, R., Vivek, N. and Upasani, V.N. (2018), "Applications of Algae in Cosmetics: An Overview", *International Journal of Innovative Research in Science, Engineering and Technology*, 7(2), 1269- 1278, https://doi.org/10.15680/IJIRSET.2018.0702038.

Lundov, M., Moesby, L., Zachariae, C. and Johansen J. (2009), "Contamination Versus Preservation of Cosmetics: A Review on Legislation, Usage, Infections, and Contact Allergy", *Contact Dermatitis*, 2009(60), 70-78, https://doi.org/10.1111/j.1600-0536.2008.01501.x.

Panico, A., Serio, F., Bagordo, F., Grassi, T., Idolo, A., De Giorgi, M., Guido, M., Congedo, M. and De Donno, A. (2019), "Skin Safety and Health Prevention: An Overview of Chemicals in Cosmetic Products", *Journal of Preventive Medicine and Hygiene*, 60(1), E50–E57, https://doi.org/10.15167/2421-4248/jpmh2019.60.1.1080.

Shafie, M.H., Kamal, M.L., Zulkiflee, F.F., Hasan, S., Uyup, N.H., Abdullah, S., Hussin, N.A.M., Tan, Y.C. and Zafarina, Z. (2022), "Application of Carrageenan Extract from Red Seaweed (Rhodophyta) in Cosmetic Products: A Review", *Journal of the Indian Chemical Society*, 99(9), 100613, https://doi.org/10.1016/j.jics.2022.100613.

Yorgancioglu, A. and Bayramoglu, E.E. (2013), "Production of Cosmetic Purpose Collagen Containing Antimicrobial Emulsion with Certain Essential Oils", *Industrial Crops and Products*, 44, 378-382, https://doi.org/10.1016/j.indcrop.2012.11.013.

ANTIMICROBIAL PROPERTIES OF THE BIOPRODUCTS FORMULATED WITH CHITOSAN AND COLLAGEN

MOHAMMED SHAYMAA OMAR MOHAMMED[1], NICOLETA RADU[1,2*], VERGINICA SCHRODER[3], RODICA ROXANA CONSTANTINESCU[4], NARCISA BABEANU[1]

[1]*University of Agronomic Sciences and Veterinary Medicine of Bucharest, Faculty of Biotechnology, Romania, 59 Marasti Blvd., District 1, Romania; nicoleta.radu@biotehnologii.usamv.ro*

[2]*National Institute of Chemistry and Petrochemistry, Biotechnology Department (ICECHIM), Bucharest Romania*

[3]*Ovidius University, Faculty of Pharmacy, Constanta, Romania, 124 Mamaia Blvd., 1 Aleea Universităţii*

[4] *The National Research & Development for Textiles and Leather - Leather and Footwear Research Institute Division, 93 Ion Minulescu, Bucharest, Romania*

Three types of formulations (stable suspensions) based on collagen, chitosan, limonene and an imidazole derivative were studied through *in vitro* tests, from the point of view of antimicrobial activity. The results obtained on 4 standardized microorganisms, namely *Pseudomonas aeruginosa*, *Escherichia coli*, *Staphylococcus aureus*, *Staphylococcus aureus* MRSA, *Candida albicans*, demonstrated that most of the obtained bioproducts have a local effect (inhibition diameters below 15 mm are obtained) and moderate effect (inhibition diameters located under 20 mm), except bioproducts containing collagen, chitosan, limonene and an imidazole derivative (antibiotic reagent) in mass ratio Col:Chit:Lim:CT=1:1:1:0.1, Col:Chit:Lim:CT=1:1:0:0.1 which exhibit a significant antimicrobial effect on *Staphylococcus aureus* and *Staphylococcus aureus* MRSA. These two formulations also exhibit significant antimicrobial effects for *Candida albicans*, for which the average inhibition diameters obtained are greater than 34 mm.

Keywords: gels, chitosan, collagen, antimicrobials

INTRODUCTION

A variant of counteracting antibiotic resistance is the finding of pharmaceutical formulations, which contain biologically active molecules, for which pathogenic microorganisms do not have resistance genes. Among the molecules of interest are limonene and chitosan. Limonene is mainly found in essential oils obtained from citrus peels which result as a by-product from the food industry (Mohammed *et al*., 2022). As far as chitosan is concerned, it is currently obtained from chitin, which is currently extracted from microfungi and crustaceans (α-chitin), by deacetylation (Babeanu *et al*., 2022). In the world, research is currently being done to obtain pharmaceutical chitosan from natural sources where chitin is in the beta form. The best sources of β-chitin are some species of squid (cephalopods of the order *Teuthida*). These species contain an endoskeleton, called a gladius, which is made of β-chitin and has the shape of a pen or a sword (Cuong *et al*., 2016). Regarding the antimicrobial activity of chitosan obtained from squid endoskeletons, Moduto *et al*. (2019) demonstrated that the solutions obtained from deacetylated squid chitin have antimicrobial action on gram-negative microorganisms involved in stomatologic diseases. Such a study carried out on *P. gingivalis* demonstrated the effectiveness of some culture media in which the concentration of the chitosan solution was greater than 10.75%, in which case the development of the microorganism is totally inhibited. The antimicrobial activity of chitosan solutions was highlighted on pathogenic microorganisms (Ibanez-Peinado, 2017; Zaghoul and Ibrahim, 2019) and on phytopathogenic fungi too (Abirami *et al*., 2020).

https://doi.org/10.24264/icams-2022.II.17

Chitosan membranes obtained from acetic acid solutions, by evaporation of the solvent and chitosan-based nanomaterials containing silver, plant extracts, clays or antibiotics such as tetracycline, gentamicin, ciprofloxacin have antimicrobial activity (Escárcega-Galaz, 2017; Al-Zahrani, 2021). Gels obtained from chitosan and sodium tripolyphosphate (TPP) containing 0.25% chitosan and 0.1% TPP show antimicrobial activity against *S. aureus, P. aeruginosa, E. coli* (Al-Zahrani, 2021). Using as raw material chitin extracted from squid, Yusharani *et al*. (2019) have obtained chitosan with a degree of deacetylation of 82-84%. With chitosan with a high degree of deacetylation, obtained from squid chitin, Cuong *et al*. (2022) have formulated chitosan-tripolyphosphate nanomaterials, using chitosan, TPP, and acetic acid as raw materials. These nanomaterials were included in the culture medium in different concentrations (50ppm; 100ppm; 150ppm; 200ppm; 250ppm) and were tested on fungal phytopathogens. The best results were obtained for concentrations higher than 200 ppm, for microorganisms of the type *A. alternata, P. digitatum* and *Lasiodiplodia sp*. The mechanism of action was highlighted by SEM studies and showed that under the action of nanomaterials with chitosan, the plasma membrane of mycelia and spores is destroyed (Xing *et al*., 2009; Cuong *et al*., 2022). Taking into account the need to create pharmaceutical formulations in which the phenomenon of antibiotic resistance is completely eliminated, in the conducted study we proposed to test the antimicrobial activity of some biopreparations, made with biomolecules obtained from natural resources such as chitosan, collagen and reagents with the potential for use in regenerative medicine, respectively limonene and clotrimazole (Mohammed *et al*., 2022). Reagents used: 2% collagen solution (from INCDPI Bucharest); glacial acetic acid, propylene glycol, pharmaceutical chitosan (DVR Pharm Brasov, Romania) limonene 97% (Merck, Bucharest, Romania), and clotrimazole (Biofarm Bucharest Romania) according to the methodology established by Babeanu *et al*. (2022). Clotrimazole dilutions were made with propylene glycol.

MATERIALS AND METHODS

The Kirby Bauer method was used to evaluate the antimicrobial activity of the produced bioproducts. The microorganisms used were: *Candida albicans* ATTC 10231, *E. coli* ATTC 11303, *P. aeruginosa* ATTC 1338, *S. aureus* ATTC 25923, *S. aureus* MRSA ATTC 33592. The microbial inoculum was made from 24-h cultures old, in physiological serum solution, according to the standard McFarland 0.5 ($1.5x10^8$UFC). The inoculum made in this way was sterilely distributed on the surface of Petri plates with a diameter of 90 mm, with a cotton swab, in the microbiological hood. After 20 minutes, between 3-5 discs of cellulose with a diameter of 6 mm, soaked in each studied bioproduct were deposited on the surface of each Petri plate. The bioproducts tested and their coding is presented in Table 1.

The evaluation of the antimicrobial activity was carried out by comparison with the antibiotic specific to each microorganism tested (Babeanu *et al*., 2022; Zaharie *et al*., 2022; Radu *et al*., 2010; Ioan *et al*., 2020). The evaluation of the antimicrobial activity was carried out on the basis of an empirical scale, established as follows: 6.1≤inhibition diameter≤15 mm=local antimicrobial activity; 15<inhibition diameter≤20 mm=moderate antimicrobial activity; inhibition diameter >20 mm = significant antimicrobial activity.

https://doi.org/10.24264/icams-2022.II.17

RESULTS AND DISCUSSIONS

Studies performed *in vitro* showed that biopreparations synthesized with collagen, chitosan, limonene and or clotrimazole have no effect on *P. aeruginosa*, which is why the results for this microorganism are not presented. Regarding *E. coli*, the results obtained revealed that the bioproducts made have local activity, the inhibition diameters obtained being smaller than 9 mm (Fig. 1), results which are in agreement with those obtained by other researchers (Abirami *et al*., 2021; Zaghloul and Ibrahim, 2019). The studies carried out on *S. aureus* highlighted a local antimicrobial activity for most of the bioproducts, except the bioproduct obtained at the mass ratio Col:Chit:Lim:CT = 1:1:1:0.1 (Fig. 2), for which an activity is obtained significant antimicrobial (inhibition diameter=20.9 mm).

Table 1. Bioproducts used in antimicrobial tests (sources: own studies)

Bioproducts	Appearance	Concentration, % /mass ratio between the components	Code
Clotrimazole	Clear	1%	CT 1%
Clotrimazole	Clear	0.1%	CT 0.1%
Chitosan 1%	Viscous, homogenous	Chitosan 1%	Chit 1%
Solution colagen:chitosan = 1:1	Viscous, homogenous	1:1	Col:Chit =1:1
Solution collagen:chitosan= 3:1	Viscous, homogenous	1:3	Col:Chit =3:1
Solution collagen:chitosan: clotrimazole= 1:1:0.1	Viscous, homogenous	1:1:0.1	Col:Chit=3:1
Solution collagen:chitosan:limonene:clotrimazole= 1:1:1:0.1	Viscous, homogenous	1:1:1:0.1	Col:Chit:Lim: CT=1:1:1:0.1
Solution collagen:chitosan:limonene: clotrimazole=1:1:1:0.5	Viscous, with particle of solid chitosan	1:1:1:0.5	Col:Chit:Lim: CT=1:1:1:0.5

Similar results are also obtained for *S. aureus* MRSA (Fig. 3), where one bioproduct has a moderate antimicrobial effect, respectively the bibioproduct named Col:Chit:Lim:CT=1:1:1:0.1, for which is obtained an average inhibition diameter of 16.18 mm; another one bioproduct exhibit a significant antimicrobial effect respectively the bioproduct named Col:Chit:Lim:CT=1:1:0:0.1, for which correspond an average inhibition diameter of 21 mm. In the case of the two bioproducts, it is interesting to note that the chitosan solution practically has no effect on *S. aureus* MRSA, and on *S. aureus* it only has a local antibacterial effect (inhibition diameter 8.8 mm).

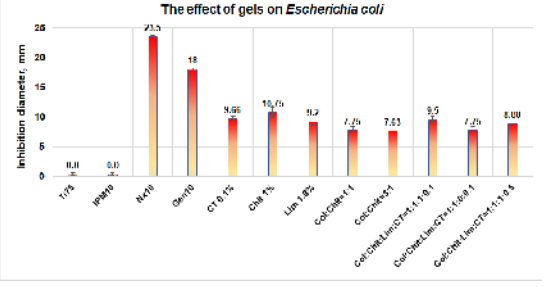

Figure 1. The effect of bioproducts made on *Escherichia coli* (sources: own studies)

Analyzing the experimental data, it can be stated that the bioproduct Col:Chit:Lim:CT = 1:1:1:0.1 has a synergistic effect on *S. aureus* MRSA, synergism due to the presence of chitosan and the antibiotic reagent derived from imidazole (clotrimazole).

Similar results were obtained by Zaghloul and Ibrahim (2019), on chitosan

https://doi.org/10.24264/icams-2022.II.17

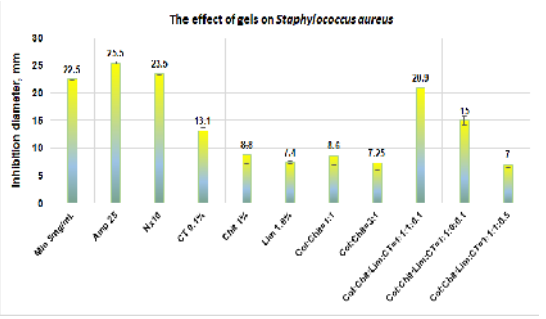

Figure 2. The effect of bioproducts made on *S. aureus* (sources: own studies)

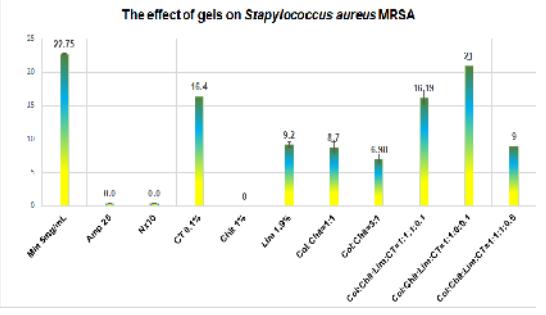

Figure 3. The effect of bioproducts made on *S. aureus* MRSA (sources: own studies)

solutions made in dilute acetic acid. Two types of chitosan were used in the experiments on *S. aureus*: chitosan obtained by the two authors from shrimp exoskeletons and respectively commercial chitosan.

In both cases, the results obtained were the same: a moderate antimicrobial effect corresponding to an inhibition diameter of 16 mm for *S. aureus* (Zaghloul and Ibrahim, 2019). Asli *et al.* (2017) have made the tests on *S. aureus* and *S. aureus* MRSA 1158c with a different type of chitosan, respectively chitosan with different average molecular mass, (1.3 kDa and 4KDa), different degrees of depolymerization less than 3, and degrees of depolymerization situated between 3 and 6.

The results obtained by them for all tested microorganisms showed that at low degrees of depolymerization, a minimum inhibitory concentration (MIC) of 16 µg/mL is obtained, while for solutions made with chitosan with degrees of depolymerization >3, is obtained a value of MIC less than 1 (Asli *et al*., 2017). Asdapoor *et al*. (2021) showed that solutions containing chitosan and clindamycin (antibiotic reagent) act synergistically on *S. aureus*, inhibiting the formation of biofilms. The mechanism of action consists of the electrostatic interaction between chitosan and the charged components of the extracellular microbial matrix the result is the loss of cell wall integrity followed by cell death (Asdapor *et al*., 2021). The mechanism of action was previously confirmed in 2009 by Xing *et al*., through the studies carried out on *S. aureus* with mixed solutions of chitosan (with a degree of deacetylation = 82%) and oleic acid, in which the destruction of the cell wall was confirmed by TEM analysis (Xing *et al*., 2009). The results obtained from the tests carried out on *C. albicans* (Fig. 4), showed that significant antimicrobial activities are obtained in the case of the bioproduct Col:Chit:Lim:CT =1:1:1:0.1, for which obtained an inhibition diameter of 34.7mm, and respectively for the codified bioproduct Col:Chit:Lim:CT =1:1:0:0.1, for which is obtained an inhibition diameter of 35.67 mm. These values are superior to the standard antibiotic used for *Candida sp.*, respectively the clotrimazole 1% solution (inhibition diameter corresponding = 31 mm). For the rest of the bioproducts, local antimicrobial activities are obtained, because the inhibition diameters obtained are below 15mm).

https://doi.org/10.24264/icams-2022.II.17

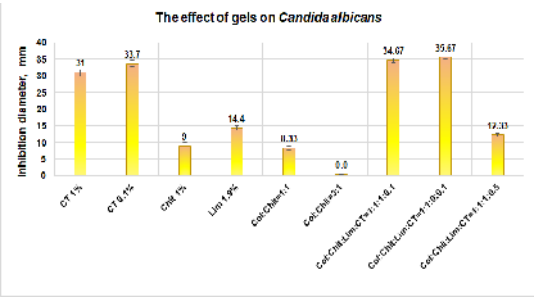

Figure 4. The effect of bioproducts made on *C. albicans* (sources: own studies)

The obtained effect does not seem to be a synergistic one, because in the presence of the 1% chitosan solution, an average inhibition diameter of 9 mm is obtained, and in the presence of the 0.1% clotrimazole solution, is obtained an average inhibition diameter of 33.7%.

In the case of the 0.1% CT solution, the large inhibition diameter obtained is probably due to the solvent in which the antibiotic was diluted, namely propylene glycol, which has the effect of reducing the degree of colonization of *C. albicans* (Henry-Stanley, 2009), and inhibiting the adhesion of pathogenic cells to the substrate (Klotz *et al*., 2004). Similar results were obtained by Zaghloul and Ibrahim (2019), in studies carried out with 1% chitosan gels, for which they obtained inhibition diameters of 15 mm for *C. albicans.* Regarding the mechanism of action, the studies carried out by Pu *et al*. by fluorescence microscopy and respectively by scanning electron microscopy (SEM) demonstrated that the exposure of *C. albicans* to chitosan solutions has the effect of permeabilizing the fungal cell membrane. This action is the basis of the anti-biofilm activity of chitosan solutions (Pu *et al*., 2014). Alburquenque *et al*. in the studies carried out with chitosan solutions on some species involved in candidiasis (microorganisms isolated from patients) such as *C. albicans, C. galabrata, C. krusei, C. tropicalis, C. lusitaniae, C. parpsilopsis*, they obtained minimal inhibitory concentrations (MIC) located between 2-128 mg chitosan /mL, at a pH = 4-4.5 (Alburquenque *et al*., 2010).

CONCLUSIONS

The bioproducts obtained with collagen and chitosan, in the presence of limonene and or an antibiotic derived from imidazole (i.e. clotrimazole) have no effect on bacteria of the *Pseudomonas aeruginosa* type but have a local antimicrobial effect on *E. coli*. In the case of *S. aureus*, only the bioproduct obtained at the mass ratio Col:Chit:Lim:CT=1:1:1:0.1 show a significant antimicrobial effect. The rest of the obtained biopreparations have a local effect. In the case of *S. aureus* MRSA, the bioproduct obtained at the mass ratio Col:Chit:Lim:CT=1:1:0:0.1 has a significant antimicrobial effect. The rest of the bioproducts act similarly to *S. aureus*, with the exception of the 1% chitosan solution, to which *S. aureus* MRSA shows resistance. In the case of *C. albicans*, significant antimicrobial activities are obtained in the case of two bioproducts: Col:Chit:Lim:CT=1:1:0:0.1 and respectively Col:Chit:Lim:CT=1:1:1:0.1, for which the inhibition diameters obtained are greater than 34%.

REFERENCES

Abirami, S., Nagarajan, D., Samrot, A.V., Mini Varsini, A., Sugasini, A. and Anand, D.A. (2020), "Extraction, Characterization, and Utilization of Shrimp Waste Chitin Derived Chitosan in Antimicrobial Activity, Seed Germination, Preservative, and Microparticle Formulation", *Biointerface Research in Applied Chemistry*, 11(2), 8725 – 8739, https://doi.org/10.33263/BRIAC112.87258739.

Alburquenque, C., Bucarey, S.A., Neira-Carrillo, A., Urzúa, B., Hermosilla, G. and Tapia, C.V. (2010), "Antifungal Activity of Low Molecular Weight Chitosan against Clinical Isolates of *Candida* spp.", *Medical Mycology*, 48(8), 1018–1023, https://doi.org/10.3109/13693786.2010.486412.

https://doi.org/10.24264/icams-2022.II.17

Al-Zahrani, S.S., Bora, R.S. and Al-Garni, S.M. (2021), "Antimicrobial Activity of Chitosan Nanoparticles", *Biotechnology & Biotechnological Equipment*, 35(1), 1874-1880, https://doi.org/10.1080/13102818.2022.2027816.

Asadpoor, M., Ithakisiou, G.N., van Putten, J.P.M., Pieters, R.J., Folkerts, G. and Braber, S. (2021), "Antimicrobial Activities of Alginate and Chitosan Oligosaccharides Against *Staphylococcus aureus* and Group B *Streptococcus*", *Front. Microbiol*, 12, 700605, https://doi.org/10.3389/fmicb.2021.700605.

Asli, A., Brouillette, E., Ster, C., Ghinet, M.G., Brzezinski, R., Lacasse, P., Jacques, M. and Malouin, F. (2017), "Antibiofilm and Antibacterial Effects of Specific Chitosan Molecules on *Staphylococcus aureus* Isolates Associated with Bovine Mastitis", *PLOS One*, 12(5), e0176988, https://doi.org/10.1371/journal.pone.0176988.

Babeanu, N., Radu, N., Enascuta, C.-E., Alexandrescu, E., Ganciarov, M., Mohammed, M.S.O., Suica-Bunghez, I.R., Senin, R., Ursu, M. and Bostan, M. (2022), "Obtaining and Characterizing Composite Biomaterials of Animal Resources with Potential Applications in Regenerative Medicine", *Polymers*, 14, 3544, https://doi.org/10.3390/polym14173544.

Cuong, H.N., Minh, N.C., Van Hoa, N. and Trung, T.S. (2016), Preparation and characterization of high purity β-chitin from squid pens (Loligo chenisis), *International Journal of Biological Macromolecules*, 93A, 442-447, https://doi.org/10.1016/j.ijbiomac.2016.08.085.

Cuong, H.N., Minh, N.C., Hoa, N.V., Giang, D.H., Hieu, N.V. and Nam, P.V. (2022), "Antifungal Activity of Squid Pen Chitosan Nanoparticles against Three Fungal Pathogens in Various Citrus Fruits *In Vitro* and *In Vivo*", *Coatings*, 12, 235, https://doi.org/10.3390/coatings12020235.

Escárcega-Galaz, A.A., López-Cervantes, J., Sánchez-Machado, D.I., Brito-Zurita, O.R. and Campas-Baypoli, O.N. (2017), "Antimicrobial Activity of Chitosan Membranes Against *Staphylococcus aureus* of Clinical Origin", in S. Enany, and L.E.C. Alexander (Eds.), *The Rise of Virulence and Antibiotic Resistance in* Staphylococcus aureus, IntechOpen, https://doi.org/10.5772/6598.

Henry-Stanley, M.J. and Wells, C.L. (2009), "Polyethylene Glycol Influences Microbial Interactions with Intestinal Epithelium", *Shock (Augusta, Ga.)*, 31(4), 390–396, https://doi.org/10.1097/SHK.0b013e31818348a5.

Ibañez-Peinado, D., Ubeda-Manzanaro, M., Martínez, A. and Rodrigo, D. (2020), "Antimicrobial Effect of Insect Chitosan on *Salmonella typhimurium*, *Escherichia coli* O157:H7 and *Listeria monocytogenes* survival", *PLOS One*, 15(12), e0244153, https://doi.org/10.1371/journal.pone.0244153.

Ioan, D.-C., Rău, I., Albu Kaya, M.G., Radu, N., Bostan, M., Zgârian, R.G., Tihan, G.T., Dinu-Pîrvu, C.-E., Lupuliasa, A. and Ghica, M.V. (2020), "Ciprofloxacin-Collagen-Based Materials with Potential Oral Surgical Applications", *Polymers*, *12*, 1915, https://doi.org/10.3390/polym12091915.

Klotz, S.A., Gaur, N.K., Lake, D.F., Chan, V., Rauceo, J. and Lipke, P.N. (2004), "Degenerate Peptide Recognition by *Candida albicans* Adhesins Als5p and Als1p", *Infect Immun*, 72, 2029–2034, https://doi.org/10.1128/iai.72.4.2029-2034.2004.

Mohammed, S.O.M., Babeanu, N., Cornea, P. and Radu, N. (2022), "Limonene – A Biomolecule with Potential Applications in Regenerative Medicine", *Scientific Bulletin. Series F. Biotechnologies*, XXVI(2) (accepted, in press).

Mooduto, L., Wahjuningrum, D.A., Agatha Prita, A. and Lunardhi, C.G.J. (2019), "Antibacterial Effect of Chitosan from Squid Pens against *Porphyromonas gingivalis* Bacteria", *Iranian Journal of Microbiology*, 11(2), 177–180, https://pubmed.ncbi.nlm.nih.gov/31341573/.

Perinelli, D.R., Fagioli, L.R., Campana, R., Lam, J.K.W., Baffone, W., Palmieri, G.F., Casettari, L. and Bonacucina, G. (2018), "Chitosan-based Nanosystems and Their Exploited Antimicrobial Activity", *Eur J Pharm Sci*, 117, 8–20, https://doi:10.1016/j.ejps.2018.01.046.

Pu, Y., Liu, A., Zheng, Y. and Ye, B. (2014), "*In vitro* Damage of *Candida albicans* Biofilms by Chitosan", *Experimental and Therapeutic Medicine*, 8, 929-934, https://doi.org/10.3892/etm.2014.1839.

Radu, N., Ghita, I. and Rau, I. (2010), "Therapeutic Effect of Polysaccharides from Plantago Species", *Molecular Crystals and Liquid Crystals*, 523(1), 236/[808]-246/[818], https://doi.org/10.1080/15421401003723078.

Xing, K., Xi, G.C., Ming, K., Cheng, S.L., Dong, S.C. and Hyun, J.P. (2009), "Effect of Oleoyl-Chitosan Nanoparticles as a Novel Antibacterial Dispersion System on Viability, Membrane Permeability and Cell Morphology of *Escherichia coli* and *Staphylococcus aureus*", *Carbohydrate Polymers*, 76(1), 17-22, https://doi.org/10.1016/j.carbpol.2008.09.016.

Yusharani, M.S., Stenley, Harmami, Ulfin, I. and Ni'mah, Y.L. (2019), "Synthesis of Water-Soluble Chitosan from Squid Pens Waste as Raw Material for Capsule Shell: Temperature Deacetylation and Reaction Time", *IOP Conf. Ser.: Mater. Sci. Eng.*, 509, 012070, https://doi.org/10.1088/1757-899X/509/1/012070.

Zaghloul, E. and Ibrahim, H. (2019), "Comparative Study on Antimicrobial Activity of Commercial and Extracted Chitin and Chitosan from *Marsupenaeus japonicus* Shells", *Egyptian Journal of Aquatic Biology and Fisheries*, 23, 291-302, https://doi.org/10.21608/ejabf.2019.31536.

Zaharie, M.G.O., Radu, N., Pirvu, L., Bostan, M., Voicescu, M., Begea, M., Constantin, M., Voaides, C., Babeanu, N. and Roman, V. (2022), "Studies Regarding the Pharmaceutical Potential of Derivative Products from Plantain", *Plants*, 11, 1827, https://doi.org/10.3390/plants11141827.

COMPARISON OF TWO DIFFERENT ETCH SYSTEMS AS ADHESION RESISTANCE IN DENTAL ADHESIVE SYSTEMS

ECE ÖZTOPRAK[1], KAAN ÖZTOPRAK[2]

[1]*DDS, PHD Pedodontic Private Practice Department, DentAnkara Tunalı Hilmi Cad. 82 Ankara-TÜRKİYE, eceoztoprak@hotmail.com*

[2]*Mustafa Kemal University, Dentistry Faculty, Oral Surgery Department, Hatay-TÜRKİYE, alpkaan83@hotmail.com*

Adhesive systems are used in many specialties in dentistry. These systems provide chemical attachment of prosthetic and restorative materials to the tooth surface. The first stage of adhesive systems is the etching process. In the commonly used Total etch systems, acid agent is applied to the tooth first to create roughness on the tooth surface, then the applied bond agent enters this rough surface to ensure retention. The acid agent used is 37% phosphoric acid gel. Normally, phosphoric acid is liquid. It should be applied in gel form in order to be applied in a controlled manner to a certain surface of the tooth and to remain on the desired surface for a long time. Commercially used phosphoric acid gels are produced by a single method and contain the carbomer chemical. Another way to produce gel is silicium dioxide. Acid gels produced with carbomer have a glossy appearance, while acids produced with Silicium have a matte appearance. In this study, we aimed to see the difference in retention of the phosphoric acid gel produced with silicium dioxide compared to the carbomeric acid gel. In this study, we prepared phosphoric acid gel with silicium dioxide and phosphoric acid with carbomer. In our study, 50 extracted caries-free human teeth were used. Orthodontic buttons were attached to the buccal surfaces of the teeth in 2 groups. Phosphoric acid gel prepared with Carbomer was applied for 40 seconds on 25 teeth and phosphoric acid gel prepared with silicium dioxide for 40 seconds on 25 teeth. Afterwards, the teeth were washed with water for 10 seconds and dried, and the orthodontic buttons were adhered with blue light for 40 seconds with Tokuyama bond and flowable composite, and a tensile test was applied to them. There was a statistically significant difference between the tensile force resistance of the buttons attached with two different methods. The teeth in which the gel prepared with silicium dioxide was used showed an average of 6% more resistance to tensile force than the other group. In this study, adhesion strength was measured for the first time by changing the gel base material in acid. We recommend this preparation of acids in adhesive systems, and we believe it can be beneficial for all dentists.

Keywords: dental adhesives, phosphoric acid, tensile test

INTRODUCTION

In dentistry, phosphoric acid is used to etch enamel and, more recently, dentin. It is thought that the acid content is directly correlated with the depth of dentin demineralization (van Meerbeek *et al.*, 1992). The buffering effect of hydroxyapatite and other dentin components limits the interaction of the etching agents with dentin (Sano et al., 1994). The dentin surface is demineralized, the tubules are opened, the smear layer and superior layer of the dentin are removed, and the intertubular dentin's microporosity is increased by the acidic chemicals (Pashley, 1992; Sattabanasuk *et al*., 2007). The tubules are where the acids mostly penetrate. It is believed that the main mechanism of bonding to dentin is the micromechanical entanglement of hydrophilic resins into this demineralized microporous dentin, resulting in the formation of a reticular interwoven hybrid tissue made up of collagen, leftover mineral particles, and resin (Nakabayashi *et al.*, 1982; van Meerbeek *et al.*, 1993). Despite being advertised for years as liquids, the majority of today's etching agents are primarily gels, either thick or thin in consistency (Guba *et al.*, 1994). Gels are thickened by manufacturers to make them easier to handle. The gel forms have the benefit of allowing the practitioner to easily manage how the acid spreads across the surface and visibly detect the acid's presence (Guba *et al.*, 1994).

https://doi.org/10.24264/icams-2022.II.18

Clinically, the demineralizing effect is seen when gas bubbles build up within the gel. Even with rigorous washing, etching gels thickened with silica microparticles leave a particulate deposit on the dentin surface; whereas, polymer-thickened gels leave a clean dentin surface (Kubo et al., 1991). Dentin may generate a layer of denatured collagen and leftover smear layer particles as a result of acid-etching, which prevents the collagen network from being totally exposed (Pashley, 1992). It is unknown if the silica component of some etching chemicals helps to prevent this residual surface layer from forming at all (Hajizadeh *et al*., 2009). Additionally, the effects of additional etching gel ingredients including surfactants, polymers, and other specific modifiers are not fully characterized (Ozcan *et al*., 2015). The aim of this study is which type of thickener in the etchant, similar acidic concentrations of various phosphoric acid etching agents make more tensile strength.

MATERIAL & METHODS

In this study, we prepared %35 phosphoric acid gel (pink color) with silicium dioxide (aerosil 200 - Evonik Industries GER) and %35 phosphoric acid (blue color) with polymer (carbopol – Lubrizol USA). In our study, 50 extracted caries-free human teeth were used. 25 of them grouped for silicium dioxide acid gel, and other 25 of them grouped for polymer acid gel. First the tooth was cleaned with brush handled by angle drive motor. Then acid applied to their mesial enamel side. Acid was kept on tooth about 40 seconds then pressure rinse with air-water mixture. Then dried with air pressure. Bond agent (Tokuyama-Japan) applied with bond brush to surfaces and given 450nm blue light directly for 10 seconds. After that, orthodontic buttons attached with flowable composite (Tokuyama-Japan) and given 450nm blue light from occlusal side for 40 seconds. After that, 0.5mm stainless steel wires binded to buttons and a tensile test (Instron-USA) was applied to them.

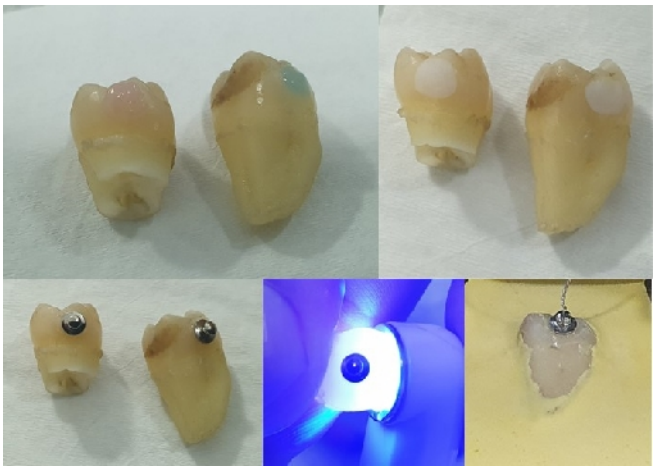

Figure 1. Process flowchart of bonding buttons

https://doi.org/10.24264/icams-2022.II.18

Table 1. Breaking Force Table

Groups	Min BF	Max BF	Average BF
Silicium group	615	960	790
Polymer group	545	850	695

Intermediate Values Used In Calculations:
T = 371.2311
Df = 48
Standard Error Of Difference = 0.283

CONCLUSIONS

In Perdigao *et al.* study, X-ray elemental analysis of both 10% phosphoric acid etching agents confirmed that silicon was present in silica-based gel but not in polymer-based gel. Photomicrographs of dentinal surfaces treated with silica-based showed that a particulate residue was left after rinsing, although the tubule orifices were open. X-ray microanalysis indicated that the residue contained silicon atoms. Cross-sectional views showed funnel-shaped tubules with dissolved peritubular dentin. Particulate debris was also evident in the tubule orifices in the cross-sectional view. When etched with polymer-based, dentinal tubules were opened, but the surface appeared clean and uncontaminated and no silicon was detected with x-ray microanalysis. They also found that there were no significant differences in the bond strengths of specimens etched with the polymer-thickened and silica-thickened gels for either enamel or dentin.(Perdigao *et al.*, 1994)

The shallow depth of intertubular dentin demineralization and the presence of a cuff of superficial peritubular dentin in all the specimens etched with silica-thickened gels may have been caused by a less aggressive effect of the respective etchant. Consequently, this may favor the establishment of high dentin bond strengths, since more calcium might be available (Yamaguchi *et al.*, 1989).

In our study, there was a statistically significant difference ($p \leq 0.05$) between the tensile force resistance of the buttons attached with two different methods. The teeth in which the acid gel prepared with silicium dioxide was used showed an average of 6% more resistance to tensile force than the other group. In this study, tensile test was measured for the first time by changing the gel base material in acid. We recommend this preparation of acids in adhesive systems, and we believe it can be beneficial for all dentists.

REFERENCES

Guba, C.J., Cochran, M.A. and Swartz, M.L. (1994), "The Effects of Varied Etching Time and Etching Solution Viscosity on Bond Strength and Enamel Morphology", *Operative Dentistry*, 19, 146–53.

Hajizadeh, H., Namazikhah, M.S., Majidinia, S., Bagheri, M. and Ghavamnasiri, M. (2009), "Effect of Different Conditioning Protocols on the Adhesion of a Glass Ionomer Cement to Dentin", *Journal of Contemporary Dental Practice*, 10(4), 9–16, https://doi.org/10.5005/jcdp-10-4-9.

Kubo, S., Finger, W.J., Müller, M. and Podszun, W. (1991), "Principles and Mechanisms of Bonding with Dentin Adhesive Materials", *Journal of Esthetic and Restorative Dentistry*, 3, 62–69, https://doi.org/10.1111/j.1708-8240.1991.tb00812.x.

Nakabayashi, N., Kojima, K. and Masuhara, E. (1982), "The promotion of Adhesion by the Infiltration of Monomers into Tooth Substrates", *Journal of Biomedical Materials Research*, 16(3), 265–273, https://doi.org/10.1002/jbm.820160307.

https://doi.org/10.24264/icams-2022.II.18

Ozcan, R., Seseogullari-Dirihan, R., Üçtaşli, M., Tay, F.R., Pashley, D.H. and Tezvergil-Mutluay, A. (2015), "Effect of Polyacrylic Acid on Dentin Protease Activities", *Dental Materials*, 31(8), 901–906, https://doi.org/10.1016/j.dental.2015.04.018.

Pashley, D.H. (1992), "Smear Layer: Overview of Structure and Function", *Proceedings of the Finnish Dental Society*, 88(Suppl 1), 215–224.

Perdigao, J., Denehy, G.E. and Swift, E.J. (1994), "Silica Contamination of Etched Dentin and Enamel Surfaces: A Scanning Electron Microscopic and Bond Strength Study", *Quintessence International*, 25, 327–33.

Sano, H., Shono, T., Takatsu, T., Hosoda, H. (1994), "Microporous Dentin Zone Beneath Resin-Impregnated Layer", *Operative Dentistry*, 19(2), 59–64.

Sattabanasuk, V., Vachiramon, V., Qian, F. and Armstrong, S.R. (2007), "Resin-Dentin Bond Strength as Related to Different Surface Preparation Methods", *Journal of Dentistry*, 35(6), 467–475, https://doi.org/10.1016/j.jdent.2007.01.002.

van Meerbeek, B., Dhem, A., Goret-Nicaise, M., Braem, M., Lambrechts, P. and Vanherle, G. (1993), "Comparative SEM and TEM Examination of the Ultrastructure of the Resin-Dentin Interdiffusion Zone", *Journal of Dental Research*, 72(2), 495–501, https://doi.org/10.1177/00220345930720020501.

van Meerbeek, B., Inokoshi, S., Braem, M., Lambrechts, P. and Vanherle, G. (1992), "Morphological Aspects of the Resin-Dentin Interdiffusion Zone with Different Dentin Adhesive Systems", *Journal of Dental Research*, 71(8), 1530–1540, https://doi.org/10.1177/00220345920710081301.

Yamaguchi, R., Powers, J.M. and Dennison, J.B. (1989), "Parameters Affecting in Vitro Bond Strength for Composites to Enamel and Dentin", *Dental Materials*, 5(3), 153–156, https://doi.org/10.1016/0109-5641(89)90003-1.

https://doi.org/10.24264/icams-2022.II.18

COMPARISON OF SURFACE PROCESSES APPLIED TO PRESERVE THE HYDROPHILIC PROPERTY OF IMPLANTS

KAAN ÖZTOPRAK[1], ECE ÖZTOPRAK[2]

[1]*Mustafa Kemal University, Dentistry Faculty, Oral Surgery Department, Hatay-Türkiye, alpkaan83@hotmail.com*

[2]*DDS, PHD Pedodontic Private Practice Department, DentAnkara Tunalı Hilmi Cad. 82 Ankara-Türkiye, eceoztoprak@hotmail.com*

Today, studies are carried out on many surface modification techniques to improve the surface properties of dental implants. The common goal of all these studies is to increase cell retention on the implant surface and to perform implantation with high biomechanical properties and biocompatibility. Anodized implants are hydrophilic due to their surface properties. The hydrophilic nature of the implant surface has been found to be beneficial for osseointegration in many studies. After the implant surface anodization process, the hydrophilicity on the surface is at the highest level and the hydrophilic feature on the surface decreases as it comes into contact with air. Many commercially hydrophilic implants lose their hydrophilic properties early in their shelf life. Researchers are in search of longer preservation of hydrophilic properties in implants. In our study, we aimed to preserve the hydrophilic feature on the titanium surface for a longer time by forming a thin layer of NaCl on the surface by cleaning the Ti Gr4 1cm^3 plate pieces immediately after the micro-arc oxidation process and dipping them into isotonic NaCl solution. The study was done in 5 groups. In the first group, titanium was cleaned after the micro-arc oxidation (MAO) process and the water contact angle (WCA) on the surface was measured. The remaining 4 groups were divided as MAO applied and 15 days passed, MAO + NaCl applied and 15 days passed, MAO applied and 30 days passed, MAO + NaCl applied and 30 days passed. Water contact angle measurements were made for all groups and their hydrophilic properties were compared. In our experiment, the highest WCA was found in the parts measured immediately after anodization in the first group. Titanium surfaces coated with NaCl showed 14% lower WCA after anodization compared to untreated titanium after 15 days. In the 30-day groups, 20% lower WCA was found in the titanium treated with NaCl compared to the untreated ones. NaCl treatment on the hydrophilic surface of titanium helped to preserve its hydrophilic property over time. In this study, it was observed that the hydrophilic properties on the surface of the implants that were treated with NaCl for the first time on hydrophilic titanium were preserved for a longer period of time. We propose to increase the osseointegration quality by performing such applications on hydrophilic implants.

Keywords: dental implants, surface treatments, hydrophilic

BACKGROUND & AIM

Due to its strong corrosion resistance and excellent biocompatibility, titanium (Ti) is a material that is frequently used in orthopedic and dental implants (Adell *et al.*, 1990). Due to titanium oxide's (TiO_2) capability to create bone-like apatite in a body environment, TiO_2 has been demonstrated to exhibit strong physicochemical bonding between a Ti implant and live bone (Hazan *et al.*, 1993). When exposed to air and atmospheric water vapor, an oxide surface layer with a thickness of 1.5–10 nm naturally develops on titanium (Sul *et al.*, 2001). TiO_2 can have crystalline or amorphous forms, depending on the manufacturing conditions. Crystalline oxides, such as rutile and anatase, exhibit a number of unique characteristics, including photocatalytic behavior, super hydrophilicity, and biocompatible characteristic (Diamanti *et al*., 2015). As a result of the mechanical qualities, corrosion resistance, non-biotoxicity, and biocompatibility, anodic oxidation is used to alter the surfaces and properties of titanium (Abdullah and Sorrell, 2007). The controlled formation of an oxide layer surface substantially thicker than that formed naturally is made possible by anodic oxidation of titanium. Depending on the

https://doi.org/10.24264/icams-2022.II.19

circumstances, including the electrolyte type, solution concentration, and applied voltage, these coatings may be thick or porous, amorphous or crystalline (Jaeggi *et al.*, 2005). Sulphuric and phosphoric acids are the electrolytes that are most frequently used to anodize titanium.

Anodized implants are hydrophilic due to their surface properties. The hydrophilic nature of the implant surface has been found to be beneficial for osseointegration in many studies. After the implant surface anodization process, the hydrophilicity (Vangolu *et al.*, 2011) on the surface is at the highest level and the hydrophilic feature on the surface decreases as it comes into contact with air. Many commercially dry-state hydrophilic implants lose their hydrophilic properties early in their shelf life. Researchers are in search of longer preservation of hydrophilic properties in implants (Lüers *et al.*, 2016). In our study, we aimed to preserve the hydrophilic feature on the titanium surface for a longer time by forming a thin layer of NaCl.

MATERIALS AND METHODS

Preparation: The 200 samples was prepared by wet hand-polishing Cp-Ti foils (unknown source, China) with dimensions of 10 mm x 10 mm x 0.5 mm, immersion in an ultrasonic bath with acetone for 10 minutes, washing with distilled water, and compressed air drying. In an electrochemical cell with 4 L %10 concentration of aqueous solution of H_3PO_4 (Birpa, 85 wt%).

Figure 1. Ti Gr4 1cm^3 plate pieces

Anodization: Titanium sheets dipped into microarc solution. Power source generated 110v DC, 10A through anode. For cathode we used stainless steel plate. Titanium plates stayed for 1 hour in the anodization process. After anodization all samples cleaned in a 180W ultrasonic bath for 20 minutes in distilled water. Then dried with air pressure. Except for MI group, other groups dipped in the isotonic 0,9 NaCl solution.

https://doi.org/10.24264/icams-2022.II.19

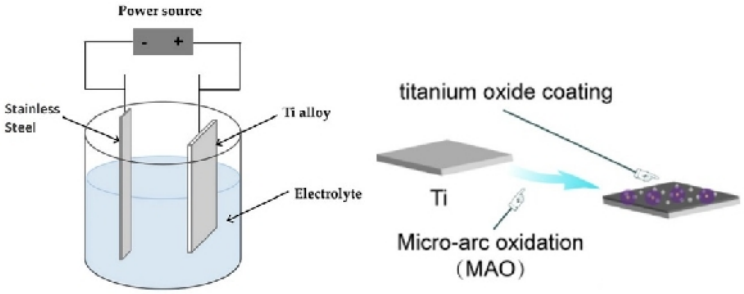

Figure 2. Ti anodizing process

The study was done in 5 groups. Every group have 40 samples. In the first group, titanium was cleaned after the micro-arc oxidation (MAO) process, and the water contact angle (WCA) on the surface was immediately measured after cleaning (MI). The remaining four groups were divided as MAO applied and 15 days passed (M15), MAO + NaCl applied and 15 days passed (MN15), MAO applied and 30 days passed(M30), MAO + NaCl applied and 30 days passed. All groups were held in the dry state in the open air. Water contact angle measurements were made for all groups and their hydrophilic properties were compared.

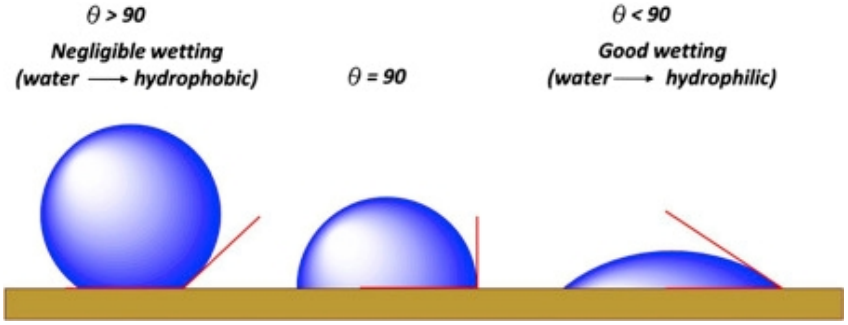

Figure 3. Water contact types

https://doi.org/10.24264/icams-2022.II.19

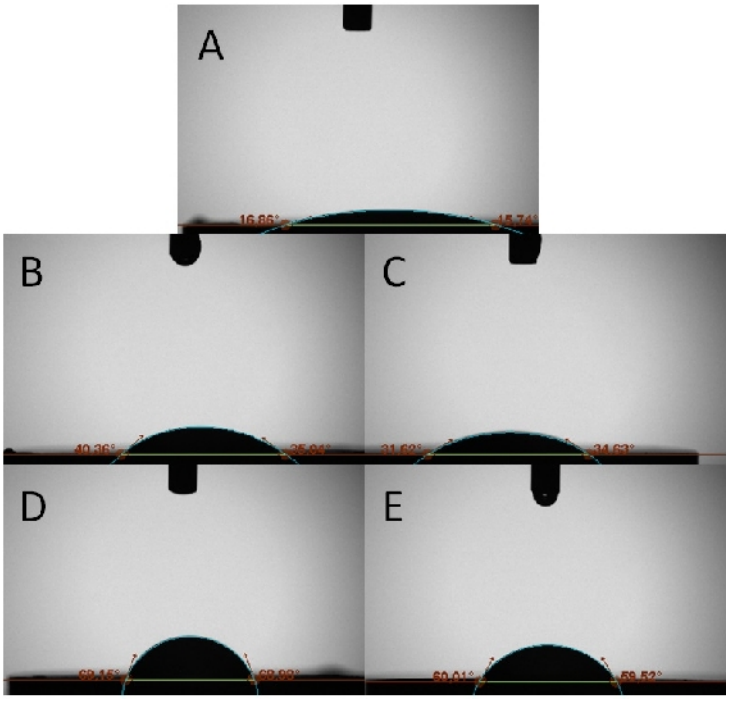

Figure 4. Contact angle samples of groups. A:MI, B:M15, C:MN15, D:M30, E:MN30

Table 1. Contact angle table of groups

Group	Lowest WCA	Highest WCA	Average	SD
MI	15,61	17,22	16,28	
M15	34,31	42,66	37,52	15,01
MN15	28,13	36,41	32,26	11,29
M30	64,58	71,11	67,25	36,04
MN30	48,18	61,74	53,80	26,53

A few standard methods for analyzing surface wettability have been modified for titanium implant surfaces. The sessile drop technique, which involves placing a drop of the desired wetting liquid on the surface of the specimen and measuring the angle between the tangent of the drop at the solid/liquid/gas three-phase boundary and the horizontal baseline of the solid surface, is the most popular method for understanding the wetting behavior of a given solid material. The so-called contact angle (CA) measures how well the surface has been moistened by the particular liquid being utilized.

In our experiment, as we expect the highest WCA was found in the parts measured immediately after anodization in the first group (MI). The (MI) group shows average of 16,28 degrees WCA. When 15 days passed the M15 group lost some hydrophilicity. WCA decreases from an average 16,28 to 37,52 degrees. Titanium surfaces coated with NaCl showed 14% lower WCA after anodization compared to untreated titanium after 15 days. In the 30-day groups, the M30 group loses more hydrophilicity. WCA degreases

https://doi.org/10.24264/icams-2022.II.19

from 15-day average of 37,52 to 67,25 degrees. 20% lower WCA was found in the titanium treated with NaCl compared to the untreated ones. NaCl remains on the titanium surface as a thin layer. This thin salt layer helps to keep hydrophilicity over time in dry state. It should be also the hydrophilic property of salt. TiO_2 layer itself has less durable hydrophilic property over time.

CONCLUSION

Salts are generally dissolves in water. When making a salt layer on some surface, the water first dissolves that salt that bound to surface. So it expected to give some hydrophilic properties (Ali *et al*., 2022). Immediately anodized titanium, the hydrophilic state high at the TiO_2 surface. NaCl solution absorbed to the surface through deep in nanoholes with high hydrophilic energy and when dried, all nanotubes filled with hydrophilic salt molecules. NaCl treatment on the hydrophilic surface of titanium helped to preserve its hydrophilic property over time in dry state. In this study, it was observed that the hydrophilic properties on the surface of the implants that were treated with NaCl on hydrophilic titanium were preserved for a longer period of time. Lüers *et al*. (2016) also get similar results in their experiment with $MgCl_2$, $CaCl_2$, PBS, and KPB types salts. We know that hydrophilic feature is good for osseointegration in previous studies. We suggest salt layers to increase the osseointegration quality by performing such applications on hydrophilic implants.

REFERENCES

Abdullah, H.Z. and Sorrell, C.C. (2007), "Preparation and Characterisation of TiO_2 Thick Films Fabricated by Anodic Oxidation", *Materials Science Forum*, 561–565, 2159–2162, https://doi.org/10.4028/www.scientific.net/MSF.561-565.2159.

Adell, R., Eriksson, B., Lekholm, U., Brånemark, P.I. and Jemt, T. (1990), "Long-Term Follow-Up Study of Osseointegrated Implants in the Treatment of Totally Edentulous Jaws", *International Journal of Oral & Maxillofacial Implants*, 5, 347–59.

Ali, M.A., Volmert, B., Evans, C.M. and Braun, P.V. (2022), "Static and Dynamic Gradient Based Directional Transportation of Neutral Molecules in Swollen Polymer Films", *Angewandte Chemie International*, 61(41), e202206061, https://doi.org/10.1002/anie.202206061.

Diamanti, M.V., Ormellese, M. and Pedeferri, M. (2015), "Application-Wise Nanostructuring of Anodic Films on Titanium: A Review", *Journal of Experimental Nanoscience*, 10(17), 1285–1308, https://doi.org/10.1080/17458080.2014.999261.

Hazan, R., Brener, R. and Oron, U. (1993), "Bone Growth to Metal Implants is Regulated by Their Surface Chemical Properties", *Biomaterials*, 14, 570–574, https://doi.org/10.1016/0142-9612(93)90172-X.

Jaeggi, C., Kern, P., Michler, J., Zehnder, T. and Siegenthaler, H. (2005), "Anodic Thin Films on Titanium Used as Masks for Surface Micropatterning of Biomedical Devices", *Surface and Coatings Technology*, 200, 1913–1919, https://doi.org/10.1016/j.surfcoat.2005.08.021.

Lüers, S., Laub, M. and Jennissen, H.P. (2016), "Protecting Ultra- and Hyperhydrophilic Implant Surfaces in Dry State from Loss of Wettability", *Current Directions in Biomedical Engineering*, 2(1), 557–560, https://doi.org/10.1515/cdbme-2016-0123.

Sul, Y.T., Johansson, C.B., Jeong, Y. and Albrektsson, T. (2001), "The Electrochemical Oxide Growth Behaviour on Titanium in Acid and Alkaline Electrolytes", *Medical Engineering & Physics*, 23(5), 329–346, https://doi.org/10.1016/S1350-4533(01)00050-9.

Vangolu, Y., Alsaran, A. and Yildirim, O.S. (2011), "Wear properties of Micro Arc Oxidized and Hydrothermally Treated Ti_6Al_4V Alloy in Simulated Body Fluid", *Wear*, 271, 2322–2327, https://doi.org/10.1016/j.wear.2010.12.039.

https://doi.org/10.24264/icams-2022.II.19

https://doi.org/10.24264/icams-2022.II.19

INVESTIGATION OF ACID RESIDUE ON THE SURFACE OF DENTAL IMPLANTS AFTER DIFFERENT SURFACE CLEANING PROCESSES

KAAN ÖZTOPRAK[1], ECE ÖZTOPRAK[2]

[1] *Mustafa Kemal University, Dentistry Faculty, Oral Surgery Department, Hatay-TÜRKİYE, alpkaan83@hotmail.com*

[2] *DDS, PHD Pedodontic Private Practice Department, DentAnkara Tunalı Hilmi Cad. 82 Ankara-TÜRKİYE, eceoztoprak@hotmail.com*

For dental implants to osseointegrate well, all clinical and production conditions must be perfect. Due to some negativities in production conditions, unwanted residual materials may remain on the implant surfaces, and these may adversely affect osseointegration. While producing implants, some surface treatments are required. These processes are generally based on the principle of increasing the surface area. Thus, they can provide attachment to the bone on more surfaces. Most methods applied to increase the implant surface area include acidic chemicals. After the acid is applied to the implant surfaces, the acid in the pits formed on the surface must be removed entirely. In cases where the acid cannot be completely removed, the remaining acid may cause bone destruction and cause implant loss. For this reason, some processes must be applied to remove residual acid. In this study, we aimed to find better ways to clean the acid residues on the implant surface. We created 2 groups of 20 implants in our study. Micro arc oxidation was applied with sulfuric acid in 2 groups and then washed with distilled water in a 180-watt ultrasonic cleaner. One group of implants was washed with pure water only, and the other group was washed with pure water and chemically neutralized. Sodium Bicarbonate 10% solution was prepared and washed for neutralization; the second group was kept in this solution for 10 minutes and washed with distilled water again. The implants in both groups were placed in 10cc ph7 distilled water and left for one day. After one day, the liquids were measured with a digital pH meter. In the measurement of the water in the group that was washed only with pure water, the average pH was 6.8, while the average pH of the water in the other group was 7. Our study concluded for the first time that basic neutralization on the implant surface could neutralize the acid residue in the microwells. We recommend chemical neutralization in implant manufacturing processes and think it can reduce implant failure rates.

Keywords: dental implants, surface treatments, acid residue

INTRODUCTION

Dental implants can get contaminated due to the ecological system in the mouth cavity with many bacteria or the environmental system outside the oral cavity with inorganic wastes (Yu *et al*., 2016). Common elemental contamination from organic carbon and traces of elements such as oxygen (O), nitrogen (N), calcium (Ca), and phosphorus (P) observed on dental implant surfaces are likely connected to failure in re-osseointegration when areas of an implant have lost osseointegration (Wheelis *et al*., 2017). It has been demonstrated that re-osseointegration occurs when a direct structural and functional union forms between an implant and bone. It has also been demonstrated that properly cleaned implants may re-osseointegrate (Schlee *et al*., 2019). As a result, surface topography, chemical purity, the thickness and composition of the oxide layer, surface cleanliness, and the presence of metallic and non-metallic chemicals on the surface appear to impact the effectiveness of implant osseointegration (Turkyilmaz, 2011). An increasing body of research (Anil *et al*., 2011; Dhaliwal *et al*., 2019) shows that implant surface topography and chemistry have a significant impact on osseointegration by influencing protein signaling and cell migration or differentiation. Surface roughness improves bone-implant contact area, mechanical interlocking, and stress distribution compared to smooth surfaces, favoring osteoblast-like cell

https://doi.org/10.24264/icams-2022.II.20

colonization (Wennerberg and Albrektsson, 2010). However, it has been demonstrated that roughened surfaces increase the deposition of pollutants (Rezaei *et al*., 2018). Nonetheless, the methods through which inorganic and organic pollutants interact with implant surfaces are unknown. Although numerous techniques of implant cleaning have been tried, none have shown reliable outcomes. Implant surface cleansing remains challenging, necessitating the development of newer, efficient procedures (Al-Hashedi *et al*., 2016; Mombelli *et al*., 2018).

To produce the requisite surface characteristics, topographical modification is often employed in titanium-based implants. This involves using a variety of surface treatments, including sandblasting, chemical etching, anodization, laser treatment, and surface coatings (Katona *et al*., 2015). Although these surface treatments can alter the characteristics of the implant surfaces, they can also result in undesirable qualities and hence contamination of the implant surfaces in rare instances. Our bones are made up of collagen, hydroxyapatite ($Ca_{10}(PO_4)_6(OH)_2$, and several anionic and cationic substituents such as carbonates (H_2CO_3), sodium (Na), magnesium (Mg), zinc (Zn), fluorine (F), chlorine (Cl), potassium (K), and silicon (Si) (Šupová, 2015). As a result, when foreign materials are implanted in the human body, they are exposed to a hostile corrosive environment that includes blood, water, Na, Cl, plasma, amino acids, and mucus in saliva (Sasikumar *et al*., 2019). Because of their favorable biocompatibility and mechanical qualities, inorganic metal oxides such as titanium oxide (TiO_2) and related alloys are extensively utilized in dental implants. The capacity of the titanium (Ti) oxide layer to tolerate corrosion in saline and acidic environments makes it an effective implant material that increases the possibility of osseointegration (Chaturvedi, 2009). However, following prolonged contact with live tissue, TiO_2 will emit trace quantities of corrosion products, resulting in dental implant contamination (Chaturvedi, 2009). Corrosion caused by body fluids can induce changes in material structure and the production of undesired inflammatory by-products, compromising the mechanical stability of the implant (Bahraminasab *et al*., 2019). Dental implants may potentially be infected during the marketing process, i.e., before any contamination from the mouth cavity. As a result, contaminations may be influenced by factors other than biological in situ effects. As a result, manufacturers must evaluate and confirm that sterile packaged medical equipment is free of surface contaminants regularly (Duddeck *et al*., 2019). Galvanic corrosion is another source of dental implant contamination. This electrochemical reaction happens when electrons may easily flow between two materials with sufficiently differing electrical potentials (Noumbissi *et al*., 2019). The surgical variables, the timing of implant surgery, site of implant placement, type of implant osteotomy, implant design, and implant stability are the essential parameters that might impact the early healing phase of the implant site and the survival rate of dental implants (Shadid *et al*., 2014). These factors significantly influence the likelihood of pollutant exposure. These pollutants have the potential to cause dental implants to fail in their function of replacing missing teeth. Furthermore, there is a financial burden on the patient and health care providers to spend on cleaning technologies. As a result, it is important to investigate the cause of dental implant failures. We will search for residual acid contaminants in this study. The purpose of this paper is also to discuss the possible effects of these pollutants on Ti dental implants.

The mouth contains Sulphur (S) compounds, as well as Na, K, Ca, PO_4, CO_2, and mucin (Oshida *et al*., 2010). As a result of the implant surfaces' sandblasting and etching, traces of sulfates, fluorides, magnesium oxides, silicates, and calcium oxides

https://doi.org/10.24264/icams-2022.II.20

are discovered (Henningsen *et al*., 2018). Pre-processed Ti surfaces are typically treated with hydrochloric acid (HCl) and sulfuric acid (H_2SO_4). S was found in the residual S_2O_8 2 or SO_4 2 from samples treated with either sodium persulfate ($Na_2S_2O_8$) or H_2SO_4. However, the Ti acid complexes (titanium sulfate) were less soluble in water and hence unsuitable for Ti surface cleaning because they might disrupt the chemical modification of the Ti surface (Takeuchi *et al*., 2003). Giner *et al*. revealed that a twofold acid etching procedure with hydrofluoric acid followed by sulfuric acid resulted in a dual roughness Ti surface that promoted osteoblast adhesion, proliferation, and differentiation, hence improving osseointegration. Non-thermal plasma treatment can entirely remove S from Ti samples, while UV treatment cannot (Giner *et al*., 2017).

MATERIAL AND METHODS

In our study, we created two groups of 20 implants each. 4L %5 by weight sulfuric acid solution prepared. Voltage and current computer-controlled anodization machine used and implants put on the anode side. In the bath we use stainless steel plates as cathode. At 110v 10A current micro-arc oxidation completed in 5 minutes. Then implants are taken out immediately. All implants were washed with distilled water in a 180-watt ultrasonic cleaner. One group of implants was washed with pure water only, and the other group was washed with pure water and chemically neutralized. Sodium Bicarbonate 10% solution was prepared and washed for neutralization, Sodium Bicarbonate group was kept in this solution for 10 minutes and washed with distilled water again. The implants in both groups were placed in 10cc pH7 distilled water and left for one day. After one day, the liquids were measured with a digital pH meter (Metravi Ph-600).

Figure 1. Ph meter

Table 1. pH data on groups

Cleaning type	Lowest pH	Highest pH	Average
Pure water group	6.7	6.9	6.8
Sodium Bicarbonate	7	7	7

$$NaHCO_3 + H_2SO_4 = Na_2SO_4 + H_2O + CO_2 \quad (1)$$

In the measurement of the water in the group that was washed only with pure water, the average pH was 6.8, while the average pH of the water in the Sodium Bicarbonate group was 7. The experiment shows that there are also left H_2SO_4 remnants on the surface after washing with pure water.

https://doi.org/10.24264/icams-2022.II.20

CONCLUSIONS

Almost all dental implants contain acidification and etching processes as fabrication. After the surface is dispersed with acid, very small micro-pits are formed on the surface. In the anodization process, these micro-wells are much smaller and reach nano-structures. It is doubtful that these small pits of implants that are naturally treated in acid can be completely cleaned and the lowest points of the holes can be completely cleansed from acid. The lengths of these pits are in the size of micrometers and the pit diameters of the implants in nanostructure take the shape of a much longer well than the diameters of the holes since they are in Nano diameter. TiO_2 nanotube arrays with an average diameter of 60~80 nm and an average length of 2~4 micrometer (Shang *et al*., 2019). Since this process takes place in acid, it is very possible for acid molecules to remain in these pits at depths that cannot be removed by water.

This study shows us that after washing the surface with pure water, we still see Sulfuric acid residues on the surface. We know from chemical equations that when sulfuric acid combines with sodium bicarbonate, sodium sulfate salt which is pH neutral is also released, carbon dioxide and water. When the sulfuric acid residues that water cannot completely remove, combine with sodium bicarbonate, a neutral sodium sulfate salt is formed by chemical reaction, which can be easily removed by dissolving in water. If this acid cannot be completely removed from the surface after the implants are etched with Sulfuric acid, it may interact with the body during implantation and affect the osseointegration significantly negatively by making primary resorption of the bone with which it is in direct contact. For this reason, our study shows that instead of removing the chemical acid residue on the surface with normal water, it can be removed in a completely healthy way after chemically neutralizing it with alkaline components. Despite the acid residues on the surface of the implants, there have been no large-scale studies so far. As a result of some implant surgeries, early implant losses that cannot be attributed to any cause can be seen. If there is acid residue left on the surface and if contact with these acid molecules directly with the bone in the surgical area, this can cause direct primary bone destruction. For this reason, our study may be a new perspective in light of the primary resorption and osseointegration problems of implants.

REFERENCES

Al-Hashedi, A.A., Laurenti, M., Benhamou, V. and Tamimi, F. (2016), "Decontamination of Titanium Implants Using Physical Methods", *Clinical Oral Implants Research*, 28, 1013–1021, https://doi.org/10.1111/clr.12914.

Anil, S., Anand, P.S., Alghamdi, H. and Jansen, J.A. (2011), "Dental Implant Surface Enhancement and Osseointegration", in: I. Turkyilmaz (ed.), *Implant Dentistry – A Rapidly Evolving Practice*, 83-108, https://doi.org/10.5772/16475.

Bahraminasab, M., Bozorg, M., Ghaffari, S. and Kavakebian, F. (2019), "Electrochemical Corrosion of Ti-Al_2O_3 Biocomposites in Ringer's Solution", *Journal of Alloys and Compounds*, 777, 34–43, https://doi.org/10.1016/j.jallcom.2018.09.313.

Chaturvedi, T.P. (2009), "An Overview of the Corrosion Aspect of Dental Implants (Titanium and Its Alloys)", *Indian Journal of Dental Research*, 20, 91–98, https://doi.org/10.4103/0970-9290.49068.

Dhaliwal, J.S., Rahman, N.A., Knights, J., Ghani, H. and de Albuquerque Junior, R.F. (2019), "The Effect of Different Surface Topographies of Titanium Implants on Bacterial Biofilm: A Systematic Review", *SN Applied Sciences*, 1, 1–16, https://doi.org/10.1007/s42452-019-0638-6.

Duddeck, D.U., Albrektsson, T., Wennerberg, A., Larsson, C. and Beuer, F. (2019), "On the Cleanliness of Different Oral Implant Systems: A Pilot Study", *Journal of Clinical Medicine*, 8(9), 1280, https://doi.org/10.3390/jcm8091280.

https://doi.org/10.24264/icams-2022.II.20

Giner, L., Mercade, M., Torrent, S., Punset, M., Perez, R.A., Delgado, L.M. and Gil, F.J. (2017), "Double Acid Etching Treatment of Dental Implants for Enhanced Biological Properties", *Journal of Applied Biomaterials and Functional Materials*, 16, 83–89, https://doi.org/10.5301/jabfm.5000376.

Henningsen, A., Smeets, R., Heuberger, R., Jung, O.T., Hanken, H., Heiland, M., Cacaci, C. and Precht, C. (2018), "Changes in Surface Characteristics of Titanium and Zirconia after Surface Treatment with Ultraviolet Light or Non-Thermal Plasma", *European Journal of Oral Sciences*, 126(2), 126–134, https://doi.org/10.1111/eos.12400.

Katona, B., Dobos, G. and Kiss, G. (2015), "Examination of the Surface Phosphorus Content of Anodized Medical Grade Titanium Samples", in: T. Berecz, K. Májlinger, I.N. Orbulov and P.J. Szabó (eds.), *Materials Science Forum*, 812, 339–344, https://doi.org/10.4028/www.scientific.net/msf.812.339.

Mombelli, A., Hashim, D. and Cionca, N. (2018), "What is the Impact of Titanium Particles and Biocorrosion on Implant Survival and Complications? A Critical Review", *Clinical Oral Implants Research*, 29(S18), 37–53, https://doi.org/10.1111/clr.13305.

Noumbissi, S., Scarano, A. and Gupta, S. (2019), "A Literature Review Study on Atomic Ions Dissolution of Titanium and Its Alloys in Implant Dentistry", *Materials (Basel)*, 12(3), 368, https://doi.org/10.3390/ma12030368.

Oshida, Y., Tuna, E.B., Aktören, O. and Gençay, K. (2010), "Dental Implant Systems", *International Journal of Molecular Sciences*, 11(4), 1580–1678, https://doi.org/10.3390/ijms11041580.

Rezaei, N.M., Hasegawa, M., Ishijima, M., Nakhaei, K., Okubo, T., Taniyama, T., Ghassemi, A., Tahsili, T., Park, W., Hirota, M. and Ogawa, T. (2018), "Biological and Osseointegration Capabilities of Hierarchically (Meso-/Micro-/Nano-Scale) Roughened Zirconia", *International Journal of Nanomedicine*, 13, 3381–3395, https://doi.org/10.2147/ijn.s159955.

Sasikumar, Y., Indira, K. and Rajendran, N. (2019), "Surface Modification Methods for Titanium and Its Alloys and Their Corrosion Behavior in Biological Environment: A Review", *Journal of Bio- and Tribo-Corrosion*, 5, 1–25, https://doi.org/10.1007/s40735-019-0229-5.

Schlee, M., Rathe, F., Brodbeck, U., Ratka, C., Weigl, P. and Zipprich, H. (2019), "Treatment of Peri-implantitis – Electrolytic Cleaning Versus Mechanical and Electrolytic Cleaning – A Randomized Controlled Clinical Trial – Six-Month Results", *Journal of Clinical Medicine*, 8(11), 1909, https://doi.org/10.3390/jcm8111909.

Shadid, R.M., Sadaq, N.R. and Othman, S.A. (2014), "Does the Implant Surgical Technique Affect the Primary and/or Secondary Stability of Dental Implants? A Systematic Review", *International Journal of Dentistry*, 2014, 204838, https://doi.org/10.1155/2014/204838.

Shang, F., Chen, S., Liang, J. and Liu, C. (2019), "Preparation and Photocatalytic Properties of ZnO Deposited TiO_2 Nanotube Arrays by Anodization", *Journal of Nanoscience and Nanotechnology*, 19(4), 2070–2077, https://doi.org/10.1166/jnn.2019.15797.

Šupová, M. (2015), "Substituted Hydroxyapatites for Biomedical Applications: A Review", *Ceramics International*, 41(8), 9203–9231, https://doi.org/10.1016/j.ceramint.2015.03.316.

Takeuchi, M., Abe, Y., Yoshida, Y., Nakayama, Y., Okazaki, M. and Akagawa, Y. (2003), "Acid Pretreatment of Titanium Implants", *Biomaterials*, 24(10), 1821–1827, https://doi.org/10.1016/s0142-9612(02)00576-8.

Turkyilmaz, I. (Ed.) (2011), *Implant Dentistry – A Rapidly Evolving Practice*, InTech, https://doi.org/10.5772/706.

Wennerberg, A. and Albrektsson, T. (2010), "On Implant Surfaces: A Review of Current Knowledge and Opinions", *The International Journal of Oral & Maxillofacial Implants*, 25(1), 63–74.

Wheelis, S.E., Wilson Jr., T.G., Valderrama, P. and Rodrigues, D.C. (2017), "Surface Characterization of Titanium Implant Healing Abutments before and after Placement", *Clinical Implant Dentistry and Related Research*, 20(2), 180–190, https://doi.org/10.1111/cid.12566.

Yu, Y, Jin, G., Xue, Y., Wang, D., Liu, X. and Sun, J. (2016), "Multifunctions of Dual Zn/Mg Ion Co-implanted Titanium on Osteogenesis, Angiogenesis and Bacteria Inhibition for Dental Implants", *Acta Biomaterialia*, 49, 590–603, https://doi.org/10.1016/j.actbio.2016.11.067.

https://doi.org/10.24264/icams-2022.II.20

https://doi.org/10.24264/icams-2022.II.20

SYNTHESIS AND CHARACTERIZATION OF ALGINATE-GELATIN HYDROGELS WITH POTENTIAL USE IN BIOMEDICAL FIELD

ILARIA QUARATESI[1], FILIP ION-ANGI[2], CRISTINA CARȘOTE[3], SEBASTIAN-BOGDAN TUTUNARU[2], MIHAELA-DOINA NICULESCU[1], ELENA BADEA[1,2*]

[1] *The National Research & Development Institute for Textiles and Leather - Leather and Footwear Research Institute Division, Ion Minulescu Str. 93, 031215 Bucharest, Romania.*

[2] *University of Craiova, Faculty of Sciences, Chemistry Department, Calea Bucuresti Str. 107 I, 200512 Craiova, Romania*

[3] *National Museum of Romanian History, Calea Victoriei Str. 12, 030026 Bucharest, Romania*

elena.badea@edu.ucv.ro

This work concerns with obtaining and characterization of new hydrogels based on sodium alginate and gelatin in the form of cross-linked polymer networks, aimed at medical applications, for example controlled release of bioactive agents (pharmaceutical industry) and bioinks (regenerative medicine). Our synthesis strategy was based on the use of mild, ecological reaction conditions in the absence of crosslinking agents and organic oxidants. Only industrially available sodium alginate and gelatin from leather wastes, produced at micro-pilot level at INCDTP-ICPI, were used, without the presence of any additional crosslinking agents, to test their ability to form strong 3D gels. Tunable physical-chemical and mechanical properties of the hydrogels have were obtained by varying the ratio sodium alginate: gelatin. Newly synthesized hydrogels were characterized by both analytical methods, such as ATR-FTIR, TG-DTG and SEM, and standard tests for mechanical resistance.

Keywords: alginate, gelatin, 3D hydrogels

INTRODUCTION

Hydrogels are polymeric systems extensively studied in recent years, due to their wide range of applications in the most diverse fields. Hydrogels are composed of polymeric networks, reticulated, elastic, with hydrophilic properties, capable of retaining impressive amounts of water or other liquids. The structural and compositional similarity with the extracellular matrix is the essential characteristic of hydrogels that ensures their applicability in the bio-medical and pharmaceutical field. In order to be able to cover a wide range of applications, hydrogels must be easy to prepare (e.g. through ecological synthesis methods, with a minimum of operations) and present biocompatibility and biodegradability. In this context, biopolymer materials such as polysaccharides and proteins, and their derivatives, have become a key element in the synthesis of hydrogels, being preferred in applications requiring biodegradability and biocompatibility. Moreover, these hydrophilic biopolymers allow fine-tuning of the physical and chemical properties of hydrogels, enabling thus to obtain materials with optimal properties such as cell adhesion, favorable molecular response, structural integrity, biodegradability, biocompatibility and controlled transport of bioactive molecules.

Due to the current demographic evolution characterized by a continuously growing population in Asia and Africa and an advanced degree of aging in Europe and North America, specialized literature abounds in the design, creation and use of more and more economically efficient and ecological materials aimed at supporting peoples' quality of life. In fact, the impact of demography is reflected by the financial

https://doi.org/10.24264/icams-2022.II.21

parameters: the global regenerative medicine market was estimated at USD 8.5 billion in 2020 and is forecast to grow to USD 17.9 billion in 2025, calculated at a compound annual growth rate (CAGR) of 15.9% (www.biospace.com, 2022).

In recent years, both polysaccharides and proteins have been used for the preparation of hydrogels in order to combine the advantages offered by the two classes of polymers. Polysaccharides, the richest source of natural carbon-based polymers, have the property of being renewable. Natural alginates, the sodium salts of alginic acid, represent one of the most studied polysaccharides in the field of tissue engineering and controlled release of active substances (Zhang *et al*., 2021; Abka-khajouei *et al*., 2022). They are found in large quantities in nature, either as structural components of brown seaweeds or capsular polysaccharides of some soil bacteria. On the other part, collagen is the most abundant protein found in mammalian bodies (about a quarter of all protein in the human body is collagen). Collagen, in the form of colloidal, gelatinous and hydrolyzed solutions, covers a huge range of applications, from high tech (e.g. nanobots), to tissue engineering and regenerative medicine, from biomedical applications to the cosmetic and nutraceutical industries. As a biomedical material, collagen meets essential criteria such as controlled degradation rate, good mechanical strength, excellent biocompatibility and low antigenicity (Sorushanova, 2019; Wang, 2021; Banerjee, 2020).

Starting from these premises, the main objective of this study was to obtain new hydrogels based on sodium alginate and gelatin in the form of cross-linked polymer networks and characterize them. This is a first step in understanding the interaction mechanism and design a tunable synthesis of hydrogels depending on the desired application, for example the controlled release of bioactive agents or bioinks production. The working method used of mild, ecological reaction conditions in the absence of cross-linking agents and organic oxidants. Newly synthesized hydrogels were characterized by both analytical methods, such as ATR-FTIR, TG-DTG and SEM, and standard tests for mechanical resistance.

MATERIALS AND METHODS

Materials and reagents: sodium alginate (Sigma, CAS-No: 9005-38-3), bovine gelatin type B (Sigma, CAS-No: 9000-70-8), gelatin GDCI-1 (obtained at the Leather Research Department, INCDTP-ICPI, Bucharest), glacial acetic acid (SC SILAL TRADING SRL, CAS-No: 64-19-7) and deionized water.

The steps of the adopted synthesis method are presented in Figure 1 (Wang, 2021).

HYDROGELS CHARACTERIZATION

FTIR-ATR Analysis

Spectral behaviour of alginate-gelatin hydrogels is illustrated in Figure 2. A specific absorption band occurred at 1724 cm^{-1} for samples treated with 2% acetic acid solution. This indicates the presence of carbonyl groups suggesting several hypotheses: the formation of carbonyl groups (dialdehyde groups), the formation of ester function groups by reaction with acetic acid or even the formation of carboxyl groups. Given the mild conditions (low temperature, 2% acetic acid, short time), we can retain two of these hypotheses: formation of dialdehyde groups or acetylation of hydroxyl groups.

https://doi.org/10.24264/icams-2022.II.21

The FTIR-ATR spectra of P3-2 and P3-3 hydrogels show the absorption band at 1724 cm^{-1}, too, confirming the oxidation/acetylation mechanism promoted by immersion of alginate-gelatin hydrogel in 2% acetic acid solution.

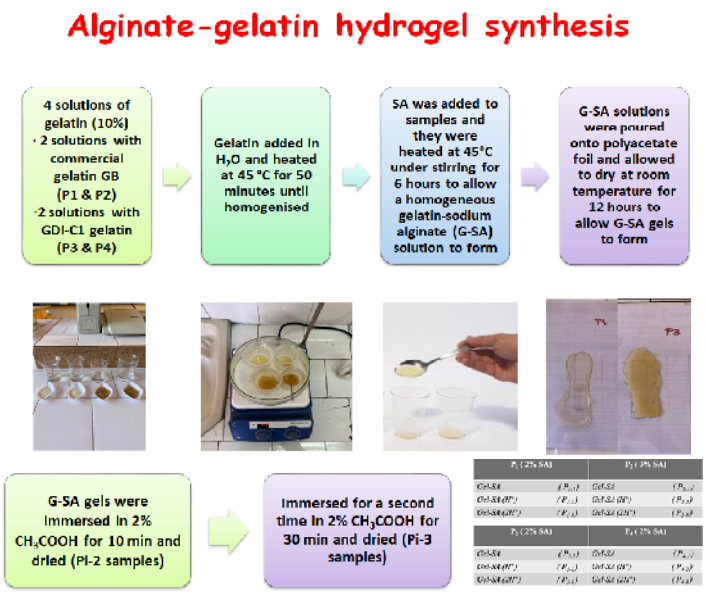

Figure 1. Schematic presentation of the alginate-gelatin hydrogels synthesis together with the list of hydrogels depending on alginate:gelatin ratio and acid immersion treatments

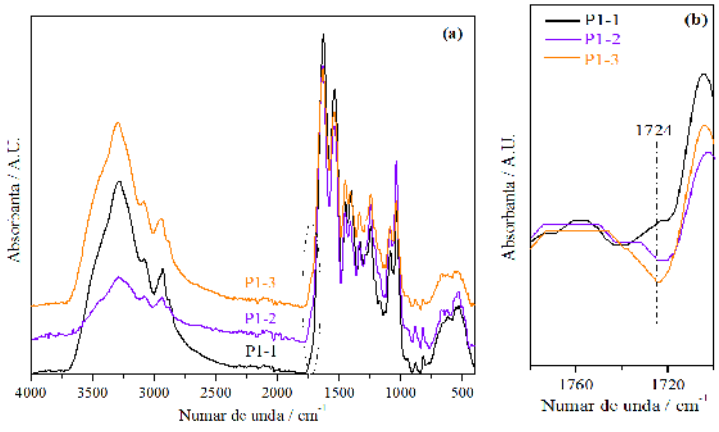

Figure 2. a) FTIR-ATR spectra of samples P1-1, P1-2 and P1-3 (b) the corresponding secondary derivatives show the occurrence of the specific band at 1724 cm^{-1} attributed to the valence vibration of the C = O carbonyl group in the carboxyl/ester function

https://doi.org/10.24264/icams-2022.II.21

TG-DTG Analysis

Several endothermic effects were observed in the hydrogels thermograms in the considered temperature range (Figure 3): while all hydrogels shown thermal effects in the intervals: (200 – 250) °C; (250 – 270) °C and (320 – 350) °C, P3-1 hydrogel (not subjected to immersion in acid solution) showed an exothermic phenomenon at temperatures above 500 °C. According to literature, alginate exhibits three thermal events (mass loss) in the intervals (25 – 200) °C, (200 – 500) °C and (500 – 800) °C (Valido *et al.*, 2022). The first event is endothermic and corresponds to alginate dehydration (residual moisture of the polysaccharide and water bound more internally to the alginate structure), while the second and third events are exothermic, and are associated with the degradation of anhydrous sodium alginate and formation of sodium carbonate (Na_2CO_3), followed by its decomposition to sodium oxide (NaO_2) and CO_2 release. The hydrogels' thermograms indicate a different behavior in the interval (200 – 500) °C. This behaviour may be attributed to a different release of water with consequent thermal stabilisation of the structure proved by the fact that sodium carbonate decomposition was not observed in the range up to 600°C.

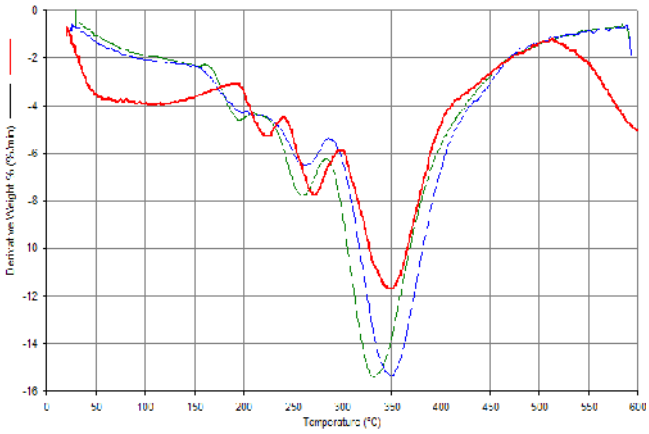

Figure 3. Thermograms obtained for alginate; gelatin hydrogels: P3-1 (red), P3-2 (green) and P3-3 (blue)

SEM Observations

SEM micrographs demonstrate that the microstructure of alginate-gelatin hydrogels, although compact, contains some areas of heterogeneity and air bubbles. Apparently, alginate would act as a filler in the gelatin matrix. However, as the degree of cross-linking increases, through successive immersion in 2% acetic acid solution, the degree of heterogeneity decreases, as well as the density of air bubbles, resulting in smoother and more regular surfaces. The microstructure of the hydrogels suggests that there may be an interaction between the two components of the polymer matrix, with alginate chains interpenetrating more homogeneously with those of gelatin.

https://doi.org/10.24264/icams-2022.II.21

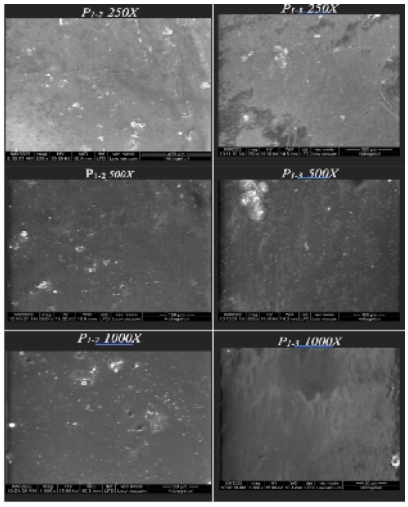

Figure 4. SEM images of samples P1-2 and P1-3 taken at progressive magnifications: 250X, 500X and 1000X

Mechanical Tests

The results of mechanical tests (ISO 7500-1) indicated that by reducing the concentration of gelatin, the mechanical parameters are significantly reduced, i.e., breaking strength and tensile strength are reduced by about 50% and elasticity is drastically reduced by more than 90%.

CONCLUSIONS

Hydrogels based on sodium alginate and gelatin were synthesized using mild, environmentally friendly reaction conditions in the absence of crosslinking agents and organic oxidants. The interpenetration of the polypeptide and polysaccharide networks was obtained by dispersing the biopolymers in deionized water under strong mechanical agitation and moderate heat treatment for 6 hours, followed by air-drying at room temperature. To promote the formation of electrostatic bonds and hydrogen bridges between the specific functional groups of the two biopolymers, a mild acid treatment with dilute acetic acid solution (2% v/v) was applied (i.e, by repeated immersion of the gels in the solution for 10-20 minutes). The effect of acid treatment was assessed by a set of analyzes: molecular analysis of hydrogels by FTIR-ATR spectroscopy, thermal stability analysis by TG-DTG, mechanical analysis and morphological analysis by SEM microscopy. These analyzes led to the conclusion of the formation of a composite system with physical-mechanical properties and thermal stability different from those of the initial biopolymers, properties prone to tailoring by immersion in acidic solution.

The main conclusions regarding the properties of the gelatin-alginate composite suggest a possible interaction between the two components of the polymer matrix, with sodium alginate chains interpenetrating with those of gelatin. At the macroscopic level, the thermal analysis suggests a thermal stabilization highlighted the behavior of the composite in the stages of release of free water and bound water, as well as in the stages

https://doi.org/10.24264/icams-2022.II.21

of thermal degradation of the polysaccharide and protein chains. The temperature range at which water release occurs expands because of the interpenetration of the two polymers, and the decomposition of sodium carbonate no longer occurs in the range up to 600°C for the acidic treated hydrogels. The mechanical analysis demonstrated a reduction in the mechanical resistance to traction and breaking, as well as the reduction in the elasticity of the hydrogel because of the reduction in the concentration of sodium alginate. These first conclusions justify us to optimize the synthesis method by eventually considering the use of ultrasound green technology.

REFERENCES

Abka-khajouei, R., Tounsi, L., Shahabi, N., Patel, A.K., Abdelkafi, S. and Michaud, P. (2022), "Structures, Properties and Applications of Alginates", *Marine Drugs*, 20(6), 364, https://doi.org/10.3390/md20060364.

Banerjee, A., Das, S., Mandal, M. and Ganguly, S. (2020), "Fluidic Embedding of Additional Macroporosity in Alginate-Gelatin Composite Structure for Biomimetic Application", *Journal of Biomaterials Science*, Polymer Edition, 31(18), 2396-2417, https://doi.org/10.1080/09205063.2020.1815278.

Sorushanova, A., Delgado, L., Wu, Z., Shologu, N., Kshirsagar, A., Raghunath, R., Mullen, A.M., Bayon, Y., Pandit, A., Raghunath, M. and Zeugolis, D.I. (2019), "The Collagen Supra-family: From Biosynthesis to Advanced Biomaterial Development", *Advanced Materials*, 31(1), 1801651, https://doi.org/10.1002/adma.201801651.

Valido, D.P., Gonçalves, W.D. Jr., de Andrade, M.E. *et al*. (2020), "Otoliths-Composed Gelatin/Sodium Alginate Scaffolds for Bone Regeneration", *Drug Delivery and Translational Research*, 10, 1716-1728, https://doi.org/10.1007/s13346-020-00845-x.

Wang, L., Zhang, H.J., Liu, X., Liu, Y., Zhu, X., Liu, X. and You, X. (2021), "A Physically Cross-Linked Sodium Alginate−Gelatin Hydrogel with High Mechanical Strength", *ACS Applied Polymer Materials*, 3(6), 3197-3205, https://doi.org/10.1021/acsapm.1c00404.

Zhang, H., Cheng, J. and Ao, Q. (2021), "Preparation of Alginate-Based Biomaterials and Their Applications in Biomedicine", *Marine Drugs*, 19(5), 264, https://doi.org/10.3390/md19050264.

*** (2022), "Regenerative Medicine Market Growth Rate of 15.9% over the Forecast Period (2020-2025)", available at: https://www.biospace.com/article/regenerative-medicine-market-growth-rate-of-15-9-percent-over-the-forecast-period-2020-2025-/, accessed on 17 Sept 2022.

https://doi.org/10.24264/icams-2022.II.21

EFFECTIVE BIOLOGICAL TREATMENT OF TANNERY WASTEWATER FROM NITROGEN COMPOUNDS

LARISA SABLIY, VERONIKA ZHUKOVA, LYUBOV KIKA

National Technical University of Ukraine "Igor Sikorsky Kyiv Polytechnic Institute", Ukraine

Even after using physico-chemical and biological methods, tannery wastewater still contains a large amount of nitrogen compounds, which reaches 90 mg/dm^3. The ingress of such wastewater into natural reservoirs leads to eutrophication. The goal is to determine the efficiency of nitrogen compounds removal during sequential wastewater treatment in anaerobic, anoxic and aerobic bioreactors with immobilized microorganisms. For the study, wastewater from a tannery, collected after cleaning in aeration tanks, was used. Model solutions with a concentration of 18.4 - 90 mg/ dm^3 were obtained by dilution. 5 sequential bioreactors were used - anaerobic (2 stages), anoxic (2 stages) and aerobic (1 stage) with a capacity of 125 ml/h. Microorganisms were immobilized in each bioreactor on artificial carrier. The effects of organic nitrogen removal in anaerobic bioreactors were 58-66%, anoxic 51-70%, aerobic 57, 5%. A decrease in the concentration of nitrogen compounds occurs as a result of the formation of N_2, NH_3 gases and the use of nitrogen by microorganisms for biomass growth. It is proposed that sequential treatment of tannery wastewater in anaerobic, anoxic, and aerobic conditions with immobilized microorganisms made it possible to obtain a high degree of nitrogen removal. The method does not require chemical materials and is ecological.

Keywords: tannery wastewater, nitrogen compounds, biological treatment, immobilized microorganisms

INTRODUCTION

After the use of physical, chemical and biological treatment methods, the wastewater of the tannery still contains quite a large amount of nitrogen compounds even under the conditions of use involving natural ecological materials (Danylkovych *et al*., 2016). The concentration of these compounds in terms of total nitrogen reaches 80-90 mg/dm^3. A significant share is organic nitrogen, which forms ammonium compounds during decomposition. Under aerobic conditions, these compounds are oxidized by microorganisms to nitrites and nitrates in the process of nitrification. The discharge of such wastewater into a natural reservoir leads to the activation of the processes of flowering and eutrophication with the deterioration of water quality in them. Therefore, the removal of nitrogen compounds from tannery wastewater is an important problem.

Nitrification and denitrification methods are most often used to wastewater treatment from nitrogen compounds (Henze *et al*., 2008, Dytczak *et al*., 2008). Disadvantages of the nitrification-denitrification technology are high energy costs for nitrification and provision of the amount of organic matter required for denitrification, which is easily biodegradable (Sabliy *et al*., 2019).

The purpose of the work is to determine the efficiency of removal of nitrogen compounds in the proposed technology of sequential wastewater treatment in anaerobic, anoxic and aerobic bioreactors with immobilized microorganisms.

EXPERIMENTAL

Wastewater from a tannery was used for the study, collected after its treatment in aeration tanks. Model solutions with concentrations of 18.4-90 mg/dm^3 were obtained by diluting them. An installation of 5 consecutive bioreactors (Fig. 1) was used - anaerobic (2 stages), anoxic (2 stages) and aerobic (1 stage). Wastewater consumption through the installation was 125 ml/h.

https://doi.org/10.24264/icams-2022.II.22

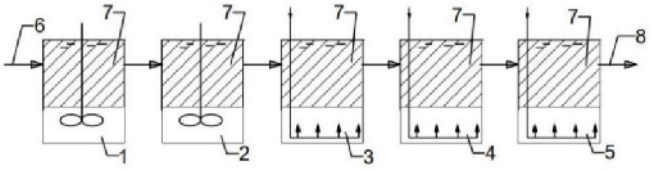

Figure. 1. Scheme of installation of bioreactors:
1 – anaerobic bioreactor of the I degree; 2 – anaerobic bioreactor of the II degree; 3 – anoxic bioreactor of the I degree; 4 – anoxic bioreactor of the II degree; 5 – aerobic bioreactor; 6 – the entrance of wastewater; 7 – fibrous carrier with immobilized microorganisms; 8 – the exit of wastewater.

Microorganisms were immobilized in each bioreactor on a fibrous kapron carrier (Fig. 2, a, b).

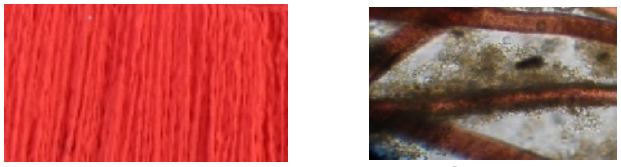

a) b)

Figure 2. Carrier for immobilization of microorganisms:
a) fibrous kapron; b) photomicrograph of carrier fibers with biofouling

The average thickness of the biological film on the fibrous carrier with a diameter of 3 mm – 1.5-3 mm was determined. Significant specific biofouling of the carrier was obtained - 32-38 mg/cm^2 (Fig. 2, b). Microscopy showed a great variety of bacterial species. In aerobic conditions, flagellated, free-swimming ciliates and conch rhizomes predominated among the protozoa. Multicellular organisms were represented by rotifers and roundworms. The high value of specific biofouling ensured the growth of biomass in the reaction zone of the bioreactor by 15-20 times compared to the activated sludge of aeration tanks and allowed to increase the efficiency of biological wastewater treatment.

RESULTS AND DISCUSSIONS

Wastewater analysis was carried out at the entrance and exit of each bioreactor according to the indicators: total nitrogen (N_{tot}); ammonium nitrogen (N_{NH4}), nitrites (N_{NO2}) and nitrates (N_{NO3}). Total nitrogen was determined by Kjeldahl, ammonium nitrogen, nitrites and nitrates were determined by colorimetric methods, respectively, with Nessler's reagent, Griess's reagent and salicylic acid, according to known methods. Organic nitrogen (N_{org}) was determined according to the formula (1):

$$N_{org} = N_{tot} – (N_{NH4} + N_{NO2} + N_{NO3}), \text{ mg/dm}^3. \quad (1)$$

The effect of wastewater treatment was determined by various nitrogen compounds according to the formula (2):

$$E = (C_{en} – C_{ex}) \cdot 100/C_{en}, \%, \quad (2)$$

where C_{en} - concentration of nitrogen compounds (for example, organic) at the entrance to this bioreactor (for example, anaerobic of the II degree), mg/dm^3; C_{ex} - concentration

https://doi.org/10.24264/icams-2022.II.22

of nitrogen compounds (for example, organic) at the exit from this bioreactor (for example, anaerobic II stage), mg/dm^3.

The results of studies on the purification of model wastewater in anaerobic bioreactors are shown in Fig. 3 and 4. The effect of organic nitrogen removal in the anaerobic bioreactor of the first degree was 58-65%, in the anaerobic bioreactor of the second degree - 60-66%. In general, in two anaerobic bioreactors, the amount of organic nitrogen decreases by 83-88%, which indicates a high degree of decomposition of nitrogen-containing compounds in bioreactors with immobilized microorganisms, compared to methane tanks (54%) (Danylkovych *et al*., 2016). In anaerobic conditions, with the participation of heterotrophic microorganisms, organic nitrogen is broken down to form ammonia - the concentration of ammonium nitrogen at the exit from bioreactors increases. The decrease in the concentration of total nitrogen (~ by 17%) is associated with the release of N_2, NH_3 gases and the consumption of nitrogen for the growth of the biomass of microorganisms.

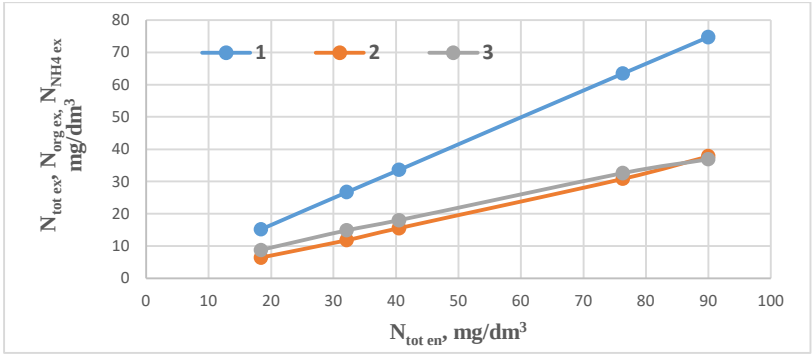

Figure 3. Graphs of dependence N_{tot}, N_{org}, N_{NH4} in an anaerobic bioreactor of the I degree: 1 - $N_{tot\ ex}$ concentration at the outlet from the concentration at the inlet $N_{tot\ en}$, 2- $N_{org\ ex}$ concentration at the outlet from the concentration at the inlet $N_{tot\ en}$, 3- $N_{NH4\ ex}$ concentration at the outlet from the concentration at the inlet $N_{tot\ ex}$

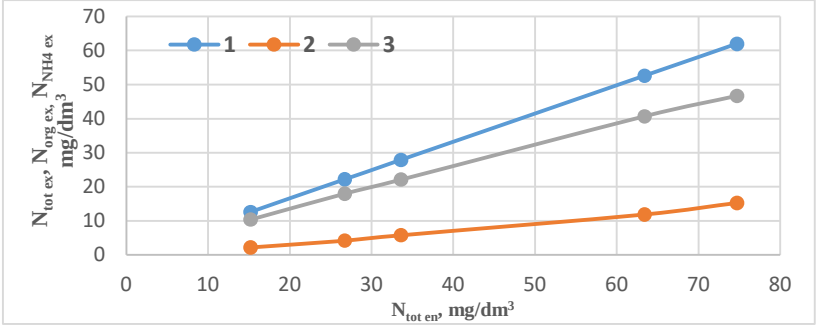

Figure 4. Graphs of dependence N_{tot}, N_{org}, N_{NH4} in an anaerobic bioreactor of the II degree: 1 - $N_{tot\ ex}$ concentration at the outlet from the concentration at the inlet $N_{tot\ en}$, 2- $N_{org\ ex}$ concentration at the outlet from the concentration at the inlet $N_{tot\ en}$, 3- $N_{NH4\ ex}$ concentration at the outlet from the concentration at the inlet $N_{tot\ ex}$

https://doi.org/10.24264/icams-2022.II.22

The results of research in anoxic bioreactors are shown in Fig. 5 and 6. The effect of decomposition of organic nitrogen in the anoxic bioreactor of the 1st degree is 52-60%, in the anoxic bioreactor of the 2nd degree - 51-70%. In general, the amount of organic nitrogen decreases by 77-82% in two anoxic bioreactors. In anoxic conditions, with the participation of heterotrophic microorganisms, the decomposition of organic nitrogen continues with the formation of ammonium, which is partially oxidized to nitrites and nitrates by nitrifying microorganisms in the presence of a limited amount of oxygen (oxygen concentration 0.1-0.2 mg/dm^3). Ammonium in anaerobic conditions in the thickness of the biofilm is oxidized to gaseous nitrogen by anammox bacteria, which use the nitrogen of nitrites formed as a result of nitrification. The decrease in the level of total nitrogen to 32% in each stage of anoxic treatment and to 52% in both stages is associated with the release of N_2 gases (in the anammox process), NH_3 and the consumption of nitrogen for the growth of the biomass of microorganisms.

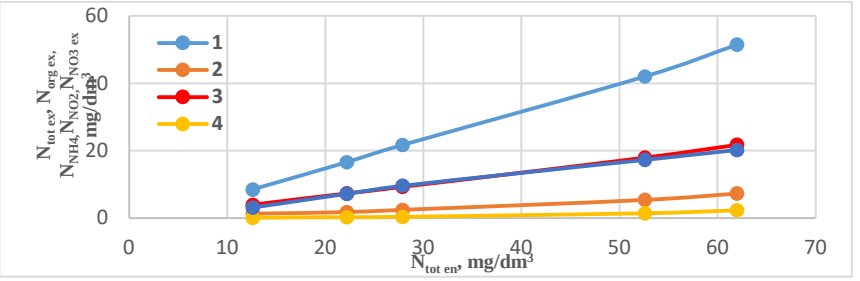

Figure 5. Graphs of dependence N_{tot}, N_{org}, N_{NH4}, N_{NO2}, N_{NO3} in an anoxic bioreactor of the I degree:
1 - $N_{tot\ ex}$ concentration at the outlet from the concentration at the inlet $N_{tot\ en}$, 2- $N_{org\ ex}$ concentration at the outlet from the concentration at the inlet $N_{tot\ en}$, 3- $N_{NH4\ ex}$ concentration at the outlet from the concentration at the inlet $N_{tot\ ex}$, 4- $N_{NO2\ ex}$ concentration at the outlet from the concentration at the inlet $N_{tot\ ex}$, 5- $N_{NO3\ ex}$ concentration at the outlet from the concentration at the inlet $N_{tot\ ex}$

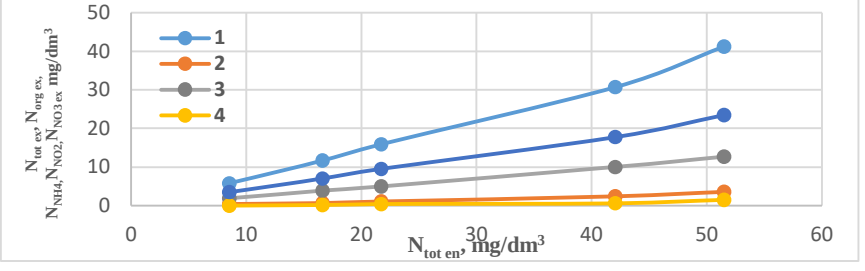

Figure 6. Graphs of dependence N_{tot}, N_{org}, N_{NH4}, N_{NO2}, N_{NO3} in an anoxic bioreactor of the II degree:
1 - $N_{tot\ ex}$ concentration at the outlet from the concentration at the inlet $N_{tot\ en}$, 2- $N_{org\ ex}$ concentration at the outlet from the concentration at the inlet $N_{tot\ en}$, 3- $N_{NH4\ ex}$ concentration at the outlet from the concentration at the inlet $N_{tot\ ex}$, 4- $N_{NO2\ ex}$ concentration at the outlet from the concentration at the inlet $N_{tot\ ex}$, 5- $N_{NO3\ ex}$ concentration at the outlet from the concentration at the inlet $N_{tot\ ex}$

https://doi.org/10.24264/icams-2022.II.22

In fig. 7 shows the results of research in an aerobic bioreactor - the last stage of anaerobic-aerobic treatment. The efficiency of ammonia oxidation reaches high values - 86-95%. The effect of decomposition of organic nitrogen reaches 57.5%. In aerobic conditions, with the participation of heterotrophic microorganisms, the residual organic nitrogen contained in the wastewater at the exit from the anoxic bioreactor of the II degree is decomposed, with the formation of ammonium compounds. These compounds are oxidized to nitrites and nitrates by nitrifying microorganisms in the presence of oxygen (oxygen concentration in the bioreactor is 1.5-2 mg/dm^3). The decrease in the content of total nitrogen to 19% is associated with the release of gaseous N_2 in the denitrification process, which occurs in the thickness of the biomass of overgrowths on the supports, and the consumption of nitrogen for the growth of the biomass of microorganisms.

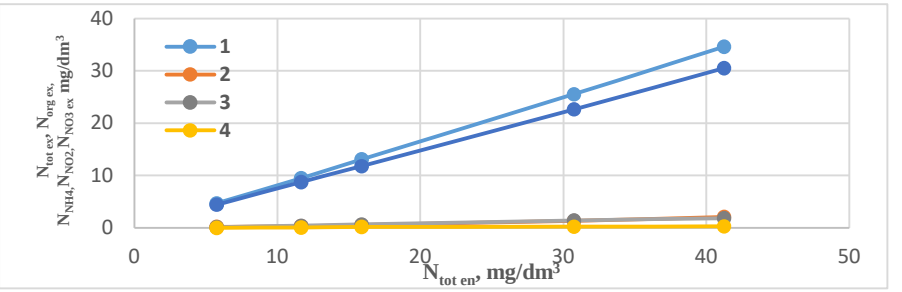

Figure 7. Graphs of dependence N_{tot} , N_{org}, N_{NH4}, N_{NO2}, N_{NO3} in an aerobic bioreactor: 1 - $N_{tot\ ex}$ concentration at the outlet from the concentration at the inlet $N_{tot\ en}$, 2- $N_{org\ ex}$ concentration at the outlet from the concentration at the inlet $N_{tot\ en}$, 3- $N_{NH4\ ex}$ concentration at the outlet from the concentration at the inlet $N_{tot\ ex}$, 4- $N_{NO2\ ex}$ concentration at the outlet from the concentration at the inlet $N_{tot\ ex}$, 5- $N_{NO3\ ex}$ concentration at the outlet from the concentration at the inlet $N_{tot\ ex}$

CONCLUSIONS

As a result of wastewater treatment at the exit from the aerobic bioreactor, the purified water contains ammonium nitrogen in a concentration of up to 0.5-1.8 mg/dm^3, nitrites - up to 0.03-0.25, nitrates - up to 5-31 mg/dm^3. This indicates the high efficiency of wastewater treatment from nitrogen compounds in bioreactors with immobilized microorganisms.

The originality of the technology is a significant decrease in the concentration of nitrogen compounds in the wastewater of a tannery when using biomass of nitrogen compound-destroying microorganisms immobilized on a fibrous carrier in successively created anaerobic, anoxic and aerobic conditions of the purification process.

Sequential treatment of tannery wastewater in anaerobic, anoxic, aerobic conditions with microorganisms immobilized on an artificial fibrous carrier is proposed. The high value of the specific biofouling of the carrier ensures the growth of biomass in the reaction zone of the bioreactor by 15-20 times compared to the active sludge of aeration tanks and allows to increase the efficiency of biological cleaning. The use of technology has shown the possibility of obtaining a high degree of removal of nitrogen compounds. Thus, for organic nitrogen, the overall cleaning effect reached 98-99%, for ammonium nitrogen - 86-95%. Thanks to this, low concentrations of ammonium nitrogen, nitrites

https://doi.org/10.24264/icams-2022.II.22

and nitrates in purified water were obtained. The wastewater treatment method does not require chemical materials, is characterized by lower electricity consumption compared to the aerobic method due to the use of anaerobic and anoxic processes, and is environmentally friendly.

REFERENCES

Danylkovych, A., Mokrousova, O. and Zhygotsky A. (2016), "Improvement of the Filling and Plasticization Processes of Forming Multifunctional Leather Materials", *Eastern European Journal of Enterprise Technologies*, 2, 6(80), 23–31, https://doi.org/10.15587/1729-4061.2016.65488.

Dytczak, M., Londry, K. and Oleszkiewicz, J. (2008), "Activated Sludge Operational Regime Has Significant Impact on the Type of Nitrifying Community and Its Nitrification Rates", *Water Research*, 42(8–9), 2320–2328, https://doi.org/10.1016/j.watres.2007.12.018.

Henze, M., van Loosdrecht, M., Ekama, G.A. and Brdjanovic, D. (2008), *Biological Wastewater Treatment: Priniciples, Modelling and Design*, IWA Publishing: London, UK, p. 526, https://doi.org/10.2166/9781780401867.

Sabliy, L., Kuzminskiy, Y., Zhukova, V., Kozar, M. and Sobczuk, H. (2019), "New Approaches in Biological Wastewater Treatment Aimed at Removal of Organic Matter and Nutrients", *Ecological Chemistry and Engineering S*, 26(2), 331-343, https://doi.org/10.1515/eces-2019-0023.

https://doi.org/10.24264/icams-2022.II.22

L. lactis BACTERIOPHAGES AND METHODS OF THEIR ELIMINATION FROM DAIRY PRODUCTS

OLGA SHYDLOVSKA, YULIIA KHMELNYTSKA
Kyiv National University of Technology and Design, Kyiv, Ukraine

Dairy products are important in human diet and nutrition. That is why dairy production is critical not only economically, but also socially and medically. In recent decades, dairy production has had problems with disturbances in fermentation processes caused by bacteriophage contamination. It is important to note that every year there are new reports about newly discovered bacteriophages that disrupt fermentation processes in the production of kefir, yogurt, and various types of cheese. *Lactococcus lactis* strains are of particular importance in dairy technology, as they are used for the production of various yogurts and cheeses. The study of the spectrum of bacteriophages infecting this strain can help to monitor the evolutionary changes of viruses and the horizontal transfer of genes. In this paper, an analysis of phages infecting L. lactis was carried out. Most bacteriophages belong to the *Siphoviridae* and *Podoviridae* families. Moreover, the authors analyzed approaches that can be used to reduce bacteriophage contamination in the production of dairy products. It has been shown that the use of disinfectants, such as ethanol on sodium hypochlorite, can reduce the titer of bacteriophages and protect products from the development of viral infection. It is also possible to use membrane filtration with UV irradiation. Moreover, all these approaches can be combined to achieve the most effective result.

Keywords: bacteriophages, *Lactococcus lactis*, biotechnology

INTRODUCTION

Bacteriophages are the most common viruses on planet Earth. This is because their hosts – bacteria – inhabit the most diverse ecological niches, namely soil, water, thermal springs, the bottom of the ocean, the surface of human skin, the gastrointestinal tract of animals, etc. It is clear that where bacteria live, we can also find bacteriophages (Batinovic *et al*., 2019).

This work is devoted to the review of bacteriophages infecting *Lactococcus lactis*, their characteristics and properties. The authors of the paper paid special attention to the analysis of possible methods of combating bacteriophage contamination of dairy production. This work shows that the development of effective methods of combating bacteriophage contamination is an important issue and requires in-depth study, since a universal and effective method has not yet been invented.

The main source of phages entering dairies is through raw milk, which can contain up to 104 IU/ml. Milk often contains phages for Lactococcus lactis and Streptococcus spp. The temperature and time combinations commonly used for pasteurization, i.e., low temperature/long time (63°C, 30 min) or high temperature/short time (72°C, 15 s), are largely insufficient to eliminate most LAB phages. Work surfaces such as floors, walls, stairs, doorknobs, office desks, equipment, detergents, and pipes can also be a source of contamination. Phages cannot be eliminated in the dairy environment because they are naturally present in raw milk, withstand most common heat treatments, spread among production facilities through liquid splashes and airborne particles, persist on equipment surfaces and biofilms, and can be found in high titers in cheese whey or other industrial effluents (Pujato *et al*., 2019).

https://doi.org/10.24264/icams-2022.II.23

REVIEW OF BACTERIOPHAGE STRAINS INFECTING *Lactococcus lactis*

L. lactis strains are widely used in the production of numerous fermented dairy products and are among the most economically important lactic acid bacteria (LAB) (Yerlikaya, 2019). All lactococcal phages belong to the order *Caudovirales*, families *Siphoviridae* (most lactococcal phages) and *Podoviridae* (few lactococcal phages). Bacteriophages infecting *L. lactis* have been divided into 10 species, and those belonging to c2, 936 or P335 species are more common in dairies. At present, 28 genomes of lactococcal bacteriophages isolated during the last 3 decades as a result of failed fermentation in dairies around the world have been identified. The GC content of the analyzed bacteriophages ranges from 34 to 36.4%. The genome length of isolates ranges from 20 to 23.2 kb for c2 phages, from 25.3 to 32.6 kb for species 936 phages, and from 25.3 to 32.6 kb for Bk5-T members. The number of putative ORFs ranges from 34 to 42 among c2 species, from 46 to 62 among 936 phages, and from 51 to 60 for Bk5-T isolates (Marcelli *et al*., 2020).

RESISTANCE OF *L. lactis* TO BACTERIOPHAGES

The type III-A system provides persistent phage immunity in part due to the absence of PAM sequence requirements (adjacent protospacer motif), tolerance of nucleotide mismatches in the target sequence (protospacer), and the efficiency of inhibition from a single spacer, especially when targeting important genes. The genetic similarity between the *L. lactis* type III-A CRISPR and other type III-A systems may predict a similar function. The *in vivo* functionality of the type III-A lactococcal system is consistent with the mechanism of action of similar systems found in *S. epidermidis*, *S. thermophilus*, and *Thermus thermophilus*. The flexibility in spacer targeting and the strength of immunity derived from a single spacer, especially when targeting essential genes, offer significant advantages for the generation of industrial strains with enhanced and programmed phage resistance (Millen, 2019).

In the study of the authors Marcelli *et al*. (2019) showed that the resistance mechanism of four bacteriophage-insensitive mutants of *L. lactis* involves changes in the phage receptor. For example, phage CHPC971 shows a low or very low adsorption rate for all four bacteriophage-insensitive mutant *L. lactis* strains compared to its sensitive strains CH LC01 and CH LC02. The studied phage is able to adsorb on L. lactis CH LC01 and CH LC02 strains, while on the other four *L. lactis* strains, adsorption was not observed or was very weak. It is important to note that rhamnose plays a direct role in the work of this receptor and may be a key molecule that provides resistance to bacteriophages.

METHODS OF REDUCING BACTERIOPHAGE CONTAMINATION IN FERMENTED *Lactococcus lactis* PRODUCTS

Complete inactivation of lactococcal phages can be achieved by treatment at 90°C for 5 minutes. Among alcohols (ethanol and isopropanol), ethanol in a concentration of 75% or more has an effective antiviral effect. Sodium hypochlorite in concentrations above 100 ppm (the maximum commercial concentration used is 200 ppm) is also capable of completely suppressing viral activity. The most effective agent widely used in the dairy industry is peracetic acid. At a concentration (0.15%, 40 °C) rapidly

https://doi.org/10.24264/icams-2022.II.23

inactivates phage suspensions (the number of viruses below the detection limit, <10 PFU/ml) after 5 minutes of treatment (Marcó *et al*., 2019)

Authors Michel *et al*. (2021) investigated an orthogonal process strategy (cross membrane filtration combined with UV-C irradiation or heat treatment) to dramatically reduce the number of bacteriophages in filtered whey. An effective mode of bacteriophage elimination was membrane filtration followed by UV irradiation at 2.25 J cm^2. At the same time, no option with heat treatment of whey was effective – mild pasteurization conditions (72–75 °C, 15–30 s, whey protein denaturation by approximately 1%) and higher combinations of temperature and time (for example, 216 s at 75 °C for P008 phage or 10.5 min at 95 °C for P680 phage; whey protein denaturation >5% to >90%, respectively). Although this technology is pilot, it can be considered for scaling up the process of purifying serum from bacteriophages on an industrial scale. It is important to note that even in an industrial pasteurizer it is possible to achieve a certain decrease in the titer of bacteriophages, the conditions of industrial pasteurization of milk (72°C for 15 s) are not sufficient for effective inactivation of even the heat-sensitive model phage P008 (Wagner, 2018).

An interesting approach to combating bacteriophage contamination is the development of transgenic strains of *L. lactis* bacteria. The authors performed plasmid transduction and proved the effectiveness of this procedure under certain circumstances. The selected phage must be able to infect both donor and recipient strains and encode a terminase that can bind plasmid DNA and package it into nascent phage heads (Marcelli, 2020).

CONCLUSIONS

Most of the bacteriophages that infect *Lactococcus lactis* belong to the *Sifoviridae* and *Podoviridae* families. Even though *L. lactis* strains resistant to phages have been isolated, the threat of reducing the efficiency of fermentation processes still exists. This is due to the ultra-fast evolution of viruses. However, today there are quite effective approaches to fight against bacteriophage contamination. Among the most common and easy to use is the use of ethanol and sodium hypochlorite solutions. Furthermore, a more serious approach of combining methods of membrane filtration and treatment of raw materials with UV irradiation can significantly reduce the titer of bacteriophages. Among the latest approaches, the development of recombinant strains can be singled out, but this technology can be too expensive for dairy industries. Today, we can conclude that the search for new approaches and the improvement of old approaches to fight against bacteriophage infections on dairy farms needs more attention from scientists and researchers. It can be said that a combination of different approaches and techniques can provide greater efficiency in reducing the phage titer in raw materials. Moreover, it can help in the complete elimination of phage from dairy raw materials. The most promising methods currently are the combination of ultrafiltration with UV irradiation.

REFERENCES

Batinovic, S., Wassef, F., Knowler, S.A., Rice, D.T., Stanton, C.R., Rose, J. and Franks, A.E. (2019), "Bacteriophages in Natural and Artificial Environments", *Pathogens*, 8(3), 100-119, https://doi.org/10.3390/pathogens8030100.

https://doi.org/10.24264/icams-2022.II.23

Marcelli, B., de Jong, A., Janzen, T., Serrano, M., Kok, J. and Kuipers, O.P. (2020), "Complete Genome Sequences of 28 Lactococcal Bacteriophages Isolated from Failed Dairy Fermentation Processes", *Microbiology Resource Announcements*, 9(12), e01535-19, https://doi.org/10.1128/MRA.01535-19.

Marcelli, B., de Jong, A., Karsens, H., Janzen, T., Kok, J. and Kuipers, O.P. (2019). "A Specific Sugar Moiety in the *Lactococcus lactis* Cell Wall Pellicle is Required for Infection by CHPC971, a Member of the Rare 1706 Phage Species", *Applied and Environmental Microbiology*, 85(19), e01224-19, https://doi.org/10.1128/AEM.01224-19.

Marcelli, B., Karsens, H., Nijland, M., Oudshoorn, R., Kuipers, O.P. and Kok, J. (2020), "Employing Lytic Phage-Mediated Horizontal Gene Transfer in *Lactococcus lactis*", *PLOS One*, 15(9), e0238988-9008, https://doi.org/10.1371/journal.pone.0238988.

Marcó, M.B., Suárez, V.B., Quiberoni, A. and Pujato, S.A. (2019), "Inactivation of Dairy Bacteriophages by Thermal and Chemical Treatments", *Viruses*, 11(5), 480-428, https://doi.org/10.3390/v11050480.

Michel, C., Samtlebe, M., Wagner, N., Neve, H., Franz, C.M., Hinrichs, J. and Atamer, Z. (2021), "Orthogonal Processing Strategies to Create 'Phage-free' Whey–Membrane Filtration Followed by Thermal or Ultraviolet C Treatment for the Reduction of *Lactococcus lactis* Bacteriophages", *International Dairy Journal*, 122, 105149-105159, https://doi.org/10.1016/j.idairyj.2021.105149.

Millen, A.M., Samson, J.E., Tremblay, D.M., Magadán, A.H., Rousseau, G.M., Moineau, S. and Romero, D.A. (2019), "*Lactococcus lactis* Type III-A CRISPR-Cas System Cleaves Bacteriophage RNA", *RNA Biology*, 16(4), 461-468, https://doi.org/10.1080/15476286.2018.1502589.

Pujato, S.A., Quiberoni, A. and Mercanti, D.J. (2019), "Bacteriophages on Dairy Foods", *Journal of Applied Microbiology*, 126(1), 14-30, https://doi.org/10.1111/jam.14062.

Yerlikaya, O. (2019), "Probiotic Potential and Biochemical and Technological Properties of *Lactococcus lactis* ssp. Lactis Strains Isolated from Raw Milk and Kefir Grains", *Journal of Dairy Science*, 102(1), 124-134, https://doi.org/10.3168/jds.2018-14983.

Wagner, N., Matzen, S., Walte, H.G., Neve, H., Franz, C.M., Heller, K.J. and Hammer, P. (2018), "Extreme Thermal Stability of *Lactococcus lactis* Bacteriophages: Evaluation of Phage Inactivation in a Pilot-Plant Pasteurizer", *LWT*, 92, 412-415, https://doi.org/10.1016/j.lwt.2018.02.056.

https://doi.org/10.24264/icams-2022.II.23

THE INFLUENCE OF SURFACTANTS IN OBTAINING NEW BYPRODUCTS, FOR AGRICULTURE APPLICATIONS

DEMETRA SIMION[1*], CARMEN GAIDĂU[1], MARIANA DANIELA BERECHET[1], MARIA STANCA[1], COSMIN ALEXE[1], GABRIELA PĂUN[2]

[1]*The National Research & Development Institute for Textiles and Leather - Leather and Footwear Research Institute Division, 93 Ion Minulescu Street, 031215, Bucharest, Romania, demetra.simion@yahoo.com*

[2]*National Institute for Research-Development of Biological Sciences, 060031 Bucharest, Romania*

The aim of the paper is to obtain new byproducts based on surfactants (gemini – polymethylene-α, ω-bis (N, N-dialkyl-N-deoxy-d-glucitolammonium iodides or bolaform – demecarium bromide) and protein hydrolysates (keratin and collagen) with micro and macro nutrients for applications in agriculture. A method was developed to include micro and macronutrients in keratin and collagen hydrolysates, in order to obtain new byproducts-bioemulsions (stable because of surfactants), with final goal of application as a new class of root fertilizers for cereals (e.g., corn). The newly obtained byproducts (bioemulsions based on surfactants) were characterized by: dynamic light scattering measurements, contact angle, optical microscopy and microbiological tests against fungal attack of *Fusarium* spp. and *Botrytis cinerea*. Better results were obtained for gemini surfactant based on sugar – polymethylene-α, ω-bis (N, N-dialkyl-N-deoxy-d-glucitolammonium iodides) due to the properties such as: biodegradability, nontoxicity and adherence to surfaces. The new fertilizer created in this research – bioemulsions based on surfactants, can support the general structure of the grains as well as the chlorophyll content, increasing the growth yield. The fertilizer is indicated for any type of crops and soils, with recommended use as additional fertilizer for plants (cereals) in the vegetation and growth phases, with a maximum need for nutrients.

Keywords: hydrolysates (keratin and collagen) with micro and macro nutrients; byproducts-bioemulsions based on surfactants; new class of root fertilizers in cereals

INTRODUCTION

In this research new byproducts based on surfactants (gemini – polymethylene-α, ω-bis (N, N-dialkyl-N-deoxy-d-glucitolammonium iodides or bolaform – demecarium bromide) and protein hydrolysates (keratin and collagen) with micro and macro nutrients were created and their applications in agriculture were studied, as a new class of root fertilizers for cereals (e.g., corn) (Tadros, 2005; Hughes *et al.*, 2021; Nuraje *et al.*, 2013; Varasteanu, 2014). The keratin and collagen hydrolysates were obtained by acid hydrolysis at 80°C for four hours. These keratin and collagen hydrolysates contain peptides and free amino acids with micro (Cu, Mg, Mo, B, Zn, Fe) and macro (N, P, K) nutrients, respectively. The new byproducts-bioemulsions are original due to the successful inclusion of surfactants/mezzo and microelements/ hydrolysates of keratin and collagen.

Bolaamphiphiles and gemini are new classes of amphiphilic surfactants, with different applications due to their high capacity for emulsification (e.g., micro and macro nutrients). Due to properties of the surfactants such as: biodegradability, nontoxicity, adherence to surfaces, they may be successfully used in processing of byproducts destined for agriculture, in improvement of surface properties. In this research a new method was elaborated for including micro and macronutrients in hydrolysates of keratin and collagen, in order to obtain new byproducts-bioemulsions, with application in agriculture. These bioemulsions were applied as a new root fertilizer to 20 corn kernels compared to a control and the evolution of the plants was followed by measuring the stems and roots 10 days before planting and 10 days after they were

https://doi.org/10.24264/icams-2022.II.24

planted by applying the treatment, i.e., spraying the plants with 10 ml every 3 days. Due to the content of protein hydrolysates with a complex composition of peptides and free amino acids, with pelliculogenic, chelating and buffering properties, the new bioemulsions provide the complete macro and micronutrient requirements for biostimulation and nutrition in the growth of cereals (e.g., corn).

EXPERIMENTAL

Materials and Methods

The following materials were used: sugar based gemini surfactant (polymethylene-α, ω-bis(N,N-dialkyl-N-deoxy-d-glucitolammoniumiodides) – Gemini, from SERVA Feinbiochemica GmbH & Co; demecarium bromide – Bola, from Sigma-Aldrich; ethanol of AnalaR grade. Phosphate buffer solution (PBS) of pH 6 is prepared in the laboratory by dissolving potassium dihydrogen phosphate in water, adjusting the pH with 1.0 M potassium hydroxide and diluting to 1.0 L with water. Triple distilled deionized water for sample preparation and all-PyrexTM glass apparatus was always used. The experimental techniques used consist in: BS-2082 Research Biological Microscope, magnification: 40x-1000x for optical microscopy; "MALVERN" zetasizer-nano equipment, with measuring range between 0.3 nm-60.0 microns and zeta potential determination with an accuracy of +/-2%; DataPhysics OCA 25 contact angle system.

RESULTS AND DISCUSSIONS

Obtaining Bioemulsions Based on Surfactants (Gemini or Bolaform) and Protein Hydrolysates (Keratin and Collagen) with Micro and Macro Nutrients

The hydrolysates (keratin and collagen) were obtained by acid hydrolysis at 80°C for four hours. Dried hydrolysates (keratin and collagen) were mixed with a solution containing micro and macro nutrients. Physico-chemical characterizations of protein hydrolysates (keratin and collagen) with micro and macro nutrients were performed according to the standard in force or literature methods for: dry substances, ash, total nitrogen and protein content, aminic nitrogen, pH and viscosity (Table 1).

Table 1. Physical-chemical characterization of protein hydrolysates (keratin and collagen) with micro and macro nutrients

Characterization	Protein hydrolysates (keratin and collagen) with micro and macro nutrients
Dry substance, %	30
Total ash, %	7
Total nitrogen, %	9
Protein substance, %	49
pH, pH units	6-7
Viscosity, cPs	2500

The samples (bioemulsions with gemini or bola) were prepared by dropping a 5-7% solution of surfactant (in water/ethanol, ratio 1:1) under continuous stirring into a aqueous solution of protein hydrolysates (keratin and collagen) with micro and macro nutrients of 10-20% at 70°C for five hours.

https://doi.org/10.24264/icams-2022.II.24

Several experiments were performed with different concentrations of protein hydrolysates (keratin and collagen) with micro and macro nutrients. The sample containing 20% protein hydrolysates (keratin and collagen) with micro and macro nutrients proved to be the most stable. The samples were labeled as presented in Figure 1. A number of three samples: protein hydrolysates (keratin and collagen) with micro and macro nutrients/ with or without surfactant (gemini or bola)/water/ethanol compared with a control sample (water), were prepared in the following working conditions: water-ethanol solvents at 1:1 ratio, temperature=70°C for five hours; surfactant concentration-c=5-7%, at pH=6 adjusting with a phosphate buffer solution (PBS), speed at 100 rpm.

1 **2** **3**

Figure 1. Photographic image of: sample 1 – protein hydrolysates (keratin and collagen) with micro and macro nutrients; sample 2 – protein hydrolysates (keratin and collagen) with micro and macro nutrients + Gemini surfactant (polymethylene-α, ω-bis(N,N-dialkyl-N-deoxy-d-glucitolammoniumiodides); sample 3 – protein hydrolysates (keratin and collagen) with micro and macro nutrients + Bola surfactant (demecarium bromide)

Characteristics of Bioemulsions Based on Surfactants (Gemini or Bolaform) and Protein Hydrolysates (Keratin and Collagen) with Micro and Macro Nutrients

Dynamic Light Scattering (DLS)

The average particle sizes of the two bioemulsions (with gemini or bola surfactant) showed increased dimensions as compared to sample 1 – protein hydrolysates (keratin and collagen) with micro and macro nutrients mixture (803 nm for sample 2; 620 nm for sample 3; 250 nm for sample 1), confirming the formation of the complex aggregates. The highest average particle size of bioemulsion with Gemini surfactant – sample 2 (Fig. 2) showed also the highest Zeta potential absolute value and improved stability as compared to bioemulsion with Bola surfactant – sample 3, and protein hydrolysates (keratin and collagen) with micro and macro nutrients – sample 1.

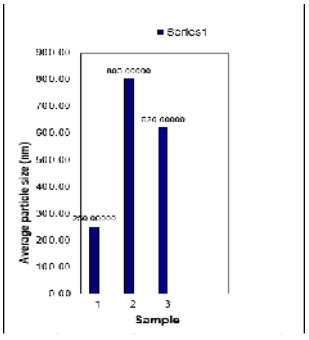

Figure 2. The average particle size for samples 1, 2 and 3

https://doi.org/10.24264/icams-2022.II.24

Zeta potential without stirring for 5 minutes showed a tendency towards agglomeration. The use of surfactants leads to obtaining stable bioemulsions.

Optical Microscopy Tests

The optical microscopy images in Fig. 3 show the agglomerated structures for samples (2 and 3) with surfactant (gemini or bola). The results are in agreement with literature data (Tadros, 2005; Hughes *et al.*, 2021; Nuraje *et al.*, 2013; Varasteanu, 2014), related to the formation of aggregate structures in bioemulsions.

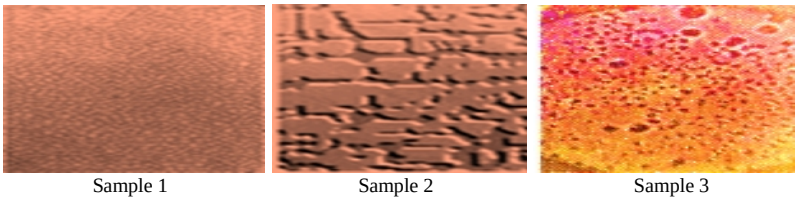

Sample 1 Sample 2 Sample 3

Figure 3. Optical microscopy images (1000x) for samples 1-3

Contact Angle Measurements

The contact angle measurements were made with a DataPhysics OCA 25 contact angle system. In Figure 4 it can be observed that Bola surfactant is the most hydrophilic and the sample 3 obtained with this surfactant is more hydrophilic than the sample 1 without surfactant and the sample 2 obtained with Gemini surfactant.

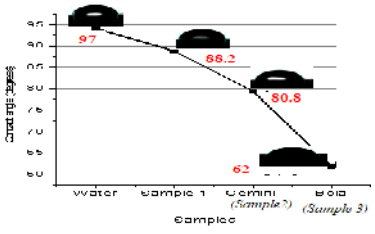

Figure 4. The contact angle measurements results for three samples and water, on a teflon surface: sample 1 – protein hydrolysates (keratin and collagen) with micro and macro nutrients; sample 2 – protein hydrolysates (keratin and collagen) with micro and macro nutrients + Gemini surfactant (polymethylene-α,ω-bis(N,N-dialkyl-N-deoxy-d-glucitolammoniumiodides); sample 3 – protein hydrolysates (keratin and collagen) with micro and macro nutrients + Bola surfactant (demecarium bromide)

Microbiological Tests

The stock cultures of microbian inoculums of *Fusarium spp ATCC 36031* and *Botrytis cinerea* were grown in Czapek-Dox nutritive medium, at 28ºC for 14 days. Two decimal dilutions of paraffin oil (10:2) were made from each culture and the cell concentration in the inoculum used was 8.92×10^3 CFU / mL for *Fusarium* spp. and 9.3×10^3 CFU / mL for *Botrytis cinerea*. The experiments were performed in Eppendorf tubes, previously sterilized at 121ºC for 15 minutes. The microbial inoculum was mixed

https://doi.org/10.24264/icams-2022.II.24

with the sample, both the microbial inoculum and the sample having constant volumes of 500 µL. All samples were tested in duplicate, and the results were expressed as a mean percentage and logarithmic reduction between the readings on the two Petri dishes corresponding to each sample (Table 2). Table 2 shows that bioemulsions based on Gemini (sample 2) or Bola surfactants (sample 3) had excellent antifungal resistance as well as sample 1 – protein hydrolysates (keratin and collagen) with micro and macro nutrients that showed antifungal properties between 98.70% and 100%.

Bioemulsion based on gemini surfactant – sample 2 had a positive influence on antifungal resistance of protein hydrolysates (keratin and collagen) with micro and macro nutrients mixture for all tested strains, meanwhile bioemulsion based on Bola surfactant – sample 3 showed slightly decreased antimicrobial resistance.

The new byproducts-bioemulsions based on surfactants and protein hydrolysates (keratin and collagen) are original due to the successful inclusion of micro and macro nutrients with high potential for cereals (e.g., corn) biostimulation and nutrition. The final goal of bioemulsions is their application as a new class of root fertilizers for cereals (e.g., corn).

Table 2. Antimicrobial resistance of new bioemulsions against fungus species

Sample	Result, UFC/mL	R%	Log_{10} red.
Botrytis cinerea		-	-
Inoculum concentration	$T_0=9,5x10^3$		
sample 1- protein hydrolysates (keratin and collagen) with micro and macro nutrients	$T_{24}= 6,2x10^1$	98,70	3,38
sample 2- protein hydrolysates (keratin and collagen) with micro and macro nutrients + Gemini surfactant (polymethylene-α,ω-bis(N,N-dialkyl-N-deoxy-d-glucitolammoniumiodides)	$T_{24}= 1,0x10^1$	99,99	4,10
sample 3- protein hydrolysates (keratin and collagen) with micro and macro nutrients + Bola surfactant (demecarium bromide)	$T_{24}= 2,12x10^2$	99,88	2,80
Fusarium spp. Inoculum concentration	$T_0=8,92x10^3$	-	-
sample 1 – protein hydrolysates (keratin and collagen) with micro and macro nutrients	$T_{24}= 5,0x10^1$	98,88	2,10
sample 2 – protein hydrolysates (keratin and collagen) with micro and macro nutrients + Gemini surfactant (polymethylene-α,ω-bis(N,N-dialkyl-N-deoxy-d-glucitolammoniumiodides)	$T_{24}= 0$	100	4
sample 3- protein hydrolysates (keratin and collagen) with micro and macro nutrients + Bola surfactant (demecarium bromide)	$T_{24}= 3,0x10^1$	99,80	1,44

The Evolution of Plant Growth

The bioemulsions created in this research, were applied as a new root fertilizer to 20 corn kernels compared to a control sample (water) and the evolution of the plants was followed by measuring the stems and roots 10 days before planting (Fig. 5a) and 10 days after they were planted (Fig. 5b) by applying the treatment, i.e., spraying the plants with 10 ml every 3 days.

https://doi.org/10.24264/icams-2022.II.24

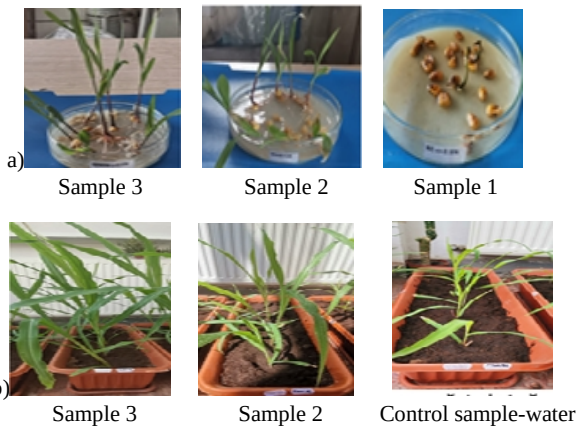

Figure 5. a), b). Images with the evolution of the plants, by measuring the treated stems and roots 10 days before and 10 days after planting, for samples 1, 2 and 3

The best results were obtained for sample 3 with Gemini surfactant.

CONCLUSIONS

New byproducts-bioemulsions were successfully made and can be used as a new class of root fertilizers for cereals (e.g., corn). The structure of new bioemulsions was demonstrated by optical microscopy.

The bioemulsions had particle sizes of: 803 nm for sample 2; 620 nm for sample 3 and 250 nm for sample 1. The new bioemulsions showed lower contact angle values which are premises for improved displaying on plant leaves or roots and a higher potential of growth biostimulation and nutrition.

Bioemulsions created with Gemini surfactants had the best results, showing an improved influence on antifungal resistance and emulsion stability.

Acknowledgements

The present work was supported by the Romanian Ministry of Research, Innovation and Digitalization, Nucleus Program, project PN 19 17 01 02/ 2022; project Eureka, PN-III-P3-3.5-EUK-2017-D-0098, FERTI-MAIZE, contract 127/2020, within PNCDI III; and PFE/2022.

REFERENCES

Hughes, J.R., Miller, A.S., Wallace, C.E, Vemuri, G.N. and Iovine, P.M. (2021), "Biomedically Relevant Applications of Bolaamphiphiles and Bolaamphiphile-Containing Materials", *Frontiers in Chemistry*, 8, article 604151, https://doi.org/10.3389/fchem.2020.604151.

Nuraje, N., Baib, H. and Su, K. (2013), "Bolaamphiphilic Molecules: Assembly and Applications", *Progress in Polymer Science*, 38, 302– 343, https://doi.org/10.1016/j.progpolymsci.2012.09.003.

Tadros, T.F. (2005), *Applied Surfactants Principles and Applications*, Wiley-VCH Verlag GmbH & Co. KGaA, Weinheim.

Varasteanu, D.S. (2014), "Surfactants Based on Proteins – Obtaining and Applications", PhD Thesis, "Politehnica" University of Bucharest.

https://doi.org/10.24264/icams-2022.II.24

HYDROGEL DRESSINGS WITH ANTIMICROBIAL AND HEALING PROPERTIES

ANDREEA ȚIGĂU[1], GEORGIANA VASILE[1], ALINA POPESCU[1], RODICA ROXANA CONSTANTINESCU[2], LAURA CHIRILĂ[1]

[1] *The National Research & Development Institute for Textiles and Leather, 16 Lucretiu Patrascanu Street, Bucharest, 030508, Romania, andreea.tigau@incdtp.ro, vasile.georgiana@incdtp.ro, alina.popescu@incdtp.ro; laura.chirila@incdtp.ro*

[2] *The National Research & Development for Textiles and Leather - Leather and Footwear Research Institute Division, 93 Ion Minulescu Street, Bucharest, 031215, Romania, rodica.roxana@yahoo.com*

The current study aimed to develop hydrogels as delivery systems based on a mixture of biodegradable and biocompatible polymers (i.e., gelatin and collagen) for encapsulating different active principles (i.e., chamomile and plantain tincture, aloe vera and propolis) to obtain dressings for treating first-degree burns injuries. The synthesized hydrogels were then immobilized on a textile material made from 100% cotton fibers. The functionalized textile materials were analyzed in terms of physical-mechanical characteristics, water absorbency and antibacterial activity. SEM analysis was used to investigate the morphology of the cotton fibers after the functionalized treatment. The antibacterial activity of the treated samples was qualitatively assessed through the Agar diffusion method by using cultures in a liquid medium of *S. aureus* and *E. coli* test strains. The obtained overall results indicated that incorporating of these active principles into the polymeric hydrogels can significantly enhance the potential efficiency of the fabrics as dressings with antimicrobial and healing accelerating properties and can be an appropriate option for treating first-degree burns injuries.

Keywords: dressings, first-degree burns injuries, hydrogels

INTRODUCTION

Wound dressings with antimicrobial and wound healing accelerating properties are emerging as valuable options to prevent wound infection and improve the wound healing process being an appropriate option for treating first-degree burns injuries (Laurano *et al*., 2022; Fan *et al.,* 2022). Compared to other types of polymeric systems, hydrogels are 3D networks consisting of physically or chemically cross-linked hydrophilic polymers, which are the best choice for a dressing material (Tavakoli and Klar, 2020; Jaya and Vivek, 2014). Dressings based on hydrogels demonstrated advanced functions in the wound process such as antimicrobial properties, adhesion and hemostasis, anti-inflammatory effects, drug delivery, self-healing, and stimulus-response (Luneva *et al.,* 2022). In order to obtain biomaterials with potential use in the treatment of first-degree burns injuries, this experimental study approached the immobilization on 100% cotton fabric of hydrogels based on collagen-gelatin as polymeric matrix which embedding different active principles, in certain formulations.

EXPERIMENTAL PART

Materials

Collagen (*ZENYH, Romania*) and gelatin (bovine skin, type B, *Sigma Aldrich, Germany*) were used as embedding agents for the bioactive agents. Tween 80 (*Sigma Aldrich, Germany*) was used as surfactant and glycerol (*Riedel-de haën|Honeywell, USA*) has been used as a solubilizing agent. Aloe vera (organic powder *Mayam, Romania*), propolis (alcoholic solution 25%, propolis extract – hydroglyceric solution 60%, propolis extract 48% – with colloidal silver 50 ppm, *Dacia Plant, Romania*),

https://doi.org/10.24264/icams-2022.II.25

plantain tincture (70% ethanolic solution, *Hofigal, Romania*) and chamomile tincture (70% ethanolic solution, *Hofigal, Romania*) were used as bioactive agents. Calcium chloride (anhydrous, *Fluka|Honeywell, USA*) was used as a cross-linking agent. For the preparation of bioactive systems, distilled water has been used. Bleached 100% cotton fabric was used for the functionalization processes.

Synthesis of the Hydrogels

For the achievement of the bioactive systems, initially, stock solutions of 5% collagen and 10% gelatin were prepared and then mixed under magnetic stirring, the mixture ratio of collagen:gelatin (by volume) was fixed at 1:1 (20 mL collagen and 20 mL gelatin). Further, over the previously prepared polymeric matrix, 13.3 mL of 5% Aloe vera solution was added, followed by the incorporation of 10 mL glycerol, which was added dropwise. The system was maintained under magnetic stirring for 10 minutes. After that, 4 mL Tween 80 and 28.5 mL distilled water separately were added under vigorous magnetic stirring. Further, after the complete homogenization of the solution, 2 mL propolis (alcoholic or hydroglyceric solution or with colloidal silver), 2 mL tincture (plantain or chamomile) were separately added, maintaining the magnetic stirring for 10 minutes at each stage. As a final step in the synthesis of the hydrogels, a solution of 1% of calcium chloride was added as a cross-linking agent. The selected experimental variants are presented in Table 1.

Table 1. The hydrogel's bioactive principle constituents for each experimental variant

Code	Active Principles					
	Propolis				Tincture	
	Alcoholic solution	Hydroglyceric solution	Colloidal silver	Aloe Vera	Plantain	Chamomile
TAP1	×			×	×	×
TAP2		×		×	×	×
TAP3			×	×	×	×
TAP4		×		×	×	
TAP5		×		×		×

Immobilization of Hydrogels on the Textile Materials

The synthesized hydrogels were immobilized on the textile materials by padding method on the laboratory padder (ROACHES, UK). The treated textile materials were then subjected to the drying operation at 50°C, for 3 minutes.

Methods

pH Analysis

The pH of the synthesized hydrogels was measured using a Multiparameter benchtop meter inoLab® Multi 9310 IDS (*Germany*). The measurements were made in triplicate.

Optical Microscopy

The synthesized hydrogels were analyzed microscopically using an OLYMPUS BX51 optical microscope (*Philippines*) equipped with the OLYMPUS UC30 photo digital camera.

https://doi.org/10.24264/icams-2022.II.25

Air and Vapor Water Permeability

The water vapor permeability was performed according to STAS 9005:1979 standard and the air permeability was performed according to SR EN ISO 9237:1999 standard.

Hydrophilicity

Hydrophilicity of functionalized textile materials was evaluated according to Romanian Standard SR 12751-89 determining fabric wettability by drop method.

Assessment of Antibacterial Activity

The antibacterial activity of the treated samples was qualitatively assessed by the Agar diffusion method according to the SR EN ISO 20645:2005 standard - Determination of antibacterial activity-agar diffusion plate test, by using cultures in liquid medium replicated at 24 hours of ATCC 6538 *Staphylococcus aureus* and ATCC 11229 *Escherichia coli* test strains. Inhibition zones were calculated using the following formula:

$$H = (D - d)/2 \quad (1)$$

where: H – the inhibition zone [mm]; D – the total diameter of specimen and inhibition zone [mm]; d – the diameter of specimen [mm]. The criteria for inhibition zones according to the standard SR EN ISO 20645:2005 are presented in the Table 2.

Table 2. Criteria for inhibition zones according to the standard SR EN ISO 20645:2005

Inhibition zone [mm]	Growth	Evaluation
>1		
1-0	absence	satisfactory effect
0		
0	little	efficiency limit
0		
0	moderate important	unsatisfactory effect

Electron Microscopy

Visualization of the morphology of the cotton fiber surfaces treated with the bioactive systems was performed by scanning electron microscopy using the Quanta 200 electron microscope (*FEI, The Netherlands*).

RESULTS AND DISCUSSION

Optical Microscopy

The images obtained by optical microscopy are shown in Figure 1. According to microscopic images, the dispersed molecule phase is presented as a compact, dense small globule mass. Normally, the destabilization of the solutions begins with the drop's flocculation of different tinctures followed by the phenomenon of coalescence and formation of two distinct phases (separation).

https://doi.org/10.24264/icams-2022.II.25

TAP1 TAP2 TAP3 TAP4 TAP5

Figure 1. Optical microscopy of the resulted bioactive systems

pH Analysis

The pH values for synthesized polymeric systems are presented in Table 3.

Table 3. The pH values of the synthesized hydrogels

Code	pH value
TAP1	4.91
TAP2	4.92
TAP3	4.92
TAP4	4.89
TAP5	4.99

The pH of the polymeric solutions is between 4.89-4.99. It is known from the literature that the skin without any injuries has a pH between 4-6 and the wound can have a pH of up to 8.9. Also, a study on the pH of commercial dressings on the market showed that the pH value is around 4-5. In conclusion, the polymeric solutions which will be used to obtain dressings for first-degree burns injuries, fall within the accepted limits for the field of application from the point of view of the pH value.

Air and Vapor Water Permeability

The values obtained for water vapor permeability and air permeability are presented in Table 4.

Table 4. Air permeability, vapor water permeability and the hydrophilicity of the obtained biomaterials

Code	Vapor water permeability	Air Permeability [l/m^2/s]		Hydrophilicity
		100 Pa	200 Pa	
TAP1	29,93	155	208.6	instantly
TAP2	26.13	201	350.2	instantly
TAP3	27.56	217.8	401	instantly
TAP4	27.74	235.2	445.8	instantly
TAP5	25.77	204.6	375.8	instantly
M	30.52	362.2	450.3	instantly

Air and water vapor permeability recorded lower values compared to the untreated fabric due to the polymeric substances deposited at the surface of the fabric in the form of a semi-permeable film, indicating a comfort decrease for all experimental variants. The most pronounced decrease in air permeability was obtained for the textile material treated with the hydrogel based on collagen-gelatin-propolis (alcoholic solution)-aloe vera-plantain tincture-chamomile tincture (code TAP1), highlighting thus the fact that the use of propolis in the form of an alcoholic solution causes a more pronounced decrease in the comfort indices compared to the hydroglyceric solution. This behavior can be attributed to the increase in alcohol concentration in the polymeric system determined by the using several alcoholic based tinctures which leads to a sealing of the

https://doi.org/10.24264/icams-2022.II.25

free zones in the fabrics geometry thus limiting the free zones in the textile substrate and subsequently the volume of air penetrating the samples.

Hydrophilicity

According to the results presented in Table 4, all the analysed samples present the good hydrophilicity, the functionalization treatments not having a negative influence on this feature. The glycerin content in a dressing improves the ability to absorb excess moisture and exudate. At the same time, glycerin has the ability to be absorbed in the fluids of the body, being diluted quickly without causing toxicity to the body. The surface of the hydrogel is not completely dry due to its high affinity to water, and the polymer is sufficiently viscous to remain on the surface of the lesion, finally allowing easy removal without causing skin damage.

Antimicrobial Activity

Images of Petri plates after 24h incubation are shown in Figure 2 and the assessment of antibacterial activity is shown in Table 5.

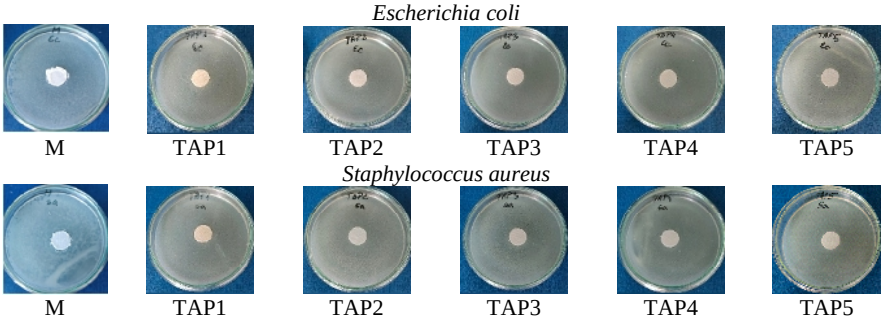

Figure 2. Images of Petri plates showing antibacterial effect after 24 h of incubation

Table 5. Evaluation of the antibacterial activity

Code	Inhibition zone (mm)		Evaluation	
	E. coli	*S. aureus*	*E. coli*	*S. aureus*
TAP1	0	0.5	Satisfactory effect	Satisfactory effect
TAP2	0	0	Satisfactory effect	Satisfactory effect
TAP3	0	0	Satisfactory effect	Satisfactory effect
TAP4	0	0	Satisfactory effect	Satisfactory effect
TAP5	0	0	Satisfactory effect	Satisfactory effect
M	0	0	Unsatisfactory effect	Unsatisfactory effect

According to ISO 20645 standard method, in the case of no inhibition zone (0 mm), without bacterial growth in the nutrient medium under the specimen, the antibacterial effect is evaluated as “satisfactory”, which indicates antimicrobial activity. By analyzing the obtained results, it can be concluded that the textile materials treated with synthesized hydrogels have an antibacterial effect against both test strains.

Scanning Electron Microscopy

The selection of the images obtained at a magnification of ×50, ×1000, and ×2000 for the textile material treated with a bioactive system are shown in Figure 3. The

https://doi.org/10.24264/icams-2022.II.25

resulting micrographs reveal that the surface of the cotton fibers is covered with a thin polymeric layer deposited both on the surface of the fibers and inside the space between the fibers. However, the micrographs cannot provide information about the thickness of the deposited layer and its uniformity.

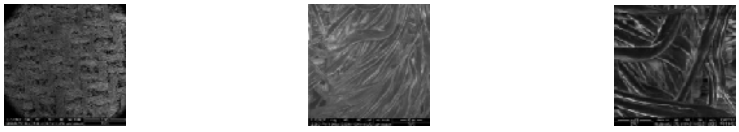

×50 ×1000 ×2000

Figure 3. Electronic images recorded for the TAP 3 variant

CONCLUSIONS

The current study was set to prepare a delivery system based on a mixture of biodegradable and biocompatible polymeric hydrogels for encapsulating different active principles. The enriched hydrogels were used to functionalize textile materials. The obtained wound dressings were subjected to different analyzes using scanning electron microscopy, physical-mechanical investigations and antibacterial tests. Results suggest that the samples enriched with the alcoholic propolis solution exhibited a more pronounced decrease in the comfort indices compared to the hydroglyceric solution. The pH of the synthesized hydrogels varies between 4.89 and 4.99, values which according to the specialized literature are suitable for wound dressings. The textile materials treated with synthesized hydrogels based on collagen-gelatin-bioactive principles have antibacterial effect against both test strains.

These overall results indicate that incorporating these active principles into the polymeric hydrogels can significantly enhance the potential efficiency of the fabrics as wound dressing material, the researches being in progress.

Acknowledgments

This work was carried out through the Nucleu Programme, with the support of MCID, project no. 4N / 08.02.2019, PN 19 17 03 01, project title: "Multifunctional integrated systems based on nanocomposites and pharmacodynamic therapeutic agents for different skin conditions – BIOPANTEX".

REFERENCES

Fan, C., Xu, Q., Hao, R., Wang, C., Que, Y., Chen, Y. and Chang, J. (2022), "Multi-Functional Wound Dressings Based on Silicate Bioactive Materials", *Biomaterials*, 287, 121652, https://doi.org/10.1016/j.biomaterials.2022.121652.

Jaya, M. and Vivek, K.S. (2014), "Cross-Linking in Hydrogels – A Review", *American Journal of Polymer Science*, 4(2), 25-31, https://doi.org/10.5923/j.ajps.20140402.01.

Laurano, R., Boffito M., Ciardelli, G. and Chiono, V. (2022), "Wound Dressing Products: A Translational Investigation from the Bench to the Market", *Engineered Regeneration*, 3(2), 182-200, https://doi.org/10.1016/j.engreg.2022.04.002.

Luneva, O., Olekhnovich, R. and Uspenskaya, M. (2022), "Bilayer Hydrogels for Wound Dressing and Tissue Engineering", *Polymers*, 14(15), 3135, https://doi.org/10.3390/polym14153135.

Tavakoli, S. and Klar, A.S. (2020), "Advanced Hydrogels as Wound Dressings", *Biomolecules*, 10(8), 1169, https://doi.org/10.3390/biom10081169.

RHEOLOGICAL CHARACTERIZATION OF SOME CELLULOSE DERIVATIVES-BASED HYDROGELS

ELENA-EMILIA TUDOROIU[1], MIHAELA-VIOLETA GHICA[1*], MĂDĂLINA GEORGIANA ALBU-KAYA[2], CRISTINA-ELENA DINU-PÎRVU[1], LĂCRĂMIOARA POPA[1], VALENTINA ANUȚA[1], BRUNO ȘTEFAN VELESCU[3], DURMUȘ ALPASLAN KAYA[4], MARIA MINODORA MARIN[2], RĂZVAN MIHAI PRISADA[1]

[1] *"Carol Davila" University of Medicine and Pharmacy, Faculty of Pharmacy, Physical and Colloidal Chemistry Department, 6 Traian Vuia Str., 020956, Bucharest, Romania, *mihaelaghica@yahoo.com*

[2] *The National Research & Development for Textiles and Leather - Leather and Footwear Research Institute Division, 93 Ion Minulescu Str., 031215, Bucharest, Romania*

[3] *"Carol Davila" University of Medicine and Pharmacy, Faculty of Pharmacy, Pharmacology and Clinical Pharmacy Department, 6 Traian Vuia Str., 020956, Bucharest, Romania*

[4] *Mustafa Kemal University, Faculty of Agriculture, Department of Field Crops, 31034, Antakya-Hatay Metropolitan Municipality, 31034, Antakya-Hatay, Turkey*

Cellulose derivatives serve as a feasible alternative to the insoluble natural cellulose considering their high solubility in the most frequent organic solvents and particularly in water. Alongside this advantageous physical property, cellulose derivatives exhibit proper biocompatibility, biodegradability, thermo-gelling nature, and mechanical characteristics. Due to their high hydrophilicity, these biopolymers possess a great capacity to absorb large amounts of water into their structural chains, forming hydrogels with multiple biomedical applications, such as wound healing. Therefore, the main objective of this present work was to assess the rheological properties of some cellulose derivatives-based hydrogels. For this purpose, different commercial varieties of methylcellulose and hydroxyethylcellulose, two of the most used cellulose derivatives, were dispersed in water and stirred continuously until a clear and transparent hydrogel was formed. Depending on the quantities used of each biopolymer, hydrogels of different concentrations were obtained, from 3 to 20%. The topical semisolid systems were rheologically investigated at 23°C using a rotational viscometer and the rheograms of the experimental data were drawn. The hydrogels showed a non-newtonian pseudoplastic behaviour, which represents a requested requirement for topical semisolid systems, both in terms of conditioning, but also of spreading on the skin surface, improving the topical administration.

Keywords: cellulose derivatives, hydrogels, rheological evaluation

INTRODUCTION

Cellulose is the most plentiful biopolymer, a crystalline and rigid molecule, insoluble in water (Popa *et al*., 2022), which due to its chemical structure can suffer several changes at hydroxyl groups, resulting cellulose derivatives (Fekete *et al*., 2014). The most regularly used cellulose derivatives are cellulose ethers (methylcellulose, sodium carboxymethyl cellulose, hydroxyethyl cellulose, hydroxypropyl cellulose,) (Tudoroiu *et al*., 2021) because they exhibit high water solubility (Lee and Yoo, 2021).

Due to their excellent availability, biocompatibility, renewability, non-toxicity, immunogenicity, thermo-gelling capacity, mechanical and rheological properties, stability, low cost, and antibacterial efficacy (He *et al*., 2021; Ho and Leo, 2021), cellulose derivatives are appealing polymers for vast applications in pharmaceutical, biomedical, and bioanalysis fields (wound dressings, drug delivery systems, tissue engineering, biosensors, or smart materials) (Abdelhak, 2019; Oprea and Voicu, 2020).

In this present work, the focus is on cellulose-based hydrogels, water-soluble bases, with high water content, cooling effect, washability, transparency, safety, porosity,

https://doi.org/10.24264/icams-2022.II.26

tolerability, and adherence to the skin. The main physical properties of these hydrogels are transitional and rheological properties that are essential in the process of their formulation (Kabir *et al*., 2018). Therefore, the purpose of this paper was to evaluate the rheological properties of some cellulose derivatives-based hydrogels, using different commercial varieties of methylcellulose and hydroxyethyl cellulose in order to select the suitable sorts to prepare hydrogels for further application as wound dressing.

MATERIALS AND METHODS

Materials

In this work, six commercial varieties of methylcellulose (MC), differing in composition and viscosity were used. They were divided into two series, each one containing three sorts. Series I includes: first sort coded as Sort MC 1, viscosity of 4000 cPs at 2% in H_2O (Janssen Chimica, Belgium), second sort coded as Sort MC 2, viscosity of 1500 cPs at 2% in H_2O (ICN Biomedicals Inc., USA), and third sort coded as Sort MC 3 (Methocel® MC), high viscosity, 27.5-32% methoxyl content, 3000-5000 mPa.s at 2% in H_2O, 20°C (Sigma-Aldrich, USA). Series II contains: first sort coded as Sort MC 1, viscosity of 15 cPs at 2% in H_2O (Janssen Chimica, Belgium), second sort coded as Sort MC 2 (Methocel® MC) with 27.5-32% methoxyl content and 10-25 mPa.s at 2% in H_2O, 20°C (Sigma-Aldrich, USA), and third sort coded as Sort MC 3, viscosity of 25 cPs at 2% in H_2O (ICN Biomedicals Inc., USA). Regarding the hydroxyethyl cellulose (HEC), three commercial varieties differing in viscosity were used. First sort coded as Sort HEC 1 with ~ 92% cellulose ether (Merck Schuchardt, Germany), second sort coded as Sort HEC 2, viscosity of 145 mPa.s at 1% in H_2O, 20°C (Loba Chemie Pvt. Ltd., India), and third sort coded as Sort HEC 3, viscosity of 4000 cPs (Sigma-Aldrich, Germany). Distilled water was used throughout the study.

Preparation of Methylcellulose Hydrogels

MC hydrogels were prepared in various concentrations according to the viscosity of the commercial sorts. For Series I, hydrogels of 3 and 4% concentration were prepared and for Series II, hydrogels of 8 and 10% were prepared. The MC powder was added slowly over half of the amount of distilled water required for preparation (heated at 80°C), gently stirring with a glass rod until the entire amount of powder was dispersed. The rest of the amount of distilled water (cold water) was added to the obtained mixture, continuously stirring. To jellify, mixtures were left to rest, continuing mixing.

Preparation of Hydroxyethyl Cellulose Hydrogels

HEC hydrogels were prepared in different concentrations according to the viscosity of the commercial varieties. Therefore, for Sort HEC 1 and Sort HEC 3, hydrogels of 4% concentration were prepared. For Sort HEC 2, hydrogel of 20% concentration was prepared. HEC hydrogels were prepared in the same way as MC hydrogels, the only difference being the use of distilled water at room temperature.

https://doi.org/10.24264/icams-2022.II.26

Analysis of Rheological Properties

Rheological determinations of all cellulose derivatives-based hydrogels were performed with a rotational viscometer (Fungilab), using standard spindles, TR 9 and TR 10. All analyses were conducted at 23°C. The operational conditions were formerly described (Albu *et al*., 2009; Ghica *et al*., 2012).

RESULTS AND DISCUSSION

To quantify the pseudoplastic behaviour of the tested hydrogels, the Power law model was used, which indicates the relation between viscosity and shear rate (eq. 1):

$$\eta = m \cdot \dot{\gamma}^{-n} \quad (1)$$

where m parameter corresponds to the viscosity resulted for the shear rate of $1 \cdot s^{-1}$ and n represents the flow behaviour index (Dănilă et al., 2019). They are evaluated by the linearization of eq. (1) through double logarithmic method (Figure 1).

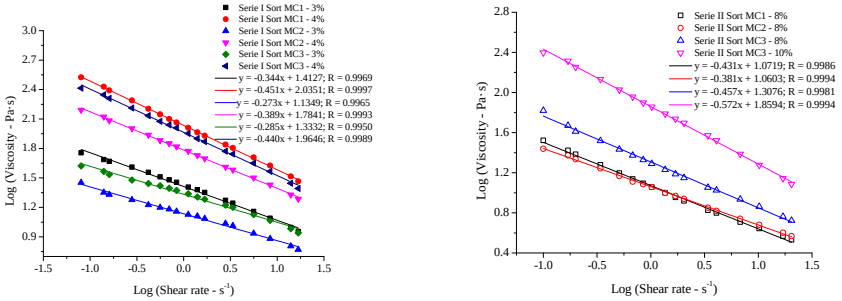

a) b)

Figure 1. Log-log plots of viscosity versus shear rate for MC hydrogels, analyzed at 23°C: a) Series I; b) Series II

Interpreting Figure 1, the viscosity of MC hydrogels from both series decreases with increase of shear rate, indicating a non-newtonian pseudoplastic behaviour at 23°C, which is a mandatory condition for topical systems, promoting the hydrogels flow and corresponding to a suitable application on the skin surface. The values for m and n parameters and correlation coefficient R specific for Power law model and the thixotropic descriptors for MC hydrogels, analyzed at 23°C are presented in Table 1 (Series I) and Table 2 (Series II).

Table 1. Values for m and n parameters and correlation coefficient R specific for Power law model, and the thixotropic descriptors analyzed at 23°C (Series I)

Gels Series I	m	n	R	S_{asc} (Pa· s^{-1})	S_{thix} (Pa· s^{-1})	T_{hyst} (%)
Sort MC 1 - 3%	25.864	0.34	0.9969	1616.187	93.197	5.76
Sort MC 1 - 4%	108.417	0.45	0.9997	5527.273	526.205	9.52
Sort MC 2 - 3%	13.642	0.27	0.9965	1009.651	62.184	6.16
Sort MC 2 - 4%	60.827	0.39	0.9993	3514.012	256.994	7.31
Sort MC 3 - 3%	21.537	0.29	0.9950	1534.456	83.833	5.46
Sort MC 3 - 4%	92.172	0.44	0.9989	4752.580	385.180	8.10

https://doi.org/10.24264/icams-2022.II.26

For all analyzed hydrogels from Series I, values of the correlation coefficient R higher than 0.9900 (between 0.9950 and 0.9997) are recorded, which means that the experimental data fitted the Power law model properly. The rheological parameter m for Sort MC 1 - 3% and Sort MC 3 - 3% has close values due to similar viscosities for the two commercial sorts (~4000 cP). Contrary, for Sort MC 2 - 3%, the m value is less than the other two, because it has a lower viscosity (1500 cP). It can be easily noticed that for all three sorts, but at 4% concentration, the m values are considerably higher than the same parameter at 3% concentration. Thus, m value is about 4.2 times higher for Sort MC 1 - 4% than for Sort MC 1 - 3%, 4.45 times higher for Sort MC 2 - 4% than for Sort MC.2 - 3%, and 4.3 times higher for Sort MC.3 - 4% than for Sort MC.3 - 3%. According to the m parameter previously detailed, Sort MC 1 - 3% and Sort MC 3 - 3% have close values of the thixotropy area (S_{thix}), while for Sort MC 2 - 3%, this thixotropic descriptor is less than the other two, because of their difference in viscosity. For all three sorts, but at 4% concentration, the S_{thix} values are significantly higher than the same descriptor at 3% concentration. Thus, S_{thix} is about 5.64 times higher for Sort MC 1 - 4% than for Sort MC 1 - 3%, 4.13 times higher for Sort MC 2 - 4% than for Sort MC.2 - 3%, and 4.6 times higher for Sort MC.3 - 4% than for Sort MC.3 - 3%. For a system to be thixotropic, the value of the thixotropy index ($T_{hyst\%}$) must be higher than 5% (Dănilă et al., 2019). It can also be noticed that the $T_{hist\%}$ for Sort MC 2 - 3% is higher than 5% compared to other sorts at the same concentration. The thixotropic behaviour is much more obvious at 4% concentration for all sorts analyzed at 23°C.

Table 2. Values for m and n parameters and correlation coefficient R specific for Power law model, and the thixotropic descriptors analyzed at 23°C (Series II)

Gels Series II	m	n	R	S_{asc} (Pa· s^{-1})	S_{thix} (Pa· s^{-1})	$T_{hyst\%}$ (%)
Sort MC 1 - 8%	11.800	0.43	0.9986	874.317	34.823	3.98
Sort MC 2 - 8%	11.489	0.38	0.9994	943.821	34.051	3.61
Sort MC 3 - 8%	20.305	0.46	0.9981	1415.572	80.017	5.65
Sort MC 3 - 10%	72.343	0.58	0.9994	3684.886	282.851	7.68

For all tested hydrogels from Series II, values of the correlation coefficient R higher than 0.9900 (between 0.9981 and 0.9994) are recorded, showing that the experimental data best fitted the Power law model. Table 2 shows that for Sort MC 1 and Sort MC 2, the rheological parameters m has very close values, while for Sort MC 3, this parameter is only about 1.74 times higher, at a concentration of 8%. This aspect can be explained by the fact that these three commercial sorts have similar viscosities (~10-25 cP). On the other hand, there is a significant increase of the m parameter for Sort MC 3 at a concentration of 10%, which is about 3.56 times higher compared to the value recorded at 8%. Sort MC 1 - 8% and Sort MC 2 - 8% have very close values of S_{thix}, while this thixotropic descriptor is about 2.30 times higher for Sort MC 3 - 8%. It can be noticed that for Sort MC 3, but in a concentration of 10%, S_{thix} increases considerably, being about 3.53 times higher than S_{thix} value at 8%. Thus, S_{thix} can be correlated with the previously determined rheological parameter m, because both descriptors have similar increases when comparing the two concentration (8 and 10%) of Sort MC 3. Regarding the thixotropic behaviour, Sort MC 1 - 8% and Sort MC 2 - 8% are not thixotropic, because $T_{hist\%}$ values are less than 5%. For Sort MC 3 - 8%, a low degree of thixotropy is observed, but at 10%, $T_{hyst\%}$ value is much higher than 5%, which indicates that this hydrogel is thixotropic at 23°C. It can also be remarked that for all sorts from Series II,

https://doi.org/10.24264/icams-2022.II.26

a high concentration of polymers is required to gelation, which could raise problems for their lyophilization.

The results of the rheological experiments conducted at 23°C for HEC hydrogels led to rheograms - viscosity as a function of shear rate - illustrated for exemplification in Figure 2a. The Power law model, previously detailed, was used to quantify the flow behaviour of HEC hydrogels. To evaluate the thixotropic behaviour of HEC hydrogels, the rheological profiles corresponding to forward and backward curves – shear stress as a function of shear rate - obtained at 23°C are presented in Figure 2b.

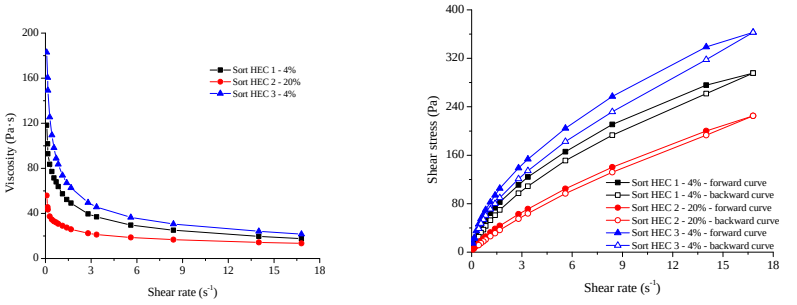

a) b)

Figure 2. a) Cumulative rheograms viscosity as a function of shear rate corresponding to HEC hydrogels, analyzed at 23°C; b) Forward and backward curves shear stress as a function of shear rate corresponding to HEC hydrogels, analyzed at 23°C

Analyzing Figure 2a, the viscosity of HEC hydrogels decreases with increase of shear rate, indicating a non-newtonian pseudoplastic character at 23°C. Figure 2b shows the thixotropic character of HEC hydrogels because the backward curve is placed under the forward curve, which means that at the same shear rate, the shear stress for the backward curve is lower.

Table 3. Values for m and n parameters and correlation coefficient R specific for Power law model, and the thixotropic descriptors analyzed at 23°C

Gels	m	n	R	S_{asc} (Pa· s^{-1})	S_{thix} (Pa· s^{-1})	T_{hyst} (%)
Sort HEC 1 - 4%	54.701	0.35	0.9897	3271.555	230.350	7.04
Sort HEC 2 - 20%	28.595	0.25	0.9966	2227.234	115.505	5.19
Sort HEC 3 - 4%	73.994	0.40	0.9970	4025.635	328.835	8.17

For Sort HEC 2 - 20% and Sort HEC 3 - 4%, values of the correlation coefficient R higher than 0.9900 are recorded, which means that the experimental data fitted the Power law model properly. For Sort HEC 1, this value is less than 0.9900. According to the Table 3, the values of the rheological parameters m are well correlated with the viscosity of the commercial sorts; thus, the highest value is registered for Sort HEC 3 - 4%, which has the highest viscosity (4000 cP), and the lowest value is registered for Sort HEC 2 - 20%, which has the lowest viscosity (145 cP). In accordance with the previously mentioned, S_{thix} has a similar variation of its values. The highest value is recorded for Sort HEC 3 - 4%, which is 2.85 times higher than the one recorded for Sort HEC 2 - 20%. It can also be observed that the lowest values of $T_{hyst\%}$ was obtained for

https://doi.org/10.24264/icams-2022.II.26

Sort HEC 2 - 20%, which presents a slightly thixotropy at 23°C. Sort HEC 1 - 4% and Sort HEC 3 - 4%, are thixotropic at 23°C because their value are higher than 5%.

CONCLUSIONS

Cellulose derivatives-based hydrogels showed a non-newtonian pseudoplastic behaviour, which represents a preferable property for the semisolid systems because this feature improves their conditioning and spreadability on the skin surface, promoting the topical administration. Considering the experimental data recorded for the flow and thixotropic parameters, Sort MC 2 and Sort HEC 3 could be selected in a concentration between 3 and 3.5% for further applications in wound healing domain.

Acknowledgement

This work was financially supported by "Carol Davila" University of Medicine and Pharmacy Bucharest, Romania, through Contract no. 33PFE/30.12.2021 funded by the Ministry of Research and Innovation within PNCDI III, Program 1—Development of the National RD system, Subprogram 1.2—Institutional Performance—RDI excellence funding projects.

REFERENCES

Abdelhak, M. (2019), "A Review: Application of Biopolymers in the Pharmaceutical Formulation", *Journal of Advances in Bio-pharmaceutics and Pharmacovigilance*, 1, 15-25, https://doi.org/10.5281/zenodo.2577643.

Albu, M.G., Ghica, M.V., Popa, L., Leca, M. and Trandafir, V. (2009), "Kinetics of *in vitro* Release of Doxycycline Hyclate from Collagen Hydrogels", *Revue Roumaine de Chimie*, 54, 373-379.

Dănilă, E., Moldovan, Z., Albu Kaya, M.G. and Ghica, M.V. (2019), "Formulation and Characterization of Some Oil in Water Cosmetic Emulsions Based on Collagen Hydrolysate and Vegetable Oils Mixtures", *Pure and Applied Chemistry*, 91(9), 1493-1507, https://doi.org/10.1515/pac-2018-0911.

Fekete, T., Borsa, J., Takács, E. and Wojnárovits, L. (2014), "Synthesis of Cellulose Derivative Based Superabsorbent Hydrogels by Radiation Induced Crosslinking", *Cellulose*, 21, 4157-4165, https://doi.org/10.1007/s10570-014-0445-6.

Ghica, M.V., Albu, M.G., Dinu-Pirvu, C. and Moisescu, S. (2012), "*In vitro* Kinetic Release and Flow Behaviour of Some Collagen-Minocycline Topical Hydrogels", *Revista de Chimie*, 63, 929-935.

He, X., Lu, W., Sun, C., Khalesi, H., Mata, A., Andaleeb, R. and Fang, Y. (2021), "Cellulose and Cellulose Derivatives: Different Colloidal States and Food-Related Applications", *Carbohydrate Polymers*, 255, 117334, https://doi.org/10.1016/j.carbpol.2020.117334.

Ho, N.A.D. and Leo, C.P. (2021), "A Review on the Emerging Applications of Cellulose, Cellulose Derivatives and Nanocellulose in Carbon Capture", *Environmental Research*, 197, 111100, https://doi.org/10.1016/j.envres.2021.111100.

Kabir, S.M.F., Sikdar, P.P., Haque, B., Bhuiyan, M.A.R., Ali, A. and Islam, M.N. (2018), "Cellulose-based Hydrogel Materials: Chemistry, Properties and Their Prospective Applications", *Progress in Biomaterials*, 7, 153-174, https://doi.org/10.1007/s40204-018-0095-0.

Lee, D. and Yoo, B. (2021), "Cellulose Derivatives Agglomerated in a Fluidized Bed: Physical, Rheological, and Structural Properties", *International Journal of Biological Macromolecules*, 181, 232-240, https://doi.org/10.1016/j.ijbiomac.2021.03.142.

Oprea, M. and Voicu, S.I. (2020), "Recent Advances in Composites Based on Cellulose Derivatives for Biomedical Applications", *Carbohydrate Polymers*, 247, 116683, https://doi.org/10.1016/j.carbpol.2020.116683.

Popa, L., Ghica, M.V., Tudoroiu, E.-E., Ionescu, D.-G. and Dinu-Pîrvu, C.-E. (2022), "Bacterial Cellulose - A Remarkable Polymer as a Source for Biomaterials Tailoring", *Materials*, 15(3), 1054, https://doi.org/10.3390/ma15031054.

Tudoroiu, E.-E., Dinu-Pîrvu, C.-E., Albu Kaya, M.G., Popa, L., Anuța, V., Prisada, R.M. and Ghica, M.V. (2021), "An Overview of Cellulose Derivatives-Based Dressings for Wound-Healing Management", *Pharmaceuticals*, 14(12), 1215, https://doi.org/10.3390/ph14121215.

VARIATIONS IN ESSENTIAL OIL MAIN COMPONENTS OF NATIVE GROWN *Salvia aramiensis* RECH FIL. GENOTYPES DEPENDING ON YEARS

MUSA TÜRKMEN, DURMUŞ ALPASLAN KAYA, FİLİZ AYANOĞLU

Mustafa Kemal University, Agriculture Faculty, Field Crops Department, 31034, Hatay, Türkiye, e-mail: musaturkmen@mku.edu.tr; dkaya@mku.edu.tr; filizayanoglu@gmail.com

The essential oils and components of sage, which is mostly consumed as a tea and spice plant, have different uses in the field of medicine and cosmetics. The high camphor and thujone contained in many sage species limit the use of the plant as tea and spice in the food sector due to its toxic and carcinogenic effects. In such cases, which directly concern human health, new species and varieties containing low camphor and thujone should be introduced to the market, and the consumer should be provided with safe food. Studies in the *Salvia aramiensis* species revealed that the camphor rate in this plant is very low and there is no thujone. Antakya sage (*Salvia aramiensis* Rech. fil.,), which is only found in the flora of Hatay in Türkiye, is important for the herbal tea market due to its chemical content. For this reason, this study was carried out in seventy-nine genotypes growing naturally in different locations for two consecutive years, in order to reveal the variation of essential oil compositions of *S. aramiensis* genotypes. In general terms, it was determined that the ratio of essential oil components of genotypes did not change much over the years. In the study, first- and second-year cineole averages of the genotypes were found as 44.40% and 45.69%, camphor averages 12.74% and 12.58%, β-pinene averages 4.70% and 5.07%, borneol averages 6.53% and 6.22%, respectively.

Keywords: Essential oil, camphor, cineole, β-pinene, borneol GC-MS, *Salvia aramiensis*

INTRODUCTION

The return to nature is gradually accelerating in the world and the use of herbal preparations as nutritional supplements, tea and spices is increasing day by day. In this context, one of the most consumed plant species is sage (*Salvia* spp.). It is known that the genus Salvia, which can spread in many different ecosystems, has about 1000 species in the world (Kintzios, 2000; Walker and Sytsma, 2007; İnce and Karaca, 2015).

Sage has ninety-seven species, 4 subspecies and 8 varieties in Türkiye. Fifty-five of these species are endemic (Hedge, 1982; Davis *et al*., 1988; İpek and Gürbüz, 2010; Vural and Adıgüzel, 1996; Dönmez, 2001; Hamzaoğlu *et al*., 2005; Celep and Doğan, 2010; Celep *et al*., 2009; Behçet and Avlamaz, 2009; Kahraman *et al*., 2009). Various studies have shown that there are around twenty Salvia species in the flora of Hatay (Davis *et al*., 1988; Türkmen and Düzenli, 1998; Düzenli and Çakan, 2001; Celep and Doğan, 2010; Ayanoğlu *et al*., 2012). Among these species, *S. aramiensis* Rech. Fill. It is included in VU: Vulnerable species group (Ekim *et al*., 2000; Celep *et al*., 2010).

Among the sage species, *S. officinalis* is the most used species as tea and spice. 1.8 cineole, camphor, thujone, pinene and borneol, which are generally monoterpene in the essential oil of Salvia species used as tea and spice, are the most common components (Lamaison *et al*., 1991; Cuvelier *et al*., 1994; Lawrence, 1998). Although each of these components has many uses in the field of medicine and cosmetics, the toxic effects of camphor and thujone components are the most important factors limiting the use of sage as tea and spice. Although the components of essential oils vary depending on the source of the plants, it is generally assumed that thujone and camphor components are common in *S. officinalis* essential oil (Lawrence, 1983; Tucker and Maciarello, 1990; Lawrence, 1998).

https://doi.org/10.24264/icams-2022.II.27

S. aramiensis is a species that grows only in Hatay in Türkiye, is used as a tea and spice, has a low camphor content and does not contain thujone in some genotypes. Demirci *et al*. (2002), in the study in which they examined the essential oil contents of *S. Aramiensis* samples taken from three different locations of Hatay, they found that the camphor content is between 7.5-10.1%. Karaman *et al*. (2007) found that the camphor ratio in the essential oil of *S. aramiensis* was 2.1%. Askun *et al*. (2010) examined the *S. aramiensis* plant from the Hatay flora in terms of essential oil components and the camphor content was determined as 5.8% in the study. Kelen and Tepe (2008), in their study investigating the chemical contents and antimicrobial properties of S. aramiensis essential oil obtained from the flora of Hatay, determined that the essential oil contains 1.8 cineole (46.0%) camphor (8.7%) and no thujone. Ayanoglu *et al*. (2012), in a study of *S. aramiensis* species in Hatay, reported that 1.8 cineole was determined as 34.94%-51.53% and camphor was around 1%, while thujone was not found. As can be seen from these studies, the camphor ratio of *S. aramiensis* essential oil varies between 2.1-11.1%, and the thujone ratio varies between 0-1.1%.

It has the potential to replace *S. officinalis* species, especially in the food sector, by giving priority to the food safety problem, which directly concerns human health, to reduce the damage to biodiversity caused by the trade made only with the collections made from natural flora, and to increase the level of competition by using high quality genotypes in growing these increasingly cultivated plants. A clonal selection study (TÜBİTAK, 119O331) conducted based on chemotype for the development of cultivars bearing the same name was conducted for two years in order to monitor the change of essential oil components over the years.

MATERIALS AND METHODS

The material of the experiment consists of *Salvia aramiensis* plants growing in Hatay natural flora. Alien pollinator, *Salvia aramiensis* Rech. Elephant. is a perennial shrub, upright plant whose trunk can grow up to 1.3 m. The body is quadrangular, with dense eglandular-tomentose (glandless-soft-hairy) and sessile glandular (glandular) hairs below, slightly pilose (soft-hairy) or subglabrous (almost glabrous) above. Leaves simple, narrowly oblong, elliptic to obovate (ellipse to obovate), 1.4-6 x 0.4-3 cm, crenulate (small-carved); Petiole 0.5-3 cm. Verticillasters have 2-10 flowers and are concentrated at the tip. Bract ovate, 5-8 x 4-8 mm, shed. Bracteoles are present. Petioles 1.5-4 mm, sepals ± tubular, 9-15 mm, in fruit elongated to 10-17 mm, violet colored, striped, short-stalked glandular hairy, few eglandular pilose hairs sometimes present or absent, upper lip triangular and suddenly narrowed and elongated at the top. Petals mauve to pink, ca. 22-30 mm long; corolla tube straight, 15-20 mm; upper lip is straight. Stamens are Type A. Anther about 3 mm, inferior theca about 2 mm, filaments about 4-5 mm. Flowering and habitat: April-May. It is found at 150-600 m in red pine forest clearing and rocky slopes. This species, which spreads only in the Amanos Mountains in Türkiye, is consumed as tea by the people in the region (Doğan *et al*. 2008).

In the study, essential oil components of seventy-nine genotypes grown in 16 different locations in Hatay region were investigated for two years. Locations and their code numbers are 1 (Alan), 21 (Belen), 24 (Çabala), 31 (Fırnız), 5 (Gökdere), 27

https://doi.org/10.24264/icams-2022.II.27

(Gümrük), 25 (Güveççi), 17 (Harlısu), 11 (Haymaseki), 13 (Höyük), 14 (İkinehir), 22 (Kömürçukuru), 4 (Kuyuluk), 2 (Kuzuculu), 32 (Üçgedik) and 26 (Yukarı pulluyazı).

The study was carried out in the autumn of 2019 and 2020. Plants in predetermined locations where *S. aramiensis* grows naturally are marked with weatherproof labels. Coordinates and altitudes of genotypes were determined. Leaf samples were taken from these marked plants for essential oil analysis. The reason essential oil analyzes are carried out in autumn is that even though the plants are in different ecologies, they experience the same physiological period, that is, the period when the plants go to rest. Thus, the analyzes made in this period when the plants are more stable reveal the situation that they are more comparable in terms of chemical properties.

Essential oils were obtained from 50 g dry leaf samples of each plant by hydrodistillation method for 3 hours in a Clevenger apparatus. While determining the essential oil components (%), essential oil samples of each plant were analyzed in GC-MS (Gas Chromatography-Mass Spectrometry) device. Analyzes were performed on a Thermo Scientific ISQ Single Quadrupole model gas chromatograph. Essential oil samples (5 µl oil diluted in 2 ml n-hexane) were determined using the TG-Wax MS model, (5% Phenyl Polysilphenylene-siloxane, 0.25 mm, 60 m long, 0.25 µm film thickness) column. The ionization energy was set to 70 eV and the mass range m/z 1.2-1200 amu. Scan mode was used for data collection. MS transfer line temperature was 250 °C, MS ionization temperature was 220 °C, column temperature was 50 °C at the beginning and increased to 220 °C with a temperature increase rate of 3 °C/min. The structure of each compound was defined with the Xcalibur program using mass spectra (Wiley 9). In addition, components have been validated using standards.

RESULTS AND DISCUSSION

The main components (cineol, camphor, β-pinene and borneol) ratios of essential oils obtained from the dry leaves of each *S. aramiensis* genotype in two consecutive studies were determined and shown in Table 1. As seen in the Table 1, there are quite large differences between genotypes in terms of the amounts of each major component. As can be seen in Table 1, there are quite enormous differences between genotypes in terms of the amounts of each major component. The cineole ratios of the genotypes varied between 15.93-76.30% in the first year of the trial and between 11.23-76.89% in the second year. According to genotypes, camphor rates were between 0,00-38,64% in the first year and between 0,009-36,64% in the second year. There were also great variations in b-pinene and borneol ratios between genotypes, and β-pinene ratios ranged from 0,00-8,50% in the first year to 0,00-12,60% in the second year, while borneol ratios in the first year 0,00-20,07% and the second year varied between 0,00-24,09%. In some genotypes, camphor, β-pinene and borneol were found to be negligible. This variation between genotypes reveals the importance of selection studies in the development of sage varieties required for the herbal tea industry.

Despite this variation between genotypes, there were no significant differences between the ratios of essential oil components of genotypes by years. It is understood that the rate of cineole increased by 2.91% compared to the previous year when considering the average cineole contents of the genotypes (Table 1). In other words, genotypes with high cineole content were high cineole content in the other year, while the cineole ratios of genotypes with low cineole content were found to be low. This is important in terms of pre-selection according to chemotypes. Considering the average camphor content of the genotypes, it was determined that the camphor rate changed by -

https://doi.org/10.24264/icams-2022.II.27

1,26% compared to the previous year. In the mean β-pinene values, there was a 7.87% difference over the years, while the average borneol ratios were found to vary by -4.74%. In the experiment, the standard deviation values of the components of the genotypes were 17.26 and 17.66 for cineole; 9.57 and 9.37 for camphor; 1.78 and 2.04 for β-pinene; 5.05 and 5.29 for borneol, respectively.

Table 1. The main components of *S. aramiensis* Rech. Fil. genotypes for two years (%) and percentage of changes

Genotypes	*1.8 cineol*		*Camphor*		*β-pinene*		*Borneol*	
	2019	2020	2019	2020	2019	2020	2019	2020
1/3	30.96	30.16	18.13	18.52	6.58	12.60	0.00	3.41
1/6	30.67	42.28	18.85	23.04	6.74	11.07	4.40	4.74
1/7	15.93	76.89	19.34	0.35	7.91	8.27	10.09	0.27
1/12	28.06	25.99	11.70	24.12	7.08	9.34	13.95	7.94
1/13	26.68	23.45	30.42	36.64	4.95	4.75	5.90	5.74
1/15	32.64	34.67	6.66	6.73	7.65	6.57	8.20	8.41
21/6	26.87	69.53	0.00	1.73	0.00	2.30	5.30	1.10
21/8	58.61	54.79	11.09	8.47	3.69	4.81	2.42	3.17
21/10	47.97	52.51	14.56	13.43	5.22	4.87	6.86	5.94
24/7	16.38	16.9	20.65	19.13	6.19	8.18	19.74	7.49
24/10	40.94	37.27	15.09	13.37	5.08	0.39	5.13	6.42
31/4	41.52	45.66	4.50	3.95	4.34	4.87	5.12	9.04
31/12	20.12	18.35	22.09	25.34	7.45	6.14	10.18	7.83
31/13	22.85	27.43	9.69	18.16	5.35	3.06	11.78	11.55
31/14	6.88	33.52	3.87	24.71	0.00	4.37	3.71	15.80
5/5	31.36	36.42	22.86	15.70	6.20	5.30	8.51	9.75
5/7	38.65	53.79	13.66	17.93	6.27	3.48	6.52	6.02
5/8	36.51	34.62	12.33	15.41	4.52	3.93	18.67	19.81
5/13	23.39	30.66	26.09	14.32	5.55	7.08	13.80	13.67
5/17	24.37	19.02	20.73	27.95	0.00	6.23	9.31	13.20
5/18	29.66	23.78	23.67	34.05	5.66	5.90	14.48	12.31
5/19	27.49	16.87	19.18	24.34	8.50	7.33	9.53	13.39
5/20	33.90	38.03	23.97	12.07	5.16	6.57	4.83	6.73
27/4	39.57	42.52	29.08	12.48	3.53	6.85	4.19	6.56
27/20	26.41	11.23	23.57	21.96	5.51	8.31	8.59	16.71
27/23	23.90	13.71	38.52	27.38	3.47	5.73	6.24	3.70
25/3	38.50	35.81	9.52	12.05	6.22	6.36	15.00	14.86
25/4	50.12	39.58	8.34	11.03	4.30	5.58	6.32	7.28
25/6	48.37	50.20	8.51	5.84	3.25	4.19	0.00	2.67
25/8	58.67	39.58	5.19	14.75	4.63	4.15	1.81	3.41
25/16	43.86	28.05	18.91	17.77	5.80	7.01	2.75	3.77
25/20	16.41	26.33	22.78	22.44	7.47	6.65	6.47	18.62
17/1	22.85	37.94	21.16	14.15	5.44	5.17	16.00	16.76
17/5	21.66	64.35	25.16	10.05	6.20	5.95	17.60	14.06
17/8	43.99	67.83	13.76	0.85	4.97	3.34	9.23	5.39
17/9	64.73	54.77	0.55	10.68	3.13	3.66	0.75	0.32
17/10	56.86	57.99	9.80	8.28	4.74	5.47	4.51	5.16
17/12	54.77	66.27	8.52	10.16	5.02	4.35	6.44	6.99
17/19	52.37	50.36	13.82	16.02	5.62	4.51	3.94	1.92
17/20	45.25	47.37	15.21	21.37	4.98	3.88	7.81	6.23
11/8	45.93	55.16	20.53	13.62	2.83	3.12	8.69	4.26
11/19	58.03	71.68	12.76	3.26	2.83	4.14	5.76	5.03
13/1	70.09	69.95	4.04	1.03	3.50	4.07	2.21	1.54
13/4	57.59	75.11	0.96	0.09	4.91	3.73	5.24	1.92
13/5	73.89	71.00	0.44	2.06	3.09	2.67	0.84	0.15
13/6	51.21	75.20	5.78	0.78	4.56	4.05	9.77	1.86

https://doi.org/10.24264/icams-2022.II.27

Genotypes	*1.8 cineol*		*Camphor*		*β-pinene*		*Borneol*	
	2019	2020	2019	2020	2019	2020	2019	2020
13/8	68.60	15.29	1.12	3.54	4.01	2.62	0.94	0.39
13/9	76.30	73.20	1.48	0.95	3.10	3.56	1.13	0.00
13/10	56.36	54.25	10.45	5.24	2.51	3.55	8.70	0.34
13/11	69.37	56.74	3.48	2.40	2.93	6.32	3.27	9.50
13/13	54.71	23.74	2.87	16.34	5.80	4.57	2.02	1.33
13/14	75.55	57.21	3.11	4.17	2.56	8.29	0.00	15.09
14/ 3	56.97	58.97	4.38	1.68	5.33	5.09	0.00	0.00
14/10	59.80	60.71	1.48	2.61	5.37	5.29	0.00	0.00
14/12	50.91	64.98	2.93	0.81	4.69	4.85	7.45	5.05
14/13	73.21	61.66	4.29	1.38	3.01	5.21	3.56	5.21
14/16	73.11	53.01	1.36	8.51	2.81	5.14	1.37	1.18
14/17	60.08	49.14	7.15	10.34	4.42	5.34	5.83	6.13
14/19	50.47	18.47	9.32	36.07	5.49	6.73	6.45	5.26
22/2	20.92	55.73	30.55	0.57	8.21	6.73	6.61	7.10
22/3	74.13	44.61	0.84	8.40	3.36	3.92	0.54	0.52
22/4	14.46	70.40	2.01	1.64	5.78	3.38	16.68	6.57
22/7	59.27	63.28	4.50	6.50	4.23	3.81	0.95	0.46
22/11	62.31	59.52	5.87	2.32	3.97	2.95	1.36	1.28
22/14	61.65	40.12	5.03	16.60	4.00	3.36	1.43	1.11
4/2	59.16	55.22	4.76	14.39	4.21	5.46	3.44	5.24
4/4	49.28	35.74	12.95	15.91	5.53	3.66	5.04	5.01
4/5	38.39	18.22	17.17	18.25	5.78	6.63	6.69	5.94
4/22	16.66	41.84	20.83	14.67	8.09	7.54	20.07	24.09
2/11	38.89	32.34	13.82	23.23	7.04	6.34	7.07	6.51
2/16	32.35	28.46	23.48	24.01	4.40	3.63	13.27	9.27
2/20	30.27	50.33	38.67	8.09	1.77	3.87	11.73	9.03
32/6	51.73	65.66	4.57	1.54	4.83	5.05	5.58	7.13
32/8	58.68	60.25	2.03	2.55	3.41	4.02	2.91	1.66
32/11	51.31	34.55	3.59	31.91	3.99	4.75	5.22	2.47
26/1	41.11	63.94	27.69	16.84	2.65	2.64	0.00	1.75
26/2	22.94	51.62	16.68	8.38	5.55	3.99	7.59	6.78
26/13	60.32	55.96	8.72	8.18	3.13	5.50	1.40	7.19
26/15	43.14	39.65	22.98	17.88	3.24	0.00	9.37	0.00
Min.	15.93	11.23	0.00	0.09	0.00	0.00	0.00	0.00
Max.	76.30	76.89	38.67	36.64	8.50	12.60	20.07	24.09
Mean	44.40	45.69	12.74	12.58	4.70	5.07	6.53	6.22
Percentage of change	2.91%		-1.26%		7.87%		-4.75%	
Standard deviation	17.26	17.66	9.57	9.37	1.78	2.04	5.05	5.29

CONCLUSIONS

As a result of this study, which was carried out on naturally grown plants for two consecutive years, it was determined that *S. aramiensis* did not contain thujone, which is especially harmful to human health, and its camphor content was low. In addition, it was observed that there was not much change in the ratios of essential oil components in the analysis made on individual plants. These results revealed that promising genotypes for herbal tea production can be obtained by selection studies within *S. aramiensis* species.

Acknowledgements

This study was supported financially by the Scientific and Technological Research Council of Turkey (TÜBİTAK; project number: 119O331), for which we are thankful.

https://doi.org/10.24264/icams-2022.II.27

REFERENCES

Aşkun, T., Başer, K.H.C., Tümen, G. and Kürkçüoğlu, M. (2010), "Characterization of Essential Oils of Some Salvia Species and Their Antibacterial Activities", *Turkish Journal of Biology*, 34, 89-95, https://doi.org/10.3906/biy-0809-2.

Ayanoğlu, F. Kaya, DA. Mert, A. and Uygur, V. (2012). Hatay yöresinde doğal olarak yetişen adaçayı (*Salvia* spp.) türlerinin kültüre alınması, verim ve kalite özelliklerinin belirlenmesi. Project Report (TÜBİTAK-109O161). 151p.

Behcet, L. and Avlamaz, D. (2009), "A New Record for Turkey: *Salvia aristata* Aucher ex Benth. (Lamiaceae), *Turkish Journal of Botany*, 33, 61–63, https://doi.org/10.3906/bot-0808-14.

Celep, F., Doğan, M. and Bagherpour, S. (2009), "A New Variety of *Salvia sericeo-tomentosa* (Lamiaceae) from South Anatolia, Turkey", *Novon: A Journal for Botanical Nomenclature*, 19(4), 432-435, https://doi.org/10.3417/2008003.

Celep, F. and Doğan, M. (2010), "*Salvia ekimiana* (Lamiaceae). A New Species from Turkey", *Annales Botanici Fennici*, 47(1), 63-66, https://doi.org/10.5735/085.047.0108.

Celep, F., Doğan, M. and Kahraman, A. (2010), "Re-evaluated Conservation Status of *Salvia* (Sage) in Turkey I: The Mediterranean and Aegean Geographic Regions", *Turkish Journal of Botany*, 34, 201-214, https://doi.org/10.3906/bot-0902-17.

Cuvelier, M.E., Berset, C. and Richard, H. (1994), "Antioxidant Constituents in Sage (*Salvia officinalis*), *Journal of Agricultural and Food Chem*istry, 42, 665–9, https://doi.org/10.1021/jf00039a012.

Davis, P.H., Mill, R.R. and Tan, K. (1988), "*Salvia* L.", *Flora of Turkey and the East Aegean Islands*, Vol. 7, Edinburgh: Edinburgh Univ. Press.

Demirci, B., Baser, K.H.C. and Tumen, G. (2002), "Composition of the Essential Oil of *Salvia aramiensis* Rech. Fil. Growing in Turkey", *Flavour and Fragrance Journal*, 17, 23-25, https://doi.org/10.1002/ffj.1027.

Dönmez, A.A. (2001), "A New Turkish Species of *Salvia* L. (Lamiaceae)", *Botanical Journal of the Linnean Society*, 137, 413–416, https://doi.org/10.1006/bojl.2001.0482.

Düzenli, A. and Çakan, H. (2001), "Flora of Mount Musa (Hatay-Turkey)", *Turkish Journal of Botany*, 25, 285-309.

Ekim, T., Koyuncu, M., Vural, M., Duman, H., Aytaç, Z. and Adıgüzel, N. (2000), *Türkiye Bitkileri Kırmızı Kitabı* (Red Data Book of Turkish Plants), Türkiye Tabiatını Koruma Derneği ve Van Yüzüncü Yıl Üniversitesi, Barışcan Ofset, Ankara.

Hamzaoğlu, E., Duran, A. and Pınar, N. (2005), "*Salvia anatolica* (Lamiaceae). A New Species from East Anatolia, Turkey", *Annales Botanici Fennici*, 42(3), 215-220, http://www.jstor.org/stable/23727241.

Hedge, I.C. (1982), "*Salvia* L.", in: Davis, P.H. (ed.) *Flora of Turkey and the East Aegean Islands*, Edinburgh, Edinburgh University Press, pp. 400-461.

İnce, A. and Karaca, M. (2015), "E-microsatellite Markers for Some Naturally Occurring *Salvia* Species in the Mediterranean Region", *Turkish Journal of Biology*, 39, 69-77, https://doi.org/10.3906/biy-1404-29.

İpek, A. and Gürbüz, B. (2010), "Türkiye florasında bulunan *Salvia* türleri ve tehlike durumları", *Tarla Bitkileri Merkez Araştırma Enstitüsü Dergisi*, 19, 30-35.

Kahraman, A., Celep, F. and Dogan, M. (2009), "Comparative Morphology, Anatomy and Palynology of Two *Salvia* L. Species (Labiatae) and Their Taxonomic Implications", *Bangladesh Journal of Plant Taxonomy*, 16, 73–82, https://doi.org/10.3329/bjpt.v16i1.2749.

Karaman, S., İlçim, A. and Çömlekçioğlu, N. (2007), "Composition of the Essential Oils of *Salvia aramiensis* Rech. fil. and *Salvia cyanescens* Boiss. & Bal", *Pakistan Journal of Botany*, 39(1), 169-172, https://doi.org/10.1002/ffj.1027.

Kelen, M. and Tepe, B. (2008), "Chemical Composition, Antioxidant and Antimicrobial Properties of the Essential Oils of Three *Salvia* Species from Turkish Flora", *Bioresource Technology*, 99, 4096-4104, https://doi.org/10.1016/j.biortech.2007.09.002.

Kintzios, S.E. (2000), *Sage: The Genus Salvia*., Harwood Academic Publishers, ISBN:90-5823-005-8, https://doi.org/10.1201/9780203304556.

Lamaison, J.L., Petitjean-Freytet, C. and Carnat, A. (1991), "Medicinal Lamiaceae with Antioxidant Properties, a Potential Source of Rosmarinic Acid", *Pharmaceutica Acta Helvetiae*, 66, 185–8.

Lawrence, B.M. (1998), "Progress in Essential Oils–Sage Oil", *Perfumer and Flavorist*, 23, 47–52.

Lawrence, B.M. (1983), "Progress in Essential Oils", *Perfumer and Flavorist*, 8(2–3), 61–66.

Tucker, A.O. and Maciarello, M.J. (1990), "Essential Oils of Cultivars of Dalmatian Sage (*Salvia officinalis* L.)", *Journal of Essential Oil Research*, 2, 139–144, https://doi.org/10.1080/10412905.1990.9697844.

Türkmen, N. and Düzenli, A. (1998), "The Flora of Dörtyol and Erzin Districts of Hatay Province of Turkey", *Turkish Journal of Botany*, 22(2), 121-141.

Vural, M. and Adıgüzel, N. (1996), "A New Species from Central Anatolia: *Salvia aytachii*, M. Vural et N. Adıgüzel (Labiatae)", *Turkish Journal of Botany*, 20, 531–534, https://doi.org/10.55730/1300-008X.2610.

Walker, J.B. and Sytsma, K.J. (2007), "Staminal Evolution in the Genus *Salvia* (Lamiaceae): Molecular Phylogenetic Evidence for Multiple Origins of the Staminal Lever", *Annals of Botany*, 100(2), 375-91, https://doi.org/10.1093/aob/mcl176.

https://doi.org/10.24264/icams-2022.II.27

HYDROGELS-BASED TEXTILE MATERIALS FOR TREATMENT OF FIRST-DEGREE BURN INJURIES

GEORGIANA VASILE[1], ANDREEA ȚIGĂU[1], ALINA POPESCU[1], RODICA ROXANA CONSTANTINESCU[2], LAURA CHIRILĂ[1]

[1]*National Research & Development Institute for Textiles and Leather, 16 Lucretiu Patrascanu Street, 030508, sector 3, Bucharest, Romania, georgiana.vasile@incdtp.ro, andreea.tigau@incdtp.ro, alina.popescu@incdtp.ro, laura.chirila@incdtp.ro*

[2]*The National Research & Development for Textiles and Leather - Leather and Footwear Research Institute Division, 93 Ion Minulescu Street, Bucharest, 031215, Romania, rodica.roxana@yahoo.com*

Hydrogels based on collagen and xanthan have found various applications as drug delivery carriers. The main strategy is to combine the traditional perspective of using essential oils with polymeric hydrogels in order to develop a potential dressing that provides wound healing for first-degree burn injuries. In this regard, the present study is aimed to develop textile materials with potential for use in the treatment of first-degree burn injuries by approaching the hydrogels based on xanthan gum and collagen as polymeric matrix loaded with essential oils (cinnamon essential oil, tea tree essential oil), propolis (hydroglyceric extract or with content of colloidal silver) and drugs (chlorhexidine, ciprofloxacin). A total of six experimental variants of hydrogels were synthesized and then were applied by padding method on a plain weave textile structure from 100% cotton. The functionalized textile materials were characterized by morphological and antibacterial point of view. The textile materials treated materials with all synthesized hydrogels based on xanthan and collagen as polymeric matrices have antibacterial activity against *S. aureus* and *E. coli* test strains, the highest inhibition zone was provided by the samples loaded with ciprofloxacin (MUP3 and MUP4 code).

Keywords: first-degree burn injuries, bioactive principles, hydrogels

INTRODUCTION

Burns are a prevalent and burdensome critical care problem. The priorities of specialized facilities focus on stabilizing the patient, preventing infection, and optimizing functional recovery (Rowan *et al*., 2015). Associated infection with burn is the main cause of mortality in patients with extensive burns. Therefore, appropriate management of burn wounds within short time is required.

Propolis is used extensively in folk remedies for treatment of burns and wounds as it shows good healing potential, skin cell proliferation properties and growth capacity (Balata *et al*., 2018). A large amount of surveys and experimental evidence sustain plant beneficial properties on wound healing as well as on a wide range of skin diseases. Essential oils derived from plants offer an alternative to aid wound and burn healing. Strong evidence about essential oils anti-inflammatory and antimicrobial properties is thoroughly described in literature (Perez-Recalde *et al*., 2018). Also, use of antibiotics in people with infected burn wounds is more complicated than in other diseases. This is because the pharmacokinetic parameters of antibiotics (absorption, distribution, metabolism and excretion) are altered in the burned person, and significant variations exist between individuals (Lu *et al*., 2017).

The aim of this study is to obtain biomaterials with potential use in the treatment of first-degree burns injuries, by approaching the immobilization on 100% cotton fabric of hydrogels based on collagen-xanthan as polymeric matrix which embedding different active principles.

https://doi.org/10.24264/icams-2022.II.28

EXPERIMENTAL PART

Materials

Bleached 100% cotton woven fabric with the weight of 168 g/m^2 has been used for all experiments. Collagen (*ZENYH, Romania*) and xanthan (*Xanthomonas campestris, Sigma Aldrich*) were used as embedding agents for the bioactive principles. Ciprofloxacin (Sigma Aldrich), chlorhexidine digluconate (Sigma Aldrich), propolis (propolis extract – hydroglyceric solution 60%, propolis extract 48% – with colloidal silver 50 ppm, *Dacia Plant, Romania*), cinnamon essential oil (*HerbalSana, Romania)* and tea tree essential oil (*Mayam, Romania*) were used as bioactive agents. Tween 80 (*Sigma Aldrich, Germany*) was used as surfactant and glycerol (*Riedel-de haën|Honeywell, USA*) has been used as a solubilizing agent. Calcium chloride (anhydrous, *Fluka|Honeywell, USA*) was used as a cross-linking agent.

Synthesis of the Hydrogels

Firstly, stock solutions of 5% collagen and 1% xanthan were prepared and then mixed (15 mL collagen and 15 mL xanthan) under magnetic stirring for 30 minutes. Thus, over the previously prepared polymeric matrix, 0.2 g ciprofloxacin or 4 mL chlorhexidine (20 µL/mL) were added, the magnetic stirring continuing for another 30 minutes. In order to improve the flexibility of the hydrogels, 7.5 mL of glycerin were added to the resulting mixture. Further, 0.9 mL essential oil (cinnamon essential oil or tea tree essential oil) and 4 mL Tween 80 were added dropwise and separately on the previously prepared mixture, maintaining the magnetic stirring for 15 minutes. 4 mL propolis were then added on the resulted mixture, the magnetic stirring continuing for 30 minutes. 0.15 mL of 5 % calcium chloride solution were added as a cross-linking agent, as a final step of the hydrogel`s synthesis. The selected experimental variants are presented in Table 1.

Table 1. The bioactive principles used for each experimental variant

Code	Drugs		Essential Oils		Propolis	
	Chlorhexidine	Ciprofloxacin	Tea Tree	Cinnamon	Hydroglyceric solution	Colloidal Ag
MUP 1	x		x	x	x	
MUP 2	x		x	x		x
MUP 3		x	x	x	x	
MUP 4		x	x	x		x
MUP 5	x		x		x	
MUP 6	x			x	x	

Functionalization treatments

The obtained hydrogels were immobilized on the textile materials by the padding method on the laboratory padder (Roaches, UK) at 85% wet pick-up. The treated textile materials were then subjected to the drying operation at 50°C for 3 minutes on the drying/curing/ heat-setting unit, model TFO/S 500 mm (Roaches, UK).

https://doi.org/10.24264/icams-2022.II.28

Methods

pH Value

The pH value of hydrogels was measured using the Multiparameter benchtop meter inoLab® Multi 9310 IDS.

Scanning Electron Microscopy

Visualization of the morphology of the cotton fiber surfaces was performed by using Quanta 200 electron microscope (*FEI, The Netherlands*).

Hydrophilicity and Comfort Indices of Functionalized Textile Materials

Hydrophilicity of functionalized textile materials was evaluated according to Romanian Standard SR 12751-89 determining fabric wettability by drop method. The water vapor permeability was performed according to STAS 9005:1979 standard and the air permeability was performed according to SR EN ISO 9237:1999 standard.

Antimicrobial Activity

The antibacterial activity of the samples was qualitatively assessed by the Agar diffusion method according to the SR EN ISO 20645:2005 standard - Determination of antibacterial activity-agar diffusion plate test, by using cultures in liquid medium replicated at 24 hours of ATCC 6538 *S. aureus* and ATCC1 1229 *E. coli* test strains. Inhibition zones were calculated using the following formula:

$$H = (D - d)/2 \quad (1)$$

where: H – the inhibition zone [mm]; D – the total diameter of specimen and inhibition zone [mm]; d – the diameter of specimen [mm].

The criteria for evaluation the inhibition zones according to the standard SR EN ISO 20645:2005 are presented in Table 2.

Table 2. Criteria for inhibition zones according to the SR EN ISO 20645:2005 standard

Inhibition zone [mm]	Growth	Evaluation
>1 1-0 0	absence	satisfactory effect
0	little	efficiency limit
0	moderate important	unsatisfactory effect

RESULTS AND DISCUSIONS

pH Value

The pH values of synthesized polymeric systems are presented in Table 3. The pH of the polymeric solutions is between 5.50 – 5.88, being within the accepted limits for the field of application. It is known from the literature that the skin without any injuries has a pH between 4 - 6 and the wound can have a pH of up to 8.9.

https://doi.org/10.24264/icams-2022.II.28

Table 3. The pH values of the hydrogels

Code	pH value
MUP1	5,62
MUP2	5,55
MUP3	5,86
MUP4	5,88
MUP5	5,50

Scanning Electron Microscopy

The electronic images obtained at a magnification of x2000 for the textile materials treated with the bioactive systems are presented in the Figure 1.

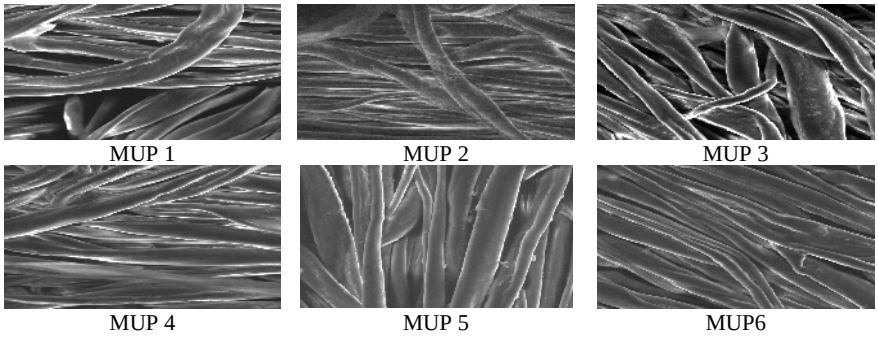

Figure 1. SEM images for functionalized textile materials

The resulting micrographs reveal that the surface of the fibers is covered with a thin polymeric layer that is uniformly distributed both on the surface of the fibers and inside the space between the fibers.

Hydrophilicity and Comfort Indices

The values obtained for hydrophilicity and comfort indices are shown in Table 4.

Table 4. Hydrophilicity and comfort indices of the functionalized textile materials

Code	Water vapor permeability [%]	Air permeability [l/m^2/s]		Hydrophilicity [s]
		100 Pa	200 Pa	
M	30.52	362.2	481.3	immediate
MUP 1	26,79	246,6	452,8	immediate
MUP 2	25,56	257,2	472	immediate
MUP 3	26,97	245,6	454,2	immediate
MUP 4	26,62	242,8	447,8	immediate
MUP 5	28,91	256,6	476,6	immediate
MUP 6	28,91	251,2	460,4	immediate

Analyzing the values obtained for air and water vapor permeability, it is found that the functionalization treatments carried out lead to a decrease of these comfort indices for all of experimental variants, there are small insignificant variations between the

https://doi.org/10.24264/icams-2022.II.28

analyzed variants. In addition, the textile biomaterials possess an excellent moisture absorption capacity.

Antimicrobial Activity

Images of Petri plates after 24h incubation are shown in Figure 2 and an assessment of antibacterial activity is shown in Table 5.

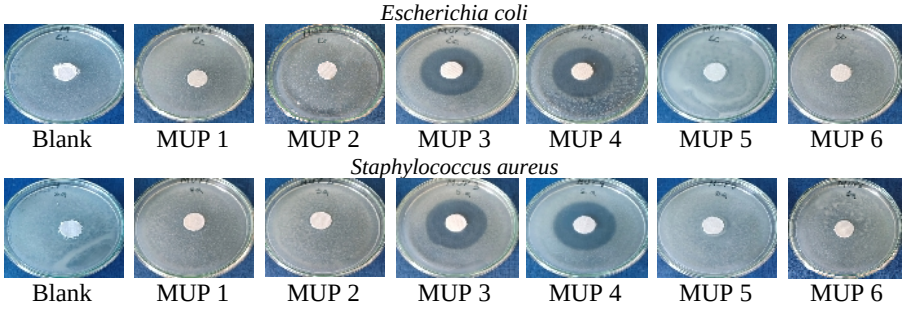

Figure 2. Images of Petri plates showing antibacterial effect after 24 h of incubation

Table 5. Evaluation of the antibacterial activity

Code	Inhibition zone (mm)		Evaluation	
	E. coli	*S. aureus*	*E. coli*	*S. aureus*
M	0	0	Unsatisfactory effect	Unsatisfactory effect
MUP 1	1.5	2	Satisfactory effect	Satisfactory effect
MUP 2	0.5	0*	Satisfactory effect	Satisfactory effect
MUP 3	18	19	Satisfactory effect	Satisfactory effect
MUP 4	17.5	16	Satisfactory effect	Satisfactory effect
MUP 5	0	0	Satisfactory effect	Satisfactory effect
MUP 6	0	0	Satisfactory effect	Satisfactory effect

**Absence of multiplication - even without the inhibition zone - can be considered as a positive effect because the formation of such an inhibition zone can be prevented by a small diffusion of the active substance*

According to ISO 20645 standard method, in the case of no inhibition zone (0 mm), without bacterial growth in the nutrient medium under the specimen, the antibacterial effect is evaluated as "satisfactory", which indicates antimicrobial activity. By analyzing the obtained results, it can be concluded that the most pronounced antibacterial effects were obtained in the case of the textile materials treated with hydrogels containing ciprofloxacin (code MUP3 and code MUP4) in comparison with the samples treated with hydrogels which containing chlorhexidine (code MUP1 and code MUP2). Also, the biomaterial obtained by treating of the textile material with the hydrogel based on collagen-xanthan-ciprofloxacin-tea tree essential oil-cinnamon essential oil-propolis (hydroglyceric solution), code MUP3, shows the greatest antibacterial effect, with inhibition zones of 18 mm for *E. coli* test strain and respectively 19 mm for the *S. aureus* test strain.

https://doi.org/10.24264/icams-2022.II.28

CONCLUSIONS

The main goal of this study was to develop textile biomaterials designed for the treatment of first-degree burns injuries, by embedding different therapeutic agents on the textile materials through an appropriate carrier system. The obtained functionalized textile materials were analyzed by using physical-mechanical tests (comfort indices) scanning electron microscopy, hydrophilicity (drop method) and antibacterial tests. The overall results suggest that the functionalization treatments lead to a decrease of comfort indices for all of experimental variants, being registered small insignificant variations between the analyzed variants. Also, the obtained biomaterials showed an excellent moisture absorption capacity and an antibacterial effect which was proved against *E. coli* and *S. aureus* test strains.

These overall results indicate that incorporating these active principles into the polymeric matrix can significantly enhance the potential efficacy of the fabrics as dressing designed for treatment of first degree burn injuries.

Acknowledgments

This work was carried out through the Nucleu Programme, with the support of MCID, project no. 4N / 08.02.2019, PN 19 17 03 01, project title: "Multifunctional integrated systems based on nanocomposites and pharmacodynamic therapeutic agents for different skin conditions – BIOPANTEX".

REFERENCES

Balata, G.F., Shamardl, H.A.E.M., Elmoneim, H.M.A., Hakami, A.A. and Almodhwahi, M.A. (2018), "Propolis Emulgel: A Natural Remedy for Burn and Wound", *Drug Development and Industrial Pharmacy*, 1–41, https://doi.org/10.1080/03639045.2018.1496449.

Lu, J., Yang, M., Zhan, M., Xu, X., Yue, J. and Xu, T. (2017), "Antibiotics for Treating Infected Burn Wounds", *The Cochrane Database of Systematic Reviews*, 7, https://doi.org/10.1002/14651858.CD012084.pub2.

Perez-Recalde, M., Ruiz Arias, I.E. and Hermida, É.B. (2018), "Could Essential Oils Enhance Biopolymers Performance for Wound Healing? A Systematic Review", *Phytomedicine*, 38, 57-65, https://doi.org/10.1016/j.phymed.2017.09.024.

Rowan, M.P., Cancio, L.C., Elster, E.A., Burmeister, D.M., Rose, L.F., Natesan, S., Chan, R.K., Christy, R.J. and Chung, K.K. (2015), "Burn Wound Healing and Treatment: Review and Advancements", *Critical Care*, 19(1), 1-12, https://doi.org/10.1186/s13054-015-0961-2.

METHODS FOR MODIFICATION OF COTTON FABRICS WITH GELATIN – GLUTARALDEHYDE AND ZNO NANOPARTICLES

DARINA ZHELEVA[1], MARGARITA KOLEVA[1], DESISLAVA ANGELOVA[1], DESISLAVA GRABCHEVA[1], PETAR TODOROV[2]

[1]*University of Chemical Technology and Metallurgy - Textile and Leather Department*

[2]*University of Chemical Technology and Metallurgy - Organic Chemistry Department*
Sofia, Bulgaria, e-mail: darinajeleva@abv.bg

Cotton fabrics have good water absorption properties, air permeability, non-toxicity, but microorganisms easily damage them. Collagen is a commonly used biomaterial that has properties such as biocompatibility, biodegradability, non-toxicity, but with poor mechanical properties. Glutaraldehyde is the main cross-linking agent for collagen and characterized by antimicrobial properties. ZnO nanoparticles exhibiting antibacterial, antifungal, anticorrosive and protective properties against UV, is widely applicable in medicine. The combination of all these components in one biocomposite with potential antimicrobial properties and healing effect can find application in medical practice. In this study, an attempt was made to improve the properties of cotton fabric by impregnating it with gelatin hydrogel cross-linked with glutaraldehyde and containing ZnO nanoparticles. Three methods of modification were applied, varying the mixing regimes of the components and the conditions. The composite materials were investigated by means of SEM, FTIR, and fluorescence analysis. The morphological analyzes of the samples modified by different methods show that the spherical particles of ZnO have changed into a flower-like structures; the particles are covered by the collagen film; and dispersed and agglomerated in certain places. FTIR analyzes prove interactions between the organic and inorganic components. This is also confirmed by the observed fluorescent properties, which are of different intensity. All these observations suggest good antibacterial properties that will be the subject of future research.

Keywords: biocomposites, cotton, gelatin, ZnO nanoparticles

INTRODUCTION

In biomedical industry, collagen has been employed to modify and functionalize different types of materials for wound treatments applications. Various forms of collagen including fibers, films, membranes, coatings, 3D printed constructs, and hydrogels have been used as scaffold for medical applications. Therefore, it is fundamental to develop wound dressings that are capable of preventing bacteria penetration into the wound or avoid microorganisms' growth (Cortés *et al.*, 2019; Dong and Lv, 2016). As a biomaterial, gelatin has advantages such as: it is a natural polymer which has not shown antigenity, it is completely resorbable *in vivo* and its physicochemical properties can be suitably modulated. Due to the large number of functional side groups it contains, gelatin readily undergoes chemical cross-linking, which is very important for its possible use as a biomaterial. One of the main disadvantage of gelatin as a material is its poor mechanical properties. Glutaraldehyde is by far the most widely used agent, due to its eficiency to stabilize collagen-based biomaterials (Khor, 1997). Cotton fabric is the most popular raw materials in textile industry due to the properties such as wearing comfortability, flexibility, water absorptivity, breathability. However, cotton products are easily damaged by microorganisms on account of its moisture retaining nature, and therefore not only cause discoloration, loss in mechanical strength, and foul odor but also result of negative health effects (Irfan *et al*, 2017). Current wound dressings have some major deficiencies including low absorption of wound fluids, low flexibility, a tendency to adhere onto the wound surface, poor mechanical strength and lack of a suitable and moist environment for wound healing. In addition, the majority of current wound dressing do not harbor antimicrobial activity. In this context, hydrogel-based wound dressings would provide a cooling sensation, a moisture environment as well as a barrier to microorganism colonization. Nanoparticles have emerged as potent treatment for bacterial infections and are routinely combined with hydrogels to form hybrid biomaterial systems (Wahid *et al.*, 2017; Tauhiduzzaman *et al*., 2021; Ayanoglu *et al*.,

https://doi.org/10.24264/icams-2022.II.29

2022). Among various metallic oxides, ZnO nanoparticles have been widely applied as antimicrobial agents, which exhibits efficient bactericidal activity against Gram-positive and Gram-negative pathogens, as well as high-pressure and heat-resistant bacteria. Some reported antibacterial mechanisms are as follows: ZnO can bind to the cell membrane and induce increased membrane permeability and cell lysis. Meanwhile, it could produce ROS (reactive oxygen species) such as singlet oxygen ($^1O_2$) and hydroxyl radicals (HO•) and inactivate pathogens. Besides, the released zinc ions could promote the growth of fibroblast and the migration of keratinocytes, thus enhancing tissue repair during wound healing. In textile fabrication, metal oxides: ZnO, TiO_2, CuO, MgO can be used to protect fabrics from UV, microbes, retard flame, conduct electricity, repel water, self-clean, etc. The nanostructures of metallic oxides release ions, and these ions cause the inactivation (Sawhney *et al.*, 2008; Raut *et al.*, 2010; Stankic *et al.*, 2016; Verbic *et al.*, 2019; Kolodziejczak-Radzimska and Jesionowski, 2014). Considering the Collagenic nature of the skin and the beneficial properties of Chitosan, the two polymers were proposed to be used in developing nanostructured wound dressing loaded with ZnO nanoparticles. These nanostructured materials confer promising characteristics to be used as anti-infectious wound dressing being biocompatible, antimicrobial against *C. albicans* and *S. aureus*, and highly hydrophilic able to absorb over 2300% water, which confer the premises of maintaining proper humidity and exudate absorption during wound healing (Tiplea *et al*., 2021). The new Collagen/(RGO/ZnO/TiO_2/SiO_2) composites demonstrate an antimicrobial activity dependent on the agent loading level (RGO is reduced graphene oxide). It is specific in respect to Gram-negative, Gram-positive bacteria and fungi (Staneva *et al.*, 2020). ZnO nanostructures have been applied on textile materials through different methods such as hydrothermal route, layer-by-layer deposition, pad-dry procedure, ultrasonic irradiation technique, and sol-gel process (Li *et al.*, 2011; Uğur *et al*, 2010; Vihodceva and Kukle, 2013). There are two main methods of chemical production of ZnO-NP and their application on textiles, i.e., *ex situ* and *in situ* synthesis (Shubha *et al.*, 2019; Montazer and Amiri, 2014). Zinc nitrate hexahydrate and potassium hydroxide were used as starting materials and the reaction was performed at 50°C. The *in situ* growth of ZnO nanostructures on cotton fabric occurred in a single-stage process. The cotton fabrics coated with ZnO nanostructures presented an antibacterial efficiency (Souza *et al.*, 2018). Pomegranate peel extract was used as a reducing agent and wood ash extract was used as an alkali source for the formation of ZnO-NP from zinc acetate. Four different methods, which varied in drying between immersion of fabric in the active solutions for synthesis and the use of padding and ultrasonication, were investigated to evaluate the most suitable one to achieve excellent UV properties of the textile (Verbic *et al.*, 2021). The authors (Hong *et al.*, 2020) reported on hydrothermal application for seedless growth of ZnO on different fabrics using [$Zn(NO_3)_2 \cdot 6H_2O$] as precursor (with nano rod structure).

The aim of this study is to prepare biocomposites from modified cotton fabric with glutaraldehyde-crosslinked gelatin and ZnO particles and to investigate the methods of modification, varying mixing regimes of the components and the conditions.

MATERIALS AND METHODS

Materials

A bleached and unmercerized, plain-woven, 100% cotton fabric, with a surface weight of 145±5 g/m^2 was used. $Zn(NO_3)_2 \cdot 6H_2O$ (CAS:10196-18-6) and NaOH were purchased from Sigma-Aldrich (Darmstadt, Germany); glutaraldehyde (25% aqueous solution) from Sigma-Aldrich (Darmstadt, Germany); citric acid monohydrate (CAS: 5949-29-1) and Gelatin (CAS: 9000-70-8), from Merck KGaA (Darmstadt, Germany). All solutions were prepare with distilled water.

https://doi.org/10.24264/icams-2022.II.29

Methods for Preparation of Composite Materials

Method 1

The gelatin (5% w/v) was dissolved in water under stirring and is added the glutaraldehyde water solution (2.5 % w/w to gelatin) for the crosslinking during 24 h. Then cotton substrates (untreated and pretreated with citric acid) was impregnated with the solution containing cross-linked gelatin and staying the immersed samples for 24 h. Then the samples were immersed in water solution of $Zn(NO_3)_2 \cdot 6H_2O$ and dried at 90°C for 30 min. Finally, the samples were soaked in sodium hydroxide solution with a ten-time stoichiometric excess to zinc ions and treated thermally at 90°C for 30 min. The obtained composites were washed with water and dried at a room temperature.

Method 2

The gelatin (5% w/v) was dissolved in water under stirring. Preparing of water solution of $Zn(NO_3)_2 \cdot 6H_2O$. Cotton substrates (untreated and pretreated with citric acid) were impregnated with solution containing gelatin and was added the solution of $Zn(NO_3)_2 \cdot 6H_2O$ and then dried at 90°C for 30 min. Next, the samples were impregnated with a glutaraldehyde water solution (2.5 % w/w to gelatin) and dried again (90°C for 10 min). Finally, the sample was soaked in sodium hydroxide solution and treated thermally at 90°C for 30 min. The obtained composite materials were washed with water and allowed to dry at a room temperature.

Method 3

The gelatin (5% w/v) was dissolved in water under stirring and cotton samples were impregnated with gelatin solution. Preparing of water solution of $Zn(NO_3)_2 \cdot 6H_2O$ and sodium hydroxide solution. Then, the solution of NaOH was added drop-wise, vigorously stirred with the solution of $Zn(NO_3)_2 \cdot 6H_2O$ at heating of 80ºC during 10 min. A white precipitate of ZnO was obtained. Then cotton substrates (untreated and pretreated with citric acid) was impregnated with the solution then dried at 90ºC for 1h and staying the immersed samples for 24 h. Finally, the samples were crosslinked with glutaraldehyde water solution and treated thermally at 90ºC for 30 min. The obtained composites were washed and dried.

Analysis

The surface morphology of the composite materials and the formation of ZnO particles were analyzed using a scanning electron microscope (SEM) JSM-5510 (Jeol Ltd., Tokyo, Japan) operated at a 10-kV acceleration voltage. FTIR analysis was carried out on an Infrared Fourier Transform spectrometer (IRAffinity-1, Shimadzu, Japan) equipped with a diffuse-reflectance attachment (MIRacle Attenuated Total Reflectance Attachment). Measurements were done using a spectral range of 600–4000 cm^{-1}. X-ray fluorescence (XRF) spectrometry was used to define the amount of ZnO in composite materials. A wavelength dispersive (WDXRF) technique was used and Rigaku Supermini200 (Bruker, Hanau, Germany) equipment was used.

RESULTS AND DISCUSSIONS

Morphological Properties of Composites

Fig.1 shows micrographs of the cotton fabric and of composite materials obtained at different modification methods. As can be seen on fig.1b the cotton material is covered by crosslinked gelatin. The micrographs of the composite obtained by *Method 1* on

https://doi.org/10.24264/icams-2022.II.29

fig.1c show that the spherical particles have changed into a flower-like shape with needle-like ends. In composite material obtained by *Method 2* on fig.1d, the individual fibers are covered with a layer with a granular structure of white spherical ZnO particles, distributed relatively homogeneous on the surface. The micrographs in fig.1e for a composite obtained by *Method 3* show crowding and agglomeration of the zinc oxide particles in certain places of the cellulose matrix. This agglomeration of the particles is likely to show a better effect due to the larger surface area of the ZnO.

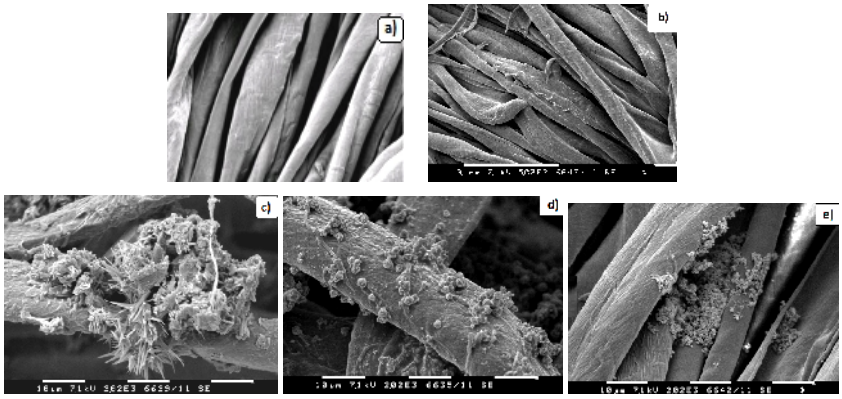

Figure 1. SEM images of the surface of a cotton fabric a) Cotton; b) Cotton-Gelatin-GA and fabrics modified by different methods: c) Modified Cotton–Method 1; d) Modified Cotton–Method 2; e) Modified Cotton–Method 3

Fluorescence Analysis of the Composites

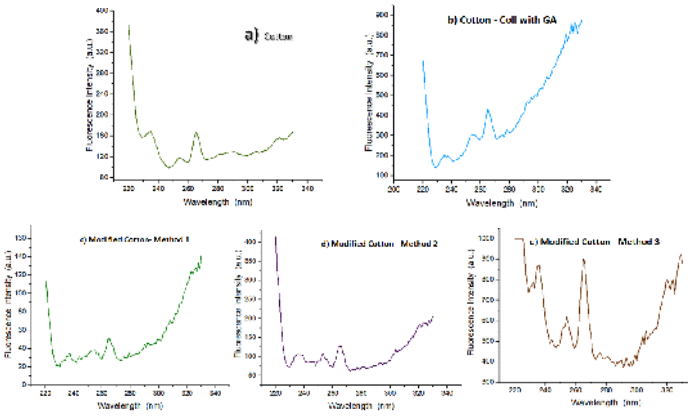

Figure 2. Fluorescence analysis of cotton fabrics: a) Cotton; b) Cotton-Gelatin-GA; c) Modified Cotton–Method 1; d) Modified Cotton–Method 2; e) Modified Cotton–Method 3

Fig.2 shows the photoluminescence spectra of samples in the solid state. After crosslinking with glutaraldehyde, collagen emits a blue–green fluorescence with higher peak intensity. The presence of zinc oxide in the crosslinked collagen film is the reason for the weakening of the fluorescence emission of collagen and for the appearance of a

https://doi.org/10.24264/icams-2022.II.29

new peak. The peak arises due to a transition between interstitial zinc and the zinc vacancy level (Samanta *et al.*, 2012). The most significant differences in the fluorescence analysis were observed in the samples modified by method 3, which is most likely due to an increase in the amount of zinc oxide and it could produce reactive oxygen species such as singlet oxygen ($^1O_2$).

FTIR Analysis

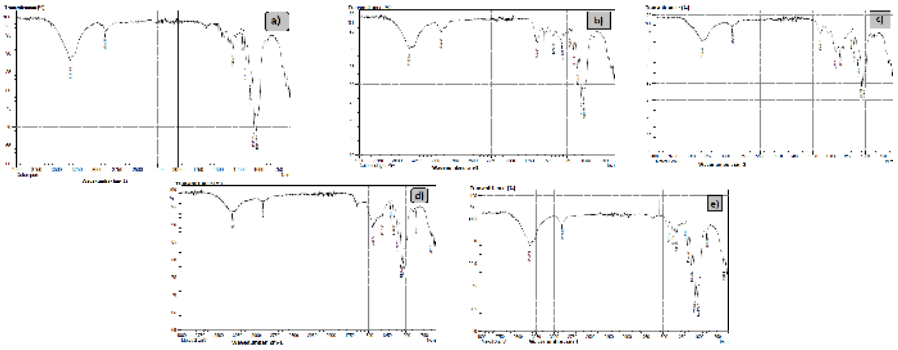

Figure 3. FTIR analysis of cotton fabrics: a) Cotton; b) Cotton-Gelatin-GA c) Modified Cotton–Method 1; d) Modified Cotton–Method 2; e) Modified Cotton–Method 3

Oxycellulose has many reactive aldehyde groups which can react with amino groups from collagen molecule to form Schiff bonds (Hu, 2015). This can be seen from the FTIR spectrum on fig.3b with the appearance of a new peak at 1450 nm^{-1}, resulting from the cross-linking of collagen with glutaraldehyde.

As reported in (Verbic *et al.*, 2021), the peak at 854 cm^{-1} confirms the formation of tetrahedral coordination of ZnO. This peak present in our spectra (fig.3c,d,e) and these peaks are most clearly expressed in the composite obtained by Method 3 (fig.3e).

CONCLUSIONS

In this study, biocomposites were obtained by modifying cotton fabric with crosslinked glutaraldehyde gelatin containing zinc oxide particles. Three methods of synthesis of ZnO by varying the components and processing conditions were investigated. It was proved that the composites obtained by method 3 show the best characteristics and exhibited promising results for antibacterial properties, which will to be investigated in the future.

Acknowledgments

This work was supported by the Bulgarian National Scientific Fund project КП-06-ДК1/11 (Textile materials to prevent the spread of SARS-CoV2 and other pathogens) of the Ministry of Education and Science, BG.

REFERENCES

Ayanoglu, M.O., Tauhiduzzaman, M. and Carlsson, L.A. (2022), "In-plane Compression Modulus and Strength of Nomex Honeycomb Cores", *Journal of Sandwich Structures & Materials*, 24(1), 627-642, https://doi.org/10.1177/10996362211021888.

Cortés, M.P., Amaya, M.C., Cañas, A., Osorio, M., Sánchez, D., Zuluaga, R., Gómez, B. and Castro, C. (2019), "Functional Textile Finishing of Type I Collagen Isolated from Bovine Bone for Potential Healthtech", *Heliyon* 5, 2, https://doi.org/10.1016/j.heliyon.2019.e01260.

Dong, C. and Lv, Y. (2016), "Application of Collagen Scaffold in Tissue Engineering: Recent Advances and New Perspectives", *Polymers*, 8(2), 42, https://doi.org/10.3390/polym8020042.

Hong, G., Kim, J., Lee, J., Shin, K., Jung, D. and Kim, J. (2020), "A Flexible Tactile Sensor Using Seedless Hydrothermal Growth of ZnO Nanorods on Fabrics", *J. Phys. Commun.*, 4, 045002, https://doi.org/10.1088/2399-6528/ab82b6.

Hu, X. (2015), "Application of Dyeing Method in Preparation of Collagen Modified Cotton", *5th Inter. Conf. on Advanced Design and Manufacturing Eng.* (ICADME), 299, https://doi.org/10.2991/icadme-15.2015.59.

Irfan, M., Perero, S., Miola, M., Maina, G., Ferri, A., Ferraris, M. and Balagna, C. (2017), "Antimicrobial Functionalization of Cotton Fabric with Silver Nanoclusters/Silica Composite Coating via RF Co-sputtering Technique", *Cellulose*, 24(5), 2331–2345, https://doi.org/10.1007/s10570-017-1232-y.

Khor, E. (1997), "Methods for the Treatment of Collagenous Tissues for Bioprostheses", *Biomaterials*, 18(2), 95-105, https://doi.org/10.1016/S0142-9612(96)00106-8.

Kolodziejczak-Radzimska, A. and Jesionowski, T. (2014), "Zinc Oxide – from Synthesis to Application: A Review", *Materials*, 7(4), 2833-2881, https://doi.org/10.3390/ma7042833.

Li, Y., Zou, Y. and Hou, Y. (2011), "Fabrication and UV-blocking Property of Nano-ZnO Assembled Cotton Fibers via a Two-Step Hydrothermal Method", *Cellulos*e, 18, 6, 1643–1649, https://doi.org/10.1007/s10570-011-9600-5.

Montazer, M. and Amiri, M. (2014), "ZnO Nano Reactor on Textiles and Polymers: Ex Situ and In Situ Synthesis, Application, and Characterization", *J. Phys. Chem. B*, 118, 1453–1470, https://doi.org/10.1021/jp408532r.

Raut, S., Vasavada, D. and Chaudhari, S. (2010), "Nano Particles—Application in Textile Finishing", *Man-Made Text. India*, 38, 31–36.

Samanta, P., Bandyopadhyay, A. (2012), "Chemical Growth of Hexagonal Zinc Oxide Nanorods and Their Optical Properties", *Appl. Nanosci.*, 2, 111–117, https://doi.org/10.1007/s13204-011-0038-8.

Sawhney, A., Condon, B., Singh, K., Pang, S., Li, G. and Hui, D. (2008), "Modern Applications of Nanotechnology in Textiles", *Text Res. J.*, 78(8), 731–739, https://doi.org/10.1177/0040517508091066.

Shubha, P., Gowda, M., Namratha, K., Shyamsunder, S., Manjunatha, H. and Byrappa, K. (2019), "*Ex-Situ* Fabrication of ZnO Nanoparticles Coated Silk Fiber for Surgical Applications", *Mater. Chem. Phys*, 231, https://doi.org/10.1016/j.matchemphys.2019.04.012.

Souza, D., Gusatti, M., Ternus, R., Fiori, M.A., Riella, H.G. (2018), "*In Situ* Growth of ZnO Nanostructures on Cotton Fabric by Solochemical Process for Antibacterial Purposes", *Journal of Nanomaterials*, 9082191, https://doi.org/10.1155/2018/9082191.

Staneva, A., Albu-Kaya, M., Martinov, B., Ivanova, I. and Vladkova, T. (2020), "Preparation and Antimicrobial Activity of Collagen /(RGO/ZnO/TiO_2/SiO_2) Composites", *JCTM*, 55, 5, 1078-1086.

Stankic, S., Suman, S., Haque, F. and Vidic, J. (2016), "Pure and Multi Metal Oxide Nanoparticles: Synthesis, Antibacterial and Cytotoxic Properties", *J. Nanobiotechnol.*, 14, 73, https://doi.org/10.1186/s12951-016-0225-6.

Tauhiduzzaman, M., Carlsson, L.A. and Ayanoglu, M.O. (2021), "Design Analysis of End Notch Flexure Sandwich Specimen with Honeycomb Core", *Journal of Composite Materials*, 55(10), 1295-1308, https://doi.org/10.1177/0021998320967050.

Tiplea, R.E., Lemnaru (Popa), G.M., Trusca, R.D., Holban, A., Albu Kaya, M.G., Dragu, L.D., Ficai, D., Ficai, A. and Bleotu, C. (2021), "Antimicrobial Films based on Chitosan, Collagen, and ZnO for Skin Tissue Regeneration, *Biointerface Res Appl Chem*, 11, 4, 11985, https://doi.org/10.33263/BRIAC114.1198511995.

Uğur, S., Sarıışık, M., Aktaş, A., Uçar, M. and Erden, E. (2010), "Modifying of Cotton Fabric Surface with Nano-ZnO Multilayer Films by Layer-by-Layer Deposition Method", *Nanoscale Res Lett*, 5, 1204, https://doi.org/10.1007/s11671-010-9627-9.

Verbic, A., Gorjanc, M. and Simoncic, B. (2019), "Zinc Oxide for Functional Textile Coatings: Recent Advances", *Coatings*, 9(9), 550; https://doi.org/10.3390/coatings9090550.

Verbic, A., Šala, M., Jerman, I. and Gorjanc, M. (2021), "Novel Green *In Situ* Synthesis of ZnO Nanoparticles on Cotton Using Pomegranate Peel Extract", *Materials*, 14, 4472, https://doi.org/10.3390/ma14164472.

Vihodceva, S. and Kukle, S. (2013), "Improvement of UV Protection Properties of the Textile from Natural Fibres by the Sol-Gel Method", *IOP Conference Series: Materials Science and Engineering*, 49, 012022, https://doi.org/10.1088/1757-899X/49/1/012022.

Wahid, F., Zhong, C., Wang, H. and Chu, L. (2017), "Recent Advances in Antimicrobial Hydrogels Containing Metal Ions and Metals/Metal Oxide Nanoparticles", *Polymers*, 9, 636, https://doi.org/10.3390/polym9120636.

III.

INNOVATIVE SYSTEMS, TECHNOLOGIES AND QUALITY MANAGEMENT

GRAIN CHARACTERISTICS COMPARISON OF DIFFERENT TYPES OF SHOE UPPER LEATHERS

FULYA ADIGÜZEL[1,2], CEMILE CEREN TOSUN[1,3], GÖKHAN ZENGIN[1], ARIFE CANDAŞ ADIGÜZEL ZENGIN[1]

[1]*Ege University, Engineering Faculty, Leather Engineering Department, 35100, Bornova, Izmir, TÜRKİYE*
candas.adiguzel@ege.edu.tr, gokhan.zengin@ege.edu.tr

[2]*Flo Casual Merchandising and Marketing Inc., Bağcılar, 34217, Istanbul, TÜRKIYE*
fulya.dguzel9@gmail.com

[3]*Uşak University, Leather, Textile and Ceramic Design Application and Research Center, 64000, Uşak, TÜRKİYE, cemile.tosun@usak.edu.tr*

In this study, it was aimed to comparatively investigate the grain properties of shoe upper leathers produced for different purposes. Thus, six different types of shoe upper leather (cracked, antique, patent, nappa, nubuck, printed) were provided from three different footwear companies. The tensile strength and elongation at break (TS EN ISO 3376), single and double edge tear strength (TS EN ISO 3377-1, TS EN ISO 3377-2), cracking and bursting resistance (TS 4137 EN ISO 3378, TS EN ISO 3379), flex resistance (TS EN ISO 5402-1) as well as dry and wet rubbing fastness tests (TS EN ISO 11640) were applied to leathers that have similar thicknesses. The results of the study gave information about the physical strength and product performances of different upper leather types. The data were evaluated comparatively and the effects of shoe upper leather types on quality and performance were evaluated.

Keywords: shoe upper leather, grain properties, quality, strength, footwear

INTRODUCTION

The leather types preferred to use in shoe production vary depending on the type of shoes and climatic conditions of the region. For example, boots manufactured by thicker leathers are generally sold to cold countries such as Russia, Moscow, and Mongolia, while the shoes produced by thin leathers with cloth lining are sold to countries with a temperate climate (Akçakale and Somçağ, 2016).

Footwear producers make their choices by considering some certain physical and chemical characteristics of upper leathers (Hossain *et al*., 2021). In this preference, the priority is the type of shoe, the duration of the footwear and the cost of the upper leathers (Ali *et al*., 2020).

The physical strength of upper leathers also reduces the number of defects in manufacturing that occur during or after the shoe production (Marconi *et al*., 2017). In this context, the physical strength of the upper leathers used in shoe production is of great importance for consumer and producer.

For this reason, in this study, it was aimed to investigate the grain characteristics of six different upper leather types. For this purpose, cracked, antique, patent, nappa, nubuck and printed upper leathers were selected from three different footwear companies and the tensile strength and elongation at break, tear strength, flex resistance, dry and wet rubbing fastness, cracking, and bursting resistance tests were performed to evaluate the results affected the grain characteristics comparatively.

https://doi.org/10.24264/icams-2022.III.1

MATERIALS AND METHODS

Materials

Six different types of shoe upper leathers were obtained from three different companies located in Istanbul and Izmir. Antique, patent, nappa, nubuck, printed and cracked type of leathers were used as the research material.

Methods

The tests were selected considering the physical effects that the shoes are exposed during their usage. Tensile strength and elongation at break, tear strength, flex resistance, dry and wet rubbing fastness, cracking, and bursting resistance tests were carried out in accordance with standards and the classification of upper leathers were given in Table 1.

Table 1. Classification of Shoe Upper Leathers

Type of Upper Leathers	Company A	Company B	Company C
Cracked	1	1	1
Nubuck	2	2	2
Nappa	3	3	3
Antique	4	4	4
Printed	5	5	5
Patent	6	6	6

Upper leathers were kept in standard atmospheric conditions (20°C temperature and 65% relative humidity) for 48 hours according to TS EN ISO 2419 for conditioning prior to physical tests (TS EN ISO 2419).

Tensile Strength and Elongation at Break

The tensile strength and elongation at break test were performed to upper leathers according to TS EN ISO 3376.

Tear Strength

Two tear resistance tests such as single and double edge were carried out by the standards methods of TS EN ISO 3377-1 and TS EN ISO 3377-2.

Flex Resistance

Flex resistance is tested with flexometer device according to TS EN ISO 5402-1. Subsequent to test, the grain characteristics of the samples were evaluated.

Dry and Wet Rubbing Fastness

For dry and wet rubbing fastness test, TSE EN ISO 11640 standard was used, and the leathers and felts were evaluated with a gray scale (TSE EN ISO 11640).

https://doi.org/10.24264/icams-2022.III.1

Cracking and Bursting Resistance Test

Cracking and bursting resistance tests were carried out in accordance with TS 4137 EN ISO 3378 and TS EN ISO 3379.

RESULTS AND DISCUSSION

Fifteen upper leathers differentiated in production type are investigated in terms of grain characteristics. First, the tensile strength and elongation at break results of upper leathers are given in Table 2.

Table 2. Tensile Strength and Elongation at Break Results of Upper Leathers

Type of upper leather	Thickness (mm)	Tensile strength (N/mm^2)	Elongation at break (%)
Cracked-A	1.35	27.50	82.52
Cracked-B	1.59	54.38	51.42
Cracked-C	1.28	10.39	63.48
Nubuck-A	1.67	27.05	50.01
Nubuck-B	2.22	26.46	45.25
Nubuck-C	2.14	20.05	39.75
Nappa-A	1.06	27.05	63.08
Nappa-B	0.97	9.92	67.40
Antique-A	1.53	17.62	43.88
Antique-B	1.11	31.78	49.68
Antique-C	1.75	19.45	44.05
Printed-A	1.08	18.44	49.46
Printed-B	1.08	12.97	49.27
Patent A	1.36	19.91	56.46
Patent -B	1.42	29.19	45.27

The tensile strength value of the shoe upper leathers should have a minimum value of $20N/mm^2$ according to UNIDO standards (UNIDO, 1996). The results are found considerably higher than the tensile strength values specified in the standard in general and required for shoe upper leathers. Printed upper leathers had the minimum tensile strength values while nubuck and cracked leathers had the highest values. The tensile strength of the upper leathers is differentiated depending on the upper leather type. Besides for the same type of leathers like cracked, nappa and antique, the values were differentiated depending on the company where the leathers were obtained.

The double and single edge tearing strength values obtained from the upper leathers are given in Table 3 and 4.

https://doi.org/10.24264/icams-2022.III.1

Table 3. The Double Edge Tear Strength Results of Upper Leathers

Type of upper leather	Thickness (mm)	Double edge tear strength value (N/mm)
Cracked-A	1.15	82.95
Cracked-B	1.61	248.80
Cracked-C	1.27	70.97
Nubuck-A	1.81	144.87
Nubuck-B	2.11	168.44
Nubuck-C	2.01	213.25
Nappa-A	1.03	80.93
Nappa-B	0.79	27.37
Antique-A	0.86	86.81
Antique-B	1.52	151.83
Antique-C	1.63	126.73
Printed-A	1.00	72.58
Printed-B	1.18	50.49
Patent-A	1.26	61.11
Patent-B	1.36	99.13

Table 4. The Single Edge Tear Strength Results of Upper Leathers

Type of upper leather	Thickness (mm)	Single edge tear strength value (N/mm)
Cracked-A	1.29	44.95
Cracked-B	1.73	88.08
Cracked-C	1.31	30.00
Nubuck-A	1.57	60.27
Nubuck-B	2.07	49.35
Nubuck-C	2.08	76.23
Nappa-A	1.11	32.06
Nappa-B	0.82	21.03
Antique-A	1.78	34.97
Antique-B	1.04	43.14
Antique-C	1.69	31.23
Printed-A	1.04	29.18
Printed-B	1.12	28.69
Patent-A	1.33	25.24
Patent-B	1.35	32.68

The single and double edge tear strength values of shoe upper leathers should have been 15N and 30N values respectively (UNIDO, 1996). All results were found considerably higher than the required values and lower tear strength values were found from thinner upper leathers. Minimum results were obtained from nappa upper leather with a value of 27.37 N/mm and 21.03 N/mm for the double and single edge tear strength respectively. The highest double and single edge tear strength values were determined from cracked type upper leather with 248.80 N/mm and 88.08 N/mm respectively.

The results of cracking and bursting strength tests are given in Table 5.

https://doi.org/10.24264/icams-2022.III.1

Table 5. The Cracking and Bursting Strength Results of Upper Leathers

	Cracking		Bursting	
Type of upper leather	Average (kg)	Average (mm)	Average (kg)	Average (mm)
Cracked-A	42.00	1262.33	0	0
Cracked-B	69.33	1204.67	0	0
Cracked-C	46.00	1093.67	28.67	1622.67
Nubuck-A	50.67	1286.67	64.67	1437.67
Nubuck-B	23.67	915.00	43.67	1168.33
Nubuck-C	56.67	1123.33	76.00	1337.67
Nappa-A	10.67	718.33	42.00	1263.00
Nappa-B	9.33	932.00	13.33	1128.00
Antique-A	23.00	1036.00	34.33	1260.00
Antique-B	22.33	848.67	28.33	1050.00
Antique-C	22.33	848.66	28.33	1050.00
Printed-A	15.00	844.67	6.67	987.00
Printed-B	12.33	859.33	4.33	1048.67
Patent-A	17.00	829.33	34.00	1160.33
Patent-B	28.00	861.33	49.00	1123.33

Since the force exceeded 90 Kg during the burst test of leathers belonging to some companies, only the cracking test was applied to those leathers.

The cracking strengths of patent, nappa and printed leathers were found lower than nubuck, cracked and antique upper leathers. It is thought that this is due to the thinness of nappa leather as well as the finishing characteristics of patent and printed leathers. The cracking test is especially important for the areas where the foot bends during the movement of the foot.

Higher fastness values were obtained from dry rubbing fastness. Printed, nappa and antique upper leathers has better dry fastness values in comparison to other upper leathers. The wet rubbing fastness values of antique, cracked, and printed leathers were found higher compared to others. Although good results were obtained in wet rubbing evaluations of nubuck and nappa leather types, it was observed that the felt values were found poor (Table 6).

Table 6. The Wet and Dry Rubbing Fastness Values of Upper Leathers

	Wet Rubbing		Dry Rubbing	
Type of upper leather	Leather	Felt	Leather	Felt
Cracked-A	4	4	4	5
Cracked-B	5	3	5	4
Cracked-C	3	2	4	3
Nubuck-A	3	1	4	1
Nubuck-B	5	1	5	5
Nubuck-C	3	2	4	3
Nappa-A	3	2	5	4
Nappa-B	3	5	4	5
Antique-A	4	3	4	4
Antique-B	3	3	5	5
Antique-C	5	5	4	4
Printed-A	4	2	5	4
Printed-B	5	4	5	5
Patent -A	2	4	4	5
Patent -B	3	5	3	5

https://doi.org/10.24264/icams-2022.III.1

100.000 steps were applied to upper leathers during the flex resistance test. As a result of the test, although wrinkles occurred on the grain side of cracked, nappa, antique, printed and patent leathers, there were no wrinkles on the grain side of the nubuck leathers. In order to prevent or completely eliminate the explosions seen on leather types except nubuck, leathers should be supported with reinforcement cloths produced with natural materials.

CONCLUSION

The grain characteristics of six different type of upper leathers such as cracked, antique, patent, nappa, nubuck and printed were aimed to investigate in terms of tensile strength and elongation at break, tear strength, flex resistance, dry and wet rubbing fastness, cracking, and bursting resistance tests and following conclusions have been drawn:

a. The thickness and the type of leathers directly affect the grain characteristics of the upper leathers; b. The results of the physical tests were found higher than the required values in general.

The physical characteristics of leathers have a direct influence on the performance of the shoes. Therefore, footwear companies should select the upper leathers depending on these characterizations. Besides, cutting, sewing and assembly operators should be informed and trained so they can reduce the number of defective shoes. Additionally, during shoe production, placing a product introductory form describing the leather properties behind the planning forms will enable the operators to have information about upper leathers.

REFERENCES

Akçakale, N. and Somçağ, H. (2016), "Yün liflerinden keçeleştirme yöntemi ile ayakkabı yapımı", *Avrasya Uluslararası Araştırmalar Dergisi*, 4(9), 213-226, https://doi.org/10.33692/avrasyad.509657.

Ali, F., Kamal, M. and Islam, M.S. (2020), "Comparative Study on Physical Properties of Different Types of Leather in Bangladesh", *International Journal of Engineering Research and Applications*, 10(2), 55-63.

Hossain, M., Azam, F.A.B. and Chowdhury, M. (2021), "Quality Assessment of Shoe Leather Based on the Properties of Strength and Comfort, Collected from Different Footwear and Leather Industries in Bangladesh", *Textile & Leather Review*, 4(1), 30-37, https://doi.org/10.31881/TLR.2020.20.

Marconi, M., Marilungo, E., Papetti, A. and Germani, M. (2017), "Traceability as a Means to Investigate Supply Chain Sustainability: The Real Case of a Leather Shoe Supply Chain", *International Journal of Production Research*, 55(22), 6638-6652, https://doi.org/10.1080/00207543.2017.1332437.

TS EN ISO 2419 (2012), "Leather - Physical and Mechanical Tests - Sample Preparation and Conditioning", Turkish Standards Institute, Ankara.

TS EN ISO 3376 (2020), "Leather - Physical and Mechanical Tests - Determination of Tensile Strength and Percentage Extension", Turkish Standards Institute, Ankara.

TS 4137 EN ISO 3378 (2006) "Leather - Physical and Mechanical Tests - Determination of Resistance to Grain Cracking and Grain Crack Index", Turkish Standards Institute, Ankara.

TS EN ISO 3377-1 (2012) "Leather - Physical and Mechanical Tests - Determination of Tear Load - Part 1: Single Edge Tear', Turkish Standards Institute, Ankara.

TS EN ISO 3377-2 (2016) "Leather - Physical and Mechanical Tests - Determination of Tear Load - Part 2: Double Edge Tear'', Turkish Standards Institute, Ankara.

TS EN ISO 3379 (2015), "Leather-Determination of Distension and Strength of Surface (Ball Burst Method)", Turkish Standards Institute, Ankara.

TS EN ISO 5402-1 (2017). "Leather - Determination of Flex Resistance - Part 1: Flexometer Method", Turkish Standards Institute, Ankara.

TSE EN ISO 11640 (2013), "Leather - Tests for Color Fastness - Color Fastness to Cycles of to-and-fro Rubbing", Turkish Standards Institute, Ankara.

UNIDO (1996), "Acceptable Quality Standards in the Leather and Footwear Industry", United Nations Industrial Development Organization, Vienna.

https://doi.org/10.24264/icams-2022.III.1

RESISTANCE OF SARS COV-2 TO SEAWATER

EMRAH AY, NIZAMI DURAN

Mustafa Kemal University, Medical Faculty, Microbiology Department, Hatay-TÜRKİYE, nizamduran@hotmail.com; emrah_ay@hotmail.com

SARS CoV-2, which is the cause of Covid-19 disease, has become the only and most important agenda of the world due to its mortality and morbidity that globally affects the whole world. The virus has profoundly affected life all over the world. The lifestyles of people have changed due to the virus. This study is planned to understand how important sea water is in SARS-CoV-2 transmission. The study aimed to determine whether there is a risk of sea water in SARS-CoV-2 transmission. The effectiveness of seawater on SARS CoV-2 viability has been investigated in different dilutions of seawater in different time periods. Experiments were carried out in three different titrations of SARS CoV-2 in Vero cell lines. Viral replication has been investigated by detecting morphological changes occurring in cells, cell viability, and the RT-PCR method. Seawater has been found to be highly potent inhibitory on SARS CoV-2 about time and dose. Especially within 300 seconds, seawater has been found to inhibit viral replication up to 1/32 dilution. These results show that viral transmission through seawater is quite difficult for people swimming in the sea during the pandemic. Seawater-mediated spread of SARS-CoV-2 is out of the question. However, these results should not be interpreted as the prophylactic activity of saline against viruses, which are obligate intracellular parasites.

Keywords: resistance, SARS CoV-2, seawater

INTRODUCTION

Coronaviruses are enveloped, positive-sense RNA viruses containing the largest known RNA genomes up to approximately 30 kb in length, that belong to the family Coronaviridae, suborder Cornidovirineae. The Orthocoronavirinae subfamily contains four genera, Alphacoronavirus, Betacoronavirus, Gammacoronavirus, and Deltacoronavirus. Coronaviruses, which have a very large host, cause respiratory infections in humans (Letko *et al*., 2020).

The SARS CoV-2 strain, which is the cause of Covid-19 disease, belongs to the genus betacoronavirus (Perlman and Netland, 2009). Coronaviruses have a single-stranded, non-segmentation RNA genome with positive polarity, and virion has 4 major structural proteins. Nucleocapsid (N) protein, transmembrane (M) protein, envelope (E) protein, and Spike (S) protein. The virus has a single-stranded RNA genome containing 29,903 nucleotides encoding 9860 amino acids (NCBI, 2020). For some types of coronavirus, it has been reported that not all structural proteins are required to create an infectious virion (Schoeman and Fielding, 2019; Vlasova *et al*., 2007).

When the phylogenetic pedigree was examined, it was found that SARS CoV-2 significantly overlapped with the SARS virus sequence isolated in 2015. In structural analysis, SARS CoV-2 is thought to result from the mutation in the "spike" glycoprotein and nucleocapsid protein of the SARS virus (Song *et al*., 2018; Xu *et al*., 2020). SARS-CoV, SARS-CoV-2, and MERS-CoV are coronaviruses that can cause different clinical severity infections that show respiratory and extra respiratory symptoms in humans (Letko *et al*., 2020). Mortality rates with SARS-CoV and MERS-CoV have been reported to be around 10% and 35%, respectively. It is in the category of betaCoVs with SARS-CoV and MERS-CoV with significant mortality and SARS-CoV-2. The virus is spherical or elliptic 60-140 nm in diameter, like other CoVs, and it is sensitive to ultraviolet rays and heat (Wu *et al*., 2020). In addition, the virus has been reported to be very sensitive to lipid solvents containing chloroform except for ether (75%), ethanol, chlorine-containing disinfectant, peroxyacetic acid, and chlorhexidine. It has been reported that SARS-CoV-2 and SARS-CoV-1 have similar stability (van Doremalen *et al*., 2020; Ong *et al*., 2020). In this study, it was planned to determine whether there is a risk of seawater in SARS-CoV-2 transmission.

https://doi.org/10.24264/icams-2022.III.2

MATERIAL AND METHOD

Virus Isolation

In the study, primary rabbit kidney cell culture, Vero E6 (African green monkey kidney cell line), Vero CCL-81, and Beas 2B (human lung epithelial cell line) cell lines were used for viral isolation. Viral isolation was successfully performed in all of these cell lines. Viral growth was confirmed both by determining the presence of cytopathological effect and by the Real-Time PCR method.

The formation of CPE in the cell lines was detected on the 3rd day in the primary rabbit kidney cell line, on the 4th day in the Vero cell lines (Both Vero E6 and the Vero CCL-81 cell lines), and in the Beas 2B cells on the 5th day. After the detection of cytopathological changes in cell cultures, cells were collected from the culture dish after the seventh day of incubation. Cells collected by centrifugation were centrifuged again at 4000 rpm for 20 minutes after the freezing-thawing process (-80°C to 37°C). For the SARS CoV-2 verification in the sample from the supernatant, the sample was studied by RT-PCR method. The presence of viral growth was performed comparatively with cells treated with different dilutions of seawater and control groups without seawater.

Cell Culture

In-vitro tests were performed on Vero E6 cells. Cell cultures were maintained with 10% fetal calf serum RPMI-1640 medium containing 10 mM HEPES, 4 IM glutamine 100 IU/ml penicillin/streptomycin. Incubation of cells was carried out at 37°C in an incubator with 95% air with 5% CO_2. Cell density was adjusted to $1x10^5$ cells per ml. Experiments were carried out by adding cell maintenance medium to 10% of the culture dish in culture dishes. Incubation of cell cultures continued for 96 hours. Cells were removed from the culture vessels with 0.25% trypsinization solution, then collected in 50 ml centrifuge tubes by centrifugation at 1250 rpm for 10 minutes, at the end of incubation. Cell number and viability were determined by hemocytometer with 1% trypan blue dye prepared in 0.9% NaCl.

Proliferation Experiments

Proliferation experiments in cell culture were performed on 24-well flat-bottom microplates. The wells were prepared with RPMI-1640 medium containing 10% fetal calf serum and $1x10^5$ cells were added per ml.

Titration of the Virus

Stock viral strains (maintained at -80°C) were rapidly dissolved in 37°C water (in a bain-marie) and re-activated in cell lines (Vero E6 cell line). The cells were then exploded by “freezing and thawing”. Cells were collected from the culture dish and centrifuged at 4000 rpm for 20 minutes, and the supernatant virus was collected as a stock solution. Also, as in our previous study, the $TCID_{50}$ of the virus was calculated (Yildirim *et al*., 2016). In the present study, three different titers of SARS CoV-2 (1, 10, and 100 $TCID_{50}$) were chosen as the doses to be studied.

Activity Studies

Preparation of Cell Cultures

The seawater sample was first sterilized by passing through membrane filters. Then, different concentrations (1, 1/2; 1/4, 1/8, 1/16, 1/32, and 1/64) were obtained by diluting with seawater phosphate buffer solution. The effectiveness of these different seawater dilutions on SARS CoV-2 was investigated.

https://doi.org/10.24264/icams-2022.III.2

Antiviral Assay (Plaque Reduction Assay)

Experiments were carried out according to the method described by Hayden *et al.* (1980) and Abbas *et al.* (2018). In experiments, the cell density was adjusted to be $1x10^5$ cells/ml. After the cells were inoculated into the plates, they were incubated for 24 hours at 37°C. The virus was titrated in three different doses (1, 10, and 100 $TCID_{50}$). Different concentrations of seawater (1: 1, 1/2, ¼, 1/8, 1/16, 1/32, and 1/64) were distributed to the wells. From each dilution to 8 wells, 100 µl of SARS CoV-2 virus suspensions at 1, 10, and 100 $TCID_{50}$ concentration was inoculated in all wells. Plates were incubated at 37°C for 1 hour for viral adsorption and penetration. Then 3 ml of RPMI-1640 medium containing 2% agarose was added. At the end of the incubation, 10% formalin was added to the wells. The plates were then incubated for two hours, at the end of the incubation, the plates were stained with 0.1% crystal violet prepared in distilled water. Cell culture wells without virus inoculations were selected as the control group. Viral plaques formed at the end of the test were counted and the percentage reduction in plaque formation compared to the control wells was calculated according to the following formula:

% inhibition=[viral count (untreated)-viral count (treated)]x100/(viral count (untreated) (1)

The experiments were repeated in triplicate.

Evaluation

Cell culture plates were evaluated daily for the presence of CPE in the cells. The presence of cells in atypical morphology such as cell rounding, constriction narrowing, and aggregation was evaluated as cytopathological changes. All microscopic evaluations were evaluated comparatively with the control group without seawater. The presence of viral reproduction was also verified by the MTT method in which cell viability can be evaluated as quantitative (Mossman, 1983). In the case of viral reproduction in the wells containing different concentrations of seawater, the determination of a decrease in cell viability was considered as the presence of viral replication, since cell viability would decrease.

Real-Time PCR

The presence of SARS CoV-2 growth in cell culture was also verified by the Real-time PCR method. In comparison with the control group using the real-time PCR method, the presence or increase of viral replication was described as an increase in the number of viral copies.

RESULTS

Effects of the Sea Water on the Replication of SARS CoV-2

In the study, the effects of different dilutions (1/1; 1/2; 1/4 1/8; 1/16; 1/32, and 1/64) of seawater on the replication of SARS CoV-2 have been investigated. In the experiments, the inhibitory effect of all dilutions of seawater against SARS CoV-2 was detected within seconds. This effect of seawater against SARS-CoV-2 was found to be directly related to your water concentration.

All dilutions of seawater were found to inhibit viral replication within 60 seconds, except for 1/32 and 1/64 dilutions against SARS CoV-2 at 100 $TCID_{50}$ titers. In all experimental groups, the presence of viral replication in each dilution was evaluated by the RT-PCR method compared to the control group. Virus replication was evaluated as a decrease or increase in terms of the number of copies. In the control group, cells were treated with SARS CoV-2 only, seawater was not added to these cell cultures.

https://doi.org/10.24264/icams-2022.III.2

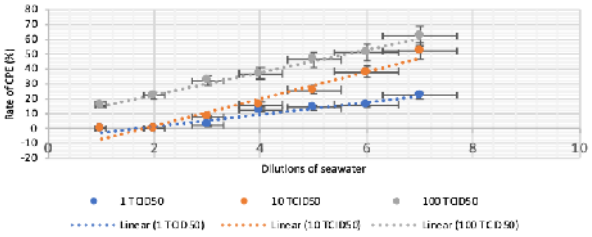

Figure 1. CPE rates were detected in cells after 60 seconds of exposure to SARS CoV-2 with different concentrations of seawater

The effectiveness of SARS CoV-2 in three different titers was investigated. After 60 seconds of exposure to seawater, it was found that the virus in 1 and 10 $TCID_{50}$ titers were completely inhibited at 1/1 and 1/2 dilutions. Decrease in seawater dilution results in an increase in viral inactivation rate. If the virus titer is 100 $TCID_{50}$, a low level of CPE was detected in the cells at 1/1 and 1/2 dilutions of seawater. When the viral titer is elevated ($1TCID_{50}$), it has been found that viral inactivation occurs to a large extent if the virus is exposed to seawater for 60 seconds (Fig. 1).

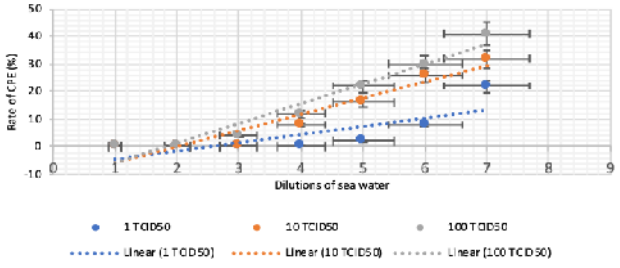

Figure 2. CPE rates were detected in cells after 120 seconds of exposure to SARS CoV-2 with different concentrations of seawater

When the exposure time to seawater was increased to 120 seconds, virus inactivation at $1TCID_{50}$ titer was 0 at 1/1, 1/2, ¼, and 1/8 dilutions. In experiments in which SARS CoV-2 was run at 10 $TCID_{50}$ titers, viral inactivation was found to be 0 in the first three dilutions (1/1, ½, and 1/4). At lower titrations of seawater, the presence of CPE was detected in cells, albeit at low levels. When the virus titer was increased to 100 $TCID_{50}$, it was found that SARS CoV-2 was fully inactivated at 1/1 and 1/2 dilutions. Whereas, in the titers of seawater less than 1/2, the presence of low rates of CPE in the cells was observed (Fig. 2).

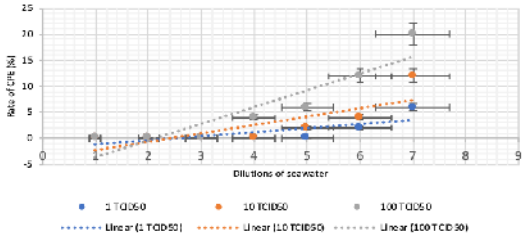

Figure 3. CPE rates were detected in cells after 180 seconds of exposure to SARS-CoV-2 with different concentrations of seawater

https://doi.org/10.24264/icams-2022.III.2

As seen in Figure 3, when the exposure time to seawater was increased to 180 seconds, it was found that the SARS CoV-2 in 1TCID$_{50}$ titer was inactivated in all dilutions from 1/1 to 1/16. When the viral titer was elevated, it was found that viral inactivation titers also increased. It was determined that the inactivation of 10 TCID$_{50}$ titers virus was seen in all dilutions from 1/1 to 1/8. It was determined that the virus with a titer of 100 TCID$_{50}$ was inactivated in all dilutions from 1/1 to 1/4 (Fig. 3).

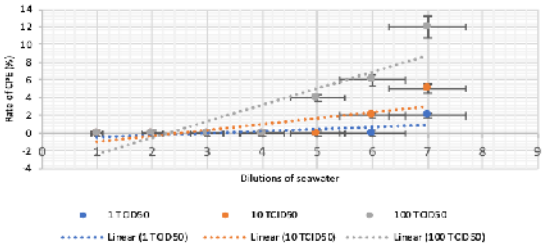

Figure 4. CPE rates were detected in cells after 240 seconds of exposure to SARS-CoV-2 with different concentrations of seawater

When the exposure time to seawater was increased to 240 seconds, it was determined that the full inactivation of the virus in 1 TCID$_{50}$ titer occurred in all dilutions from 1/1 to 1/32. Complete inactivation was observed against SARS CoV-2 in 10 TCID50 titers, from 1/1 to 1/16, while in dilutions from 1/1 to 1/8 against the virus in 100 TCID$_{50}$ titers (Fig. 4).

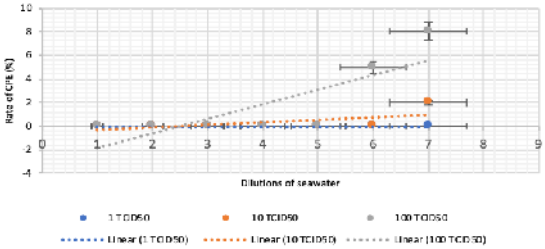

Figure 5. CPE rates were detected in cells after 300 seconds of exposure to SARS-CoV-2 with different concentrations of seawater

When the exposure to seawater was increased up to 300 seconds, viral inactivation was detected in all dilutions of 1 TCID$_{50}$ titer of the virus from 1/1 to 1/64 of the dilution. When the viral titer was chosen as 10 TCID$_{50}$, only a 1/64 dilution of seawater showed a very small amount of CPE in the cells. When the viral titer was determined as 100 TCID$_{50}$, viral inactivation occurred in all dilutions from 1/1 to 1/16 of seawater. However, at 1/32 and 1/64 dilutions, 5 and 8% CPE was detected in the cells, respectively (Fig. 5).

DISCUSSION

SARS CoV-2 pandemic has profoundly affected people all over the world. People's lifestyles have undergone major changes to prevent viral transmission. The main transmission path of SARS-CoV-2 is contact. Carrying out studies on direct or indirect transmission is extremely important in terms of developing new strategies to protect against SARS-CoV-2. For this reason, in our planned study, we have reached important findings regarding the survival of SARS-CoV-2 in seawater. It is a known fact that SARS-CoV-2 is an infectious agent that can easily spread in contact with contaminated surfaces or materials. In this study, which investigated the subject of transmission of SARS CoV-2

https://doi.org/10.24264/icams-2022.III.2

by seawater, it was determined that transmission from infected individuals would not be possible through seawater. This study has shown that seawater can inactivate SARS CoV-2 in seconds even at very low concentrations (up to 1/64 dilution).

CONCLUSION

As a result, it can be said clearly that SARS-CoV-2 cannot be transmitted through seawater. This shows the results that solutions with a high salt concentration can be used effectively in SARS-CoV-2 disinfection. It is important to keep in mind that gargling with high salt concentration solutions may not be important in preventing infection. Because when the virus reaches the mucosal surfaces, it quickly enters the epithelial cells for replication. For this reason, it should be remembered that garaging with solutions with high salt concentrations cannot be prevented viral replication. High salt concentration solutions can only be used safely to eradicate viral contamination in inanimate environments.

REFERENCES

Abbas, S.Y., El-Bayouki, K.A.M., Basyouni, W.M. and Mostafa, E.A. (2018), "New Series of 4 (3H)-quinazolinone Derivatives: Syntheses and Evaluation of Antitumor and Antiviral Activities", *Medicinal Chemistry Research*, 1-12, https://doi.org/10.1007/s00044-017-2083-7.

Hayden, F.G., Cote, K.M. and Douglas, R.G. Jr. (1980), "Plaque Inhibition Assay for Drug Susceptibility Testing of Influenza Viruses", *Antimicrobial Agents and Chemotherapy*, 17, 865-870, https://doi.org/10.1128/AAC.17.5.865.

Letko, M., Marzi, A. and Munster, V. (2020), "Functional Assessment of Cell Entry and Receptor Usage for SARS-CoV-2 and the Other Lineage B Betacoronaviruses", *Nature Microbiology*, 5, 562-569, https://doi.org/10.1038/s41564-020-0688-y.

Mosmann, T. (1983), "Rapid Colorimetric Assay for Cellular Growth and Survival: Application to Proliferation and Cytotoxicity Assays", *Journal of Immunological Methods*, 65, 55-63, https://doi.org/10.1016/0022-1759(83)90303-4.

National Center for Biotechnology Information (2020), "Severe Acute Respiratory Syndrome Coronavirus 2 Reference Genome", Accessed on 2 August 2020.

Ong, S.W.X., Ong, S.W.X., Tan, Y.K., Chia, P.Y., Lee, T.H., Ng, O.T., Wong, M.S.Y. and Marimuthu, K. (2020), "Air, Surface Environmental, and Personal Protective Equipment Contamination by Severe Acute Respiratory Syndrome Coronavirus 2 (SARS-CoV-2) from a Symptomatic Patient", *JAMA*, E1-E3, https://doi.org/10.1001/jama.2020.3227.

Perlman, S. and Netland, J. (2009), "Coronaviruses Post-SARS: Update on Replication and Pathogenesis", *Nature Reviews Microbiology*, 7, 439-450, https://doi.org/10.1038/nrmicro2147.

Schoeman, D. and Fielding, B.C. (2019), "Coronavirus Envelope Protein: Current Knowledge", *Virology Journal*, 16, 2-22, https://doi.org/10.1186/s12985-019-1182-0.

Song, W., Gui, M., Wang, X. and Xiang, Y. (2018), "Cryo-EM Structure of the SARS Coronavirus Spike Glycoprotein in Complex with its Host Cell Receptor ACE2", *PLoS Pathogens*, 14(8), 1-19, https://doi.org/10.1371/journal.ppat.1007236.

Xu, X., Xu, X., Chen, P., Wang, J., Feng, J., Zhou, H., Li, X., Zhong, W. and Hao, P. (2020), "Evolution of the Novel Coronavirus from the Ongoing Wuhan Outbreak and Modeling of its Spike Protein for Risk of Human Transmission", *Science China Life Sciences*, 63, 1-4, https://doi.org/10.1007/s11427-020-1637-5.

Wu, F., Wu, F., Zhao, S., Yu, B., Chen, Y.M., Wang, W., Song, Z.G., Hu, Y., Tao, Z.W., Tian, J.H., Pei, Y.Y., Yuan, M.L., Zhang, Y.L., Dai, F.H., Liu, Y., Wang, Q.M., Zheng, J.J., Xu, L., Holmes, E.C. and Zhang, Y.Z. (2020), "A New Coronavirus Associated with Human Respiratory Disease in China", *Nature*, 579, 265-269, https://doi.org/10.1038/s41586-020-2008-3.

van Doremalen, N., Bushmaker, T., Morris, D.H., Holbrook, M.G., Gamble, A., Williamson, B.N., Tamin, A., Harcourt, J.L., Thornburg, N.J., Gerber, S.I., Lloyd-Smith, J.O., de Wit, E. and Munster, V.J. (2020), "Aerosol and Surface Stability of SARS-CoV-2 as Compared with SARS-CoV-1", *The New England Journal of Medicine*, 382, 1564-1567, https://doi.org/10.1056/NEJMc2004973.

Vlasova, A.N., Vlasova, A.N., Zhang, X., Nagesha, H.S., Haynes, L.M., Fang, Y., Lu, S. and Saif, L.J. (2007), "Two-way Antigenic Cross-reactivity between Severe Acute Respiratory Syndrome Coronavirus (SARS-CoV) and Group 1 Animal CoVs is Mediated through an Antigenic Site in the N-Terminal Region of the SARS-CoV Nucleoprotein", *Journal of Virology*, 81, 13365-13377, https://doi.org/10.1128/JVI.01169-07.

Yildirim, A., Duran, G.G., Duran, N., Jenedi, K., Bolgul, B.S., Miraloglu, M. and Muz, M. (2016), "Antiviral Activity of Hatay Propolis Against Replication of Herpes Simplex Virus Type 1 and Type 2", *Medical Science Monitor*, 22, 422-30, https://doi.org/10.12659/MSM.897282.

SYNERGISTIC EFFICACY OF EUCALYPTOL WITH ACYCLOVIR AGAINST HSV-2

EMRAH AY, NIZAMI DURAN

Mustafa Kemal University, Medical Faculty, Microbiology Department, Hatay-Türkiye, emrah_ay@hotmail.com; nizamduran@hotmail.com

The increasing drug resistance in herpes viruses in recent years brings with it new treatment approaches. In recent years, it has been tried to overcome drug resistance, especially with the use of herbal products in combination with existing drugs. In this study, we aimed to investigate the effectiveness of eucalyptol in combination with acyclovir. A Vero cell line was used for toxicity tests and viral culture isolation studies in the study. The non-toxic concentrations of eucalyptol and acyclovir were determined by the MTT method. Antiviral efficacy studies were performed within non-toxic concentrations. Antiviral activity was determined by calculating the IC50 values of the compounds against HSV-2. In addition, it was evaluated by the RT-PCR method. The 50% inhibitory concentration (IC50) and Fractional inhibitory concentration (FIC) index values determined during 24 hours and 48 hours of action showed that Eucalyptol exhibited a potent activity. This efficacy was found to be stronger when used in combination with acyclovir. These results show that the combination of Eucalyptol and acyclovir may be beneficial against resistant HSV infections. We suggest that the results of these studies, which are planned as in-vitro, be supported by in-vivo studies.

Keywords: Eucalyptol, antiviral, HSV-2, acyclovir, synergy.

INTRODUCTION

Herpes simplex virus (HSV) infections are shared all over the world and cause serious complications in immunocompromised patients. The drug of choice for treatment is acyclovir, a nucleoside analog of guanosine that needs to be phosphorylated three times. Initial phosphorylation is completed by the virally encoded thymidine kinase protein, which allows acyclovir to be activated only in virus-infected cells. Cellular thymidylate kinases provide second and third phosphorylations. Acyclovir triphosphate is a DNA chain terminator that acts by inhibiting viral DNA polymerase (Groves, 2016; Tognarelli *et al*., 2019).

The widespread use of acyclovir has resulted in the emergence of acyclovir-resistant HSV strains. It has been reported that acyclovir-resistant strains can occur mostly in patients whose immune system is suppressed (Sadowski *et al*., 2021; Schnitzler, 2019).

A wide variety of synthetic and natural products are being studied against HSV to solve the increasing drug resistance in herpesviruses. Eucalyptol is one of the phytochemicals on which a wide variety of studies have been conducted.

HSV infections with reduced susceptibility to acyclovir are mainly reported in immunocompromised patients. The prevalence of drug resistance in these patients varies between 3.5-10%. It has been reported that acyclovir resistance may be even higher in bone marrow or transplant recipients (>25%) (Ho *et al*., 2020; Sadowski *et al*., 2021).

It has been reported that HSV resistance to acyclovir is less than 1% in immunocompetent patients. However, the presence of acyclovir-resistant HSV has been reported among immunocompetent individuals, especially in cases of recurrent herpetic keratitis. It has also been reported that acyclovir prophylaxis predisposes to antiviral-resistant recurrent herpetic keratitis. Eucalyptol (1,8-cineol) is a naturally occurring monocyclic monoterpene ether. It has an aromatic scent. Due to its pleasant spicy aroma

https://doi.org/10.24264/icams-2022.III.3

and taste, eucalyptol is used as a flavoring agent and in cosmetics (Juergens *et al*., 2020). In this study, we aimed to investigate the effectiveness of eucalyptol in combination with acyclovir.

MATERIALS AND METHODS

Determination of Cytotoxic Dosage of Eucalyptol

First of all, non-toxic concentrations of eucalyptol in healthy cells were determined. Vero (African green monkey kidney cell line) was used for this purpose. Antiviral activity studies were performed on the concentrations of the molecule determined as non-toxic on Vero cells. The MTT method was used for cytotoxicity tests.

Cell Culture Experiments

In cell culture studies, RPMI-1640 cell growth medium containing 10% fetal calf serum (FBS), 10 mM HEPES, 100 IU/ml penicillin/streptomycin with 4mM glutamine was used. Cultures were incubated at 37 °C in a cell incubator with 5% carbon dioxide.

The cell concentration was set to be $1x10^6$ cells/ml for cell proliferation and generation experiments, and 1x105 cells/ml for activity studies. Incubation of the cells was continued until they covered the surface of the culture dish for 3-7 days.

The passage of cells covering the culture dish surface was performed using a 0.25% trypsinization solution. Cells were removed from the culture dish surface with the versen-trypsin solution and incubated at 1500 rpm for 15 min collected by centrifugation. Cell viability was then determined by trypan blue staining.

Proliferation Assays

Proliferation experiments were performed in 12, 24, 48, and 96-well flat-bottom culture plates. In the experiments, activity studies were carried out by adjusting the wells to 1x105 cells per ml with RPMI-1640 medium containing 10% fetal calf serum. Dimethyl sulfoxide (DMSO) was used to dissolve chemical compounds in the culture medium. The selected concentration of DMSO used as the solvent in the experiments was included in the experiments as a negative control.

MTT (3-(4,5-Dimethylthiazol-2-yl)-2,5-diphenyltetrazolium bromide) Method

The MTT method allows living cells to be detected colorimetrically and quantitatively (Mosmann *et al*., 1983). This method is based on the principle that the MTT dye of intact mitochondria can cleave the tetrazolium ring in cells. MTT is reduced to colored, water-insoluble formazan by a mitochondrial-dependent reaction, which is actively absorbed into cells. The MTT-reducing property of the cells is taken as a measure of cell viability. The dye density obtained as a result of MTT analysis correlates with the number of viable cells. In the experiments, different concentrations of eucalyptol were treated with virus-infected cells and their effects on viral replication were investigated. In the study, negative (DMSO) and positive control (Acyclovir) were also studied together in the MTT method. At the end of the incubation, 10 µl of MTT was added to each well and the plates were incubated for 4 hours under the same

https://doi.org/10.24264/icams-2022.III.3

conditions. Absorbance measurements were performed at 570 nm with a spectrophotometer.

HSV-2 Isolation

RPMI 1640 medium containing 10% fetal calf serum was used as a viral production medium. The vero cell line was used as the cell line for viral isolation. HSV-2 strain was obtained from Hatay Mustafa Kemal University Faculty of Medicine Cell Culture Laboratory virus stocks. The viral strain was reactivated by removing the virus strain from the deep freezer, thawing it in a water bath at 37°C, and inoculating the Vero cell culture covering the culture dish's surface. Following inoculation, the herpes simplex virus began to determine the characteristic CPE patterns from the 3rd day. Incubation was continued until day 7. The collected cells were centrifuged at 4000 rpm for 20 minutes after the freeze-thaw process. The sample taken from the supernatant was confirmed for herpes simplex virus type 2 by RT-PCR.

Titration of HSV-2

For this purpose, the HSV-2 strain removed from -80 °C was thawed at 37 °C and incubated in Vero cell lines for 96 hours. Then, the viral culture vessel was freeze-thawed and the cells were blasted. The cells were collected from the culture dish and centrifuged at 4000 rpm for 20 minutes and the supernatant was organized as a virus solution. Subsequently, the virus suspension was infected with Vero cells in 96-well flat-bottomed microplates, and the infectious dose calculation was performed as stated in the literature. Vero cells were produced by inoculating ($1x10^5$ cells/ml) into 96-well microplates. When cell growth covered the surface of the wells, the medium was taken from each well and 50 µl of 10-fold diluted stock virus solution (from to $10^{-1}$to 10^{-6}), prepared in serum-free RPMI-1640 medium, was added to the cells. For viral adsorption, after incubation at 37 °C for 2 hours, 50 µl of medium containing 5% FBS was added to each well and incubated at 37 °C for 7 days in an atmosphere of 5% CO_2.

At the end of the incubation, viral dilutions were examined for the presence of CPE. Viral titer was calculated according to the Reed and Muench method. All experiments were performed independently of each other in triplicate (Reed and Muench, 1938; Allahverdiyev *et al*., 2004).

Viral DNA Isolation from Cell Culture

HSV-2 infected cell cultures incubated with treatment compounds were collected by centrifugation at 1250 rpm for 10 min. Viral DNA isolation was performed from the collected cell pellets using the Zymo Research Viral DNA Kit according to the test package insert as follows. Collected cell pellets were suspended in 800 µl of ZR Viral DNA Buffer with the help of a vortex. The cell suspension, which was kept at room temperature for 10 minutes, was transferred into the Zymo-Spin IC Column and centrifuged at 15000 rpm for 1 minute. After pouring the supernatant, 300 µl of DNA Wash Buffer was added into the column and centrifuged for 1 min. This step was repeated once. 10 µl of DNA Elution Buffer was added to the Zymo-Spin IC Column and placed in a sterile eppendorf, and after 1 minute of incubation at room temperature, it was centrifuged at 15000 rpm for 1 minute. DNA samples obtained in sterile eppendorf were stored at -20 °C until the PCR study.

https://doi.org/10.24264/icams-2022.III.3

Determination of Viral Load by Real-Time PCR

In viral load determination studies, 1 µl of DNA was used from DNA samples kept at -20°C. GoTaq PCR Mastermix (Promega, USA) was used for RT-PCR analyses. The reaction protocol was performed in the following steps using the Montana 4896 RT-PCR (Anatolia, Turkey). Denaturation was applied for 2 minutes, at 95 °C for 15 seconds, and at 60 °C for 60 seconds, for a total of 40 cycles. Each sample was worked in duplicate. The results were evaluated logarithmically considering the CT values of the samples. The primer sequences used are given below. (Forward 5'-ATCAACTTCGACTGGCCCTT -3', Reverse 5'- CCGTACATGTCGATGTTCAC -3') (Cunningham *et al*., 1996; Lakeman *et al*., 1995).

RESULTS

While the non-toxic concentration of eucalyptol on Vero cells was determined as >62.5 µg/ml, this value for Acyclovir was found to be toxic at a concentration of 62.5 µg/ml after 48 hours of incubation (Figures 1 and 2).

The 50% inhibitory concentration (IC_{50}) and Fractional inhibitory concentration (FIC) index values determined during 24 hours and 48 hours of action showed that Eucalyptol exhibited a potent activity. This efficacy was found to be stronger when used in combination with acyclovir.

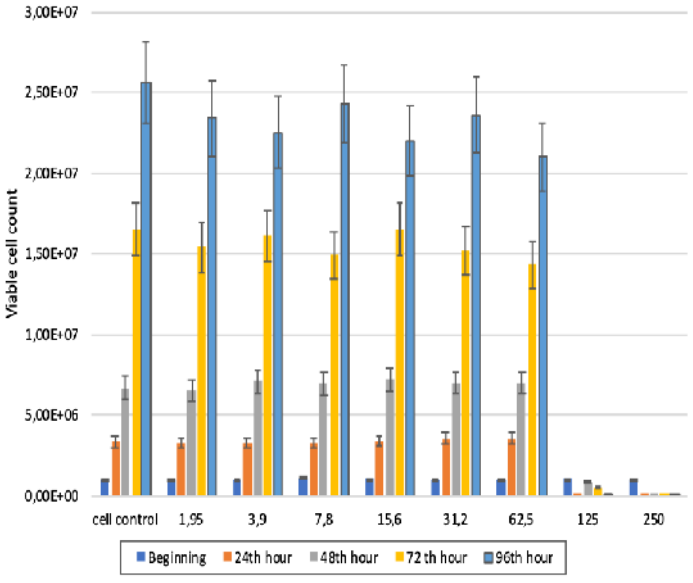

Figure 1. The non-toxic concentration of eucalyptol on Vero cells

https://doi.org/10.24264/icams-2022.III.3

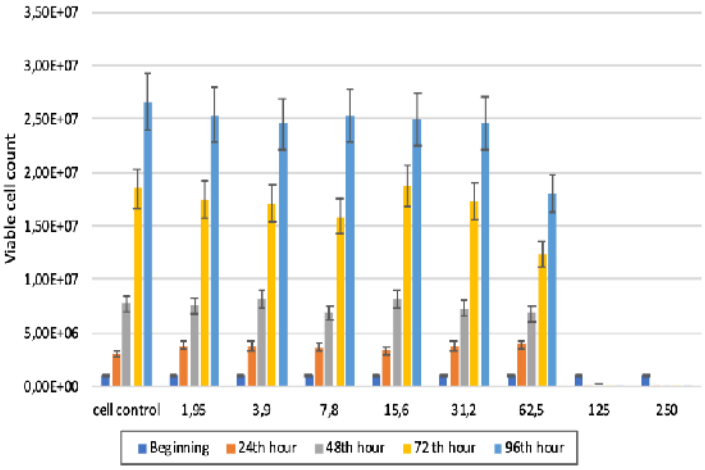

Figure 2. The non-toxic concentration of Acyclovir on Vero cells

The antiviral activities of eucalyptol at a concentration of 62.5 and acyclovir at a concentration of 31.2 µg/ml against the virus at a titer of 100 TCID50 of HSV-2 are given in Figure 3. According to this figure, it was determined that eucalyptol was quite potent, and the efficacy was significantly increased in the case of the acyclovir combination. ($p<0.05$).

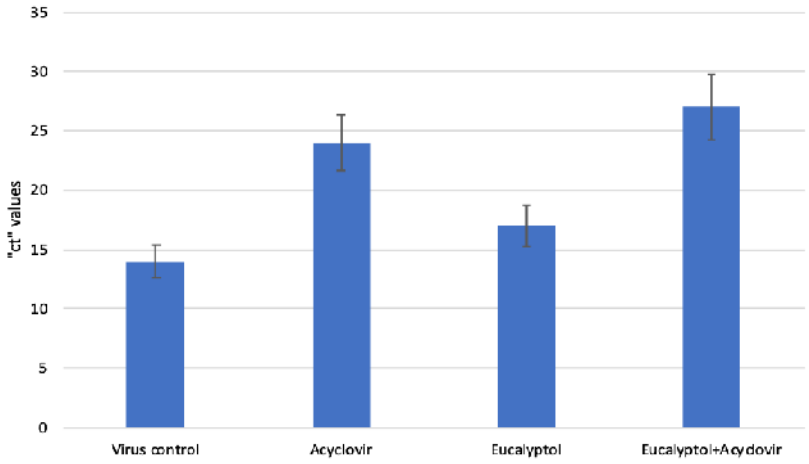

Figure 3. Single and combined activities of eucalyptol and acyclovir against HSV-2

The antiviral activities of acyclovir and eucalyptol at different concentrations were evaluated by considering the percentage of CPE. Similarly, it was determined that the combination of eucalyptol and acyclovir exhibited extreme antiviral activity (Figure 4).

https://doi.org/10.24264/icams-2022.III.3

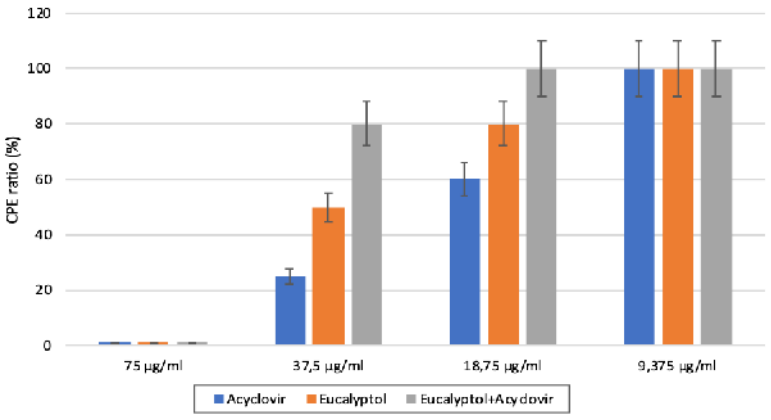

Figure 4. Evaluation of the efficacy of eucalyptol and acyclovir against HSV-2 in terms of CPE

CONCLUSION

These results show that the combination of Eucalyptol and acyclovir may be beneficial against resistant HSV infections. We suggest that the results of these studies, which are planned as *in-vitro*, be supported by *in-vivo* studies.

REFERENCES

Allahverdiyev, A., Duran, N., Ozguven, M. and Koltas, S. (2004), "Antiviral Activity of the Volatile Oils of *Melissa officinalis* L. against Herpes Simplex Virus Type-2", *Phytomedicine*, 11(7-8), 657-661, https://doi.org/10.1016/j.phymed.2003.07.014.

Cunningham, E.T., Jr., Short, G.A., Irvine, A.R., Duker, J.S. and Margolis, T.P. (1996), "Acquired Immunodeficiency Syndrome-Associated Herpes Simplex Virus Retinitis. Clinical Description and Use of a Polymerase Chain Reaction-Based Assay as a Diagnostic Tool", *Archives of Ophthalmology*, 114(7), 834-480, https://doi.org/10.1001/archopht.1996.01100140048006.

Groves, M.J. (2016), "Genital Herpes: A Review", *American Family Physician*, 93(11), 928-934.

Ho, D.Y., Enriquez, K. and Multani, A. (2020), "Herpesvirus Infections Potentiated by Biologics, *Infectious Disease Clinics of North America*, 34(2), 311-339, https://doi.org/10.1016/j.idc.2020.02.006.

Juergens, L.J., Worth, H. and Juergens, U.R. (2020), "New Perspectives for Mucolytic, Anti-inflammatory and Adjunctive Therapy with 1,8-Cineole in COPD and Asthma: Review on the New Therapeutic Approach", *Advances in Therapy*, 37(5), 1737-1753, https://doi.org/10.1007/s12325-020-01279-0.

Lakeman, F.D. and Whitley, R.J. (1995), "Diagnosis of Herpes Simplex Encephalitis: Application of Polymerase Chain Reaction to Cerebrospinal Fluid from Brain-Biopsied Patients and Correlation with Disease, *The Journal of Infectious Diseases*, 171(4), 857-863, https://doi.org/10.1093/infdis/171.4.857.

Mosmann, T. (1983), "Rapid Colorimetric Assay for Cellular Growth and Survival: Application to Proliferation and Cytotoxicity Assays", *Journal of Immunological Methods*, 65(1-2), 55-63, https://doi.org/10.1016/0022-1759(83)90303-4.

Sadowski, L.A., Upadhyay, R., Greeley, Z.W. and Margulies, B.J. (2021), "Current Drugs to Treat Infections with Herpes Simplex Viruses-1 and -2", *Viruses*, 13(7), 1228, https://doi.org/10.3390/v13071228.

Schnitzler, P. (2019), "Essential Oils for the Treatment of Herpes Simplex Virus Infections", *Chemotherapy*, 64(1), 1-7, https://doi.org/10.1159/000501062.

Tognarelli, E.I., Palomino, T.F., Corrales, N., Bueno, S.M., Kalergis, A.M. and González, P.A. (2019), "Herpes Simplex Virus Evasion of Early Host Antiviral Responses", *Frontiers in Cellular and Infection Microbiology*, 9, 127, https://doi.org/10.3389/fcimb.2019.00127.

https://doi.org/10.24264/icams-2022.III.3

EFFECT OF ENZYMATIC BATING ON WET BLUE LEATHER PROPERTIES

RENATA BIŠKAUSKAITĖ, VIRGILIJUS VALEIKA

Kaunas University of Technology, Polymer Chemistry and Technology Department, Radvilėnų pl. 19, 50299 Kaunas, Lithuania, renata.biskauskaite@ktu.lt; virgilijus.valeika@ktu.lt

The use of enzymes in leather processes has increased in recent years. Enzymes have gained more recognition because of their properties, such as specific activity, simple application, mild enzymatic reaction conditions, and non-polluting effluent generations. However, not all enzymatic operations are well investigated, and there is still a lack of knowledge on ferment usage in post-tanning processes. The aim of this study was to investigate the enzyme implementation in wet blue bating and its effect on semi-finished product. The various enzyme preparations were used for bating at different concentrations and process times. The amount of removed collagen proteins, the shrinkage temperature after bating and rechroming were assessed; on top of that, the amount of chrome compounds in semi-finished product and in the effluent was determined. The results showed that enzymatic bating had an effect on wet blue leather. The greatest difference was obtained using Zime SB enzyme preparation. The results obtained during the study are promising, even so, further research on mechanical properties, dying, and fatliquoring effects needs to be investigated to see enzymatic effect on the finished product.

Keywords: enzymes, wet blue, bating.

INTRODUCTION

Leather is a by-product of slaughter houses and meat industries that is used and sold worldwide (Dixit *et al*., 2015). Conventional leather processing from skin to finished product includes various operations in which harsh chemicals and water are used. These operations can be divided into three main groups: pre-tanning, tanning, and post-tanning (Ramasami and Prasad, 1991). During leather manufacturing, from 1000 kg of raw material only 20% of finished product is made and more than 60% of solid and liquid waste is accumulated. This waste contains hazardous chemicals that have a negative environmental impact (Sivaram and Barik, 2019).

Due to growing concerns for the environment, researchers are trying to find alternatives on how to achieve the best leather quality with less waste. Enzymes seem to be one of the solutions; they are gaining more recognition because of their properties, such as specific activity, simple application, mild enzymatic reaction conditions, and generation of non-polluting effluents (Choudhary *et al*., 2004).

Traditionally, ferments are used in bating process. This step with enzymes is crucial for deep leather cleaning and better penetration of substances for further processes. However, due to technology improvement enzyme preparations now have many applications also in the pre-tanning processes: soaking, de-hairing, de-greasing and fiber opening (De Souza and Gutterres, 2012; Kanagaraj *et al*., 2020; Senthilvelan *et al*., 2012). Nevertheless, there is limited information on ferment usage in post-tanning operations, though these processes are also extremely important for finished leather.

Song *et al*. (2017), did research on the protease effect on crust leather dyeing. The study showed better fastness properties against rubbing and better dyes absorption in treated leather. Using enzymes directly in dyeing results in high dye uptake, and leather has brighter and more even colour (Kanth *et al*., 2009). In addition, the use of ferments in the dyeing step can decrease the chemical oxygen demand compared to the conventional process (Colak and Ortafidan, 2016).

https://doi.org/10.24264/icams-2022.III.4

Recent studies showed a new perception for enzyme applications in the rebating process. Enzymatic treated wet blue resulted in better uptake of chromium and other chemicals used in further operations, uniform dyeing and decrease in the pollution load (Jayakumar *et al*., 2019). Researchers studied acid protease ability to affect proteins in wet blue leather. The results indicated that elastin was more affected than collagen. This study provides a basis to understand the rebating mechanism (Li *et al*., 2019). Accordingly, the aim of this research was to study the enzymatic rebating process and its effect on the semi-finished product. Understanding enzymatic operation can help improve conventional leather processes with new technologies.

EXPERIMENTAL

Materials

Bovine wet blue (purchased from tannery "TDL Oda", Lithuania) was cut into 5x10 cm series of samples in such a way that all leather parts would be presented in each experiment.

The chemicals used for the analysis were of analytical grade. Analytical and technical grade materials were used for the technological processes.

The acid bating enzyme preparation (EP) Zime SB (River Chimica, Italy) and NovoBate WB (Novozymes, Denmark) were used for the rebating process execution.

Other technical products used for the technological processes were the following: Cromeco 33 Extra (contains 25% of chromium (III) oxide, 33% basicity) produced by Gruppo Chimico Dalton (Italy); Neutragene MG-120 (for increasing the chromium compounds' basicity).

Technological Processes

Rebating, rechroming, and neutralisation were performed as follows:

Washing: water 300%; temperature 40 °C, 30 min, drain.

Rebating (for control samples this step was excluded): water 200%, EP 1% or 5%; temperature 40 °C, 1 hour or 3.5 hours, drain.

Rechroming: water 150%, Chromeco 33 Extra 4%, temperature 40 °C, 30 min; Neutrage MG-120 0.15%, 10 min; Neutrage MG-120 0.15%, 50 min, drain.

Washing: water 150%; temperature 40 °C, 30 min, drain.

Neutralisation: water 150%; temperature 35-40 °C; $NaHCO_3$ 1.5%; 30 min; NaHCOO 2.0%; 1.5 hour, drain.

Washing: water 100%; temperature 40-45 °C; 30 min, drain.

Notes: The percentage amounts of materials were based on wet blue leather weight. Regime for all processes: run continuously.

Analysis Methods

The amount of collagen proteins removed was estimated from the amount of hydroxyproline in the pickling solution using a photo colorimetric method (Zaides *et al*., 1964). Chromium compound exhaustion was estimated by determining the concentration of chromium in the mixture of used chroming and washing solution. The concentration of chromium in solution was determined according to the method described in the literature (Golovteeva *et al*., 1982). The amount of chrome compounds

https://doi.org/10.24264/icams-2022.III.4

in the leather was determined according to the standard (Standard ISO, 2009). The shrinkage temperature of the chromed and rechromed leather samples was determined as described in the literature using special equipment and replacing the distilled water with glycerol (Golovteeva *et al*., 1982).

RESULTS AND DISCUSSION

Eight rebating variants were tested for chromed leather bating:

1. Water 200%, Zime SB 1%, temperature 40 °C, 1 hour, drain;
2. Water 200%, Zime SB 5%, temperature 40 °C, 1 hour, drain;
3. Water 200%, NovoBate WB 1%, temperature 40 °C, 1 hour, drain;
4. Water 200%, NovoBate WB 5%, temperature 40 °C, 1 hour, drain;
5. Water 200%, Zime SB 1%, temperature 40 °C, 3.5 hours, drain;
6. Water 200%, Zime SB 5%, temperature 40 °C, 3.5 hours, drain;
7. Water 200%, NovoBate WB 1%, temperature 40 °C, 3.5 hours, drain;
8. Water 200%, NovoBate WB 5%, temperature 40 °C, 3.5 hours, drain.

The percentage amounts of materials were based on wet blue leather weight. The regime for all processes: run continuously. After rebating, the effect of the enzymatic process on wet blue was evaluated by collagen protein in bating solution and changes in shrinkage temperature compared to control, which was wet blue without bating (Table 1).

Table 1. Influence of enzyme on the amount of collagen in the solution and shrinkage temperature

Rebating variant	Indexes	
	Removed collagen amount, g/kg wet blue	Shrinkage temperature, °C
1	0.014	119.7
2	0.051	119.4
3	0.039	118.0
4	0.128	114.0
5	0.014	119.9
6	0.059	119.3
7	0.036	116.0
8	0.106	114.7
Control	-	113.8

The results indicate that the amount of removed collagen increased with EP concentration and with the processing time. However, the concentration of EP used had a greater impact than the processing time; with 5% EP removed collagen amount after one hour was more than three times higher compared to 1% EP. The shrinkage temperature after rebating also changed with different EP concentrations and time. NovoBate WB had a larger effect on collagen; using its higher concentration, shrinkage temperature decreases. These results show that EP amount for the process was too high, derma of leather was too much affected.

The main reason for rebating stays the same as conventional bating before rechroming: to prepare material for other operations. Because of that, it is very

https://doi.org/10.24264/icams-2022.III.4

important to analyse if rebating process has any impact in finished product. All variants with control were washed, rechromed and neutralise as in conventional process.

Table 2. Influence of rebating process on rechroming and shrinkage temperature

Rebating variant	Indexes		
	Shrinkage temperature, °C	Cr_2O_3 exhaustion, %	Cr_2O_3 in leather, %
1	123.8	68.1	6.78
2	124.1	77.3	6.81
3	122.7	66.4	6.80
4	122.3	67.6	6.46
5	123.2	71.6	6.89
6	123.1	80.1	6.77
7	122.2	70.5	6.49
8	123.1	68.9	6.46
Control	123.0	58.6	6.50

From Table 2, results showed a huge influence on chroming process. Using EP led to higher chromium exhaustion, these results correlate to collagen removed amount; fibrils during rebating were loosening and more chromium oxide was able to cross-link to leather. With Zime SB chromium exhaustion can exceed 80 percent. Due to the more effective process, there is less chromium in the waste water. However, shrinkage temperatures after rechroming are similar to control, there was no significant improvement.

CONCLUSIONS

The results obtained during this study show a bating effect on wet blue leather. Shrinkage temperature after bating increases, also during rechroming process chromium uptake is higher using EP. These results are very promising. However, there should be more studies on other physical properties as well as further processes evaluation if there are effects on dying and fatliquoring. To evaluate it is very important for finished product application; for each use of leather, there are different regulations.

REFERENCES

Choudhary, R.B., Jana A.K. and Jha, M.K. (2004), "Enzyme Technology Applications in Leather Processing", *Indian Journal of Chemical Technology (IJCT)*, 11, 659-671.

Colak, S.M. and Ortafidan, T. (2016), "Eco-friendly Dyeing Process with Enzymes", *Proceedings of the 6th International Conference on Advanced Materials and Systems (ICAMS 2016)*, 329-334, https://doi.org/10.24264/icams-2016.III.3.

De Souza, F.R. and Gutterres, M. (2012), "Application of Enzymes in Leather Processing: A Comparison between Chemical and Coenzymatic Processes", *Brazilian Journal of Chemical Engineering*, 29(3), 473-482, https://doi.org/10.1590/S0104-66322012000300004.

Dixit, S., Yadav, A., Dwivedi, P.D. and Das, M. (2015), "Toxic Hazards of Leather Industry and Technologies to Combat Threat: A Review", *Journal of Cleaner Production*, 87, 39-49, https://doi.org/10.1016/j.jclepro.2014.10.017.

Golovteeva, A.A., Kutsidi, D.A. and Sankin, L.B. (1982), *Laboratornyj praktikum po khimiyi i tekhnologiyi kozhy i mekha*, Legkaiya i Pischevaiya Prom. Moscow (In Russian).

Jayakumar, G.C., Karthik, V., Asan Fathima, A.D., Tamil Selvi, A., Muralidharan, C. and Kanth, S.V. (2019), "High Exhaustion System (HES) for Leather Process: Role of Biocatalyst as an Exhaustive Aid for Wet-End", *XXXV IULTCS Congress 2019 – Proceeding*, 256-261, Dresden.

Kanagaraj, J., Panda, R.C. and Kumar, V. (2020), "Trends and Advancements in Sustainable Leather Processing: Future Directions and Challenges – A Review", *Journal of Environmental Chemical Engineering*, 8(5), https://doi.org/10.1016/j.jece.2020.104379.

Kanth, S.V., Venba, R., Jayakumar, G.C. and Chandrababu, N.K. (2009), "Kinetics of Leather Dyeing Pretreated with Enzymes: Role of Acid Protease", *Bioresource Technology*, 100(8), 2430-2435, https://doi.org/10.1016/j.biortech.2008.11.026,

Li, H., Zhu, D., Li, Y., Cao, S., Jiang, C. and Yu, T. (2019), "Analysis of the Functional Components of Acid Protease and Investigation of Bating Mechanism of Wet-blue", *XXXV IULTCS Congress 2019 – Proceedings*, 359-365, Dresden.

Ramasami, T. and Prasad, B.G.S. (1991), "Environmental Aspects of Leather Processing", *Proceedings of the LEXPO XV*, 43–71.

Senthilvelan, T., Kanagaraj, J. and Mandal, A.B. (2012), "Application of Enzymes for Dehairing of Skins: Cleaner Leather Processing", *Clean Technologies and Environmental Policy*, 14(5), 889-897, https://doi.org/10.1007/s10098-012-0458-5.

Sivaram, N.M. and Barik, D. (2019), *Energy from Toxic Organic Waste for Heat and Power Generation*, Woodhead Publishing, 55-67, https://doi.org/10.1016/B978-0-08-102528-4.00005-5.

Song, J.E., Kim, S.M. and Kim, H.R. (2017), "Improvement of Dye Affinity in Natural Dyeing Using *Terminalia chebula retzius* (Tchebula) Applied to Leather", *International Journal of Clothing Science and Technology*, 29, 610-626, https://doi.org/10.1108/IJCST-03-2017-0029.

Zaides, A., Mikhailov, A. and Pushenko, O. (1964), "Modiphitsirovanyi method opredeleniya oksiprolina", *Biokhimiya*, 1, 5-6 (in Russian).

*** (2009), Standard ISO 5398-2: 2009. Leather - Chemical determination of chromic oxide content - Part 2: Quantification by colorimetric determination.

https://doi.org/10.24264/icams-2022.III.4

https://doi.org/10.24264/icams-2022.III.4

IMPROVING THE FOOTWEAR ERGONOMICS BY PERSONALIZING ITS SHAPE

LILIIA CHERTENKO, DARIIA KAPTIUROVA, OLEXANDER BONDAR

Kyiv National University of Technologies and Design, Nemyrovich-Danchenko str., 01011 Kyiv, Ukraine, chertenko.lp@knutd.com.ua

The paper examines the possibility and relevance of developing and manufacturing comfortable ergonomic shoes with individual anthropometric insoles in the context of a standard footwear enterprise. The comfortableness of the shoes is achieved due to the correct anthropometrically justified shape of the last and the load-relieving anatomical insole-sole. All initial information for designing is obtained by 3D scanning of a customer's foot and its imprint on polyurethane foam on a specialized professional 3D scanner. Designing of the last is carried out in LastMaker and PowerShape software environment while designing of the insole is performed in PowerShape based on the configuration of the lower surface of the designed last, which corresponds to the relief of the plantar surface of the foot. The anatomical insole was manufactured by milling on a 3-ways CNC machine. The general process of manufacturing shoes complies with the standard technology approved at the manufacturing facility. The individuality of the shoe shape is achieved due to the individually designed shoe last and anatomical insole. Experimental wear showed that shoes produced in this way meet comfortableness requirements to a greater extent than those manufactured using standard lasts and components. The proposed shape of the insole facilitates even distribution of body weight over the entire surface of the foot sole. When walking, such an insole ensures proper functioning of all parts of the foot at each stage of a step. The goal of improving the ergonomicity and sustainability of the shoes being developed is also achieved with the help of a special upper design that combines the insole-lining and upper elements, which reduces the number of shoe components and the technological process for its manufacture.

Keywords: footwear last, 3D design, foot parameters

INTRODUCTION

The new progressive fashion stands out due to its focus on human health and comfort. However, there are still many unresolved issues in the development and manufacturing of ergonomic footwear. The number of foot diseases causes great concern among European and American specialists. Many of these diseases, such as valgus deformity, flat feet, heel spurs, etc., are acquired and can be caused by uncomfortable, poorly fitted shoes.

Thus, the main problem of today's shoe industry is the large number of low-quality shoes worn by people. The survey indicated that from 46 to 81% of participants wear shoes that are too tight because they are literally unable to choose shoes with the suitable fullness from the available range (Buldt *et al*., 2018).

Recent questionnaires and surveys (Chertenko *et al*., 2022) have shown a large number of problems with the comfortableness of women's shoes presented in the mass market.

Ergonomicity and comfortableness of shoes are often sacrificed for the sake of achieving aesthetics as the main factor of competitiveness. After all, it is no secret that buyers, who shape the assortment of fashion stores or boutiques, often ignore the requirements for the ergonomicity of shoes. Thus, ultimately, consumers are forced to wear shoes that cause discomfort or even pain and disruption of movement biomechanics.

However, the current global trend of sustainable fashion is focused on the maximum ergonomicity of products used by people. Therefore, today, due to the shift of the fashion vector towards consumer needs, we have a chance to combine ergonomicity and aesthetics. Another trend of current global fashion involves personalization and customization of products according to the needs of a specific consumer.

Therefore, the major goal of the paper was the development of a convenient shape and ergonomic design of shoes, which is able to ensure the normal functioning of the

https://doi.org/10.24264/icams-2022.III.5

human foot, comfortable wear and an attractive look of shoes. At the same time, we set the goal of individualizing the shape in the context of serial shoe production.

We assume that the ergonomicity and comfortableness of shoes can be enhanced by the manufacture of anatomical insoles that match the shape of a foot, as well as by improving the shape of a last. However, the new advanced ergonomic last shape and ergonomic insoles must meet certain practical requirements, they must be easy to use and require little physical effort in their production and use. Otherwise, the modifications are unlikely to be accepted voluntarily and supported in the long run (Yardley *et al*., 2008).

As a rule, shoes consist of a number of components, each of which can affect walking mechanics (Menant *et al*., 2008). Shoes with milled individual or ergonomic insoles can be both closed-toe (loafers, sneakers, running shoes, boots, ankle boots, shoes, moccasins, etc.) and open (strap shoes, mules, clogs, etc.).

In a significant number of people, certain foot pathologies are caused by inappropriate shoe shape, size, overall anthropometric data that do not correspond to the specific population group (Deselnicu *et al*., 2016). A human foot not only plays an important role in support and movement, but can also affect a person's lifestyle. Decreasing the comfortableness of shoe sizes is the major cause of discomfort, pain, calluses, valgus deformity, ulcers, etc. Accidents and foot diseases lead to a decrease in mobility, which results in the exacerbation of other diseases.

The most important component in the production of shoes is a shoe last. This is the three-dimensional shape of the foot that is used to create shoes. The shape and size of a foot, comfortableness parameters, fashion and design type of shoes affect their manufacturing (Sarghie *et al*., 2013).

Traditionally, shoes are classified based on length and width (balls' circumference). But in addition to the length, girth and shape of the feet, the sole surfaces of human feet can also differ. Walking with completely flat insoles can cause improper load on the feet muscles. Parameters such as axial angle, Hallux-Valgus angle, distribution of body weight on each foot are important for the mechanics of walking. These data for the two feet of the same person may differ (Costea *et al*., 2014). Anatomic insoles are, in fact, used to ensure the correct load on one's feet, as well as for the even distribution of weight between both limbs. For collecting information about a human foot, the most advanced and accurate technique is foot 3D scanning.

Profiled increased-comfort insoles are removable (insertable) and fixed. The shape of the designed last will depend on the type of insole. When using a fixed insole, the relief of the lower surface of a last corresponds to the relief of the upper surface of the insole. This relief depends on the purpose of the shoes and on the anatomical features of a foot. While manufacturing mass-produced shoes, the relief of the insole has averaged parameters. Shoes with such insoles are produced by companies like Birkenstock, Orteks, Walkx, etc. These insoles have won the favor of many consumers due to the increased comfortableness of the manufactured shoes.

The top surface of the insole corresponds to the shape of the foot sole, the side protrusions of the insole (from 5 to 20 mm high) are located on the side surface of the shoe. In the instep part, there is always a hard instep support. A heel socket with a depth of at least 6 mm is placed in the heel part. The arch support of the longitudinal arch of the foot is provided by pad thickness 8-15 mm (Fainberh and Husev, 1984). To support the transverse arch of the foot, a metatarsal pad (Seitz roller) with a height of 2 to 4 mm can be used.

MATERIALS AND METHODS

All the initial information necessary for designing the shape of the last and the anatomical insole was obtained using 3D scanning (Fig.1). We used a Scanner Foot in

https://doi.org/10.24264/icams-2022.III.5

3D with a working scanning area of 400x180x180 mm and a scanning accuracy of 1.3 mm. The data obtained during scanning can be used to estimate the foot health, analyze the morphological and statistical dimensions of the foot, for the footwear design, the selection of shoes and insoles in shoe stores or orthopedic salons (Kimura *et al*., 2012).

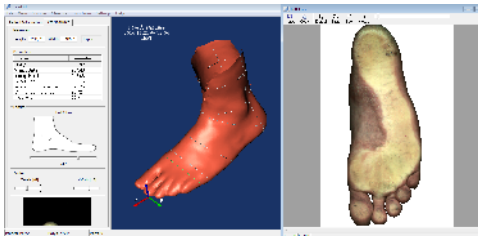

Figure 1. The results of the foot 3D scanning

Information obtained by 3D scanning of foot prints on special foam was also used to design the shape of the insoles (Fig. 2 a). The paper experimentally proved the possibility of obtaining a digital 3D shape of the plantar surface of the foot without the use of plaster casting. One foam block with a foot print was scanned on the Foot In3D scanner (Fig. 2b), so we don't need to perform additional procedures for making a plaster positive.


a

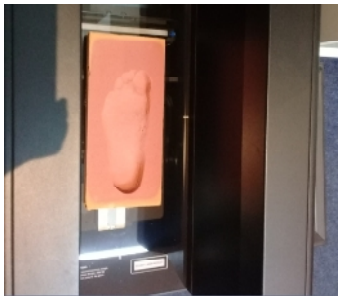
b

Figure 2. Obtaining a footprint using polyurethane foam

The results of foot scanning according to the standard procedure on a 3D scanner and scanning of polymer foam with a foot imprint demonstrated the need to use a polymer foam that perfectly reproduces the relief of the foot due to the uniform compression of the soft tissues of the foot. As the results of the comparison of 3D models showed, scanning the foot on the scanner does not provide such detailed information as the reflection on the polymer foam (Fig. 3).

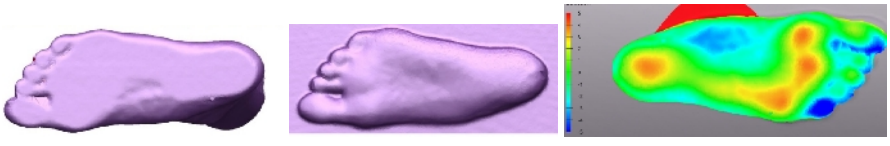

Figure 3. Comparison of the 3D model of a foot imprint on the foam and the foot scanned on a 3D scanner

The results showed significant deviations in the relief of the plantar surface, especially in the ball area and heel area (up to 4 mm).

https://doi.org/10.24264/icams-2022.III.5

RESULTS AND DISCUSSION

The main process of designing lasts and insoles based on the received data took place in the 3D PowerShape environment (Fig. 4). According to the 3D shape of the customer's foot, an ergonomic model of the last was developed, as well as a supporting anatomical sole, wich commons an insole and outsole. In order to increase the comfort of the footwear, the ball girth was increased, the toe part was slightly expanded in accordance with the recommendations of the orthopedic doctor, taking into account the features of the normal biomechanics of the foot during movement.

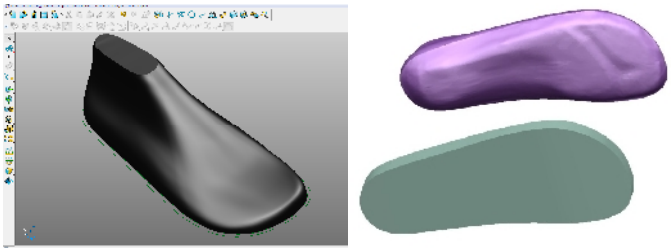

Figure 4. The designed shoe last and insole (Power Shape 3D software)

Preparation for the manufacture of designed anatomical sole took place in the ArtCAM software, which allows you to develop the processing trajectory and set the 3D processing parameters for the CNC milling (Fig. 5a). After that that sole was made using a standard 3-ways CNC machine from EVA material (Fig. 5b). Sheets of EVA-pores with a thickness of 10 mm were pre-glued in two layers, and in the areas of increased thickness (the area supporting the internal arch) a third layer was added.

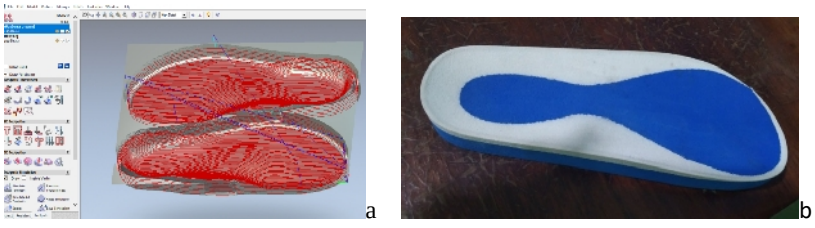

a b

Figure 5. The main stages of insole modeling in ArtCAM

A collection of ergonomic women's shoes, consisting of three models of summer open sandals with anatomical insoles, was offered to the customer based on the developed individual shape of the last (Fig. 6).

Figure 6. A collection of summer women's shoes with an anatomical sole

https://doi.org/10.24264/icams-2022.III.5

A sample of sandals was made at the shoe factory. The upper part of the shoe (straps) has a structural unity with the insole-lining (Fig. 7).

Figure 7. Sandals pattern and sandals on the last

The upper part of that construction is more comfortable, because the number of seams that can rub the foot is reduced. Also this model uses natural materials (cattle skin), which is an ecological material with high hygienic properties (moisture permeability and breathability, durability). The lacing allows you to adjust the width, which eliminates the possibility of discomfort when wearing shoes that are too narrow in the instep and ball area. The upper part has design supported and fixed the instep part of the foot. The test wearing of the shoe sample confirmed the comfort of the form.

To compare the sensations, the customer was offered to wear standard models of shoes manufactured at the factory. Two models of standart sandals with different sole shapes and also the developed personal sandal with anatomic sole were selected for test.

I II III

Figure 8. The tested models of the sandals: model I, model II and model III

The customer alternately wore three pairs of shoes from Fig. 8 for one day for 7-8 hours each. It was suggested to evaluate the feeling of comfort while wearing according to the questionnaire. The maximum score (10) was assigned to the most comfortable shoes, the minimum score (1) to the least comfortable. The results of test are shown on Fig. 9.

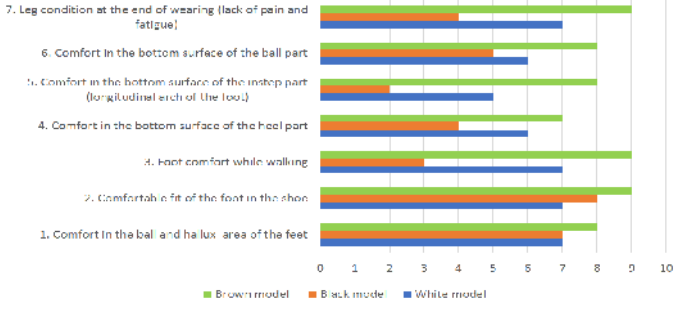

Figure 9. Comparing the comfort rating of the personal ergonomic shoes and the standard shoe

https://doi.org/10.24264/icams-2022.III.5

Such an increase in subjective comfort index can be explained in terms of foot anatomy and movement biomechanics. The fact is that the proposed shape of the insole, designed on the basis of the plantar relief of the foot, taking into account the recommendations of an orthopedist, facilitates even distribution of body weight over the entire surface of the foot, which significantly reduces the load on the heel and other areas of peak pressure. When walking, such an insole ensures proper functioning of all parts of the foot at each stage of a step. As a result, the general feeling of tiredness in the foot and lower leg is significantly reduced.

CONCLUSIONS

The shoes developed in this work were designed based on the 3D shape of a foot using advanced computer technologies and equipment. Test wear demonstrated a high degree of comfortableness of such shoes for the customer. At the same time, there has been suggested an original design of the upper of the shoe made according to the principle of moccasins, when the insole and the elements of the upper comprise a single part, which reduces the number of operations for assembling the uppers of the shoe, as well as the amount of excess material that is usually spent on the lasting edge. The anatomical insole also performs the function of the sole, and, therefore, it eliminates the need for the use of additional parts and the process of assembling them, which also significantly increases the value of the proposed shoe design from the perspective of sustainability. However, the design of the upper of the developed sandals needs to be improved from an aesthetic point of view, as well as from the perspective of the rationality of the templates' shape in order to promote a more economical use of genuine leather from which the upper of the shoes is made. In addition, in the future, we are planning to investigate the possibility of utilizing a single averaged shape of the last for individual anatomical insoles with different configurations.

REFERENCES

Buldt, A.K. and Menz, H.B. (2018), "Incorrectly Fitted Footwear, Foot Pain and Foot Disorders: A Systematic Search and Narrative Review of the Literature", *Journal of Foot and Ankle Research*, 11, https://doi.org/10.1186/s13047-018-0284-z

Chertenko, L. and Booth, B.G. (2022), "Modelling Shape and Parameterising Style: An Approach to the Design of High-Fashion Shoe Lasts", *Footwear Science*, 14(2), https://doi.org/10.1080/19424280.2022.2095041.

Costea, M., Vasilescu, A.M., Hortal, G. and Mihai, A. (2014), "Plantar Footprints Analysis - Case Study (Part 2), *Leather and Footwear Journal*, 14(4), 243-250, https://doi.org/10.24264/lfj.14.4.4.

Deselnicu, D.C., Vasilescu, A.M. and Mihai, A. (2016), "New Products Development through Customized Design Based on Customers' Needs. Part 1: Footwear Comfort Parameters", *Procedia Technology*, 22, 1043-1050, https://doi.org/10.1016/j.protcy.2016.01.148.

Fainberh, L. and Husev, L. (1984), *Metodycheskye rekomendatsyy po naznachenyiu prysposoblenyi ortopedycheskykh vkladnukh VP*, Kyiv (in Russian).

Kimura, K., Utsumi, T., Kouchi, M., Mochimaru, M. (2012), "3D Foot Scanning System INFOOT - Automated Anatomical Landmark Detection and Labeling", *Asian Workshop on 3D Body Scanning Technologies*, Tokyo, Japan, 17-18 April 2012, 44-46, https://doi.org/10.15221/A12.044.

Menant, J.C., Steele, J.R., Menz, H.B., Munro, B.J. and Lord, S.R. (2008), "Effects of Footwear Features on Balance and Stepping in Older People", *Gerontology*, 54, 18–23, https://doi.org/10.1159/000115850.

Sarghie, B., Costea, M. and Mihai, A. (2013), "3D Modelling of Shoe Lasts Using Templates Based on Anthropometrical Measurements of the Foot Case Study", *Leather and Footwear Journal*, 13(3), 221-234, https://doi.org/10.24264/lfj.13.3.5.

Yardley, L., Kirby, S., Ben-Shlomo, Y., Gilbert, R., Whitehead, S. and Todd, C. (2008), "How Likely are Older People to Take up Different Falls Prevention Activities?", *Preventive Medicine*, 47, 554–558, https://doi.org/10.1016/j.ypmed.2008.09.001.

COMPARATIVE STUDIES OF PHYSICAL-MECHANICAL PROPERTIES OF NOBLE FURS

ANA-MARIA CIOBANU, DENIS-ANDREI DRUȘAN, MĂDĂLINA IGNAT, ROXANA CONSTANTINESCU, VLAD BĂRBULESCU, CIPRIAN CHELARU

The National Research & Development Institute for Textiles and Leather - Leather and Footwear Research Institute Division, Bucharest, Romania

The current work aims to highlight the structural differences of noble furs, more precisely of nutria fur and nutriette fur, especially following their behavior in various physical-mechanical analyzes. Noble furs have always had a special role in people's lives, over time the mankind crossed the seas and continents in search of the precious furs (noble furs). Since the 17th century, noble furs have been so appreciated that they have been used in certain geographical areas instead of money. In the past, noble furs were used only by those with a very good financial situation, but nowadays, noble furs are used on a large scale to make clothes, collars, and hats. The main purpose of this article is, therefore, to determine which of the two noble furs has superior physical and mechanical qualities. The reason why these two furs were chosen was that one is believed to be an imitation of the other on the market. The two types of fur were carefully analyzed by subjecting them to different types of physical-mechanical tests, the most relevant being: "Determination of tensile strength and percentage elongation", "Determination of tear strength", "Determination of shrinkage index", "Resistance at plucking the fur". All the tests were performed according to actual standards in ICPI accredited laboratory. The obtained results showed that although the two noble furs seem similar at first sight, the original has a superior quality, but also nutriette fur has proven to have some appreciable physical-mechanical properties.

Keywords: furs, physical-mechanical, nutria, nutriette

INTRODUCTION

The processing of furs and their use as clothing has a long history. If in the prehistoric period furs demonstrated the hunting virtues (trophies) and were used as such for bedding or to protect the body, much later, people discovered the useful and aesthetic value of clothing in these furs. Of course, for the achievement of this qualitative leap, the most important contribution had the evolution of the techniques of harvesting and processing of furs (Chirita, 1983).

Particularly high-quality fur types are awarded with the term of "noble fur", but the distinction to the other fur types is blurred and was not always the same in the various fashion epochs. The terms "semi-precious" and "non-precious" skins are also used gradually in trade (Deselnicu and Albu, 2007).

Among the noble furs is the nutria fur, which is highly valued, in its natural color it is light to rich brown, the most valuable furs being in the darker shades, but it may also be dyed. The designation of "noble" can be given to a common fur if it is considered to be an imitation of a noble fur. So, an upper hair lambskin, in itself a common fur, takes on a noble character if it is colored as an imitation silver fox. We also speak of noble lamb as Nutriettes, which are actually a fake nutria (Pastarnac *et al*., 1985).

The chemical composition of animal skins with fur consists of water, minerals, protein substances and fat substances and does not differ fundamentally from the chemical composition of animal skins used in tanneries. However, the quantitative rations of the different structural elements differ considerably (Chirita, 1983).

Nutrias grow most intensely until the age of one year. In good maintenance conditions, they can grow and develop until the age of two. The long and thick hair on the spine exceeds 30 mm in length, the fluff being 20 mm. The standard nutria hair

https://doi.org/10.24264/icams-2022.III.6

color is brownish gray, the back has a darker shade, the abdomen lighter, the flanks have an intermediate color. The hair is thick and quite fragile, but shiny. The fluff is fine, twisted in a wavy shape, thin, beautiful, gray with a blue or brown shade. In Romania, in addition to standard nutria, colored nutrias are also grown: black, beige, silver and brown of different shades. In many colored varieties, the fluff on the abdomen is shorter than the standard nutria, but after the thickness of the fluff they are just as thick or even exceed the fur of the standard nutria (Chirita, 1983).

A large influence on the commercial value of nutria furs is their size. At the age of 6-7 months, the nutrias give a fur that can fit the size of the standard.

In the present-day fur production, physical and mechanical properties of skin tissue are essential.

The skins of fur-bearing animals possess a number of fundamental structural features. They usually have a very thin dermis, due to the fact that the hair coat is strongly developed.

The hairy covering is the totality of hairs that cover the animal's body. The hairy covering of most fur skins consists of hairs distinct from each other, in shape, size, color and structure (Chirita, 1983).

EXPERIMENTAL

Materials and Methods

The objective of the study was to present the differences in terms of physical and mechanical properties of noble furs, more precisely of nutria fur, compared to nutriette fur. So, the materials used were a piece of nutria fur and one of nutriette fur and were conditioned according to the standard.

To achieve the objective, the two types of fur were carefully analyzed by subjecting them to different types of physical-mechanical tests, according to actual standards, performed in ICPI accredited laboratory, the most relevant being: *Determination of tensile strength and percentage elongation* SR EN ISO 3376:2020, *Determination of tear strength* SR EN ISO 3377-1:2012, *Determination of shrinkage index* SR 5053:1998, *Resistance at plucking the fur* STAS 4180-90 Pt.4.4.

The equipment used was the traction test machine “Tinius Olsen”.

RESULTS AND DISCUSSIONS

In the present paper, the studied nutria fur is a standard brown one, which can be observed in the pictures below, alongside the nutriette fur.

https://doi.org/10.24264/icams-2022.III.6

Figure 1. Images of standard nutria fur (left) and nutriette fur (right)

In the displayed graph it can be seen the behavior of the two furs at an elongation of 30N. The nutria fur registered an average value of 33.94% after testing 10 samples, while the nutriette fur had an average value of 23.92% at the same test, carried out under the same conditions.

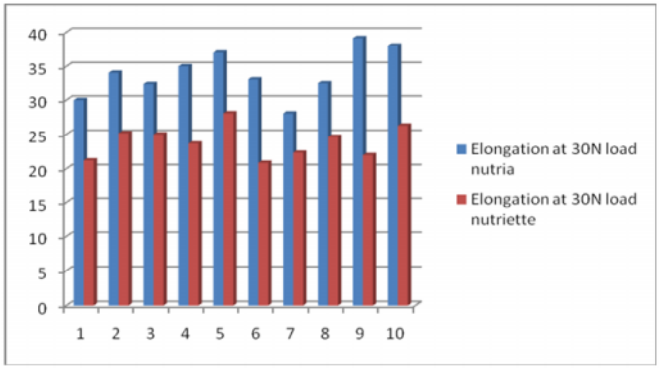

Figure 2. Variation of elongation at 30N for the two types of furs

The second graph shows the differences in values at elongation at break for the two furs, the analysis being also performed on a number of 10 samples. In this case it can also be seen that the nutria fur is shown to be superior to the nutriette fur, the average value registered being one of 65.34%, compared to one of 45.32%.

https://doi.org/10.24264/icams-2022.III.6

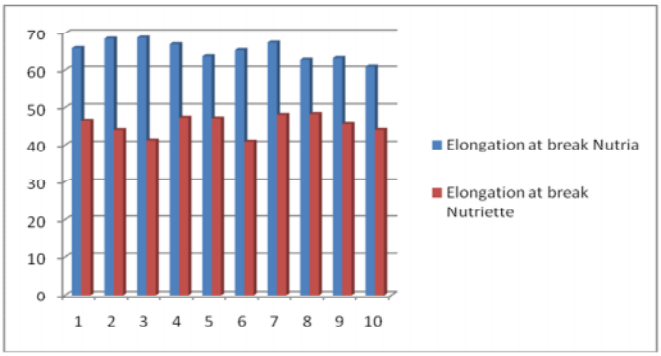

Figure 3. Variation of elongation at break for the two types of furs

The third graph shows the breaking load, the differences between the two furs being similar to the two previous analyses. In other words, the nutria fur has proven to have a better breaking load than the nutriette fur, the average value for it being 153.12 N, compared to 139.25 N.

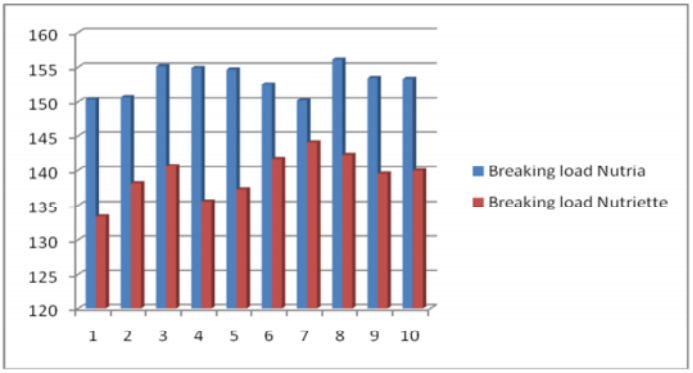

Figure 4. Variation of breaking force for the two types of furs

The elongation at 30N, the elongation at break and the breaking load are results obtained from a single complex analysis called “Tensile strength and percentage elongation”, made with the help of the traction test machine “Tinius Olsen” and fully respecting the specific standard for this analysis (SR EN ISO 3376:2020).

Regarding the tearing strength of the two furs, the nutria fur seems to be better again, the average value being 26.83 N, while the nutrient fur reached an average value of 20.03 N. To obtain these numbers, 10 samples cut from each fur were tested once again. The results can be better seen in the graph below.

https://doi.org/10.24264/icams-2022.III.6

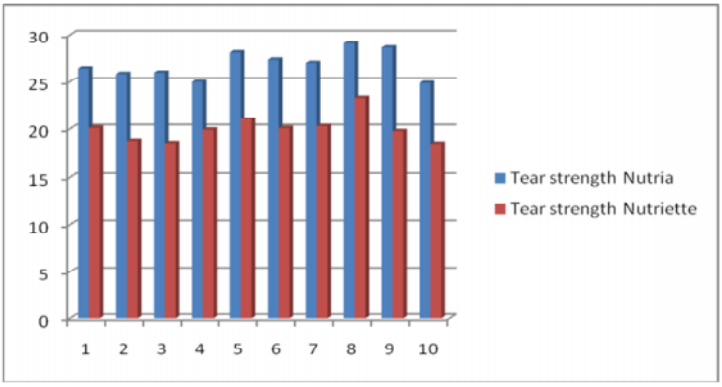

Figure 5. Variation of tear strength for the two types of furs

This analysis is also performed using the traction test machine "Tinius Olsen" fully following its standard (SR EN ISO 3377-1:2012).

Another extremely relevant analysis for this study is "Determination of the shrinkage index", which revealed that once again nutria fur is visibly better. According to this analysis, performed based on its standard (SR 5053:1998), at the temperature of 70°C the nutria fur has a shrinkage index of 3.2%, while the nutriette fur holds a value of 4.12%.

The only analysis that gave identical results was the one referring to the quality of the hair, "Resistance at plucking the fur" (STAS 4180-90 Pt.4.4) and was proven that both furs are great in this regard.

CONCLUSIONS

Although the two noble furs seem similar at first sight, the original is always of superior quality. As mentioned at the beginning of this study, the nutriette fur was specifically designed to be a more affordable nutria fur substitute. It should be noted that although it did not rise to the level of nutria fur, the nutriette fur has proven to have some appreciable physical-mechanical properties.

REFERENCES

Chirita, Gh. (1983), *Leather and Fur Processing Technology* (in Romanian), Vol. 1, Technical Press, Bucharest.

Deselnicu, V. and Albu, L. (2007), *Modern Technologies for Leather and Fur Processing* (in Romanian), Certex Press, Bucharest.

Pastarnac, N., Sirbu, V., Stroia, S. and Gruia, R. (1985), *Breeding Furs and Their Primary Processing* (in Romanian), Ceres Press, Bucharest.

*** (1998), SR 5053:1998 – Skins and Furs under Processing and Finished Skins and Furs. Determination of the Shrinkage Index (in Romanian).

*** (2012), SR EN ISO 3377-1:2012 – Leather – Determination of Tear Load.

*** (2020), SR EN ISO 3376:2020 – Leather – Physical and Mechanical Tests.

*** (2008), STAS 4180-90 – Finished Woolen Sheepskins. Sheep Leather Fined on Wool (in Romanian).

https://doi.org/10.24264/icams-2022.III.6

https://doi.org/10.24264/icams-2022.III.6

THE EFFECTS OF DIFFERENT LACQUERS USED IN FINISHING ON LEATHER COLOR CHANGE

SULTAN ÇİVİ, ANIL ÖZÇELİK, ESER EKE BAYRAMOĞLU

Ege University, Leather Engineering Department, IZMIR, TURKIYE,
sultancivi@gmail.com, ozcelikanil@gmail.com, eserekebay@gmail.com

Although there are many factors affecting the final color of the leather, it is wondered whether it has a significant contribution since final coat is the last step for the production of leather in finishing. It is necessary to determine which lacquer emulsion or emulsions are causing this situation, which may result in cost, time, and quality losses. For this reason, in this study, firstly, three different lacquer emulsions, namely Nitrocellulose, Cellulose Aceto Butyrate and Polyurethane, were applied to the leathers dyed with the same finishing composite (base coat) at the final stage. These lacquer emulsions are widely used in leather finishing. Water-soluble forms of these materials, including solvent-soluble types, were chosen for use in this study because they are more environmentally friendly and easier to apply. After that, leather colors were analyzed for color parameters determination by using Konica Minolta brand CM 3600d Spectrophotometer and compared with the color changes before and after the lacquers were applied. Finally, The NCSS (Number Cruncher Statistical System) 2022 Statistical Software (NCSS LLC, Kaysville, Utah, USA) program was used to statistically evaluate the results. As a result, it was attempted to identify the lacquer emulsions that causes the color change in the leather.

Keywords: finishing, laquer, color change

INTRODUCTION

The finishing process, which is the final stage of the leather production process in tanneries, is critical in ensuring that the final product has the appropriate resistance properties. Finishing enhances the appearance of leather by reducing surface defects and scratches, providing shine, feel, color match, color effects, and aiding in the preservation of the leather's natural appearance (Winter *et al*., 2015).

Three foundation coats - Base Coat, Pigment Coat, and TopCoat - make up finishing (Sasikala *et al*., 2007). The surface characteristics of the leathers are chemically altered to fix the finishing chemicals in the base coat. The leathers are given a uniform color by the pigment coat. To enhance physical qualities, fillers and binders are additionally utilized. To protect the leather finish, topcoat is made up of lacquers based on polyurethane and cellulose derivatives (Tamilselvi *et al*., 2019). Topcoat can provide leather excellent fastness and mechanical qualities because it is reasonably hard and more abrasion-resistant (Wu *et al*., 2021). The final appearance and texture of the leather surface are determined by the finish. Additionally, it has a considerable impact on the finished leather's fastness qualities. Nowadays, there is an increasing preference for water-based topcoat systems over organic, solvent-containing varnishes and topcoats (Dix and Kirchner, 2002).

Isocyanates, polyols, and/or NH-functional chemicals are combined to form polyurethanes (Dix and Kirchner, 2002). To guarantee the leather has strong light fastness, the top coating is made of solvent-based aliphatic polyurethanes (PU). Solvent-based PUs are nevertheless prohibited because of their toxicity and environmental issues. The creation of water-based polyurethane (WPU) has shown to be a successful method for reducing organic solvent emissions significantly. In most cases, hydrophilic alteration is necessary for PU to dissolve in water. WPU can be classified into three groups based on the hydrophilic elements that make up the PU backbone: anionic

https://doi.org/10.24264/icams-2022.III.7

(carboxylic ion), cationic (ammonium ion), and nonionic (polyethylene glycol). The most popular water-based leather finishing material among them is anionic WPU because of its excellent dispersion stability and ease of mass manufacture (Wu *et al*., 2021).

By processing cellulose with a solution of nitric and sulfuric acids, nitrocellulose (NC) is created. The cellulose's hydroxyl groups (OH) are changed to nitrate groups (NO3) during this process, improving its ability to dissolve in solvents and transforming it into a transparent lacquer. Solvent-based NC lacquer, when applied as a topcoat, can enhance leather in a number of ways, including superior water resistance, good dry and wet friction fastness, filth resistance, and resistance to mechanical stress. Its distinctive high shine feature can be utilized for leathercraft, shoes, and other items. It enhances the value and beauty of leather, making it desirable in leather goods. To lessen the concerns that volatile organic compound (VOC) emissions pose to the environment and human health, water-based NC polish emulsions have recently been created. There are generally three ways to make aqueous NC dispersions. One involves emulsifying NC with the addition of surfactants. First, NC is dissolved in small volumes of organic solvents. Next, the NC solution is emulsified in water using surfactants, and the water-based product is produced by vacuum distillation after the organic agents have been removed. Phase inversion is the second strategy. The surfactant solvent combinations are used to first emulsify the NC, and then water is added while being vigorously stirred. These results in the transformation of the water-in-oil (W/O) emulsion created in the initial stage into an oil-in-water (O/W) emulsion. The third method is self-emulsification, which involves covalently immobilizing hydrophilic groups within the NC to increase its hydrophilicity and aid in its dispersion in water (Wu *et al*., 2021). Nitrocellulose emulsions give the leather a natural feel. It flows well and has a low surface tension. Spraying it is simple, and it dries rapidly.

By esterifying cellulose with acetic, butyric, and anhydrides, cellulose is converted to cellulose acetate butyrate (CAB). When cellulose is entirely soluble in the solvent, CAB synthesis is carried out under homogenous conditions. A significant commercial cellulose derivative product called cellulose acetate butyrate (CAB) has been employed in coating materials, optical films, filtration membranes, and polymers (Dehmen, 2018). The most versatile cellulose ester type, CAB Solvent has an optimum solubility and is compatible with other popular paint polymers. Esters, ketones, glycol ethers, glycol ether esters, aromatic hydrocarbon solvents, and combinations of alcohols are among the solvents in which it is soluble (Turkchem, 2017). Its water-soluble versions are utilized to produce leather. The surfaces made from CAB aid in the manufacturing of relatively high levels of flexible, abrasion-resistant, high-gloss, and flame-resistant leather by both leather and artificial leather manufacturers (Cellulosic Resins and Their Uses, 1972).

In this investigation, white finishing-process dye was applied to chrome-tanned bovine crust leathers, and color measurements were taken. Then, three different topcoats - Polyurathane (PU), Nitrocellulose (NC), and Cellulose Aceto Butyrate—were applied, and the color was once more measured. It was determined whether there had been a color change between before and after the topcoat using the findings of the color measurement. As a result, the impact of the topcoat on color change was examined.

https://doi.org/10.24264/icams-2022.III.7

EXPERIMENTS

Finishing Applications

Bovine crust leathers that had been chrome-tanned were employed in this study. The leathers used for the study were finished using the recipe listed in Table 1.

Table 1. Finishing recipe

Product	Formula 1	Formula 2	Notes
VDB-2 1004	150		Verpol White Pigment
AA 4750	50		Piel Color Synthetic Waks
UR 1443	100		Piel Color Aliphatic Polyurethane
RE 2350	70		Piel Color Acrylic Polymer
Water	200	100	
UR 1786*		100	Piel Color Polyurethane Top Coat
LA 6016**		100	Piel Color NC Hydrolac
LW 5343***		100	Stahl CAB Hydrolac

Application :
1) 3xspray - hydraulic press 90C/90 bar- 4xspray
2) 2xspray -hydraulic press 100C/100 bar
*Experiment 1
**Experiment 2
***Experiment 3

Referring to the lacquer coat's color measurements all leathers were finished with the same white base coat and the color was measured.The Experiment 1 leathers received a water-soluble Polyurethane topcoat (UR 1786), the Experiment 2 leathers received Nitrocellulose hydrolac (LA 6016), and the Experiment 3 leathers received Cellulose Aceto Butyrate Hydrolac (LW 5343). All leathers were then measured for color once again to to compare the color change.

Color Measurement Tests of Leather Samples

Color measurement was carried out twice, after the paint coat (first measurement) and after the topcoat was applied (Experiment 1, Experiment 2 and Experiment 3). Color difference determination was realized on Konica Minolta brand CM 3600d Spectrophotometer. Firstly, Standard white calibration process was practised in device. Measurement was carried out by reading 15 points from the grain surface of the samples into the reading area of the instrument. The results were reported as average values of these measurements.

Statistical Evaluation of Results

While evaluating the findings obtained in the study, NCSS (Number Cruncher Statistical System) 2022 Statistical Software (NCSS LLC, Kaysville, Utah, USA) program was used for statistical analysis. Dunn's test was used to determine the group that caused the difference.

https://doi.org/10.24264/icams-2022.III.7

RESULTS AND DISCUSSION

In color measurements, evaluations were made according to the ΔE*ab (D65) results obtained from L* a * b color area measurements. Various quantitative methods have been developed to avoid the complexity that arises in the verbal expression of the concept of color. L* a * b color space, defined by CIE (International Commission on Illumination) in 1976, is widely used in color measurements. In this method, the L aperture indicates the +a red direction, -a the green direction, +b the yellow direction and -b the blue direction. ΔE*ab is the numerical value showing the size of the color difference (Turkchem, 2017)

In this study, ΔL values were compared to measure the lightness change of leather samples and ΔE values were compared to measure the total color change.

Comparison of ΔL Measurement Results

Comparison of ΔL results of leather samples is given in Table 2.

Table 2. Comparison of ΔL Values (Kruskal-Wallis Multiple-Comparison Z-Value Test (Dunn's Test))

Section 1

Variable	ΔL Experiment 1	ΔL Experiment 2	ΔL Experiment 3
ΔL Experiment 1	0.0000	3,3723	0,9882
ΔL Experiment 2	3,3723	0.0000	2,3841
ΔL Experiment 3	0,9882	2,3841	0.0000
First_measurement	4,0258	0,6535	3,0377

Section 2

Variable	First_measurement
ΔL Experiment 1	4,0258
ΔL Experiment 2	0,6535
ΔL Experiment 3	3,0377
First_measurement	0.0000

Regular Test: Medians significantly different if z-value > 1,9600.
Bonferroni Test: Medians significantly different if z-value > 2,6383.

According to the Table 2, a significant difference was found in the Experiment 1 and Experiment 3 compared to the first measurement. Based on this information, it can be said that Polyurethane and Cellulose Aceto Butyrate topcoat materials change the degree of lightness.

Comparison of ΔE Measurement Results

The ΔE results of the leather samples are given in Table 3.

https://doi.org/10.24264/icams-2022.III.7

Table 3. Comparison of ΔE Values (Kruskal-Wallis Multiple-Comparison Z-Value Test (Dunn's Test))

Section 1 Variable	First_measurement	ΔE Experiment 2	ΔE Experiment 3
First_measurement	0.0000	0,1621	4,104
ΔE Experiment 1	0,1621	0.0000	3,9419
ΔE Experiment 2	4,104	3,9419	0.0000
ΔE Experiment 3	0,481	0,3189	3,623

Section 2 Variable	ΔE Experiment 3
First_measurement	0,481
ΔE Experiment 1	0,3189
ΔE Experiment 2	3,623
ΔE Experiment 3	0.0000

Regular Test: Medians significantly different if z-value > 1,9600.
Bonferroni Test: Medians significantly different if z-value > 2,6383.

According to the Table 3, a significant difference was found between the first measurement and the second Experiment 2. According to this information, it can be said that Nitrocellulose topcoat material change the color.

CONCLUSION

Finishing practitioners have noticed that some topcoat materials change color during the finishing process, which is the final stage of leather production in which various performance properties and the final color are applied to the leather. In order to investigate this situation, to reformulate with the finishing process in this study, and color measurement analyses were performed. Three different topcoats were applied to leather samples, namely Polyurethane, Nitrocellulose, and Cellulose Aceto Butyrate, and color measurements were taken again. Statistical methods were used to compare all color measurements taken. According to the statistical evaluation results, the topcoat materials Polyurethane and Cellulose Aceto Butyrate changed the whiteness of the leathers measured as lightness difference. The Nitrocellulose topcoat material was found to change the color of the leathers.

REFERENCES

Dehmen, O.G. (2018), "Synthesis of Cellulose Acetate Butyrate Based Polymeric Films and Their Applications", İstanbul Teknik Üniversitesi Fen Bilimleri Enstitüsü Yüksek Lisans Tezi.

Dix, J.P. and Kirchner, W. (2002), *Applications in the Leather Industry*, ISBNs: 3-527-30286-7 (Hardback); 3-527-60058-2 (Electronic).

Sasikala, L., Ganesan, P. and Hariharan, S. (2007), "Processing of Leather for Garments – An Overview", *Man-made Textiles in India*, 50(10), 356-360.

https://doi.org/10.24264/icams-2022.III.7

Tamilselvi, A., Jayakumar, G.C., Charan, K.S., Sahu, B., Deepa, P.R., Kanth, S.V. and Kanagaraj, J. (2019), "Extraction of Cellulose from Renewable Resources and Its Application in Leather Finishing", *Journal of Cleaner Production*, 230, 694-699, https://doi.org/10.1016/j.jclepro.2019.04.401.

Turkchem, (2017), "Konika minolta cihazları ile kesin renk ölçümü", http://www.turkchem.net/konica-minolta-cihazlari-ile-kesin-renk-olcumu.html.

Winter, C., Schultz, M.E.R. and Gutterres, M. (2015), "Evaluation of Polymer Resins and Films Formed by Leather Finishing", *Latin American Applied Research*, 45, 213-217, https://doi.org/10.52292/j.laar.2015.400.

Wu, X., Wu, J., Mu, C., Wang, C. and Lin, W. (2021), "Advances in Antimicrobial Polymer Coatings in the Leather Industry: A Comprehensive Review", *Industrial & Engineering Chemistry Research*, 60(42), 15004−15018, https://doi.org/10.1021/acs.iecr.1c02600.

*** (1972), "Cellulosic Resins and Their Uses", *Pigment and Resin Technology*, 1(3), 23-27, https://doi.org/10.1108/eb040803.

https://doi.org/10.24264/icams-2022.III.7

FOOTWEAR INDUSTRY LEATHER CUTTING ISSUES AND RECOMMENDATION OF WASTAGE MINIMIZATION RESEARCH INNOVATIVE TECHNIQUES

DURAIRAJ DHANAPAL, SITAWALA MUNDIA

Technology Copperstone University, Leather Department, Kitwe –Zambia, e-mail: dhanapal_d2k@yahoo.com

Leather from different parts of the animal, its characteristics, and this has to be taken into account when using leather in several products. The main parts of the hide and skin such as the shoulder, butt, belly, and axillae are different properties in terms of strength, flexibility, and durability (Mesa *et al*., 2019). They consumed for many types of footwear such as shoes, boots, sandals, slippers, etc. Footwear is divided into many categories such as athletic shoes also known as sneakers, galoshes, high heels, and many others. The leather clicking operation is very important for making shoe uppers mostly cow leather. Buff, goat skins are used for upper making. This operation is required a high level of skill efficiency (Elamvazhuthi *et al*., 2009). Right now, African country's footwear industry is very faster developing based on leather sources This research already focused on the leather cutting section layout design, operation methods, time study, standard operating procedure, assorting, grading, nesting, machine maintenance, allocation sheet Stroke report, die cabinet, daily report techniques all are implemented and recommended to the African middle scale footwear sectors.

Keywords: leather, implementation, higher productivity.

INTRODUCTION

Leather is a natural material the hide/skin thickness varies all over the animal, and to get it to the right thickness it is usually split on special cutting machines or buffed to an even thickness. The main parts of the hides and skins vary property stated that K.T Sarkar (2005), such as shoulder, Butt, Belly, and Axillae. Particularly Footwear has become an important component of fashion accessories. Shoemaking is considered a traditional handcraft profession however now it has been largely taken over by the industrial manufacture of footwear (Nguyen, 2004). Nowadays a lot of materials are used for making shoes such as leather, fabrics, plastic, rubber, wood, jute fabrics, metal, etc. This leather cutting operation needs a high level of skills and knowledge otherwise the expensive leather has to be wasted. Nowadays medium sectors /African footwear sectors meet huge challenges in this primary operation of leather cutting process the quality parameters such as cost minimization, waste minimization, production efficiency, unskilled manpower, production targets, financial factors, etc. This research work was particularly focused on cutting waste minimization in Zambia's small/medium scale companies. This innovative research implemented the leather assorting, workplace cutting layout, cutting operation, time study management, standard operating procedure (SOP), leather quality grading techniques, cutting machine maintained methods, material saving techniques, cutting allocation sheet methods, cutting die allocation, damage dies cabinet systems, die checking marble stone, daily cutting stroke reports system.

https://doi.org/10.24264/icams-2022.III.8

RESEARCH METHODOLOGY

Selection of Leather

In footwear production commonly used for Goat skin, cow leather, buff leather, pig leather, and sheep skin. Finishing is a very important role in footwear production. Leather finishing has a lot of varieties such as full grain leather, correct grain leather, suede leather, patent leather, PU coated leather, Semi-aniline finish, pigmented finish, etc. (Alves *et al*., 2012). Defected such as grain feel off, defected surface, poor thickness, improper finishing shade, looseness, color feel off, poor strength, testing failure, more chemical contents are shorted out the correct selection and the assorted process was followed for this research work.

Advanced Leather Grading Method

Grading is a very important factor in the footwear industry, nowadays SATRA five-point grading systems are commonly used in many countries, and grading is the key point. Commonly Grain defects, vein marks, color feel-off, poor strength, flaying cuts, and machinery defects are major problems in finished leather (Brun and Ciccullo, 2022). From this research leather inspection records, color swatches, sample shoes, inspection tools kits, and multi-light boxes are very important for the leather grading process. Based on the challenge upgraded cutting efficiency and cutting average standard was properly handled by the cutting section in the Middle sectors. This research referred to the SATRA five points grading rules and motivated the trained assorting skills. SATRA Leather grading level AQL level 1 light inspection (Accepted quality level), AQL level 2.5 – Normal inspection and AQL Level 4 (Minor leather inspection) was implemented.

Manual Nesting and Innovative Cutting Techniques

Before cutting nesting technical skill was very important for the upper leather cutting operator, finished leather has loose fiber leathers, brand marks, operation scars, open flaws, closed Flaws, wire marks, and scratches. Growth marks, fat wrinkles, veins, flay cuts, discolored finishing area, border dry area, insect or parasitic damage, etc. (Solomon, 2021). The nesting and dies interlocking technical skill, and cutting direction training were implemented by this valuable research.

Cutting Implementation and Machines Maintenance

The workplace is one of the important factors due to the research we trained key points about lack of cutting, loose leather components, uneven grain, components color matching issues, proper SOP, hourly QC report, stroke report, leather norms consumption systems, workplace safety prevention was implemented and it suggested to avoid up normal component cutting. Cutting board has two types of material cutting board (white color) and leather cutting board (green or Red Colour). Regularly every 2 hours color management systems such as yellow, blue, Green, and Red, are colors normally used for cutting board management systems. Board four edges were colored and 180-degree angle, the 360-degree angle changed based on that particular area not damaged, uniform board thickness was maintained Due to research techniques recommended below 16 mm thickness board not suitable for the leather cutting

https://doi.org/10.24264/icams-2022.III.8

operation, proper light effect, ventilation, waste piece collection bag or tank also allotted in all cutting machines, machines maintained record sheet upgraded in the cutting section (Sarkar, 2005).

Cutting Stroke Record Implementation

The footwear industry nowadays has fast developments in African countries such as Ethiopia, Kenya, Zambia, South Africa, Morocco, and Egypt. etc. India China and Europe have more developed footwear industries and advanced technologies, but upcoming African countries lack technical ethics and technology, and implementation is required for every operation. In this regard, Copperstone University's Leather Department research was analyzed and reduced the leather cutting issues. Implemented the operator cutting stroke efficiency. As per the international SATRA standard operator cutting efficiency per day 2500 Stroke (8 Hours) capacity and lining and other material cutting operator 3200 strokes (8 hours) based on the statement we provided better innovative cutting training and motive prevention techniques.

RESULTS AND DISCUSSION

Vietnam, Bangladesh, India, and China, have more footwear industries, right now some Europe customers give a special focus to African countries, because the African continent has a lot of cattle population and at the same time price wise also very cheap than Asian countries, Zambia having 2.3 million cattle population in African countries, footwear industry very fast movement along with other African countries (Baldacci *et al*., 2014).

Table 1. Monthly Leather Cutting Data

Before implementation in leather cutting					
S.No week wise	Leather Cutting Norms for one pair (S.Ft)	Total Leather Cuttability per day	Total No. of pairs	Total Leather Cutting Consumption S.Ft	Leather Shortage (Extra Norms)
1	2.87	6*1550	9300	26691	3.25%
2	3.83	6*1350	8100	31023	2.86%
3	3.36	6*1425	8550	28728	3.74%
4	3.25	6*1280	7680	24960	4.15%
Total			33630	111402	14%

After implementation in leather cutting					
S.No Week wise	After Cutting Methods Implementation	Total No. of Pair After Implementation	Shortage Norms in S.Ft	Leather Saving Norms (in S.Ft.)	International Leather Cutting Loss Norms (S.Ft) Based On Grade
1	6*1650	9900	1.28%	0	A,B,C grade 1.20%
2	6*1425	8550	0	1.25%	C,D grade 1.5-1.70 %
3	6*1523	9138	0	1.85%	A,B,C grade 1.20 %
4	6*1375	8250	0	2.10%	A,B,C grade 1.20 %
Total	118676	35838			

https://doi.org/10.24264/icams-2022.III.8

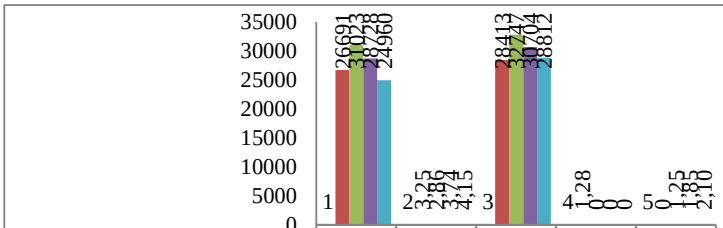

Totel Leather Cutting Consumption in S.Ft	1	2	3	4	5
Total Leather Shortage in S.Ft	26691	3,25	28413	1,28	0
After Implementatio Cutting norms	31023	2,86	32747	0	1,25
After Implement Norms Shortage in %	28728	3,74	30704	0	1,85
After implement Norms Saving in %	24960	4,15	28812	0	2,10

Figure 1. Leather cutting Consumption Norms detail

Based on this valuable estimation prevention training and workers' motivation factors were also improved by this research. After implementing the innovative cutting techniques for existing productivity and after implementing production efficiency, the leather consumption record was recorded and compared The first two-month leather cutting efficiency was evaluated and the final result was better than previous leather cutting consumption values skilled manpower is another important parameter for manufacturing footwear Educated operators, hard-working innovative-minded supervisors, and operators are important to upgrade innovative thoughts (Cipriani, 2002). After one month the same company's (Copper belt Footwears) leather cutting section's total productivity leather consumption, quality of cut components status, and leather cutting waste consumption ratio were gradually reduced by this innovative research and recommendation.

CONCLUSION

This research analyzed and identified the leather components cutting current issues and refers to the quality implementation techniques in each cutting process (Sonobe *et al*., 2007). After this cutting implementation, 2.10% of leather norms were saved, and cutting quality productivity also improved by this cutting implementation methods, incase 1 S.Ft leather 1.50 USD market values based on this research every month average 2492.196 S.Ft leather is saved by cutting department (Cipriani, 2002). So every month footwear company leather cutting section 3738.294 USD per month benefit for the above research. In this way, Zambia's medium sectors footwear company upgraded the innovative cutting techniques and regular productivity with quality standards of leather cutting, and wastage was reduced.

https://doi.org/10.24264/icams-2022.III.8

REFERENCES

Alves, C., Brás, P., de Carvalho, J.V. and Pinto, T. (2012), "New Constructive Algorithms for Leather Nesting in the Automotive Industry", *Computers & Operations Research*, 39(7), 1487-1505, https://doi.org/10.1016/j.cor.2011.08.021.

Baldacci, R., Boschetti, M.A., Ganovelli, M. and Maniezzo, V. (2014), "Algorithms for Nesting with Defects", *Discrete Applied Mathematics*, 163, 17-33, https://doi.org/10.1016/j.dam.2012.03.026.

Brun, A. and Ciccullo, F. (2022), "Factors Affecting Sustainability-Oriented Innovation in the Leather Supply Chain", Strategic Change, 31(3), 305-321, https://doi.org/10.1002/jsc.2500.

Cipriani, S. (2002), "Study of the Quality Control and Management on the African Leather Sector", 2002 African meeting publication.

Elamvazhuthi, I., Kamaruddin, S. and Azmi, M.S. (2009), "Automation of Nesting and Cutting Process of Leather Furniture: A Case Study", *International Journal of Mechanical Engineering*, 9(10), 14-18.

Mesa, J.W., Onyancha, D.O. and Sang Magut, P.K. (2019), "Assessment of the Quality of Leather Footwear for School Children Made by SMEs in Kariokor Kenya", *International Journal of Scientific and Research Publications*, 9(7), https://doi.org/10.29322/IJSRP.9.07.2019.p91118.

Nguyen, V. (2004), "Analysis of the Luxury Goods and Apparel and Footwear Industries", available at https://www.scribd.com/document/207086522/Analysis-of-Luxury-Goods-and-Apparel-and-Footwear-Industries.

Sarkar, K.T. (2005), "Defects of Hiding and Skins", in *Theory and Practice of Leather Manufacture*, Macmillan India Press, Madras, pp. 50-52.

Solomon, B.B. (2021), "Leather Cutting Waste Minimization Techniques in Ethiopian Footwear Industry: Case Study ELICO - Universal Leather Products Industry", https://doi.org/10.21203/rs.3.rs-274284/v1.

Sonobe, T., Akoten, J.E. and Otsuka, K. (2007), "The Development of Leather Footwear Industry in Ethiopia; How Different is it from the Asian Experience?", *Global Development Network Conference*, Beijing China.

https://doi.org/10.24264/icams-2022.III.8

https://doi.org/10.24264/icams-2022.III.8

STUDIES REGARDING STRUCTURAL PROPERTIES OF CHEMICAL INDUSTRY EQUIPMENT

DENIS-ANDREI DRUȘAN[1], ANA-MARIA CIOBANU[1], MĂDĂLINA IGNAT[1], ROXANA CONSTANTINESCU[1], CIPRIAN CHELARU[1], VLAD BĂRBULESCU[1], ANGELA CHELU[2]

[1]*The National Research & Development Institute for Textiles and Leather - Leather and Footwear Research Institute Division, Bucharest, Romania*

[2]*University POLITEHNICA of Bucharest - Faculty of Mechanical Engineering and Mechatronics*

An adequate and optimized equipment plays a very important role in the chemical industry. Due to the way an equipment is designed, it can be subject to certain types of structural deformations. This aim of this study is to show the importance of fortifies openings that are made to connect the pipes with pressure vessels. The development of chemical and petrochemical installations led to the need for continuous research of the vessel's coatings for a better understanding of design of these structures to be operate in maximum safety. The openings contribute to destabilization of structure for a pressure vessel and make it dangerous to use.

Keywords: pressure vessel, stress concentrators, internal pressure.

INTRODUCTION

In mechanical engineering, revolution coatings, as structural elements are in a top position and are used in the construction of equipment, pipelines, etc. Pressure vessels, reactors used in the chemical and petrochemical industries, nuclear reactors, pipelines used in drilling operations, oil and natural gas carrying, are in the category of coatings.

The development of the chemical and petrochemical industries, installations using such equipment has also led to the need for continuous research of the coatings for a deeper understanding of the problems involved in the design of these structures, whose operation must be done in maximum safety. Pressure vessels are part of complex systems and installations. Therefore, openings in their sheaths and pipes required to allow connection to the system to which they belong. All these openings lead to geometric discontinuities in the sheaths and to stress concentrators (Jinescu, 1983). Fittings are technological elements, through which the connection is made for pipes, tubes, or other components/devices of the equipment (Pavel, 1998).

The complex geometry of machine components and structures makes it impossible to use the fundamental formulas of the strength of materials. Existence of section changes, holes, channels, notches and changes in geometric configuration lead to a complex stress distribution (Radeș, 2010) and can occur areas with height local stress, called concentration of mechanical stresses. Stress concentration factor $\mathbf{a}_k$ (formula 1 and formula 2), can be written as:

- in case of tension or bending stresses (for normal stresses):

$$\alpha_\sigma = \frac{\sigma_{max}}{\sigma_{nom}} \quad (1)$$

where

σ_{max} - maximum normal stresses

τ_{max} - maximum tangential stresses

- in case of shear or twisting stresses (for tangential stresses):

$$\alpha_\tau = \frac{\tau_{max}}{\tau_{nom}} \quad (2)$$

https://doi.org/10.24264/icams-2022.III.9

where

σ_{nom} - normal stresses - empirically determined

τ_{nom} - tangential stresses - empirically determined

Geometric discontinuities change the distribution of stresses in their vicinity so that the stress equations are no longer valid. Such discontinuities are also called “stress peaks” and the regions in which they occur are called areas of stress concentrators. In this paper is defined the factor of concentration of stresses at the openings in coatings methods for evaluating its effect. The method of area replacement is to ensure that the reaction force of the material is greater than or equal to the pressure load. According to this method, the stress concentration factor, α_σ, in the joint (Fig. 1) is obtained in the form (Jinescu, 1986):

$$\alpha_\sigma = \frac{2 \cdot B \cdot T}{A \cdot D_m} \tag{3}$$

where

$$\left.\begin{aligned} A &= 0{,}8 \cdot \sqrt{D_m \cdot T} \cdot T + 0{,}8 \cdot \sqrt{d_m \cdot t} \cdot t \\ B &= \left(\frac{d_m}{2} + 0{,}8 \cdot \sqrt{D_m \cdot T}\right) \cdot \frac{D_m}{2} + 0{,}8 \cdot \sqrt{d_m \cdot t} \cdot \frac{d_m}{2} \end{aligned}\right\} \tag{4}$$

Figure 1 – section A - represents the areas of the cross sections subjected to pressure; Figure 1 – section B – represents the cross-sectional area subjected to stress.

where

D_m - average diameter of the cylindrical container;

d_m - average diameter of the connection;

T - wall thickness of the cylindrical container;

t - thickness of the connection wall.

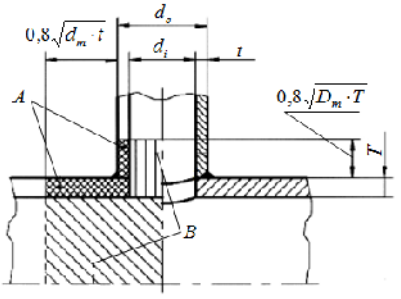

Figure 1. Cylindrical cover with non-penetrating connection

From a practical point of view, there is the problem of attenuating the stress concentration. The strength of the container or fitting cover can be improved by adding material around the hole. This addition of material in the area of influence of the concentration effect is called compensation, strengthening of the holes (Fig. 2) (Jinescu,

https://doi.org/10.24264/icams-2022.III.9

1986). If the coating is provided with several concentrators, it may be more economical to thicken the entire coating instead of local consolidations.

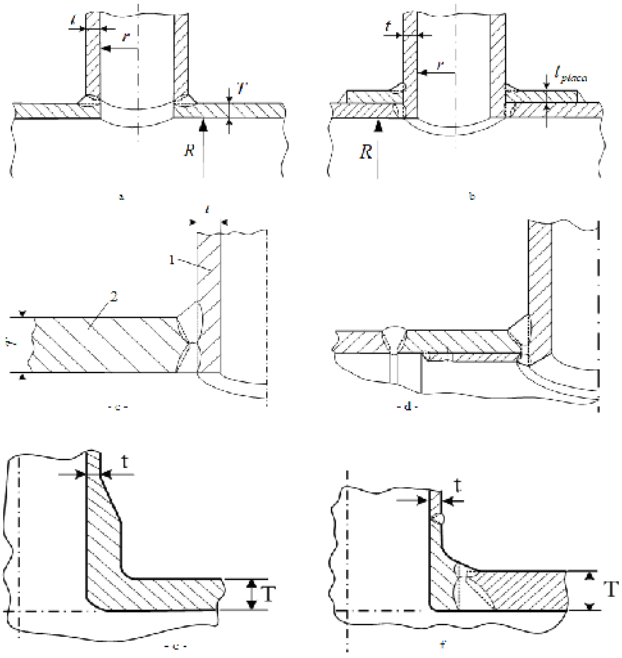

Figure 2. Opening without compensation (a, c); Reinforcement of holes with reinforcement plate (b; d); Consolidation of the holes by thickening the connection (e; f)

EXPERIMENTAL

Determining the maximum diameter of the opening that does not require compensation for the cylindrical body of a column.

The radius of curvature for spherical or cylindrical coatings is obtained as follows:

$$r_{is} = \frac{D_e}{2} \quad e_{a,s} = \frac{D_i}{2} \tag{5}$$

Maximum length of the coating contributing to the strengthening of the opening, measured along the average surface of the coating:

$$l_{so} = \sqrt{(2r_{is} + e_{c,s}) \cdot e_{c,s}} \tag{6}$$

The maximum diameter of an opening without compensation according to SR EN 13445 is given by the relation:

$$d_{max1} = \min\left(0{,}5 \cdot D_i; \frac{e_a \cdot l_{so} \cdot \frac{f - 0{,}5 \cdot P}{P} - r_{is} \cdot l_{so}}{0{,}5 \cdot r_{is} + 0{,}5 \cdot e_a}\right) \tag{7}$$

$$d_{max2} = 0{,}15 \cdot \sqrt{(2r_{is} + e_a) \cdot e_a} \tag{8}$$

$$d_{max} = \max\left(d_{max1}; d_{max2}\right) \tag{9}$$

https://doi.org/10.24264/icams-2022.III.9

RESULTS AND DISCUSSIONS

In a cylindrical shell joined by a domed or hemispherical bottom, with the large base of a conical shell, with a flat bottom or with any type of flange, the distance w, must comply with the condition:

$$w \geq w_{min} = \max\left(0{,}2\sqrt{\left(2r_{is} + e_{c,s}\right) \cdot e_{c,s}};\ 3e_{a,s}\right) \tag{10}$$

$$r_{is} = \frac{D_e}{2} - e_{a,s} = \frac{D_i}{2} = 700\ mm \tag{11}$$

Maximum length of the casing which contributes to the strengthening of the opening, measured along the average surface of the casing:

$$l_{so} = \sqrt{\left(2r_{is} + e_{c,s}\right) \cdot e_{c,s}} = \sqrt{(2 \cdot 700 + 12) \cdot 12} = 130{,}17\ mm \tag{12}$$

$$d_{max1} = \min\left(0{,}5 \cdot 1400;\ \frac{12 \cdot 130{,}17 \cdot \frac{139{,}33 - 0{,}5 \cdot 0{,}12}{0{,}12} - 700 \cdot 130{,}17}{0{,}5 \cdot 700 + 0{,}5 \cdot 12}\right) \tag{13}$$

$$d_{max1} = \min(700; 4836{,}385) = 700\ mm \tag{14}$$

Diameter that does not require compensation:

$$d_{max2} = 0{,}15 \cdot \sqrt{(2 \cdot 700 + 12) \cdot 12} = 19{,}52\ mm \tag{15}$$

Maximum diameter that does not require compensation:

$$d_{max} = \max(700; 19{,}52) = 700\ mm \tag{16}$$

The distance between an opening and a discontinuity of the coating must be:

$$w \geq w_{min} = \max\left(0{,}2\sqrt{(2 \cdot 700 + 12) \cdot 12} = \max\left(26{,}03; 36\right)\right. \tag{17}$$

$$w \geq w_{min} = 36\ mm \tag{18}$$

Calculations show that the openings on the cylindrical body of the column do not require compensation. The check ports and two other connections will be compensated with a reinforcing ring because they have large stress concentrators.

CONCLUSIONS

The traditional way to compensate for an opening or connection is to “thicken” material close to the opening, in addition to the minimum required thickness of the coating.

Important disadvantages of the compensation method:

- does not provide information on the stresses in the casing and connection.
- the method cannot be extended to situations where we have additional loads other than internal pressure.

The advantage of the method is that of its simplicity of application.

https://doi.org/10.24264/icams-2022.III.9

REFERENCES

Budynas, R.G. and Nisbett, J.K. (2006), *Shigley's Mechanical Engineering Design*, McGraw−Hill.
Jinescu, V.V. (1983), *Calculation and Construction of Chemical, Petrochemical and Refinery Equipment* (in Romanian), vol. 1, Didactical and Pedagogical Press, Bucharest.
Jinescu, V.V. (1986), *Technological Equipment for Process Industries* (in Romanian), vol. 3, Technical Press, Bucharest.
Pavel, A. (1998), *Tubular Junctions (Connections and Tees)* (in Romanian), Briliant, Bucharest.
Peterson, R.E. (1974), *Stress Concentration Factor*, Wiley.
Pilkey, W.D. and Pilkey, D.F. (2008), *Peterson's Stress Concentration Factors*, John Wiley&Sons, Inc., https://doi.org/10.1002/9780470211106.
Radeş, M. (2010), *Material Resistance* (in Romanian), vol. 1, Printech, Bucharest.
Vullo, V. (2014), *Circular Cylinder and Pressure Vessels; Stress Analysis and Design*, Springer, https://doi.org/10.1007/978-3-319-00690-1_11.
Young, W.C. and Budynas, R.G. (2002), *Roark's Formulas for Stress and Strain*, McGraw−Hill.
*** (2014), European Standard, "Unfired Pressure Vessels – Part 3: Design", SR EN 13445-3.

https://doi.org/10.24264/icams-2022.III.9

https://doi.org/10.24264/icams-2022.III.9

NEW APPROACHES TO THE TREATMENT OF DRUG-RESISTANT BACTERIA

NIZAMI DURAN

Mustafa Kemal University, Medical Faculty, Microbiology Department, Hatay-Türkiye, nizamduran@hotmail.com

Today, the treatment of infectious diseases is getting more difficult every day due to increasing drug resistance against microorganisms. In order to overcome the increasing drug resistance globally, a wide variety of studies are carried out on probiotic microorganisms. In this study, we aimed to investigate the synergistic activities of the bioactive components of *L. casei* and *S. thermophilus* probiotic microorganisms against ESBL-positive *E. coli* and *K. pneumoniae* strains against these two microorganisms. The non-toxic concentrations of *L. casei* and *S. thermophilus* bioactive components in Vero cell culture were determined. Antibacterial activities against ESBL-positive *E. coli* and *K. pneumoniae* at determined non-toxic concentrations were evaluated by studying MIC and MBC concentrations. Firstly, non-cytotoxic concentrations of bioactive metabolites of *S. thermophilus* and *L. casei* were determined on Vero cells. It has been determined that the bioactive metabolites of both *S. thermophilus* and *L. casei* cause toxicity of <32 µg/ml. For this reason, studies have been studied at levels lower than this concentration for antimicrobial efficacy studies. Antimicrobial activities of *L. casei* and *S. thermophilus* alone and in combination against *E. coli* were given. Here, it was determined that the activities of probiotic microorganisms created a synergistic effect when used in combination. It was determined that the activities of *L. casei* and *S. thermophilus*, when used in combination, had a synergistic effect against *K. pneumoniae*. In this study, where we aimed to produce a new and effective drug/solution in the treatment of wounds infected with drug-resistant bacteria (*E. coli* and *K. pneumoniae*), which are very difficult to treat, our findings may be hopeful.

Keywords: drug, resistance, probiotic bacteria

INTRODUCTION

Today, probiotics are recommended as suitable alternatives to antibiotics for treating diseases (Hossain and Sadekuzzaman, 2017). Probiotics are live microorganisms that can show beneficial effects after ingestion by the host (Araya *et al*., 2002). Various studies in recent years have shown that oral or topical use of bacterial probiotics can be effective in the treatment of skin disorders (Yeşilova *et al*., 2012; Argenta *et al*., 2016; Sekhar *et al*., 2014; Drago *et al*., 2011; Nole *et al*., 2014).

It has been reported in a study that local application of *Streptococcus thermophilus* to the skin can increase the ceramide level of the skin in the epidermis and may be useful in the treatment of atopic dermatitis (Di Marzio *et al*., 2003). It has also been shown that the use of topical ceramide on its own can accelerate the wound-healing process (Tsuchiya *et al*., 2013).

Previous studies have reported that some lactic acid bacteria have antagonistic activities against microorganisms that contribute to wound infections, such as Staphylococcus aureus (Besser *et al*., 2019). Although the efficacy of probiotics in wound treatment has been investigated in various studies, the combined efficacy of the bioactive components of Lactobacilli and streptococci and these bioactive components against ESBL-producing *E. coli* and *K. pneumonia* have not been studied. The most serious problem in *E. coli* and *K. pneumoniae* is drug resistance; these microorganisms secrete broad-spectrum beta-lactamase enzyme. There are severe difficulties in the treatment of infections of these two ESBL-producing microorganisms. Our main aim in

https://doi.org/10.24264/icams-2022.III.10

this study is to develop an effective formulation/drug against ESBL-producing *E. coli* and *K. pneumoniae*.

MICROORGANISMS

Probiotic Microorganisms

Lactobacillus casei, *Streptococcus thermophilus*, EBSL positive *Escherichia coli*, ESBL-positive *Klebsiella pneumonia*.

Probiotic Microorganisms

In the study, *L. casei* and *S. thermophilus* strains were removed from -80 ºC, dissolved in a 37 ºC water bath, then disbanded in Tryptic Soy Broth (TSB) medium and incubated in an incubator with 5% carbon dioxide for 48 hours. At the end of the incubation, 100 µl of bacterial strains were taken and passaged into Mueller-Hinton agar. At the 24th hour of incubation following the passage, bacterial strain verification was performed from the colonies with the help of Gram staining and biochemical tests. Confirmation of the species determination was carried out with biochemical tests and an automated culture system.

Bioactive Metabolites

Probiotic microorganisms were inoculated from a pure culture sample with the help of a loop into a 500 ml TSB medium. The inoculated TSB culture dishes that were not tightly closed were incubated in a 5% CO_2 incubator. At the end of the incubation, the samples taken into 50 ml glass centrifuge tubes were centrifuged at 4000 rpm for 20 minutes and the supernatants were collected. After centrifugation, the collected supernatants were filtered with membrane filters.

Bacterial Culture: ESBL-producing *E. coli* and *K. pneumoniae* Strains

Cultivation of strains was performed on Eosin Methylene Blue (EMB) medium, antimicrobial tests were performed on Müeller-Hinton broth and Mueller-Hinton agar medium. Cultivations were carried out at 37 °C for 24 hours. Microorganisms were identified with Gram stain, conventional biochemical tests, and automated culture systems when needed.

A healthy cell line (Vero cell line) was used for the detection of non-toxic concentrations of bioactive metabolites of probiotic microorganisms. The vero cell line was obtained from the culture collection of Hatay Mustafa Kemal University Microbiology Cell Culture Laboratory. Stock cultures were taken from the deep freeze and thawed in a water bath pre-warmed to 37 ºC. Then, the cells were incubated in a cell culture medium containing 10% fetal calf serum and antibiotics in a 5% CO_2 incubator at 37 °C, and their cultivation was carried out.

Cell Culture

Evaluations of the cultured cells were carried out daily with an inverted microscope, after the cells covered the surface of the culture dish at a rate of 70-80%, the cells were removed from the surface of the culture dish with trypsinization solution and passaged

https://doi.org/10.24264/icams-2022.III.10

into different culture dishes. For this purpose, the medium in the culture dishes was removed, and the debris was removed by washing the cells with PBS at least twice before the trypsinization solution was added.

After this process, 0.25% trypsinization solution was added to the culture dishes and incubated at 37 ºC for 10 minutes to remove the cells attached to the culture dish surface. The cells were then collected by centrifugation at 1500 rpm for 10 minutes. Then, the cell pellet to be resuspended in RPMI-1640 medium was counted and the cell density was adjusted to $1x10^6$ cells.

Determination of Bioactive Metabolite Doseages

Flat-bottomed 96-well microplates were used to determine the non-toxic doses of bioactive metabolites obtained from *L. casei* and *S. thermophilus* bacteria. Different concentrations of bioactive metabolites were studied.

The bioactive components at these concentrations were added to the media of Vero cells and the cells were incubated under the same conditions. Cytotoxic/non-cytotoxic concentrations of bioactive components were determined by MTT (3-(4,5-Dimethylthiazol-2-yl)-2,5-diphenyltetrazolium bromide) analysis method after the cells were incubated for 24 hours.

MTT [3-(4,5-Dimethylthiazol-2-yl)-2,5-diphenyltetrazolium bromide] Method

The cytotoxic concentrations of these bioactive metabolites on healthy cells were determined by the MTT method, which is a calorimetric and quantitative method. The MTT test was performed in flat-bottomed 96-well plates by adjusting the cell density to $1x10^6$ cells/ml (Mossman, 1983).

It was incubated for 6 hours for the adhesion of cells to the bottom of the plate (at 37 °C and 5% CO_2). Thus, the metabolic activity of the incubated cells was achieved to reach high levels. During this time, serial dilutions of the biologically active components were prepared (from 1025 µl/ml to 1 µl/ml concentration) and added to 4 wells from each dilution on the adherent cells. At least four wells were determined as cell control and medium control groups.

To determine the effect of bioactive metabolites on cells, the cells were incubated for 24 hours at 37 °C in an incubator with 5% carbon dioxide. At the end of the incubation, 10 µl of MTT was added to each well and the plates were incubated for 4 hours under the same growth conditions.

Absorbance measurements were performed at 570 nm with a spectrophotometer. Proliferation was expressed as the ratio of cells in wells treated with bioactive metabolites to control cells and IC_{50} values were calculated using the SPSS program (SPSS. Inc, Chicago).

Detection of MIC (Minimum Inhibitory Concentration) and MBC (Minimal Bactericidal Concentration)

MIC (minimum inhibitory concentration) values of probiotic microorganism bioactive components against *E. coli* and *Klebsiella pneumonia* were determined by the microdilution method. The concentration in which the growth turbidity was not detected visually was accepted as the MIC value.

In addition, 10 µl Mueller-Hinton agar was inoculated from the last dilution in which growth turbidity was observed and all subsequent dilutions were incubated at 37

https://doi.org/10.24264/icams-2022.III.10

°C for 24 hours. The dilution concentration that inhibited bacterial growth by 99% was determined as MBK (minimal Bactericidal Concentration). All experiments were repeated three times.

RESULTS

Firstly, non-cytotoxic concentrations of bioactive metabolites of *S. thermophilus* and *L. casei* on Vero cells were determined. It was determined that the bioactive metabolites of both *S. thermophilus* and *L. casei* caused toxicity at the level of 16 µg/ml. For this reason, studies were carried out at levels lower than this concentration (16 µg/ml) for antimicrobial efficacy studies (Figures 1 and 2).

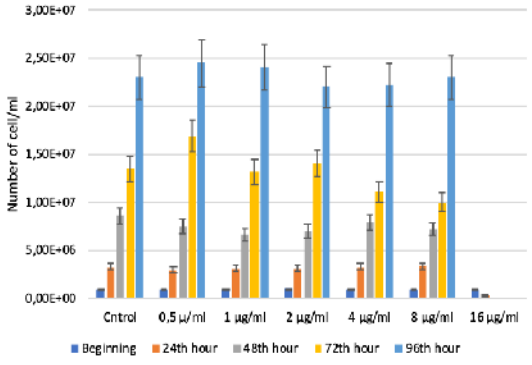

Figure 1. Non-toxic concentrations of bioactive metabolites of *S. thermophilus* on Vero cells

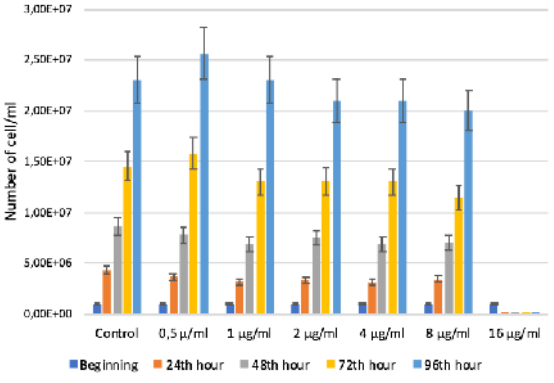

Figure 2. Non-toxic concentrations of bioactive metabolites of *L. casei* in Vero cell line

https://doi.org/10.24264/icams-2022.III.10

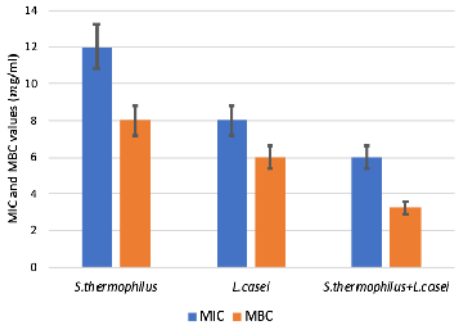

Figure 3. Synergistic activity of *L. casei* and *S. thermophilus* against *E. coli*

Figure 3 shows the antimicrobial activities of single and combined uses of *L. casei* and *S. thermophilus* against *E. coli*. Here, it was determined that the activities of probiotic microorganisms create a synergistic effect when used in combination (Figure 3).

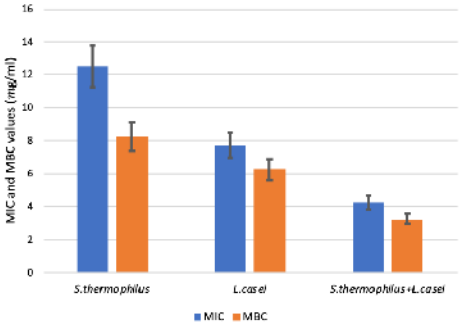

Figure 4. Synergistic activity of *L. casei* and *S. thermophilus* against *K. pneumoniae*

As in Figure 3, MIC and MBC values of single and combined uses of *L. casei* and *S. thermophilus* against *K. pneumonia* are given in Figure 4. As seen from the figure, it has been determined that the activities of both *L. casei* and *S. thermophilus*, when used together, have a synergistic effect against *K. pneumoniae* (Figure 4).

DISCUSSION

Broad-spectrum beta-lactamases (ESBL) were first identified in the 1980s and detected in *Klebsiella* species and later in *E. coli* and other genera of the *Enterobacteriaceae* family. Antibiotic resistance is a global problem that affects the whole world due to the widespread and incorrect use of antibiotics in the world.

As a result of beta-lactamase, enzyme production is one of the most important resistance mechanisms among *Enterobacteriaceae* members such as *E. coli* and *K. pneumoniae*, which inactivate beta-lactam group drugs by breaking down. To date, hundreds of beta-lactamase enzymes have been identified. It has been reported that nearly half of these enzymes are extended-spectrum beta-lactamases (ESBL, extended-spectrum beta-lactamases).

https://doi.org/10.24264/icams-2022.III.10

ESBLs can be easily transferred between plasmids and bacteria from one bacteria to another. ESBL production in bacteria leads to resistance to cephalosporins and aztreonam. ESBL production, especially seen in Enterobacteriaceae members such as *Klebsiella pneumonia* and *Escherichia coli*, and the easy spread of these enzyme genes to other species have become a serious health problem both in our country and in the world.

Infectious agents created by ESBL-positive strains require a long stay in intensive care units, resulting in serious morbidity and mortality. These microorganisms are among the most important hospital infection agents worldwide and may cause problems in treatment due to multiple antibiotic resistance (Kaftandzieva *et al*., 2014).

CONCLUSION

In the present study, we showed that probiotic microorganism metabolites can be beneficial in overcoming bacterial resistance against ESBL strains, which is one of the most crucial resistance problems in bacteria. We think that when these results are supported by advanced studies, they can be an important alternative solution for a serious problem for the whole world.

REFERENCES

Araya, M., Morelli, L., Reid, G., Sanders, M., Stanton, C. and Pineiro, M. (2002), *Joint FAO/WHO Working Group Report on Drafting Guidelines for the Evaluation of Probiotics in Food*, London, Canada: World Health Organization, Food, and Agriculture Organization of the United Nations.

Argenta, A., Satish, L., Gallo, P., Liu, F. and Kathju, S. (2016), "Local Application of Probiotic Bacteria Prophylaxes against Sepsis and Death Resulting from Burn Wound Infection", *PloS one*, 11(10), e0165294, https://doi.org/10.1371/journal.pone.0165294.

Besser, M., Terberger, J., Weber, L., Ghebremedhin, B., Naumova, E.A. and Arnold, W.H. (2019), "Impact of Probiotics on Pathogen Survival in an Innovative Human Plasma Biofilm Model (*hp*BIOM)", *Journal of Translational Medicine*, 17(1), 243, https://doi.org/10.1186/s12967-019-1990-4.

Di Marzio, L., Cinque, B., Cupelli, F., De Simone, C., Cifone, M.G. and Giuliani M. (2008), "Increase of skin-ceramide levels in aged subjects following a short-term topical application of bacterial sphingomyelinase from Streptococcus thermophilus", *International Journal of Immunopathology and Pharmacology*, 21, 137-143, https://doi.org/10.1177/039463200802100115.

Drago, L., Iemoli, E., Rodighiero, V., Nicola, L., De Vecchi, E. and Piconi, S. (2011), "Effects of *Lactobacillus salivarius* LS01 (DSM 22775) Treatment on Adult Atopic Dermatitis: A Randomized Placebo-Controlled Study", *International Journal of Immunopathology and Pharmacology*, 24(4), 1037-1048, https://doi.org/10.1177/039463201102400421.

Hossain, M.I., Sadekuzzaman, M. and Ha, S.D. (2017), "Probiotics as Potential Alternative Biocontrol Agents in the Agriculture and Food Industries: A Review", *Food Research International*, 100(1), 63-73, https://doi.org/10.1016/j.foodres.2017.07.077.

Kaftandzieva, A., Trajkovska-Dokic, E., Kotevska, V., Cekovska, Z. and Jankoska, G. (2014), "Genotypes of ESBL Producing *Escherichia coli* and *Klebsiella pneumoniae* about Resistance to Antimicrobial Drugs", *Prilozi*, 35(2), 31-38, https://doi.org/10.2478/prilozi-2014-0004.

Mosmann, T. (1983), "Rapid Colorimetric Assay for Cellular Growth and Survival: Application to Proliferation and Cytotoxicity Assays", *Journal of Immunological Methods*, 65, 55-63, https://doi.org/10.1016/0022-1759(83)90303-4.

Nole, K.L.B., Yim, E. and Keri, J.E. (2014), "Probiotics and Prebiotics in Dermatology", *Journal of the American Academy of Dermatology*, 71(4), 814-821, https://doi.org/10.1016/j.jaad.2014.04.050.

Sekhar, M.S., Unnikrishnan, M., Vijayanarayana, K., Rodrigues, G.S. and Mukhopadhyay, C. (2014), "Topical Application/Formulation of Probiotics: Will It Be a Novel Treatment Approach for Diabetic Foot Ulcer?", *Medical Hypotheses*, 82(1), 86-88, https://doi.org/10.1016/j.mehy.2013.11.013.

Tsuchiya, S., Ichioka, S., Sekiya, N., Tajima, S., Iwasaki, T. and Numata, S. (2013), "The Effect of a Hydrocolloid Dressing Containing Ceramide-2 on Split-Thickness Wounds in a Laser-Induced Erosion Model", *Advances in Skin and Wound Care*, 26(5), 224-229, https://doi.org/10.1097/01.ASW.0000428952.00149.77.

Yeşilova, Y., Çalka, Ö., Akdeniz, N. and Berktaş, M. (2012), "Effect of Probiotics on the Treatment of Children with Atopic Dermatitis", *Annals of Dermatology*, 24(2), 189-193, https://doi.org/10.5021/ad.2012.24.2.189.

https://doi.org/10.24264/icams-2022.III.10

NEW FORMULATION EFFECTIVE AGAINST SARS CoV-2 AND H1N1

NIZAMI DURAN

Mustafa Kemal University, Medical Faculty, Microbiology Department, Hatay-Türkiye, nizamduran@hotmail.com

People apply a wide variety of over-the-counter treatments as food supplements against respiratory tract infections. In this study, we investigated the antiviral efficacy of piperine, capsaicin, and glycyrrhetinic acid (GA) against coronaviruses (SARS-CoV-2) and Influenza viruses (H1N1), which are associated with acute respiratory infections. TCID50 concentrations of SARS-CoV-2 and H1N1 isolates were determined. Then, the effectiveness of phytochemicals against these viral isolates at non-toxic concentrations was investigated. For this purpose, the MTT method and RT-PCR techniques were used. Non-toxic concentrations of Capsaicin, Piperine, and GA on Vero cells were determined as 0.625 µg/ml, and Ceramide at 1.25 µg/ml and lower concentrations. It was determined that Capsaicin and Piperine showed very significant antiviral activity against SARS CoV-2 when compared to standard drugs at concentrations of 0.312 µg/ml. The effectiveness of GA was determined to be lower (0.625 µg/ml) than these two phytochemicals. Capsaicin, piperine, and GA exhibited antiviral activity on SARS-CoV-2 and H1N1 viral replication, especially the activity of the combination of capsaicin plus piperine against SARS CoV-2 was stronger than the activity against N1N1 than against H1N1. In addition, it was determined that the triple combination of these components exhibited stronger antiviral activity than single and double combinations, resulting in a significant decrease in the number of viral copies. We think that this new formulation containing three different phytochemical compounds is effective against SARS-CoV-2 and influenza viruses, which are the most important causes of morbidity and mortality from respiratory tract viruses, and can be effective, especially for prophylactic purposes.

Keywords: SARS CoV-2, phytochemicals, influenza virus.

INTRODUCTION

Piperine is a phytochemical found in the fruits and roots of plants such as *Piper nigrum* L. and *Piper longum*. It has very rich pharmacological activities such as antimicrobial, anti-inflammatory, immunosuppressive, anti-cancer, neuroprotective, and antioxidant effects (Derosa *et al*., 2016; Haq *et al*., 2021; Imran *et al*., 2022).

Capsaicin is a compound found in chili peppers that has burning and irritating properties. Capsaicin is the phenolic responsible for hot peppers' characteristic taste and pungency (8-methyl-N-vanillyl-6-none amid). Capsaicin (N-vanillyl-8-methyl-6-(E)-none amide) is a unique and important compound from the group component of capsaicinoids. This component is found only in plants of the genus Capsicum (Srinivasan, 2016; Wang *et al*., 2022).

It is the primary source of chili pepper's pungency or bitterness. Traditionally, capsaicin has been used to relieve pain. Recently, some studies have shown that capsaicin has important therapeutic effects on many diseases such as diabetes, hypertension, cancer, and obesity (Wang *et al*., 2022).

The use of natural products is increasing due to their low toxicity on healthy cells, and natural products have been used frequently in research against many infectious agents all over the world (Rodrigues *et al*., 2016).

One of the natural products used in folk medicine for many years is the licorice root plant. Licorice root has been used to relieve stomach ailments due to its widespread pharmacological effects. One of licorice root's most important active components (Glycyrrhiza glabra) is Glycyrrhetinic acid. Glycyrrhetinic acid is a hydrolytic product of Glycyrrhizic acid, a component of licorice root. Glycyrrhetinic acid is a compound

https://doi.org/10.24264/icams-2022.III.11

obtained from licorice root extract and is a bioactive triterpene glycoside with anti-inflammatory, anti-ulcer, anti-allergic, antidote, anti-oxidant, anti-tumor, and antiviral and anti-bacterial activity (Pastorino *et al*., 2018).

Influenza viruses and coronaviruses, which have an important place in respiratory tract viruses, are important respiratory tract pathogens causing morbidity and mortality in every flu season due to the rapidity of viral replication and easy transmission. These viruses have created endemics and pandemics throughout human history. Humanity has experienced a SARS-CoV-2 pandemic, whose impact is still felt, and has been exposed to similar or even more serious pandemic and endemic influenza epidemics (Kim *et al*., 2018).

The SARS-CoV-2 pandemic is an important viral agent with very serious consequences all over the world. Although there are many drug studies today, the search for a wide variety of active molecules continues to prevent mucosal transmission against SASR CoV-2 and other respiratory pathogens due to the lack of an effective molecule and insufficient protection of vaccines (Kirtipal *et al*., 2020).

In this study, we investigated the antiviral effectiveness of a new formulation containing various phytochemicals against SARS CoV-2 and H1N1.

MATERIALS AND METHODS

Cell Culture Studies

The Vero cell line was used as cell culture in the present study. Cell cultures were incubated in RPMI-1640 broth containing 10% fetal calf serum, 10 mM HEPES, 100 IU/ml penicillin/streptomycin with 4mM glutamine, in an incubator with 5% carbon dioxide at 37 °C. The cultivation of cells was adjusted to $1x10^5$ cells per ml. Cell culture studies were carried out in 100, 200, and 500 ml culture dishes, in containers containing 10 percent of the culture vessel.

Cell cultures were incubated by waiting until cell growth covered the culture dish surface.

During this period, the medium was changed when a change in the pH of the medium was observed. Cells were removed from the culture dish surface with 0.25% trypsinization solution and incubated at 1250 rpm for 10 min. collected by centrifugation. Cell viability and number were determined by hemocytometer after staining with 1% trypan blue dye prepared in 0.9% NaCl.

Proliferation Assays

Proliferation experiments in cell culture were performed in 96-well flat-bottomed microplates. Cells were inoculated into the wells with RPMI-1640 medium containing 10% fetal calf serum, with $1x10^5$ cells per ml.

ACTIVITY STUDIES

Preparation of Cell Cultures

Firstly, non-toxic concentrations of compounds (piperine, capsaicin, and glycyrrhetinic acid) were determined in Vero cell cultures. For this purpose, the concentrations of the compounds containing different concentrations were added to the

https://doi.org/10.24264/icams-2022.III.11

medium and their non-toxic concentrations on the cells were determined. Dimethyl sulfoxide (DMSO) was used to dissolve chemical compounds. Effects on cell growth were performed by evaluating both morphologically and in terms of cell viability with an inverted microscope. Antiviral activity studies were performed on non-toxic concentrations to be determined.

In cytotoxicity tests, cell density was set to $1x10^5$ cells/ml. After the cells were inoculated into the culture dishes, they were incubated for 6 hours for the cells to adhere to the culture dish surface, then the chemical compounds were added to the cells. Cultures containing only the amount of DMSO used as the solvent were selected as the control group. In addition, cultures without chemicals were evaluated as a negative control. All experiments were performed in triplicate and repeated 3 times.

DETECTION OF SARS COV-2 AND H1N1 BY SYBR GREEN RT-PCR METHOD

The activity of the compounds against SARS CoV-2 was determined by RT-PCR demonstration of viral replication in Vero cells treated with these three compounds. For this purpose, viral RNA isolations were performed by taking 300 ml of culture filtrates treated with compounds. For this, a commercially available viral RNA isolation kit was used. Subsequently, viral copy numbers were determined using primers specific for SARS-CoV-2.

(hCOVassay1 primer: Forward: 5'GCCTCTTCTCGTTCCTCATCAC 3'Reverse: 5'AGCAGCATCACCGCCATTG 3', hCOVassay2 primer: Forward: 5' AGCCTCTTCTCGTTCCTCATCAC 3' Reverse: 5' CCGCCATTGCCAGCCATTC 3'). For viral copy number determination, 500 ng, 100 ng, and 50 ng dilutions of the SARS-CoV-2 genome were made and the viral load in each sample was determined in terms of copy number (Marinowic *et al*., 2021).

The replication level of H1N1 was determined according to the method described by (Yang *et al*., 2009).

3-(4,5-DIMETHYLTHIAZOL-2-YL)-2,5-DIPHENYLTETRAZOLIUM BROMIDE (MTT) METHOD

The MTT method is a frequently used practical method for determining cell viability. MTT is a substance actively absorbed into cells and is reduced to colored, water-insoluble formazan by a mitochondrial-dependent reaction (Mosmann *et al*., 1983). The MTT-reducing property of cells is considered a measure of cell viability. The dye density obtained as a result of MTT analysis correlates with the number of viable cells. In the MTT method, the decrease in cell viability following viral inoculation was evaluated in favor of viral replication, while high cell viability was evaluated as an antiviral effect.

In the study, the highest dosage of chemical compounds determined as non-toxic was used in antiviral effectiveness tests. After adding the compounds to the cultures inoculated with SARS CoV-2, they were incubated for 96 hours at 37°C in a 5% carbon dioxide incubator. Then, 10 µl of MTT was added to each well and the plates were incubated for 4 hours under the same conditions, and absorbance measurements were made at a 570 nm spectrophotometer.

https://doi.org/10.24264/icams-2022.III.11

Titrating the Virus Strains

Viral strains extracted from -80 ºC were rapidly thawed in a double boiler at 37 ºC and then incubated in cell lines for 96 hours. Then, the viral culture vessel was freeze-thawed and the cells were blasted. The cells were collected from the culture dish and centrifuged at 4000 rpm for 20 minutes and the supernatant was collected as a virus solution.

Then, the virus suspension was infected with Vero cells in 96-well flat-bottom microplates, and the infectious dose calculation was performed as stated in the literature. Vero cells were produced by inoculating ($1x10^5$ cells/ml) into 96-well microplates. When cell growth covered the surface of the wells, the medium was taken from each well and 50 µl of 10-fold diluted stock virus solution (from $10^{-1}$to 10^{-6}), prepared in Serum-free RPMI-1640 medium, was added to the cells. For viral adsorption, after incubation for 2 hours at 37 ºC, 50 µl of the medium was added to each well and incubated for 7 days. At the end of the incubation, viral dilutions were examined for the presence of CPE and noted. Viral titer was calculated by Reed and Muench method.

All experiments were performed independently of each other in triplicate (Reed and Muench, 1938; Allahverdiyev *et al*., 2004).

RESULTS

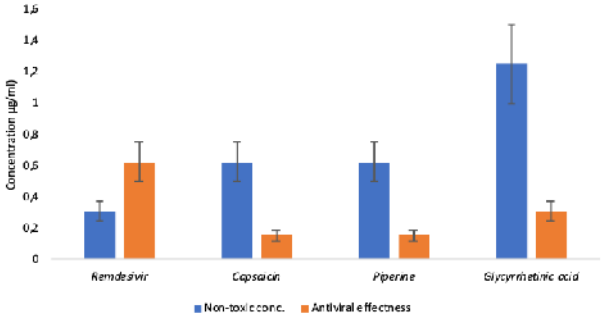

Figure 1. Concentrations of non-toxic and antiviral activity of Capsaicin, Piperine, and glycyrrhetinic acid against SARS CoV-2

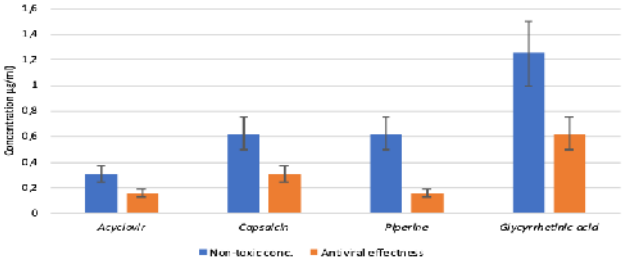

Figure 2. Concentrations of non-toxic and antiviral activity of Capsaicin, Piperine, and glycyrrhetinic acid against H1N1

https://doi.org/10.24264/icams-2022.III.11

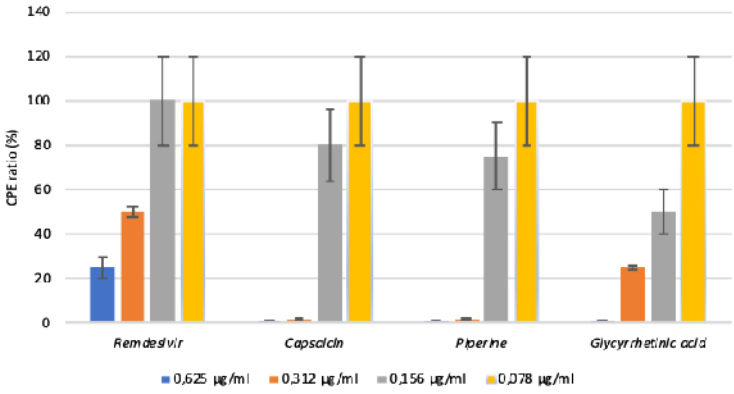

Figure 3. Evaluation of the efficacy of Capsaicin, Piperine and Glycyrrhetinic acid on SARS CoV-2 in terms of the presence of CPE

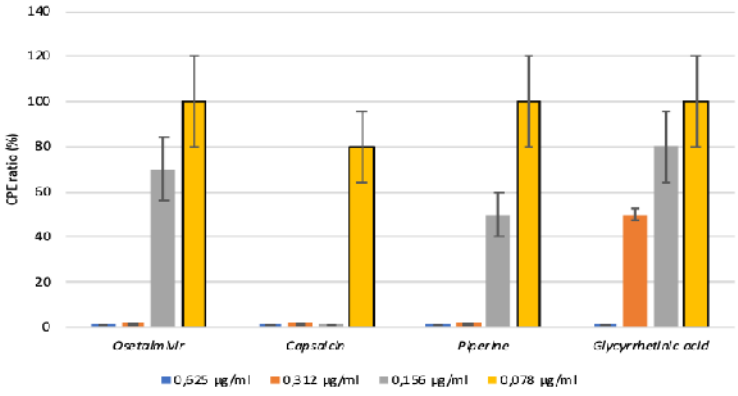

Figure 4. Evaluation of the efficacy of Capsaicin, Piperine and Glycyrrhetinic acid on H1N1 in terms of the presence of CPE

Non-toxic concentrations of Capsaicin, Piperine, and GA on Vero cells were determined as 0.625 µg/ml and 0.625 µg/ml 1.25 µg/ml, respectively. It was determined that Capsaicin and Piperine showed very significant antiviral activity against SARS CoV-2 when compared to standard drugs at concentrations of 0.312 µg/ml. The effectiveness of GA was determined to be lower (0.625 µg/ml) than these two phytochemicals.

In the study, capsaicin, piperine, and GA exhibited antiviral activity on SARS CoV-2 and H1N1 viral replication, especially the activity of the combination of capsaicin plus piperine against SARS CoV-2 was stronger than the activity against N1N1 than against H1N1. In addition, it was determined that the triple combination of these components (capsaicin, piperine, and GA) exhibited stronger antiviral activity than single and double combinations, resulting in a significant decrease in the number of viral copies.

https://doi.org/10.24264/icams-2022.III.11

CONCLUSION

Capsaicin, piperine, and GA are important plant phytochemicals. These phytochemicals were found to be particularly effective against respiratory viral agents. Important respiratory pathogens such as coronaviruses and influenza viruses are viruses with a broad host spectrum that can mutate frequently. Over the years, such viral agents can lead to severe epidemics with endemics and pandemics for humans. Our study findings show that these phytochemicals, effective against these pathogens, can be used both for synthesizing new drugs and prophylaxis during epidemics in winter.

REFERENCES

Allahverdiyev, A., Duran, N., Ozguven, M. and Koltas, S. (2004), "Antiviral Activity of the Volatile Oils of *Melissa officinalis* L. against *Herpes simplex* Virus Type-2", *Phytomedicine*, 11(7-8), 657-661, https://doi.org/10.1016/j.phymed.2003.07.014.

Derosa, G., Maffioli, P. and Sahebkar, A. (2016), "Piperine and Its Role in Chronic Diseases", *Advances in Experimental Medicine and Biology Series*, 928, 173-184, https://doi.org/10.1007/978-3-319-41334-1_8.

Haq, I.U., Imran, M., Nadeem, M., Tufail, T., Gondal, T.A. and Mubarak, M.S. (2021), "Piperine: A Review of Its Biological Effects", *Phytotherapy Research*, 35(2), 680-700, https://doi.org/10.1002/ptr.6855.

Imran, M., Samal, M., Qadir, A., Ali, A. and Mir, S.R. (2022), "A Critical Review on the Extraction and Pharmacotherapeutic Activity of Piperine, *Polymers in Medicine*, 52(1), 29-34, https://doi.org/10.17219/pim/145512.

Kim, H., Webster, R.G. and Webby, R.J. (2018), "Influenza Virus: Dealing with a Drifting and Shifting Pathogen", *Viral Immunology*, 31(2), 174-183, https://doi.org/10.1089/vim.2017.0141.

Kirtipal, N., Bharadwaj, S. and Kang, S.G. (2020), "From SARS to SARS-CoV-2, Insights on Structure, Pathogenicity, and Immunity Aspects of Pandemic Human Coronaviruses", *Infection, Genetics and Evolution*, 85, 104502, https://doi.org/10.1016/j.meegid.2020.104502.

Marinowic, D.R., Zanirati, G. and Rodrigues, F.F.V. (2021), "A New SYBR Green Real-Time PCR to Detect SARS-CoV-2", *Scientific Reports*, 11, 2224, https://doi.org/10.1038/s41598-021-81245-0.

Mosmann, T. (1983), "Rapid Colorimetric Assay for Cellular Growth and Survival: Application to Proliferation and Cytotoxicity Assays", *Journal of Immunological Methods*, 65, 55-63, https://doi.org/10.1016/0022-1759(83)90303-4.

Pastorino, G., Cornara, L., Soares, S., Rodrigues, F. and Oliveira, M.B.P.P. (2018), "Licorice (*Glycyrrhiza glabra*): A Phytochemical and Pharmacological Review", *Phytotherapy Research*, 32(12), 2323-2339, https://doi.org/10.1002/ptr.6178.

Reed, L.J. and Muench, H. (1938), "A Simple Method of Estimating Fifty Percent Endpoints", *American Journal of Epidemiology*, 27, 493-497, https://doi.org/10.1093/oxfordjournals.aje.a118408.

Srinivasan, K. (2016), "Biological Activities of Red Pepper (*Capsicum annuum*) and Its Pungent Principle Capsaicin: A Review", *Critical Reviews in Food Science and Nutrition*, 56(9), 1488-500, https://doi.org/10.1080/10408398.2013.772090.

Wang, F., Xue, Y., Fu, L., Wang, Y., He, M., Zhao, L. and Liao, X. (2022), "Extraction, Purification, Bioactivity and Pharmacological Effects of Capsaicin: A Review", *Critical Reviews in Food Science and Nutrition*, 62(19), 5322-5348, https://doi.org/10.1080/10408398.2021.1884840.

Yang, J.R., Lo, J., Liu, J.L., Lin, C.H., Ho, Y.L., Chen, C.J., Wu, H.S. and Liu, M.T. (2009), "Rapid SYBR Green I and Modified Probe Real-Time Reverse Transcription-PCR Assays Identify Influenza H1N1 Viruses and Distinguish between Pandemic and Seasonal Strains", *Journal of Clinical Microbiology*, 47(11), 3714-3716, https://doi.org/10.1128/JCM.01646-09.

https://doi.org/10.24264/icams-2022.III.11

INVESTIGATION OF THE PROCESS OF SOAKING WHEN PROCESSING OSTRICH SKINS

ILYOS ISMATULLAEV[1], JURABEK ULUGMURATOV[1], AVAZ KENJAEV[1], KHASHIM BEGALIEV[1], FAZLI AKYÜZ[2]

[1]*Tashkent Institute of Textile and Light Industry, Tashkent, 100100, Uzbekistan, begaliev1961@inbox.ru*

[2]*Istanbul University Cerrahpasa, Vocational School of Technical Science, Textile, Clothing, Shoes and Leather, Leather Technology Department, Leather Technology, Buyukcekmece, İstanbul, 34500, Turkey, fazli.akyuz@iuc.edu.tr*

In this work, the results of a study of the process of soaking in the processing of exotic leather raw materials of ostrich skins were carried out. In order to reduce the negative impact of wastewater from the tanning industry on the environment and to accelerate the soaking process, an enzyme preparation of microbial origin Letan SE2 and a surfactant CH-22C, which meets the requirements of the European regulations REACH and ECHA, were used. When these chemicals are used in the soaking process, mucopolysaccharides and non-collagen proteins are intensively removed from the interfiber space, the moisture content in the skin tissue of the ostrich skin increases, and uniform soaking in thickness and area is ensured. Intensive and correct soaking process improves the quality of subsequent processing of the ostrich skin. The paper shows the possibility of carrying out the soaking process using environmentally friendly chemicals, the use of which allows reducing the level of technogenic impact of chemicals on the environment, which is very important for the preservation of natural objects.

Keywords: ostrich, skins, the process of soaking

INTRODUCTION

Recently, exotic leather obtained from ostrich skins as a material for the leather and footwear industry has become in demand by designers for the manufacture of shoes, accessories, clothing, and furniture decoration. The uniqueness of the ostrich skin gives a characteristic pattern due to large follicles from feathers, good wear resistance and plasticity (Sukhinina, 2014). The originality of the texture of the ostrich skin made it possible to create exclusive leather products, which ensured a high demand for a semi-finished ostrich product in the global fashion industry and a high price compared to other types of leather (Cooper, 2001; Belleau *et al*., 2002).

Ostrich farming as a poultry industry in Uzbekistan was founded in 2016. Currently, ostrich breeding is widely spread in many regions of the republic, especially in the Fergana region in the city of Rishtan. The first and largest specialized farm in Uzbekistan with a full cycle of breeding black African ostriches was the Anglo-Uzbek farm “Straus farm” (Straus Farm, 2017).

Many studies aimed at improving the technology of processing ostrich skins provide information about the peculiar structure of the ostrich skin and the technology for processing ostrich skin (Ulugmuratov *et al*., 2019; Ulugmuratov *et al*., 2020).

The present research was aimed at studying one of the important and initial processing of ostrich skins, as the soaking process. In order to reduce the level of technogenic impact of the applied chemicals on the environment, an enzyme preparation of microbial origin and an environmentally friendly surfactant were used, which is very important for the preservation of natural objects and, in general, for improving the ecological situation in Uzbekistan.

https://doi.org/10.24264/icams-2022.III.12

MATERIALS AND METHODS

In experimental study, 20 sets of wet-salted raw skins obtained from 12-14 months old ostriches at slaughter stage were processed. The average weight of a set of skins was 4-6 kg, and the area was 140-160 dm^2.

Currently, they also pay great attention to the use of environmentally friendly non-ionic and ionic surfactants (surfactants), industrial wastewater containing non-biodegradable surfactants complicates purification and has a detrimental effect on the environment. To minimize this negative impact on the environment, it is necessary to reduce the consumption of harmful substances or replace them with environmentally friendly enzyme preparations and surfactants that meet the requirements of the European Chemical Agency (ECHA) and the European REACH regulation (European chemicals agency (REACH); REACH-Registration. html). In studies to solve the above problems, an enzyme preparation of microbial origin Letan SE2 (ODAK kimyevi maddeler) and a surfactant - CH-22C (Shebekinskaya Industrial Chemistry LLC., 2018), were used. The soaking agent CH-22C meets the requirements of the European regulations REACH and ECHA. Table 1 shows the physicochemical characteristics of the chemical materials used in research.

Table 1. Physicochemical properties of surfactants CH-22C, Letan Biosit B-40 and Letan SE2

Parameters	Surfactant CH-22C	LETAN BIOSIT B-40	LETAN SE 2
Chemical characterization	Composition based on biodegradable nonionic and anionic surfactants, REACH compliant	Organic sulfur compounds	Mixture of aliphatic substances
Active substance content, %	37	-	-
Hydrogen exponent, 1% solution	6.0-8.5	Approx 10	Approx 8-9
Appearance	Clear colorless liquid	Light colored liquid	Clear colorless liquid
Ionogenic character	Anionic	Non-ionic	Non-ionic
Steadiness	Resistant to electrolytes. acids and alkalis in common concentrations. Resistant to chromium and aluminum salts		
Consumption in the process of soaking from the mass of wet-salted skins	Up to 2.0	0.05-0.10	0.10-0.25

The mass of a part of the skins was determined on an analytical balance with an accuracy of 5 mg, the thickness of the skins was measured using a special thickness gauge with an accuracy of 0.01 mm. The following methods according to International Union of Leather Technologists and Chemists Societies (IULTCS) official methods of analysis for leather (The IULTCS Official Methods of Analysis., 2020), were used to determine the physical and chemical properties of the processed leathers: IUC 2 (2017) for sampling, IUC 3 (2017) for preparation of chemical test samples, IUC 4 (2018) for

https://doi.org/10.24264/icams-2022.III.12

determination of matter soluble in dichloromethane, IUC 5 (2005) for determination of volatile matter, IUC 7 (1977) determination of sulphated total ash and sulphated water insoluble ash, IUC 10 (1984) determination of nitrogen and hide substance, IUP 1 and 3 (2012) for sample preparation and conditioning, IUP 2 (2017) for sampling location, IUP 4 (2016) for measurement of thickness, IUP 16 for measurement of shrinkage temperature up to 100°C.

To determine the content of mucopolysaccharides in the soaking solution, the solutions were initially subjected to preliminary washing to remove protein and evaporated (Kachetkova, 1967). Several methods were tested in the work: spectrophotometric, the method for determining the protein with a biuret reagent and Flores (State pharmacology, Issue 2, 1990). The first two methods did not lead to results. When using the spectrophotometric method, it became impossible due to the presence of NaCl in the test solutions. When using the biuret method, the protein concentration in the samples used was found to be too low. The method for determining protein according to Flores turned out to be sensitive also in solutions containing inorganic salts (Suzuki, 2006).

RESULTS AND DISCUSSION

Correct performance of the soaking process should ensure sufficient and uniform watering of the raw material throughout the entire thickness and area with minimal loss of gel substance, the maximum possible extraction of salt from the raw material, residues of blood, dirt and soluble proteins (albumin and globulins) and other preservatives, as well as complete protection raw materials from bacterial influences. Insufficient and uneven watering of the skins during the soaking process can cause a screed of the facial surface of the skin in subsequent processes or the appearance of stiffness. Excessive losses of protein substances during soaking lead to looseness of the finished skin up to fragrance (lagging of the facial layer of the skin from the underlying layer).

Table 2. Parameters of the soaking process when processing ostrich skins

Processes	Name of chemical materials	Temperature, °C	Consumption of chemical materials, %	Duration of the process, hr
Soaking - 1	Water	20	400	18 hr
	Bactericide, Letan Biosit B-40		0.2	
	surfactant, CH-22C		0.3	
Soaking - 2	Water	20	400	18 hr
	Surfactant, CH-22C		0.3	
	Enzyme preparation Letan SE2		X=0.1; 0.20; 0.30; 0.40; 0.50	

The processing of ostrich skins was similar to the following technology developed by Turkish researchers (Chiftchi *et al*., 2012; Bitlisli *et al*., 2004; Afsar *et al*., 2002). In contrast to this technology, during the soaking process, an enzyme preparation Letan SE2 and an environmentally friendly surfactant CH-22C were used to intensify the soaking process. The parameters of the soaking process when processing ostrich skins are shown in Table 2.

https://doi.org/10.24264/icams-2022.III.12

The structure of the ostrich skin tissue, consisting of thick, densely spaced parallel collagen bundles and a large amount of mucopolysaccharides and fatty inclusions, prevents the penetration of an aqueous solution into its thickness during soaking. Experimental studies have shown that the watering of ostrich skins in soaking solutions using only surfactants is not enough than for skins treated in solutions with the addition of the Letan SE2 enzyme preparation. At the same time, the moisture content in the control samples is comparatively lower (by 5-7%) with the same duration of the soaking process. The mass fraction of moisture in experimental samples, with the use of an enzyme preparation in the process of soaking, reaches a value of 68-70%. To determine the optimal consumption of the enzyme preparation, experimental studies were carried out on pieces of ostrich skin. The skin was cut into pieces measuring 5×5 cm, mainly from the tail section closer to the crown of the hide and pieces in experimental studies of the soaking process. In the process of soaking on ostrich skin samples, analyzes were carried out to determine the content of leached mucopolysaccharides in the soaking liquid. Initially, the solutions were pre-washed to remove protein and evaporated (The IULTCS Official Methods of Analysis, 2020). Then the resulting residue was weighed, first taking into account the content of surfactants, NaCl, and then after their deduction. At a concentration of 0.5%, the highest value of leached mucopolysaccharides was obtained. Moreover, the results minus the surfactant and salt differ from the control by 2.0-2.5 times.

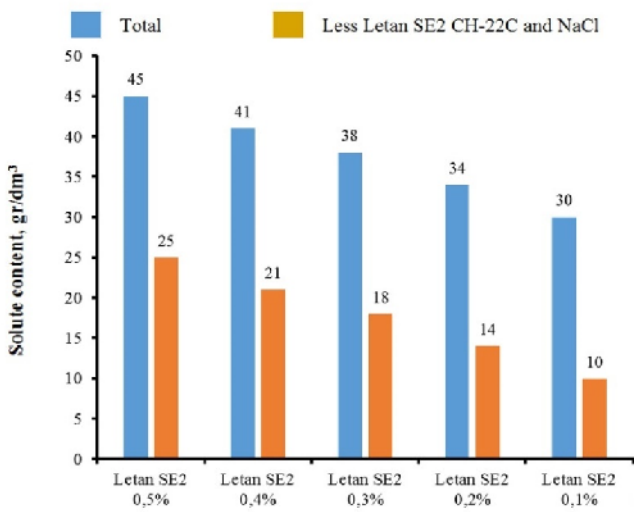

Figure 1. Dependence of the leachable mucopolysaccharides content in soaking solutions obtained after the second soaking

Figure 1 shows the results of determining the content in the soaking solution obtained after the second soaking of skin samples with the participation of CH-22C and Letan SE2. The concentration of the latter is in the range of 0.10–0.5%. In the control experiment, the enzyme preparation was absent.

https://doi.org/10.24264/icams-2022.III.12

The role of the enzyme preparation is not limited to the leaching of mucopolysaccharides, but the breakdown of non-collagen proteins contained in the skin tissue of the hide occurs.

The experimental results were processed using the method of mathematical statistics.

In experimental samples using enzyme preparation Letan SE2, the content of water washable non-collagen proteins is 2.5 times higher than in the control sample.

The results of experimental studies have been tested and confirmed on whole parts of the ostrich skin (skins of the body, legs, neck and wings). According to the studies carried out, the optimal concentration of CH-22C and Letan SE2 are 0.3% and 0.25-0.35%, respectively. With an increased consumption of the Letan SE2 enzyme preparation of 0.4-0.5%, excessive loosening of the structure of the skin tissue is observed, which is undesirable. At that time, the Turkish company ODAK recommends the use of Letan SE2 from 0.1 to 0.35%, depending on the type of leather raw materials. With the removal of mucopolysaccharides and non-collagen proteins from the interfiber space, the moisture content in the skin tissue of the skins increases and a uniform soaking of the skin tissue of the skins is provided in thickness and area.

CONCLUSIONS

The possibility of carrying out the soaking process with the use of environmentally friendly chemicals allows reducing the level of technogenic impact of chemicals on the environment, which is very important for the preservation of natural objects of the Republic. The obtained research results on the soaking process are the basis for the development and improvement of a competitive, environmentally friendly technology for processing ostrich skins.

REFERENCES

Afsar, F., Gulumser, G., Ozgunay, G. and Akyuz. F. (2002), "A Study on Processing of Ostrich Leathers and Determination of Their Properties", *Ege Univ. Derg.*, 39(3), 137-144.

Belleau, B.D., Summers, T.A. and Von Hoven, T. (2002), "Marketing Exotic Leather: American Alligator, Ostrich and Emu", *Journal of the American Leather Chemists Association*, 97(2), 65-73.

Bitlisli, B.O., Basharan, B., Sari, O., Aslan, A. and Zengin, G. (2004), "Some Physical and Chemical Properties of Ostrich Skins and Leathers", *Indian Journal of Chemical Technology*, 11, 654-658.

Chiftchi, F., Demir, H. and Ekiz, B. (2012), "The Effects of Certain Factors on Leather Quality and Yield in Ostrich", *J. Fac. Vet. Med. Istanbul Univ.*, 38(2), 121-133.

Cooper, R.G. (2001), "Ostrich (*Struthio camelus* var. *domesticus*) Skin and Leather: A Review Focused on Southern Africa", *World's Poultry Science Journal*, 57(02), 157-178, https://doi.org/10.1079/WPS20010012.

European Chemicals Agency (ECHA), https://echa.europe.eu/.

Kachetkova, N.K. (1967), *Methods of Carbohydrate Chemistry*, Mir., 38-42.

ODAK kimyevi maddeler, http://www.odakkimya.net.

REACH-Registration, http//www.cirs-reach.com/news-and-articles/.

Shebekinskaya Industrial Chemistry LLC (2018), http://www.shebkoghim.ru.

State Pharmacology, Issue 2 (1990), *General Methods of Analysis. Medicinal Plant Material*, 11th ed., Medicine, 30-33.

Straus Farm (2017), https://web.facebook.com/strausfarm/?rc=p&_rdc=1&_rdr, accessed on July 18 2017.

Sukhinina, T.V, (2014), "Semi-Finished Product from Ostrich Skins as a Material for the Leather and Footwear Industry", *Leather and Footwear Industry*, 4, 26-30.

Suzuki, Y. (2006), "Characteristics of a Protein Error in Determination of Serum Protein in the Presence of Inorganic Salt", *Analytical Sciences. The Japan Society for Analytical Chemistry*, 22, 269-274, https://doi.org/10.2116/analsci.22.269.

The IULTCS Official Methods of Analysis., (2020), Society of Leather and Chemists, Northampton, U.K.

https://doi.org/10.24264/icams-2022.III.12

Ulugmuratov, J.F., Ismatullaev, I.N., Begaliev, Kh.Kh., Akhmedov, B.B. and Kadirov, T.J. (2019), "Study of leather extraction technology from ostrich skin raw materials" Textile problems, 2. p.71-77.
Ulugmuratov, J.F., Hamitov, A.A., Ismatullaev, I.N., Mirzaev, N.B., Begaliev. Kh.Kh. and Akhmedov. B.B. (2020), "Degreasing in the treatment of ostrich skins using environmentally safe surfactants process research", Textile problems, 4, p.90-99.

https://doi.org/10.24264/icams-2022.III.12

LASER FINISHING IN THE DECORATION OF LEATHER PRODUCTS

NATALIIA PERVAIA, NATALIA BORSHCHEVSKA, OLGA ANDREYEVA, TYMOFII LYPSKYI

Kyiv National University of Technologies and Design, 2 Nemyrovych-Danchenko Str., 01011, Kyiv, Ukraine, email: nataliiapervaia@gmail.com, borshoes@gmail.com, wayfarer14@ukr.net, timofii79@gmail.com

Today, the use of laser finishing of leather products is becoming more popular than traditional methods. However, there is not much information on the effect of laser energy on the leather structure during finishing, so additional research is need. Crust leather produced by a new unified resource-saving technology with the use of polymer compounds at the stage of tanning and liquid finishing was used for research. The different leather samples were taken for research the laser effect. Leather samples with a thickness of 1.40-1.45 mm were subjected to laser engraving at a depth of laser ablation from 0.1 mm to 0.7 mm in steps of 0.1 mm. It was found that the structure of the dermis under the action of laser radiation has not undergone morphological changes: the samples preserved the natural histological structure, collagen bundles are not deformed, the layers are evenly spaced without increasing the density of the structure. There is some increase in the distances between the structural elements of the dermis. It was found in the area of direct action of the laser beam there are signs of welding of collagen fibers, but on the surface of the sample of leather were no found chemicals substance. The influence of laser finishing on the structure and physical-mechanical properties of leather for footwear and leather goods was determined. It was found that increasing the depth of ablation to 50-52% of the thickness of the leather adversely affects it`s physical and mechanical properties, thereby deteriorating the performance of footwear and leather goods. The results of complex research of the effect of laser radiation on the physical and mechanical properties of the leather for the shoes uppers and leather goods allowed to establish rational technological parameters of the laser finish. Such information expands the possibilities of introducing laser equipment into serial production in order to create a modern range of finished products due to the creative design of models and unification of products.

Keywords: laser finishing, leather products, properties of leather.

INTRODUCTION

Replacing traditional intensive operations with laser technology opens up new opportunities for innovative solutions and is a key issue for the economic success of the footwear and leather goods industries. Today, laser technologies are used both for finishing materials and for the manufacture of products. Materials are processed at very high temperatures, which can cause melting or evaporation of almost any material due to the high concentration of power and energy in a very small area (Grigor'janc, 1989). However, due to the reasonable choice of technological parameters, the use of laser technology has recently become significantly more widespread, as it has a number of advantages over conventional methods and is becoming increasingly economically attractive for cutting and finishing leather products.

Figure 1. The sequence of action of laser radiation on natural leather: a) absorption and heating; b) melting; c) evaporation

https://doi.org/10.24264/icams-2022.III.13

Most laser technologies were based on thermal action, the need to heat material a given temperature. The absorption of thermal energy for natural leather is volumetric view and the depth of penetration of laser radiation is determined by physical properties of the leather, which is an anisotropic inhomogeneous material (Fig. 1).

To determine the impact of thermophysical processes occurring during laser finishing on the physical and mechanical properties of natural crust leather for footwear and leather goods, a microscopic analysis of topological and morphological changes in the structure and indicators of physical and mechanical properties of leather

MATERIALS AND METHODS

Crust leather was produced using a new unified resource-saving technology using polymer compounds at the stage of tanning and liquid finishing. In addition, tanning includes pre-processing of abated pelt with a polymeric compound based on ethylene carboxylic acid instead of pickling, which allows us to decrease the duration of the process as well as the tanning agent consumption by 25 %. The liquid finishing includes using a polymeric compound based on maleic acid after the neutralization process (before dying), which allows us to decrease the processing duration by 20 %, dying agents and tannins consumption by 50 %, to increase the grade of quality, to increase the crust leather yield of thickness by 1.4 %, and area by 0.3 %. For comparison, used crust leather, made by a known technology (Andreyeva *et al*., 2019).

The effect of laser radiation on the microstructure of dermal collagen was examined using scanning electron microscopy (SEM) on a Tescan Mira 3 LMU (Czech Republic). For more complete information a first layer of conductive material in the form of platinum was sprayed on the front surface of the leather sample after laser finishing, which covered the surface of the sample and the area of direct action of the laser beam (Krishtal *et al*., 2009).

Crust leather finishing was performed on a CO2 laser machine Comelz CZ/M (Italy). Crust leather samples with a thickness of 1.40-1.45 mm were subjected to laser engraving at a depth of laser ablation from 0.1 mm to 0.7 mm in steps of 0.1 mm.

Stages of conducting the research: 1. Determination of the effect of laser radiation on the physical and mechanical properties of crust leather to establish the main dependencies between important indicators and parameters of laser ablation. 2. Establishing rational technological parameters of laser engraving. 3. Research of the effect of laser engraving on the structure of leather crust for the upper of shoes and leather goods

RESULTS

In order to determine the effect of laser radiation on the physical and mechanical properties of the leather, the effect of the depth and area of laser ablation on the parameters of the strength limit during stretching and elongation under a stress of 10 MPa was determined. The ablation depth varied from 0.1 mm to 0.7 mm, and the area was 1%, 25%, 50% of the working area of the tested sample. Cracking of the front surface of the samples occurred almost simultaneously with their rupture. The obtained values were compared with the values of leather samples without engraving. Based on the conducted studies, the effect of the depth of laser ablation on the strength limit

https://doi.org/10.24264/icams-2022.III.13

during stretching was established (Fig. 2), while the ablation area of the samples was 1% of the working area of the sample.

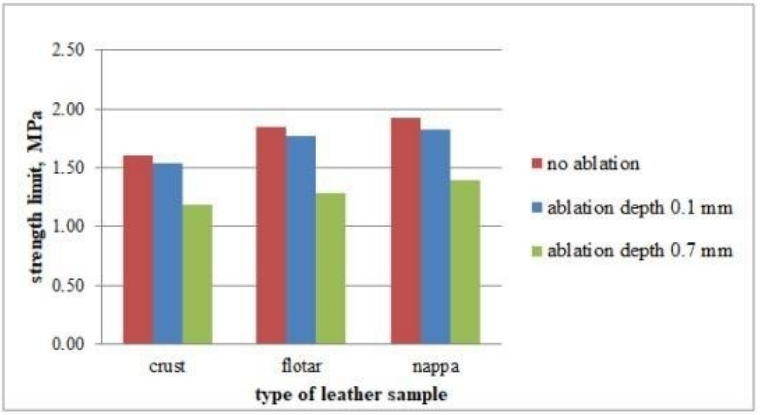

Figure 2. Diagram of the influence of the ablation depth on the strength limit

According to the results of the experimental research, it was determined that the increase in the area and depth of laser ablation affects the decrease in the tensile strength index. When the ablation area increases to 50% of the total area of the sample, and the depth up to 0.7 mm, the index of the tensile strength limit decreases by 1.1 times (Fig. 3).

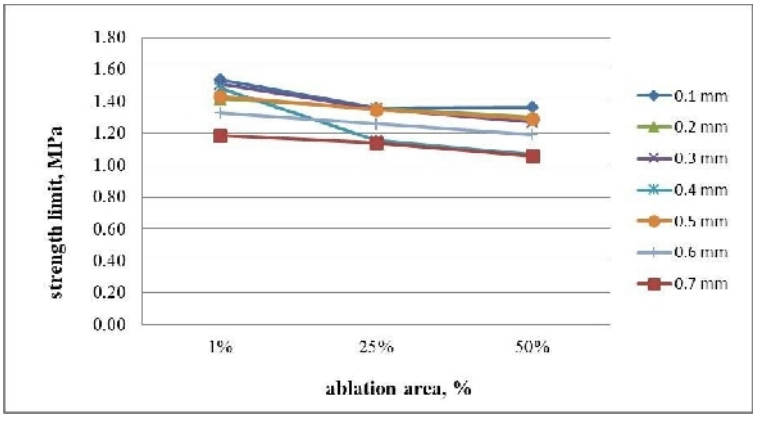

Figure 3. The influence of the area and depth of laser ablation on the strength resistance of crust leather

Based on the analysis of the obtained results, it is not recommended increase the area of engraved elements by more than 25-35% of the total area of the product part with an ablation depth of 0.3-0.4 mm on the relevant shoe parts. It is also not

https://doi.org/10.24264/icams-2022.III.13

recommended increase the area of engraved elements by more than 40% of the area of the part with an ablation depth of 0.4-0.5 mm on the parts of leather goods.

According to the results of electron scanning microscopy it was found that the structure of the dermis under the action of laser radiation has not undergone morphological changes: the samples preserved the natural histological structure, collagen bundles are not deformed, the layers are evenly spaced without increasing the density of the structure (Fig. 4 a, b). There is some increase in the distances between the structural elements of the dermis (Fig. 4 c).

It was found in the area of direct action of the laser beam there are signs of welding of collagen fibers, but on the surface of the sample of leather were no found chemicals substance. There is no amorphous carbon, which turned the upper layer of leather removed from the area of engraving by gas flow.

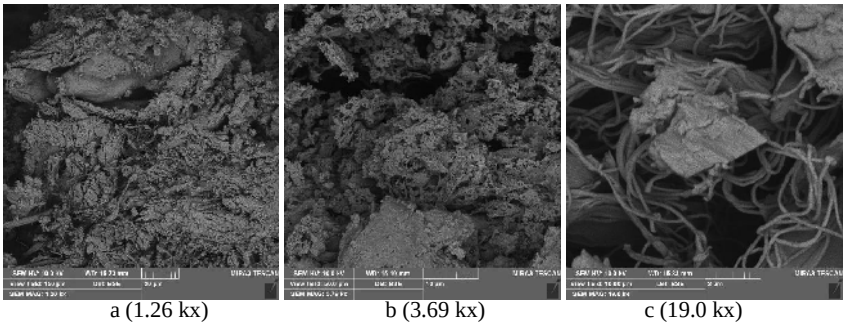

a (1.26 kx) b (3.69 kx) c (19.0 kx)

Figure 4. Electron scanning microscopy image of the cross-section leather samples in the area of laser ablation

Such changes are a consequence of thermophysical processes, which depends on the absorption coefficient of the material, the wavelength of the laser and duration of exposure. The duration of laser radiation in turn determines the temperature and size of the heated layers.

Increasing the distance between the structural elements of the dermis determined to higher vapor permeability (Danylkovych, 2006; Rybalchenko *et al*., 2010). When the ablation depth increased to 0.7 mm (50% of the total thickness of the sample) compared to the sample without ablation, the skin vapor permeability increased by 5% (Borshchevska, 2020). As the ablation area increased to 50%, this indicator increased to 8.5%. This result is a consequence of the release of the capillary-porous structure of the leather. Physical and mechanical properties of the leather are preserved with a sufficiently fluffy structure. The tensile strength index varied from 15.0 to 12.5 MPa at a depth of laser ablation from 0.1 mm to 0.7 mm and a minimum ablation area of 1% of the working area of the sample

CONCLUSION

The depth of laser ablation, equal to 25-30% of the leather thickness, and the area of engraved elements less than 50% of the total area of the part are rational technological parameters for laser finishing leather, which provides good hygienic properties and does not impair the performance of products.

https://doi.org/10.24264/icams-2022.III.13

The results of complex research of the effect of laser radiation on the physical and mechanical properties of the crust leather for the shoes uppers and leather goods allowed to establish rational technological parameters of the laser finishing. Such information expands the possibilities of introducing laser equipment into serial production in order to create a modern range of finished products due to the creative design of models and unification of products. (Fig. 5). Improving the aesthetic properties of leather products was achieved through the development of a unique design using laser engraving.

Figure. 5. Creative design of leather goods and shoos with using laser engraving

REFERENCES

Andreyeva, O., Pervaia, N., Maistrenko, L., Mokrousova, O., Harkavenko, S. and Nikonova, A. (2019), "A Unified Technology of Crust Leather Production Using Polymeric Compounds Development, *Leather and Footwear Journal*, 19(3), 193-202, https://doi.org/10.24264/lfj.19.3.4.

Borshchevska, N.M. (2020), "Doslidzhennia vplyvu lazernoho hraviruvannia na fizyko-mekhanichni vlastyvosti naturalnykh shkir dlia verkhu vzuttia ta shkirhalantereinykh vyrobiv" [in Ukrainian], *Visnyk KNUTD. Tekhnichni nauky*, 5 (150), 46-55, https://doi.org/10.30857/1813-6796.2020.5.4.

Danylkovych, A. (2006), "Praktykum z khimii ta tekhnolohii shkiry ta khurta" [Workshop on Chemistry and Technology of Leather and Fur] [in Ukrainian], Kyiv: Feniks.

Grigor'janc, A. (1989), "Osnovi lazernoj obrabotki materialov" [Basics of Laser Material Processing] [in Russian], Moskva.

Krishtal, M.M., Yasnikov, I.S., Polunin, V.I., Filatov, A.M. and Ulianenkov, A.G. (2009), *Skaniruyushchaya elektronnaya mikroskopiya i rentgenospektralnyy mikroanaliz* [in Russian], Moskva: Tekhnosfera, 166 p.

Rybalchenko, V.V., Konoval, V.P. and Drehulias, E.P. (2010), *Materialoznavstvo vyrobiv lehkoi promyslovosti. Metody vyprobuvan: navchalnyi posibnyk* [in Ukrainian], Kyiv: KNUTD, p. 395.

https://doi.org/10.24264/icams-2022.III.13

https://doi.org/10.24264/icams-2022.III.13

3D VIRTUAL PROTOTYPING OF FUNCTIONAL KNITTED GARMENTS FOR PERSONS WITH SPECIAL NEEDS

GEORGETA POPESCU[1], DOINA TOMA[1], CLAUDIA NICULESCU[1], ALINA POPESCU[1], ADRIAN SALISTEAN[1], IONELA BADEA[1], MINELA NENECIU[2], SARA WECHSLER[2], IONUT DANIEL ION[2], MIRELA GRETI PUIU[2], CRINA RAICAN[2]

[1] *National Research & Development Institute for Textiles and Leather, 16 Lucretiu Patrascanu Street, 030508, Sector 3, Bucharest, Romania, e-mail: office@incdtp.ro*

[2] *SC DATSA TEXTIL SRL, 7 Bazalt Street, 120068, Buzau, Romania, e-mail: office@datsa.ro*

The field of functional clothing is vast and varied, with each function having its own set of specifications, material needs, and corresponding technologies and methods. Garments for persons with special needs are part of the functional clothing category and are meant to improve the quality of life of those whose body shape, mobility or dexterity differs from the norms. Virtual prototyping of garments provides high potential for design, product development and marketing processes. This paper presents the virtual prototyping of functional knitted garments for persons with special needs (elderly people, people with disabilities, operational staff from defense/public order/security structures) highlighting the importance of personalization and its competitive advantages. The steps to develop the virtual prototypes were: i) 2D pattern design from data in the dimensional table of the model and in correlation with the real sizes of knitted garments using Pattern Design Software (PDS) from OPTITEX; ii) Simulation knitted garments prototypes on the avatar using Optitex 3D Suite Software; iii) Evaluating the fit of the product on the body. The possibility to check the aspect of the product and how it is matching on the 3D model of the human body, without requiring physical development of a prototype is the main advantage of the virtual prototypes. If the product does not fit properly on the 3D surface of 3D model (mannequin / avatar), the designer can easily modify the shapes of parts and then check the new shape by repeating the steps of 3D simulation process in virtual space.

Keywords: functional knitted garments, virtual prototyping, persons with special needs.

INTRODUCTION

The design and customization of garments for people with atypical changes in conformation is relevant for research in the field of garments and constitutes a major challenge if we take into account the changes in conformation produced in recent years, due to: the obesity, which has become a major public health problem worldwide which led to problems with size matching and clothing products comfort; the aging of the population with the change in body shape after the age of 60, which represents an important factor at the European and world level, which imposes the reintegration of the elderly, in family life, associative and social life; activity at computer, a static activity that causes deviations of the spine, causing conditions such as scoliosis, kyphosis, kyphoscoliosis or spondylosis; various native or acquired disabilities during life (Gupta, 2011).

The CareKnits project aims to offer a wide range of methods, advanced technologies and tools dedicated to the design and manufacture of clothing adapted to the shape of the wearer by implementing, integrating and interfacing already validated digital technologies throughout the process from creation/ design to product realization.

Today, advanced computer simulation techniques and garments virtual prototyping are indispensable for the development of garments and their fitting on the 3D body models within a virtual environment, as well as real-time virtual clothes try-on (Jevsnik *et al*., 2012 and 2017).

https://doi.org/10.24264/icams-2022.III.14

This paper presents the virtual prototyping of functional knitted garments for persons with special needs (elderly people, people with disabilities, operational staff from defense/public order/security structures) highlighting the importance of personalization and its competitive advantages for the beneficiary of this project, SC DATSA TEXTIL SRL.

EXPERIMENTAL

In order to design and manufacture functional knitted textile products intended for people with special needs, the anthropometric database of the Romanian population between the ages of 6 and 60+ was filtered, according to certain criterions. The data were obtained in the anthropometric surveys carried out by INCDTP between 2008 and 2014, in Bucharest, at the National Institute of Diabetes, Nutrition and Metabolic Diseases "Prof. Dr. N. Paulescu" and in other public institutions, through 3D scanning. Measurement was done with the 3D Body Scanner Vitus XXL Anthroscan. It contains a family of software modules (ScanWorX) for 3D body visualization and automatic processing and evaluation of anthropometric data.

The Specific Anthropometric Database

The primary 3D anthropometric database of INCDTP contains 6150 scanned bodies of which: 2850 for children, girls and boys, 1800 adult subjects, women and men, 1500 obese and elderly subjects and 150 subjects from public order structures. Primary anthropometric database was filtered according to certain criteria (e.g., sex, age and Body Mass Index, etc.) to constitute the databases specific to people with special needs, namely Anthropometric database for: obese women; obese men; women aged 60+; men aged 60+; workers in public order structures.

Each anthropometric dimension of the specific databases was subjected to a one-dimensional statistical processing by calculating the statistical parameters for the main dimensions of the body (bust and hip girth, for women and chest and waist girth, for men). Dimensional typology selection (establishing body shape variants to be included in the anthropometric dimensions table) took into account the frequency of the investigated sample, different combination of possible value of main dimensions. Thus, frequency values bigger than 5% were selected. Determination of types body, for each group of people with special needs, was done by analyzing the frequency of the difference between Ps (hip girth) and Pb (bust girth), on women and Pt (waist girth) and Pb (chest girth), on men. The type bodies with the highest frequency were selected, and for them the sizes of the garments and the body dimensions that will be used in the design of the patterns, were established.

For people with severe physical disabilities and important changes in posture, a module of the ScanWorX software allows visualization of the scanned 3D body, visualization of the disability and manual retrieval of anthropometric dimensions in the areas of interest for pattern construction (Bruniaux *et al*., 2016; Nakić *et al*., 2019).

Creation of Virtual Prototypes for People with Special Needs

Optitex Pattern Making - PDS software provided by INCDTP was used to create virtual prototypes of functional knitted products for people with special needs. The major advantage of this software consists in its perfect integration with the Optitex 3D

https://doi.org/10.24264/icams-2022.III.14

design/modeling/simulation solution. Thus, the created patterns can be visualized on different body types by creating three-dimensional samples. Changes made to the patterns are automatically transferred to the virtual clothing model.

To create the virtual prototypes, the following steps were taken: development of the conceptual model adapted to the body type; 2D design of the basic patterns in accordance with the data from the size table or those taken from the avatar in correlation with the real dimensions of the knitted product using the Pattern Design Software (PDS) from OPTITEX; placing the 2D patterns on the parametrized mannequin/avatar with the help of the Optitex 3D Suite software, simulating their sewing; evaluating the fit of the product on the body; redesigning the 2D patterns after evaluating the body-product correspondence and resumption the verification of the correspondence; designing 2D model patterns and placing them on the parametrized mannequin/avatar; checking the appearance and body-product correspondence of the virtual model/prototype (Nakić *et al*., 2019).

In order to create the virtual prototype, functional knitted textile products were selected from the most common range, used by elderly people / obese people / with non-standardized atypical conformations / with different disabilities / operational personnel from defense structures / public order / security.

RESULTS AND DISCUSSIONS

Based on the mentioned algorithm, 12 virtual prototypes of functional knitted textile products were made. In the following tables are exemplified five of them.

Table 1. Dress for the elderly female

Conceptual model	*Parameterized mannequin and basic patterns: vB body type, size 48*	*Model patterns, virtual prototype on the body and checking the body-product fitting by viewing the tension map.*
	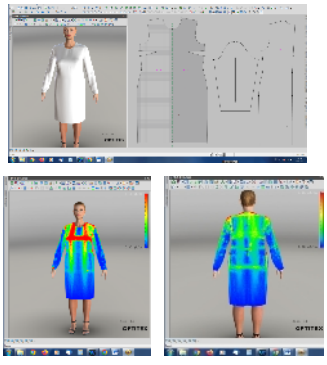	

The model is designed for people of different sizes and body type vB. The virtual prototype made with model patterns when analyzing the degree of body-product fit, on the mannequin parameterized according to body type and size, using the tension map, shows a high pressure in the shoulder area (normal for a product with shoulder support) and breasts. After correcting the model patterns in the breast area, when resuming the product simulation, a correct positioning of the product on the body and a reduction of the tension exerted in the breast area were highlighted.

https://doi.org/10.24264/icams-2022.III.14

Table 2. Jacket for elderly men

Conceptual model	*Parameterized mannequin and basic patterns: vD body type, size 56*	*Model patterns, virtual prototype on the body and checking the body-product fitting by viewing the tension map.*
	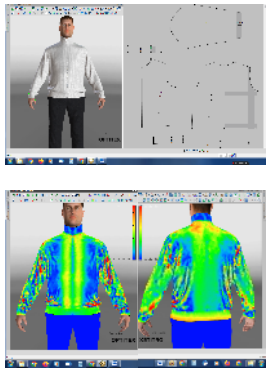	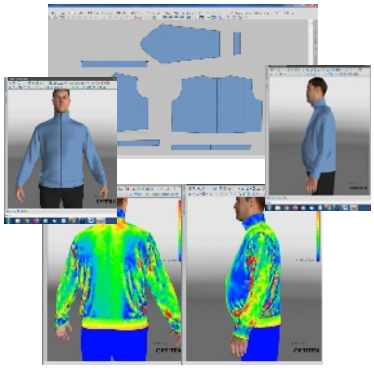

Visualization of the product made with the basic patterns, on the parameterized mannequin, indicates a proper placement and correct patterns. The analysis of the tension map of the product made with the model patterns, shows a good fit on the body without pressure on the body and sleeves well placed on the hands, without creases.

Table 3. Blouse for women with atypical conformation (developed hips)

Conceptual model	*Avatar, its dimensions and basic patterns.*	*Model patterns, virtual prototype simulation on avatar, checking the body-product fitting by viewing the tension map.*
	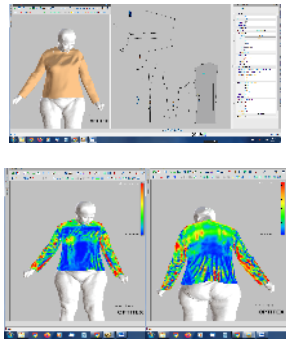	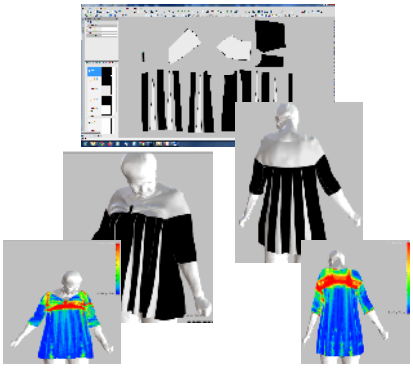

A model with a flared line that masks the atypical conformation and boat neckline that gives the feeling of a balanced body has been designed. The body dimensions were taken from the avatar resulting from the scanning protocol. The analysis of the map of the pressure exerted by the prototype executed with the basic patterns shows the need to change the basic patterns, on the middle line of the back. The simulation of the body – product correspondence made with the corrected model patterns shows a tension exerted in the area around the neck and shoulders (the model is with a plate), normal due to the overlap of the materials.

https://doi.org/10.24264/icams-2022.III.14

Table 4. Blouse / Dress for the person with advanced scoliosis

Conceptual model	*Avatar, its dimensions and basic patterns.*	*Model patterns, virtual prototype simulation on avatar, checking the body-product fitting by viewing the tension map.*
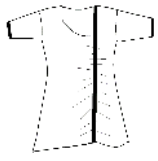	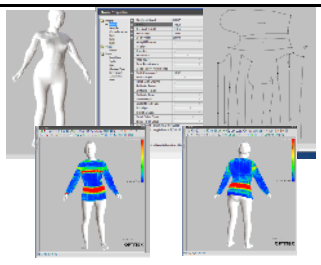	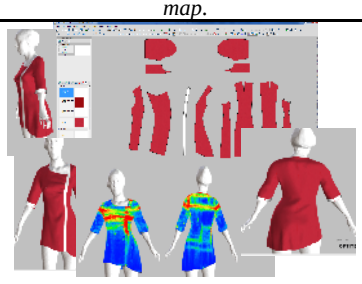
The model is designed for people with major body asymmetry, in order to hide this problem. From checking the fit of the body-product made with the basic patterns, the high tension in the hip area and the asymmetry at the end of the product can be observed. The virtual prototype made with model patterns has a good drape. The end of the product is correct, masking the person's asymmetry.		

Table 5. Sweater for operatives in defense/public order/security structures

Conceptual model	*Parameterized mannequin and basic patterns. According to SR 13544/2010: C body type, size 56*	*Model patterns, virtual prototype on the body and checking the body-product fitting by viewing the tension map.*
	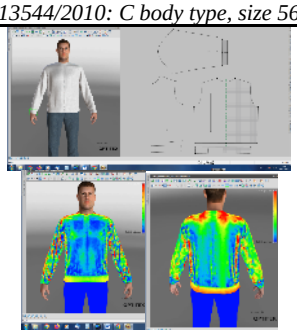	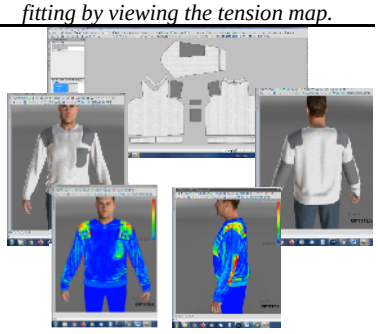
The basic patterns were designed for Body type C, Size 56, Height 182 cm using the dimensions from SR 13544/2010. The simulation of the fit of the product on the mannequin parameterized to the body dimensions shows a good fit with pressure in the shoulder area, which is normal for a product with support on the shoulders. In the area of the elbows, the jacket has reinforcements as a protection area against friction, a fact that stiffens a little and slightly presses the elbows.		

CONCLUSIONS

The main advantage of virtual prototypes consists in the fact that clothing products can be designed to fit directly on a parametrized mannequin/avatar of a wearer, without it physically existing at the time of the trials and then transferred to production.

In a small number of steps, the shape and dimensions of the patterns, colors, types of knits and other parameters that influence the shape, appearance and comfort of clothing products can be changed.

https://doi.org/10.24264/icams-2022.III.14

The use of 3D virtual prototyping offers many advantages as: the possibility to check the aspect of the product and how it is matching on the 3D model of the human body, without requiring physical development of a prototype; the reduction of the time to produce the first prototype; a significant reduction of the manufacturing costs; the reduction of waste; the possibility of diversifying the model – by combining or altering the textures of materials; the possibility of co-creation service; improved communication between the development and production departments; online promotion of the created model.

The results obtained in the design and creation of the virtual prototype, which included the function of modeling the product according to the technical characteristics of the materials, are used to define the technological parameters and programming of knitting machines of the functional knitted textile products.

Acknowledgement

This work was supported by a grant of the Ministry of Research, Innovation and Digitization /Intermediate Body for Research – Competitiveness Operational Programme 2014-2020/ Priority Axis 1 – Research, Technological Development and Innovation supporting the economic competitiveness and business development/ Investment Priority 1.1/ Specific Objective: 1.3 Increasing private investment in RDI, Action: 1.2.1 Stimulating companies' demand for innovation through RDI projects undertaken by companies individually or in partnership with R & D institutes and universities for the purpose of product and process innovation in the economic sectors presents potential for growth, / Project type – Innovative technological project/ project Code SMIS2014 - 121567/ "Development of RDI capacity for obtaining functional knitted textile products in order to increase the competitiveness of DATSA TEXTIL SRL through innovation / CareKnits".

REFERENCES

Bruniaux, P., Cichocka, A. and Frydrych, I. (2016), "3D Digital Methods of Clothing Creation for Disabled People", *FIBRES & TEXTILES in Eastern Europe*, 24, 5(119), pp. 125-131, https://doi.org/10.5604/12303666.1215537.

Gupta, D. (2011), "Design and Engineering of Functional Clothing", *Indian Journal of Fibre & Textile Research*, 36(4), pp. 327-335.

Jevsnik, S., Pilar, T., Stjepanovic, Z. and Rudolf, A. (2012), "Virtual Prototyping of Garments and Their Fit to the Body", Chapter 50 in B. Katalinic (ed.), *DAAAM International Scientific Book 2012*, pp. 601-618, Published by DAAAM International, ISBN 978-3-901509-86-5, ISSN 1726-9687, Vienna, Austria, https://doi.org/10.2507/daaam.scibook.2012.50.

Jevsnik, S., Stjepanovic, Z. and Rudolf, A. (2017), "3D Virtual Prototyping of Garments: Approaches, Developments and Challenges", *Journal of Fiber Bioengineering and Informatics*, 10(1), pp. 51-63, https://doi.org/10.3993/jfbim00253.

Nakić, M. and Bogović, S. (2019), "Computational Design of Functional Clothing for Disabled People", *Tekstilec*, 62(1), pp. 23-33, https://doi.org/10.14502/Tekstilec2019.62.23-33.

THE DEVELOPMENT OF A SMALL-SCALE PPG-UAV FOR EMERGENCY RESPONSE ACTIONS

ADRIAN SALISTEAN, DOINA TOMA, MIHAELA JOMIR, IONELA BADEA

National Research & Development Institute for Textiles and Leather, 16 Lucretiu Patrascanu Street, 030508, Sector 3, Bucharest, Romania, adrian.salistean@incdtp.ro

In this paper is shown the development processes of an Unmanned Aerial Vehicle (UAV) that can be used for remote sensing, logistics or other emergency actions. The UAV is an ultralight aerial unit with an adaptable mission configuration. Thus, the configuration can be tailored to the type of intervention: observation, logistics, detection of certain personnel that are using Personnel Protective Equipment (PPE) equipped with radio ID transponders etc. The UAV is in fact a scaled down Powered Paraglider (PPG). The PPG-UAV uses a textile wing manufactured from a low weight double rip-stop nylon 6.6 fabric with extra coatings for air permeability reduction and added UV protection. The paraglider is linked with an Automated Command and Control (ATC) unit designed with increased modularity in mind allowing rapid reconfiguration based on the nature of the intervention. In this paper we summarize the fabric development followed by the paraglider pre-dimensioning, simulation using a numerical experimental model. The process is conducted on computer software developed within our institute. After the design phase the virtual prototype is preloaded for CNC cutting of the wing patterns, prototype assembly. The prototype is validated using computational algorithms combined with live testing in either static tests and/or simulated emergency live situations.

Keywords: Unmanned Aerial Vehicle (UAV), Powered Paraglider (PPG), Technical Textiles

INTRODUCTION

The objective of this project is to improve the service and operational response capacity for the National Emergency Situation Management System in Romania. In emergency situations all response structures act against the timer, and any means to reduce the response time can make the difference between life and death. Using the latest Unmanned Aerial Vehicles (UAV) technology, the response time can be reduced by allowing convenient remote sensing using many technologies like embedded-electronics, auto-pilot, high-capacity low weight batteries, materials that are strong yet lightweight, wireless communication, digital imaging, image processing software, positioning systems GPS, GNSS and so on. The value of an UAV for remote sensing, besides hardware and electronics, stay also in the software used that can automatically derive orthoimages by overlapping digital images and LiDar sensor point clouds. The fields of computer vision and deep learning AI can give a definitive advantage in remote sensing and data processing. Photogrammetric software supports can be embedded in UAV microcontroller and can control flight planning, calibration of cameras and triangulation for the creation of orthoimages such as 3D virtual landscapes in which a surveyor can interact with. For field survey high precision positioning data is required, and this is done by measuring through differential GPS, GNSS coordinates and corrected with internal inertial system data (Knache, 1992).

The specific objective of this project is to develop integrated support system in a way that is tailored for the specific operational requirements of emergency response actions. The system is composed of two components: protective equipment and support system for intervention actions. The support system is an Unmanned Aerial Vehicle (UAV) system that can be tailored to the nature of the intervention: disaster localization and monitoring, small scale logistics transport, detection of intervention staff using a

https://doi.org/10.24264/icams-2022.III.15

special Personal Protective Equipment (PPE) equipped with a special radio ID transponder, etc.

METHODS AND RESULTS

A comparative fabric design was done at the start of the projects. There were developed two fabrics using two woven types developed accordingly to the presented weave diagrams and characteristics (Cristian *et al*., 2012):

- Fiber composition of yarn: 100% PA6.6HT;
- Linear density of yarns: 30 den/32 f;
- Warp yarn count: 495 threads/10 cm;
- Weft yarn count for version 1: 504 threads/10 cm (fig. 1a);
- Weft yarn count for version 2: 508 threads/10 cm (fig.1b).

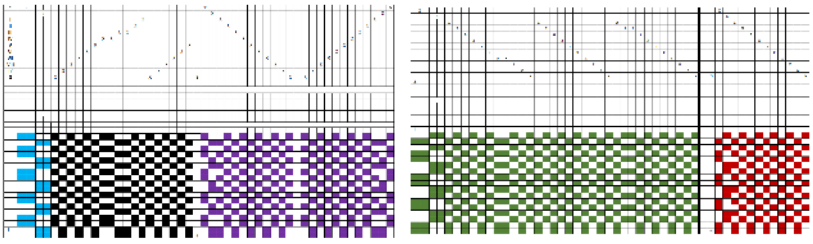

(a) (b)

Figure 1. Weave structure for version 1 (a. Ripstop) and version 2 (b. Double ripstop)

Several fabric variants were developed as follows:

- ripstop weave (F1 and F3) and
- double-ripstop weave (F2 and F4).

Each weave variant was also made in two finishing variants:

- calendering (F1 and F2) and
- polyurethane coating (F3 and F4).

Table 1. All variants fabrics test results

Test Name		Fabric F1	Fabric F2	Fabric F3	Fabric F4
Mass (g/m^2)		40	51	47	59
Yarn count	Warp	495	495	495	495
(threads/10cm)	Weft	504	508	504	508
Breaking strength	Warp	440	554	422	541
(N)	Weft	445	484	410	480
Elongation at	Warp	28.6	23.6	26.7	24.9
breaking force (%)	Weft	32.7	26.2	38.4	29.1
Tearing strength	Warp	34.4	21.3	65.2	20.7
(N)	Weft	32.7	22.5	65.5	20.7
Bursting strength (KPa)		330.3	368.4	330.2	370.8
Bursting strength (mm)		35.4	36.3	42.5	43.2
Air permeability (l/m^2/sec) at 200Pa		10.53	10.34	0	0

https://doi.org/10.24264/icams-2022.III.15

Test Name	Fabric F1	Fabric F2	Fabric F3	Fabric F4
Raw material	100% PA66HT	100% PA66HT	100% PA66HT	100% PA66HT
Coating	Calendered	Calendered	PU coating	PU coating
Weave type	Ripstop	Double-ripstop	Ripstop	Double-ripstop

- Air permeability: the lowest air flow was on the coated ones (F3 and F4)
- Mass: lightest is the F1 variant.
- Breaking resistances: all variants show relative similar values but with slightly higher values with the double-ripstop variants F2 and F4. Increased tear strength is observed on the F3 variant, probably to the tearing mode which blocks the rupture propagation (Buyuk *et al*., 2019). This tearing behavior also exhibits on the F1 variant.
- Analyzing the test results we choose F3 as the working variant for the UAV textile structure prototype manufacturing due to the tearing behavior that presented the highest tear strength and can prove useful in maintaining canopy integrity.

The prototype manufacturing preparation starts at pre-dimensioning (Flores *et al*., 2014), this is done in a software program developed by the institute and this software includes a database (Fig. 2a, Fig. 2b) that stores a collection of materials commonly used in parachute manufacturing. The database contains the current stock of available materials that are to be used in the prototype manufacturing. The materials from the database can be selected manually or automatically by the software based on the technical parameters of the required material resulted from the calculation.

The methods used by the software for the pre-dimensioning are empirical and interpolation engineering methods commonly used in parachute design. On the virtual model more computational checks are computed using FEM methods for the parachute dynamic behavior in the deployment phase, flight attitude and landing.

Using the virtual model obtained after the pre-dimensioning phase, a drawing of the 3D model (Fig. 2c) is extracted. The 3D model undergoes a flow simulation and mechanical structural check for several phases of flight, starting at launch, stabilized flight, maneuvering flight and then landing. Maximum load estimation of forces on the canopy is done on launch/deployment phase, because at this moment the forces acting on the parachute constructive elements can exceed tens of times the forces encountered on stabilized flight, depending on the deployment altitude and speed. However, this is no longer valid for paragliders, because of the paraglider launching conditions, the forces acting on the canopy are quite low. Thus, in the case of paragliders in order to obtain the design forces, the simulation is made at the maximum load for a paraglider, namely at 80 km/h on a tight turn with 2-3 times the G-force acting on the canopy. During this phase in the design, we can calculate/estimate the fabric stretching and how it affects the wing aerodynamics. For the particular model developed in this project we are using NACA0012 airfoil for which we have precise measurements data done experimentally.

https://doi.org/10.24264/icams-2022.III.15

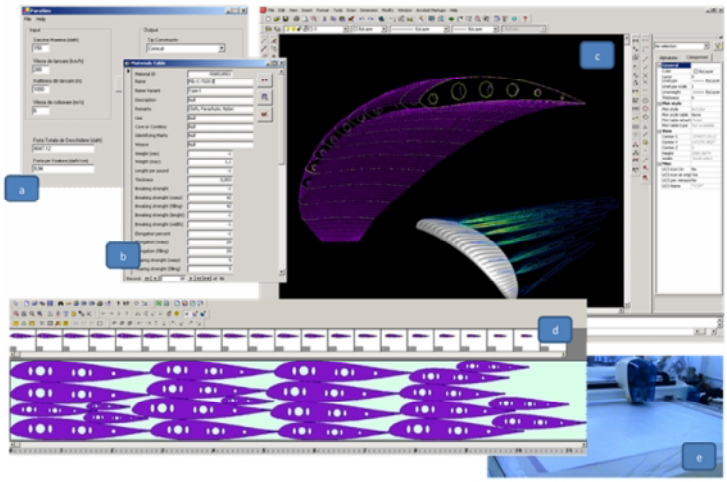

Figure 2. Computational workflow in parachute/paraglider design

Dimensional parameters can be modified if so desired after the simulation in done and checked for conformity (Ashby, 1999). 3D model resulted after this phase can be broken down into component parts and flatted down into patterns. The manufacturing markings are made on the fabric weft (Fig. 2d). The patterns are then sent to the cutting machine that performs fabric cutting (Fig. 2e). After this the parts are picked by an operator, marked and stitched according to the manufacturing process. The sewing is usually done with two needle seams on all structural parts.

Figure 3. Assembled main wing

Main Operational and Performance Requirements for the UAV Support System:

A1: Collecting information from where events occurred: fires, explosions, industrial accidents, floods, etc.;

A2: Detection of the NBC contamination level of an area;

https://doi.org/10.24264/icams-2022.III.15

A3: Patrolling of some areas (border, communication routes, infrastructure - electrical networks, transport pipelines etc.) for the purpose of preventive detection of emergency situations.

On the basis of the collected data, it is possible to move to the second phase of efficient incidents management through:

B1: Persistent surveillance of the area where events occur that have a continuous spatial and temporal evolution (fires, floods, natural disasters, industrial accidents, etc.);

B2: Appropriate equipment for intervention staff with PPE tailored specifically to the event produced;

B3: Locating and tracking in real time intervention teams;

B4: Search for missing persons in natural environments covered with dense vegetation;

B5: Temporary provision of radio communication coverage of mobile radio communications networks in isolated / hard-to-reach areas or where terrestrial networks are unavailable / degraded;

B6: Small-scale logistics transport in remote areas.

The airframe that can host the payload according to the operational requirements consists mainly in the propellers shroud and the servo actuators supports and control arms for wing steering (Fig. 4).

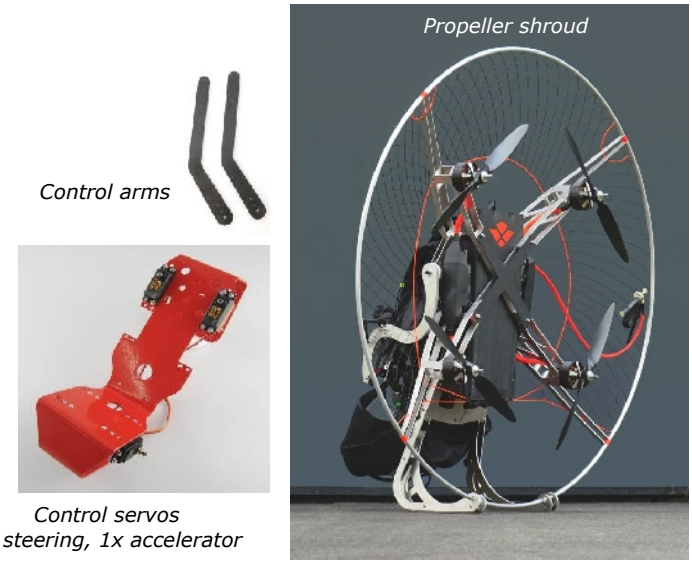

Figure 4. UAV airframe main components

The propulsion system consists in a quad propeller assembly where each propeller speed can be controlled independently. This assembly nullifies the propeller torque normally associated with single propeller assemblies and also gives extra steering and attitude control in addition to the wing controls.

https://doi.org/10.24264/icams-2022.III.15

CONCLUSIONS

The resulted flexible ram-air wing is a PPG glider with a 6.8 m projected wing span.

The fabrics used in the manufacture of the wing have superior characteristics of weight and resistance. The fabric used is a double rip-stop nylon 6.6 fabric with urethane amino modified poly siloxane coating for UV protection.

The propulsion system is comprised of an electrical quad propellers system for increased manoeuvrability and portability.

The modular configuration of UAV support system and load variants implemented so far on the prototype are:

- Video suite: permanently mounted (for observation, monitoring, cartography and GIS);
- Sensor detection and localization sensor set: optional (for locating missing persons, fire detection and wind direction detection);
- Detection and localization of personnel that are using Personnel Protective Equipment (PPE) (Toma *et al*., 2018) equipped with radio ID transponders;
- Cargo unit: optional (for emergency transport of medicines and supplies in remote areas, small cargo, up to 10kg).

At the time of writing for this article we are undergoing live tests in order to assess the system performances, operational limits and identification of possible design/manufacturing flaws.

REFERENCES

Ashby, D.L. (1999), "Potential Flow Theory and Operation Guide for the Panel Code PMARC_14", NASA TM-1999-209582.

Buyuk, M.F., Adnan, M., Antonin, H. and Karel, A. (2019), "Theoretical Model: Analysing Theoretically the Air Flow through Car Seatfoam Material", *Industria Textila*, 70, 4, 324-330, https://doi.org/10.35530/IT.070.04.1559B.

Cristian, I., Nauman, S., Boussu, F. and Koncar, V. (2012), "A Study of Strength Transfer from Tow to Textile Composite Using Different Reinforcement Architectures", *Applied Composite Materials*, 19, 3-4, 447-458, https://doi.org/10.1007/s10443-011-9215-x.

Flores, R., Ortega, E. and Onate, E. (2014), "Simple and Efficient Numerical Tools for the Analysis of Parachutes", *Engineering Computations*, 31(5), https://doi.org/10.1108/EC-10-2012-0247.

Knache, T.W. (1992), *Parachute Recovery Systems – Design Manual*, Para Publishing, Santa Barbara, California, 230-231.

Toma, D., Chirila, L., Popescu, A., Chirila, C. and Iordache, O. (2018), "Multifunctional Finishing Treatments Applied on Textiles for Protection of Emergency Personnel", *Industria Textila*, 69, 5, 357–362, https://doi.org/10.35530/IT.069.05.1585.

https://doi.org/10.24264/icams-2022.III.15

ACCOMPLISHING AND OPTIMIZING ROBOTIC SELF-NAVIGATION INTELLIGENCE FOR WAREHOUSE LOGISTICS THROUGH SENSOR FUSION AND ANTENNA LOCALIZATION

SEBASTIAN SBIRNA[1], SIMONA SBIRNA[2]

[1]*Ørsted, Dept. of Digital Transformation, Nesa Allé 1, 2820 Gentofte, Denmark, sebas@orsted.com; seby.sbirna@gmail.com*

[2]*University of Craiova, Faculty of Science, Chemistry Department, 107i Bucharest Street, Craiova, Romania, simona.sbirna@edu.ucv.ro; simona.sbirna@gmail.com*

Logistics automation has been the subject of many developments linking robotic hardware with improved quality and safety of work for warehouse employees. It is also a field where robotic navigation, route optimization and precise maneuvering are crucial to the competitiveness of the engineering product on the market. This research demonstrates a mathematical modeling method through which robots can navigate warehouse floors efficiently, using indoor positioning of high accuracy. Moreover, the paper also describes the hardware considerations taken into account when measuring the accuracy of the robot from achieving its destination on the floor plan. A prototype is creating, showing the sensor fusion interlinks for obstacle avoidance and distance mapping. Finally, the prototype and the algorithm are tested against eight static, as well as dynamic performance tests, in order to validate the performance of the system in static and dynamic interference environments. The goal of this paper is to present the engineering perspectives of optimizing a self-driving warehouse robot through utilization of the emerging technologies related to indoor positioning. This is presented through a prototype development of an Automated Guided Vehicle which will perform indoor positioning of itself across a warehouse floor plan and be able to avoid obstacles while driving towards its destination. Both the hardware description and the algorithmic modeling will be presented, accompanied by an extensive set of testing experiments, presented to determine the feasibility of our proposed developments in this field.

Keywords: robotics, navigational robots, trigonometric algorithm modeling.

INTRODUCTION

Robots development has met tremendous developments within the last years, as it can be seen in various papers Gupta *et al*. (2021), Lim *et al*. (2016), Kruse *et al*. (2013), Palamas and Ware (2013), Müller *et al*. (2004).

The logistics and planning of warehouse storage and transportation of stock is in a never-ending development. Modern companies have since the industrial revolution found out that optimization was a fundamental way to lower costs.

A new era of logistics has started, much more complex than people have experienced before. Previously, people would receive orders and walk to the location of that order for the specific object. Now, the objects are delivered to the person, this phenomenon being called "goods-to-person". Logistics automation (LA) is a commodity that companies are strongly focusing on, to make sure they are competitive in the market. LA is a way to improve the efficiency of the logistic operations within the warehouse or distribution centers. Optimization through innovation is a substantial part of the development happening in the field of logistics.

Replacement of employees by Automated Guided Vehicle (AGV) robots can cheapen the production costs and transfer the risk of work injuries on the shoulders of the robots – Balaji *et al*. (2022), Hasan *et al*. (2021). Employees in warehouses are instead allowed to focus more on management and planning, since the robots can lift, move and, in general, work faster and on heavier loads. However, more issues are to be considered when placing a robot in a warehouse.

https://doi.org/10.24264/icams-2022.III.16

The challenge is to make the robot self-navigating, obstacle avoiding, and able to pick, plug, to move objects and so on. The AGVs must be able to know their own position, where they are heading and how they may get there.

To keep our research focused on the development of a functional AGV which may eliminate the costs of redesigning warehouses, the following problem statement has been defined: "How can one create an AGV utilizing an innovative indoor positioning and navigation system?" We have to mention that the present paper will not have in focus the design development of the chassis of the AGV

Using encoders to control the motors of the AGV should significantly improve the accuracy of the algorithm and reduce the number of triangles that need to be computed and analyzed in order to reach the final target point. A method of detecting obstacles has also been implemented.

HARDWARE DESCRIPTION

Our engineering research is focused on the creation, optimization and testing of an AGV with essential logistic functionality. In order to help develop ideas about already existing navigational robots, conducting an analysis on previous research is fundamental in our process. There are three very clear aspects which all previous researches agree to be needing taking into consideration: map building, path planning and obstacle avoidance – Michalson *et al*. (2012).

The robot hardware system is divided into three main parts, a communication and localization part, an obstacle avoidance part and a motor part. The robot is meant for indoor automatic navigation within warehouses, therefore appropriate hardware choices must be considered, making it a specialized unit which is considered to function optimally under the assumption of an indoor (low interference) setting.

Communication and Localization Part

The advancements of technology have recently allowed fast communication and data transmission to be carried out by wireless networks and services. One area of ICT in which radio waves are used very frequently and in which they are vital to the functionality of the embedded systems is within localization, mapping and positioning.

UWB (Ultra-Wideband) is a recently-emerged wireless technology that uses very low power of spectral density (~ 0.5 mW) and a high frequency range (known possible range: from 3.1 to 10.6 GHz) in order to achieve, among other uses, accurate positioning of robotic systems even in small rooms (because of its mean error range of 100 mm). Theoretically, only very little interference is possible even on already used frequency bands, due to it using less power than the background noise.

By using an anchor/tag combination of 4 UWB transceiver anchors (which have similar functionality as a satellite in a GPS system) across the warehouse room, the system is able to determine the location of the tag and identify its coordinates on a map with user-specified xOy axes. We implemented such a system of localization across our testing warehouse room environment, and the signal of our system allows very accurate timing measurements (0.16 μs), penetrating through 1 or 2 thick concrete walls, which is enough for most indoor room localization scenarios. The maximum range that it can achieve, based on tests, is 200 meters in clear line-of-sight.

Whereas this paper does not focus on the design engineering of mechanical parts for such a robot, an image of one of our developed AGV prototype is presented in Figure 1.

https://doi.org/10.24264/icams-2022.III.16

Figure 1. Prototype chassis and component representation of the AGV

Obstacle Avoidance Part

The obstacle avoidance sensor was selected to be able to detect objects in a cone field from a certain distance in front of the robot vehicle, ensuring that the robot would not collide with other objects. Furthermore, it is necessary to be able to measure distances, allowing the AGV to gradually move close to an object, and to function in various environments without disturbances from e.g. ambient light. The sensor should be kept lightweight for low weight, power consumption and cost. The Ultrasonic Rangefinder sensor (USS) works through an internal clock, taking the time between the sensor emitting and receiving the sound wave, giving the sensor a cone-like field of view. Through cross-implementation of such sensors, an even wider angle of detection could be achieved. However, using several ultrasonic sensors may cause interference problems, where one sensor catches the ping of another (referred to as “ghost echo”).

Motor Part

A lot of research went into finding a motor suitable for our case, in order to lower the risk of movement hardware failure. From investigations of other research involving driving AGV robots, three main types of motors have been identified as potentially suitable: DC motors, Servo motors and Stepper motors. On the background of the investigation of the different motors, we have selected a brushed DC motor equipped with an encoder as the optimal motor for this project, as it balances out hardware expenses with the ability to provide decent amount of power with good precision. Our small AGV prototype, presented in Figure 1, was able to achieve speeds of 250 mm/s using two brushed DC motors. For the motor specifications we chose to prioritize torque over RPM, keeping in mind that the robot was essentially meant to function in a warehouse environment. The high torque allows the robot to carry more weight.

UWB LOCATION AND COMMUNICATION – SYSTEM TESTING

In order to test the location of the robot across the warehouse floor, we have analyzed the movement and location patterns of the AGV in a 3500 mm x 4800 mm room, with the UWB anchors placed on each of the four corners of the room.

The robot would be found at coordinates notated in “*x*-mm, *y*-mm” measured from the anchor to the robot’s position. We have performed three different sets of tests, one where the UWB system would be in clear sight of all the other anchor transceivers.

https://doi.org/10.24264/icams-2022.III.16

Then, separate test sets will be performed, where static and, respectively, dynamic interference would be added, due to both static and moving solid objects.

Testing without Interference

The first test only focused on the reliability of the UWB location. This means that there was no interference of any kind and the wireless tag was in clear sight of all the anchors. When examining the results from the system, it was clear that the found coordinates are really close to the true position, with only small differences (10-20 mm). This shows that the UWB positioning can be reliable if it is in clear sight of all the anchors. The second test was done in a similar way, modifying the number of calibrations and the original coordinates. We have noticed that the robot is found to be within 10-30 mm of its initial coordinates, showing that more static calibration measurements does not make the pinpointing more precise. Then, three more tests were executed without interference. The results are gathered in Table 1.

Table 1. Average UWB test results (without interference)

Number of samples	Number of calibrations	Original *x* coordinate (mm)	Original *y* coordinate (mm)	Average *x*-values (mm)	Average *y*-values (mm)	Average error *x* (mm)	Average error *y* (mm)
1	10	1000	1000	1018.37	1088.53	18.37	-11.47
1	30	900	900	912.74	931.47	12.74	31.47
10	10	1000	1000	978.81	961.19	-21.19	-38.81
10	30	1000	1000	1010.94	976.33	10.94	-23.67
10	30	1000	2000	1027.86	2060.86	27.86	60.86

Testing with Static Interference

Afterwards, we have chosen to test the same AGV system with introducing static interference, to get a more realistic view on how the UWB would behave in an environment where interference can happen, such as a warehouse. This was verified through a set of two more tests, in which we placed a static object between the robot and the axis. We note that interference has a tremendous impact on the results, leading to positioning errors of up to 200 mm. The errors are also very different depending on which location anchor is the one being interfered with. It appears that the coordinate attribute of the anchor that is having its signal interfered is pushing the axis coordinate location estimate further away from the original coordinate. The results are presented in Table 2.

Table 2. Average UWB test results (with static interference)

Number of samples	Number of calibrations	Original *x* coordinate (mm)	Original *y* coordinate (mm)	Average *x*-values (mm)	Average *y*-values (mm)	Average error *x* (mm)	Average error *y* (mm)	Interference axis
10	30	1000	2000	981.67	2105.83	-18.33	105.83	*x*
10	30	1000	2000	1206.44	1821.44	206.44	-178.56	*y*

Testing with Random Dynamic Interference

The last executed test was performed in a moving state of the robot, while the AGV was moving along the y-axis following a linear path, keeping the same x-coordinate constant.

https://doi.org/10.24264/icams-2022.III.16

The wireless environment had been naturally polluted by signals of various electronic equipment, just as it would be in an actual warehouse setting. Then, we are performing a signal reliability test, in which we are interested only in computing the x-coordinate of the AGV, since the robot should be keeping the x-coordinate constantly close to its original value, while moving on the *y*-axis. The results are shown in Table 3.

Table 3. Average UWB test results (with random dynamic interference)

Number of samples	Number of calibrations	Original *x* coordinate (mm)	Average *x*-values (mm)	Average error *x* (mm)	Free moving axis	Interval of movement (mm)
10	30	1590	1580.38	-9.62	*y*	0 - 3000

We can conclude that, even though the UWB location system produces errors regardless of the presence of interference or not, the error found due to static interference may sometimes be substantial. Therefore, it must be made sure that all the UWB anchors are in clear sight of the tag on the robot, otherwise it will not be able to maneuver accurately enough.

ULTRASONIC RANGEFINDER SENSOR – OBJECT DETECTION TESTING

In order to investigate the behavior and reliability of the USS obstacle detection sensor, a total of six tests were carried out, each measuring a different property of the sensor. The tests were conducted by setting up various real floorplan scenarios that the robot could encounter, so that we measure the most accurate responses of the sensor in various conditions.

The following types of tests were conducted: code testing; accuracy of length measurements; objects' material response; angle measurements; "ghost echo" test and also height test. For all of these tests, the USS was mounted on a box to simulate the height it would have had if it was mounted on the robot, since, when this testing was performed, several parts of the actual robot were not yet manufactured, thus requiring us to get a static estimate of the sensor's performance. Since each test is rather long in description of data and execution, we will present the aggregate insights which have been found about the USS sensor below. We have determined that taking an average of 5 sensor readings per obstacle distance measurement best produces a balance between speed of computation and accuracy of the measurements.

Regarding the accuracy on different types of object materials, various types of wood objects have yielded no change in measurement error, regardless of their different wood properties. When testing on a porous object (a blackboard sponge), it could be seen that the sponge absorbs some energy of the sound waves, as the measurement readings were largely inconsistent, therefore this test determined that the USS would not allow the AGV to avoid obstacles made of materials which can absorb a large amount of sound wave energy.

For this sensor, we have determined the angle of the sensor's field of view to be 30° for objects detected at 300 mm or more from the sensor. When trying to detect object in very close proximity of the sensor (100 mm or less), the field of view drops to below 15°, however we could assume that the robot would not approach objects this close without first identifying them from further away. For short-sight collisions, the sensor is reliable for scenarios where an object is placed in its straight line-of-sight.

https://doi.org/10.24264/icams-2022.III.16

CONCLUSIONS

The present paper has described an optimized Automated Guided Vehicle (AGV) which can efficiently navigate a warehouse floor plan using a combination of indoor, ultra-wideband wireless positioning sensors, and ultrasonic sensors for obstacle distance measurement and avoidance.

Using the method of wireless energy wave multilateration, this paper has proven that ultra-wideband technology may be used in future indoor robot navigation endeavors, however, as it can be seen from our tests, it must be mentioned that this method does suffer from high sensitivity to signal blocking and static interference.

On the other hand, the system has proven to be very stable to dynamic interference and wireless signal pollution.

The Ultrasonic Rangefinder sensor has proven to be an accurate choice for obstacle detection and avoidance within a cone field-of-view in front of the robot, however point-blank collisions could be detected even at small distances.

Whereas our prototype has only been using one of such USS sensors, we argue that a larger, multilateral field-of-view detection of obstacles can be achieved by utilizing an array of such sensors.

However, as we have discovered, such implementations will have to deal with the capturing of ultrasonic signal echo from one USS to another close-by USS within this sensor array, thereby requiring mitigation of this problem, known as "ghost echo".

Accurate indoor positioning sensors are at its early stages of development, however, with more research done into the algorithmic modeling area of localization, we can expect that wireless sensors will be in the forefront of providing the necessary hardware considerations of allowing high positioning accuracy in otherwise difficult-to-achieve scenarios.

REFERENCES

Balaji, H., Shaikh, Sh., Phalke, A. and Jadhav, Sh. (2021), "Design and Methodology of Automated Guided Vehicle – A Review", *IOSR Journal of Mechanical and Civil Engineering (IOSR-JMCE)*, Special Issue - AETM'16, pp. 29-35.

Gupta, A., Singh, A., Bharadwaj, D., Mondal, A.K. (2021), "Humans and Robots: A Mutually Inclusive Relationship in a Contagious World", *International Journal of Automation and Computing (IJAC)* – renamed as *Machine Intelligence Research (MIR)*, 18, pp. 185–203, https://doi.org/10.1007/s11633-020-1266-8.

Hasan, H.S., Abidin, M.S.Z., Mahmud, M.S.A. and Said, M.F.M. (2021), "Ultra-wideband Based on Automated Guided Vehicle for Localization", *International Transaction Journal of Engineering, Management & Applied Sciences & Technologies (ITJEMAST)*, 12(2), pp. 12A2C 1-8, https://doi.org/10.14456/ITJEMAST.2021.24.

Kruse, T., Pandey, A.K., Alami, R. and Kirsch, A. (2013), "Human-aware Robot Navigation: A Survey; Robotics and Autonomous Systems", *Robotics and Autonomous Systems*, 61(12), pp. 1726-1743, https://doi.org/10.1016/j.robot.2013.05.007.

Lim, J., Lee, S., Tewolde, G. and Kwon, J. (2016), "Indoor Localization and Navigation for a Mobile Robot Equipped with Rotating Ultrasonic Sensors Using a Smartphone as the Robot's Brain", *International Journal of Handheld Computing Research*, 7, pp. 1-11, https://doi.org/10.4018/IJHCR.2016010101.

Michalson, WR., Barrett, J. M., Gennert, M.A. and Center, J.L. (2012), "Analyzing and Modeling an IMU for Use in a Low-cost Combined Vision and Inertial Navigation System", *IEEE International Conference on Technologies for Practical Robot Applications*, pp. 19-24.

Müller, F., Buschmann, C. and Fischer, S. (2004), "Grid-based Navigation for Autonomous Mobile Robots", *Proceedings of the 1st Workshop on Positioning, Navigation and Communication*, https://doi.org/10.1007/978-3-642-35197-6_14.

Palamas, G. and Ware, J.A. (2013), "Sub-goal Based Robot Visual Navigation through Sensorial Space Tessellation", *International Journal of Advanced Research in Artificial Intelligence*, 2(11), pp. 38-45, https://doi.org/10.14569/IJARAI.2013.021106.

https://doi.org/10.24264/icams-2022.III.16

TECHNICAL AND HARDWARE IMPLEMENTATION OF A MODULAR TMS PROTOTYPE SYSTEM BY USING DATA MODELING, SENSOR COMPUTING AND WARNING SYSTEMS

SEBASTIAN SBIRNA[1], SIMONA SBIRNA[2]

[1]*Ørsted, Dept. of Digital Transformation, Nesa Allé 1, 2820 Gentofte, Denmark, sebas@orsted.com; seby.sbirna@gmail.com*

[2]*University of Craiova, Faculty of Science, Chemistry Department, 107i Bucharest Street, Craiova, Romania, simona.sbirna@edu.ucv.ro; simona.sbirna@gmail.com*

The great necessity of realizing appropriate monitoring of cooling and heating systems seems to be essential in the current context, as we approach the reality of interconnected smart cities and vehicles, which can regulate their energy consumption and, at the same time, maintain high standards on the equilibrium that they provide. This work outlines the essential technical considerations when modeling a working device prototype designed for monitoring of temperature inside vehicles and other areas. The main focus of this paper is to present and explain the algorithm that has been developed throughout three months of intensive prototyping of such a system. The scope of our final prototype includes an automatic alarm function for extreme cases, along with visual feedback in the form of messages on an LCD screen and color-coded LED signals. There is a specific focus regarding the collection and processing of accurate data for vehicles, with the consequence of releasing appropriate warnings to drivers or system owners. The main research focus is on explainability and reproducibility of our decisions behind the programming approach. Finally, we have demonstrated the means through which the mentioned solution is adaptable and cost-efficient, together with short considerations that would take the prototype into mass production.

Keywords: computerized monitoring, production engineering, sensor programming

INTRODUCTION

Owing to the constant expansion of technology and globalization, what was considered as an unreachable dream during the last century is now a common reality: easy delivery of food with refrigerated vehicles, directly to restaurants, shops or even right in front of your door.

Nevertheless, in order for the food to arrive to the customers in the proper conditions and in accordance with the respective regulations, these vehicles need to be properly equipped with temperature monitoring systems (TMS) that alert the clients of the system when there is a change in temperature that requires their attention. This research was conducted within the Department of Engineering and Science from Aalborg University Copenhagen, using helpful advice from Faculty of Science of the University of Craiova – Sbirna and Veng Søberg (2015).

Our research was done using Arduino as prototyping platform, Arduino being an open-source electronic prototyping platform allowing users to create interactive electronic objects (https://www.arduino.cc), which has been received with great interest from the programmers' community, new groups of interest appear very often, and there are a lot of projects available – Shakirovich Ismailov and Botirovich Jo'rayev (2022), Jadav *et al*. (2022), Shaheen *et al*. (2021), Roldán *et al*. (2015), Devika *et al*. (2014), Mellis *et al*. (2007).

The core concepts behind the sensor features will be discussed, along with the implementation of such features into the C++ programming language, custom-configured for Arduino projects – Hughes (2016).

https://doi.org/10.24264/icams-2022.III.17

PRODUCT DESCRIPTION

The system is divided into three main parts, namely: a sensor part, a monitoring part and a warning part. The two output parts will be placed near the driver and the input part will be placed in the storage compartment to measure the temperature. The system is a dependent system because it is optimized for cooling trucks, and the features that it has are designed to be used in such vehicles. It can be used independently in other places, but some of its features might be unnecessary and/or redundant, depending on the application.

The Sensor Part

The sensor part of the system (Figure 1) is where the temperature is measured with three sensors. They work individually and are not dependent on each other. The sensors are meant to be placed in three different locations in the cooling compartment of the truck, one in the front, one in the middle and one in the back. Thus, the sensors are separated from the monitoring and warning part of the system.

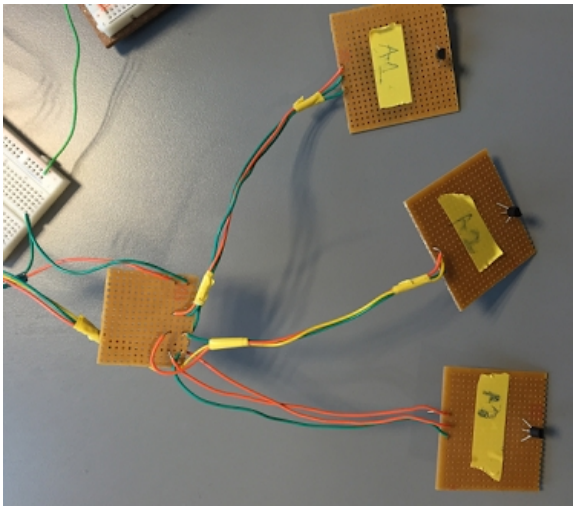

Figure 1. The sensor part of the system

The Monitoring Part

The monitoring part of the system (Figure 2) is its central part, where the current temperature in the cooling compartment is displayed. The wanted temperature range can be adjusted via buttons placed nearby, and, also, pressing a button can stop the sound alarm. If the alarm is stopped, it will start again after some time if the temperature is still outside the acceptable range, and after being stopped two times while the temperature is still outside the acceptable range, it will not be possible to be stopped a third time before it is adjusted correctly.

The display shows the temperature from each of the three sensors individually and also tells the driver if the temperature is “hot”, “warm”, “good”, “cool” or “cold”.

https://doi.org/10.24264/icams-2022.III.17

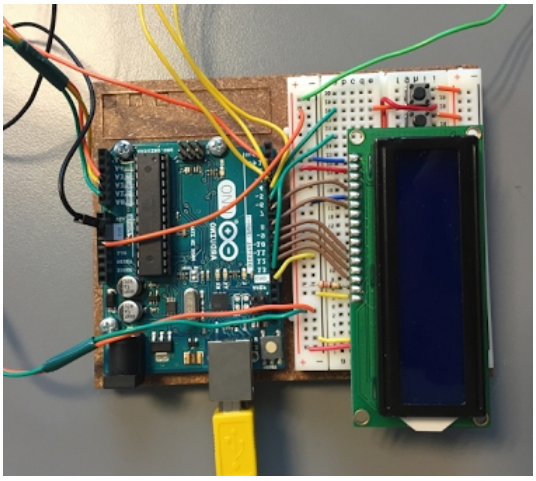

Figure 2. The monitoring part of the system

The Warning Part

The warning part of the system (Figure 3) alerts the driver that something is wrong with the temperature in the cooling compartment of the vehicle, without disturbing the driver more than necessary. The warning board announces the driver both visually and audibly to make sure that the driver notices the warning. It consists of a small speaker (Piezo) and three LEDs. They indicate if the temperature is high, good or low. The red LED is lighting when the temperature goes above a superior given temperature limit, the blue one when the temperature goes beneath an inferior given temperature limit and the green one when the temperature is within the limit range. The speaker informs by audio signals whenever the temperature is reaching an extreme level (“hot” or “cold”).

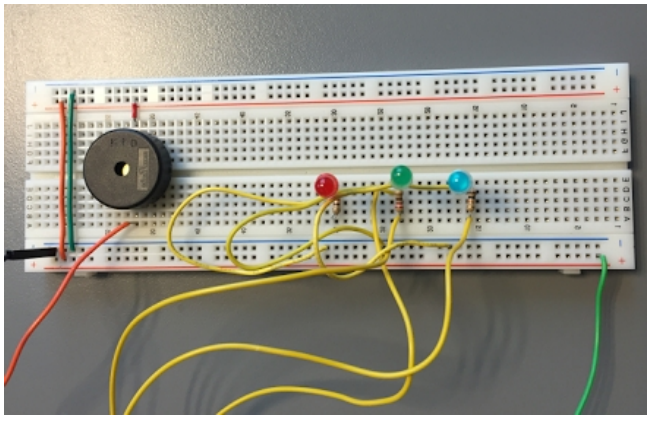

Figure 3. The warning part of the system

https://doi.org/10.24264/icams-2022.III.17

TEMPERATURE RANGES

The main goal of the sensor is to provide both temperature monitoring and warning functionalities to the clients, so one of our first questions in the development process was: "when will the sensor show that the temperature is good, and what will it do otherwise?"

We decided to set the initial "goodTemperature" at 5.0°C, with a no-warning range (a "good" range of values) between ± 0.9°C of the "goodTemperature" ("good" state); a mild-warning range between 1.00 and 1.9°C above or below the "goodTemperature" ("warm" or "cool" state); and a strong-warning range from 2.0°C above or below "goodTemperature" onwards ("hot" or "cold" state).

These ranges of values will be extremely important for our further computations within the sensor code, for they constitute a means to analyzing, giving meaning and working easier with the raw sensor values.

CODE SUBROUTINES

Each individual subroutine of the code for this sensor has to be presented, along with its role in the greater whole of the program – Pan and Makinwa (2022). The functions have been ordered in accordance to their order in the execution flow and will be presented in what follows.

• Subroutine no. 1 – void setup()

The first function to be executed, setup() mainly takes care of the pin mode configurations and displays a welcome message for the client on the LCD, after which it shows the hard-coded "goodTemperature" on the screen and lets the user decide if this temperature value needs adjustment or not.

• Subroutine no. 2 – void setGoodTemperature()

This function will take care of appropriately updating the "goodTemperature" according to the needs of the clients, through the pressing of two buttons (left for decrease, right for increase) which increase or decrease the value by 1.0°C each time one of the buttons is pressed (the buttons can also be long-pressed for a continuous increase or for a continuous decrease of the "goodTemperature" value, until the button is released).

• Subroutine no. 3 – void setGoodTemperatureLCD()

This function updates the value of "goodTemperature" on the LCD screen every time a button is pressed and from setGoodTemperature().

• Subroutine no. 4 – void loop()

This is the function which will be executed over and over again by the Arduino, as soon as setup() and its relevant subfunctions end, and until the program is stopped or reset, so all functions which will be called from loop() or from its subfunctions will also be executed endlessly, allowing us to do most of our mathematical calculations within this function; while the translation of the results into something more easy to work with, as well as the update of the warning devices, will be done in subfunctions of loop().

• Subroutine no. 5 – int checkTemperatureState(float temperature)

The function checkTemperatureState() is the one which assigns an integer number between -2 and 2 (hence, a temperature state) to each of the measured temperature values. The states are saved in a vector named, for good practice, "temperatureState" – Pan and Makinwa (2022) and only after these assignments will the function setState() be executed.

https://doi.org/10.24264/icams-2022.III.17

• Subroutine no. 6 – void setState(int i, int currentState)

This function is part of the program because of a problem that needed to be solved, the warning sound being supposed to turn on just after one or more thermosensors have measured a “hot” or “cold” value, and is supposed to turn off only after no thermosensors have measured a “hot” or “cold” value in the last cycle (Figure 4).

Figure 4. Displaying temperature on the monitoring part of the system

• Subroutine no. 7 – void updateLCD()

This function first calls updateLCDMessages() and then updates the second (bottom) row of the LCD with the current temperatures read from each of the three sensors. Because of size limitations, the sign “°C” is only shown once on the LCD, at the bottom right corner, to inform the user that the temperatures are in degrees Celsius (Figure 4).

• Subroutine no. 8 – void updateLCDMessages(int tmpState)

This function takes care of updating the first (top) row of the LCD with the temperature states corresponding to the values read from each of the three sensors. The states will be shown in capital letters, with one whitespace in between each of the states.

• Subroutine no. 9 – void updateLEDs()

This function updates the LEDs of the prototype each time it is executed, by first turning off all the LEDs and then turning back on only those that correspond to the currently registered temperature states. Because the time during which all the LEDs are off is extremely short (one or a few milliseconds), the eye cannot notice this change.

• Subroutine no. 10 – void updatePiezo()

By long-pressing both buttons of the equipment, the user may switch off the purposefully-done annoying sound of the Piezo. However, due to forgetfulness or lack of responsibility, a user may simply want to turn off the sound warning as soon as it starts, without also taking the necessary action of adjusting the temperature accordingly.

• Subroutine no. 11 – void piezoWarning()

This function may or may not be executed, depending on some criteria, and is responsible for: switching the sound warning on or off; deciding how high a pitch is given as output; as well as resetting the remaining number of times that a user can switch off the alarm, the alarm sound starting the first time a “cold” or “hot” temperature state is detected, and will stop completely only when all the calculated temperature states are neither “hot” nor “cold”.

https://doi.org/10.24264/icams-2022.III.17

CONCLUSIONS

The paper has presented most of the programming paradigms behind our chosen approach to achieve certain functionality by using specific components. Through many different incremental updates and improvements across the allowed timespan of our research, a reliable, consistent and easy-to-use temperature monitoring system has been developed. A great advantage of our system is that it is designed to be modular, so that if, in the future, users would need to add extra monitoring services, or perhaps adjust its appearance, it would be possible with very little obstructing factors, as while it is still in its prototype phase, it could easily be implemented by solving the necessary manufacturing hindrance factors (such as replacing connections through breadboards with soldered components or an open-circuited design of the system with a laser-cut acrylic glass casing).

An addition to the program of the system that would be very representative for our product would be the implementation of wireless communication functionality between different modules of the system, so each would gain a lower level of interdependency between components, the risk of errors would be minimized and our product would blend into most of the refrigerated vehicles available, regardless of their internal design.

It is worth mentioning the fact that, in the final product version of the program, new libraries and functionality might be implemented for many different areas.

Some of the improvements could be: data logging, wireless communication between sensors and micro-controller, more warning modules and/or states, the addition of moisture reading and warning, the ability of clients to change the mild and strong warning threshold values, showing of the readings and warning states in Fahrenheit grades and many more.

These changes can only be taken into account if the cost of manufacturing and services will increase by a reasonable amount, since one of the main reasons that a client should choose our solution over the competition's is the low cost and high reliability of the product and of its services.

REFERENCES

Devika, S.V., Khamuruddeen, Sk., Khamurunnisa, Sk., Thota, J. and Shaik, K. (2014), "Arduino Based Automatic Plant Watering System", *International Journal of Advanced Research in Computer Science and Software Engineering (IJARCSSE)*, 4(10), pp. 449-456.

Hughes, J.M. (2016), *Arduino in a Nutshell: A Desktop Quick Reference*, O'Reilly Media, Inc., Sebastopol, California, USA.

Jadav, V., Machhi, N., Biawat, D., Das, R. and Mali, J. (2022), "Review for Arduino Based Portable Ventilator for COVID-19", *International Journal of Creative Research Thoughts (IJCRT)*, 10(1), pp. d214-d217.

Mellis, D.A., Banzi, M., Cuartielles, D. and Igoe, T. (2007), "Arduino: An Open Electronics Prototyping Platform", *Proc. Chi*, pp. 1-11.

Pan, S. and Makinwa, K.A.A. (2022), *Introduction. In: Resistor-based Temperature Sensors in CMOS Technology. Analog Circuits and Signal Processing*, Springer Nature Switzerland AG, Cham, https://doi.org/10.1007/978-3-030-95284-6.

Roldán, J.J., Joossen, G., Sanz, D., del Cerro, J. and Barrientos, A. (2015), "Mini-UAV Based Sensory System for Measuring Environmental Variables in Greenhouses", *Sensors*, 15, pp. 3334-3350, https://doi.org/10.3390/s150203334.

Sbirna, S. and Veng Søberg, P. (2015), "P1 Project: MOE 1, Group 4, Semester Project", Aalborg University, Copenhagen, Denmark.

Shaheen, Y.S.A., Alkafrawi, H.M.I., Al Aga, T.R.S., Elkafrawi, I.M. and Omar Imaeeg, M.A. (2021), "Arduino Mega Based Smart Traffic Control System", *Asian Journal of Advanced Research and Reports*, 15(12), pp. 43-52, https://doi.org/10.9734/ajarr/2021/v15i1230449.

Shakirovich Ismailov, A. and Botirovich Jo'rayev, Z. (2022), "Study of Arduino Microcontroller Board", *Science and Education Scientific Journal*, 3(3), pp. 172-179.

https://doi.org/10.24264/icams-2022.III.17

NEUTRALISATION AND BATING OF HIDE UNHAIRED USING SODIUM SILICATE AND SODIUM SULPHIDE

GERDA ŠLEKIENĖ[1], RENATA BIŠKAUSKAITĖ[1], VIKTORIIA PLAVAN[2], VIRGILIJUS VALEIKA[1]

[1] *Kaunas University of Technology, Polymer Chemistry and Technology Department, Radvilėnų pl. 19, 50254, Kaunas, Lithuania, gerda.slekiene@ktu.lt; renata.biskauskaite@ktu.lt; virgilijus.valeika@ktu.lt*

[2] *Kyiv National University of Technologies and Design, Technologies of Polymers and Chemical Fibers, Applied Ecology Department, Nemirovich-Danchenko str. 2, 01011 Kyiv, Ukraine, plavan.vp@knutd.edu.ua*

Various methods of neutralisation of hide unhaired with sodium silicate and sodium sulphide have been investigated seeking to reduce or refuse ammonium sulphate conventionally applied for the neutralisation. Due to the high release of ammonia into the environment, alternative materials are being sought that do not impair the properties of the hide being processed and that a high-quality chromed semi-finished product of leather can be obtained. In the research, different methods of hide neutralisation and their influence on subsequent hide treatment processes qualitative indexes of the obtained leather were analysed and described. It has been found that after unhairing with sodium silicate and sodium sulphide hide, it is appropriate to neutralise and bate the hide by adding 1 % ammonium sulphate, 0.8 % lactic acid and 0.15 % proteolytic enzyme preparation OROPON ON2. To obtain the best quality of chromed semi-finished product of leather, it is advisable to pickle the hide using not more than 1 % sulfuric acid. In this way, neutralised-bated, pickled and chromed leather's quality meets the quality requirements for chromed semi-finished product of leather.

Keywords: unhairing, pelt, neutralisation, ammonia, lactic acid

INTRODUCTION

The leather industry earns special attention because of its strong potential for foreign exchange earnings and employment generation prospects. This industry has developed enormously over the past decades; since then, leather has become a material of choice in the world of fashion. However, this industry, like many others, is facing stringent environmental regulations worldwide, due to vast usage of toxic chemicals and generation of hazardous waste (Khambhaty, 2020).

Despite the fact that liming with sulphides is still the most commonly used process for obtaining unhaired pelts, new methods of hide/skin unhairing-derma opening up are being intensively developed. The main disadvantage of sulphide liming is that the cleaning of unhairing solutions, polluted with lime, sulphides and products of protein degradation remains very difficult and expensive (Sirvaityte *et al*., 2016).

After liming, lime in the unhaired pelt is no longer required, and in most cases, it has a detrimental effect on subsequent tannage. Accordingly, the lime must be removed. Unfortunately, the deliming is not simple neutralisation of lime, and, due to this, only specific chemical materials can be applied. The deliming materials have to have ability to react with lime forming soluble in water compounds; to decrease the pH of the pelt; to remove swelling of the derma tissue (Sivakumar *et al*., 2015).

Removal of the calcium is achieved by decreasing the pH value with acidic chemicals. By acidifying the collagen at pH – 12.5, the amino groups are protonated. Thereby, positive charges neutralise negative charged collagen, and the fibre structure opens, facilitating chemicals to penetrate. In conventional deliming, ammonium salts

https://doi.org/10.24264/icams-2022.III.18

are preferred for this application because they enable comparable short process times and buffer the pH to around 9. When the pH value is not stable, the selection of convenient bating enzymes for the following working step is not possible (Prokein *et al*., 2020; Covington, 2009). Unfortunately, ammonium salts generate considerable amount of ammonia, making tannery environment unhealthy (Sivakumar *et al*., 2015).

Probably, the best way to avoid the pollution caused by the sulphide-lime unhairing is to refuse the employing of lime overall. Many new methods are developed that allow replacing lime with other materials. Firstly, it is enzymatic unhairing. There are a few possible ways to adopt enzymes for the unhairing process. The first one is when the enzymes are applied for a pure enzymatic process, in such a case, the unhairing effect is achieved, owing to the enzyme used (Shrinivas and Naik, 2011; More *et al*., 2017). The next way is to use enzyme and oxidising agents. In such a case, enzymes are used for the main unhairing and oxidisers are used for degrading of hair remnants. Proteases that act in an alkaline or acidic medium are used in such cases (Valeika *et al*., 2012). Unfortunately, so far, such unhairing methods have been applied merely at laboratory scale (Khambhaty, 2020).

The next possibility is to replace lime with other alkalis such as sodium hydroxide (Valeika *et al*., 2000) or sodium aluminate (Sirvaityte *et al*., 2016). In addition, the application of soluble silicates is very promising (Sirvaityte *et al*., 2015).

It is very important that absence of lime in a pelt allows the use of wide spectra of neutralising materials (Zeng *et al*., 2011; Sirvaityte *et al*., 2007; Crudu *et al*., 2012) because there is no lime and there is no possibility to form insoluble calcium compounds.

The main aim of the present research was to investigate neutralisation of unhaired hide using sodium silicate to reduce the use of ammonia compounds or replace them and to assess the influence of the neutralisation on chromed leather properties.

EXPERIMENTAL

Salted cowhide was used as a raw material for this study. The soaked and washed hide was cut into 5x10 cm pieces and experimental series were prepared from these pieces. An unhairing-opening (experimental) up of derma structure of samples was carried out as follows: H_2O – 100%, temperature 20-22°C, Na_2SiO_3 2%, 2 hours run continuously, Na_2S (100%) 1%, 2 hours run continuously, H_2O – 50%, NaOH 0.5%, 2 hours run continuously, later 5 minutes every 4 hours, total process duration 24 hours; drain. Washing: H_2O – 100%, temperature 36-38°C, 0.5 hour run continuously, drain; again H_2O – 100%, temperature 36-38°C, 0.5 hour run continuously, drain. The pickling and chroming of neutralised-bated samples were carried out accordingly to conventional technology.

The enzyme preparation (EP) OROPON ON2 “TFL” (Switzerland) was employed for the bating process. The amount of collagen protein was estimated from the amount of hydroxyproline in the solution, and the amount of hydroxyproline was determined using a photo-colorimetric method (Zaides *et al*., 1964). The shrinkage temperature of hide samples, the pH of pelt and chromed leather, and the amount of chrome compounds in leather were determined according to standards (Standard ISO, 2002; Standard ISO, 1977; Standard ISO, 2009). Shrinkage temperature of chromed leather was determined as described in the literature using special equipment and replacing the distilled water with glycerol (Golovteeva *et al*., 1982). The concentration of chromium

https://doi.org/10.24264/icams-2022.III.18

in solution was determined according to the method described in the literature (Golovteeva *et al*., 1982).

RESULTS AND DISCUSSION

Twelve compositions were tested to neutralise the pelt after unhairing with sodium silicate and sodium sulphide. For all variants, some of the neutralisation conditions were the same: H_2O 40% (percent are based on pelt weight), temperature 36-38°C, run continuously. Bating (in neutralisation solution) conditions were the same for all variants: H_2O 100%, EP OROPON ON2 0.15%, 1 hour run continuously. Neutralisation variants:

1. $(NH_4)_2SO_4$ 2%, 30 min.; $(NH_4)_2SO_4$ – 2%, 30 min. (control);
2. $(NH_4)_2SO_4$ 2%, 1 hour;
3. $(NH_4)_2SO_4$ 1%, 1 hour;
4. Lactic acid 2.4%, 30 min.; lactic acid 2.4%, 30 min.;
5. $(NH_4)_2SO_4$ 1%, 20 min.; lactic acid 0.8%, 20 min.; lactic acid 0.8%, 20 min.;
6. H_3BO_3 1.5%, 30 min.; H_3BO_3 1.5%, 30 min.;
7. $(NH_4)_2SO_4$ – 1% 20 min.; $NaCH_3COO$ 0.15%, CH_3COOH 1% 20 min.; $NaCH_3COO$ 0.15 %, CH_3COOH 1 % 20 min.;
8. $NaCH_3COO$ 0.2 %, CH_3COOH 1.5% 20 min.; H_3BO_3 1.5%, 20 min.; lactic acid 0.4% 20 min.;
9. $(NH_4)_2SO_4$ – 1%, 20 min.; lactic acid 0.4% 20 min.; lactic acid 0.4% 20 min.;
10. $(NH_4)_2SO_4$ – 1%, 30 min.; lactic acid 0.4% 30 min.;
11. $(NH_4)_2SO_4$ – 1% 10 min.; $NaCH_3COO$ 0.2%, CH_3COOH 0.5% 50 min.;
12. $NaCH_3COO$ 0.2 %, CH_3COOH 0.5% 10 min.; lactic acid 0.4% 50 min.

The quality of neutralisation was assessed determining pH of solution and pelt after process; shrinkage temperature and porosity of pelt; amount of removed collagenous proteins (Table 1) and observing the colouring of cross-section of pelt by phenolphthalein.

Table 1. Indexes of neutralisation process

Neutralisation variant	Index				
	pH of solution	pH of pelt	Shrinkage temperature of pelt, °C	Porosity of pelt, %	Removed collagen proteins, g/kg of pelt
1 (control)	8.52	8.36	63.8	66.5	0.40
2	8.82	8.54	62.7	65.6	0.51
3	9.09	8.83	63.0	64.2	0.42
4	3.01	3.51	47.7	58.2	0.26
5	4.26	6.86	62.5	63.9	0.40
6	8.18	8.59	63.2	59.1	0.77
7	4.51	4.28	57.8	65.3	0.27
8	4.52	4.90	60.3	64.0	0.40
9	8.27	8.37	63.7	65.2	0.09
10	8.92	-	-	-	-
11	8.48	8.31	63.8	67.01	0.11
12	5.95	-	-	-	-

Note: Shrinkage temperature of pelt after unhairing 57.0 °C, porosity 55.8 %.

The pelts were completely neutralised during two hours of treatment with the neutralising materials and the enzyme by almost all neutralisation methods (1-9 and 11),

https://doi.org/10.24264/icams-2022.III.18

with the exception of variants 10 and 12, which resulted in a reddish discolouration of the pelt's cross-section by the application of phenolphthalein.

As the most promising 2nd and 9th variants were chosen for the further experiments. Therefore, the pelt after neutralisation according to 1 (control), 2 and 9 variants was pickled using conventional technology (percent are based on pelt weight): H_2O 100%, NaCl – 5.5%, 15 min.; HCOONa 1%, 20 min.; H_2SO_4 0.5%, 15 min.; H_2SO_4 0.5%, 15 min.; H_2SO_4 0.5%, 5 hours; regime run continuously. The results are presented in Table 2.

Table 2. Indexes of pickling dependently on neutralisation method

Neutralisation variant	Index				
	pH of solution	pH of pelt	Shrinkage temperature of pelt, °C	Porosity of pelt, %	Removed collagen proteins, g/kg of pelt
1 (control)	2.74	2.84	43.0	56.8	0.03
2	2.73	2.78	42.7	64.4	0.04
9	2.70	2.77	40.5	55.8	0.05

The obtained data show similar action of pickling on variously neutralised pelt. Herewith, there are some differences in shrinkage temperature and porosity after pickling.

The pickled samples were chromed according to conventional technology. The results are presented in Table 3.

Table 3. Indexes of chroming dependently on neutralisation method

Neutralisation variant	Index				
	pH of solution	Shrinkage temperature of leather, °C	Cr_2O_3 in leather, %	Exhaustion of Cr_2O_3, %	Porosity of pelt, %
1 (control)	3.23	84.3	2.42	46.9	67.6
2	3.23	86.7	2.32	44.9	68.3
9	3.19	90.0	2.37	51.6	66.9

The chroming was low quality independently on the neutralisation method. The main reason was too low pH after chroming and, accordingly, bad chromium fixation. Since the pH of pickled pelt and chroming solution depends on pH after pickling, presumably, the amount of acid for pickling of such pelt should be reduced.

Therefore, pelt was neutralised according to the 9th method and pickled in three ways: 1 – conventionally (1.5% H_2SO_4); 2 – using 1% H_2SO_4; 3 – using 1% H_2SO_4 and 1% CH_3COOH (other conditions were the same). Conventional chroming was carried out for the pickled pelts. The results are presented in Table 4.

Table 4. Indexes of pickling and chroming dependently on pickling method

Pickling variant	Indexes						
	Pickling			Chroming			
	pH of solution after pickling	pH of pelt after pickling	Shrinkage temperature after pickling, °C	pH of leather after chroming	Exhaustion of Cr_2O_3, %	Cr_2O_3 in leather, %	Shrinkage temperature of leather, °C
1	2.73	2.86	35.7	2.90	63.4	3.43	104.1
2	3.73	3.72	48.7	3.38	76.7	4.61	114.0

https://doi.org/10.24264/icams-2022.III.18

3	3.54	3.21	43.7	3.04	61.4	3.36	101.1

Summarising the results in Table 4 it can be concluded that it is preferable to add 1 % sulphuric acid during pickling to produce qualitative semi-finished chromed product.

CONCLUSIONS

The pelt obtained by unhairing-derma opening up with the use of sodium silicate and sodium sulphide can be qualitative neutralised and bated with 1 % of ammonium sulphate, 0.8 % of lactic acid and adding 0.15 % of the enzymatic preparation OROPON ON2 for the bating. Since the conventional pickling process produces a too acidic pelt, less sulphuric acid (1%) needs to be added to the pickling of such pelt. The chromed semi-finished product obtained after such pickling and chroming had a high shrinkage temperature (114°C), a high content of chromium compounds in the derma (4.6%) and a relatively high exhaustion of chromium compounds during the chroming was reached.

REFERENCES

Covington, A.D. (2009), *Tanning Chemistry: The Science of Leather*, RSC Publishing, Cambridge.

Crudu, M., Gaidau, C., Crudu, A., Popescu, M. and Ionescu, M. (2012), "Innovative Material-Technology System for Reduction of Environmental Pollution with Salts", *Polymer Chemistry and Technology: Proceedings of Scientific Conference Chemistry and Chemical Technology*, Kaunas, Lithuania.

Golovteeva, A.A., Kutsidi, D.A. and Sankin, L.B. (1982), *Laboratornyj praktikum po khimiyi i tekhnologiyi kozhy i mekha*, Legkaiya i Pischevaiya Prom. Moscow (in Russian).

Khambhaty, Y. (2020), "Applications of Enzymes in Leather Processing", *Environmental Chemistry Letters*, 18(3), 747-769, https://doi.org/10.1007/s10311-020-00971-5.

More, S.Y., Bholay, A.D. and Nalawade, P.M. (2017), "Eco-Friendly Applications of Bacterial Extracellular Alkaline Protease", *IOSR Journal of Environmental Science, Toxicology and Food Technology*, 11(4), 81–87, https://doi.org/10.9790/2402-1104018187.

Prokein, M., Chrobot, A., Renner, M. and Weidner, E. (2020), "Free of Salt High-pressure Deliming of Animal Hides", *Environmental Science and Pollution Research*, 27, 35567–35579, https://doi.org/10.1007/s11356-020-09765-2.

Shrinivas, D. and Naik, G.R. (2011), "Characterization of Alkaline Thermostable Keratinolytic Protease from Thermoalkalophilic *Bacillus halodurans* JB 99 Exhibiting Dehairing Activity", *International Biodeterioration and Biodegradation*, 65(1), 29–35, https://doi.org/10.1016/j.ibiod.2010.04.013.

Sirvaitytė, J., Beleska, K. and Valeika, V. (2016), "Lime Free Unhairing: Sodium Aluminate as an Alternative Towards a Cleaner Process", *Journal of the American Leather Chemists Association*, 111(11), 406-412.

Sirvaityte, J., Beleska, K., Valeikiene, V., Plavan, V. and Valeika V. (2015), "Immunization Action of Sodium Silicate on Hair: Part 2 Hair-save Process Based on Lime Substitution by Sodium Silicate", *Journal of the Society of Leather Technologists and Chemists*, 99(5), 231-237.

Sirvaitytė, J., Valeika, V., Beleska, K. and Valeikiene, V. (2007), "Action of Peracetic Acid on Calcium in Limed Pelt", *Journal of the Society of Leather Technologists and Chemists*, 91(3), 123-127.

Sivakumar, V., Ponnusawmy, C., Sudalaimani, K., Rangasamy, T., Muralidharan, C. and Mandal, A.B. (2015), "Ammonia Free Deliming Process in Leather Industry Based on Eco-benign Products", *Journal of Scientific and Industrial Research*, 74(9), 518-521.

Valeika, V., Balciuniene, J., Beleska, K. and Valeikiene, V. (2000), "Lime-free Unhairing: Part 3 Influence of Unhairing Method on Chemical, Physical and Mechanical Properties of Pelt and Leather", *Journal of the Society of Leather Technologists and Chemists*, 84(4), 165-169.

Valeika, V., Beleska, K. and Sirvaityte, J. (2012), "Alkali-free Method of Hide Preparation for Tanning", *Brazilian Journal of Chemical Engineering*, 29(2), 315–323, https://doi.org/10.1590/S0104-66322012000200012.

Zaides, A., Mikhailov, A. and Pushenko, O. (1964), "Modiphitsirovanyi method opredeleniya oksiprolina", *Biokhimiya*, 1, 5-6 (in Russian).

Zeng, Y.H., Lu, J.H., Liao, X.P., He, Q. and Shi, B. (2011), "Non-ammonia Deliming Using Sodium Hexametaphosphate and Boric Acid", *Journal of the American Leather Chemists Association*, 106(1), 257- 263.

*** (1977), Standard ISO 4045:1977. Determination of pH.

https://doi.org/10.24264/icams-2022.III.18

*** (2002), Standard ISO 3380: 2002. Leather – Physical and mechanical tests – Determination of shrinkage temperature up to 100 degrees C.
*** (2009), Standard ISO 5398-2: 2009. Leather - Chemical determination of chromic oxide content - Part 2: Quantification by colorimetric determination.

https://doi.org/10.24264/icams-2022.III.18

EFFICACY OF CAPSAICIN ON CELL ADHESION AND INVASION OF ORAL PATHOGENS

ERHAN TEK[1], NIZAMI DURAN[2]

[1]*Mustafa Kemal University, Veterinary Faculty, Microbiology Department, Hatay-Türkiye, etek@mku.edu.tr*

[2]*Mustafa Kemal University, Medical Faculty, Microbiology Department, Hatay-Türkiye, nizamduran@hotmail.com*

Streptococcus pyogenes, *Streptococcus mutans*, and *Candida albicans* are important human pathogens and their infections in the mouth, mouth, and throat are important. Prophylaxis against oral and respiratory tract infections is of great importance in terms of both reducing the use of antibiotics and lowering the infection frequency. This study investigated the antimicrobial activity of Capsaicin against *S. mutans*, *C. albicans*, and *S. pyogenes*. Non-cytotoxic concentration of Capsaicin was determined in the Vero cell line by the MTT method. Efficacy studies were performed within these determined non-cytotoxic concentrations. The efficacy of single and different combinations of these three biological components on cell adhesion and invasion. The non-toxic concentration of capsaicin on Vero cells was <1.35 µg/ml. Capsaicin exhibited significant antimicrobial activity against *S. pyogenes*, *S. mutans*, and *C. albicans*. Moreover, capsaicin was statistically significantly effective against host cell adhesion and invasion against *S. mutans*, *S. pyogenes* and *C. albicans* compared to the control group. The results showed that capsaicin is a highly potent antibacterial agent against *S. pyogenes*, and *S. mutans*, as well as an important prophylactic agent for fungal infections. As a result, we think that capsaicin is a useful molecule for the provision and maintenance of both respiratory diseases and oral health.

Keywords: *S. pyogenes*, *S. aureus*, *C. albicans*, throat infection, proliaxia, lozenge

INTRODUCTION

A wide variety of microorganisms can cause infections in the human oral cavity. The mouth is a unique region colonized by bacteria, fungi, viruses, and even protozoa. Throat infections are mainly caused by viruses, and bacterial and fungal pathogens are also important infectious agents for the oral region (Zhang *et al*., 2018).

Among the pathogens that cause throat infections, *Streptococci*, *staphylococci*, and *Candida* are among the most important pathogens that come to mind first (Vlastarakos *et al*., 2007). *Streptococcus pyogenes* can cause late complications of rheumatic fever and glomerulonephritis. In addition, it is one of the most frequently detected bacterial agents of pharyngitis and skin infections. *Streptococcus pyogenes* is one of the leading pathogenic bacteria infecting children and adolescents and can cause a wide variety of infections. It is reported that more than 600 million throat infections are caused by *S. pyogenes* in the world annually (Fiedler *et al*., 2015; Walker *et al*., 2014).

Dental caries is one of the most common infectious diseases in the world. It is a serious threat to oral and dental health. One of the main pathogens that play an important role in the development of dental caries is *Streptococcus mutans*. *S. mutans* is an acidogenic and acidic Gram-positive bacterium that naturally lives in the oral cavity. The natural habitat of *S. mutans* is the human oral cavity, more specifically dental plaque, a multi-species biofilm that forms on the hard surfaces of the tooth (Krzyściak *et al*., 2014; Struzycka, 2014).

Candida can cause serious infections, especially in children, the elderly, and immunocompromised hosts. *Candida albicans* is a pathogenic yeast that causes oral, vaginal, and systemic infections. In recent years, it has been reported that there is a

https://doi.org/10.24264/icams-2022.III.19

significant increase in the frequency of *C. albicans* infections due to the prolonged human lifespan and the increase in immunosuppressed hosts (Silva *et al*., 2012; Poulain, 2015). In this study, we found that capsaicin was effective against *Streptococcus pyogenes*, *S. mutans*, and *C. albicans*.

MATERIALS AND METHODS

Strains Used in the Study

Vero cell line, *Streptococcus pyogenes*, *Streptococcus mutans*, and *Candida albicans* strains were obtained from the culture collection of Hatay Mustafa Kemal University Faculty of Medicine, Department of Medical Microbiology and Capsaicin was obtained commercially.

Cell Culture

The cytotoxicity and invasion and adhesion tests were performed on the Vero cell line. In cell culture experiments, RPMI 1640 broth containing 10% fetal calf serum, 10 mM HEPES, and 100 IU/ml penicillin/streptomycin with 4 mM glutamine was used for cell growth and maintenance. Incubation of cells was carried out in an incubator at 37°C, 5% CO_2, and 95% air. For the production of cells, it was carried out in culture dishes of different volumes (100, 250, and 500 ml) as $1x10^6$ cells/ml. When the cells were grown as a monolayer on the culture dish surface, the passage of the cells was carried out. The cells were removed from the culture dish with trypsinization solution and transferred to 50 ml centrifuge tubes, at 1500 rpm for 15 min. collected by centrifugation. Cell viability and number were determined under the microscope in a hemocytometer with 1% trypan blue dye prepared in 0.9% NaCl.

Activity assays were performed in 96-well flat-bottom microplates. Cells were inoculated into the wells with RPMI 1640 medium containing 10% fetal calf serum at $1x10^6$ per ml. In the experiments, dimethyl sulfoxide (DMSO) (Sigma, MI, USA) was used to dissolve Capsaicin.

Cell Viability Determination

Cell viability assay was performed with trypan blue dye. The basis of staining method is based on staining dead cells exposed to Trypan blue dye due to the deterioration of their membrane integrity. Cells removed by trypsinization during both the passage of Vero cells and activity studies were evaluated microscopically after treatment with trypan blue and incubated with dye at room temperature. Stained cells were considered dead, and unstained cells were considered alive. The mixture, which was incubated for 15 minutes at room temperature, was examined under a microscope to determine viability. Cell count was performed with a hemocytometer.

ACTIVITY STUDIES

Preparation of Cell Culture

Firstly, non-toxic concentrations of Capsaicin were determined in Vero cell culture. Activity studies were performed within these non-toxic concentrations. Studies

https://doi.org/10.24264/icams-2022.III.19

to determine the cytotoxic effect were performed with the MTT (3-(4,5-Dimethylthiazol-2-yl)-2,5-diphenyltetrazolium bromide) method as described below. For activity studies, cell cultures were prepared with 1x106 cells in each ml of Vero cells. After 6 hours of incubation for cell adhesion, amounts of capsaicin containing different concentrations were added to the culture medium.

Cultures containing only the concentration of DMSO used as the solvent were used as the control group. Cultures without capsaicin were determined as the negative control group. All experiments were performed in triplicate, repeating 2 times. After incubation, the cells that continued to proliferate by adhering to the culture dish surface were treated with 0.25% trypsinization solution and transferred to centrifuge tubes. Cells were collected by centrifugation at 1500 rpm for 10 minutes in a refrigerated centrifuge (+4 C) and cell viability was determined.

Efficacy of Capsaicin on Microorganism Reproduction in Vero Cell Line

For the adhesion of the cells, capsaicin was added to the cells incubated for 24 hours and incubated at 37 °C for 1 hour. Then, suspensions of microorganisms at a density of 1x106/ml were prepared from 24-hour cultures. These suspensions were transferred onto cell cultures in which capsaicin was inoculated and incubated at 37 °C for 3 hours. To determine the growth densities of microorganisms, both absorbance measurements and the samples taken from each well were inoculated into Mueller-Hinton agar and growth controls were carried out. Colony counts were calculated as CFU/ml. Thus, the activities of capsaicin on microorganisms were evaluated by quantitation.

Effects of Capsaicin on Cell Adhesion and Invasion of *S. pyogenes, S. mutans* and *C. albicans*

For this purpose, fresh cultures of microorganisms passaged on Mueller-Hinton and Saboraud Dextrose agar were used. Before these procedures, the Vero cell line was prepared with $1x10^6$ cells per ml. Capsaicin was inoculated into the cells at non-toxic concentrations on the cells that covered at least 80% of the culture dish surface. Following inoculation, the cultivation of cells was carried out at 37 °C for 2 hours. Then, microorganism cultures prepared from 24-hour cultures of microorganisms (for bacteria: $1x10^8$/ml; for C.albicans $1x10^6$/ml) were added to cell culture media treated with capsaicin. Incubation of cultures at 37 °C for 3 hours was carried out to finalize the adhesion experiments. PBS solution was added to the wells of the plate and aspirated gently. This process was repeated 3 times and the cells were washed. After this stage for adhesion tests; cells were treated with 0.025% Triton X-100 and incubated with this solution for at least 5 minutes at room temperature. At the end of the incubation, the mixture consisting of cells and microorganisms was homogenized and the samples taken from each well of the plate were inoculated into agar media. Bacterial colony counts were performed 24 hours after incubation.

Invasion Experiment

As mentioned above, Capsaicin treatment in cell cultures was added to the wells of the plate by preparing a solution of Gentamicin and Fluconazole for adhesion tests of bacteria to cells. After the addition of the antibiotic solution, the culture plates were incubated for a short time (approximately 10 minutes) at 37°C. During this time, the cell surface and microorganisms in the medium were inactivated. Then, PBS solution was

https://doi.org/10.24264/icams-2022.III.19

added to the wells of the plate and the cell surfaces were washed 3 times as in the adhesion experiments above. After this step, 0.025% Triton X-100 was added to the cells and incubated for about 5 minutes at room temperature. The lysate formed in the wells was homogenized and the sample taken from each well was inoculated on Mueller-Hinton agar, and colony counts were carried out after 24 hours of incubation at 37°C.

RESULTS

The non-toxic concentration of capsaicin on Vero cells was <1.35 µg/ml. Capsaicin exhibited significant antimicrobial activity against *S. pyogenes*, *S. mutans*, and *C. albicans* (Figure 1).

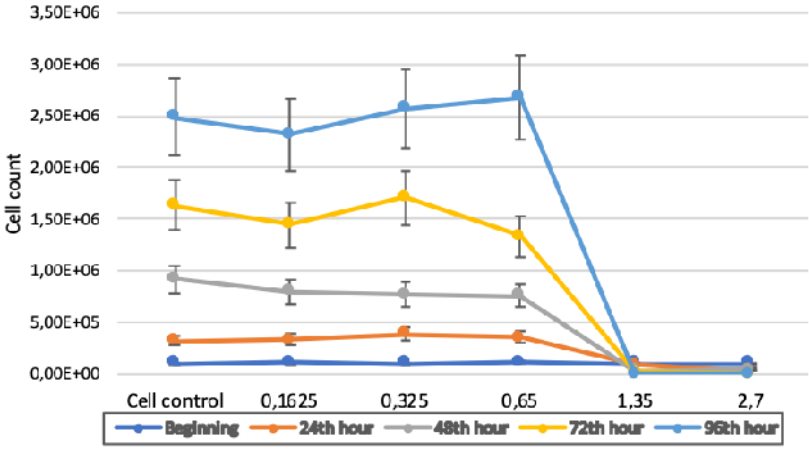

Figure 1. Determination of the non-toxic concentration of capsaicin in Vero cell culture

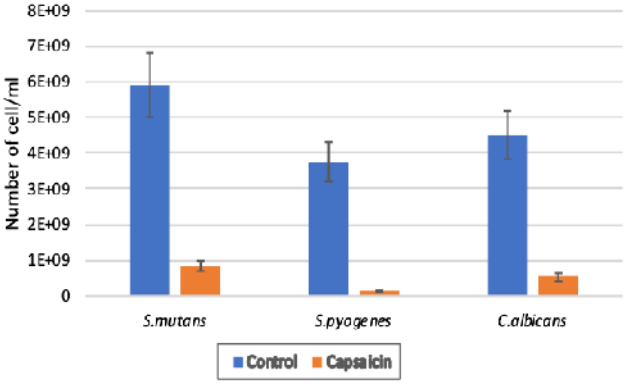

Figure 2. Antimicrobial activity of capsaicin against *S. mutans*, *S. pyogenes* and *C. albicans*

https://doi.org/10.24264/icams-2022.III.19

As seen in Figure 2, capsaicin exhibited significant antimicrobial activity against *S. mutans*, *S. pyogenes*, and *C. albicans*. It was determined that there was a significant inhibition of growth against all three pathogens in the number of microorganisms.

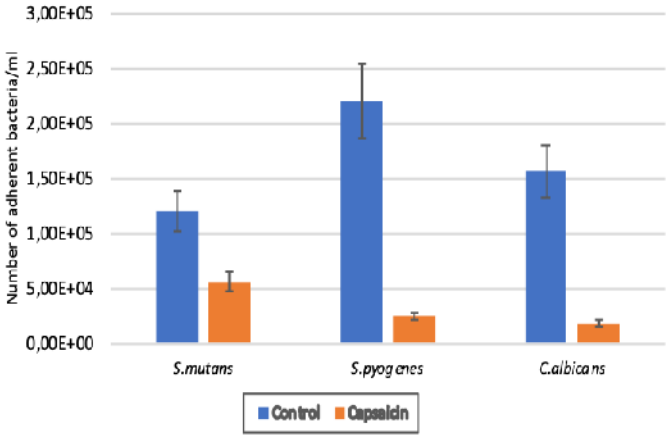

Figure 3. Effects of capsaicin on adhesion of microorganisms to Vero cells

As can be seen from Figure 3, Capsaicin inhibited the adhesion of microorganisms to Vero cells. This activity is very strong against *S. pyogenes* and *C. albicans*.

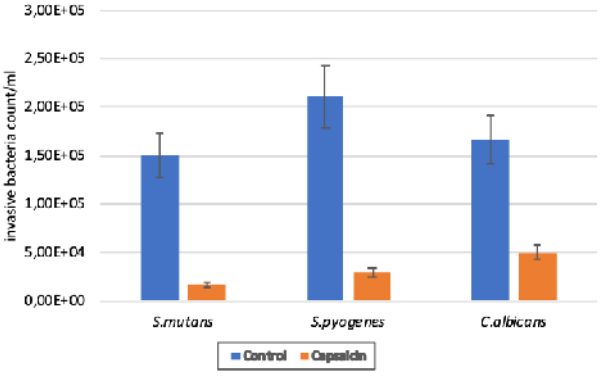

Figure 4. Effects of capsaicin on the invasion of microorganisms into Vero cells

It has been determined that capsaicin is very effective against cell invasion of cells that have made host cell adhesion (Figure 4).

CONCLUSION

Oral and dental diseases and respiratory tract infections are among the most common diseases in humans. *S. pyogenes*, *S. mutans*, and *C. albicans* can cause

https://doi.org/10.24264/icams-2022.III.19

significant infections in the oral region. Today, various throat lozenges containing antiseptic, local anesthetic, and alcohol are used to relieve the symptoms of sore throat. Capsaicin showed very strong activity against *S. pyogenes*, *S. mutans*, and *C. albicans*, which are among the important oral pathogens. Capsaicin both significantly reduces the host cell adhesions of these pathogens and prevents the invasion of microorganisms with low adhesion into the cell. It is a potent agent both against oral and respiratory pathogens and against other human pathogens colonizing the host cell and causing inoculation for humans. The results should be verified with further studies. We believe that capsaicin can be used as a prophylaxis against such pathogens.

REFERENCES

Fiedler, T., Köller, T. and Kreikemeyer B. (2015), "*Streptococcus pyogenes* Biofilms-Formation, Biology, and Clinical Relevance", *Frontiers in Cellular and Infection Microbiology*, 5, 15, https://doi.org/10.3389/fcimb.2015.00015.

Krzyściak, W., Jurczak, A., Kościelniak, D., Bystrowska, B. and Skalniak, A. (2014), "The Virulence of *Streptococcus* Mutans and the Ability to Form Biofilms", *European Journal of Clinical Microbiology & Infectious Diseases*, 33(4), 499-515, https://doi.org/10.1007/s10096-013-1993-7.

Poulain, D. (2015), "*Candida albicans*, Plasticity, and Pathogenesis", *Critical Reviews in Microbiology*, 41(2), 208-217, https://doi.org/10.3109/1040841X.2013.813904.

Silva, S., Negri, M., Henriques, M., Oliveira, R., Williams, D.W. and Azeredo, J. (2012), "*Candida glabrata*, *Candida parapsilosis*, and *Candida tropicalis*: Biology, Epidemiology, Pathogenicity, and Antifungal Resistance", *FEMS Microbiology Reviews*, 36(2), 288-305, https://doi.org/10.1111/j.1574-6976.2011.00278.x.

Vlastarakos, P.V., Nikolopoulos, T.P., Maragoudakis, P., Tzagaroulakis, A. and Ferekidis, E. (2009), "Biofilms in Ear, Nose, and Throat Infections: How Important Are They?", *Laryngoscope*, 117(4), 668-673, https://doi.org/10.1097/MLG.0b013e318030e422.

Walker, M.J., Barnett, T.C., McArthur, J.D., Cole, J.N., Gillen, C.M., Henningham, A., Sriprakash, K.S., Sanderson-Smith, M.L. and Nizet, V. (2014), "Disease Manifestations and Pathogenic Mechanisms of Group A *Streptococcus*", *Clinical Microbiology Reviews*, 27(2), 264-301, https://doi.org/10.1128/CMR.00101-13.

Zhang, Y., Wang, X., Li, H., Ni, C., Du, Z. and Yan F. (2018), "Human Oral Microbiota and Its Modulation for Oral Health", *Biomedicine and Pharmacotherapy*, 99, 883-893, https://doi.org/10.1016/j.biopha.2018.01.146.

https://doi.org/10.24264/icams-2022.III.19

A NEW MODULAR SOLUTION OF PERSONNEL PROTECTIVE EQUIPMENT FOR THE EMERGENCY RESPONDERS

DOINA TOMA, ADRIAN SALISTEAN, GEORGETA POPESCU, SABINA OLARU, IONELA BADEA

National Research & Development Institute for Textiles and Leather, 16 Lucretiu Patrascanu Street, 030508, Sector 3, Bucharest, Romania, e-mail: office@incdtp.ro

Emergency responders, due to the specifics of their work, are exposed to a combination of several different risks and there may be several possible consequences for their safety and health. The relative risk significantly influences the decisions regarding the compromise that must be made between the level of protection, functionality and comfort provided to the emergency worker. The aim of this research was to develop modular PPE systems that protect the emergency responders from injury while acting/ operating effectively in hazardous environments and provide the highest level of protection against a range of possible threats. The modular PPE system, built upon a duty uniform, integrates state-of-the-art protective technologies; provides basic protection from most likely threats (for example: fire, extreme weather etc.); enhances daily-wear comfort; provides increased localized protection as needed (for example: knees, forearms); includes next-to-skin layer and outer layer to provide varying levels of protection as needed; the modular layers easily donned and undonned. This modular approach: i) provides several advantages, including preserving comfort and flexibility until the intervention mission requires the use of the next level of protection; ii) it is a guarantee that emergency responders are not in a position of choosing between their safety and the effectiveness of the mission; iii) the use of modular layers could be the most cost-effective option, because only certain layers may become damaged or be in need of decontamination following an incident.

Keywords: protection, duty uniform, modular layers.

INTRODUCTION

Emergency responders, due to the specifics of their work, are exposed to a combination of several different risks and there may be several possible consequences for their safety and health. An assessment of the risks specific to emergency response actions revealed the presence of the following types: physical risks (falling objects, ballistic projectiles / fragments, sharp edges and objects, slippery surfaces, excessive vibrations etc.); environmental risks (high heat, humidity, strong wind, insufficient light, excessive noise etc.); chemical risks (inhalation /absorption on the skin, contact with chemicals in liquid/vapor/powder form, ingestion, injection, chemical explosions etc.); biological hazards (pathogens carried/propagated by blood, tuberculosis or airborne pathogens, biological toxins, biogenic allergens etc.); thermal hazards (radiant and convective heat, flame, hot liquids or gases, hot solids or molten substances etc.); electrical hazards (electric shock, electric arc, static charge generation etc.); radiation risks (ionizing radiation - alpha / beta particles, gamma rays, X-rays, non-ionizing radiation etc.) (Milczarek, 2011; Willis *et al*., 2011). The relative risk significantly influences the decisions regarding the compromise that must be made between the level of protection, functionality and comfort provided to the emergency responder. The aim of the project is to provide emergency responders with a modular PPE system built upon a duty uniform that provides limited protection and physiological benefits (for example, moisture wicking) in combination with a series of modular, mission-specific layers, to provide specialized protection. This modular approach: i) provides several advantages, including preserving comfort and flexibility until the intervention mission requires the use of the next level of protection; ii) it is a guarantee that emergency

https://doi.org/10.24264/icams-2022.III.20

responders are not in a position of choosing between their safety and the effectiveness of the mission; iii) the use of modular layers could be the most cost-effective option, because only certain layers may become damaged or be in need of decontamination following an incident.

EXPERIMENTAL

Materials

Considering: i) the specifics of the intervention missions: the confrontation with a multitude of known and unknown threats; ii) the capabilities necessary for the health and safety of the emergency responder: ensuring increased protection against threats without wearing specialized equipment and without compromising comfort and maneuverability; iii) the performance requirements imposed by the specific European standards, a solution for the realization of an PPE system intended for use in emergency intervention actions, is a multilayer structure: a) the inner layer, in contact with the skin/Underwear PPE – which covers the sensorial and thermophysiological comfort functions, ensures thermal protection; b) intermediate layer (base): Duty uniform – with the function of barrier against the risk factors with the highest probability of occurrence in case of an intervention action (thermal risks: convection heat, flame; external risks: splashes with liquids; mechanical hazards: cutting, abrasion etc.); c) outer layer: modular protective layers – Specialized PPE for intervention missions in case of: fires, dangerous materials, weapons of mass destruction, firearms, extreme weather conditions, etc.

The methodology used for the design and achievement of the modular PPE system for emergency response actions is based on a multidisciplinary approach to the development and management of "complex systems" (Speicher, 2018; Reichow, Conway and Sappelsa, 2017). Starting from the needs analysis, the key needs of the PPE system were identified, which were the basis for establishing the key performance parameters and the high-performance parameters. The established performance parameters were translated into design requirements, based on which the raw materials, the realization technologies, the conception (design) of the PPE system were identified (Advanced Personal Protection System, 2014).

Starting from the key needs identified: User Comfort; Certification of protection properties in accordance with the legislation in the field of PPE; Durability for Daily Wear; Usability/Functionality; Aesthetics; Multi-service Applicability; User acceptability; Reasonable cost and taking into account the performance requirements imposed on the materials, it was decided to use them for manufacturing: inner layer (in contact with the skin) – underwear PPE – for a knitted fabric made of yarn 93/5/2% meta-aramid/ para-aramid/antistatic fibers; intermediate layer (base) – Duty uniform – for a woven fabric made of yarn 29/59/10/2% aramid/ FR viscose /polyamide /antistatic fibers; outer layer – specialized PPE for firefighters – for a combination of materials: a) fabric 78/20/2% para-aramid/ meta-aramid/antistatic fibers (with fire protection role) + b) 3-D spunlace non-woven made of para-aramidic / meta-aramidic fibers + ePTFE / PU-bicomponent membrane (acting as a thermal-moisture barrier) + c) non-woven made of FR viscose/ aramid fibers + viscose FR / aramid / polyamide fiber fabric (with the role of thermal liner); outer layer – specialized PPE for intervention missions in

https://doi.org/10.24264/icams-2022.III.20

extreme weather conditions – for a multilayer textile support laminated in 3 layers: 100% PES fabric + PTFE film + 100% PES knit.

Prototype Design

Based on the protection requirements and the minimum required performance parameters specified, the following experimental program was established for the realization of the prototypes of intervention PPE systems in the modular structure.

Table 1. Experimental program

Prototype variant of PPE intervention system	Prototype component of PPE intervention system	Constructive variant
Prototype PPE system for intervention in emergency situations Variant V1	*Modular layer 1:* Underwear PPE – inner layer (in contact with the skin)	Suit consisting of a blouse with long / short sleeves and long / short pants
	Modular Layer 2: Duty Uniform – base layer	Suit consisting of blouse and pants
Prototype PPE system for intervention in emergency situations Variant V2	*Modular layer 1:* Underwear PPE – inner layer (in contact with the skin)	Suit consisting of a blouse with long sleeves and long pants
	Modular Layer 2: Duty Uniform – base layer (intermediate)	Suit consisting of blouse and pants
	Modular layer 3: Specialized PPE for firefighters (outer layer)	Outer suit: Jacket and pants Detachable underwear: Jacket + pants
Prototype PPE system for intervention in emergency situations Variant V3	*Modular layer 1*: Underwear PPE – inner layer (in contact with the skin)	Suit consisting of a blouse with long sleeves and long pants
	Modular Layer 2: Duty Uniform – base layer (intermediate)	Suit consisting of blouse and pants
	Modular layer 3: Specialized PPE for interventions in extreme weather conditions (outer layer)	Jacket with detachable hood and lining

Three variants of the prototypes of PPE systems for intervention in emergency situations were made (Figure 1, 2, 3), respectively.

Figure 1. Prototype PPE system for intervention in emergency situations Variant V1

https://doi.org/10.24264/icams-2022.III.20

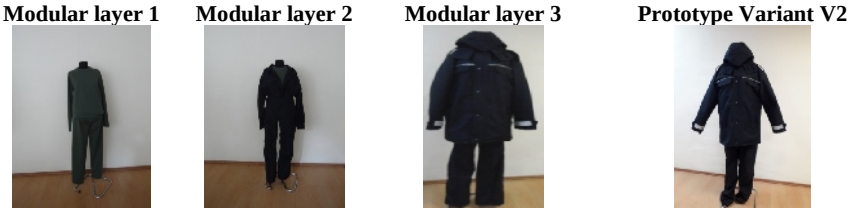

Figure 2. Prototype PPE system for intervention in emergency situations Variant V2

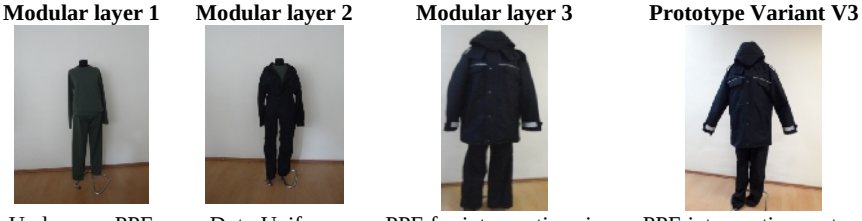

Figure 3. Prototype PPE system for intervention in emergency situations Variant V3

RESULTS AND DISCUSSION

In order to evaluate the performances of the prototypes of PPE intervention systems in the modular structure, the specific laboratory tests performed for the verification of the protection parameters were performed, in accordance with the requirements of the applicable standards, respectively: SR EN ISO 11612:2015 – Protective clothing. Clothing to protect against heat and flame. Minimum performance requirements; SR EN 469:2020 – Protective clothing for firefighters. Performance requirements for protective clothing for firefighting activities; SR EN 342:2018 – Protective clothing. Ensembles and garments for protection against cold; SR EN 343:2019 – Protective clothing. Protection against rain: SR EN ISO 13688:2013 – Protective clothing – General requirements.

The PPE intervention system Variant V1 has characteristics according to the specifications of the following standards: a) SR EN ISO 11612:2015: point 6.3 (resistance to limited flame spread) – the mean value of afterflame time and afterglow time: 0 s, code letter A1; point 6.4 (dimensional change) within the limits imposed, less than ± 3%; point 6.5.1 (tensile strength) above the min. value imposed, 300 N in warp and weft (for fabric of DU); point 6.5.2 (tear strength) above the min. value imposed, 15 N in warp and weft (for fabric of DU); point 6.5.3 (burst strength) above the min. required value, 200 kPa (for knitted fabric of UPPE); point 6.9.2 (pH value) within the required limits, >3.5 and <9.5; b) SR EN ISO 13688:2013: point 4.2 (innocuousness -

https://doi.org/10.24264/icams-2022.III.20

content of carcinogenic amines) within the imposed limits, undetectable; point 4.3 (design); section 4.4 (comfort).

The PPE intervention system Variant V2 has characteristics according to the specifications of the following standards: a) SR EN ISO 11612:2015: point 6.3 (resistance to limited flame spread) – the mean value of afterflame time and afterglow time: 0 s, code letter A1; point 6.4 (dimensional change) within the limits imposed, less than ± 3%; point 6.5.1 (tensile strength) above the min. value imposed, 300 N in warp and weft; point 6.5.2 (tear strength) above the min. value imposed, 15 N in warp and weft; point 6.5.3 (burst strength) above the min. required value, 200 kPa; point 6.9.2 (pH value) within the required limits, >3.5 and < 9.5; b) SR EN 469:2020: point 6.1 (resistance to limited flame spread) – the mean value of afterflame time and afterglow time: 0 s, code letter A1 (for specialized PPE for firefighters); point 6.5 (thermal resistance) – dimensional changes after exposure 5 minutes at 180°C, below 5% (for materials made of specialized PPE for firefighters); point 6.6 (tensile strength) above the min. value imposed for the outer material of the PPE for firefighters, 450 N in warp and weft; point 6.7 (tear strength) above the min. value imposed for the outer material of the PPE for fighters, 25 N in warp and weft; point 6.8 (surface wetting), above the min. value imposed, 4 (ISO degree scale); point 6.9 (dimensional change) below the required minimum values, ± 3% (for all materials of the PPE for firefighters); point 6.10 (resistance to penetration of liquid chemicals), rejection rate > 80% for each of the liquid chemicals mentioned in the standard; point 6.11 (resistance to water penetration) over 20 kPa, level 2 performance (for the multilayer assembly with a moisture barrier of the PPE for firefighters); point 6.12 (water vapor resistance), below 30 m2Pa/W, performance level 2; c) SR EN ISO 13688: 2013: point 4.2 (innocuousness – content of carcinogenic amines) within the imposed limits, undetectable; point 4.3 (design); section 4.4 (comfort); point 5 (aging).

The PPE intervention system Variant V3 has characteristics according to the specifications of the following standards: a) SR EN 343:2019: point 4.2 (resistance to water penetration) above the min. required value, 13000 Pa; point 4.3 (water vapor resistance) below the max. value imposed, 55 m2Pa/W; point 4.4 (tensile strength) above the required value, 450 N in warp and weft; point 4.5 (tear strength) above the imposed value, 25 N in warp and weft; point 4.6 (dimensional changes) below the required minimum values, ± 3%; b) SR EN 342:2018: point 4.2 (thermal resistance) above the required min. value, 0.31 m2K/W; point 4.3 (air permeability) within the limit values imposed for performance class 3 (AP <5 mm/s); point 4.4 (resistance to water penetration) above the min. value imposed, 13000 Pa; point 4.5 (water vapor resistance) below the max. value imposed, 55 m2Pa/W; point 4.6 (tear strength) above the min. value imposed, 25 N in warp and weft; c) SR EN ISO 11612:2015: point 6.3 (resistance to limited flame spread) – the mean value of afterflame time and afterglow time: 0 s, code letter A1; point 6.4 (dimensional change) within the limits imposed, less than ± 3%; point 6.5.1 (tensile strength) above the min. value imposed, 300 N in warp and weft; point 6.5.2 (tear strength) above the minimum value imposed, 15 N in warp and weft; point 6.5.3 (burst strength) above the min. required value, 200 kPa; point 6.9.2 (pH value) within the required limits, >3.5 and < 9.5; d) SR EN ISO 13688:2013: point 4.2 (innocuousness – content of carcinogenic amines) within the imposed limits, undetectable; point 4.3 (design); section 4.4 (comfort).

https://doi.org/10.24264/icams-2022.III.20

CONCLUSIONS

The aim of this research was to develop modular PPE systems that protect the emergency responders from injury while acting/ operating effectively in hazardous environments and provide the highest level of protection against a range of possible threats.

To meet this objective the modular PPE system: integrates state-of-the-art protective technologies including flame resistance, water repellency; provides basic protection from most likely threats (for example: fire, extremes weather etc.); enhances daily-wear comfort; provides increased localized protection as needed (for example: knees, forearms); includes next-to-skin layer and outer layer to provide varying levels of protection as needed; the modular layers easily donned and undonned.

The test and evaluation process consisted of objective and subjective testing. The objective laboratory testing quantitatively determined if a fabric could meet the minimum performance requirements. The testing objective consisted of material testing and system level testing. However, laboratory data cannot accurately assess the operational suitability and effectiveness of a PPE system when used under operational conditions. Critical attributes, such as comfort, appearance, durability, freedom and range of motion, could not be fully evaluated under laboratory conditions. That is why this research will continue with the Wear Trial of the PPE system under operational conditions. This subjective evaluation will be essential to differentiating the performance of the modular layers integrated into the PPE system prototypes.

Acknowledgements

This work was carried out through the Nucleu Programme, with the support of MCID, project no. 4N/08.02.2019, PN 19 17 02 01, project title: "Advanced multifunctional logistics, communications and protection systems to improve the safety, operability and efficiency of emergency workers – SiMaLogPro".

REFERENCES

Milczarek, M. (2011), "A Literature Review on Occupational Safety and Health Risks", European Agency for Safety and Health at Work (EU-OSHA) Emergency Services, pp. 23-45.

Reichow, S., Conway, T. and Sappelsa L. (2017), "Project Responder 5", Final Report, Homeland Security Studies and Analysis Institute, pp. 23-45.

Speicher, N. (2018), "Next Generation First Responder Integration Handbook, Part 3: Technical Supplement Version 3.0", Homeland Security, Science and Technology Directorate, pp. 98-104.

Willis, H.H., Castle, N.G., Sloss, E.M. and Bartis, J.T. (2011), "Protecting Emergency Responders, Personal Protective Equipment Guidelines for Structural Collapse Events", pp. 115-119.

*** (2014), "Advanced Personal Protection System (APPS), Wildland Firefighter Personal Protection Equipment (WLFF PPE) Clothing System Program", Final Report, by Responder Techologies (R-Tech) Program Department of Homeland Security (DHS), Science and Technology Directorate (S&T) Washington, D.C. and U.S. Army Natick Soldier Research, Development and Engineering Center Natick, MA, pp. 20-38.

https://doi.org/10.24264/icams-2022.III.20

ACTIVITY OF OLEIC ACID ON BIOFILM FORMATION OF *S. aureus*

ELIF YAPRAK, NIZAMI DURAN

Mustafa Kemal University, Medical Faculty, Microbiology Department, Hatay-TÜRKİYE, nizamduran@hotmail.com; dyteliyaprak@gmail.com

Oleic acid is a naturally occurring fatty acid in animal and vegetable oils and has been shown to have a wide variety of pharmacological effects. It aimed to investigate the efficacy of oleic acid on the adhesion and invasion of *S. aureus* to the host cell and biofilm production. The standard *S. aureus* strain (ATCC 25923) was used in the experiments. Cytotoxicity tests of oleic acid were performed in the Vero cell line. Bacterial adhesion and invasion rates and activities on slime formation in cells treated with oleic acid were evaluated compared to the control group. Slime formation tests were evaluated phenotypically on Congo red agar. In the study, it was determined that oleic acid was effective in both cellular adhesion and invasion in terms of colony number in cell cultures treated with 0.156 µg/ml concentration of oleic acid. In addition, it was determined that slime production was significantly inhibited in bacterial cultures treated with oleic acid. Oleic acid prevents cells from attaching to bacteria and has an inhibitory effect on the virulence of bacteria. This activity of oleic acid may be due to its modulatory effect on cellular processes, and its bacterial virulence may be related to its effect on bacterial metabolism.

Keywords: oleic acid, adhesion, invasion, biofilm

INTRODUCTION

Oleic acid is a monounsaturated fatty acid. It is found in nature in vegetable and animal oils. Oleic acid is the most abundant fatty acid in human adipose tissue and is second only to palmitic acid in human tissues overall. Oleic acid is an unsaturated fatty acid found as a glyceryl ester in various vegetable oils such as hazelnut and olive oil (Sales-Campos *et al*., 2013; Carrillo *et al*., 2012; Carrillo *et al*., 2012).

Oleic acid constitutes 500-85% of the total fatty acids that form a triglyceride complex in olive oil. Scientific studies have shown that oleic acid and its derivatives exhibit a variety of biological activities, including antimicrobial and anticancer activities. In the literature, it has been reported that oleic acid and extracts containing oleic acid have various biological effects such as antibacterial, antifungal, antiviral, and antioxidant activity (Sales-Campos *et al*., 2013; Carrillo *et al*., 2012). Although rich pharmacological activities of oleic acid have been reported, studies on its effectiveness in host cell adhesion and invasion and its effects on bacterial virulence are limited.
In this study, the activities of oleic acid on the cultured cells and the biofilm formation of *S. aureus* were evaluated.

Bacterial Strain

Standard *Staphylococcus aureus* (ATCC 25923) strain from the bacterial culture collection of Hatay Mustafa Kemal University Faculty of Medicine, Department of Medical Microbiology was used in the experiments.

Strains, Cell Culture, and Oleic Acid

The Vero cell line, which was used for both cytotoxicity tests and in-vitro efficacy tests in the study, was obtained from the culture collection of Hatay Mustafa Kemal University Faculty of Medicine, Department of Medical Microbiology, and oleic acid was obtained commercially.

https://doi.org/10.24264/icams-2022.III.21

In the study, RPMI 1640 broth containing 10% fetal calf serum, 10 mM HEPES, and 100 IU/ml penicillin/streptomycin with 4 mM glutamine was used for cell growth and maintenance in cell culture experiments.

Incubation of cells was carried out in an incubator at 37 °C, 5% CO_2, and 95% air. For the production of cells, they were incubated in culture dishes of different volumes (100, 250, and 500 ml) as $1x10^6$ cells/ml, in containers containing 10 percent of the culture vessel. For the proliferation of the cells, the growth was followed daily for 3 days, and passage procedures were performed when the cells were grown in a monolayer manner on the surface of the culture dish. The cells were removed from the culture dish with the prepared trypsinization solution and transferred to 50 ml centrifuge tubes at 1500 rpm for 15 minutes. The cell pellet was collected by centrifugation.

Activity assays were performed on flat-bottomed microplates. Dimethyl sulfoxide (DMSO) used to dissolve oleic acid was used. Tests for the determination of the non-toxic concentration of DMSO were performed using the Vero cell line. The non-toxic concentration of DMSO was chosen as the solvent concentration.

Activity Studies

Firstly, non-toxic concentrations of oleic acid in Vero cell culture were determined. Activity studies were performed within these non-toxic concentrations. Studies to determine the cytotoxic effect were performed with the MTT (3-(4,5-Dimethylthiazol-2-yl)-2,5-diphenyltetrazolium bromide) method as described by Mossman (Mossman *et al*., 1983). For activity studies, cell cultures were prepared with $1x10^6$ cells in each ml of Vero cells. After 6 hours of incubation for cell adhesion, amounts of chemical compounds containing different concentrations were added to the culture medium.

After incubation, the cells that continued to proliferate by adhering to the culture dish surface were treated with 0.25% trypsinization solution and transferred to centrifuge tubes. Cells were collected by centrifugation at 1500 rpm for 10 minutes in a refrigerated centrifuge (+4 °C) and cell viability was determined.

Cell Adhesion Tests

Fresh cultures of *S. aureus* passaged on Mueller-Hinton agar were used for this purpose. Before these procedures, the Vero cell line was prepared with 1x106 cells in each ml. Then, Oleic acid (different concentrations (of 5, 10, 15, 20, and 25 µg/ml) was added to the cells. After inoculation, they were incubated at 37 °C for 2 hours.

Then, a $1x10^8$ concentration of bacteria solution prepared from 24-hour fresh cultures of *S. aureus* was added to cell culture media treated with oleic acid. Adhesion tests were performed by incubating at 37 °C for 3 hours. The wells were washed with PBS solution. This procedure was repeated 3 times. The cells were then treated with 0.025% Triton X-100 and incubated with this solution for 5 minutes at room temperature. At the end of the incubation, the samples taken from the wells were inoculated into Mueller-Hinton agar and a bacterial count was performed.

Invasion Tests

For invasion tests, after bacterial adhesion to the cells, the cell surface was washed with an antibiotic solution (gentamicin solution; 200 µg/mL). Cells with an antibiotic solution at 37 °C for 15 min. incubated. Thus, bacteria on the cell surface were

https://doi.org/10.24264/icams-2022.III.21

inactivated. Then, the wells were washed 3 times with PBS solution. Then, 0.025% Triton X-100 was added to the cells and incubated for 5 minutes at room temperature. The lysate formed in the wells was homogenized and the sample taken from each well was inoculated with Mueller-Hinton agar for the bacterial count and incubated (24 hours at 37 °C).

Slime Production

The presence of the effect of oleic acid on the slime production of *S. aureus* was evaluated by the Congo-red method, one of the phenotypic methods.

Slime production from bacteria exposed to these chemical compounds and different combinations of these compounds was compared with slime-positive Saureus strains by inoculation on a Congo-red medium. In the evaluation made after a 48-hour incubation at 37 °C following the microorganism inoculation, the presence of black colonies in Congo-red medium was evaluated as slime production positive, and the presence of light-colored colonies was evaluated as negative slime production.

Results

Oleic acid exhibited döşe-dependent activity on the adhesion of *S. aureus* to Vero cells. Compared to the control group, it was determined that there was no effect on cell adhesion in the presence of 5 µg/ml oleic acid, but bacterial adhesion was inhibited statistically in the presence of 10, 15, 20, and 25 µg/ml oleic acid (Figure 1).

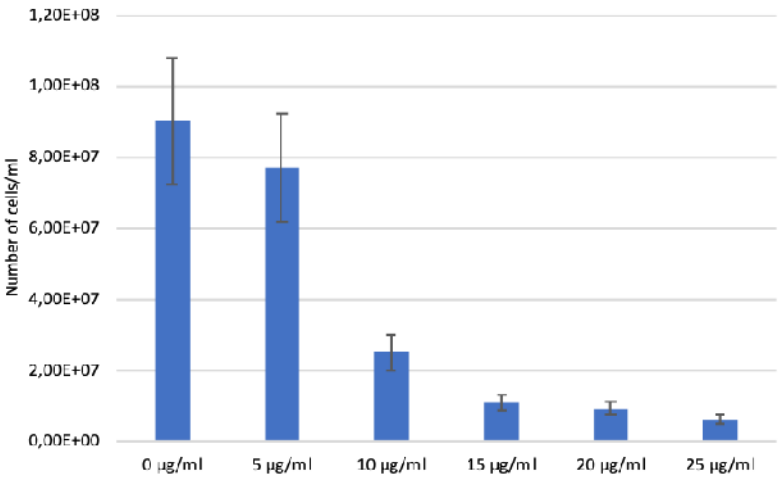

Figure 1. Efficacy of *S. aureus* adhesion to Vero cells at different concentrations of oleic acid

A similar relationship was also obtained in the invasion tests performed following the adhesion experiments. Unlike the adhesion tests, oleic acid significantly inhibited the invasion of *S. aureus* into the host cell at 5 µg/ml and all other concentrations (Figure 2).

https://doi.org/10.24264/icams-2022.III.21

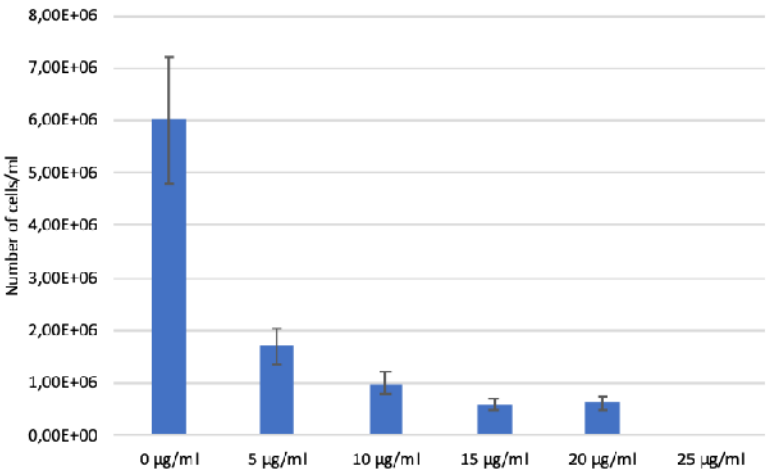

Figure 2. Efficacy of *S. aureus* invasion into Vero cells at different concentrations of oleic acid

The efficacy results of oleic acid on the biofilm-forming capacity of S.aureus are given in Figure 3. As can be seen from the figure, although oleic acid produced a reduction in bacterial biofilm formation at 5 and 10 µg/ml concentrations, this inhibition was not significant when compared to the control group. However, oleic acid significantly inhibited biofilm formation at concentrations of 15, 20, and 25 µg/ml (Figure 3).

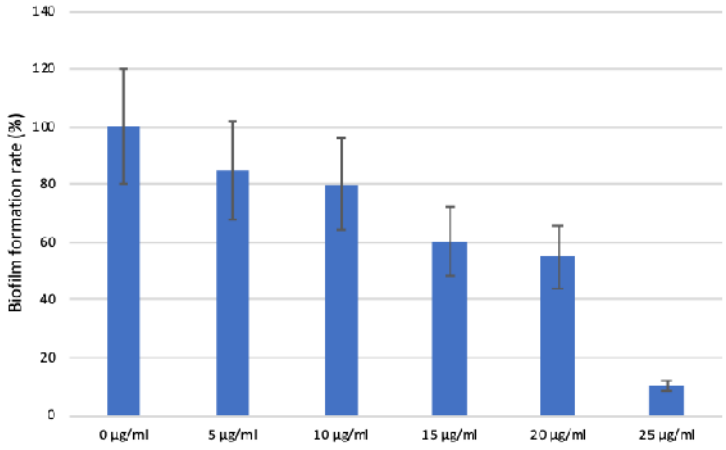

Figure 3. The concentration-related activity of oleic acid on biofilm formation of *S. aureus*

https://doi.org/10.24264/icams-2022.III.21

DISCUSSION

In recent years, it has been reported in various studies that oleic acid has very important contributions to human health and diseases (Ghavam *et al*., 2021; Yamagata *et al*., 2021; Li *et al*., 2014). In our study, it was determined that when the intracellular oleic acid level is high, both the cell resistance of the host cell against the pathogen increases and the biofilm formation capacity of *S. aureus*, which is one of the most important virulence factors, is inhibited.

CONCLUSIONS

The fact that oleic acid makes the host cell resistant to bacterial adhesion and invasion can be considered an indicator of its being a cellular modulator. These results will be very valuable in the treatment of virulent *S. aureus* strains. The combined use of oleic acid with any antibiotic can increase drug efficacy by inhibiting biofilm formation.

REFERENCES

Carrillo, C., Cavia, M.ª del M. and Alonso-Torre, S.R. (2012), "Antitumor Effect of Oleic Acid; Mechanisms of Action: A Review", *Nutrición Hospitalaria*, 27(6), 1860-5, https://doi.org/10.3305/nh.2012.27.6.6010.

Carrillo, C., Cavia, M.ª del M. and Alonso-Torre, S. (2012), "Role of Oleic Acid in the Immune System; Mechanism of Action: A Review", *Nutrición Hospitalaria*, 27(4), 978-990, https://doi.org/10.3305/nh.2012.27.4.5783.

Ghavam, M., Afzali, A. and Manca, M.L. (2021), "Chemotype of Damask Rose with Oleic Acid (9 Octadecenoic Acids) and Its Antimicrobial Effectiveness", *Scientific Reports*, 11(1), 8027, https://doi.org/10.1038/s41598-021-87604-1.

Li, S., Zhou, T., Li, C., Dai, Z., Che, D., Yao, Y., Li, L., Ma, J., Yang, X. and Gao, G. (2014), "High Metastatic Gastric and Breast Cancer Cells Consume Oleic Acid in an AMPK Dependent Manner", *PLoS One*, 9(5), e97330, https://doi.org/10.1371/journal.pone.0097330.

Mosmann, T. (1983), "Rapid Colorimetric Assay for Cellular Growth and Survival: Application to Proliferation and Cytotoxicity Assays", *Journal of Immunological Methods*, 65(1-2), 55-63, https://doi.org/10.1016/0022-1759(83)90303-4.

Sales-Campos, H., Souza, P.R., Peghini, B.C., da Silva, J.S. and Cardoso, C.R. (2013), "An Overview of the Modulatory Effects of Oleic Acid in Health and Disease", *Mini-Reviews in Medicinal Chemistry*, 13(2), 201-210, https://doi.org/10.2174/1389557511313020003.

Yamagata, K., Uzu, E., Yoshida, Y., Kato, C. and Tagami, M. (2021), "Oleic Acid and Oleoylethanolamide Decrease Interferon-γ-Induced Expression of PD-L1 and Induce Apoptosis in Human Lung Carcinoma Cells", *European Journal of Pharmacology*, 903, 174116, https://doi.org/10.1016/j.ejphar.2021.174116.

https://doi.org/10.24264/icams-2022.III.21

https://doi.org/10.24264/icams-2022.III.21

IV.

ECOLOGICAL PROCESSES FOR CIRCULAR AND NEUTRAL ECONOMY

PROTEIN EXTRACTS FROM FISH HEAD AS NATURAL FERTILIZER FOR CORN PLANTS

MARIANA DANIELA BERECHET, DEMETRA SIMION,
MARIA STANCA, COSMIN ANDREI ALEXE

The National Research & Development Institute for Textiles and Leather - Leather and Footwear Research Institute Division, 93 Ion Minulescu St., sector 3, Bucharest, Romania; marianadanielaberechet@yahoo.co.uk; demetra.simion@yahoo.com; maria.stanca@icpi.ro; cosminandrei.alexe@yahoo.com

The amino acid composition in the hydrolysates of fish proves to be a most promising source of protein. Two extracts from fish by-products (P1, from the head and fins of sturgeon and P2, from the cartilage of sturgeon head and fins) were obtained as liquids that were dried at 40°C. Liquid extracts were characterized physico-chemically (dry matter 3.86% and 4.25%, protein content 1.44% and 3.25%), and particle size (247nm, 94% and 4148nm, 65% majority populations for P1 and P2) and zeta potential (-27.4mV and -15.8mV) were measured. The smaller particle size for the P1 extract led to its choice for treatments applied in the growth of corn seeds. Four samples of concentrations of 0.5%, 1%, and 1.5% and control concentrations were experimented, each on 25 corn seeds, observing the growth of plants over a period of 13 days. A 13% higher increase of the corn plants was obtained in the case of the sample treated with 1.5% fish protein extract, P1. Throughout the experiments, the P1 sample with 1.5% fish protein extract had higher increases than the control sample. These results suggest that extracts from the head by-products of sturgeon fish could be used in agriculture as a nutrient in the growth of corn plants.

Keywords: protein extracts from fish head, majority populations of particle sizes, nutrients in the growth of corn seed

INTRODUCTION

The increase in the quantity of fish by-products not used worldwide, and in particular in countries engaged in large-scale fishing, has led to the investigation of their possible uses (Petrova *et al*., 2021). The amino acid composition in fish hydrolysates is a most promising source of protein for human consumption, for animal feed, for use in pharmaceuticals, cosmetics or in technologies of encapsulation of some compounds (Kumoro *et al*., 2022; Tørris *et al*., 2018). Depending on the species, gender, size, age, cultivation methods and the season of the year of harvest, fish meat contains between 15 and 24% protein (Karl *et al*., 2014). Fish proteins demonstrate unique functional characteristics that can become excellent vehicles for water retention, strong gel formation, stable foam formation, lipid binding and the formation of stable lipid emulsions (Kristinsson *et al*., 2007; Lee *et al*., 2016). Fish protein extract can be obtained from any kind of fish or fish residues. But in practice, it is usually produced from fish by separating the oil, removing bones and drying from which the final product can have a higher protein content (85% to 95%) and lower content of ash and water than fishmeal (Shaviklo, 2015). In addition to animal proteins, the protein extract from fish contains other important micronutrients, such as various vitamins, minerals and trace elements, which are beneficial during the child's growth period, maintaining well-being and accelerating recovery after malnutrition and various diseases, but also in animal nutrition. From a technological and economic point of view, the production of protein extract from fish is very effective because the protein loss is less than 4%, compared to other methods of processing fish (freezing, threading, canned food) in which it can reach from 40% to 60%. Characterized by high nutritional value, low caloric content, protein extract can be prepared from whole edible fish, can be used as food supplements, with high potential to

https://doi.org/10.24264/icams-2022.IV.1

reduce the state of malnutrition in a viable way economically worldwide, with a long shelf life, good storage stability and no need for refrigeration during transport and storage, all these being important advantages (Pires *et al*., 2012). Fish extract has a low level of antinutritional components, and can be used directly in the preparation of some food products (Lee *et al*., 2016). Fish extract typically possesses a smaller particle size than fishmeal and is of uniform color and texture (Shaviklo, 2015). The high content of amino acids in fish extract has encouraged its uses in human applications such as a milk substitute and treatments of patients with edema, hypoalbuminemia, malnutrition, patients in the post-surgical stage and in wound healing (Kumoro *et al*., 2022). In addition, peptides with various molecular weights contained in fish extract also demonstrate remarkable bioactivities such as anti-cancer, anti-inflammation, anti-microbial, antihypertensive, antioxidant, anti-aging, antidiabetic, antigermycide, anticoagulant and calcium binding activities, thus promoting human health and well-being (Hu *et al*., 2019; Khan *et al*., 2020; Shaviklo, 2015). The excellent functional characteristics of fish extract, such as solubility, viscosity, foaming properties, emulsifying properties, water retention capacity and oil absorption capacity suggest that fish extract could be used as an encapsulation or coating material in the field of nanotechnology (Khan *et al*., 2020; Kristinsson *et al*., 2007). Petrova *et al.* (2021) used protein hydrolysates from cod fish as peptones in microbiological culture media with good results in growing the strain of *Staphylococcus aureus* and *Salmonella enteriditis.*

This work aims to valorize the fish by-products by obtaining protein extracts from the head of sturgeon fish. They were characterized physico-chemically and the particle size and zeta potential were measured. Testing experiments were made in the growth of corn seeds by applying treatments with concentrations of 0.5%, 1% and 1.5% of fish extract obtained.

EXPERIMENTAL

Materials

The heads of sturgeon fish were bought from local fishermen (Figure 1). The chemical compounds used in the experiments were reagents for analysis.

Figure 1. Sturgeon head

Methods

Obtaining Protein Extracts from Fish Head

The protein extracts from the fish were obtained from the heads of sturgeon by boiling 4h, in distilled water, at a temperature of 90°C (Figure 2). Two types of fish head extracts were obtained: one from the fish head and fins (P1) and one from the

https://doi.org/10.24264/icams-2022.IV.1

cartilage extract from the fish head and fins (P2). After boiling the extracts were decanted and filtered through gauze and kept at 4°C (Figure 3). The fish extracts obtained were dried in the oven at 40°C.

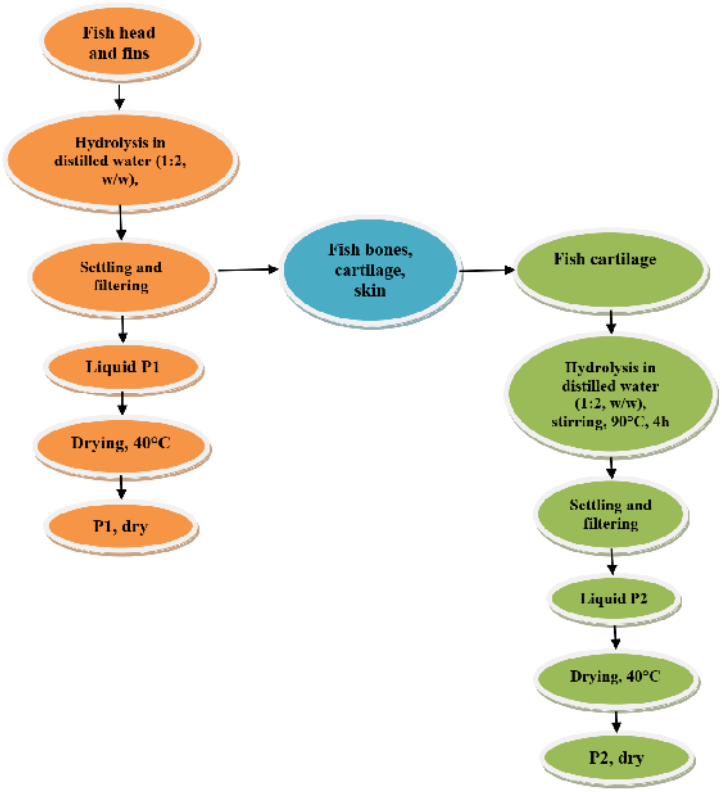

Figure 2. The scheme of obtaining protein extracts from fish head, P1 and P2

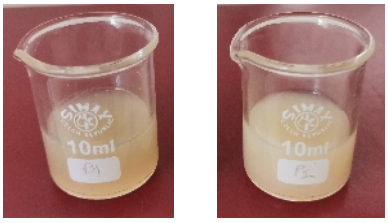

(P1) (P2)

Figure 3. Liquid protein extracts from fish head: P1 and P2

Physico-Chemical Characterization of Protein Extracts from Fish Head

The physico-chemical analyses of the obtained fish extracts were analyzed according to standardized and internal methods: SR EN ISO 4684:2006 (dry matter), SR EN ISO 4047:2008 (ash content), SR ISO 5397:1996 (total nitrogen and protein).

https://doi.org/10.24264/icams-2022.IV.1

DLS Analysis of Protein Extracts from Fish Head

The particle size and Zeta potential of the fish head extracts was measured by the dynamic light scattering technique (DLS) with the Nano-ZS Zetasizer device from Malvern (Malvern Hills, UK).

The Use of Fish Head Extract as a Nutrient in the Growth of Corn Seeds

Experiments have been conducted to stimulate the growth of corn seeds by applying treatments with fish head protein extract, P1. Three extract concentrations of 0.5%, 1% and 1.5% were used and corn plants grown over a period of 13 days were measured. Four samples consisting of 25 corn seeds each were observed: a water-treated control sample without fish extract, a sample treated with 0.5% fish extract, a sample treated with 1% fish extract and a sample treated with 1.5% fish extract.

RESULT AND DISCUSSION

A head extract of sturgeon fish (P1) and a head and fins cartilage extract of sturgeon fish (P2) and dried at 40°C (Figure 4) were obtained.

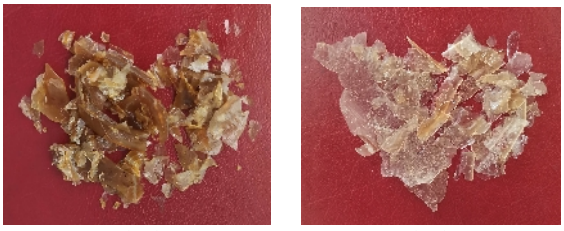

(P1) (P2)

Figure 4. Dried protein extracts from fish head, P1 and P2

Liquid protein extracts from the obtained fish were characterized physico-chemically by dry matter, ash, total nitrogen, protein and pH content (Table 1). Close values for dry matter were obtained: 3.86% (P1) and 4.25% (P2), for total nitrogen: 0.48% (P1) and 0.52% (P2), and a pH of 6.8 for both samples, while the ashes and the content in the propane have higher values for the P2 sample obtained from cartilage.

Table 1. Physical-chemical characteristics of fish head extracts P1 and P2

Characteristics	P1	P2
Dry matter (%)	3.86	4.25
Ash (%)*	0.14	2.12
Total nitrogen (%)*	0.48	0.52
Protein content (%)*	3.00	3.25
pH (units of pH)	6.83	6.80

* Values reported at dry substance

The DLS analysis showed smaller particle sizes in the case of the P1 sample compared to the P2 sample (Table 2), with a particle average of 905 nm in the case of the P1 sample compared to 1549 nm for the P2 sample.

https://doi.org/10.24264/icams-2022.IV.1

Table 2. Particle sizes and zeta potential of P1 and P2 fish head protein extracts

Head fish protein extracts	Particle populations (%) and size (nm)						Average, d, nm	Pdl	Zeta potential, mV
	Majority population 1		Majority population 2		Majority population 3				
	Size	%	Size	%	Size	%			
P1	40	5	247	94	-	-	905	0.687	-27.4
P2	27.5	2	501.6	33	4148	65	1549	0.700	-15.8

The particle sizes of the majority populations of 40nm (5%) and 247nm (94%) for the P1 sample, smaller than 501.6nm (33%) and 4148nm (65%) for the P2 sample, have determined the choice of sample P1 to be used in treatments for growing corn seeds (Table 3).

Table 3. Average (cm) growing of corn seeds treated with protein extract, P1

Days	5	6	7	8	9	13
Control, average, CM	4.1	6	7.8	9.3	12.5	19.2
P1, 0.5%, average, CM	3.3	4.8	6.1	7.3	8	12.7
P1, 1%, average, CM	4.7	5.6	6.3	7.8	8.4	12.4
P1, 1.5%, average, CM	5.1	7	8.8	11	14.5	21.5

Corn seeds treated with 1.5% P1 protein extract have increased more than the control with better growth values throughout the experiments (Figure 3).

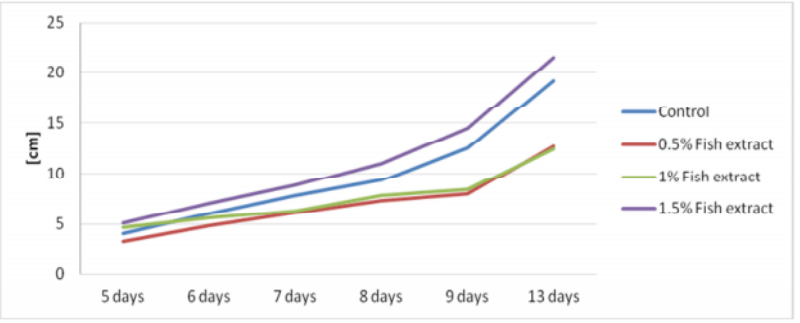

Figure 3. The increase in corn plants stem length, [cm]

Fish by-products can be capitalized and used in pharmaceuticals, cosmetics or natural fertilizers in agriculture.

CONCLUSION

Two protein extracts from the head of sturgeon fish, P1 and P2, were obtained and were characterized physico-chemically, also measuring the particle size. The P1 protein extract in a concentration of 1.5% applied as a treatment in the growth of corn seeds led to 13% higher results in the growth of corn plants compared to the control. These experiments suggest that protein extracts from fish by-products could be used as nutrients in agriculture.

https://doi.org/10.24264/icams-2022.IV.1

Acknowledgement

The present work was supported by the Romanian Ministry of Research, Innovation and Digitalization, CNDI-UEFISCDI, project number 260/2021, PN-III-P3-3.5-EUK-2019-0249, GEL-TREAT, E!13432 and project number 4N/2019–PN 19 17 01 02 (CREATIV_PIEL), National Program Nucleu.

REFERENCES

Hu, S., Yu, J., Wang, Y., Li, Y., Chen, H., Shi, Y. and Ma, X. (2019), "Fish Consumption Could Reduce the Risk of Oral Cancer in Europeans: A Meta-analysis", *Archives of Oral Biology*, 107, 104494, https://doi.org/10.1016/j.archoralbio.2019.104494.

Karl, H., Lehmann, I., Manthey-Karl, M., Meyer, C. and Ostermeyer, U. (2014), "Comparison of Nutritional Value and Microbiological Status of New Imported Fish Species on the German Market", *International Journal of Food Science and Technology*, 49(11), 2481–2490, https://doi.org/10.1111/ijfs.12543.

Khan, S., Rehman, A., Shah, H., Aadil, R.M., Ali, A., Shehzad, Q., Ashraf, W., Yang, F., Karim, A., Khaliq, A. and Xia, W. (2020), "Fish Protein and Its Derivatives: The Novel Applications, Bioactivities, and Their Functional Significance in Food Products", *Food Reviews International*, 38(8), https://doi.org/10.1080/87559129.2020.1828452.

Kristinsson, H.G., Theodore, A.E. and Ingadottir, B. (2007), "Chemical Processing Methods for Protein Recovery from Marine By-products and Underutilized Fish Species", in: Shahidi, F. (Ed.), *Maximising the Value of Marine by-products*, Woodhead Publishing Series in Food Science, Technology and Nutrition, Bosa Boca, 144–168, https://doi.org/10.1533/9781845692087.1.144.

Kumoro, A.C., Wardhani, D.H., Kusworo, T.D., Djaeni, M., Ping, T.C. and Azis, Y.M.F. (2022), "Fish Protein Concentrate for Human Consumption: A Review of Its Preparation by Solvent Extraction Methods and Potential for Food Applications", *Annals of Agricultural Sciences*, 67(1), 42–59, https://doi.org/10.1016/j.aoas.2022.04.003.

Lee, H.J., Park, S.H., Yoon, I.S., Lee, G.W., Kim, Y.J., Kim, J.S. and Heu, M.S. (2016), "Chemical Composition of Protein Concentrate Prepared from Yellowfin Tuna *Thunnus albacares* Roe by Cook-Dried Process", *Fisheries and Aquatic Sciences*, 19, 12, https://doi.org/10.1186/s41240-016-0012-1.

Petrova, I., Tolstorebrov, I., Zhivlyantseva, I. and Eikevik, T.M. (2021), "Utilization of Fish Protein Hydrolysates as Peptones for Microbiological Culture Medias", *Food Bioscience*, 42, 101063, https://doi.org/10.1016/j.fbio.2021.101063.

Pires, C., Costa, S., Batista, A.P., Nunes, M.C., Raymundo, A. and Batista, I. (2012), "Properties of Protein Powder Prepared from Cape Hake By-products", *Journal of Food Engineering*, 108(2), 268–275, https://doi.org/10.1016/j.jfoodeng.2011.08.020.

Shaviklo, A.R. (2015), "Development of Fish Protein Powder as an Ingredient for Food Applications: A Review", *Journal of Food Science and Technology*, 52, 648–661, https://doi.org/10.1007/s13197-013-1042-7.

Tørris, C., Småstuen, M.C. and Molin, M. (2018), "Nutrients in Fish and Possible Associations with Cardiovascular Disease Risk Factors in Metabolic Syndrome", *Nutrients*, 10(7), 952, https://doi.org/10.3390/nu10070952.

DECORATIVE PLATES FROM EPOXYDIC COMPOSITES

CIPRIAN CHELARU[1], MĂDĂLINA IGNAT[1], RODICA ROXANA CONSTANTINESCU[1], ANA-MARIA CIOBANU[1], DENIS DRUȘAN[1], VIRGINIA BURGHELEA[2]

[1]*The National Research & Development Institute for Textiles and Leather - Leather and Footwear Research Institute Division, 93 Ion Minulescu, Bucharest, Romania, cchelaru_cciprian@yahoo.com, madalina.fleancu@yahoo.com, rodica.roxana@yahoo.com, ciobanu_ana09@yahoo.com, drusan.denis.andrei@gmail.com*

[2] "Politehnica" University of Bucharest, Polizu 1, Bucharest, Romania, *v.burghelea_2008@yahoo.com*

Leather waste obtained in the leather industry represents a potential source of pollution for the environment, for plants and animals. The ecological treatment of this waste involves quite high costs and only companies with large production capacities can afford them. This paper proposes a method of transforming this waste into ash rich in chromium III and using it as a pigment (green), together with other substances, to obtain new materials. In this sense, it is proposed to use compounds that can incorporate and block the diffusion of the substances back into the environment. To achieve this, a mixture of epoxy polymers, biphenol A and biphenol F, will be used, in a 1:1 ratio, which after the polymerization reaction, with Ancamine 2686, will result in an inert mass. The polymer tiles can then be used as decorative elements for the facades of some buildings.

Keywords: leather waste, epoxy polymer, polymerization

INTRODUCTION

Leather tanning is one of the oldest human activities and remains the most important operation in the flow of leather processing. The resulting fragments of tanned leather from these operations constitute the chromed leather waste, can add up to 25% of the raw hide subjected to process. As hundreds of tons of hides are tanned, large amounts of tanned leather with chromium reach to the order of tons. The specialized scientific literature of the last years presents studies regarding the capture of chromium and retanning using the residual chromium from tanneries. Chromium recovery is based on biological processes (Aliane *et al*., 2001; Pinto *et al*., 2006; Rengaraj *et al*., 2003), complexation-ultrafiltration (Park *et al*., 2008; Turtoi *et al*., 2001; Strathman, 1980), ion exchange processes (Strathman, 1980; Langhammer *et al*., 2008; Wenling *et al*. (2008), adsorption on various materials (Animes *et al*., 2007; Su and Juang, 2002; Junxi *et al*., 2008), electro-coagulation (Morales-Barrera and Cristiani-Urbina, 2008), electrochemical recovery. Studies dedicated to the recovery of residual chromium have been directed towards the production of chromium-based pigments (Sivakumar *et al*., 2000; Lazau *et al*., 2007), ceramic materials, including refractory ceramics (Lazau *et al*., 2007), the incorporation of residual chromium in cement (Sivakumar *et al*., 2000; Lazau *et al*., 2007; Gupta *et al*., 2001). For the residual chromium in tanneries, the possibility of reintroducing it in leather processing was studied, but also capturing it in a complex of residual minerals (Pontikes *et al*., 2009), with the possibility of accumulating on this complex to produce ceramic glazes and glass (Wang *et al*., 2007). Chromium has different effects on organisms. The effect of chromium accumulation on aquatic life - fish - is not known, but high concentrations of metals from spills can damage gills as well as fins. For the animals, it can cause respiratory problems, birth defects, infertility, tumors. It is beneficial for crops to contain controlled amounts of chromium because the plants absorb chromium III from the environment. Cancer occurs 15-30 years after the first exposure of the body, by localization in the organs, chromium causes malignant tumors. The health risks of chromium depend on its oxidation state. Metallic chromium has low toxicity. Chromium III is beneficial for health but within certain limits. Chromium VI is toxic.

https://doi.org/10.24264/icams-2022.IV.2

The toxicity of chromium is well known and a suitable way for its removal is desired. One solution is to use the chromium leather waste ash, together with a mix of polymeric products made from bisphenyl A (BPA) and bisphenol F (BPF) to obtain traffic floors or decorative plates for buildings and other. Bisphenyl A was discovered in 1891 by the Russian chemist Aleksandr Dianin and in 1958 the polycarbonate plastics were discovered by the Bayer and General Electric (Rengaraj *et al*., 2003). From all the BPA produced, 65-70% go to the polycarbonates production (Park *et al*., 2008; Turtoi *et al*., 2001), 25-30% is used for epoxy and vinyl ester resins production (Rengaraj *et al*., 2003; Park *et al*., 2008) and 5% is use in the manufacture of high-performance plastics and as a minor additive in PVC, thermal paper, and several other materials. Bisphenol F (BPF) is used in plastics and epoxy resins production as tank and pipe linings, bridge deck toppings, industrial flooring, structural adhesives, electrical varnishes and several other materials (Arthanareeswaran *et al*., 2007). It is used in obtaining liners, lacquers, adhesives, coating of drinks and food cans (Arthanareeswaran *et al*., 2007). BPF is used in dentistry as restorative materials, adhesives, oral prosthetic etc. (Arthanareeswaran *et al*., 2007). The final product can be obtained if a curing agent is present. Ancamine 2686 is a proper candidate that can operate at room temperature for liquid epoxy resin. Ancamine 2686 provides high mechanical build and very good chemical and mechanical resistance (Strathman, 1980). Quartz is a mineral substance (silica oxide) naturally found in nature. Depending on the granulation, this one can be use as filer in the main composition, to bring more "light". By exploiting its piezoelectric properties, the polymeric floor can incorporate some devices that can generate electricity.

EXPERIMENTAL

Materials

Bisphenyl A (BPA), IUPAC name 2,2'-bis (4-hydroxyphenyl) propane – organic compound, solid, colourless, melting point 158-159°C, with a good solubility in organic solvents and poor solubility in water.

Bisphenol F (BPF), IUPAC name 4,4′-dihydroxydiphenylmethane – organic compound, solid, melting point 162-164°C, with a good solubility in organic solvents.

Ancamine 2686 – organic compound, liquid, yellow, 100-400 mPa·s at 25°C.

Quartz (Uricani) – is a mineral substance (silica oxide) – 99,99%.

Chromium leather ash – 61% Cr_2O_3.

Figure 1. Materials

Equipment

Hot plate – Magnetic Stirrers with Hot Plates (Velp Scientifica) with 50-370°C temperature interval. Oven – (Nabertherm) with 50–1200°C temperature interval.

Ultrasonic bath – Elmasonic S 15H (Elma) – with 30 – 80°C interval and 01-30-∞ min variable time setting.

https://doi.org/10.24264/icams-2022.IV.2

Stereomicroscope – S8AP0 (Leica). Magnification is from 10x to 160x, it has incident and transmitted light and possibility to observe the samples with polarized light.

Durometer – device specially designed to measure the hardness of materials such as polymers, elastomers, and rubbers. The Shore A Hardness Scale measures the hardness of flexible mold rubbers that range in hardness from very soft and flexible, to medium and somewhat flexible, to hard with almost no flexibility at all.

Micro hot table is a device that has the possibility to heat with a preset speed, allowing to visualize the sample behavior, from the upper part of the equipment, with the help of a stereomicroscope.


Hot plate


Oven


Ultrasonic bath


Optical stereomicroscope


Micro-hot table


Durometer

Figure 2. Equipment

RESULTS AND DISCUSSIONS

For this experiment, tanned leather waste was used (Figure 3-a), subjected to heat treatment, in stages. The chromium leather waste was initially treated at 150°C in order to burn the organic part, resulting in a carbonized waste (Figure 1-3). After this process, chromium leather waste was heated at 800°C to eliminate all the organic parts (Figure 3-c).


a) Leather waste


b) Leather waste at 150°C


c) Leather waste at 800°C

Figure 3. Leather waste in different stages

Based on obtained chromium ash, a number of 8 recipes were developed – Table 1.

https://doi.org/10.24264/icams-2022.IV.2

Table 1. Components used for epoxydic samples

No.	Chromium leather ash	Epoxydic resin	Hardener	Uricani quartz
		%		
1	-	40.00	20.00	40.00
2	0.10	39.96	19.98	39.96
3	0.20	39.92	19.96	39.92
4	0.30	39.88	19.94	39.88
5	0.40	39.84	19.92	39.84
6	0.50	39.80	19.90	39.80
7	0.60	39.76	19.88	39.76
8	1.00	39.60	19.80	39.60

The quantities of each recipe specified in the Table 1 were placed in a cylindrical plastic container to facilitate mixing, which was later used as a mold for the final sample. The components from each container were subjected to mechanical mixing (manual) – 3 min, ultrasonic mixing (with degassing) – 20 min, mechanical mixing (manual) – 3 min, rest – 1 h.

After the synthesis, discoidal samples were obtained, illustrated in Figure 4.

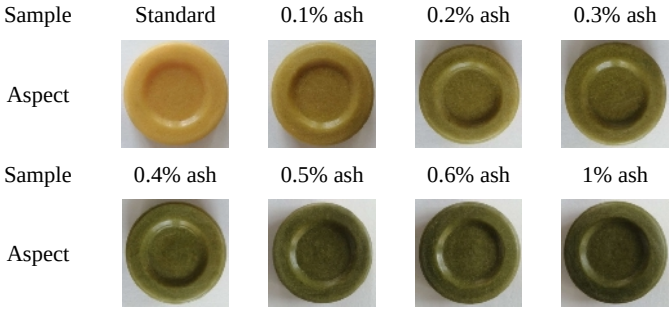

Figure 4. Composite materials base on leather waste ash

After synthesis, all the samples were subjected to a series of tests, to obtain relevant data for characterisation. Microscopy test reveals that all samples are homogeneous for the entire surface and areas with component segregation are not visible. At the same time, the same test shows that the samples contain air bubbles – Figure 5.

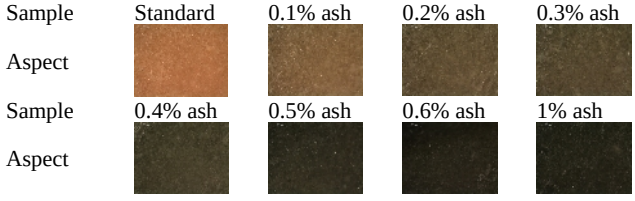

Figure 5. Microscope aspect of composite materials base on leather waste (20x)

https://doi.org/10.24264/icams-2022.IV.2

The height of the obtained samples was between 0.81 and 0.86 cm, area between 42.08 and 43.01 cm^2. Based on these values, sample density is between 0.2675 g/cm^3 and 0.2813 g/cm^3. After a mathematical conversion, it follows that 1 m^2 decorative plate with a height of 0.8 cm will have an average weight of 2.3 kg. The values can be observed in Figure 6 (obtained samples) and Figure 7 (calculated decorative 1 m^2 plate).

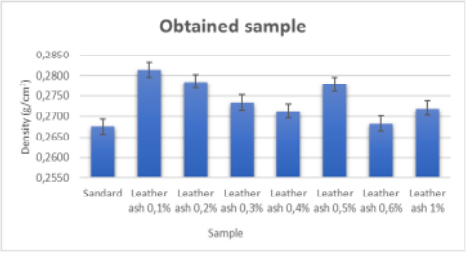

Figure 6. Sample density (g/cm^3)

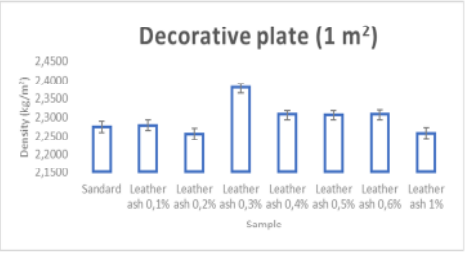

Figure 7. Plate weight (kg/cm^2) for a plate with 0.8 cm thickness

Obtained samples were tested also for hardness, and values registered were between 93°ShD and 96°ShD, on a scale of 0-100 (Figure 8).

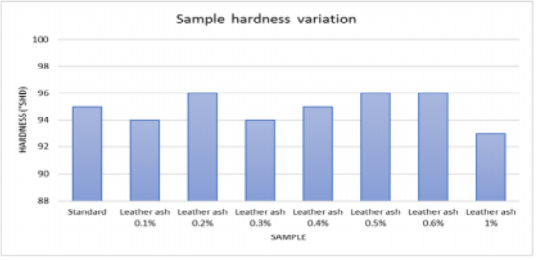

Figure 8. Sample hardness (°ShD)

CONCLUSION

Chromium leather waste can be used as raw material in a different product, and by embedding it in a proper matrix is possible to prevent its potentially toxic action on the environment.

By using a polymeric material, it is possible to obtain decorative plates that can be used in constructions. The obtained decorative 1 m^2 tiles have an average weight of 2.3 kg, which means that they will not create an additional problem for the facade of the buildings.

Due to the high hardness of the obtained samples, over 93°ShD, the obtained material can also be used as traffic floor.

In the same way special protective paints for corrosive environments, cast parts and / or processed by various technologies can be obtained, as well as other applications in various fields (art, aeronautics, consumer goods).

Acknowledgements

This study was funded by the Ministry of Research and Innovation through the Program 1 - Development of the National R&D System, Subprogram 1.2 - Institutional

Performance - RDI excellence funding projects, Contract no. 4PFE/30.12.2021: "INCDTP in the vanguard of excellence research" – TEX&PEL FOR FUTURE.

REFERENCES

Aliane, A., Bounatiro, N., Cherif, A.T. and Akretche, D.E. (2001), "Removal of Chromium from Aqueous Solution by Complexation–Ultrafiltration Using a Watersoluble Macroligand", *Water Research*, 35(9), 2320–2326, https://doi.org/10.1016/S0043-1354(00)00501-7.

Animes, K.G, Amar, N.S. and Ray, S. (2007), "Trivalent Chromium Removal by Electrocoagulation and Characterization of the Process Sludge", *Journal of Chemical Technology and Biotechnology*, 82(5), 496–503, https://doi.org/10.1002/jctb.1700.

Arthanareeswaran, G., Thanikaivelan, P., Jaya, N., Mohan D. and Raajenthiren, M. (2007), "Removal of Chromium from Aqueous Solution Using Cellulose Acetate and Sulfonated Poly(Ether Ether Ketone) Blend Ultrafiltration Membranes", *Journal of Hazardous Materials*, 139(1), 44–49, https://doi.org/10.1016/j.jhazmat.2006.06.006.

Gupta, V.K., Gupta, M. and Sharma, S. (2001), "Process Development for the Removal of Lead and Chromium from Aqueous Solutions Using Red Mud, an Aluminium Industry Waste", *Water Research*, 35(5), 1125-1134, https://doi.org/10.1016/S0043-1354(00)00389-4.

Junxi, L., Hong, L., Chuan, W., Xiangzhong, L., Yexiang, T., Xiaoli, X. and Guofeng, C. (2008), "Synthesis, Characterization and Re-Activation of a Fe/Ti System for the Reduction of Aqueous Cr(VI)", *Journal of Hazardous Materials*, 151(2-3), 761–769, https://doi.org/10.1016/j.jhazmat.2007.06.044.

Langhammer, H.T., Müller, T., Böttcher, R. and Abicht, H.-P. (2008), "Structural and Optical Properties of Chromium-Doped Hexagonal Barium Titanate Ceramics", *Journal of Physics: Condensed Matter*, 20(8), 085206, https://doi.org/10.1088/0953-8984/20/8/085206.

Lazau, R.I., Pacurariu, C., Becherescu, D. and Ianos, R. (2007), "Ceramic Pigments with Chromium Content from Leather Wastes", *Journal of the European Ceramic Society*, 27(2-3), 1899–1903, https://doi.org/10.1016/j.jeurceramsoc.2006.04.078.

Morales-Barrera, L. and Cristiani-Urbina, E. (2008), "Hexavalent Chromium Removal by a *Trichoderma inhamatum* Fungal Strain Isolated from Tannery Effluent", *Water, Air, and Soil Pollution*, 187(1-4), pp. 327–336, https://doi.org/10.1007/s11270-007-9520-z.

Park, D., Yun, Y-S. and Jong, M.P. (2008), "XAS and XPS Studies on Chromium-Binding Groups of Biomaterial During Cr(VI) Biosorption", Journal of Colloid and Interface Science, 317(1), 54–61, https://doi.org/10.1016/j.jcis.2007.09.049.

Pinto, C.A., Valenzuela-Diaz, F.R., Sansalone, J.J., Dweck, J., Cartledge, F.K. and Büchler, P.M. (2006), "X-Ray Diffraction Study of Particulate Tannery Waste Solidified in Cement", *Materials Science Forum*, 530(31), 478–484, https://doi.org/10.4028/www.scientific.net/MSF.530-531.478.

Pontikes, Y., Rathossi, C., Nikolopoulos, P., Angelopoulos, G.N., Jayaseelan, D.D. and Lee, W.E. (2009), "Effect of Firing Temperature and Atmosphere on Sintering of Ceramics Made from Bayer Process Bauxite Residue", *Ceramics International*, 35(1), 401-407, https://doi.org/10.1016/j.ceramint.2007.11.013.

Rengaraj, C.S., Joo, C.K., Kim, Y. and Yi, J. (2003), "Kinetics of Removal of Chromium from Water and Electronic Process Wastewater by Ion Exchange Resins: 1200H, 1500H and IRN97H", *Journal of Hazardous Materials*, B102, 257-275, https://doi.org/10.1016/S0304-3894(03)00209-7.

Sivakumar, M., Malaisamy, R., Sajitha, C.J., Mohan, D., Mohan, V. and Rangarajan, R. (2000), "Preparation and Performance of Cellulose Acetate–Polyurethane Blend Membranes and Their Applications II", *Journal of Membrane Science*, 169(2), 215–228, https://doi.org/10.1016/S0376-7388(99)00339-7.

Strathman, H. (1980), "Selective Removal of Heavy Metal Ions from Aqueous Solutions by Diafiltration of Macromolecular Complexes", *Separation Science and Technology*", 15(4), 1135–1152, https://doi.org/10.1080/01496398008076291.

Su, L.H. and Juang, R.S. (2002), "Heavy Metal Removal from Water by Sorption Using Surfactant-Modified Montmorillonite", *Journal of Hazardous Materials*, 92, 315–326, https://doi.org/10.1016/S0304-3894(02)00026-2.

Turtoi, D., Zainescu, G., Tudorache, El., Belcu, M., Mocioi, M. and Simonescu, Cl. (2001), "The Recovery of Chromium from Tannery Wastewaters", 12 Romanian International Conference on Chemistry and Chemical Engineering, Bucharest, Romania, 60-65.

Wang, Y.S., Pan, Z.Y., Lang, J.M., Xu, J.M., Zheng, Y.-G. (2007), "Bioleaching of Chromium from Tannery Sludge by Indigenous *Acidithiobacillus thiooxidans*", *Journal of Hazardous Materials*, 147(1-2), 319–324, https://doi.org/10.1016/j.jhazmat.2007.01.005.

Wenling, H., Fei, Z. and Bin, H. (2008), "Simultaneous Separation and Speciation of Inorganic As(III)/As (V) and Cr(III)/Cr(VI) in Natural Waters Utilizing Capillary Microextraction on Ordered Mesoporous Al_2O_3 Prior to their On-Line Determination by ICP-MS", *Journal of Hazardous Materials*, 151(1), 58–64, https://doi.org/10.1016/j.jhazmat.2007.05.044.

TECHNOLOGICAL CONSIDERATIONS REGARDING THE MECHANICAL RECYCLING OF WASTE FROM POLYETHYLENE AND POLYPROPYLENE PACKAGING

DOINA CONSTANTINESCU[1], BOGDAN BOATA[1], MIHAELA IORDACHE[1], MARIA DANIELA STELESCU[2], MIHAI GEORGESCU[2], MARIA SÖNMEZ[2]
[1]*SC MONOFIL SRL, Uzinei, 1, Savinesti, Piatra Neamt, Romania*
[2]*National Research and Development Institute for Textiles and Leather - Division Leather and Footwear Research Institute, Ion Minulescu, 93, sector 3, 031215, Bucharest, Romania*

Plastic materials have found applications in almost all fields as a result of their properties and low price. More than 30% of the production of plastics is intended for obtaining packaging. Since they are non-biodegradable and represent a hazard to the environment, strategies and directives have been adopted at national, European, and global level, regarding the recycling of packaging waste. The main ecological method of recycling them is mechanical recycling. The paper presents the main stages of an industrial mechanical recycling process, namely: collection, sorting, grinding, washing, drying, (purification), granulation, packaging, storage and marketing. This underlines the fact that in order to obtain high-performance PE or PP raw materials from recyclable polymer waste from packaging, the recycling process requires advanced sorting to separate them into polymer classes, because the mixtures of the polymers involved are incompatible in their melted state. This incompatibility leads to the lower processability and physical-mechanical performance of the products manufactured from these types of recycled polymer waste. In addition to the sorting methods currently used in the industry, new advanced methods of selective sorting of waste according to the type of polymer were also presented, such as: spectroscopic method, selective dissolution of polymers, thermal adhesion method, froth flotation method, electrostatic separation methods. It was emphasized that by using state-of-the-art technologies such as electron beam treatment followed by the electrostatic separation of waste mixtures from packaging, it is possible to obtain recycled polymers with high purity (90-97%) at advantageous production costs.

Keywords: plastic waste, PE, PP, packages, mechanical recycling, electrostatic separation

INTRODUCTION

Plastics have shown a significant development in the last 50 years, due to their high-performance properties that have allowed their use for a wide range of applications. In addition, they are light, cheap and can be easily processed into different products. The total amount of plastics generated in 2020 in the EU is 53.9 Mt, comprising: 45.7 million tonnes from plastics production (polymerisation) (about 84.8%), 4.6 million tonnes of post-consumer recycled plastics (about 8.5%) and 3.6 million tonnes of pre-consumer recycled plastics (about 6.7%). Plastics consumption in the EU in 2020 was 5.6 Mt and of this consumption, the largest amount (33.5%) is due to packaging. Because plastics, respectively plastic packaging are not biodegradable, and the end-of-life products from this class can pollute the environment, different strategies and directives have been adopted at national, European or worldwide level. Thus, the European Court of Auditors, through directive 94/62/EC on packaging and packaging waste, provides that the recycling rate of plastic packaging waste for 2025 to reach 50%, and for 2030 55%. The analysis of the 2006-2020 recycling evolution showed that the Compound Annual Growth Rate (CAGR) for this period was about 5.4%. Of the amount of plastics packaging waste collected in the EU in 2020 (17,946 kt), only 46% (8,171 kt) were recycled, 54% are still sent to energy recovery (6,689 kt) or landfill (3,085 kt). In Romania, in 2020, 44% were recycled from the collected plastic packaging waste (http://www.plasticseurope.org).

https://doi.org/10.24264/icams-2022.IV.3

The main types of polymers used to make the packaging are: low density (LDPE) polyethylene (PE) or high density (HDPE), polypropylene (PP), polyethylene terephthalate (PET), and other types. The main uses of these types of polymers (in virgin and recycled form, respectively) are presented in Table 1.

Table 1. The main types of polymers used to obtain packaging
(Kokkılıç *et al.*, 2022; Azeez, 2019; http://www.plasticseurope.org/)

Polymer	Percentage*	Applications of virgin plastic	Applications of recycled plastic
LDPE	17.4%	Reusable bags, trays and containers, agricultural film, food packaging film, wire and cable coatings, etc.	Trash bags, decking, shipping envelopes, housewares, buckets, wire and cable jacketing, carpet
HDPE	12.9%	Milk and detergent bottles, blowmolded beverage bottles, heavy-duty films, toys, utensils, housewares, pipe and processing equipment, wire and cable insulations, fibers for clothing, gas pipes, etc.	Decking, flower pots, crates, pipe, detergent bottles, food storage containers, swimming pool installation, corrosion protection for steel pipelines, folding chairs and tables, electrical and plumbing boxes, housewares, industrial wrapping and gas pipes etc.
PP	19.7%	Food packaging, sweet and snack wrappers, hinged caps, microwave containers, pipes, automotive parts, bottles, medical syringes, beakers, drinking straws, office furniture, clear bags, carpets, etc.	Plant pots, packaging articles, automotive parts, bottle tops, carpets, household components, 3D printing filament
PET	8.4%	Bottles for water, soft drinks, juices, cleaners, packaging film, soft drink bottles, other beverage, food & medicine containers, X-ray and photographic film, as fibers for clothing and carpets, staple fiber, etc.	Clothing, carpet, clamshell containers, water bottles, food packaging, house ware, lighting product, power tools, sports tools, water and soft drink bottles, thermally stabilized films, etc.

*Percentage of the total amount of plastics obtained in the EU, reported in 2020

Polyethylene (PE) is one of the most important polymers used in the production of packaging. In contrast to the large volume of packaging production, PE is one of the post-consumer recycled plastics capitalized in products with low use value. Consequently, there is a strong need to increase the recycling rate of the PE in order to manage and recover PE waste in an environmentally friendly way. The challenge lies in finding a cost-effective method for sorting, decontaminating food-grade PE, eliminating the hazardous impact caused by improper disposal, and stabilizing mechanical performance during the recycling process to ensure safe reuse and close the loop back into production.

The paper aims to present some aspects regarding the mechanical recycling of plastic waste, especially those from polyethylene and polypropylene packaging, and to bring up some considerations from a technical and technological point of view that could lead to the production of recycled plastics of high quality, with mechanical properties close to those of virgin polymers.

https://doi.org/10.24264/icams-2022.IV.3

Industrial Technologies and Facilities for Mechanical Recycling of Plastic Waste

Mechanical recycling is the most important and environmentally friendly method of recovering recyclable plastics and consists of the processing of plastic waste into secondary raw material or products without significantly changing the chemical structure of the material. This recycling approach mainly includes a number of steps such as collection, sorting, washing and grinding of the plastic wastes (Al-Salem *et al*., 2009). Figure 1 shows the main structure of a "state-of-the-art" **mechanical recycling facility** for the recovery of recyclable plastics from sorted post-consumption packaging, from S.C. Monofil SRL, Săvineşti, Romania. The first stage of the process is **the sorting** (manual or automatic) of recyclable plastics from non-recyclable plastics and other foreign substances. At the same time, the first grouping of waste according to the type of polymers is achieved. Manual sorting can be facilitated by material identification codes but the possibility of human error should not be neglected. Then follows the operation of **grinding** into flakes, followed by **washing and drying** the flakes (by dehydration and centrifuge). Dry flakes, if homogeneous, are directed to storage and then to processing by extrusion-granulation.

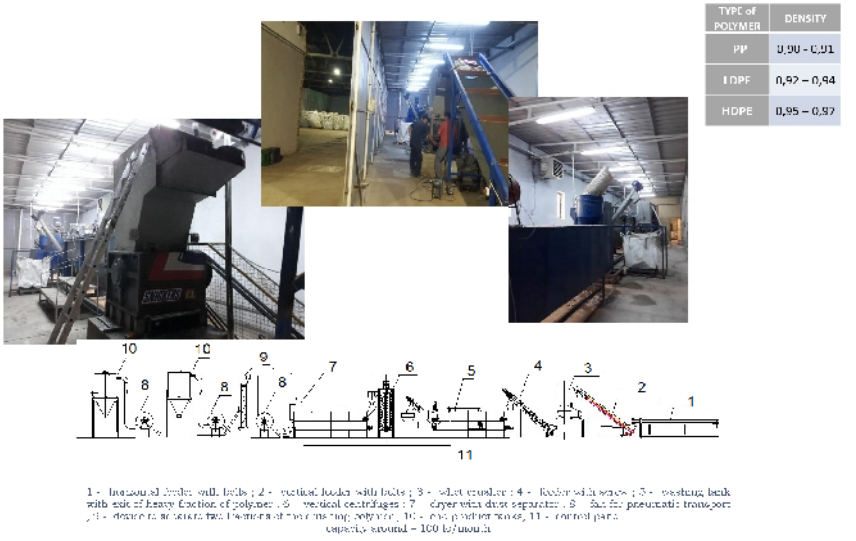

Figure 1. Technological flow and recycling facility of recyclable plastics from post-consumer packaging sorted from S.C. Monofil SRL

Certain types of materials such as HDPE or PET, require advanced purification in order to be used in the food industry, etc. This operation may include: chemical cleaning, optical sorting, washing for the label's removal, treatments at high temperatures and low pressures, etc.

The last stage is the **extrusion-granulation**, when the homogeneous waste flakes are melted and transformed into granules; in this operation can be added: plasticizers, antioxidants, compatibility agents, dyes, etc., to improve the properties of recycled waste. The recycled plastic material is obtained in the form of granules, which are then **packaged**, **stored** and **distributed** to consumers.

https://doi.org/10.24264/icams-2022.IV.3

Post-consumption packaging waste presents a series of **contaminations** that visibly affect the physico-mechanical characteristics and processability of the resulting recycled polymers. Of these, soluble mechanical impurities and dust are removed by classic processes in sorting and recycling facilities that operate on the principle of densimetric separation. Majority of the packages existing on the market are produced from two polymers, PE and PP, which have densities of less than 1g/cm^3, Table 2. The two polymers are immiscible in the molten state and therefore, the contamination of one of these polymers with the other (for example, HDPE contaminated with PP), leads to obtaining a recycled material with poor physico-mechanical and processing properties. The solutions adopted industrially for the removal of these contaminations consisted of:

1. Use of selective solvents for each of the mentioned polymers according to Table 2. This process is not cost-effective from an economic point of view due to the high costs as well as ecological in terms of solvent recovery.
2. Adding mineral additives in the technological process for the compatibility of the two immiscible polymers, PE and PP. This process was adopted by IMERYS for the production of HDPE for pipes that had a content of max 15% PP residual.
3. The use of polymers, such as LLDPE (linear LDPE), which ensures the compatibility of the two polymers at a concentration of maximum 10% PP in PE. This process is successfully used in the production of consumer goods and plastic pipes.

Table 2. Selected solvent in accordance with density

Polymer type	Polymer density	Solvent	Solvent density
Polypropylene (PP)	0.90-0.91	EtOH:H_2O (4:3)	0.92
Low-density polyethylene (LDPE)	0.92-0.94	EtOH:H_2O (1:1)	0.94
High-density polyethylene (HDPE)	0.95-0.97	H_2O	1.00
Polystyrene (PS)	1.05-1.07	10%NaCl/H_2O	1.08
Polyethylene terephthalate (PET)	1.38-1.39	$MgCl_2$ - saturated	1.34

Advanced Methods of Separation / Sorting of Waste According to the Type of Polymer

Certain types of polymers such as PP, LDPE and HDPE, are difficult to separate efficiently because of the small difference between their densities (Tall, 2000). In order to obtain high quality recycled plastic granules, numerous studies have been performed in which advanced methods of separation / sorting of waste have been successfully used, depending on the type of polymer. These methods are based on the properties of the basic polymers used in the packaging, which are presented in Table 3. A brief description of these advanced methods of sorting plastic waste is presented in Table 4.

Table 3. Physical proprieties according to each type of plastic
(Lim *et al.*, 2022; Cho and Cho, 2020)

Plastic type	Thermal adhesion temperature, °C	Gravity specific	Work function, eV
LDPE	85-100	0.92-0.94	4.92
HDPE	120-140	0.95-0.97	4.77
PP	125-145	0.89-0.91	5.04
PS	105-140	1.05-1.07	4.22
PET	135-140	1.31-1.39	4.42

https://doi.org/10.24264/icams-2022.IV.3

Table 4. Advanced methods of polymer waste separation

Method	Description	References
Spectroscopic method	The spectroscopic methods include Fourier transform near-infrared spectroscopy (FT-NIR), mid-infrared spectroscopy (MIR), Raman spectroscopy, laser induced breakdown spectroscopy (LIBS) or X-ray fluorescence. They allow the separation of plastic materials with densities close in value.	Adarsh *et al*., 2022; Bonifazi *et al*., 2018
Selective dissolution of polymers	The solubility-based processes include stages of dissolving a series of incompatible polymers in a common solvent at various temperatures or in different solvents, so that one polymer is separated each time. These processes differ in the method employed to recover the polymer after the dissolution stage. The method requires high amount of energy and use of chemical solvents, is not considered sustainable.	Pappa *et al.*, 2001
Thermal adhesion method	The method using the different softening or melting temperatures of various types of plastics. LDPE can be separated from HDPE through this method because their thermal-adhesion temperatures are different (Table 3).	Tall, 2000; Lim *et al.*, 2022
Froth flotation method	Froth flotation is a physicochemical separation process based on the differences in surface properties of materials. The principle behind froth flotation is the attachment of the hydrophobic particles to air bubbles to be floated and recovered to the concentrate, while the hydrophilic particles are wetted by water and stay in the liquid phase	Kokkılıç *et al*., 2022
Electrostatic separation	This technology makes it possible to separate different materials based on the differences between effective surface work function (Table 3).	Silveira *et al.*, 2018

Obtaining Recycled PE of High Purity by Electron Beam Treatment Followed by Electrostatic Separation of Packaging Waste Mixtures

Electrostatic separation methods allow obtaining materials of high purity (90-97%). This process offers high efficiency, low cost, and no concerns regarding secondary pollution (Wu *et al*., 2013; Silveira *et al*., 2018). It requires the waste to be dry and to have a size of 0.1-13 mm. In order to be able to apply this method, the waste flakes must be processed to acquire the electric charge. This stage can be achieved using: vibration, rotary drum, rotary blades, fluidized bed, cyclone, propeller-type tribo-charger, etc. Once the particles have acquired an electric charge, they can be separated electrostatically due to the difference between effective surface work function, Table 3. The most commonly used types of electrostatic separators are: the free-fall, roll, plate, and fluidized bed types. (Wu *et al*., 2013). The separation process depends on many factors such as: residence time in the charger, air velocity, rotating speed, vibrating frequency, the relative humidity of the ambient in the charger, etc. For these reasons, it requires the optimal establishment of electrical and geometric parameters to allow efficient separation of waste.

In a study presented at the ICARS 2022 conference (Gosh *et al*., 2022) the charge induced by accelerated electrons was tested for the electrostatic separation of polyolefins, in a batch/discontinuous type procedure. It has been found that a pretreatment with low electron doses before electrostatic separation leads to specific charging of polymers, such as polyolefins, almost independently of additives and fillers (exempted talc). In the case of a 1-year with return on investment (ROI) and an annual flow rate > ~ 3750 t, the total price of sorted polymer materials amounts to less than ~ EUR 1000 / t and demonstrates that accelerated electron technology can provide cost-effective recycling systems for polymer waste. This procedure must be transferred to a continuous procedure so as to be integrated into a continuously operating thermoplastics recycling facility.

https://doi.org/10.24264/icams-2022.IV.3

CONCLUSIONS

Plastics waste, and especially those from packaging, contain a mixture of polymers. For this reason, in the process of mechanical recycling of this waste, a sorting and separation by class of polymers is needed, in order to obtain recycled plastics of high quality, which could replace virgin plastics. Since the methods currently used in the industry need to be improved, several methods have been developed for the efficient separation of polymers from waste, but they are in an early stage. Of these new methods (spectroscopic method, selective dissolution of polymers, thermal adhesion method, froth flotation method, electrostatic separation methods), electrostatic separation methods allow obtaining materials of high purity (90-97%), and process offers high efficiency, low cost, and no concerns regarding secondary pollution. The method requires processing of the waste flakes to acquire the electric charge. Through a pre-treatment with low doses of electrons followed by electrostatic separation, an efficient separation of polymers from packaging waste (purity of over 90%) can be achieved in continuous flow and at low cost.

Acknowledgements

This work was supported by a grant of the Ministry of Research, Innovation and Digitization, CNCS/CCCDI – UEFISCDI, project number 712PED/2022, within PNCDI III.

REFERENCES

Adarsh, U.K., Bhoje Gowd, E., Bankapur, A, Kartha, V.B., Chidangil, S. and Unnikrishnan, V.K, (2022), "Development of an Inter-confirmatory Plastic Characterization System Using Spectroscopic Techniques for Waste Management", *Waste Management*, 150(2022), 339–351, https://doi.org/10.1016/j.wasman.2022.07.025.

Al-Salem, S., Lettieri, P. and Baeyens, J. (2009), "Recycling and Recovery Routes of Plastic Solid Waste (PSW): A Review", *Waste Management*, 29, 2625–2643, https://doi.org/10.1016/j.wasman.2009.06.004.

Azeez, T.O. (2019), "Thermoplastic Recycling: Properties, Modifications, and Applications", in: G.A. Evingür, Ö. Pekcan and D.S. Achilias (eds.), *Thermosoftening Plastics*, https://doi.org/10.5772/intechopen.81614.

Bonifazi, G., Capobianco, G. and Serranti, S. (2018), "A Hierarchical Classification Approach for Recognition of Low-Density (LDPE) and High-Density Polyethylene (HDPE) in Mixed Plastic Waste Based on Short-Wave Infrared (SWIR) Hyperspectral Imaging", *Spectrochimica Acta Part A: Molecular and Biomolecular Spectroscopy*, 198(2018), 115–122, https://doi.org/10.1016/j.saa.2018.03.006.

Cho, Y.J. and Cho, B.G. (2020), "Status and Future Prospects for Plastics Recycling", *Journal of the Korean Institute of Resources Recycling*, 29(4), https://doi.org/10.7844/kirr.2020.29.4.31.

Gosh, U., Constantinescu, D. and Stelescu, D. (2022), "Economic and Technical Aspects of Sorting of Mixed Thermoplastic Waste", *ICARS 2022*, IAEA Viena.

Kokkılıç, O., Mohammadi-Jam, S., Chu, P., Marion, C., Yang, Y. and Waters, K.E. (2022), "Separation of Plastic Wastes Using Froth Flotation – An Overview", *Advances in Colloid and Interface Science*, 308, 102769, https://doi.org/10.1016/j.cis.2022.102769.

Lim, J., Ahn, Y., Cho, H. and Kim, J. (2022), "Optimal Strategy to Sort Plastic Waste Considering Economic Feasibility to Increase Recycling Efficiency", *Process Safety and Environmental Protection*, 165, 420–430, https://doi.org/10.1016/j.psep.2022.07.022.

Pappa, G., Boukouvalas, C., Giannaris, C., Ntaras, N., Zografos, V., Magoulas, K., Lygeros, A. and Tassios, D., (2001), "The Selective Dissolution/Precipitation Technique for Polymer Recycling: A Pilot Unit Application", *Resources, Conservation and Recycling*, 34(1), 33-44, https://doi.org/10.1016/S0921-3449(01)00092-1.

Silveira, A.V.M., Cella, M., Tanabe, E.H. and Bertuol, D.A. (2018), "Application of Tribo-Electrostatic Separation in the Recycling of Plastic Wastes", *Process Safety and Environmental Protection*, 114, 219–228, https://doi.org/10.1016/j.psep.2017.12.019.

Tall, S. (2000), "Recycling of Mixed Plastic Waste – Is Separation Worthwhile?", PhD Thesis, Department of Polymer Technology, Royal Institute of Technology, Stockholm, Sweden.

Wu, G., Li, J. and Xu, Z. (2013), "Triboelectrostatic Separation for Granular Plastic Waste Recycling: A Review", *Waste Management*, 33, 585–597, https://doi.org/10.1016/j.wasman.2012.10.014.

***http://www.plasticseurope.org/ (visited 29.09.22).

https://doi.org/10.24264/icams-2022.IV.3

LEATHER INDUSTRY IN ROMANIA - AN OVERVIEW

CLAUDIA MONICA DUMITRA[1], LAURENTIA ALEXANDRESCU[2], MIRELA PANTAZI-BAJENARU[2], DANA CORINA DESELNICU[1, 3], AUGUSTIN SEMENESCU[1,3]

[1]*University POLITEHNICA of Bucharest, Splaiul Indepentei no. 313, Bucharest, Romania, monica.dumitra@upb.ro, dana.deselnicu@upb.ro, augustin.semenescu@upb.ro*

[2]*The National Research & Development Institute for Textiles and Leather - Leather and Footwear Research Institute Division, 93 Ion Minulescu st., 031215, Bucharest, Romania, email: icpi@icpi.ro*

[3]*Academy of Romanian Scientists, Splaiul Independenței 54, 050094, Bucharest, Romania*

Considering that the technological process is constantly increasing, and changes are made in all industries, the leather industry also encountered challenges that were overcome. The leather industry, in the face of the current difficulties, seeks to maintain within the European Union, its trend and the technical knowledge acquired. Technological advances provide this industry with tools capable of improving the yield, quality, and speed of cost recovery. For this subsector of the national economy to be competitive, it must identify, assimilate, and exploit the latest and most modern technologies. Romania has once an important competitor in the Europe market and in this paper, we are presenting an overview of the leather industry in Romania since it can play a very important role in the country's economy. Thus, this work presents aspects encountered at the level of the leather industry in Romania such as number of producers in the leather industry, evolution of the number of Romanian tanning and leather companies, evolution of labor productivity in companies in the leather and substitutes industry, number of footwear manufacturing companies, top 5 players on the footwear market. These aspects were obtained by the authors through their own processing of the data provided by Statistics.

Keywords: leather industry, footwear, labor productivity, personnel cost, GDP

INTRODUCTION

Since ancient times, the skin of domestic and hunted animals began to be used to produce footwear, clothing, accessories, decorative products, or other purposes. The evolution of the processing of hides and skins had several different stages, starting with the craft level and subsequently reaching industrial processing. The leather industry has experienced continuous development due to the specific characteristics of products obtained from leather (Ciubotaru and Visan, 2003). Currently, at the level of this industry, a great diversity of productions is processed due to the modern technologies used in processing and finishing. Animal skin differs from one species to another or even within the same species, depending on the different living conditions of animals such as environmental, geographical, sex, age, etc. (Bacardit *et al*., 2015). However, leather production is a process that generates pollution, and the leather industry contributes to the emergence of environmental protection problems, both regionally and globally (Oluwasevi *et al*., 2021; Brugnoli *et al*., 2013).

The raw materials used in the leather industry are obtained from the skins of domestic animals, wild and game animals, reptiles, and marine animals. Among the main sources of raw materials in the leather industry are cattle, sheep, goats, horses, pigs, deer, foxes, wolves, nutria, crocodiles, snakes, lizards, walruses, seals, sharks, etc. (Kurian and Nithya, 2009). Animals whose skin is used in the leather industry are slaughtered not for this aspect, but for meat, wool, milk, etc. Exceptions to this rule are animals whose fur is particularly valuable such as that derived from foxes, wolves, leopards, bears, etc. (Joseph and Nithya, 2009).

https://doi.org/10.24264/icams-2022.IV.4

At the level of Romania, the leather industry represents one of the traditional industries of the country, being an important sector of the national economy, satisfying the consumption needs of the population through leather products 9 (Memedovic and Mattila, 2008). The manufacturing companies are divided according to the resulting finished products such as shoe companies, companies producing soft or hard skins, companies producing leather goods, etc. In recent years, modernization and refurbishment actions have been carried out that have helped to develop the potential of the leather and footwear industry to achieve high-performance products (Bondrea *et al*., 2017).

LEATHER INDUSTRY IN ROMANIA

The leather, footwear, gloves, and fur sector are characterized by a special degree of complexity determined by the large number of basic technologies applied, totally different from one sector to another, as well as by the diversity of types of raw materials and materials used, namely semi-finished products and finished products. An unfavorable aspect of the leather processing industry is the ecological impact of the technologies used on the environment due both to the inefficiency of the treatment plants and to the use of technologies without recovery and recirculation systems. There are also discrepancies in the automation and computerization of technological processes, especially in the manufacture of shoes, leather goods, fur and gloves that lend themselves more to design, production and control systems using computing. However, through the modernization and refurbishment actions in recent years, the possibility of achieving high-performance products and maintaining an acceptable level of production by partially equipping it with new, modern equipment has been created.

The leather industry is an industry with a tradition of over 100 years in Romania, which developed intensively between 1965-1980, being represented in most of the counties of the country and with a significant share in the economy of Timis, Sibiu, Cluj, Bihor, Bucharest and Suceava counties. Many capacities in the footwear and leather goods sectors in the EU countries have been moved to our country, capitalizing on the advantages of the Romanian market.

Romania is part of the international and bilateral agreements operating in the leather industry (The Association Agreement of Romania with the European Community and its Member States; Central European Free Trade Agreement – CEFTA; Agreement between Romania and the States of the European Free Trade Association – EFTA; Free trade agreements with the Republic of Moldova, Turkey, and Israel.)

Based on the economic cooperation agreements related to the leather-footwear industry, but also for raw materials, the markets and for the products were opened through reciprocity. In relations with Turkey and CEFTA member countries, the leather industry in Romania is directly affected by large exports of hides and skins. Raw skins in our country are purchased at low prices by specially established foreign firms. Due to the reciprocal elimination of customs duties, they are exported abroad where they are processed and finished in tanneries and then reintroduced into the country, at high prices, in order to process various leather goods which in turn are exported. The companies that develop activities at the level of the leather industry in Romania are structured according to the final asset they produce footwear enterprises, clothing and leather goods enterprises, upholstery enterprises. In general, they are either embedded in a larger concern, or they are small independent units that develop a low turnover.

https://doi.org/10.24264/icams-2022.IV.4

Despite the decline recorded by all industries after 1989, the leather industry in Romania is trying to maintain its presence in the European Union. Immediately after 1989, the Romanian leather industry finds that the technology at its disposal has a gap of 15-20 years compared to the rest of Europe. For example, in Romania the degree of automation in a tannery was only 5%, and in a shoe factory 20%, while western countries were discussing full automation possibilities of the flow (Olle *et al*., 2014). The structural changes that have taken place in the world economy in the last two decades, as a result of the advances in information and communication technology, the liberalization of international trade, capital and technological flows, the increase in the supply of labor at a global level and the liberalization of its market have had an impact in the leather industry in Romania, which represents an important sector of the national economy.

In Romania, the leather industry is focused on the production of shoes. Currently, Romanian footwear manufacturers face two challenges. On the one hand, they must face competition coming mainly from China and Turkey, countries that produce very cheap shoes, and on the other hand, the growing competition in the segment of fashion, stylish shoes. In the domestic market, there is strong competition, in which both domestic and foreign companies participate. The best footwear brands on the domestic market indicate that consumer options are oriented towards good quality shoes, the purchase decision being influenced by the style and materials used, but also by the price of the products. Even if in the fight with Asian countries Romania has lost ground mainly due to wage differences, as a result of its favorable geographical position, expertise, well-qualified labor force and much less paid than in the West, Romania remains one of the largest shoe producers in Europe and the world. Given that the tanning market industry is a global industry, and Romanian tanners are dependent on access to raw materials and export markets, it is essential to find new suppliers of raw materials. The footwear market is full of competition, dozens of domestic and international brands are fighting for about 65 euros that a Romanian spends on average on shoes every year. Romanian footwear companies manufacture a wide range of products, from everyday shoes to luxury items.

COLLECTING AND ANALYZING DATA AND INFORMATION FROM LEATHER ENTERPRISES IN ROMANIA

As previously presented, the leather industry in Romania covers various industrial products and processes, imports and exports are carried out within it and are among the oldest industries in our country. The footwear, clothing, furniture, automotive and leather goods industries are the most important selling points for tannery production in the EU. Data such as the number of manufacturers in the leather industry, the number of employees in the leather industry, the cost of personnel, the evolution of the number of footwear enterprises, categories of enterprises, etc. will be presented below.

https://doi.org/10.24264/icams-2022.IV.4

Figure 1. Number of producers in the leather industry in Romania 2008 - 2016 (own processing of data provided by Statista)

This statistic shows the number of manufacturers in the manufacturing industry in Romania from 2008 to 2016 and it can be seen that in recent years you analyze this number is similar, being about 1550.

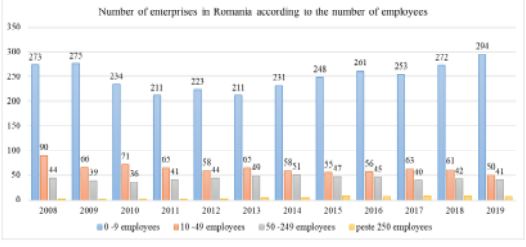

Figure 2. Evolution of the number of Romanian tanning and leather companies (own processing of data provided by Statista)

If we refer to the number of employees who are in the leather industry, from Figure no. 2 it can be noted that most are those that have several up to 9 employees, a feature kept throughout the analyzed period 2008 – 2019. On the other hand, the fewest companies are those that have at least 250 employees.

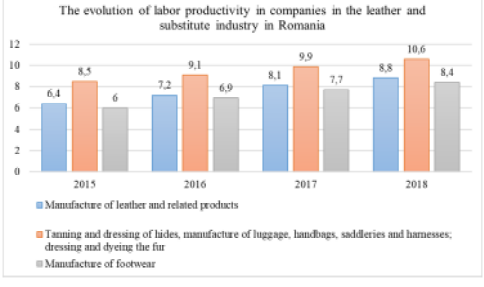

Figure 3. Evolution of labor productivity in companies in the leather and substitutes industry in Romania (own processing of data provided by Statista)

https://doi.org/10.24264/icams-2022.IV.4

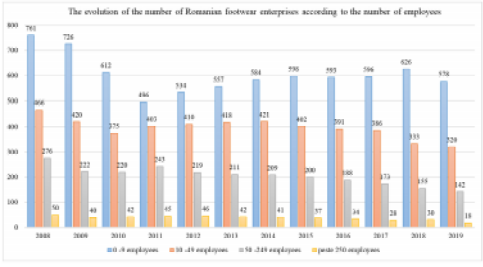

Figure 4. Number of footwear manufacturing companies in Romania in the period 2008 - 2019 (own processing of data provided by Statista)

Regarding the number of Romanian companies producing shoes, it can be noted that even in the case of this sector in the leather processing industry, the number of companies that have over 250 employees is much lower than those companies that have several up to 9 employees, which can be seen in Figure 4.

Figure 5. Personnel cost in the Romanian leather industry between 2008 and 2016 (own processing of data provided by Statista)

In Figure 5, the annual personnel costs of the leather and related products manufacturing industry in Romania between 2008 and 2016 are highlighted. In 2016, this industry had personnel costs of approximately 335.2 million euros. In Figure 6 can be seen the top 5 players on the footwear market in Romania in 2019, namely, Deichmann, CCC, Benvenuti, Decathlon and Nike. Thus, Deichmann is the market leader for both men's, women's, and children's shoes.

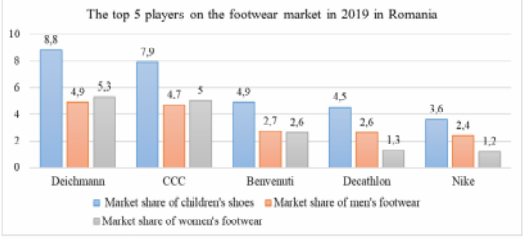

Figure 6. Top 5 players on the footwear market in 2019 in Romania (own processing of data provided by Statista)

https://doi.org/10.24264/icams-2022.IV.4

CONCLUSIONS

At the level of Romania, the leather industry developed significantly between 1965 and 1980, being especially present in Timiș, Sibiu, Cluj, Bihor, and Bucharest counties. In the 70s - 80s, at the country level, the production of products from the leather industry was sized to meet the needs of the domestic market, and the recorded surplus to be exported. Since 1989, the Romanian leather industry has entered direct competition with products made worldwide in industries like those in countries such as Turkey, India, China, Mexico, etc. Thus, the demand for leather products at the level of the domestic market has decreased significantly. As mentioned, the leather industry in Romania is considered a traditional industry. To meet demands many companies carried out modernization and refurbishment actions that help in keeping the leather industry on top. Also, it must be said that international arguments in this industry help in maintaining a growing market. The tools, human resources, and waste revolution contribute to the national economy no matter the product process. As could be seen, although the number of companies decreased from 2008, there are still important players/companies in the Romanian market that bring value to leather in Romania, they are known internationally and yet have an important contribution to GDP growth in Romania.

REFERENCES

Bacardit, A., Baquero, G., Sorolla, S. and Ollé, L. (2015), "Evaluation of a New Sustainable Continuous System for Processing Bovine Leather", *Journal of Cleaner Production*, 101, 197-204, https://doi.org/10.1016/j.jclepro.2015.04.012.

Bondrea, A.D., Lăzăroiu, G., Mocanu, R., Stan, A.N., Bălănescu, L., Mihăescu, L. and Berbece, V. (2017), "The Energy Method to Protect the Environment from Waste in the Leather Industry", *8th International Conference on Energy and Environment (CIEM)*, Bucharest, 105-109, ISBN:978-1-5386-3943-6, ISSN: 2067-0907.

Brugnoli, F., Gonzalez-Quijano, G. and Albu, L. (2013), "The First Environmental Social Report of the European Leather Industry", *Leather and Footwear Journal*, 13(1), 21-48, https://doi.org/10.24264/lfj.13.1.3.

Ciobotaru, V. and Vişan V. (2003), "Favourable Economical Effects by Using Ecological Technologies for Finishing Leathers", *International Conference – Management of Technological Change*, Greece.

Grand View Research (2021), "Leather Goods Market Size, Share & Trends Analysis Report by Product, by Type, by Region and Segment Forecasts, 2021-2028".

Joseph, K. and Nithya, N. (2009), "Material Flows in the Life Cycle of Leather", *Journal of Cleaner Production*, 17(7), 676-682, https://doi.org/10.1016/j.jclepro.2008.11.018.

Memedovic, O. and Mattila, H. (2008), "The Global Leather Value Chain: The Industries, the Main Actors and Prospects for Upgrading in LDCs", *International Journal of Technological Learning, Innovation and Development*, 1(4), 482-519, https://doi.org/10.1504/IJTLID.2008.021965.

Olle, L., Bou, J., Shendrik, A. and Bacardit, A. (2014), "Sustainable Solvent-free Finishing of Patent Leather Using Carbonyl-functional Resins", *Journal of Cleaner Production*, 65, 590-594, https://doi.org/10.1016/j.jclepro.2013.07.058.

Omoloso, O., Mortimer, K., Wise, W.R. and Jraisat L. (2021), "Sustainability Research in the Leather Industry: A Critical Review of Progress and Opportunities for Future Research", *Journal of Cleaner Production*, 285, 125441, https://doi.org/10.1016/j.jclepro.2020.125441.

***, https://www.statista.com/

STRATEGIES TO MAKE FOOTWEAR SUSTAINABLE AND CIRCULAR: A NEW WALK TOWARDS THE EUROPEAN GREEN RULES

MARIA JOSÉ FERREIRA[1]*, VERA V. PINTO[1], PATRÍCIA COSTA[1], ALBANO FERNANDES[2], TIAGO MACHADO[2]

[1]*CTCP – Portuguese Footwear Research and Technological Centre & GreenShoes4.0 Consortium, Rua de Fundões – Devesa Velha, 3700-121, São João da Madeira, Portugal, www.ctcp.pt; https://greenshoes.ctcp.pt, * mjose.ferreira@ctcp.pt*

[2]*AMF – Rua S. Cipriano, nº 658, 4835-461 Guimarães, Portugal, www.amfshoes.com*

To stay on pace with Paris Agreement goals on climate change, the 1.5°C pathway and Green Deal objectives, the footwear sector must speed up its efforts to reduce greenhouse gas (GHG) emissions to contribute to an absolute reduction of 50% by 2030 (or equivalent science-based targets) and achieve Net Zero by 2050. Footwear needs to move away from a linear pattern of growing consumption of planet resources towards a sustainable and more circular living where we use less resources and reduce emissions and climate change. To do so, the industry, whole value chain and consumers need to commit and take concrete actions. The objective of this article is to inspire footwear companies to measure their products environmental footprint, using the European Product Environmental Footprint methodology, and present the actions with higher potential of increasing sustainability and reduce the aggregate GHG footprint of new products.

Keywords: footwear, product environmental footprint, recycling, circular economy

INTRODUCTION

GHG emissions continue to rise and there is a growing likelihood that temperatures will temporarily exceed the threshold of 1.5°C above pre-industrial levels in the next five years. Rising temperatures are fuelling a variety of social, environmental, and economic impacts, from heatwaves and fires, to flooding. To contribute to limit global warming to 1.5°C is fundamental that footwear businesses measure footwear environmental footprint, define specific actions, and act.

The European Product Environmental Footprint (PEF) methodology/tool supports companies to measure the environmental performance of their products. The PEF tool introduces several improvements compared to other existing Life Cycle Analysis (LCA) methods including, clear identification of the environment impact categories to be considered, data sets to be used, minimum data quality requirements and detailed procedure to estimate the PEF.

Within project LIFE17 ENV/PT/000337 nine partners including AMF, APICCAPS, ATLANTA, CEC, CTCP (coordinator), EVATHINK, ICPI, INESCOP, FICE and PESTOS (https://www.greenshoes4all.eu/), were engaged in experimenting the EU draft PEF method and deploying new recycled materials. This paper presents works done by AMF shoe manufacturer and CTCP R&D centre with the objective of estimating and reducing footwear products environmental footprint.

To complement this works in the frame of national project GreenShoes4.0, CTCP studied and established a set of sustainable actions with high potential to contribute to the goal of reducing the global carbon footprint of footwear products by 50%. These actions will be synthetically presented to inspire companies to plan and give firm steps to reduce the environmental footprint of new products.

https://doi.org/10.24264/icams-2022.IV.5

EXPERIMENTAL

Materials

Three shoe models were selected by AMF and CTCP and LCA studies conducted to evaluate the magnitude and significance of potential environmental impacts throughout their life cycle. The work included identifying the most relevant impact categories, life cycle stages and processes. The systems boundaries integrate the entire life cycle (cradle to cradle), including the following: the raw material acquisition and pre-processing, manufacturing, distribution, and end-of-life. Additional, more greener solutions (e.g., incorporating recycled and lighter materials) were studied, and their environmental performance compared. Table 1 presents the models and a general description of main materials and components.

Table 1. Footwear environmental footprint impact categories assessed

Model	Description	
	Original	Sustainable
XFAST 	Upper: Microfiber (PA/PU) Lining: PA/PE Insole: Synthetic fibre/resin/PP Insock: PU/PE/PVP foam Outsole: EVA	Upper: Recycled cotton/PE Lining: Recycled PES/Corn fibres Insole (lighter: PE + Synthetic resins Lighter insock: (PU/PE/PVP foam) Outsole: EVA
TUBELESS 	Upper: Microfiber (PA/PU) Lining: PA/PE Insole: Kevlar Insock: PU/PE/PVP foam Outsole: Rubber	Upper: Recycled cotton/PE Lining: Recycled PES/Corn fibres Insole: Lighter Kevlar Lighter insock: (PU/PE/PVP foam) Outsole: Rubber
REDBRICK 	Upper: Leather Lining: PA/PE Insole: Kevlar Insock: PU/PE Outsole: PU/TPU	Version 1 Upper: Leather Lining: PA/PE Insole: Lighter Kevlar Insock: Lighter (PU/PE/PVP foam) Outsole: PU/TPU Version 2 Upper: Polyamide microfiber Lining: PA/PE Lighter insock: (PU/PE/PVP foam) Lighter Insole: PE + Synthetic resins Outsole: Recycled PU/TPU

Legend: EVA – Ethylene Vinyl Acetate; PA – Polyamide; PE – Polyester; PU – Polyurethane; TPU – Thermoplastic polyurethane; PP – Polypropylene; PVP – Poly(vinyl phosphate)

Methods

A Product Environmental Footprint (PEF) study is a standardised LCA study aiming to ensure that environmental information is comparable and reliable. The PEF calculation gives quantitative information on the impacts of products, taking into consideration the entire value chain (from the extraction to the end life stages). Estimating a PEF involves, namely: defining the goal and scope (e.g., functional unit, reference flow), life cycle inventory (e. g. primary data collection), impact assessment,

https://doi.org/10.24264/icams-2022.IV.5

interpretation and reporting, and final verification and validation (Fig. 1a). Measuring the product sustainability/environmental impacts involves (Fig. 1b):

1. Classification: assignment of all input and output flows collected in the inventory to the relevant impact categories.
2. Characterization: process to model environmental mechanisms linking the environmental pressures represented by inventory data to each EF impact category, and to quantify the impact magnitude.
3. Normalization: understand better the relative contribution of the studied system to the reference system for each indicator result, and which impact categories are more critical for the product system under study.
4. Weighting: process of converting normalized results of the different impact categories by using numerical factors based on the expressed relative importance of the impact categories considered.
5. Interpretation: can be used for hotspot analysis to identify the most relevant impact categories, life cycle stages, processes, and elementary flows.

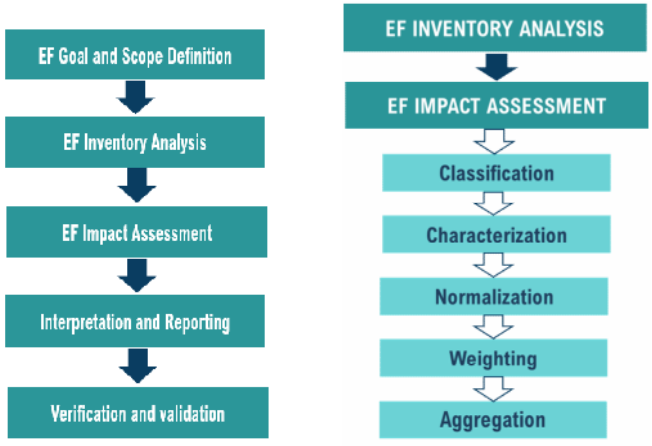

(a) (b)

Figure 1. Steps of EF methods (a) and of the impact assessment phase (b).

In this work specific primary data was collected at AMF company. Since the use phase of footwear is usually insignificant its impact was not considered. Regarding secondary data, Ecoinvent database v3.7 and other data sets were used. The software used to model the data was OpenLCA 1.9. The impact categories were calculated using the EU EF updated method (adapted).

RESULTS AND DISCUSSION

The PEF method assesses 16 impact categories (Table 2), covering, namely, climate change, acid rain, human toxicity, and particulate matter as well as impacts due to the use of water, land, and resources. Table 3 presents an example of the characterised, normalised, and weighted results obtained. Table 4 details the results for 3 of the 7 most relevant impact categories. These 3 categories, “Climate change”; “Fossil resources use”; and “Minerals/metals resources use”, represent about 57% of the total impact.

https://doi.org/10.24264/icams-2022.IV.5

Table 4 details also the environmental impact associated to the product "Life cycle stage" and "Materials, components and/or processes", giving indications to make changes to reduce the products PEF/environmental impact.

Among these, "Climate Change" is the most relevant impact category and was chosen to present and discuss the environmental impact of the shoe models. Fig. 2 presents the results of the Climate Change impact category, Global Warming Potential indicator (GWP100), in kg CO_2 eq, calculated for each pair of footwear before and after redesign (sustainable). Within this study was possible to reduce AMF shoes carbon footprint (kg $CO_{2\ eq}$) up to between 14 to 32% considering the more sustainable versions.

Table 2. Footwear environmental footprint impact categories assessed

EF Impact Category	Impact category Indicator	Unit
Climate change, total + fossil + biogenic + land use and land use change	Radiative forcing as global warming potential (GWP100)	kg CO2-eq
Ozone depletion	Ozone Depletion Potential (ODP)	kg CFC-11-eq
Human toxicity, cancer	Comparative Toxic Units for humans (CTUh)	CTUh
Human toxicity, non-cancer	Comparative Toxic Units for humans (CTUh)	CTUh
Particulate matter	Impact on human health	disease incidence
Ionising radiation, human health	Human exposure efficiency relative to U235	kBq U235-eq
Photochemical ozone formation, human health	Tropospheric ozone concentration increase	kg NMVOC-eq
Acidification	Accumulated Exceedance (AE)	mol H+-eq
Eutrophication, terrestrial	Accumulated Exceedance (AE)	mol N -eq
Eutrophication, freshwater	Fraction of nutrients reaching freshwater end compartment (P)	kg P-eq
Eutrophication, marine	Fraction of nutrients reaching marine end compartment (N)	kg N-eq
Ecotoxicity, freshwater	Comparative Toxic Unit for ecosystems (CTUe)	CTUe
Land use	Soil quality index and others	Dimensionless (pt)
Water use	User deprivation potential (deprivation-weighted water consumption)	m3 world eq
Resource use, minerals and metals	Abiotic resource depletion (ADP ultimate reserves)	kg Sb eq
Resource use, fossils	Abiotic resource depletion – fossil fuels, ADP	MJ

https://doi.org/10.24264/icams-2022.IV.5

Table 3. PEF example of results: characterised, normalised and weighted results

Impact category	Characterised results		Normalised	Weighted
	Reference unit	Total impacts	Total impacts (Person-years)	Total impacts (Points)
Acidification	mol H+ eq	4,46E-02	8,02E-04	4,97E-05
Climate change	kg CO2 eq	8,7	1,07E-03	2,26E-04
Ecotoxicity, freshwater	CTUe	1,60E+02	3,74E-03	7,19E-05
Eutrophication, freshwater	kg P eq	3,54E-03	2,20E-03	6,17E-05
Eutrophication, marine	kg N eq	9,57E-03	4,90E-04	1,45E-05
Eutrophication, terrestrial	mol N eq	7,98E-02	4,51E-04	1,67E-05
Human toxicity, cancer	CTUh	3,85E-09	2,28E-04	4,86E-06
Human toxicity, non-cancer	CTUh	1,12E-07	4,87E-04	8,96E-06
Ionising radiation	kBq U-235 eq	6,42E-01	1,52E-04	7,62E-06
Land use	Pt	7,81E+01	9,53E-05	7,56E-06
Ozone depletion	kg CFC11 eq	4,59E-06	8,56E-05	5,40E-06
Particulate matter	disease inc.	4,04E-07	6,79E-04	6,08E-05
Photochemical ozone formation	kg NMVOC eq	2,89E-02	7,11E-04	3,40E-05
Resource use, fossils	MJ	1,24E+02	1,90E-03	1,58E-04
Resource use, minerals and metals	kg Sb eq	1,28E-04	2,01E-03	1,52E-04
Water use	m3 depriv.	8,20E+00	7,15E-04	6,08E-05
Total (single score)	n/a	n/a	n/a	9,41E-04

Table 4. Footwear most relevant impact categories, stages and process (example)

Impact category	% Contribution	Life cycle stage	% Contribution	Material / component / process	% Contribution
Climate change	24,0%	Raw materials in final product	55,5%	Outsole	22,3%
				Insole	8,0%
				Interlayer	7,8%
				Insock	6,9%
				Upper	3,5%
		Raw materials that go to waste	3,0%	Interlayer	1,4%
		Waste	19,8%	Urban waste	15,7%
		End of Life	7,3%	Transport passenger car	3,8%
				Municipal solid waste	3,2%
Resource use, fossils	16,8%	Raw materials in final product	68,0%	Outsole	35,1%
				Insole	9,9%
				Insock	7,5%
				Interlayer	5,6%
		Waste	15,4%	Urban waste	12,0%
		Raw materials that go to waste	2,8%	Interlayer	1,3%
Resource use, minerals and metals	16,1%	Waste	90,9%	Urban waste	84,0%

https://doi.org/10.24264/icams-2022.IV.5

Fig. 3 details the main contributors to Climate Change (Global Warming Potential indicator, GWP100, in kg CO_2 eq) for each pair of footwear before and after redesign. These results indicate that "Materials selection (and their pre-processing)", including, raw materials, components, adhesives, and packaging, is the most relevant life cycle stage, representing around (65 to 90) % of the total GWP100 in kg CO_2 eq. The heavier components, e.g., upper, insole and outsole, are the main EF contributors. Manufacturing, including namely electricity and waste; and EoL represent, respectively, around (4 to 26) % and (6 to 7) % kg CO_2 eq of the total GWP100. These range of results are related with the production processes and type of models. Distribution account around 2 % of the total GWP100 in kg CO_2 eq. Therefore, reducing the weight of the materials incorporated and wastes generated, and selecting materials that are recycled and recyclable increases sustainability / decreases environmental impact.

FUTURE STEPS

GreenShoes4.0 Project

The Portuguese footwear sector has evolved from being an industry driven, resource-based activity to a market led knowledge-based industry, taking advantage of design and technology to preserve Portugal's shoemaking capability.

To remain competitive, it needs to concentrate on the creative phase, master the whole product and process life cycle and add value to each phase, embracing societal, environmental, digital and market trends and opportunities.

GreenShoes4.0 (Footwear, Leather Goods and Advanced Material, Equipment and Software Technologies) is a Portugal 2020 R&D collaborative project, promoted by a consortium of 15 companies covering the whole footwear value chain. It includes leather, insoles/soles, software, production equipment, logistics and leather goods and footwear leadership, as well as 8 R&D bodies with multidisciplinary and complementary capabilities (Fig. 4).

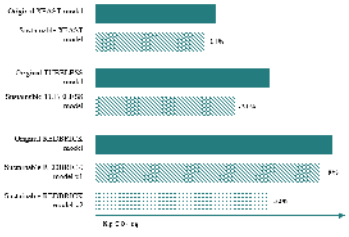

Figure 2. AMF shoes: Results of climate change impact category before and after sustainable

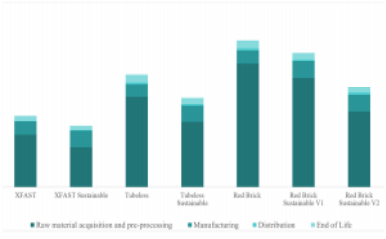

Figure 3. AMF shoes: Detailed contributor to Climate Change, GWP100), kg CO_2 eq.

GreenShoes4.0 seeks to mobilise the whole sector with the aim of researching, developing and creating in the following three areas:

1. New footwear and leather goods concepts aiming the circular and digital green economy, incorporating the materials developed, and produced and commercialised by new agile technologies.
2. Leathers, polymers and components for the footwear and leather goods of the future.

https://doi.org/10.24264/icams-2022.IV.5

3. New production technologies and digitalization of the entire value chain of the cluster and solutions to valorise the waste materials generated during the sector industry's productive phase and by used products.

Figure 4. The GreenShoes4.0 consortium

ACTIONS TO INCREASE SUSTAINABILITY AND REDUCE FOOTWEAR ENVIRONMENTAL FOOTPRINT

Based in life cycle analysis studies and experience of working with footwear and allied trade companies in Portugal and Europe, CTCP proposes a set of sustainable actions with potential of contributing towards the target of reducing 50% in the overall carbon footprint of products:

1. Design: Product ecodesign for longer life, repairability and circular use/recyclability.
2. Materials & Components: Upper, lining, and bottom materials and components that have low environmental, carbon and water footprint, are lighter, and recycled.
3. Materials Efficiency: Using materials more efficiently and reducing wastes.
4. Go Circular: Increasing production waste and products at the end-of-life circularity.
5. Research: Developing materials, components, and processes with lower environmental, carbon and water footprint (impact).
6. Energy: Increasing efficiency and adopting lower carbon and renewable energy.
7. Business Models: Increasing collaboration in the value chain from supply to retail and creating circular, digital enable, or traceable business models.
8. Processes: Deploying lower impact production processes.
9. Chemicals: Reducing chemical critical substances according REACH and other regulations.
10. Packaging: Rethink packaging to promote reuse and recycling and reduce weight.

Fig. 5 illustrates these actions estimated relative contribution to reduce the footwear footprint. The Figure shows that acting on the design phase, material and components selection and circularity will give a relevant contribution. The quantified reductions will depend on the company and products baseline, the specific objectives established, and the concrete measures undertaken. Ongoing work in GreenShoes4. establishes is fundamental to radically change the design and production approach and train designers and all the collaborators about the implications of their choices and procedures, namely sensibilizing for the following aspects:

1. Minimize the number and weight of all materials, components, adhesives, chemicals, and choosing light weight sustainable materials.
2. Incorporate materials and components that promote the product durability, longer use and repairability, namely upper in leather, removable insocks, soles

https://doi.org/10.24264/icams-2022.IV.5

that can be substituted or easily repaired by roughing and gluing a new bottom material.
3. Use recycled and recyclable materials and components.
4. Reduce the material required per pair / item and increasing material usage, namely upper shapes that allow maximum cut efficiency and minimize cutting and sewing wastes.
5. Minimise the number of production steps, finishing operations and chemicals used along the processes, selecting water-based solutions when needed.
6. Increase energy efficiency, reduce energy consumption, and use renewable green energy for production and transportation.
7. At the end-of-life increase the circular use of footwear, namely are made with one material, or materials that don't need to be separated before recycling or are modular and can be more easily disassembled before upcycling.

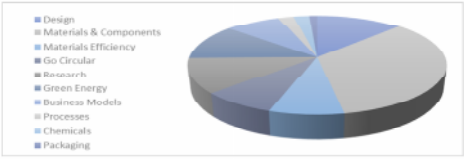

Figure 5. Where to act to reduce footwear and bags environmental footprint

CONCLUSIONS

This study involved the estimation of the environmental footprint of three footwear models based on PEF method. The reduction of footwear environmental footprint can be achieved by careful selection of materials and components, namely recycled and recyclable materials, reduction of materials amount (mass), reduction of waste generation by implementing more efficient production processes (e.g., more efficient cutting process), among others. Within this study was possible to reduce AMF shoes carbon footprint (kg CO2 eq) up to between 14 to 32%. To reduce the products environmental footprint companies, need to prioritize actions and bet in the ones with higher potential of achieving the reduction desired in a sustainable way, with social, environmental and economical balance. Based in life cycle analysis studies done within these projects and experience of working with footwear and allied trade companies in Portugal and Europe, CTCP identified and set of sustainable actions with potential of contributing towards the target of reducing 50% in the overall carbon footprint of footwear products.

Acknowledgements

CTCP, the Portuguese Footwear Technology and Research Centre, and the All the Partners of Projects Consortiums thank the support of the European project LIFE17 ENV/PT/000337 and of the National project GreenShoes4.0 - Calçado, Marroquinaria e Tecnologias Avançadas de Materiais, Equipamentos e Software, Projeto mobilizador Portugal 2020 Nº 46082.

REFERENCES

***, https://www.greenshoes4all.eu/

https://doi.org/10.24264/icams-2022.IV.5

LOW CARBON FOOTPRINT COMPOSITE BASED ON CHLOROPRENE RUBBER AND ELASTOMER WASTE

MIHAI GEORGESCU, MARIA SÖNMEZ, LAURENŢIA ALEXANDRESCU, MIHAELA NIŢUICĂ (VILSAN), MARIA DANIELA STELESCU, DANA GURĂU, DENIS-ANDREI DRUȘAN, ANA-MARIA CIOBANU, CIPRIAN CHELARU

The National Research & Development Institute for Textiles and Leather - Leather and Footwear Research Institute Division, 93, Ion Minulescu St., 031215, Bucharest, Romania, mihai.georgescu@icpi.ro

The aim of the paper consists in the treatment of post-consumer and technological waste of elastomers and plastomers, according to the 4R principle (reduction, reuse, recycling and recovery) by transforming them into raw materials with added value and integrating them into different industries. This will lead to the developing of new processing concepts regarding obtaining new biodegradable composite materials, with various waste contents (10-50 wt%). The composite is based on chloroprene rubber, and added post-consumer recycled rubber particles, with size of 45 mesh, eco-reinforcing material, and active fillers, plasticizers, vulcanizing agents, antioxidants. In order to enhance the compatibility and their level of interaction, the elastomer waste was finely ground (cryogenic mill) and functionalized with potassium oleate. Rubber waste acts as a filling material which leads to lower carbon footprint of the composite and lower mass. Tensile, tear strength, elasticity, hardness, abrasion resistance, melt flow index and morphological study (FT-IR) of those composites were examined in order to determine their viability in various application areas. The transformation of waste (cryogenically ground, and functionalized) into new products with added value will lead to remarkable improvements in the life cycle of raw materials and the sustainable use of this waste, contributing to increasing sustainability, improving eco-efficiency and economic efficiency and reducing the carbon footprint on the environment.

Keywords: composite, rubber waste, eco material, carbon footprint

INTRODUCTION

Chloroprene rubber, also known as neoprene, has excellent physical properties, and is characterized by good resistance to elements, flame, ozone and oils. Due to the presence of halogen in the rubber molecule, chloroprene resists burning better than any other hydrocarbon rubbers (Maya *et al*., 2018). Rubbers represent a class of materials that have become an environmental and economic issue, so the evaluation of the end-of-life management of these materials is of primary relevance. The emerging challenges of depletion of raw materials and an increase in rubber demand can be met through circular economy by slowing, closing, and narrowing resource loops. In recent years increasing recycling rates or increasing the product lifetime has become the primary goal for sustainable development. Besides tires, 50% of the world's rubber production is used for the consumption of general rubber goods (GRG). The processed waste can be transformed into cheaper and more sustainable material to feed their production. This cycle of producing tires and GRG from their used, worn-out materials increases sustainability. The use of worn-out tires and scrap GRG granulates in new products can significantly reduce the carbon footprint up to one-third compared to the products produced without recycled material (European Tyre and Rubber Manufacturers' Association, Circular Economy, https://www.etrma.org/key-topics/circular-economy/).

Nowadays, thanks to the development of new processes, there are several different options that can be identified for the end-of-life management of these materials. One of the most common solutions is to use the rubbers as fuel to burn this waste with associated energy recovery (Isayev, 2013; Ramarad *et al*., 2015). Another solution is to recycle this

https://doi.org/10.24264/icams-2022.IV.6

material through a mechanical process, by grinding the waste to convert it into powder or granulates, that can be used for different applications: bituminous mixtures, concrete, reinforcing fillers in polymers, rubber pads (Farina *et al*., 2017; Isayev, 2013; Li *et al.*, 2010; Si *et al.*, 2018; Sienkiewicz *et al*., 2017; Zanetti *et al.*, 2015). If rubber materials, in the last part of their life cycle, are not directed towards a recycling process, the remaining destination is landfill disposal, with the consequent possible development of diseases and ecological contaminations (Molino *et al.*, 2018). However, to fulfil the objectives defined by a circular economic model and therefore try to keep the quality of materials unchanged for as long as possible, it is necessary to rely on other processes, which allow a recovery of the material while preserving its physico-mechanical properties.

In this research the composite is based on chloroprene rubber, and added post-consumer recycled rubber particles, having the size of 0.5 µm, ground reinforcing material, and active fillers, such as plasticizers, vulcanizing agents, antioxidants. In order to enhance the compatibility and their level of interaction, the wood waste was finely ground (cryogenic mill) and functionalized with potassium oleate. Using rubber waste as a filling material leads to the lower carbon footprint composite and the decrease in mass.

EXPERIMENTAL

Materials

Materials used to obtain the composites were: c*hloroprene rubber*, from SAFIC ALCAN; *stearin* – powder, white colour, molecular weight 284,48 g/mol; *zinc oxide*, microparticles, white powder, precipitate 93-95%; *magnesium oxide*, microparticles, fine powder, precipitate 93-95%, *silicon dioxide*, molecular mass 60,08 g/mol, white colour, particle size < 0,5 mm; c*hlorinated paraffin* – solid state, powder; *N-Isopropyl-N'-phenyl-1,4-phenylenediamine*, brown flat granules, molar mass: 226,317 g/mol, density: 1.04 g/cm^3; *sulfur*, vulcanization agent (fine yellow powder, melting point: 115°C); *tetramethylthiuram disulfide* – vulcanization agent (density 1.40 g/cm^3), melting point <146°C, an ultrafast curing accelerator); all ingredients are from Bayer company.

Rubber waste was collected from the soles and footwear manufacturers, cryogenically ground at 8.000-10.000 rpm for 20s and screened through a 45-mesh screen (down to 0.5µm).

Methods

Functionalization

The functionalization of rubber waste with potassium oleate was achieved by mixing in a heated mechanical stirrer with 80 rotations/min, at a temperature of 80°C for 8 hours. The ratio between elastomer waste and potassium oleate – 50%.

Composites Processing

The rubber is plasticized for 90s, speed 40 rpm and 45°C, mechanically mixed in a Brabender Plasti-Corder. The other ingredients like fillers, plasticizers and elastomeric waste are slowly added, in 4 min 30s, twin screw speed set to 20rpm and temperature rises to 90°C. Compound homogenization for another 2 minutes, speed 60 rpm and temperature reaches over 100°C. The total processing times was 8 minutes. Table 1 shows

https://doi.org/10.24264/icams-2022.IV.6

tested formulations. The mixture is removed from the mixer chamber and finished on the electric roller, by adding the antioxidant and vulcanizing agents. The processing parameters are as follows: temperature 23-30°C, friction of the rollers 1:2, and 50 rotations/min, for 5 min and homogenization for another 2 min.

Table 1 shows the formulations of compound based on chloroprene rubber, with semi-active – MgO and ZnO white mineral fillers, and flame-retardant materials such as chlorinated paraffin, stearin.

This formulation has been altered to have a reduced carbon footprint, by adding functionalized waste in various amounts, 10, 20, 30, 50% waste respectively, compared to the amount of chloroprene rubber. The waste used was rubber (CC1-CC4).

Table 1. Polymer composites based on polychloroprene rubber compounded with rubber waste

Ingredients / Symbol	M.U.	CO	CC1	CC2	CC3	CC4
Processing on Brabender						
Chloroprene Rubber	g	190	190	190	190	190
Stearin	g	2.28	2.28	2.28	2.28	2.28
Zinc oxide	g	9.5	9.5	9.5	9.5	9.5
Magnesium oxide	g	7.6	7.6	7.6	7.6	7.6
Silicon dioxide	g	57	38	19	0	0
Chlorinated paraffin	g	57	57	57	57	19
functionalized rubber waste	g	0	19	38	57	95
Antioxidant IPPD	g	5.7	5.7	5.7	5.7	5.7
Processing on Roller						
Sulfur	g	2.85	2.85	2.85	2.85	2.85
Accelerator	g	2.28	2.28	2.28	2.28	2.28

RESULTS AND DISCUSSIONS

It can be seen in Figure 1 that the torque in the first part which lasts 90 secs at 40 rpm, the elastomer is added into the mixer and therefore the torque increases initially.

The first loading peak corresponds to the introduction of elastomers. As the torque increases, so does the temperature due to friction.

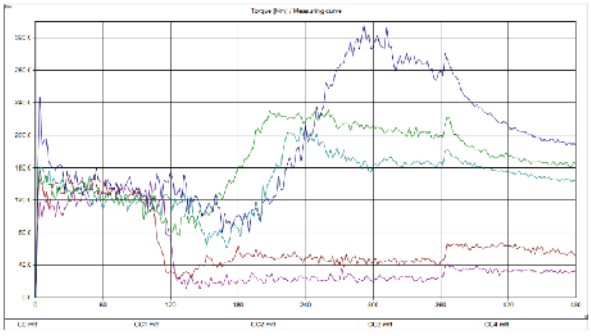

Figure 1. The variation of torque vs time recorded by the Brabender Plasti-Corder during the processing of rubber mixtures (C0-CC4)

https://doi.org/10.24264/icams-2022.IV.6

After the loading peak is reached, the torque begins to decrease, mainly due to the homogenization and plasticization of the elastomer, as well as due to the increase in temperature due to shear.

Then the other ingredients are added and the speed is reduced to 20 rpm for 4':30".

After 90 Sec first part, the torque begins to increase due to the incorporation of the ingredients, but also as a result of elastomer reinforcement and energy transfer.

After incorporating the fillers and other ingredients, the second loading peak is observed when a maximum torque is achieved.

The torque starts to decrease, indicating the homogenization of the mixture.

Then the homogenization of the compounds takes place for 120 sec at 60 rpm.

As a result, a maximum value of torque is obtained due to the compaction and homogenization of the rubber mixture.

This is generally followed by a decrease in the value of the torque, which indicates both the homogenization of the mixture and the increase of the mixture temperature due to the friction at a higher rotation speed (60 rpm).

FTIR Spectroscopy

The structural determinations were carried out on an IR molecular absorption spectrometer with double beam, in the range of 4000-600 cm^{-1}, using 4200 FT-IR equipped with ATR diamond crystal and sapphire head. The solid-state samples were set in the ATR and the equipment recorded the transmittance spectra of the sample and then compared it with the background spectra previously recorded. The recorded spectra of the samples were compared with the pure elastomer spectrum. After the tests were carried out, the following were found:

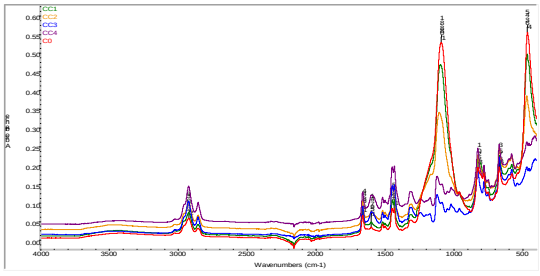

Figure 2. FTIR spectra of composites based on chloroprene rubber / rubber waste modified with potassium oleate

In the case of composites based on chloroprene rubber (control sample CO) and mixtures containing rubber waste modified with oleate CC1-CC4), both bands originating from rubber and the presence of additional bands due to the specific ingredients used in processing (silicon dioxide at 1088.81 cm^{-1}, 463 cm^{-1} as well as the presence of the potassium oleate surface modified rubber waste at 1597 cm^{-1}) can be identified.

The physical-mechanical characteristics of the composites – CC series (based on chloroprene rubber and elastomeric waste) are shown in Table 3.

https://doi.org/10.24264/icams-2022.IV.6

Table 3. Physical-mechanical characteristics

Physical-mechanical characteristics	Symbol			
	CC1	CC2	CC3	CC4
Hardness, °Sh A	55	49	49	47
Elasticity, %	18	16	16	20
Tensile strength, N/mm^2	11.86	12.22	13.87	14.18
Elongation at break, %	660	780	670	620
Remanent elongation, %	24	28	24	28
Tear strength, N/mm	46.5	47.9	49.2	50.2
Specific weight, g/cm^3	1.41	1.37	1.33	1.28
Abrasion resistance, mm^3	224.91	395.76	183.94	163.39

The ***hardness*** decreases by a maximum of 8°ShA in the samples that contain less silicon dioxide and more rubber waste.

Elasticity varies unevenly across the samples.

The ***tensile*** and ***tear strength*** gradually increase as the silicon dioxide active filler is replaced by the elastomeric waste, and show good values, of 14.18 N/mm^2 and 50.2 N/mm respectively for sample CC4.

Elongation at break shows good behaviour, and values over 620%.

Specific weight of the mixtures decreases as the amount of the powder increases, indicating, along with the other properties, a good compatibility between the chloroprene polar rubber and the rubber powder.

The abrasion increases with the increase in the amount of powder, shows a maximum value for the CC2 mixture (20 phr silicon dioxide and 20 phr rubber powder), followed by a decrease (an improvement) in the values for the CC4 sample.

Obtaining chloroprene rubber sheets (simple diagram – Figure 3). First part unvulcanized rubber sheet then processed and vulcanized on roller mix.

Figure 3. Obtaining and vulcanisation of rubber sheets

The Life Cycle Assessment methodology was used to carry out the analysis and the main environmental impact categories evaluated were: Climate change, Ozone depletion, Photochemical ozone formation, Acidification, Eutrophication, Ecotoxicity, Resource use. The first step, the analysis focused on the identification and quantification of main environmental hotspots. The results of the hotspots analysis reveal that the main contribution to the environmental impacts of the composite is the material consumption and type and the energy used. In this regard the material has an impact of up to 60% of total. The comparison underlines how the using of recycled of rubber waste allows to reduce the carbon footprint with 20%. Using the rubber waste lower the GWS from 3.02 kg eqCO_2 in processing phase to 2.4 kg eqCO_2.

CONCLUSIONS

- Composites based on Chloroprene rubber and semi-active fillers compounded with functionalized post-consumption rubber waste were obtained.

https://doi.org/10.24264/icams-2022.IV.6

- The values of the tensile and the tearing strength increase as the silicon dioxide active filler is replaced by the elastomeric waste, showing good compatibility with the matrix.
- Elongation at break has good values, over 620%.
- Abrasion resistance increases in samples with rubber wastes, property important for soles.
- The density of the mixtures decreases as the amount of rubber waste increases and replace other components with heavier density.

The use of recycled of rubber waste allows to reduce the carbon footprint with 20%, while maintaining good physico-mechanical properties.

Acknowledgements

This paper is funded by the Ministry of Research and Innovation within Program 1 – Development of the national RD system, Subprogram 1.2 - Institutional Performance - RDI excellence funding projects, Contract no. 6PFE/2018-PERFORM-TEX-PEL, the LIFE program in the frame of LIFEGREENSHOES 4 ALL (LIFE17ENV/PT/000337) project and PN 19 17 01 03/2019 project: "Biodegradable composites from technological and post-consumption polymeric wastes by designing and applying 4R eco-innovative technologies (4R-ECO-MAT)".

REFERENCES

Farina, A., Zanetti, M.C., Santagata, E. and Blengini, G.A. (2017), "Life Cycle Assessment Applied to Bituminous Mixtures Containing Recycled Materials: Crumb Rubber and Reclaimed Asphalt Pavement", *Resources, Conservation and Recycling*, 117, 204–212, https://doi. org/10.1016/j.resconrec.2016.10.015.

Isayev, A.I. (2013), "Recycling of rubbers", in: *The Science and Technology of Rubber*, fourth ed., 697–764, https://doi.org/10.1016/B978-0-12-394584-6.00020-0.

Li, X., Xu, H., Gao, Y. and Tao, Y. (2010), "Comparison of End-of-Life Tire Treatment Technologies: A Chinese Case Study", *Waste Management*, 30, 2235–2246, https://doi.org/10.1016/j.wasman.2010.06.006.

Maya, M.G., Soney, C.G., Thomasukutty, J., Lekshmi, K. and Sabu, T. (2018), "Development of a Flexible and Conductive Elastomeric Composite Based on Chloroprene Rubber", *Polymer Testing*, 65, 256–263, https://doi.org/10.1016/j.polymertesting.2017.12.006

Molino, A., Donatelli, A., Marino, T., Aloise, A., Rimauro, J. and Iovane, P. (2018), "Waste Tire Recycling Process for Production of Steam Activated Carbon in a Pilot Plant" *Resources, Conservation and Recycling*, 129, 102–111, https://doi.org/10.1016/j.resconrec.2017.10.023.

Ramarad, S., Khalid, M., Ratnam, C.T., Chuah, A.L. and Rashmi, W. (2015), "Waste Tire Rubber in Polymer Blends: A Review on the Evolution, Properties and Future", *Progress in Materials Science*, 72, 100-140, https://doi.org/10.1016/j.pmatsci.2015.02.004.

Si, R., Wang, J., Guo, S., Dai, Q. and Han, S. (2018), "Evaluation of Laboratory Performance of Self-Consolidating Concrete with Recycled Tire Rubber", *Journal of Cleaner Production*, 180, 823–831, https://doi.org/10.1016/j.jclepro.2018.01.180.

Sienkiewicz, M., Janik, H., Borzędowska-Labuda, K. and Kucinska-Lipka, J. (2017), "Environmentally Friendly Polymer-Rubber Composites Obtained from Waste Tyres: A Review", *Journal of Cleaner Production*, 147, 560-571, https://doi.org/10.1016/j.jclepro.2017.01.121.

Zanetti, M.C., Fiore, S., Ruffino, B., Santagata, E., Dalmazzo, D. and Lanotte, M. (2015), "Characterization of Crumb Rubber from End-of-Life Tyres for Paving Applications", *Waste Management*, 45, 161–170, https://doi.org/10.1016/j.wasman.2015.05.003.

***, European Tyre and Rubber Manufacturers' Association, Circular Economy, https://www.etrma.org/key-topics/circular-economy/ (accessed July, 2021).

BENEFITS OF HYDROGEN-RICH GAS (HRG) ON BIOMASS COMBUSTION PERFORMANCES

GHEORGHE LAZAROIU[1], LUCIAN MIHAESCU[2], GABRIEL-PAUL NEGREANU[2], IONEL PISA[2], RODICA MANUELA GRIGORIU[1], ELENA-ADRIANA JARCU[3]

[1]*University Politehnica of Bucharest, Energy Production and Use Department gheorghelazaroiu@yahoo.com*

[2]*University Politehnica of Bucharest, Technical Thermodynamics, Engines, Thermal and Frigorific Equipment Department, gabriel.negreanu@gmail.com*

[3]*University Politehnica of Bucharest, Hydraulics Department, Hydraulic Machinery and Environmental Engineering, mierloiu.adriana@yahoo.com*

Due to accelerated globalization, climate change and the increased costs of classical fuels, the notion of biomass is growing in recent years. Harnessing fuels as well as biofuels or hydrogen-rich gas (HRG) helps in a sustainable and environmentally friendly development of the energy sector. Although biofuels cover a vast field in terms of calorific value, maintaining a certain level of humidity is a real problem in practice. Thus, the primary combustion is difficult, and the combustion plants and their performances are restricted. Ideally, the humidity is recommended to be a maximum of 30%. Hydrogen-rich gas (HRG) is obtained from electrolysis, without the need to separate the two gaseous elements H_2 and O_2. Stoichiometric combustion is performed with oxygen from the gaseous fuel, the rest at the level of excess air being completed from the oxidizing medium. The experiments are carried out on pilot installations from University Politehnica of Bucharest and the advantages of co-combustion of solid biofuels with hydrogen-rich gas are highlighted. As a result, you want to increase the speed and combustion and decrease the CO emission. The limits of mass participation of avian waste mixed with biomass for co-combustion will be studied, with the highlighting of the influence of humidity and calorific value.

Keywords: Biofuels, HRG, co-combustion.

THE CONCEPT OF BIOFUEL

Today the concept of biomass encompasses the biodegradable part from a very wide range of fuels, industrial and agricultural waste such as: wood waste, agricultural, vegetable waste (fruit trees, vines), industrial and household waste, biogas, fermentation products, etc. (Bertrand *et al*., 2016). Energy crops are on the backsliding, especially due to relatively high costs, as well as resorting to fertilizers (Lazaroiu *et al*., 2020b).

The share of biofuels in the current energy balance is low, but a sharp development is expected mainly under the impetus of ecology. In our country, the production of energy from biofuels is about 2.1%. Biofuels may be used in a pure state or in a state of processing, in which case the notion of derived biofuel shall arise (Ubando *et al*., 2020).

From the category of derived biofuels, from solid ones, it is mentioned:

- Alcohol-type fuels (ethanol and methanol);
- Gaseous gas and pyrolysis gases;
- Biogas resulting from anaerobic fermentation.

The primary combustion of biofuels is, however, a difficult problem, starting from the very powering of combustion plants. Maintaining a certain level of humidity also restricts combustion technology as well as its performance.

If for wood biomass there are achievements, for the other categories of solid fuels, the researches have still remained at the initiation stage.

https://doi.org/10.24264/icams-2022.IV.7

ENERGY CHARACTERISTICS OF SOLID BIOFUELS AND COMBUSTION TECHNOLOGIES

Biofuels cover a very wide area for calorific value. But, the value of calorific power alone is not a sufficient indication for combustion processes. Elementary analysis is edifying analysis, it also leads to the value of calorific power. A simpler but sufficient analysis from the point of view of information is the technical analysis, which includes:

$$W_t^i + V^i + C_f^i + A^i = 100 \quad (1)$$

where:

W_t^i is the total humidity, in %

V^icoefficient of volatile materials, %

C_f^i fixed carbon, %

A^i ash (mineral mass), %

The index *i* indicates the fuel reference status.

Volatile materials allow the ignition process to be carried out. Fixed carbon is the carbon mass of organic carbon and also the main source of energy obtained by combustion.

The combustion process consists of three phases:

- Preparation for ignition (σ_p);
- Ignition and combustion of volatile substances (σ_v);
- Ignition and combustion of carbon (σ_c).

The size of the preparation time for ignition depends on the moisture and ash content, the sum of which is also called the ballast of fuel.

$$\sigma_p = f(W_t^i, A^i) \quad (2)$$

For solid biofuels with low humidity, the ash content is usually very low, the ignition time is less than 10% of the total combustion time $\sigma_a(\sigma_a = \sigma_p + \sigma_v + \sigma_c)$. But a high moisture content totally disrupts this balance.

Biofuels have a very high content of volatile substances, so ignition of fixed carbon (coke) is made easier.

Because combustion is controlled by the combustion of fixed carbon, the emission of carbon oxide will be high when the energy recovery of biofuels (Saxena *et al*., 2009; Lazaroiu *et al*., 2018a).

For direct combustion of solid biofuels, the solutions are (Lazaroiu and Mihaescu, 2021):

- For low power (below 1.2 MW) – layered combustion;
- For medium power (over 1.2 MW) – combustion in air current (similar to combustion sprayed for coal).

In both cases, the combustion of high ballast biofuels requires a heat input fuel (usually natural gas) to ease ignition, but also to reduce CO emission.

Replacing the natural gas used as a thermal support fuel with hydrogen brings advantages related to a much higher burning speed. Thus, the laminar rate of burning, *u*, of hydrogen compared to that of methane, at an excess of air λ = stoichiometric combustion, is 7 times higher (Methane 0.39 m/s; Hydrogen 2.96 m/s). The laminar burning rate, *u*, is expressed in m/s, and represents the speed at which the flame front advances, having the opposite direction with the direction of flow (Iordache and Chisaliga, 2022; Turner, 2004).

https://doi.org/10.24264/icams-2022.IV.7

The use of hydrogen instead of methane as a thermal support fuel has the advantage of releasing the point heat very quickly. In addition, the two gaseous fuels also have a similar value for the adjacent combustion temperature, having a value of around 2300°C. Rapid heat development allows the solid biofuel to be heated exactly in the areas necessary to ignite and complete the combustion, respectively.

Hydrogen-rich gas (HRG) is obtained from electrolysis, but does not include the separation of the two gaseous components H_2 and O_2. Stoichiometric combustion is performed with oxygen from the gaseous fuel, the rest at the level of excess air being completed from the oxidizing medium. It should be noted that the unit price of HRG is slightly lower than that of methane at the level of reporting to the heat released (Lazaroiu *et al*., 2018b; Saroj *et al*., 2020).

PRESENTATION OF THE CONCEPT OF TECHNOLOGY PROPOSED FOR THE COMBUSTION OF BIOFUEL IN A LAYER

The combustion of poultry waste depends on its calorific value which is influenced by its humidity. The poultry waste used in tests included the primary state of harvest with an average humidity of about 50%. This aspect involves an inhibition of the ignition process, especially for solid biomass a maximum humidity of 30% being usually required. The hydrogen-rich gas flame has a very high burning speed which allows for the correction of the negative thermo-physical aspects of ignition for humid raw poultry waste.

Experimental research was carried out on a pilot boiler located at UPB, this boiler is equipped with all the necessary facilities for experimental tests, allowing the determination of the flow rate of biofuel, HRG, thermal power output and polluting emissions (Lazaroiu *et al*., 2017; Aneke and Wang, 2016; Pîșă *et al*., 2016; Gejguš *et al*., 2016; Lazaroiu *et al*., 2020a).

During the experiments, a thermal power of 48 kW was achieved in the boiler, compared to the 55 kW nominal power.

The figure 1 shows the co-combustion scheme for wet poultry waste with hydrogen-rich gas (Lazaroiu *et al*., 2020c; Lazaroiu *et al*., 2021).

The combustion of avian waste responds to two objectives:

- Ecological (reduction of stored quantities);
- Heat generation (for poultry breeding halls).

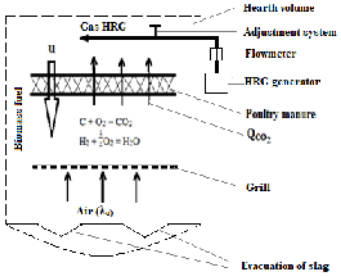

Figure 1. Co-combustion technology scheme using HRG

The validation tests will highlight the advantages of the new pilot demonstration installation.

https://doi.org/10.24264/icams-2022.IV.7

The use of co-combustion with hydrogen-rich gas will increase the mass share of avian waste above the previously determined values.

It is estimated that the maximum dose of HRG will be 40-50 liters for a quantity of 2-3 kg of avian waste-biomass mixture. The share of the thermal contribution of hydrogen in the above mentioned quantity is equivalent to an equivalent contribution of natural gas of 4-6%.

The energetic characteristics of the biofuel required the participation of hydrogen-rich gas to achieve an efficient combustion. The layered combustion of solid biofuels is under a strong influence of the density of the layer, the gaseous diffusion becoming much more permissive to a loosening of the layer.

Depending on the density of the solid fuel layer, combustion develops, according to two models shown in Figures 2 and 3.

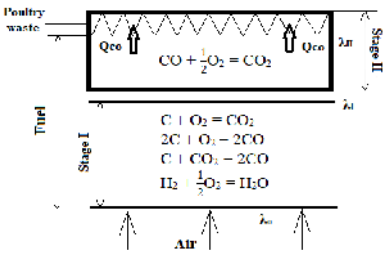

Figure 2. Scheme of the combustion model for a low porosity (high density) fix fuel bed, with two burning stages

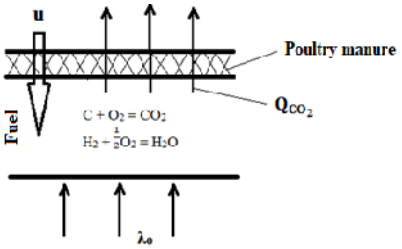

Figure 3. Scheme of the combustion model for a high porosity (low density) fix fuel bed

The burning rate will be influenced both by the quality of the waste biomass mixture (H_i^l, kJ/kg) and by the participation of hydrogen in co-combustion (% HRG).

Figure 4. Pilot plant, 55 kW boiler

Figure 4 shows the 55 kW pilot plant with the following furnace dimensions:

- length x width x height = 0.75 x 0.55 x 0.6 m;
- combustion volumetric space: 0.25 m^3;

https://doi.org/10.24264/icams-2022.IV.7

The dimensions of the fixed bars grate are:

- length: 0.52 m; width: 0.015 m; Space between bars: 0.015 m; Overall grill surface: 0.286 m^2; net surface of the grill: 0.19 m^2.

EXPERIMENTAL RESEARCH ON CO-COMBUSTION OF SOLID GAS BIOFUELS HRG, IN AIR CURRENT COMBUSTION TECHNOLOGY

This technology, as presented in Chapter 2, allows the combustion of biofuel particles with a diameter not exceeding 30 mm in air and flue gas suspension [9, 10].

The injection of HRG to raise the ignition and combustion capacity of biomass on the grid of a 1 MW thermal installation is shown in Figure 5.

The technology allows the capture of the thermal power of installations over 1 MW, the total power being a consequence of the number of burner models. The experiments were carried out at the pilot boilers from the University Politehnica of Bucharest and of 2 MW, a boiler equipped with a burner with the turmoil of the flame. HRG gas was introduced into the place of natural gas in one case, and into the body of the eddy burner in the second case. The fuel used was formed by the shredder of wood waste, with a humidity of 30%. The thermal input of HRG gas was on average 5%. The CO emission value was between 40 and 85 ppm, representing very low values.

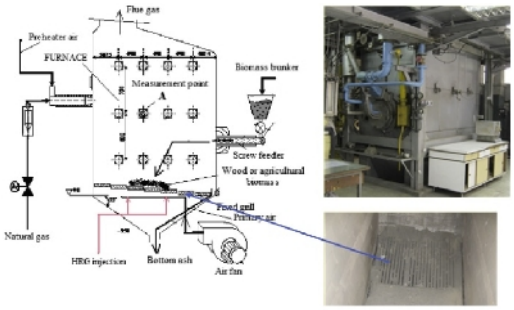

Figure 5. Use of HRG gas injection at a 2 MW thermal installation.

CONCLUSIONS

Experiments have highlighted the advantages of co-combustion of solid biofuels with hydrogen-rich gas. The aim was to increase the burning rate, reflected in the decrease in CO emission.

Two types of testing have been carried out, comprising two combustion technologies, namely:

- Layered burning with application for avian waste;
- Burning in air current, with application for wood and agricultural waste.

Experimental measurements have highlighted the theoretical premises, relating to the increase in the performance of the combustion of solid biofuels under the influence of hydrogen-rich gas, manifested in particular in the decrease in CO emission.

https://doi.org/10.24264/icams-2022.IV.7

Acknowledgment

This work was supported by a grant of the Ministry of Research, Innovation and Digitization, CNCS - UEFISCDI, project number PN-III-P4-PCE-2021-0777, within PNCDI III, contract PCE 5/2022.

REFERENCES

Aneke, M. and Wang, M. (2016), "Energy Storage Technologies and Real Life Applications – A State of the Art Review", *Applied Energy*, 179, 350–77, https://doi.org/10.1016/j.apenergy.2016.06.097.

Bertrand, E., Pradel, M. and Dussap, C.G. (2016), "Economic and Environmental Aspects of Biofuels", in: C.R. Soccol, S.K. Brar, C. Faulds, L.P. Ramos (eds.), *Green Fuels Technology*, Springer, 525-555, https://doi.org/10.1007/978-3-319-30205-8_22.

Gejguš, M., Aschbacher, C. and Sablik, J. (2016), "Comparison of the Total Costs of Renewable and Conventional Energy Sources", *Res Pap Fac Mater Sci Technol Slovak Univ Technol*, 24(37), 99–104, https://doi.org/10.1515/rput-2016-0010.

Iordache, I. and Chisaliga, D. (2022), *Hydrogen and Natural Gas in Romania* (in Romanian), ed. Didactica și Pedagogica, ISBN 978-606-31-1539-4, 174 p.

Lazaroiu, Gh. and Mihaescu, L. (2021), *Innovative Renewable Waste Conversion Technologies*, Springer, https://doi.org/10.1007/978-3-030-81431-1.

Lazaroiu, Gh., Ciupageanu, D.A., Grigoriu, R.M. and Simion, I. (2020a), "Energy Recovery from Poultry Manure: A Viable Solution to Reduce Poultry Industry Energy Consumption", *18th International Conference on Renewable Energies and Power Quality (ICREPQ'20)*, https://doi.org/10.24084/repqj18.272.

Lazaroiu, Gh., Mihaescu, L, Vatuiu, T., Pisa, I., Bondrea, D.A., Negreanu, G.P., Jarcu, E.A. and Berbece, V. (2018a), *Solid Biomass Source of Clean Energy* (in Romanian), vol. 2, Politehnica Press Bucharest, ISBN 978-606-515-840-5, 124 p.

Lăzăroiu, Gh., Mihăescu, L. and Pîşă, I. (2018b), "New Efficient And Ecologic Energy Vector", in V. Bădescu, G.C. Lăzăroiu, L. Barelli (eds.), *Power Engineering Advances and Challenges Part A: Thermal, Hydro and Nuclear Power*, ISBN: 978-1-138-70585-2, CRC Press Taylor & Francis Group, pp. 339-381.

Lazaroiu, Gh., Mihaescu, L., Bondrea, D.A., Pisa, I., Stanescu, L.A., Negreanu, G.P., Jarcu, E.A., Berbece, V., Dragne, M.I. and Ciupageanu, D.A. (2020b), *Towards a Circular Energetics* (in Romanian), vol. 3, Politehnica Press Bucharest, ISBN 978-606-515-840-4, 182 p.

Lăzăroiu, Gh., Mihăescu, L., Negreanu, G.P., Pîşă, I., Pop, E., Grigoriu, R.M. and Ciupageanu, D.A. (2021), "Experimental Researches on Poultry Manure Combustion in Co-Combustion with Biomass", *10th International Conference on Thermal Equipment, Renewable Energy and Rural Development (TE-RE-RD 2021 – Jubilee Edition)*, https://doi.org/10.1051/e3sconf/202128602013.

Lazaroiu, Gh., Mihăiescu, L., Grigoriu, R.M., Ciupageanu, D.A. and Simion, I. (2020c), "Efficient Poultry Industry Waste Management Approach in The Bioeconomy Framework", *Proceedings of the 8th International Conference on Advanced Materials and Systems – ICAMS 2020*, https://doi.org/10.24264/icams-2020.IV.12.

Lazaroiu, Gh., Pop, E., Negreanu, G., Pisa, I., Mihaescu, L., Bondrea, A. and Berbec, V. (2017), "Biomass Combustion with Hydrogen Injection for Energy Applications", *Energy*, 127, 351-357, https://doi.org/10.1016/j.energy.2017.03.133.

Pîşă, I., Lazaroiu, Gh., Mihaescu, L., Prisecaru, T. and Negreanu, G.P. (2016), "Mathematical Model and Experimental Tests of Hydrogen Diffusion in the Porous System of Biomass", *International Journal of Green Energy*, 13(8), 774-780, https://doi.org/10.1080/15435075.2016.1161629.

Saroj, C.D., Dhirendra, K.A., Ambica, N.T. and Mohanty, P. (2020), "A Review on Performance of Biogas and Hydrogen on Diesel Engine in Dual Fuel Mode", *Fuel*, 260, 116337, https://doi.org/10.1016/j.fuel.2019.116337.

Saxena, R.C., Adhikari, D.K. and Goyal, H.B. (2009), "Biomass-based Energy Fuel through Biochemical Routes: A Review", *Renewable and Sustainable Energy Reviews*, 13(1), 167-178, https://doi.org/10.1016/j.rser.2007.07.011.

Turner, J.A. (2004), "Toward a Hydrogen Economy: Sustainable Hydrogen Production", *Science*, 305(5686), 972–4, https://doi.org/10.1126/science.1103197.

Ubando, T., Felix, C.B. and Chen, W.H. (2020), "Biorefineries in Circular Bioeconomy: A Comprehensive review", *Bioresource Technology*, 299, 122585, https://doi.org/10.1016/j.biortech.2019.122585.

PROTEIN COMPOSITES FROM COLLAGEN BY-PRODUCTS FOR SAFE USE IN CIRCULAR ECONOMY

MIHAELA-DOINA NICULESCU[1], BRANDUSA GEORGIANA DUMITRIU[2], MADALINA IGNAT[1], SIMONA SAVIN[3], COSMIN ANDREI ALEXE[1], GABRIELA PAUN[3]

[1]*The National Research & Development Institute for Textiles and Leather - Leather and Footwear Research Institute Division, 93 Ion Minulescu Street, Bucharest, Romania, mihaelaniculescu59@yahoo.com*

[2]*BIOTEHNOS SA, 3-5 Gorunului Street, Otopeni, Romania, dumitriu_brandusa@yahoo.com*

[3]*The National Institute of Research and Development for Biological Sciences, 296 Independenței Bd. District 6, Bucharest, Romania, gpaunroman@gmail.com*

Sustainable economy means reducing the carbon footprint and minimizing the amount of waste released from productive activities. This paper presents the characterization of composites obtained from by-products of the leather industry based on collagen and keratin extracts. The protein composites have specific properties for the agricultural field and industrial applications in accordance with the current recommendations for a sustainable economy. Chemical-enzymatic hydrolysis of leather and wool by-products was performed for protein extraction. The composites were obtained by addition and crosslinking of collagen and keratin extracts with tannins from vegetable by-products. The characterization of composites was performed based on the results of analytical investigations by physico-chemical methods: volumetry, potentiometry, Texture Analysis, Dynamic Light Scattering, colorimetry, microscopy. It has been found that new collagen and keratin extracts contain small and medium components size, useful for the biostimulation of agricultural crops, but also contain large size components which give adhesive and film-forming properties, useful in industrial applications.

Keywords: by-products, composites, biocompatibility

INTRODUCTION

The circular economy is a model of production and consumption, which involves extending the life cycle of products and reducing waste to a minimum. When a product reaches the end of its life, its materials are kept within the economy wherever possible and they can be productively used again, thereby creating further value.

The leather processing industry (cattle, sheep, pigs, birds, fish) as well as the food industry generate significant amounts of by-products. As a result of biotechnological processing, industrial protein waste generates amino acids and peptides, which constitute alternative sources of nutrients for agriculture, as biostimulators and fertilizers (Epure *et al*., 2018), but can also be used in various other applications: adhesives (Sun *et al*., 2020), packaging (Ahmed *et al*., 2022), surfactants (Li *et al*., 2021), auxiliaries for leather processing (Ammasi *et al*., 2020), or as a metal chelating agent in decontamination actions (Lin *et al*., 2021). Furthermore, collagen from protein waste from the fish industry can be successfully used in various biomedical applications, including wound healing, tissue engineering and regeneration, drug delivery and other therapeutic applications (Subhan *et al*., 2021). Based on the proteins extracted from the by-products, we can generate materials with added value without using substances obtained through chemical synthesis, if we use extracts from vegetable waste that contain significant amounts of phenolic and polyphenolic acids, which function as crosslinking agents for protein compounds (peptides, polypeptides, amino acids) recovered from waste (Kaczmarek *et al*., 2020).

https://doi.org/10.24264/icams-2022.IV.8

The intelligent use of secondary protein resources is an ecological alternative to synthetic materials and contributes to reducing the carbon footprint, in the context of the circular economy.

This paper presents the characterization of new composites obtained from by-products of the leather industry based on collagen and keratin extracts for the agricultural field and industrial applications in accordance with the current recommendations for a green economy. For the safety of contact during the use of this composites, a cytotoxicity study was carried out, which will be presented in this work.

EXPERIMENTAL PART

Materials

The bovine leather by-products were collected from the Leather and Footwear Research Institute Division, Romania and wool was purchased from sheep farmers, for collagen and keratin extraction, as gelatin with average molecular weight over 35 kDa and collagen and keratin hydrolysate with average molecular weight 16 - 24 kDa.

The pomegranate peel was collected from food industry to obtain tannin extract.

Chemical reagents of analytical grade, like ammonia (25%), sodium carbonate, potassium hydroxide, tartric acid, oxalic acid, were purchased from Chimreactiv SRL (Bucharest, Romania). Ethoxylated alkyl non-ionic detergent from Borron SE for wool degreasing. Alcalase 2.4 L (protease from Bacillus licheniformis with 2.4 U/g) were purchased from Sigma-Aldrich (Bucharest, Romania). Glycerol were products of SC Chimopar SA Romania. Polyvinyl alcohol from SC REMED PRODIMPEX SRL.

Stabilized mouse connective tissue fibroblast cell line (NCTC clone 929) from the European Collection of Cell Cultures (ECACC - Sigma-Aldrich, USA).

Procedures

Bovine gelatin (GPU-B) was obtained by thermal hydrolysis of semi-processed leather by-products at 80°C temperature and pH 5.5-6.0. The collagen hydrolysate (HPU-B) was obtained by chemical-enzymatic hydrolysis at 63±2°C and pH 8.0-9.0. The keratin hydrolysate (KHU-B) was obtained by alkaline-enzymatic hydrolysis at pH 8.0-8.5 for 24-32 hours.

Pomegranate peel extract was used for crosslinking. The pomegranate peel extract (with 6% dry substance, 1.5% tanning substances) was obtained by hydrolyzing the pomegranate peel powder in water at pH=3.0-4.0, centrifugation and vacuum filtration (Cano-Lamadrid *et al.*, 2022).

The composites based on collagen or collagen and keratin were made by continuously stirring the gelatin, collagen or keratin hydrolysate additivated-crosslinked with glycerol, pomegranate peel extract at 40°C for 90-120 minutes, mixing with 5% polyvinyl alcohol solution and ultrasonication for 30 minutes at 40°C, casting as films and drying in vacuum at 55°C. The following types of films were made: PH1 collagen film, PH2 collagen and keratin film, PGA gelatin film. Also, PM control film, were made only of polyvinyl alcohol.

For the characterization of gelatin GPU-B, other films were cast: film FGS only from gelatin at the standard concentration 6.67% (GS) and film FGC only from gelatin at a concentration three times higher than the standard (GC).

The cytotoxic potential was determined by *in vitro* tests by colorimetric determination of cell viability using the standard MTT test (3-(4.5-dimethylthiazol-2-yl)-2.5 diphenyltetrazolium bromide). The plates were incubated for 24 and 48 hours at

https://doi.org/10.24264/icams-2022.IV.8

37°C in an air atmosphere with 5% CO_2. Finally, the absorbance was measured at the wavelength of 570 nm. To study the morphology, the culture of mouse fibroblast cells (NCTC), fixed in methanol and stained with Giemsa solution, was analyzed microscopically 48 hours after the addition of the protein compositions.

Analytical Methods

The collagen and keratin extracts and their complexes were analysed by gravimetric methods, dry substance (SR EN ISO 4684:2006) and total ash (SR EN ISO 4047:2002), by volumetric methods, in terms of total nitrogen and protein substance (SR ISO 5397:1996), aminic nitrogen (ICPI protocol) by potentiometric method for pH measurement (SR EN ISO 4045:2008).

Texture tests of gelatin and composites based on collagen and keratin were carried out using a TEX'AN texture analyser.

Dynamic Light Scattering was used for size particle determination and distribution by ZetaSizer device Nano ZS (Malvern, UK).

To evaluate biocompatibility, the absorbance was measured at a wavelength of 570 nm, using a Mithras LB 940 plate reader (Berthold Technologies). The morphology of mouse fibroblast cell cultures was observed with a Zeiss AxioStar Plus microscope equipped with a digital camera driven by AxioVision 4.6 software (Carl Zeiss, Germany).

RESULTS AND DISCUSSIONS

To obtain collagen and keratin composites, the following protein extracts were prepared: GPU-B gelatin, HPU-B collagen hydrolysate, KHU-B keratin hydrolysate, with the chemical characteristics presented in Table 1.

Table 1. Characteristics of protein extracts

Characteristics	MU	Gelatin	Hydrolysates	
		GPU-B	HPU-B	KHU-B
Volatile matter	%	7.29	4.25	7.54
Total ash	%	0.88	1.44	7.80
Total nitrogen	%	16.33	16.77	12.60
Protein substance	%	91.71	94.24	76.35
Amino nitrogen	%	0.45	0.85	0.62
pH analytical solution	-	5.60	7.54	7.68

An important characteristic for the industrial applications of gelatin is the strength of the gelatin. The strength of gelatin with standard concentration (GS), compared to gelatin approximately 3 times more concentrated (GC) was determined using a TEX'AN texture analyzer. The results of the analyses are presented in Figure 1 (a) and (b).

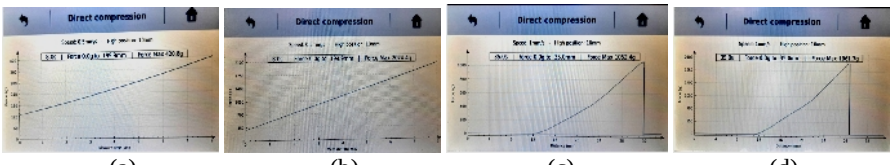

(a) (b) (c) (d)

Figure 1. Determining the strength of gelatin: (a) GS, (b) GC and of gelatin films: (c) FGS, (d) FGC

https://doi.org/10.24264/icams-2022.IV.8

Analytical data indicate that concentrated gelatin (GC) has a strength, expressed in grams, almost 5 times higher than that of gelatin with standard concentration (GS), respectively 2074.4 g versus 420.8 g. Both tests highlight the fact that a higher concentration, compared to the standard concentration, confers a higher resistance, and for the films associated with them, FGS and FGC the deformation force up to the breaking point is almost double, namely 1961 g compared to 1052 g.

The analysis of collagen and keratin hydrolysates by Dynamic Light Scattering (DLS) presented in Figure 2, (a) for HPU-B collagen hydrolysate and (b) for HKU-B keratin hydrolysate, highlights the existence of small peptide fragments, in the specific "nano" field in this case for free amino acids and oligopeptides.

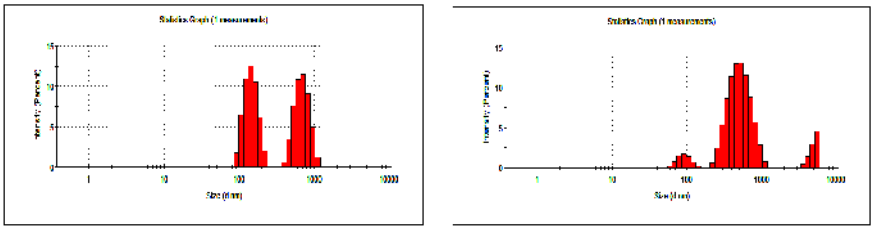

(a) (b)

Figure 2. Particle size in protein hydrolysates: (a) collagen; (b) keratin

The particle size distribution in collagen and keratin hydrolysates is presented in Table 2:

Table 2. Particle size distribution in protein hydrolysates

Sample	Particle size share		
	10-100 nm	100-1000 nm	1000-10000 nm
Collagen hydrolysate, HPU-B	1.8	97.0	1.2
Keratin hydrolysate, HKU-B	4.2	85.6	10.2

The reflected light intensity measurements indicate both populations of small particles, in the range of 10-100 nm and mainly populations of medium particles, located in the range of 100-1000 nm, dominant for collagen hydrolysates, but also large particles, in the range of 1000-10000 nm, spread over a wider range in keratin hydrolysates. DLS analysis corresponds with the higher content of amino nitrogen, which indicates a lower average molecular weight (Sörensen method) of collagen hydrolysate compared to keratin hydrolysate.

In this research, films were made from collagen and keratin extracts by additivating and crosslinking them with polyvinyl alcohol, glycerol, pomegranate peel extract, in three variants: with gelatin (PGA); with collagen hydrolysate (PH1); with collagen and keratin hydrolysates (PH2). The deformation forces up to the breaking point were determined in comparison with the control film, made of polyvinyl alcohol (PM). The results of determining the breaking point for these films are presented in Figure 3.

It is observed that although the appearance of the curves differs from one sample to another, the values of the deformation forces up to the breaking point are located near the maximum detection limit of the device, from 4995.2 g for the control film, to 5008.2 g for the film with additive-crosslinked collagen hydrolysate.

https://doi.org/10.24264/icams-2022.IV.8

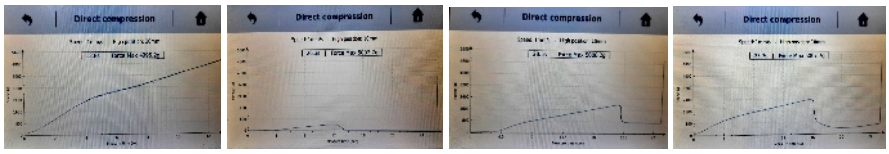

(a) (b) (c) (d)

Figure 3. Determining the strength of films: (a) PM; (b) PGA; (c) PH1; (d) PH2

It is also noted that the additivation-crosslinking of gelatin, Figure 3(b) causes an increase in the deformation forces up to the breaking point by approximately 2.5 times compared to the film formed from concentrated gelatin, without additivation-crosslinking, Figure 1(d).

The biocompatibility of the composites was quantified by cell viability, shown in Figure 4, (A) after 24 hours and (B) after 48 hours. The results were reported as viability percentages depending on the control sample (cells incubated without solution from the analysed sample) considered to have 100% viability.

It is found that the samples analyzed after 24 hours have no cytotoxic effect, remaining viable between the values of 96.84% and 89.28% in the concentration range 100-1000 μg/ml for sample PH1; 98.00% and 98.94% in the concentration range 100-750 μg/ml for sample PH2; 99.05% and 96.63% in the concentration range 100-1000 μg/ml for the PGA sample and 90.33% and 98.74% in the concentration range 100-1000 μg/mL for the PM sample. After 48 hours of incubation, over the entire concentration range, 100-1000 μg/ml, samples PH1, PH2, PM do not have a cytotoxic effect, but the PGA sample has a non-cytotoxic effect at a concentration of 100 μg/ml, slightly cytotoxic at in the range of concentrations 500-750 μg/ml and moderately cytotoxic at a concentration of 1000 μg/ml.

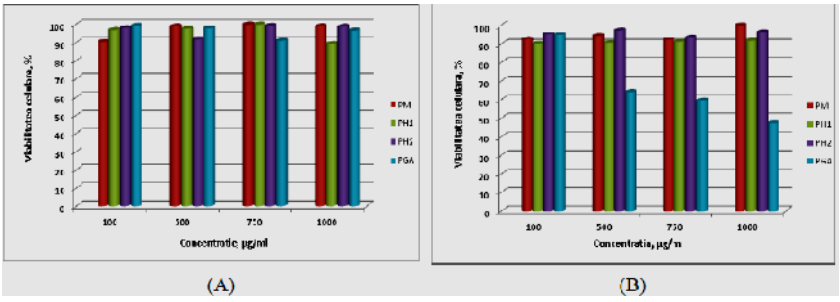

Figure 4. Cell viability: (A) after 24 hours; (B) after 48 hours

The microscopic evaluation led to the following observations: (i) the culture control (MC) shows the specificity of the cell line of mouse fibroblasts, NCTC-type, clone 929, with normal, elongated cells, having 2-3 extensions and monochrome cytoplasm; the positive control (M+), namely 3% oxygenated water, added to the culture medium (MEM) in an amount of 2 μl/ml generates cytotoxicity on the cells; (ii) for the PH1 sample in the concentration range 100-1000 μg/ml, the cells are uniform, monochrome cytoplasm, without cellular debris, with a cell density comparable to the culture control, without cytotoxicity; (iii) for the PH2 sample in the concentration range 100-1000 μg/ml, the cells have a normal appearance, without cytotoxicity; (iv) for the PGA sample at the concentration of 100 μg/ml cells are uniform, comparable to the culture control, without cytotoxic effect, at the concentration of 500-750 μg/ml cells are uniform, but rare, slight

https://doi.org/10.24264/icams-2022.IV.8

cellular debris appears, with slightly cytotoxic effect, at a concentration of 1000 μg/ml, cells are uniform, rounded, rarer, small cellular debris is present, the effect being moderately cytotoxic; (v) for the control sample PM, in the concentration range 100-1000 μg/ml, the cells have a normal appearance, without cytotoxicity.

CONCLUSIONS

The new collagen and keratin extracts contain small and medium components size, useful for the biostimulation of agricultural crops and contain large size components which give adhesive and film-forming properties, for industrial applications.

The protein extracts processed or not by additivation, crosslinking or just by simple physical conditioning, lead to obtaining composites with specific properties for the production of plant growth biostimulators, nutrients for crops and agricultural land, adhesives, for agriculture and industrial applications alike (wood, paper, leather, etc.).

The biocompatibility tests demonstrate the fact that the collagen and keratin hydrolysates from the composites do not have cytotoxic potential, but some composites with gelatin at concentrations higher than 500 μg/ml may show a slight cytotoxic effect in comparison with a control that does not have such an effect.

Acknowledgements

This work was supported by a grant of the Romanian National Authority for Scientific Research and Innovation CCCDI - UEFISCDI, project PN-III-P3-3.5-EUK-2019-0250, contract no. 262/2021, and by Ministry of Research, Innovation and Digitization, Program 1, contract no. 4 PFE/2021.

REFERENCES

Ahmed, M., Verma, A.K. and Patel, R. (2022), "Physiochemical, Antioxidant, and Food Simulant Release Properties of Collagen-Carboxymethyl Cellulose Films Enriched with *Berberis lyceum* Root Extract for Biodegradable Active Food Packaging", *Journal of Food Processing and Preservation*, 46(4), e16485, https://doi.org/10.1111/jfpp.16485.

Ammasi, R., Victor Sundar, J., Chellan, R. and Chellappa, M. (2020), "Amino Acid Enriched Proteinous Wastes: Recovery and Reuse in Leather Making)", *Waste Biomass Valorization*, 11, 5793–5807, https://doi.org/10.1007/s12649-019-00912-6.

Cano-Lamadrid, M., Martínez-Zamora L., Castillejo, N. and Artés-Hernández, F. (2022), "From Pomegranate Byproducts Waste to Worth: A Review of Extraction", *Foods*, 11(17), 2596, https://doi.org/10.3390/foods11172596.

Epure, D.G., Cioineag, C.F., Becheritu, M., Gaidau, C., Stepan, E. and Gidea, M. (2018), "Use of Biofertilizant Based on Collagen Hydrolysate for Cereal Seed Treatment", *AgroLife Scientific Journal*, 7(1), 48-55.

Kaczmarek, B. and Mazur, O. (2020), "Collagen-Based Materials Modified by Phenolic Acids-A Review", *Materials*, 13(16), Article No. 3641, https://doi.org/10.3390/ma13163641.

Li, Y., Sun, D.Y., Jiang, C.H., Ding, H.Y. and Wang, Q.J. (2021), "Preparation of Polypeptide Surfactants Using Chromium-Containing Waste Leather: Effect of Hydrophilic and Lipophilic Groups", *Journal of Surfactants and Detergents*, 24(6), 923-931, https://doi.org/10.1002/jsde.12513.

Lin, S.T., Hu, X., Li, L.H., Yang, X.Q., Chen, S.J., Wu, Y.Y. and Yang, S.L. (2021), "Preparation, Purification and Identification of Iron-Chelating Peptides Derived from Tilapia (*Oreochromis niloticus*) Skin Collagen and Characterization of the Peptide-iron Complexes", *LWT - Food Science and Technology*, 149, Article no. 111796, https://doi.org/10.1016/j.lwt.2021.111796.

Subhan, F., Hussain, Z., Tauseef, I., Shehzad, A. and Wahid, F. (2021), "A Review on Recent Advances and Applications of Fish Collagen", *Critical Reviews in Food Science and Nutrition*, 61(6), 1027-1037, https://doi.org/10.1080/10408398.2020.1751585.

Sun, J., Su, J.J., Ma, C., Göstl, R., Herrmann, A., Liu, K. and Zhang, H. (2020), "Fabrication and Mechanical Properties of Engineered Protein-Based Adhesives and Fibers", *Advanced Materials*, 32(6), https://doi.org/10.1002/adma.201906360.

OBTAINING AND CHARACTERIZING A POLYMER COMPOUND BASED ON NBR ELASTOMER AND FUNCTIONALIZED POST-CONSUMER RUBBER WASTE

MIHAELA (VILSAN) NITUICA, MARIA SÖNMEZ, MARIA DANIELA STELESCU, LAURENTIA ALEXANDRESCU, MIHAI GEORGESCU, CIPRIAN CHELARU, DENIS-ANDREI DRUSAN, ANA-MARIA CIOBANU, DANA GURAU

The National Research & Development Institute for Textiles and Leather - Leather and Footwear Research Institute Division, 93 Ion Minulescu St., sector 3, Bucharest, Romania, mihaela.nituica@icpi.ro

This work presents the obtaining and characterization of elastomeric compounds based on butadiene-co-acrylonitrile rubber and NBR rubber waste (from the footwear industry) that replaces the active silicon dioxide filler. The rubber waste was cryogenically ground to micrometric dimensions and functionalized with monoethylene glycol (MEG). After grinding, it is functionalized with monoethylene glycol (MEG) in a proportion of 20% at a temperature of 60°C. By recycling and reusing vulcanized rubber waste (NBR), as well as by means of advanced technologies, it is possible to contribute to the improvement of product quality, the protection of the environment through waste recycling, and most importantly the protection of human health through the elimination of noxious substances during their burning and, of course, increasing the turnover of economic agents. The polymer compounds obtained after conditioning at ambient temperatures were characterized according to the standards in force for the footwear industry, in terms of physical-mechanical normal state and accelerated aging at 70°C for 168 h and FT-IR spectroscopy. The polymer composites based on NBR rubber and functionalized rubber waste present optimal values according to the standards and are used in the processing of general-purpose footwear.

Keywords: NBR elastomer, rubber waste, FT-IR spectra, polymer compound, waste recycling

INTRODUCTION

At the global level recently, the industry of processing vulcanized materials aims to recycle them (United Nations Environment Programme, 2015), and the diversification of the chemical compositions and structures of vulcanized rubber is the main reason because it is not biodegradable. The increase in the number of finished products made of vulcanized rubber (tyres, car parts and shoe soles), represents a threat to the environment, as well as to human health (Formela, 2021). By recycling and reusing vulcanized rubber waste (nitrile rubber), as well as advanced technologies, it is possible to contribute to the improvement of product quality, to environmental protection through waste recycling, and most importantly to the protection of human health through the elimination of noxious substances during their burning and, of course, increasing the turnover of economic agents (United Nations Environment Programme, 2015; Chittella *et al*., 2021). The progress made in recent years in the management of elastomer waste has made rubber products, especially used ones, to be perceived as a potential source of valuable raw materials (Sienkiewicz *et al*., 2017). Thus, a series of decisions and regulations appeared in the regulation of waste recycling and reuse. The Romanian government has issued a series of decisions for waste management. One of these decisions is Governmental Decision no. 85/2002 – "Introduction of the waste management record and the European waste catalog". The cryogenically ground rubber (elastomer) waste used in powder form, in elastomeric compounds, has particles with regular shape, a smooth surface and shows a low level of oxidation (Nituica *et al*., 2022). Butadiene-co-acrylonitrile (NBR) rubber mixtures generally contain fillers, plasticizers, antioxidants, vulcanizing agents to improve tensile and tear strength,

https://doi.org/10.24264/icams-2022.IV.9

workability, etc. (Alexandrescu *et al*., 2014). Thus, active fillers such as silicon dioxide can be successfully replaced by ground (powder) and functionalized elastomeric waste (Stelescu *et al*., 2020; Nituica *et al*., 2021). The compounds based on NBR rubber and elastomeric waste (from the footwear industry) processed through the mixing technique, in the presence of vulcanization systems, leads to the obtaining of technical products with characteristics necessary for use in the footwear industry (Nituica *et al*., 2022). The vulcanization of the compounds has a major impact on the final properties of the products, representing an important property, and the use of vulcanized rubber waste as filler is important in obtaining elastomeric compounds (Roucoules *et al*., 2007; Alexandrescu *et al*., 2019).

EXPERIMENTAL PROCEDURE

Materials

The materials used were: 1) NBR - butadiene-co-acrylonitrile rubber: acrylonitrile content – 34%, Mooney viscosity (100%) – 32±3, density – 0.98 g/cm^3; 2) ST – stearin: white flakes, molecular weight 284.48 g/mol, dynamic viscosity 9,87 mPa.s at 70°C, volumetric weight approx. 400-500 kg/m^3, moisture – 0.5% max, ash – 0.025% max; 3) ZnO – zinc oxide microparticles (white powder): precipitate 93-95%, density – 5.5 g/cm, specific surface – 45-55 m^2/g; 4) SiO_2 – silicon dioxide: density 1.9-4.29 g/cm^3, molar mass – 60.1 g/mol; 5) $CaCO_3$ – chalk: white powder, molecular weight 100.09; 6) rubber waste – ground rubber from the footwear industry; 7) functionalized rubber waste – ground rubber from the footwear industry functionalized with MEG (monoethylene glycol); 8) mineral oil; 9) IPPD 4010 – N-isopropyl-N'-phenyl-p-phenylenediamine: density – 1.1 g/cm^3, solidification point of over 76.5°C, flat granules brown to dark violet in color; 10) S – Sulphur: vulcanization agent, fine yellow powder, insoluble in water, melting point: 115°C, faint odor; 11) Th – tetramethylthiuram disulfide: curing agent, density – 1.40g/cm^3, melting point <146°C, ultrafast curing accelerator.

Methods

Preparation of Polymer Compound Based on NBR Rubber and Non-Functionalized/ Functionalized Rubber Waste

The polymer compounds obtained are based on butadiene-co-acrylonitrile rubber (NBR) and non-functionalized/functionalized butadiene-co-acrylonitrile rubber waste with monoethylene glycol (MEG), Table 1. Phases of the laboratory-scale technological process for making polymer compounds based on NBR elastomer and non-functionalized/functionalized NBR rubber waste with MEG (monoethylene glycol) are the following: analysis and reception of raw materials; dosing of raw materials; mixing the polymer compound in Brabender mixer; rheological characterization on a Monsanto Rheometer for establishing the optimal vulcanization parameters in the electric press; making the samples (with dimensions according to the elastomer processing standards) in the electric press for quality control of the mixture; quality control of samples made of elastomeric compound based on NBR rubber and non-functionalized/functionalized waste.

The polymer compounds were processed by mixing technology on the Brabender Plasti-Corder (capacity 350 cm^3) with the possibility of adjusting the working parameters (temperature and mixing speed) according to Table 2, with strict observance of the order of introduction of the ingredients.

https://doi.org/10.24264/icams-2022.IV.9

Table 1. Formulation of compounds based on NBR rubber and non-functionalized/functionalized rubber waste

Symbol	MU	B0	$B0_2$	BCP_1	BCP_2	BCP_3	BCP_4
Mixing in the Brabender Plasti-Corder							
Butadiene-co-acrylonitrile (NBR)	g	150	150	150	190	190	190
Stearin	g	1.8	1.8	1.8	2.85	2.85	2.85
ZnO (active powder)	g	7.5	7.5	7.5	9.5	9.5	9.5
SiO_2	g	45	-	30	19	0	0
$CaCO_3$ (kaolin)	g	37.5	37.5	37.5	37.5	37.5	37.5
Non-functionalized rubber waste (50%)	g	-	75	-	-	-	-
Functionalized rubber waste (NBR)	g	-	-	15	30	45	75
Mineral oil	g	15	15	15	15	15	15
IPPD 4010 antioxidant		4.5	4.5	4.5	4.5	4.5	4.5
S (Sulfur)	g	2.25	2.25	2.25	2.25	2.25	2.25
Th (tetramethylthiuram disulfide)	g	0.9	1.5	0.9	0.9	0.9	0.9

B0 – composite without rubber waste; $B0_2$ – composite with 50% non-functionalized rubber waste (butadiene-co-acrylonitrile rubber waste)

Butadiene-co-acrylonitrile rubber waste (NBR rubber waste from consumer goods and the footwear industry) was used in elastomeric mixtures in powder form. The waste was ground with a cryogenic mill, in three cycles, at a speed of 12,000-14,000 rpm to a final size of 0.35 mm. After grinding, it was functionalized with monoethylene glycol (MEG) in a proportion of 20% at a temperature of 60°C.

Table 2. Working method using the Brabender Plasti-Corder mixer

The order of introduction of the ingredients	Mixing time (min.)	Mixing speed	Temperature, °C
NBR rubber (plasticization)	1’ 30”	40 rpm	40°C
Ingredients (without vulcanizing agents)	3’	35 rpm	40°C
Vulcanizing agents (S and Th)	1’30”	40 rpm	40°C
Homogenization time	4’	100 rpm	80 °C
TOTAL	10’	35-100 rpm	40°C-80°C

After the mixing process, the elastomeric polymer compounds based on NBR rubber and rubber waste are tested from a rheological point of view on a Monsanto Rheometer, at 165°C, for 24’, to establish the optimal vulcanization times for pressing in the electric press, in standard molds. After pressing, 150x150x2 mm samples are obtained by pressing in elastomer-specific molds, by compression between its plates. The optimal parameters for obtaining the samples are: working temperature 165°C; pressing time – 5 minutes; cooling time (water cooling) – 10 minutes; pressure – 300 kN. The samples are subjected to characterizations according to the standards in force.

Characterization of Elastomeric Compounds

The elastomeric compounds based on NBR rubber and rubber waste were tested in terms of rheological, physical-mechanical and structural properties (Infrared Spectroscopy) using appropriate techniques.

The elastomeric compounds based on NBR rubber were tested in compliance with the physical-mechanical standards in effect, under normal condition and accelerated ageing: hardness, °ShA – ISO 48-4:2018; elasticity, %, ISO 4662:2017; tensile strength, N/mm^2 – SR ISO 37-2020; tear strength, ISO 34-1:2015 – N/mm; elongation at break, N/mm^2 – SR ISO 37-2020; abrasion, mm^3, SR ISO 4649/2011. Accelerated ageing was carried out

https://doi.org/10.24264/icams-2022.IV.9

according to SR ISO 188/2011, using the hot air circulation oven method at 70 ± 1°C and 168h. After performing the aging process, the samples are subjected to conditioning for 16 hours up to 7 days, then they are subjected to physical-mechanical determinations, and the results obtained are compared with those obtained under normal conditions.

Fourier Transform Infrared Spectroscopy (FT-IR Spectroscopy) were performed with a double beam IR molecular absorption spectrometer, in the range 4000-400 cm^{-1}, using the FT-IR Thermo Nicolet iS 50 equipped with ATR with diamond crystal.

RESULTS AND DISCUSSION

Physical-Mechanical Characterization of Polymeric Compounds

The physical-mechanical characterization of samples under normal and accelerated aging conditions was carried out on elastomer-specific equipment.

Table 3. Physical-mechanical characterisation of compounds based on NBR rubber and non-functionalized/functionalized rubber waste

Symbol	B0 (control)	$B0_2$	BCP_1	BCP_2	BCP_3	BCP_4
Normal condition						
Hardness, °Sh A	60	55	57	54	47	46
Elasticity, %	20	19	16	19	17	18
Tensile strength, N/mm^2	11.3	8.82	8.68	7.29	4.87	3.06
Elongation at break, %	180	940	740	700	540	380
Abrasion resistance, mm^3	218.39	157.03	223.02	250.63	165.13	66.67
Accelerated aging at 70°C and 168 h						
Hardness, °Sh A	66	61	61	60	53	50
Elasticity, %	24	20	20	18	18	18
Tensile strength, N/mm^2	14.47	8.0	8.0	5.76	3.73	2.8
Elongation at break, %	980	600	600	560	420	360

From the recorded physical-mechanical characteristics, Table 3, it appears that: hardness decreases significantly especially for samples BCP_3 and BCP_4, samples containing 30% and 50% functionalized elastomer waste, respectively, which indicates a stiffness of the characterized samples; elasticity and tensile strength decrease compared to the control sample – B0 by replacing the active charge (SiO_2) with functionalized rubber waste (in different proportions – 10-50%); elongation at break shows a maximum value especially for sample BCP_1 (10% functionalized rubber waste), then decreases with the increase in the amount of elastomeric waste, and the lowest value of elongation at break is for sample BCP_4 – 380%; the abrasion resistance increases with the increase in the amount of rubber waste, by approximately 14% compared to the control sample, having a maximum value for the BCP_2 sample (20% functionalized rubber waste and 20% active filler), followed by a decrease of 69 % for the BCP_4 sample (the active filler being replaced with 50% functionalized rubber waste). Changes in the physical-mechanical characteristics are significant. After the accelerated aging process at 70°C, for 168 h, small variations in hardness of ±1°ShA are observed for the samples with 10-20% functionalized waste and 20% active filler, and for the samples BCP_3 and BCP_4, where the active filler is replaced with functionalized rubber waste, it decreases by ±10°ShA, while variations of elasticity from 17% to 25%, tensile strength from 41% to 80% and elongation at break from 38% to 80% are noticed as well. The changes in the physical-

https://doi.org/10.24264/icams-2022.IV.9

mechanical characteristics are significant for the samples where the active filler was totally replaced with the rubber waste functionalized with MEG.

FT-IR Spectrometric Analysis

The FT-IR spectra recorded for the polymer compounds based on NBR elastomer are shown in Figure 1 (a, b, c). The stretching vibration bands are based on those obtained in the reference spectrum of butadiene-co-acrylonitrile rubber (NBR elastomer).

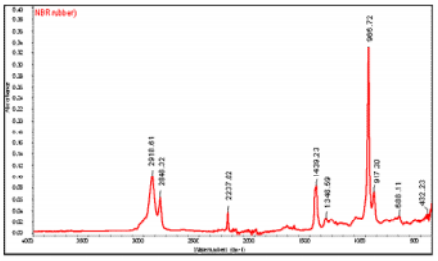

a) FT-IR spectrum from NBR rubber

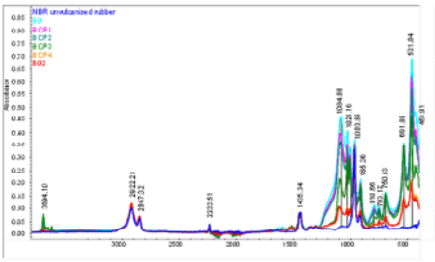

b) FTIR spectrum of composites based on NBR rubber and NBR waste functionalized with MEG/non-functionalized

Figure 1. FT-IR spectra of compounds based on NBR rubber with non-functionalized/functionalized rubber waste (B0, $B0_2$, BCP_1, BCP_2, BCP_3, BCP_4)

In the FT-IR spectrum recorded for NBR rubber, the band at 2237.02 cm^{-1} confirms the presence of stretching groups of -CN bonds from nitrile as well as the stretching vibration of double bonds from butadiene =C-H at 966.72 cm^{-1} (Alhareb *et al*., 2015). In the FTIR spectrum of functionalized and non-functionalized NBR waste, the bands originating from NBR rubber (2917.74, 2848.41, 1454.95, 966.76 cm^{-1}), the presence of silicon dioxide/kaolin (1081.4, 794.28 and 457.01 cm^{-1}) can be visualized (Khalil, 2007). As it can be seen in the case of sample B0 (compound based on NBR rubber without NBR waste), a very high intensity of the bands at 1084.88 and 458.91 cm^{-1} can be observed, compound bands originating from silicon dioxide and kaolin. The high intensity proves that the highest amount of SiO_2 is used in this sample. Moreover, the intensity of these bands decreases as the amount of SiO_2 decreases (samples BCP_1 and BCP_2). Instead, in the case of samples BCP_3 and BCP_4, silicon dioxide is replaced with NBR waste. However, in this region (1084.88 cm^{-1}) characteristic bands can be identified, but these come from kaolin. The presence of monoethylene glycol could not be detected for the samples containing functionalized NBR waste (10, 20, 30 and 50% functionalized NBR waste), because it is either covered with a layer of NBR rubber or is used in low quantities. The presence of compound bands comes from SiO_2 and kaolin, the intensity of these varying depending on the amount added to the mixture.

CONCLUSIONS

The elastomeric compounds were tested by appropriate techniques. In the FT-IR spectra recorded for samples based on NBR rubber and rubber waste in a proportion of 10, 20, 30 and 50%, functionalized with MEG, the bands originating from NBR rubber, from kaolin and silicon dioxide can be visualized. The presence of monoethylene glycol could not be observed for samples containing functionalized NBR waste because it is

https://doi.org/10.24264/icams-2022.IV.9

either covered with a layer of NBR rubber or is used in low quantities. The presence of compound bands originating from SiO_2 and kaolin could be highlighted at 1084.88 and 458.91cm^{-1}, their intensity varying depending on the amount used. From the comparison of the samples that do not contain silicon dioxide, BCP_3 and BCP_4, it is observed that by replacing SiO_2, with rubber waste, there is a decrease in hardness, elasticity and tensile strength, while abrasion resistance increases. The changes in the physical-mechanical characteristics are significant for the samples where the active filler was totally replaced with the rubber waste functionalized with MEG. The polymer composites based on NBR rubber and functionalized rubber waste show optimal values according to the standards and are used in the processing of general-purpose footwear.

Acknowledgements

This research was financed by the Romanian Ministry of Research, Innovation and Digitalization through Nucleu Program, PN 19-17 01 03/2019 project: "Biodegradable composites from technological and post-consumption polymeric wastes by designing and applying 4R eco-innovative technologies (4R-ECO-MAT)", and 4PFE/30.12.2021: "INCDTP in the Vanguard of Excellence Research" – TEX&PEL FOR FUTURE.

REFERENCES

Alexandrescu, L., Deselnicu, V., Sonmez, M., Georgescu, M., Nituica, M., Zainescu, G., Deselnicu, D.C. and Pang, X. (2019), "Biodegradable Polymer Composite Based on Recycled Polyurethane and Finished Leather Waste", *IOP Conf. Series: Earth and Environmental Science 401*, 012006, https://doi.org/10.1088/1755-1315/401/1/012006.

Alexandrescu, L., Sonmez, M., Nituica, M., Gurau, D. and Popa, N. (2014), "Hybrid Polymeric Structures Based on Butadiene-co-Acrylonitrile and Styrene-Butadiene Rubber Reinforced with Nanoparticles", *Leather and Footwear Journal*, 14(1), https://doi.org/10.24264/lfj.14.1.4.

Alhareb, A.O., Akil, H.B.M. and Ahmad, Z.A.B. (2015), "Poly(methyl Methacrylate) Denture Base Composites Enhancement by Various Combinations of Nitrile Butadiene Rubber/Treated Ceramic Fillers", *Journal of Thermoplastic Composite Materials*, 30(8), 1–22, https://doi.org/10.1177/0892705715616856.

Chittella, H., Yoon, L.W., Ramarad, S. and Lai, Z.W. (2021), "Rubber Waste Management: A Review on Methods, Mechanism, and Prospects", *Polymer Degradation and Stability*, 194, 109761, https://doi.org/10.1016/j.polymdegradstab.2021.109761.

Formela, K. (2021), "Sustainable Development of Waste Tires Recycling Technologies – Recent Advances, Challenges and Future Trends", *Advanced Industrial and Engineering Polymer Research*, 4(3), 209-222, https://doi.org/10.1016/j.aiepr.2021.06.004.

Khalil, K.M.S. (2007), "Cerium Modified MCM-41 Nanocomposite Materials via a Nonhydrothermal Direct Method at Room Temperature", *Journal of Colloid and Interface Science*, 315(2), 562–568, https://doi.org/10.1016/j.jcis.2007.07.030.

Nițuică, M., Sonmez, M., Georgescu, M., Stelescu, M.D., Alexandrescu, L. and Gurau, D. (2021), "Biodegradable Polymer Composites Based on NBR Rubber and Protein Waste", *Leather and Footwear Journal*, 21(4), 229-236, https://doi.org/10.24264/lf.21.4.3.

Nițuică, M., Sonmez, M., Georgescu, M., Stelescu, M.D., Alexandrescu, L., Gurau, D. and Pantazi-Bajenaru, M. (2022), "Polymer Composite Based on NBR Rubber Compounded with Rubber Waste Functionalized with Potassium Oleate", *Leather and Footwear Journal*, 22(1), 45-52, https://doi.org/10.24264/lf.22.1.5.

Roucoules, V., Siffer, F., Ponche, A., Egurrola, U. and Vallat, M.F. (2007), "Strengthening the Junction Between EPDM and Aluminium Substrate via Plasma Polymerisation", *The Journal of Adhesion*, 83(10), 875-895, https://doi.org/10.1080/00218460701699732.

Sienkiewicz, M., Janik, H., Borzedowska-Labuda, K. and Kucinska-Lipka, J. (2017), "Environmentally Friendly Polymer-Rubber Composites Obtained from Waste Tyres: A Review", *Journal of Cleaner Production*, 147, 560-571, https://doi.org/10.1016/j.jclepro.2017.01.121.

Stelescu, M.D., Manaila, E., Nituica, M. and Georgescu, M. (2020), "New Materials Based on Ethylene Propylene Diene Terpolymer and Hemp Fibres Obtained by Green Reactive Processing", *Materials*, 13, 2067, https://doi.org/10.3390/ma13092067.

*** (2015), United Nations Environment Programme, Global Waste Management Outlook, available at: https://www.unenvironment.org/resources/report/global-waste-management-outlook.

MAKING FOOTWEAR BASED ON CIRCULAR ECONOMY - REWEART

MIRELA PANTAZI-BAJENARU, MIHAI GEORGESCU, LAURENTIA ALEXANDRESCU, DANA GURAU

The National Research & Development Institute for Textiles and Leather - Leather and Footwear Research Institute Division, 93 Ion Minulescu St., Bucharest, Romania, email: icpi@icpi.ro

The REWEART project will help meet the objectives of the EU's Environmental Policy. What is more, it will contribute to the implementation of EU commitments under UNFCCC Kyoto Protocol, EU GHG emission reduction commitments in 2020 under the Climate and Energy Package, Green Deal and Fashion Pact. Following the objectives of resource and energy reduction as well as waste cuts all along the product life cycle, the main ambition of REWEART project is to refer to natural ecosystems, which produces no waste, and uses only renewable resources (solar energy and water). REWEART project aims at generalising the use of proactive waste management at design stage and at anticipating and improving reactive management. The project offers us an exceptional opportunity to conceive a new business model and related services and tools, enabling, at design stage, the selection of the most suitable materials and processes to create a new footwear product 100% recycled, organic, as working hypothesis. A cost effectiveness evaluation has been made possible to make affordable new products available to the market, while a concurrent environmental impact analysis ensures that the new solutions are positive for the environment. The project results have been assessed against a set of performance yardsticks addressing environmental, social and economic impact. This paper presents the activities carried out within the LIFE REWEART project during its entire period of development.

Keywords: vegane, organic, recycled footwear

INTRODUCTION

REWEART is a LIFE project co-financed by the European Commission that aims to develop a new business model to create new 100% recycled, organic footwear.

Project duration: 01.09.2018-31.03.2022.

AIMS & OBJECTIVES

The main objective of REWEART was generalising the use of proactive waste management at footwear design stage and anticipating and improving reactive management. The project aimed to conceive a new business model and related services and tools, enabling, at design stage, the selection of the most suitable materials and processes to create a new footwear product 100% vegan, recycled and organic. The project objectives and outputs were:

- To demonstrate a new shoe production model;
- To guarantee transferability and replicability of shoe manufacturing;
- To provide public administration tools for assessing shoe manufacturing policies and strategies;
- To increase awareness and support shoe sector by providing cost-effective solutions that include more efficient techniques that may also improve profitability;
- To identify and involve all relevant stakeholders related to shoe issues.

https://doi.org/10.24264/icams-2022.IV.10

CONSORTIUM

The consortium was created based on the combination of different environments, experience and expertise of the partners, includes all the skills, recognized expertise and competences needed to achieve all aspects of the work program. The consortium includes 6 institutions from 3 countries.

PROJECT PARTNERS

- ✓ INCDTP – Division: Leather and Footwear Research Institute (ICPI) (Romania) – *Coordinator*;
- ✓ ATEVAL (Spain);
- ✓ FERRE AGRUPACIÓN, S.A. (Spain);
- ✓ HILATURAS FERRE, S.A. (Spain);
- ✓ MUSTANG, S.R.L. (Italy);
- ✓ VESICA PISCIS FOOTWEAR, S.L. (Spain).

ACTIVITIES AND RESULTS

The actions and means to achieve the objectives were organized as follows:

Specifications and Selection of Components

The materials from the market were selected, the materials were developed based on recycled materials, the shoe models and the shoe manufacturing procedure was defined and the production line (pilot). We selected 27 suppliers and 38 materials to produce shoes and their components that meet the requirements of an organic, vegan and recycled shoe, to different stretches. We used 14 models and developed over 100 models to test different features, materials, etc.

Demonstration Pilot Plant for Footwear

Developed pilot plant components for the production of shoes, as follows:

Pilot Unit for Shoe Production

REWEART manufacturing process proposed for the vegane shoes, is based on the STROBEL lasting system, which consist on the attachment of a non-woven textile to the upper by stitching. After this, the assembly of the upper material to the sole is done by stitching, with minimum use of adhesive, water based anyway. With this approach, we propose a prototype line consisting on a cutting machine, two/three types of stitching machines (upper and lining assembly and side stitching) and then just a lasting station by hand and an upper-sole joining with pressure and final stitching. The PILOT STATION for manufacturing footwear was developed (Fig. 1).

https://doi.org/10.24264/icams-2022.IV.10

Figure 1. Pilot station

Pilot for Rubber Milling; Performed by INCDTP

INCDTP has set up a small pilot facility for rubber compounds elaboration and prepared tentative outsole blends (trial-error) with rubber + wood until they achieved a final one based on optimum processability. The objective was to obtain a polymer composite based on natural rubber and wood waste which can be considered a prototype.

Yarn Production and ICT Tool

Selection of Materials for Weaving at INCDTP

Since the field of application of the present prototype is the manufacture of footwear fabrics, a thread with sufficient twist is sought to avoid breakage. At the same time, a fine thread is sought in order to have sufficient flexibility to make different weights that will be achieved through the twisting of the manufactured thread.

Processing of Threads at INCDTP

Different fabrics were made (Fig. 2) which were tested for: tensile strength and elongation, tear strength, abrasion/ friction resistance, pilling effect, seam strength, air permeability, resistance on surface hanging, fibrous composition of the woven fabrics.

Figure 2. Fabrics produced at INCDTP

Variety of yarns used to make fabrics: (a) new yarns, made within the project used mainly as weft yarns; (b) new yarns used in warp and weft; (c) the combination of new yarns, with yarns that have a min 95% cotton fibers (virgin, recovered) and with min 97% flax fibers, linen.

https://doi.org/10.24264/icams-2022.IV.10

ICT Tool

The ICT REWEART tool permits:
- Customization of the shoe and their parts to the available fabrics
- Recycling of garments to manufacture a bag, shoe or belt.
- Configurate 3D one of the products (shoe, belt, bag) by taking a picture of the garment to be recycled and use it as input for the customization process.

Demonstration and Validation of Unit for Vegane-Recycled-Organic Shoes

This activity permits the full demonstration of the footwear manufacturing process using the materials developed in previous actions. 2000 pairs of shoes were made. INCDTP contributed with five shoe designs (Fig. 3) as options to be manufactured.

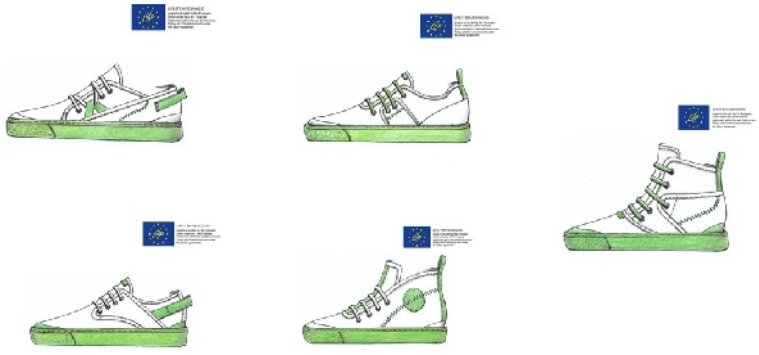

Figure 3. The models designed by INCDTP

We planned and achieved the manufacturing of 24 different designs, over 13 models using 12 different upper materials, 3 lining materials, 2 insock materials and 5 outsole materials, in all cases achieving 100% recyclability and easy shoe disassembly to facilitate recyclability. 6 of the fabrics woven at INCDTP were also used (Fig. 4).

Figure 4. Footwear made with woven materials at INCDTP

https://doi.org/10.24264/icams-2022.IV.10

LCA

GaBi ts Software (Professional) was used for the LCA analysis. LCAs were calculated for 12 shoe models. In addition we've calculated some variations for the SIDDHARTA model, using outsoles from different suppliers and different compositions, showing slightly different results, from 6.6 to 5.8 Kg CO_2eq/pair. The results in terms of reduction of the carbon footprint of the manufactured models, fall in the range 3.04 Kg CO_2eq /pair in the case of sandals (SRINIVASA model) to 6.25 Kg CO_2eq /pair in the case of sneakers with TPU outsole SIDDHARTA model), with an average of 5.5 Kg CO_2eq/pair.

Typical values of carbon footprint for casual or man shoes made of different materials (leather, polymeric, etc.) range from 10 to 14 Kg CO_2eq/pair.

The water footprint has also been reduced to almost zero, as all recycling procedures are based on mechanical processes leading to near zero water consumption.

As per energy consumption, typical values for casual/man shoes contribute from 3 to 6% of the total carbon footprint (5.05 kWh/pair). In the case of these VEGANE-RECYCLED-ORGANIC models the contribution is 0.5 kWh/pair.

ENVIRONMENTAL BENEFITS

i) Direct / quantitative environmental benefits:

As a direct result of the project, there will be some environmental benefits after footwear companies implement some of the recommendations for manufacturing a shoe with minimum environmental impacts. The shoes can be 100% recyclable and we have also provided recommendations to manufacture a 100% recyclable, organic and vegane shoe, so all expected project impacts have been achieved.

REWEART has permitted a reduction of 85% i.e., so consumption of 1.08 m^3/1,000 pairs is foreseen. As per CO_2 eq, typical current models amount for 13,5Kg CO_2 eq per pair and we have reached, for the different models manufactured, values in the range 3,5 to 6,23 Kg CO_2 eq/pair (Fig. 5) and in cases where we can recycle the outsole, a value of 2.21. As per water footprint, considering a typical process consum of 7.23m^3/1,000 pairs, we have achieved a reduction of 85%, which means 1.08 m^3/1,000 pairs.

At the end of the project, we use outsoles made of virgin TPU (65% weight) but we can recycle 100% of outsoles materials and 100% of upper materials, so REWEART shoes are 100% recyclable. A total of 120gr of upper materials are recycled material and 250gr virgin TPU.

One pair of shoes at the end of project contain the following recycled materials:

- Sandals 148gr per pair: outsole material (EVA 5% content recycled) 15gr + 72gr insole (100% recycled cork) + 13gr upper fabric (100% recycled cotton)= 100gr or 68% made of recycled material and 100% recyclable.

- Shoes (Leonardo model) 370gr per pair: upper material (77gr, 100% recycled), insole (39 gr, 100% recycled), insock and laces (14gr, 100% recycled)= 130gr or 35% made of recycled material and 100% recyclable.

The objective of a shoe 100% organic, vegane, reusable and recyclable has been achieved.

https://doi.org/10.24264/icams-2022.IV.10

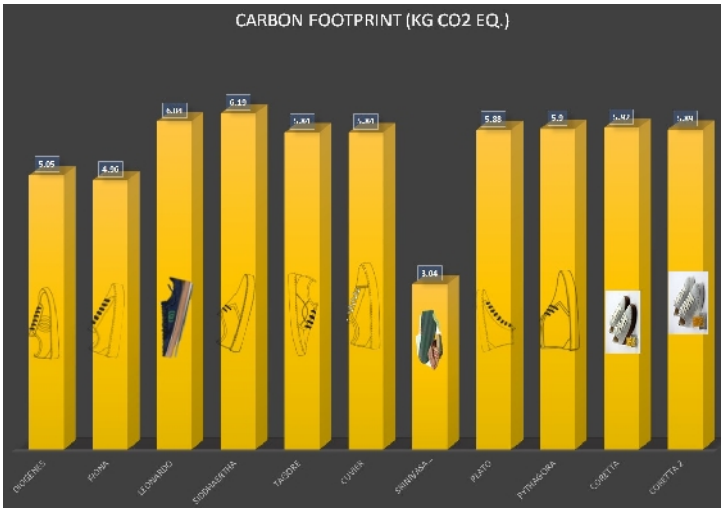

Figure 5. Carbon footprint for the different models manufactured

(ii) The case of REWEART is a real eco-design in production among footwear companies, taking environmental issues into account from the product design stage, as for example: (i) Use of minimum energy; (ii) Use of "eco" materials with minimum environmental impact; (iii) Zero waste production; (iv) Methodology for re-use of garments into shoes with the help of an advanced IT tool; (v) Reduction of GHGs emissions; (vi) Reduced packaging and water consumption.

CONCLUSIONS

REWEART project has demonstrated the concept of full recyclability of footwear properly and re-using them as components for the creation of new articles, making use of an advanced 3D configurator and incorporating B2C elements which provide our initiative the look of something that can be global with local manufacturing.

All materials used for project trials were organic, chemicals free and animal free, achieving a product 100% ORGANIC, VEGANE and RECYCLED.

LIFE REWEART has achieved the objective of zero waste, as all components can be recycled, has reduced the water footprint to zero, carbon footprint up to 85% (against regular footwear) and energy consumption to 10% compared to traditional process.

Acknowledgements

This study was funded by the Ministry of Research and Innovation through the Program 1 - Development of the National R&D System, Subprogram 1.2 - Institutional Performance - RDI excellence funding projects, Contract no. 4PFE/30.12.2021: "INCDTP in the vanguard of excellence research" – TEX&PEL FOR FUTURE.

REFERENCES

*** www.life-reweart.eu

https://doi.org/10.24264/icams-2022.IV.10

ECOLOGICAL FRIENDLY PRODUCTION PROCESS AND WASTE TREATMENT FOR CIRCULAR ECONOMY IN LEATHER TANNING INDUSTRIES

SENGODA GOUNDER RAJAMANI[1], ARNOLD MULDER[2]

[1]*Chairman, Asian International Union of Environment (AIUE) Commission, India, e-mail: dr.s.rajamani@gmail.com, Mobile: +91 9840063210*

[2]*AMECON, Delft, The Netherlands*

Ecological friendly processes with recovery of salt, chemicals and water for reuse in the tanning process as well as from liquid and solid waste are necessary for the promotion of circular economy.Recent developments in cleaner production and treatment process by reducing volume of effluent and pollution discharges, recovery of quality salt in the segregated streams such as saline soak liquor, spent chrome liquor and adoption of advanced aerobic oxidation process in the treatment system resulted in the recovery of purified salt, quality chromium and water for reuse. The achievements of innovative cleaner production and effluent treatment for promotion of circular economy are: Reduction in water usage in soaking process from 6000-8000 liters to less than 3000 liters/ ton of hides, Separate treatment of saline streams and recovery of quality salt, chromium in the form of cake / powder and Replacement of physiochemical treatment into biological treatment reduction in chemical usage and sludge generation by more than 60%. Viable cleaner production and sustainable treatment technologies had been engineered and are being implemented in many major leather clusters and Common Effluent Treatment Plants.

Keywords: cleaner production, chrome recovery, circular economy

INTRODUCTION

The treatment and disposal of tannery effluent with high salinity and Total Dissolved Solids (TDS) is a major challenge in most of the land locked tannery clusters. This resulted in development of appropriate cleaner production process to reduce the volume of water usage and pollution discharges. The segregation of streams such as saline soak liquor, spent chrome liquor enable to adopt advanced aerobic oxidation process, membrane system, recovery of quality chromium in the form of cake/powder, purified salt (sodium chloride) and water for reuse.

The merits of the developed cleaner production and effluent treatment are: (i) Reduction in water usage in soaking process from 7000 liters to less than 3000 liters/ton of hides (Buljan *et al*., 1997), (ii) Segregation of high saline streams from soaking operations and spent chrome liquor for separate treatment and recovery of quality salt, chromium in form of cake/powder, water for reuse under Zero Liquid Discharge (ZLD) concept (Buljan and Rajamani, 1997; Schaapman *et al*., 1990; Rajamani, 2020), (iii) Upgradation of physiochemical treatment into biological treatment process with reduction in chemical usage to reduce sludge generation by 60-70%, (iv) Advanced oxidation treatment using ozone for achieving COD reduction, colour and turbidity removal to the required level in the composite effluent (Rajamani, 2022) and (v) Integration of treated tannery effluent with treated domestic sewage for achieving TDS norms and use of the entire treated effluent for irrigation.

Viable cleaner production and sustainable treatment technologies had been engineered and are being implemented in a Leather Complex with about 200 new tanneries, a Common Effluent Treatment Plant (CETP) with capacity of 20 mld. This is

https://doi.org/10.24264/icams-2022.IV.11

one of biggest leather cluster with adoption of new and innovative cleaner productions with circular economy.

Sustainable Cleaner Technologies for Circular Economy

The raw hides & skins available in the market for leather tanning contains 30-50% of salt (Sodium Chloride) on total weight basis. These hides & skins are taken for soaking operations without proper salt dusting. The volume of water usage is 6000-8000 liters per ton of hides and TDS concentration ranges from 40000 to 60000 mg/l. The entire soak liquor is mixed with other sectional streams and discharged as a composite stream and the TDS level is in the range of 20000-25000 mg/l. This high TDS level in the effluent affects the performance of biological treatment system and inability to achieve discharge parameters particularly TDS which is being enforced in many Indian States and other countries as well.

In order to meet the challenges in achieving the environmental regulations and to improve the in effluent treatment system with recovery of quality chemicals, salt and water for reuse, the following cleaner productions have been developed for implementation:

- Improved method for desalting of skins by using simple system such as DODECA by tanneries at source and centralized mechanical desalting of hides by adopting proven equipment which are portable as well.
- Sulphide reduced liming process by the use of suitable enzymes to extent feasible for reduction of sulphide load by 60-70% in the effluent.
- Safe and sustainable disposal of waste fleshing by conversion into fertilizer, composting by using with dewatered bio-sludge and other degradable organic matter (Langerwerf *et al*., 1997).
- Segregation of chrome stream and adoption of improved Common Chrome Recovery System (CCRS) and recovery of chromium in the form of cake or powder. The supernatant also further processed and converted into reusable chemical and quality water.
- Reduction in sludge generation by biological treatment with minimum chemical usage, anaerobic digestion of sludge with bio-energy generation and conversion into composting (Suthanthararajan *et al*., 2001).

Segregation of Streams in Tanneries

All the tanneries in addition to the adoption of suitable cleaner productions, the streams are segregated as follows for separate treatment.

- Saline soak liquor from pre-soaking, main soaking and washing.
- Spent chrome liquor from chrome tanning operations.
- All other streams starting from liming, deliming, washing and all remaining wet finishing operations are collected as a composite stream.

The concept of sustainable cleaner production and circular economy is shown in Figure 1.

https://doi.org/10.24264/icams-2022.IV.11

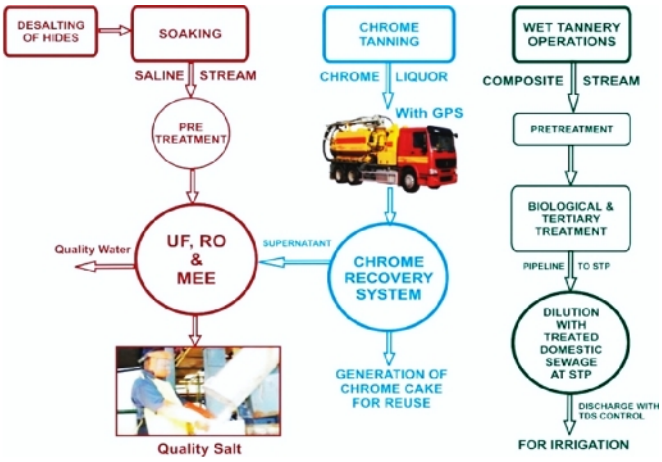

Ultra Filtration (UF), Reverse Osmosis (RO), Multiple Effect Evaporator (MEE)

Figure 1. Innovative Cleaner Production for Sustainable Treatment with TDS Control

Saline Soak Liquor

Saline Soak Liquor is generated from the three stage operations of namely (i) Pre or Dirt soaking (Soaking I), (ii) Main soaking (Soaking II) and (iii) Wash after main soaking (soaking III). During the conventional three stages of soaking using pits and paddles more than 6-8 m^3 of effluent is discharged per ton of raw material process. By the use of drums for soaking after viable desalting and cleaner production process, the volume of water usage and effluent discharge is reduced to less than 4 m^3/ton of raw hides and skins.

The saline soak effluent from each tannery is discharged into the exclusive conveyance system to CETP for separate treatment under ZLD concept with recovery of quality water and reusable salt. The treated saline stream is partly reused in pickling / soaking and balance is evaporated for generation of reusable salt (mainly sodium chloride) and water. The salt is having more than 99% purity and has got market demand for industrial and other uses in land locked areas. The overall TDS level in the other composited stream is reduced by about 60% (i.e. from more than 20000 mg/l to less than 10000 mg/l). Due to this reduction, the environmental authorities permit the sustainable option of mixing the treated composite effluent with treated domestic sewage available near the tannery cluster and enable meet all the discharge parameters including TDS.

Sustainable Desalting Process

The tanneries processing salted goat, sheep, cow & buff calf skins in small scale can adopt desalting frames and rotary drums. DODECA (12 frame) wooden frames can be adopted for small size skins weighing up to 4-5 kgs. For medium size hides weighing up to 10 kg can be desalted using rotary drums with perforated holes.

Majority of tanneries in the cluster are in small & medium scale, they are not having the capability and land space to have mechanical desalting system required for big size hides. Hence, it is necessary to adopt mechanical desalting as a centralized facility. It is

https://doi.org/10.24264/icams-2022.IV.11

proposed to provide two centralized desalting facility for a capacity of about 80-100 tons per day during the implementation. The desalting process, clarification of the dusted salt solution, reuse in pickling, etc. are shown in Figure 2.

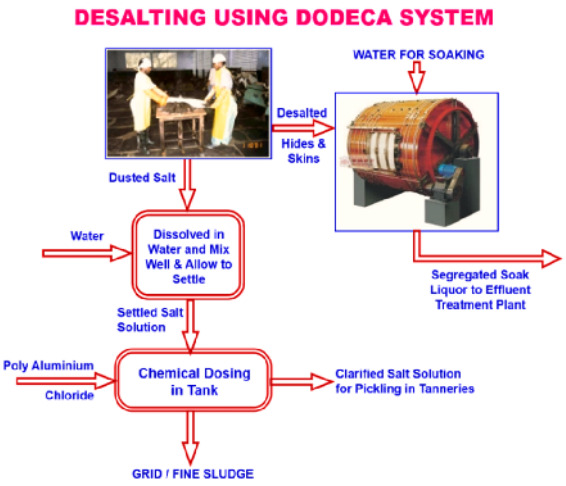

Figure 2. Desalting Process for TDS Management

The salt collected from desalting process would contain grit and organic ingredients. This can be clarified by adding 200 liters of water for 20 kg dusted of salt and grit will settle in bottom of the tank. The supernatant can be collected in a separate tank and added with poly aluminium chloride (PAC) dosing. The suspended and organic settleable matter settles in the bottom as a sludge. This can be disposed in the sludge dewatering system installed in individual tanneries. The clarified supernatant which contains 7-8% salt solution can be used for pickling by adding required balance salt, sulphuric acid and water. The desalting process would reduce the TDS content in the saline soak liquor from the range of 40000-50000 to 20000-30000 mg/l.

Improved Chrome Recovery System

The effluent discharge from chrome tanning operation is about 4-6% of total volume of wastewater from chrome tanneries. Conventionally, the tanneries provide individual chrome recovery system by using MgO (magnesium oxide) as alkali and the recovered chrome slurry is regenerated as basic chromium sulphate (BCS) by mixing with sulphuric acid (H_2SO_4) (Buljan and Rajamani, 1997). BCS is in the form of liquid is reused in the tanning process. In this conventional process, there are limitation and management and reuse of Chromium. The discharge of entire supernatant from chrome system with high TDS (25000-40000 mg/l), Chlorides (8000-15000 mg/l), Sulphate (4000-8000 mg/l), etc. to the CETP along with other streams results in increase of overall TDS in composite stream, constraints in adopting biological treatment system particularly anaerobic system achieving TDS level in the treated effluent is not feasible.

The concept of the improved CCRS (Rajamani, 2018; Rajamani, 2016) (i) Collection of spent chrome liquor from individual tanneries through tankers fitted with

https://doi.org/10.24264/icams-2022.IV.11

GPS, (ii) Screening, pretreatment, separation of Chromium as a slurry in the reactor by using suitable alkali, (iii) Dewatering of chrome slurry using Chamber Filter Press and recovery of Chromium in the form of cake and (iv) The supernatant with high TDS of more than 30000 mg/l is taken for further treatment integrated with saline soak stream treatment system for recovery of quality salt and water by adopting membrane system.

SUSTAINABLE SOLID WASTE MANAGEMENT FOR CIRCULAR ECONOMY

The tanneries during beam house operation generate large amount of fleshing. It is estimated 20-30 kg of fleshing generated during the process of 1000 kg of hides & skins. Only part of fleshing is taken for commercial process and about 50% of fleshing mainly from skins and small hides are becoming waste.

The following options are proposed for the disposal of fleshing: (i) Conversion into composting using other organic degradable waste and bio-sludge, (ii) Conversion into biological liquefaction and feed to anaerobic reactor for bio-energy generation and bio-sludge (Rajamani, 2021) and (iii) Mixing with dewatered bio-sludge from digester and converting into bio-fertilizer. These solid waste management options have been implemented in a separate industrial type building within the CETP.

COMPOSTING AND GENERATION OF BIO-FERTILIZER

It is estimated that about 5-10 tons of partly dewatered bio-degradable sludge would be generated from soak liquor treatment, composite treatment and anaerobic digester. This bio-degradable sludge can be processed further by adding waste fleshing and degradable organic waste available in the local area. The ratio of the mix would be generally 1:1:1 and the composting process would take about 15-20 days. Proper bio-seeding generated from sewage treatment plant (STP) / bio-spray is being periodically applied for accelerating the composting process.

RESULTS AND DISCUSSION

- Improved desalting using DODECA method removes the salt content from 60% to 30% on weight basis.
- Modified and improved soaking process reduces the water usage and effluent discharge from the level of 600-800% to 300-400%.
- Improved chrome recovery system generates chromium in the form of cake / powder.
- Entire supernatant is further process and recovered in the form of quality salt and water for reuse.
- Segregation & treatment of saline soak liquor under ZLD system generates quality water and salt.
- TDS level in the composite stream reduced from about 20000 mg/l to less than 10000 mg/l.
- Improved cleaner production and segregated treatment enable to comply the environmental regulations and discharge norms.
- Scope for replicability in many tannery clusters.

https://doi.org/10.24264/icams-2022.IV.11

CONCLUSION

This unique and sustainable technological developments in cleaner production aiming at circular economy will reduce the level of TDS in the effluent discharge by 50%, hazardous category sludge generation by 60% and meets the environmental norms. Many full-scale systems are being implemented in India and other countries.

Acknowledgment

Contributions of Department for Promotion of Industry and Internal Trade (DPIIT)-Govt. of India, Indian Leather Technology Association (ILTA), IAFLI, UNIDO, National Mission for Clean Ganga (NMCG), National Green Tribunal (NGT), Mega Leather Cluster (MLC)-Kanpur, Schoolnet India Limited, Asian International Union Environment (AIUE) Commission, Asian International Forum and others commission members from various countries, AMECON & TNO Netherlands, Central Leather Research Institute (CSIR-CLRI), European Union including Italy and Spain, The Netherlands and other Countries such as China, Japan, Romania, Turkey, Taiwan and Russian Federation, New Zealand are acknowledged. Leather Industry Associations and Common Effluent Treatment Plants (CETPs) in India are acknowledged.

REFERENCES

Buljan, J. and Rajamani, S. (1996), "Technology Package – A System for Recovery and Reuse of Chromium from Spent Tanning Liquor Using Magnesium Oxide and Sulphuric Acid", TECHPACK / UNIDO / RePO / 1.

Buljan, J., Reich, G. and Ludvik, J. (1997), "Mass Balance in Leather Processing", Paper presented in IULTCS Congress, London, UK.

Langerwerf, J.S.A., Rajamani, S., Ramasami, T., Raghavan, K.V., Van Groenestijn, J.W. and Mulder, A. (1995), "Implementation and Dissemination of the Results of the TNO-CLRI Co-operation Programme", Paper presented in XXIII IULTCS Congress, Friedrichshafen, Germany.

Rajamani, S. (2016), "Innovative Environmental Technologies including Water Recovery for Reuse from Tannery and Industrial Wastewater – Indian and Asian Scenario", Proceedings of the 6th International Conference on Advanced Materials and Systems (ICAMS 2016), Bucharest, Romania, 513-518, https://doi.org/10.24264/icams-2016.IV.13.

Rajamani, S. (2018), "Sustainable Environmental Technologies Integrated with Cleaner Production – Recent Developments in World Leather Sector", Paper presented in XIVth International Scientific-Practical Conference, Ulan-Ude, Russia.

Rajamani, S. (2020), "Sustainable ZLD System by Adopting Centralized Treatment of Segregated Streams for Recovery of Reusable Quality Chemical, Salt & Water – First of its kind in India & Asia", *Leather News India Journal*.

Rajamani, S. (2021), "Biological Liquefaction and Anaerobic Digestion of Waste Fleshing's Integrated with Sludge and Bio-Energy Generation – A Novel and Sustainable Development", Paper presented in XXXVI IULTCS Congress 2021, Addis Ababa, Ethiopia.

Rajamani, S. (2022), "State-of-the-Art Technology of Advanced Oxidation Process Using Ozone in Water and Industrial Wastewater Treatment – A First of Its Kind Treatment System in India", Paper presented International Workshop organized by CSIR-CSMCRI, Gujarat & NAM S&T Centre, New Delhi.

Schaapman, J.E., Rajamani, S., Gupta, S.N., Mitra, R.B. and Pelckmans, H.H.A. (1990), "Cleaner Technology in the Leather Industry – Chrome Recovery and Reuse", Paper presented in Water Pollutional Control Federation 63rd Annual Conference, Washington DC, USA.

Suthantararajan, Rajamani, S., Kalyanaraman, C., Umamaheswari, B. and Ravindranath, E. (2001), "Anaerobic Digestion of Sludge from Highly Saline Wastewater Streams from Tanneries with Special Anaerobic Sludge Digester with Liquid Separator (ASDLS) System and Generation of Bio-Energy", Paper presented in the 2001 IULTCS Congress held at Cape Town, South Africa.

GREEN BIOSYNTHESIS OF ZINC NANOPARTICLES

MARYNA ROHOVA[1], VLADYSLAV KOVALENKO[1],
VOLODYMYR TKACHENKO[2], INNA LYCH[3], IRYNA VOLOSHYNA[1]

[1] *Kyiv National University of Technology and Design*

[2] *National University of Food Technologies*

[3] *Shpytky Academic Lyceum "Skif" of the Dmytrivka Village Council of the Bucha district of the Kyiv region*

Currently there is a growing need for the development of an environmentally friendly process of synthesis of nanoparticles, during which no toxic chemicals are used. That is why an important area of research in nanotechnology sphere is the synthesis of metal nanoparticles by microorganisms such as bacteria and yeast (detoxification often occurs by reduction of metal ions/formation of metal sulfides). Bacteria are the organism of choice due to their fast growth, high efficiency and low cost. Metal nanoparticles exhibit antimicrobial properties, but the properties of nanoparticles depend on their size and shape, making them specific for different applications. Nevertheless, the desired size and shape of nanoparticles can be obtained by optimizing the synthesis process through manipulating their reaction conditions. Microbial synthesis of nanoparticles is an alternative to chemical and physical methods, as it is non-toxic and biocompatible. Despite the relevance of the application of the "green synthesis" method in the field of nanotechnology, biosynthesis by bacterial organisms has certain disadvantages, such as a high probability of pathogenicity, labour-intensive cultivation, and pollution problems. Ultimately, there is a need to explore more potential microorganisms for the synthesis of metal nanoparticles. The paper provides a review of literature data on the biosynthesis of zinc nanoparticles using lactic acid microorganisms. It was shown that bacteria are capable of synthesizing both extracellular and intracellular nanoparticles in the wavelength range of 315-392 nm. Data on the manifestation of antimicrobial properties by zinc nanoparticles against various gram-positive and gram-negative bacterial microorganisms and micromycetes.

Keywords: nanoparticles, green biosynthesis, *Lactobacillus*

INTRODUCTION

In recent years, green synthesis has been a new method not featuring some of the disadvantages of physical and chemical methods. In this approach, bacteria, archaebacteria, fungi and plants can be used without the use of toxic and expensive materials to produce metal nanoparticles (MNPs) (Baraton, 2002; Shkotova *et al*., 2019).

Since such particles are close to molecules in size, nanomaterials are able to exhibit unique physical and chemical properties close to the properties of individual molecules. The nanometre measurement range of sizes 1÷100 nm opens up new properties and fields of application of substances and materials (Baraton, 2002).

A unique property of nanoparticles is a developed specific surface of ~1000 m^2/g, open to the action of environmental molecules. The smaller is the size of the nanoparticle, the greater is the number of atoms in relation to the volume present on the surface and the higher is its reactivity (Baraton, 2002; Pomastowski *et al*., 2020).

Optical properties of nanoparticles are radically different from the properties of bulk material. Shall the shape and size of the particles change, the spectral characteristics change significantly for almost all nanoparticles. By varying the geometric parameters of nanoparticles, it is possible to achieve the required optical properties. When proceeding to the consideration of ensembles of nanoparticles, it is necessary to take into account the interaction between individual particles. The spectral properties of hybrid nanoparticles differ from the properties of the components they are composed of (Rodrigo, 2012; Shkotova *et al*., 2019).

https://doi.org/10.24264/icams-2022.IV.12

Nanoparticles have such chemical properties as catalytic and adsorption. The physical properties of nanoparticles arise due to surface or quantum-dimensional effects. Magnetic characteristics are of great importance for nanoparticles: here the difference between compact magnetic materials and the corresponding nanoparticles is most clearly revealed (Baraton, 2002).

One of the main reasons for the change in the physical and chemical properties of small particles as their size decreases is the increase in the relative share of "surface" atoms that are in different conditions (coordination number, symmetry of the local environment, etc.) than atoms inside the bulk phase. From the energy point of view, the decrease in particle size leads to an increase in the role of surface energy (Baraton, 2002; Voloshyna *et al*., 2019).

BIOSYNTHESIS OF ZINC NANOPARTICLES

Nanoparticles of zinc oxide (ZnO) have attracted attention due to their unique properties, in particular, the properties of combating a wide range of pathogenic microorganisms. Bacterial, fungal and yeast cultures are used for intracellular or extracellular synthesis of ZnO nanoparticles by microbial cells or enzymes, proteins and other biomolecular compounds. Numerous studies indicate that nanoparticles of ZnO have great potential in biological applications, in particular as antimicrobial agents (El-Sayed *et al*., 2021).

Lactobacillus gasseri

Research was conducted on the biosynthesis of zinc oxide nanoparticles (ZnO-NP) using lactobacillus strains. Biosynthesized zinc nanoparticles thanks to *Lactobacillus gasseri* were investigated using the UV-visible absorption spectrum in the wavelength range from 345 to 350 nm. This range is typical for the wavelengths of zinc nanoparticles. Biosynthesized nanoparticles of ZnO exhibits a surface plasmon resonance (SPR) band at 377 nm. In addition, the presence of glucose in the MRS medium used for the biosynthesis of zinc nanoparticles tends to decrease the value of the oxidation-reduction potential. A white precipitate at the bottom of the flask indicates the presence of zinc nanoparticles. ZnO molecules evolve slowly and form spherical and cubic shaped structures with a size of 22 nm. (El-Sayed *et al*., 2021). In addition, the integrated biosynthesis of ZnO-NPs in yogurt had a positive effect on the shelf life of yogurt for four weeks without changes in sensory evaluation (El-Sayed *et al*., 2021).

Lactobacillus johnsonii

Extracellular biosynthesis of ZnO nanoparticles was carried out (average size between 4 and 9 nm) using *Lactobacillus johnsonii* culture fluid. The result of UV spectroscopy shows a broad peak of the absorption band at 406 nm. The time factor plays an important role in biosynthesis: maximum synthesis can be observed 24 hours after inoculation, but after 48 hours of incubation production decreases. A similar result was observed in the biosynthesis of titanium nanoparticles. UV spectroscopy showed that the optical properties of Zn nanoparticles indicate the presence of an absorption peak of Zn nanoparticles at 392 nm. In addition, the FTIR peak diagram of titanium confirmed the stronger ability of proteins to bind metal and increase the possibility of coating metal nanoparticles with proteins to prevent particle agglomeration. TEM image of Zn and Ti nanoparticles recorded a spherical shape and had average particle diameters of 18–105 nm (Al-Zahrani *et al*., 2018; Pomastowski *et al*., 2020).

https://doi.org/10.24264/icams-2022.IV.12

Lactobacillus paracasei

The potential of *Lactobacillus paracasei* LC20 isolated from sweet whey was investigated as a new, effective and affordable source for the synthesis of ZnO nanocomposites after cultivation. It was established that *L. paracasei* LC20 is capable of synthesizing Zn nanoparticles, the presence of which, in turn, was confirmed by a white precipitate using the MRS medium (Krol *et al*., 2018). *L. plantarum* can also be targeted for Zn nanoparticle synthesis in the range of 7–19 nm (Krol *et al*., 2018).

Lactobacillus acidophilus

Currently, the antimicrobial effect of Zn and Ag nanoparticles on *Lactobacillus acidophilus* bacteria is sufficiently well studied due to the potential impact of these nanoparticles on human microflora. Cell morphological changes were observed during the experiment, but many cells remained normal in shape. Only a small amount of intracellular contents leaked through the nanoparticle treatment, and more live than dead cells were observed after exposure to metal nanoparticles. According to the results obtained in the study, it can be concluded that Zn and Ag nanoparticles have a slight inhibitory effect on *Lactobacillus acidophilus* (Selvarajan *et al*., 2013).

Lactobacillus plantarum

In the course of zinc nanoparticles synthesis thanks to *Lactobacillus plantarum* the Fourier-IR spectroscopy analysis revealed the presence of proteins, carboxyl and hydroxyl groups on the surface of both biosynthesized Zn nanoparticles, which act as reducing agents and stabilizers. Surface plasmon resonance for biosynthesized of nanoparticles was 349 nm and 351 nm. Biosynthesized Zn nanoparticles exhibit antibacterial and inhibitory activity against pathogenic bacteria depending on the concentration (Krol *et al*., 2018; Mohd Yusof *et al*., 2020a).

Lactic acid bacteria have mechanisms of tolerance to zinc ions. The main mechanism of resistance of *Lactobacillus* strains to zinc ions largely depends on the ability of microorganisms to interact with zinc ions through the processes of biosorption or bioaccumulation (Mohd Yusof *et al*., 2020b).

Lactobacillus sporogens

Lactobacillus sporogens is also used for the synthesis of zinc nanoparticles. Absorption of radiation using UV-visible spectroscopy occurs in the range of 315 nm. X-ray diffraction analysis showed that zinc nanoparticles have a hexagonal cell structure with an average size of 145.7 nm (Mishra *et al*., 2013).

Antimicrobial Activity of Zn Nanoparticles

Effective antimicrobial activity of Zn nanoparticles against various gram-positive and gram-negative bacterial pathogens and micromycetes, such as *Clostridium difficile*, *Clostridium perfringens*, *E. coli*, *Salmonella typhi*, *Candida albicans and Aspergillus flavus* (Mohd Yusof *et al*., 2019), *Pseudomonas aeruginosa*, *Acinetobacter baumanii*, *Klebsiella pneumonia* and *Staphylococcus aureus* (Mishra *et al*., 2013; Salman *et al*., 2018) was established by the agar well diffusion method.

Among gram-positive bacteria, the diameter of the inhibition zone formed by zinc oxide nanoparticles against *S. aureus* showed a significant increase as compared to *B. subtilis.* Among gram-negative bacteria, the diameter of the zone of inhibition formed

https://doi.org/10.24264/icams-2022.IV.12

by zinc oxide nanoparticles against *K. pneumonia* showed a significant increase as compared to *E. coli* and *P. aeruginosa*. Effect of zinc oxide nanoparticles on *K. pneumoniae*, *P. aeruginosa*, *E. coli*, *S. Aureus* and *B. subtilis* showed strong antibacterial activity against *S. aureus* and *K. pneumoniae* (Rajan *et al*., 2016).

CONCLUSION

Therefore, due to their properties, lactic acid microorganisms and micromycetes are capable of synthesizing zinc nanoparticles, which are capable of exhibiting antibacterial properties.

REFERENCES

Al-Zahrani, H.A., El-Waseif, A.A. and El-Ghwas, D.E. (2018), "Biosynthesis and Evaluation of TiO_2 and ZnO Nanoparticles from *in vitro* Stimulation of *Lactobacillus johnsonii*", *Journal of Innovations in Pharmaceutical and Biological Sciences*, 5(1), 16-20.

Baraton, M.I. (2002), *Synthesis, Functionalization, and Surface Treatment of Nanoparticles*, Am. Sci., Los-Angeles.

El-Sayed, H.S., El-Sayed, S.M. and Youssef, A.M. (2021), "Novel Approach for Biosynthesizing of Zinc Oxide Nanoparticles Using *Lactobacillus gasseri* and Their Influence on Microbiological, Chemical, Sensory Properties of Integrated Yogurt", *Food Chemistry*, 365, 130513, https://doi.org/10.1016/j.foodchem.2021.130513.

Krol, A., Railean-Plugaru, V., Pomastowski, P., Złoch, M. and Buszewski, B. (2018), "Mechanism Study of Intracellular Zinc Oxide Nanocomposites Formation", *Colloids and Surfaces A*, 553, 349-358, https://doi.org/10.1016/j.colsurfa.2018.05.069.

Mishra, M., Paliwal, J.S., Singh, S.K., Selvarajan, E., Subathradevi, C. and Mohanasrinivasan, V. (2013), "Studies on the Inhibitory Activity of Biologically Synthesized and Characterized ZnO Nanoparticles Using *L. sporogens* against *Staphylococcus aureus*", *Journal of Pure and Applied Microbiology*, 7(2).

Mohd Yusof, H., Abdul Rahman, N., Mohamad, R., Zaidan, U.H. and Samsudin, A.A. (2020a), "Biosynthesis of Zinc Oxide Nanoparticles by Cell-Biomass and Supernatant of *Lactobacillus plantarum* TA4 and Its Antibacterial and Biocompatibility Properties", *Scientific Reports*, 10(1), 19996, https://doi.org/10.1038/s41598-020-76402-w.

Mohd Yusof, H., Mohamad, R., Zaidan, U.H. and Abdul Rahman, N. (2019), "Microbial Synthesis of Zinc Oxide Nanoparticles and Their Potential Application as an Antimicrobial Agent and a Feed Supplement in Animal Industry: A Review", *Journal of Animal Science and Biotechnology*, 10, 57, https://doi.org/10.1186/s40104-019-0368-z.

Mohd Yusof, H., Mohamad, R., Zaidan, U.H. and Abdul Rahman, N. (2020b), "Sustainable Microbial Cell Nanofactory for Zinc Oxide Nanoparticles Production by Zinc-Tolerant Probiotic *Lactobacillus plantarum* Strain TA4", *Microbial Cell Factories*, 19(10), https://doi.org/10.1186/s12934-020-1279-6.

Pomastowski, P., Król-Górniak, A., Railean-Plugaru, V. and Buszewski, B. (2020), "Zinc Oxide Nanocomposites-Extracellular Synthesis, Physicochemical Characterization and Antibacterial Potential", *Materials (Basel)*, 13(19), 4347, https://doi.org/10.3390/ma13194347.

Rajan, A., Cherian, E. and Baskar, G. (2016), "Biosynthesis of Zinc Oxide Nanoparticles Using *Aspergillus fumigatus* JCF and Its Antibacterial Activity", *International Journal of Modern Science and Technology*, 1(2), 52-57.

Rodrigo, S.G. (2012), *Optical Properties of Nanostructured Metallic Systems*, Springer Heidelberg Dordrecht, New York, https://doi.org/10.1007/978-3-642-23085-1.

Salman, J.A.S., Kadhim, A.A. and Haider, A.J. (2018), "Biosynthesis, Characterization and Antibacterial Effect of ZnO Nanoparticles Synthesized by *Lactobacillus* spp.", *Journal of Global Pharma Technology*, 10(03), 348-355.

Selvarajan, E. and Mohanasrinivasan, V. (2013), "Biosynthesis and Characterization of ZnO Nanoparticles Using *Lactobacillus plantarum* VITES07", *Materials Letters*, 112, 180-182, https://doi.org/10.1016/j.matlet.2013.09.020.

Shkotova, L., Bohush, A., Voloshina, I., Smutok, O. and Dzyadevych, S. (2019), "Amperometric Biosensor Modified with Platinum and Palladium Nanoparticles for Detection of Lactate Concentrations in Wine" (in Ukrainian), SN Applied Sciences, 1(4), 306, https://doi.org/10.1007/s42452-019-0315-9.

Voloshyna, I.M., Shkotova, L.V., Skorokhod, S.O., Appolonova, I.Ye. and Zholobak, N.M. (2019), "*Lactobacillus* Bacteria: Biological and Therapeutic Properties" (in Ukrainian), *Mikrob. Zhurnal*, 81(6), 131–146, https://doi.org/10.15407/microbiolj81.06.131.

https://doi.org/10.24264/icams-2022.IV.12

ASPECTS REGARDING THE PHYSIOLOGICAL AND COMFORT PARAMETERS IN SHOES MADE OF LEATHER SUBSTITUTES

CRISTINA SECAN*, SUNHILDE CUC

University of Oradea, Faculty of Energy Engineering, Textiles-Leather and Industrial Management Department, B.St.Delavrancea str., No. 4, 410087, Oradea, Romania, E-Mail: cris_secan@yahoo.com; sunhilde_cuc@yahoo.com

The issue of replacing natural leather with leather substitutes is increasingly common in the leather goods industry. In this paper, it was addressed the issue of ensuring the physiological and comfort parameters when wearing leather substitute shoes. The aim of the paper is to analyze how the sanogenetic indicators influence the hygienic properties of footwear products starting from the porosity of the materials subjected to experimental determinations. Poromeric skin substitutes will be used, which allow the passage of water vapor and air. Both types of leather substitutes for shoe uppers and some types of textile materials for linings will be subjected to laboratory analysis, using the pycnometric method. In conclusion, the values obtained for porosity fall between 47 and 58%, limits also provided by the specialized literature. It is noted that the porosity values of leather substitutes are close to those of chrome-tanned leather, so as a result, the value of leather substitutes use will increase (they have sanogenetic properties similar to natural leather). Currently, leather substitutes are used more and more in the manufacture of footwear products, because they maintain a thermal transfer balance between the foot and the surrounding environment, favoring the elimination of moisture produced by the foot when wearing the footwear in the outdoor environment.

Keywords: leather substitutes, porosity, comfort.

INTRODUCTION

Footwear products made of leather substitutes have an increasing tendency to look like those made of natural leather (Cociu and Mălureanu, 1993), but there are still problems related to their functionality, given by the state of comfort they give to the body. Thus, footwear products must ensure both the physiological needs and the protection of the body from the environment, and the required properties are (Porav and Secan, 2016a; Porav and Secan, 2016b): water vapor permeability (SR 9123:1994), absorption desorption (SR 8994/1:1994), lightness, resistance to water seeping, thermal insulation capacity, etc. During wearing, the hygienic, physical-mechanical and thermal properties are of particular importance.

The foot temperature in shoes with natural leather uppers is **lower** than in those with leather substitute uppers, and the relative humidity in shoes with natural leather uppers is approx. 64% compared to that with substitute uppers that is approx. 78% (Malureanu and Mihai, 2003).

Leather substitutes have a poly-layered structure, and the layers are made of polyvinyl chloride or other vinyl polymers on a textile support and can be poromeric, which allow the passage of water vapor and air, or non-poromeric, which do not possess hygienic properties (Bucevschi, 1984; Bucevschi and Negreanu, 1990).

Porosity is the most important property with a role in mass transfer or thermal insulation, by pore understanding the space occupied by the gaseous phase and delimited by the solid phase. Thus, natural leather being a capillary-porous system, after tanning, it has its own porosity, but in the case of leather substitutes, the porosity must be created by expansion, in their manufacturing process (Secan, 2008a; Secan and Mitu, 2008; Secan, 2008b).

https://doi.org/10.24264/icams-2022.IV.13

The present paper presents the results of the research on the porosity of some leather substitutes and textile materials for uppers and linings.

THE EXPERIMENTAL PART

In order to highlight how the sanogenetic indicators influence the hygienic properties of footwear products (SR 8994/15:1994), materials with different structures are studied, which generally represent leather substitutes intended for the manufacture of shoe uppers, but also textile materials for linings, that have undergone some experimental determinations.

Simple replacement samples were used that were numbered from 1...7, but also textile samples numbered from 1...8. The respective number actually represents the code of the material.

The description of the materials and their destination is presented below (Secan, 2010):

- The following types of substitutes are used for uppers:
  - Material 1 - substitute PVC type on tricot used for uppers;
  - Material 2 - substitute PVC type material on both uppers;
  - Material 3 - substitute material of PVC type on non-woven for uppers;
  - Material 4 - substitute PU type material on the fabric layer used for the uppers;
  - Material 5 - substitute of PVC/knitted fabric type used for uppers;
  - Material 6 - substitute PU type/non-woven material used for uppers;
  - Material 7 - upper fabric.
- For linings we have the following types of textile materials:
  - Material 1 - thermo-adhesive fabric used for lining the shoe top;
  - Material 2 - non-woven material used for lining the heel counter stiffener;
  - Material 3 - substitute material of PU type on non-woven surface used for linings;
  - Material 4 - fine cloth fabric used for intermediate lining;
  - Material 5 - substitute PU type material on non-woven backing used for linings;
  - Material 6 - is identical to material 3;
  - Material 7 - impregnated fabric for lining the shoe top;
  - Material 8 - fabric used for intermediate linings.

Porosity is determined with the relationship (Mitu, 2000):

$$P_z = \frac{\gamma_r - \gamma_a}{\gamma_r} \cdot 100\% \quad (1)$$

γ_r– the actual specific mass or density of the material (kg / m^3);

γ_a– volumetric mass, i.e., the mass of the unit volume of material, including the pore volume.

The real specific mass or density of materials is determined taking into account their real, inhomogeneous structure. The method is based on immersing the material in certain non-polar liquids, which have the ability to displace air from the pores of the material. Such liquids are: toluene, nitrobenzene, benzene, etc.

The volumetric mass is calculated with the relation (Mitu, 2000):

https://doi.org/10.24264/icams-2022.IV.13

$\gamma_a = \frac{Ms}{\delta \cdot 1000}$ (g / cm^3) or kg / m^3 (2)

M_s–mass per unit area, (g / m^2)

δ–material thickness, mm.

Knowing the dimensions **a** and **b** of a sample of material, as well as its mass Mm expressed in grams, the mass of the surface unit MS is established, with the relationship (Mitu, 2000):

$$Ms = \frac{M_m \cdot 10^4}{a \cdot b} \text{ (g / m}^2\text{)} \quad (3)$$

Mm - mass of the material sample, (g)

a and **b** is the size of the sample in cm.

The actual specific mass or density of the material is determined using the pycnometric method which is based on weighing the sample in air, obtaining the Mm value and then introducing it into the pycnometer with the chosen liquid, which will displace the air from the pores of the material.

The density calculation relation is the following (Mitu, 2000):

$$\gamma_r = \frac{Mm}{Vm} = \frac{Mm}{\frac{M_2 - M_1}{\gamma_\varphi}} = \frac{Mm \cdot \gamma_\varphi}{M_2 - M_1} \quad (4)$$

where:

M_2 –represents the pycnometric mass of liquid and immersed sample, g;

M_1 –mass of pycnometer with liquid, g;

V_m –sample volume, cm^3;

γ_φ –the density of the immersion liquid used (in the case of toluene).

γ_φ = 0.867 g / cm^3.

RESULTS AND INTERPRETATIONS

The porosity of the materials subject to the determinations is presented in Table 1, respectively Table 2.

Table 1. Porosity of leather substitutes for shoe uppers

No.	Sample mass Mm (g)	Thickness d (mm	Mass per unit area Ms(g/m^2)	Volumetric mass γ_a (g/cm^3)	Mass of pycnometer with liquid M1 (g)	Mass of pycnometer with liquid and sample M2 (g)	Specific mass or density γ_r (g/cm^3)	Porosity Pz (%)
1	0.176	1.13	440	0.389	66.428	66.599	0.887	56.16
2	0.192	0.9	480	0.533	65.803	65.986	0.909	41.43
3	0.22	1.09	550	0.504	65.389	65.608	0.87	42.179
4	0.141	0.63	352.5	0.559	65.057	65.173	1.05	47.12
5	0.147	1.02	367.5	0.36	64.403	64.545	0.897	59.92
6	0.194	1.16	485	0.418	64.016	64.203	0.899	53.55
7	0.095	0.99	237.5	0.239	65.978	66.071	0.885	73.06

https://doi.org/10.24264/icams-2022.IV.13

Table 2. Porosity of textile materials for linings

No.	Sample mass Mm (g)	Thickness d (mm)	Mass per unit area Ms (g/m^2)	Volumetric mass γ_a (g/cm^3)	Mass of pycnometer with liquid M1 (g)	Mass of pycnometer with liquid and sample M2 (g)	Specific mass or density γ_r (g/cm^3)	Porosity Pz (%)
1	0.147	0.7	367.5	0.525	67.139	67.284	0.879	40.31
2	0.13	0.86	325	0.377	66.855	66.972	0.963	60.88
3	0.19	0.8	475	0.593	66.57	66.732	1.01	41.96
4	0.074	0.33	185	0.56	65.61	65.68	0.9165	57.83
5	0.123	0.75	307.5	0.41	64.896	65.015	0.896	54.24
6	0.151	0.83	377.5	0.454	64.652	64.796	0.909	50.07
7	0.084	0.46	210	0.456	64.526	64.605	0.92	50.63
8	0.077	0.35	192.5	0.55	63.724	63.795	0.94	41.51

Taking into account the importance of the porosity owned by the materials used only for shoe uppers, the following graph is presented below:

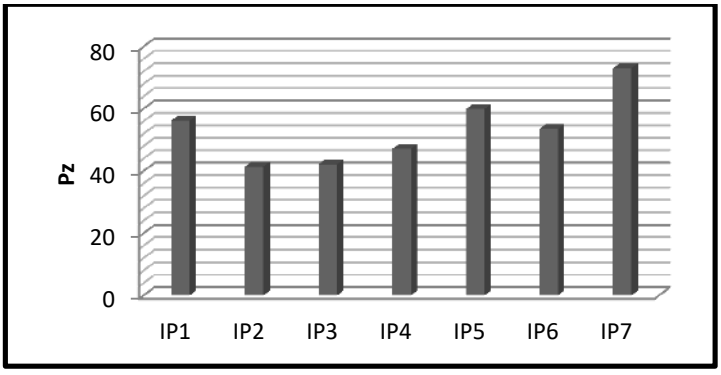

Figure 1. Porosity variation for types of substitutes intended for shoe uppers

In Figure 1, higher porosity values can be observed for material 2 woven type, followed by PU polyurethane on tricot support and PVC polyvinyl chloride on tricot support (material 6 and material 1). There are lower values for the PU polyurethane substitute, on a non-woven support (material 7). Impregnated or printed materials (materials 5, 4, 3) have lower porosity values.

Figure 2 shows the porosity variation for textile materials intended for linings.

https://doi.org/10.24264/icams-2022.IV.13

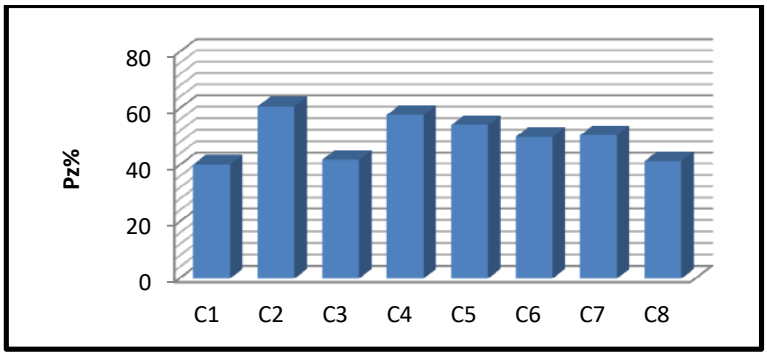

Figure 2. Porosity variation in types of textile materials intended for linings

The highest value of porosity is observed in the case of material 2, which is a non-woven used for the lining of the heel counter stiffener, respectively a material that is very resistant to wear, but also vapor permeability and moisture absorption capacity. Comparing material 7, which is an impregnated woven fabric with material 4, which is a fine yarn fabric, lower porosity values are observed for material 7. Material 1, which is a thermo-adhesive fabric used for doubling the shoe tops, has the lowest porosity value in order to avoid plastic deformations in the process of spatial formation.

In order to provide a suggestive illustration of the obtained data, the graph below (fig. 3) shows the porosity variation for all the studied materials. Thus, a comparative analysis of the values of this parameter can be made, starting from the structure and composition of each type of material.

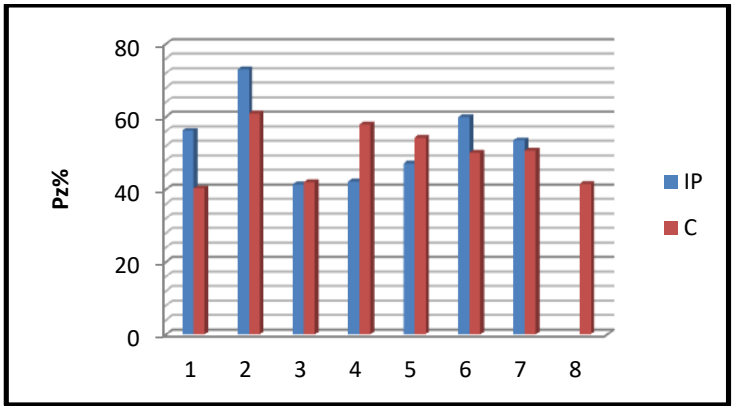

Figure 3. Porosity variation with different types of substitutes

CONCLUSIONS

After processing the experimental data, it is noticed that the porosity varies between 45 and 60%, i.e. within the limits indicated by the specialized literature which states that

https://doi.org/10.24264/icams-2022.IV.13

for the upper part of the footwear the limits are between 47 and 58%, and for the lower part the limits are between 29 and 47%.

The exception is material 7, which is actually a fabric enriched with rubber patterns (PVC, etc.) and which is hydrophobized; treatment actually applied on textile materials intended for footwear. The values for porosity are entered in the table above, to which benchmarks are associated for interpretation.

Making a comparison between leather and leather substitutes, following the analysis of the graphs obtained, a proximity of porosity values is observed for leather substitutes, intended for shoes uppers with chrome-tanned leather, a fact that justifies the tendency to use these days as much as possible footwear products made from leather substitutes, which have sanogenetic properties similar to natural leather.

It is therefore recommended that leather substitutes with porosity should be used in the manufacture of footwear products, so that they possess the ability to transmit and release moisture, maintaining a thermal transfer balance between the foot and the surrounding environment, taking into account the fact that footwear is a system composed of several layers of materials.

REFERENCES

Bucevschi, M.D. (1984), *Technology of Leather Substitutes* (in Romanian), Rotaprint, Iaşi.

Bucevschi, M.D. and Negreanu, D.S. (1990), *Artificial and Synthetic Leather* (in Romanian), Technical Press, Bucharest.

Cociu, V. and Mălureanu, G. (1993), *Fundamentals of the Technology of Products Made of Leather and Substitutes* (in Romanian), Rotaprint, Iaşi, part II.

Malureanu, G. and Mihai, A. (2003), *Fundamentals of Footwear Design* (in Romanian), Performantica, Iaşi.

Mitu, S. (2000), *The Comfort and Functions of Clothing Products* (in Romanian), "Gh. Asachi" Press, Iaşi.

Porav, V. and Secan, C. (2016a), "An Analysis the Influence of the Textile Material Doubling Process by Thermofusing on Vapor Permeability", *Annals of the Oradea University, "Fascicle of Textile – Leatherwork"*, The International Scientific Conference, "Innovative Solutions for Sustainable Development of Textiles Industry", vol. XVII, University of Oradea Press, ISSN 1843-813X, p.107.

Porav, V. and Secan, C. (2016b), "The Influence of Doubling of Textile Materials through Thermofusing on Their Hydrophilicity", *Annals of the Oradea University, "Fascicle of Textile – Leatherwork"*, The International Scientific Conference, "Innovative Solutions for Sustainable Development of Textiles Industry", vol. XVII, University of Oradea Press, ISSN 1843-813X, p. 111.

Secan, M.C. (2008a), "Study on the Influence of the Structure of Leather Substitutes on Water Vapour Permeability" (in Romanian*), Textiles of the Future, The Annual Symposium of the Specialists in the Knitting-Clothing Industry*, Faculty of Textiles-Leather, November 2008.

Secan, M.C. and Mitu, S. (2008), "Experimental Research on Establishing Limits of Comfort Parameters for Products Made of Leather and Substitutes" (in Romanian), *Textiles of the Future, The Annual Symposium of the Specialists in the Knitting-Clothing Industry*, Faculty of Textiles-Leather, November 2008.

Secan, M.C. (2008b), "Research Concerning the Influence of Certain Sanogenetic Indicators on the Hygienic Properties of Footwear Products", *Annals of the University of Oradea, Fascicle of Textiles-Leatherwork*, The International Scientific Symposium "Innovative Solutions for Sustainable Development of Textile Industry", vol. IX, University of Oradea Press, pp. 291-296.

Secan, C. (2010), "Contributions to the Optimization of the Use of Leather Substitutes in the Footwear Manufacturing Process" (in Romanian), PhD Thesis.

*** (1994), SR 8994/15:1994, *Leather Substitutes. Determination of Perspiration Resistance* (in Romanian).

*** (1994), SR 8994/1:1994, *Leather Substitutes. Determination of Permeability, Absorption and Desorption of Water Vapor* (in Romanian).

*** (1994), SR 9123:1994, *Leather Substitutes. Determination of Water Permeability* (in Romanian).

https://doi.org/10.24264/icams-2022.IV.13

BEHAVIOUR OF NITRILE RUBBER-BASED MIXTURES TO COMPOSTING TESTS

MARIA DANIELA STELESCU, MIHAELA NIȚUICĂ (VILSAN), MIHAI GEORGESCU, DANA GURĂU, LAURENȚIA ALEXANDRESCU, MARIA SÖNMEZ

The National Research & Development Institute for Textiles and Leather - Leather and Footwear Research Institute Division, 93 Ion Minulescu Street, 031215 Bucharest, Romania; dmstelescu@yahoo.com

The paper presents the behavior of some samples based on nitrile rubber reinforced with inorganic and organic type of filler, respectively, to composting. The organic filler used was obtained as waste in the leather and footwear industry. Before use, the waste was ground and then functionalized with potassium oleate in order to improve compatibility with the polymer matrix. The samples of rubber mixtures were obtained on a Brabender mixer, the vulcanization agents were added on a laboratory roller, and the vulcanization of the samples was performed in a hydraulic laboratory press, at 165°C, with a pressing force of 300 kN. The aerobic composting test was performed at laboratory scale, using solid, standardized and homogeneous synthetic waste. After a thermophilic incubation period of 42 days (at 58°C), followed by a period of mesophilic incubation (at the room temperature) of 42 of days, a decrease of some physico-mechanical properties was noticed (hardness, 100% modulus, tensile strength), of the gel fraction, and of the crosslinking densities, the largest decrease of these characteristics being observed in the sample with the highest content of organic filler. The results obtained may indicate that the biodegradation of the rubber samples is favored by the organic fillers.

Keywords: NBR, leather waste, composting test, gel fraction, crosslinking density

INTRODUCTION

Acrylonitrile butadiene copolymers (nitrile rubbers) are used to obtain rubber products (technical articles) with high resistance to oils and petroleum products, with a low gas permeability, a very good abrasion resistance, and with a resistance to aging, heat and ozone superior to natural rubber (Degrange *et al.*, 2005; Shen *et al.*, 2016). Nitrile rubber mixtures (NBR) generally contain fillers (to improve the tensile and tear strength), plasticizers to improve processability, vulcanizing agents, antioxidants, etc.

Vulcanized rubber materials are not biodegradable and for these reasons, after use, they represent a problem for the environment. Due to the current concerns regarding environmental protection, in recent years there have been several studies regarding the replacement of inorganic fillers in rubber mixtures with organic, biodegradable ones (Przepiorkowska *et al.*, 2007; Prochoń and Przepiórkowska, 2013; Mendez-Hernandez *et al.*, 2018). However, there are not many studies on the evaluation of the biodegradation properties of these types of rubber mixtures (Prochoń *et al.*, 2012).

This paper aims to analyze the behavior of samples based on reinforced nitrile rubber both with inorganic and organic fillers to biodegradation and disintegration by composting. Thus, a part of the inorganic filler was replaced with cryogenically ground leather waste or with ground waste based on leather and vulcanized butadiene-styrene rubber (SBR). The testing of the samples regarding the aerobic composting behavior was performed in laboratory conditions, during an incubation period of 84 days, of which 42 days at 58°C (thermophilic incubation), followed by 42 days at the ambient temperature (mesophilic incubation). The modification of the physico-mechanical characteristics, the gel fraction, and the crosslinking densities of the samples were determined.

https://doi.org/10.24264/icams-2022.IV.14

EXPERIMENTAL

Materials

In the obtaining of the samples based on nitrile rubber (NBR) subjected to disintegration into compost, both inorganic and organic fillers were used. The organic fillers were functionalized with potassium oleate in order to improve their compatibility with the nitrile rubber. Table 1 shows the composition of the analyzed samples, in parts per 100 parts of rubber (by weight). The main characteristics of the materials used were presented in a previous paper (Nițuică *et al.*, 2021).

Table 1. The composition of the samples

Ingredients	Symbol samples		
	B0 (control)	BCB_4	$BCPP_4$
Polymer matrix: NBR rubber	100	100	100
Plasticizer: mineral oil	10	10	10
Stearin	1.2	1.2	1.2
Inorganic filler:			
- Silicon dioxide (SiO_2)	30	-	-
- Kaolin	25	5	5
Organic filler:			
- Functionalized leather waste with potassium oleate	-	-	50
- Leather and SBR rubber mixed waste functionalized with potassium oleate	-	50	-
Antioxidant: IPPD 4010	3	3	3
Vulcanizing agent:			
- Sulphur (S)	1.5	1.5	1.5
- Zinc oxide (ZnO)	5	5	5
- Tetramethylthiuram disulfide (Th)	0.6	0.6	0.6

Preparation of Samples

The rubber mixtures were obtained on an internal Brabender PlastiCorder mixer. The addition of the sulfur and vulcanization accelerators was carried out on a laboratory roller, and the vulcanization process took place in a hydraulic laboratory press at 165°C, a pressing force of 300 kN, and vulcanization time 5 minutes. The method of obtaining the samples was presented in detail in the paper by Nițuică *et al.*, 2021. The paper also presents the procedure of waste functionalization (leather, and a mix of leather and butadiene-styrene-SBR rubber waste, respectively), characteristics presented in Brabender processing diagrams, as well as rheological characteristics of mixtures.

Measurements

Composting tests of NBR rubber samples was performed using solid, standardized and homogeneous synthetic waste, in accordance with ISO 20200. The aim was to determine the degree of disintegration of the test materials at the laboratory scale, in conditions that simulate an intensive process of aerobic composting. For the test, a transparent plastic box with a lid was used, provided with a hole on both sides of the box (reactor). From the vulcanized rubber sheets, dumbbell-type specimens (with a thickness of 2 mm and a length of 115 mm) were punched, then they were weighed and placed in the plastic box. From each sample, min. 6 test pieces were analyzed. For the composting

https://doi.org/10.24264/icams-2022.IV.14

test, synthetic solid waste (inoculated with matured compost) was used as a solid matrix, in the amount of 1100 g, whose composition is specified in Table 2. Over the synthetic solid waste, 1345 g of distilled water were added, representing 55% of the total mass quantity. These were mixed, and then together with the samples (test pieces) were placed in the box (reactor). The reactor with the samples were inserted into the oven at 58°C, it was weighed daily and the evaporated water was replaced with distilled water, evenly distributed. After 42 days, the first series of samples was removed from the box, washed and wiped, dried for 24 hours in the oven at 58°C and then 1 hour at 100°C. After conditioning at room temperature, the samples were reweighed and then tested. After the thermophilic incubation period (at high temperature), the second series of samples, which remained in the box, was maintained for another 42 days at a mesophilic incubation (at ambient temperature). During this period, the reactor was weighed twice a week and distilled water was added to return the mass to 70% of the mass measured at the beginning of the test. The second series of test pieces was removed on the 84th day, and the same procedure of washing, wiping, drying and conditioning was applied.

Accelerated ageing evaluation was carried out according to ISO 188 using the hot air oven method. Test duration was of 168 h and temperature of 70±1°C.

For the samples: (a) in normal state, (b) after accelerated aging, (c) after the thermophilic incubation period (after 42 days) and (d) after the thermophilic incubation period and the mesophilic incubation period (in total 82 days), the physico-mechanical characteristics were determined, namely: tensile strength (using dumb-bell shaped specimens according to ISO 37), hardness in Shore A degrees (according to ISO 48-4) and elasticity (according to ISO 4662).

Table 2. Composition of synthetic solid waste

Material	Mass	Characteristics	Company
Sawdust	400 g	Sawdust of natural wood, sieved with dimensions of max 3 mm	P.W. "Hobby", P. Matuszewski, Poland
Food for rabbits	300 g	Protein 15.6%, fat 2.8%, fiber 18.5%	Cunipic Animals De Companyia, Spain
Matured compost	200 g	Compost Garden	Agro C.S., Prirodni product, Czech Republic
Corn starch	100 g	Starch soluble from potatoes, P.A. $(C_6H_{10}O_5)_n$	Lachner, Czech Republic
Sucrose	50 g	Saccharosa P.A., D(+)szacharoz G.R.($C_{12}H_{22}O_{11}$, M=342.30 g/mol)	Lachner, Czech Republic
Corn oil	40 g	Unrefined corn oil, polyunsaturated fat 54%	S.C. Man Ro S.R.L, Romania
Urea	10 g	P.A. purity 99.5%	Chimreactiv S.R.L., Romania

In order to be able to evaluate the degree of biodegradation of the samples after the thermophilic and mesophilic incubation period, respectively, the gel fraction and the crosslink density were determined using the Flory–Rehner equation for tetrafunctional networks. For this, the samples were immersed for 168 hours in toluene at room temperature. The procedure and the calculation formulas are presented in several previous papers, with the specification that: the molar volume of toluene is 106.5 cm^3/mol and the Flory-Higgins polymer (NBR) – solvent (toluene) interaction parameter (χ_{12}) is 0.3795 (Stelescu *et al*., 2022; Basu *et al*., 2021).

https://doi.org/10.24264/icams-2022.IV.14

RESULTS AND DISCUSSIONS

Analysis of the Samples after the Composting Test of the Samples

During the composting process, the sequence of specific odors mentioned in the ISO 20200 standard was detected, as well as the change in the appearance of composting and the color shifting from slightly yellowish due to the high concentration in sawdust, to dark brown. Figure 1 shows the images of the samples: the initial stage, at 42 days, and at 84 days, after washing, wiping and drying. As shown in Figure 1, after the composting test period, the samples have not disintegrated because, according to the literature (Prochoń *et al.*, 2012), the samples of cross-linked rubber have a high resistance to biodegradation. According to the results obtained during weighing, the samples showed mass variations both negative and positive, of a maximum of ±10%. These variations in mass may be due to the biodegradation reactions that occurred at the interface between the samples, the solid synthetic waste in the wet state (with the composition specified in Table 2) and the microorganisms developed during the thermophilic and mesophilic incubation period, respectively. These changes could be observed with the naked eye immediately after washing and wiping the samples (see Figure 2), but after drying them, the samples darkened (see Figure 1).

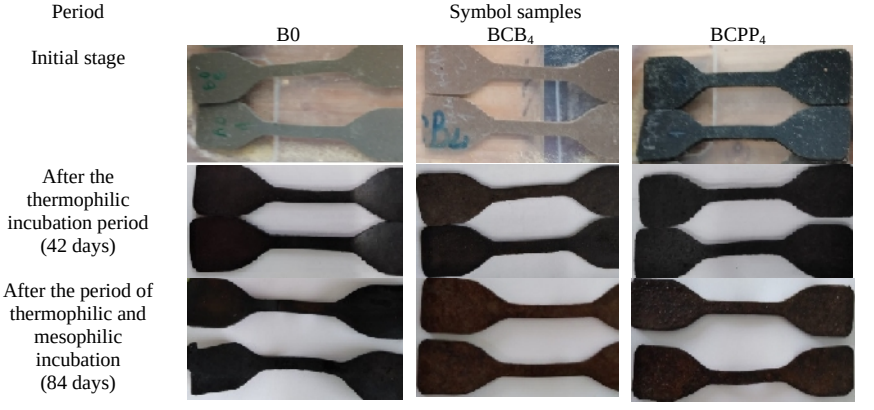

Figure 1. The images of the samples in the initial state, after the thermophilic and mesophilic incubation period respectively (the samples are washed, wiped and dried)

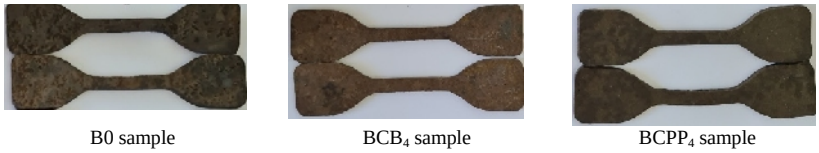

B0 sample BCB_4 sample $BCPP_4$ sample

Figure 2. Images of the samples washed and wiped, after the thermophilic incubation period

Physico-Mechanical Characteristics

The physico-mechanical characteristics of the samples in the normal state, after accelerated aging, after the thermophilic and mesophilic incubation period are shown in Figure 3. From analyzing the obtained characteristics the following can be observed: (a) the characteristics are influenced by the type of filler introduced into the mixture

https://doi.org/10.24264/icams-2022.IV.14

(inorganic or organic); (b) the values of the characteristics obtained after accelerated aging or after the thermophilic incubation period may indicate an increase in the degree of crosslinking due to maintaining the samples at a high temperature (Liu *et al.*, 2016; Jiang *et al.*, 2019); (c) for samples tested after thermophilic and mesophilic incubation periods (84 days) a decrease in characteristics is observed that may indicate a partial biodegradation of samples, and this is more significant in the sample with a higher content of organic waste ($BCPP_4$).

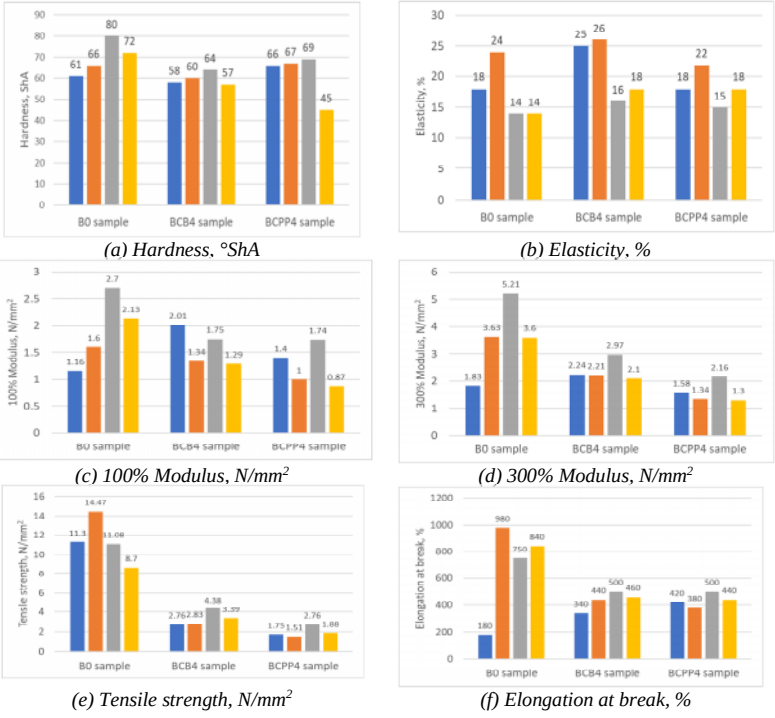

(a) Hardness, °ShA *(b) Elasticity, %*

(c) 100% Modulus, N/mm² *(d) 300% Modulus, N/mm²*

(e) Tensile strength, N/mm² *(f) Elongation at break, %*

Figure 3. Physico-mechanical characteristics of the samples for: normal state (blue), after accelerated aging 168hx170°C (orange), after the thermophilic incubation period of 42 days (gray), and after the thermophilic and mesophilic incubation period 84 days (yellow)

Gel Fraction

The gel fraction and the crosslink density of the samples is shown in Figure 4. A tendency to increase the gel fraction and the crosslink density of the samples after the thermophilic incubation period can be observed, due to the crosslinking reactions that may occur during the maintenance of the samples for a period of 42 days at 58°C (Liu *et al.*, 2016; Jiang *et al.*, 2019). The values of the gel fraction and the crosslink density decrease significantly after maintaining the samples at a thermophilic and mesophilic incubation period (84 days), the largest decrease being observed in the sample with a high content of organic filler ($BCPP_4$ sample).

https://doi.org/10.24264/icams-2022.IV.14

(1) Gel fraction, % (2) Crosslink density x $^{10-4}$, mol/cm^3

Figure 4. Gel fraction and crosslink density of samples for: normal state (dark gray), after the thermophilic incubation period of 42 days (yellow), and after the thermophilic and mesophilic incubation period 84 days (green)

CONCLUSIONS

After analyzing the biodegradation behavior by composting of samples based on NBR rubber reinforced with inorganic and organic filler type, respectively, it was observed that after a period of 42 days of thermophilic incubation, followed by a period of 42 days of mesophilic incubation, there is a decrease in: hardness, 100% modulus, 300% modulus, tensile strength, gel fraction and crosslinking density, and these decreases are more pronounced in the sample with a higher content of organic waste.

Acknowledgements

This research was financed by ANCSI through PN 19 17 01 03/2019 project.

REFERENCES

Basu, D., Banerjee, S.S., Debnath, S.C., Malanin, M., Amirova, L., Dubois, P., Heinrich, G. and Das, A. (2021), "Unusual Low Temperature Relaxation Behavior of Crosslinked Acrylonitrile-Butadiene Co-Polymer", *Polymer*, 212, 123309, https://doi.org/10.1016/j.polymer.2020.123309.

Degrange, J.M., Thomine, M., Kapsa, Ph., Pelletier, J.M., Chazeau, L., Vigier, G., Dudragne, G. and Guerbé, L. (2005), "Influence of Viscoelasticity on the Tribological Behaviour of Carbon Black Filled Nitrile Rubber (NBR) for Lip Seal Application", *Wear*, 259, 684–92, https://doi.org/10.1016/j.wear.2005.02.110.

Jiang, B., Jia, X., Wang, Z., Wang, T., Guo, F. and Wang, Y. (2019), "Influence of Thermal Aging in Oil on the Friction and Wear Properties of Nitrile Butadiene Rubber", *Tribology Letters*, 67(86), https://doi.org/10.1007/s11249-019-1201-8.

Liu, J., Li, X., Xu, L. and Zhang, P. (2016), "Investigation of Aging Behavior and Mechanism of Nitrile-Butadiene Rubber (NBR) in the Accelerated Thermal Aging Environment", *Polymer Testing*, 54, 59-66, https://doi.org/10.1016/j.polymertesting.2016.06.010.

Mendez-Hernandez, M.L., Salazar-Cruz, B.A., Rivera-Armenta, J.L., Estrada-Moreno, I.A. and Chavez-Cinco, M.Y. (2018), "Preparation and Characterization of Composites from Copolymer Styrene-Butadiene and Chicken Feathers", *Polymeros*, 28, 368–372, https://doi.org/10.1590/0104-1428.08217.

Nițuică (Vîlsan), M., Sonmez, M., Georgescu, M., Stelescu, M.D., Alexandrescu, L. and Gurau, D. (2021), "Biodegradable Polymer Composites Based on NBR Rubber and Protein Waste", *Leather and Footwear Journal*, 21(4), 229-236, https://doi.org/10.24264/lfj.21.4.3.

Prochoń, M. and Przepiórkowska, A. (2013), "Innovative Application of Biopolymer Keratin as a Filler of Synthetic Acrylonitrile-Butadiene Rubber NBR", *Journal of Chemistry*, 787269, https://doi.org/10.1155/2013/787269.

Prochon, M., Janowska, G., Przepiorkowska, A. and Kucharska-Jastrzabek, A. (2012), "Thermal Properties and Combustibility of Elastomer-Protein Composites: Part I. Composites SBR – Keratin", *Journal of Thermal Analysis and Calorimetry*, 109, 1563–1570, https://doi.org/10.1007/s10973-011-2028-1.

Przepiorkowska, A., Chronska, K. and Zaborski, M. (2007), "Chrome-tanned Leather Shavings as a Filler of Butadiene–Acrylonitrile Rubber", *Journal of Hazardous Materials*, 141, 252–257, https://doi.org/10.1016/j.jhazmat.2006.06.136.

Shen, M., Peng, X., Meng, X., Zheng, J. and Zhu, M. (2016), "Fretting Wear Behavior of Acrylonitrile–Butadiene Rubber (NBR) for Mechanical Seal Applications", *Tribology International*, 93, 419–428, https://doi.org/10.1016/j.triboint.2015.09.029.

Stelescu, M.D., Airinei, A., Bargan, A., Fifere, N., Georgescu, M., Sonmez, M., Nituica, M., Alexandrescu, L. and Stefan, A. (2022), "Mechanical Properties and Equilibrium Swelling Characteristics of Some Polymer Composites Based on Ethylene Propylene Diene Terpolymer (EPDM) Reinforced with Hemp Fibers", *Materials*, 15, 6838, https://doi.org/10.3390/ma15196838.

https://doi.org/10.24264/icams-2022.IV.14

V.

CREATIVE INDUSTRIES AND CULTURAL HERITAGE

DIVERGENCE OF UPPER MATERIALS TO SPECIFIC FOOTWEAR CONSTRUCTION: SEEKING A CULTURE OF SUSTAINABLE MATERIAL SOLICITATION

MUHAMMAD NAIMUL HASAN[1*], ANOWER JAHAN TAMANNA[1], MD. ARMANUL HAQUE[2]

[1] *Khulna University of Engineering & Technology, Mechanical Engineering Faculty, Leather Engineering & Technology Department, Khulna-9203, Bangladesh, hasannamkuet@gmail.com*

[2] *Leatherex Footwear Industries Ltd. Dhaka-1341, Bangladesh*

Footwear is equally a fashion and function apparel item constructed of leather and non-leather materials. This research aims to investigate the selection of materials for footwear fabrication corresponding to shoe functionality and fashion aspects of consumers. Here, an attempt is taken to build a network among the consumer perception of cherry-picking shoes, sustainable fashion, and the physicomechanical behavior of versatile upper materials focusing on leather and non-leather. A psychometric rating scale is used to rate the relationship of sustainability attitude regarding both materials and users. The chosen materials are leather, pleather, and fabric. The leather items are suede, semi-aniline, and corrected grain leather whereas non-leather materials are canvas cotton, PUCF, and PVCF. The randomly selected materials with a thickness of 1.2-2.4 mm for the dress (oxford), casual, and boot shoe fabrication were brought under rigorous physicomechanical tests following ISO and SATRA methods. Besides, a quantitative statistical analysis of psychophysical material information test was carried out among 132 valid respondents. Though cent-percent of finished leather and most of the canvas fabric samples have satisfied standards of physicomechanical characteristics whereas pleather was underneath. The weighted score for green materials solicitation for sustainable use was 2.5 ± 0.01on a psychometric rating scale of 5.00, quite unsatisfactory due to a deficiency of materials knowledge among consumers. Moreover, the Pearson correlation coefficient is about 0.99152 and a p-value of $0.03 \angle 0.05$ has been observed which provided strong evidence of a statistically significant positive correlation among the variables on the sustainability attitude scale of material cherry-picking.

Keywords: Footwear, upper materials, sustainability.

INTRODUCTION

Footwear is a wearing attire that has been designed for the feet to protect, adorn and comfort. In addition, most recently footwear has become a significant part of fashion associates, performance items, and even considered an energy harvester (Ujević *et al*., 2009; Soloman, 2021; Goonetilleke and Weerasinghe, 2011). The footwear generally consists of two principal parts recognized as upper and bottom. The footwear industry uses diverse types and styles of shoe materials such as leather, synthetic materials, poromerics, rubber, leatherette, naugahyde, vegan or faux leather, multiple textiles, composites, foamposities, etc., materials are among the rudimentary materials most frequently used in footwear assembly. Each material has its specific characteristics. Design and material assortment measures meaningfully affect not only the shoe's lifecycle but also its end-of-life supervision (Ujević *et al*., 2009; Staikos and Rahimifard, 2007; Meyer *et al*., 2021). The usage of the terms artificial leather, synthetic leather, leatherette, imitation leather, faux leather, man-made leather, bonded leather, pleather, textile leather, or polyurethane (PU)-leather is restricted in Europe by the European standard EN 15987 (Meyer *et al*., 2021). From the viewpoint of a global perspective, footwear worldwide production has reached 24.3 billion pairs in 2021 with an economy of $105.8 billion. The manufacturing sites are deeply focused on the territory of Asia. Bangladesh shares more than 1.6% of the world's total footwear consumption and secured its position in the world's top ten shoe consumption matrix -2021 (World Footwear Yearbook 2021). According to the Export Promotion Bureau, leather and leather products is the second-largest sector of Bangladesh in terms of exports, after ready-made garments, exported leather and leather products were worth $1.2 billion in the FY

https://doi.org/10.24264/icams-2022.V.1

2020-2021. Which is about 2.43 percent of the total export earnings of the country ($38.758 billion). In Bangladesh, there are 42 automated and over 4500 non-automated large and cottage-level footwear production units that continuously satisfy the national and international demand for various kinds of footwear (Hasan *et al*., 2016). Despite its stretched expansion and contribution to Bangladesh's economy, research on footwear materials has not been broadly undertaken.

This study inspected the dynamics of the sustainable upper materials consumption practice, selection culture, and approach in certain categories of footwear apparel production in Bangladesh. Here, a comparative analysis of physicomechanical properties of shoe upper leather and alternative materials (pleather and canvas fabric) was done to give a guide to the footwear manufacturers both local and exporters regarding the solicitation of quality materials for footwear production and sustainable development of the sector. Moreover, a psychometric test on consumers' behavioral intention to use leather-made foot apparel through a structured questionnaire was conducted to elucidate the cultural facts about non-leather footwear use.

MATERIALS AND METHODS

Materials

There were eighteen different types of footwear upper materials samples among which nine were chrome tanned leather, three of each PVCF (Polyvinyl Chloride-Coated Fabric) and PUCF (Polyurethane Coated Fabric), and three canvas textiles were collected randomly from prominent export-oriented footwear industries around Dhaka city. The SATRA- thickness gauge tester (0.01mm least count) was used to measure the thicknesses of test samples. The details of the test specimens are provided in Table 1.

Methods

In any experimental research, sampling, conditioning, and machine calibration are the prime importance to meet results accuracy. Prior to testing, all the samples were conditioned in a standard atmospheric of 48 hours, 27±2°C, and 65±2% of RH (Relative Humidity). Sharp press knives with 18 mm deep and 200 cutting edge angle (ISO 2419) were used for cutting the specimen (Dutta, 1990; Bayes *et al*., 2013). Triplicate tests of different physical and mechanical experiments were carried out in the laboratory to assess the quality of shoe upper materials (leather and non-leather) and minimize errors. The carried out tests, equipment, method of analysis, etc., are shown in Table 2.

Statistical Analysis

A survey was conducted among 132 valid subjects (73 men, age - 27 year, and 59 women, age - year) to perform statistical analysis. The observation was based on a structured questionnaire. The order of questions is focused on a sustainability attitude scale modeling shown in Fig. 1. And administered to comprehend the perception of subjects' (consumer) decision approach to buying and using leather and non-leather made footwear in their daily life, and knowledge of footwear quality linked with material sustainability. A psychometric scale (Likert scale) was used to evaluate the skepticism of consumers' dissuasive attitude toward the application of material sustainability knowledge and culture in purchasing footwear. The numerical ratings of 5 – 1 were allotted to the feasible Likert answers of intensely approve – intensely disapprove in order to reach a minimum mean value. The weighted score (WS) was computed using Eq. (1).

https://doi.org/10.24264/icams-2022.V.1

Table 1. Sample specification

ID No.	Shoe Style	Upper Category	Color	Thickness (mm)	Yarn Count Warp	Yarn Count Weft
S1	Casual	Cow, corrected grain	Black	1.22		
S2		Cow, corrected grain	Black	1.23		
S3		Cow, corrected grain	Black	1.28		
S4	Boot	Cow, Suede	Brown	1.92		
S5		Cow, suede	Brown	2.11		
S6		Cow, suede	Brown	2.38		
S7	Dress	Cow, semi-aniline	Red	1.31		
S8		Cow, semi-aniline	Red	1.32		
S9		Cow, semi-aniline	Red	1.33		
S10		PUCF (woven backer)	Grey	1.21	45	45
S11	Dress	PUCF (woven backer)	Grey	1.24	45	45
S12		PUCF (woven backer)	Grey	1.31	45	45
S13	Casual	Canvas (cotton)	Blue	1.23	75	110
S14		Canvas (cotton)	Black	1.22	75	110
S15		Canvas (cotton)	Blue	1.25	75	110
S16	Boot	PVCF (non-woven baker)	Pink	1.91		
S17		PVCF (non-woven baker)	Pink	1.89		
S18		PVCF (non-woven baker)	Pink	2.21		

$$WS = \sum_{1}^{n} \frac{nx}{N} \quad (1)$$

where, x = number of responses; n = rating score of question; and N = total number of valid subjects. The Pearson correlation test was also conducted with the hypothesis maintaining a 95% confidence interval with df. = n-1. The null hypothesis is no correlation between the parameters of materials sustainability and the specific shoe construction and vice versa is the alternative hypothesis has been considered.

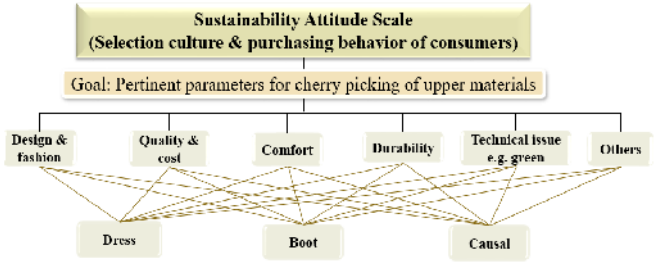

Figure 1. Material selection model for specific footwear construction

Table 2. Tests, analysis method, and equipment

Experiments	Method of analysis	Equipment
Thickness of upper materials	ISO 2589 (Leather); ISO 9073-2(Textile)	Thickness gauge, SATRA STD 483 (Leather), STD 484 (synthetic & other materials)
Sampling location and preparation (Leather)	ISO 2418-9	-
Sample conditioning	ISO 2419/ ISO 554	
Tensile Strength (TS) & Elongation (E)	ISO 3376	Tensile tester, STD 172
Stitch Tear (double hole) strength (ST)	ISO 3377/ SATRA- PM 5	Tensile tester, STD 172
Tongue Tear strength (TT)	ISO 3377	Tensile tester, STD 172
Finish film Adhesion (FA)	SATRA-TM 408	Adhesion of Finish tester, STD 112

https://doi.org/10.24264/icams-2022.V.1

Experiments	Method of analysis	Equipment
Water Vapor Permeability (WVP)	ISO 14268/ SATR- PM 172	Water Vapor permeability machine STM 473
Grain Crack Index (GCI); Load (L) & Distension (D)	ISO 3378-9/ SATRA- STM 104	Digital Lastometer, STM-463
Flex Resistance (FR)	ISO 5402/ SATRA-TM 147	Flexing machine, STM 141
Yarn count Ne (textile)	ISO 7211-5	-
Rub Fastness (RF) (wet & dry)	ISO 11642/ SATRA-TM 08 ISO 105-X10 (PU & PVC)	Rub Fastness tester, STM 462/ (coloring ISO 105-A02 & Staining ISO 105-A03)
Fastness to Water spot (FW).	ISO 15700	-

RESULTS AND DISCUSSION

The physicomechanical test results have been provided in Table 3. Among all the experiments, the most significant mechanical properties for shoe upper materials selection are Tensile Strength (TS) and Stitch Tear (ST) strength (ISO 3377-1:2011; ISO 3376:2020). The results for both parameters vary a little among the corrected grain, suede, and semi-aniline leather whereas in the case of pleather (PUCF & PVCF) wide-ranging range of gaps are observed from the shoe upper standard values and even from naturally grown sample leather used in this research work.

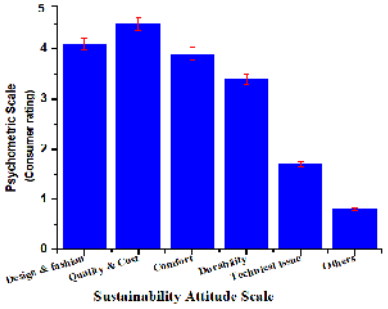

Figure 2. Sustainability scale rating

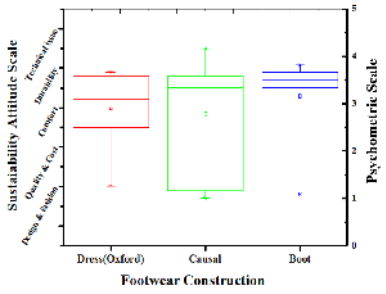

Figure 3. Consumer perceptions of specific footwear

The three categories of upper leather for the dress (Oxford), boot, and casual have shown a very high mechanical stability (TS, ST, WVP, and GCI), demonstrating the utmost values which scenario is crystal clear in the data table. TS, ST, and, WVP values have exceeded the specification of > 15 N/mm^2 (ISO 3376), min 78 N/mm (ISO 3377), and min 0.8 (ISO 14268), and, > 35 N (ISO 3378-9) respectively for chrome-tanned shoe-upper leather (ISO 3377-1:2011). The percentage of elongation (% E), TT, FR, RF (wet & dry), FW, etc., are also in minimum requirements. On the other hand, pleather did not achieve any of the technical requirements properties under the yardstick of ISO or SATRA recommendation. This diminutive performance of % E highlighted that the Pleather has poor elasticity, TS, ST, and, WVP to adjust to the user's feet and the actions (forward torque 14.2 N.m) consequent from the wearer of footwear. The normal range of pressures on the foot surface is about 150–400 KPa during a simple way of walking at the dorsal foot dorsum (Ruperez *et al*., 2009; Rupérez, 2012).

Moreover, during the footwear fabrication, the resultant 3600 force provided on the upper materials by pincers of toe lasting machine easily tears the surface of pleather due to making processes.

https://doi.org/10.24264/icams-2022.V.1

Table 3. Physicomechanical tests result of upper materials

Upper material types	Shoe Type	Thickness, mm Mean ± SD	TS, N/mm² Mean ± SD	E, % Mean ± SD	ST, N/mm Mean ± SD	TT, N/mm Mean ± SD	WVP, mg/cm².h Mean ±SD	FA, N/m Mean	GCI/ L (N); D(mm) Mean L	D	FR, (25000, Cycle), Break pipiness rating	RF, wet (128) & dry (1024)	S, mm Mean ±SD
Corrected grain	Casual	1.24 ± 0.03	19.18 ± 0.65	47 ± 2.0	81.5 ± 0.53	36.71 ± 1.08	0.8 ± 0.04	0.5	35.54	7.45	2	4/5	4.35 ± 0.16
Suede	Boot	2.14 ± 0.23	22.44 ± 1.10	67 ± 11.0	86.07 ± 3.88	40.88 ± 1.63	0.9 ± 0.06	-	38.27	7.12	3	4	3.97 ± 0.28
Semi-aniline	Dress	1.32 ± 0.01	18.46 ± 0.50	45 ± 3.0	78.29 ± 1.61	31.86 ± 0.48	0.9 ± 0.02	0.4	36.23	7.32	3	4/5	2.79 ± 0.32
PUCF	Dress	1.25 ± 0.05	10.03 ± 0.51	27 ± 3.0	52.67 ± 0.68	14.36 ± 0.80	0.55 ± 0.06	0.2	18.56	5.95	6	2/3	1.97 ± 0.15
PVCF	Boot	2.01 ± 0.18	10.87 ± 1.97	22 ± 1.0	28.55 ± 1.74	16.48 ± 0.97	0.38 ± 0.06	0.1	17.25	6.89	6	2/3	3.97 ± 0.22
Canvas	Casual	1.23 ± 0.02	17.07 ± 0.41	31 ± 2.0	78.92 ± 0.26	27.35 ± 1.01	1.85 ± 0.02	-	29.40	7.25	-	-	2.69 ± 0.11

The psychometric scale (Likert rating) has represented in Fig. 2. where the results revealed that technical issues (e.g., green material) were less addressed by the consumer

https://doi.org/10.24264/icams-2022.V.1

on purchasing shoes. The perception of men and women are presented in an aggregated way in the bar diagram. The rating of products quality and cost has the topmost score of 4.5 ± 0.23 that's signified quality improvement and price down must be the challenging issue in case of material solicitation. Moreover, comfort has been rated undisputed parameter. It is clear from the box plot in Fig. 3 that a positive correlation existed between the choice of categories of footwear and the sustainability scale e.g., quality and cost, and durability.

Most of the data are concentrated on the 50% region in the case of dress (median 3.1) and boot (median 3.5) shoes. In addition, the Pearson coefficient for dress (Oxford), boot and casual footwear has been calculated and were 0.99152 (p-value 0.03644); 0.92188 (p-value 0.00891), 0.83979 (p-value 0.0166) respectively. So, the p-value was less than 0.05 ($p \leq 0.05$) observed is an indication of a strong relationship exists between the scale of sustainability and the consumer choice of different footwear styles during purchase and usage and the null hypothesis has been rejected.

CONCLUSION

The inquiry of sustainable properties of leather material with alternatives has been crystal clear to the manufacturer and the answer has been inherent with natural leather's internal geometric structure. The physicomechanical properties of leather are the ultimate proof of the most unique material indeed. The breathability property is the prime importance for footwear production which was measured by water vapor permeability. This property is absent in pleather. The psychometric test also signified that consumer perception of buying and using footwear is based on comfort, quality, durability, and cost. The manufacturer should have to consider materials physiognomy along with consumer perception to sustain a culture of selecting suitable materials for specific footwear to fulfill the aspiration of the sustainability of the sector.

REFERENCES

Bayes, T.J.W. *et al*. (2013), *Basic Shoemaking: A Step by Step Guide to Shoemaking*, SATRA Technology Centre Limited, Northamptonshire, ISBN 978-0-907924-20-3.

Dutta, S.S. (1990), *An Introduction to the Principle of Physical Testing of Leather*, Indian Leather Technologists' Association, Kolkata, ISBN 81-901423-0-5.

Goonetilleke, R.S. and Weerasinghe, T.W. (2011), "Getting to the Bottom of Footwear Customization", *Journal of Systems Science and Systems Engineering*, 20(3), 310-322, https://doi.org/10.1007/s11518-011-5171-0.

Hasan, M.N., Paul, T., Hasan, M.N. and Hashem, M.A. (2016), "Estimation of VOCs Emission from Different Adhesives Used in Shoe Manufacturing", *International Conference on Mechanical, Industrial and Energy Engineering*, 4, 1-4, https://www.researchgate.net/publication/354528841.

Rupérez M.J., Giner, C.E. and Monserrat, E. (2012), "Simulation of the Behavior of the Calfskin Used as Shoe Upper Material in Footwear CAD", *Computer-Aided Design*, 44(12), 1205-1216, https://doi.org/10.1016/j.cad.2012.06.009.

Ruperez, M.J., Monserrat, C. and Alcañíz, M. (2009), "A Study of the Viability of Obtaining a Generic Animation of the Foot while Walking for the Virtual Testing of Footwear Using Dorsal Pressure", *Journal of Biomechanics*, 42(13), 2040-2046, https://doi.org/10.1016/j.jbiomech.2009.06.054.

Soloman, B.B. (2021), "Leather Cutting Waste Minimization Techniques in Ethiopian Footwear Industry: Case Study ELICO - Universal Leather Products Industry", Research Square, Bahir Dar University, https://doi.org/10.21203/rs.3.rs-274284/v1.

Staikos, T. and Rahimifard, S. (2007), "A Decision-making Model for Waste Management in the Footwear Industry", *International Journal of Production Research*, 45(18-19), 4403-4422, https://doi.org/10.1080/00207540701450187.

Ujević, D., Kovačević, S., Wadsworth, L.C., Schwarz, I., and Šajatović, B.B. (2009), "Analysis of Artificial Leather with Textile Fabric on the Backside", *Journal of Textile and Apparel Technology and Management*, 6(2), 1-9, https://www.researchgate.net/publication/277112454.

*** (2011), ISO 3377-1:2011 Leather-Physical and Mechanical Tests-Determination of Tear Load—Part 1: Single Edge Tear, ISO: Geneva, Switzerland.

*** (2021), *World Footwear Yearbook* (https://www.worldfootwear.com/).

https://doi.org/10.24264/icams-2022.V.1

SHAPING THE RANGE OF FOOTWEAR IN DIFFERENT MATERIALS ACCORDING TO A PERSON'S PSYCHO-TYPE

MARYNA LESHCHYSHYN, ANTONINA BABYCH, VICTORIA KERNESH

Kyiv National University of Technologies and Design, Ukraine, marfiichuk@gmail.com, basienka@ukr.net, kievfoot@ukr.net

The article is to highlight and substantiate the results of marketing research, determine human psycho-types regarding the design of shoes, materials, heel shape and toe, so it is possible to: improve the range of manufacturers, predict the use of modern classic leather and textile materials, for the production of products of this segment; improving its quality; increasing demand for footwear from Ukrainian manufacturers and the percentage of finished goods. Marketing research was conducted with the help of respondents of the shoe store brand "Kachorovska", Kyiv (Ukraine), which helped to properly form the range of women's shoes according to the psycho-type and temperament of the buyer. These data helped to create a system that allows you to properly and efficiently shape the range of shoes and thus fully satisfy the buyer and achieve the desired percentage of sales. The article considers the state of the domestic footwear market and presents the results of marketing research of consumer preferences taking into account the human psycho-type during the formation of the range of women's shoes from different materials, and clarifies how its range meets the needs of the population. In this paper, a comparative analysis of the choice of shoe models of the appropriate human psycho-type for the formation of the range, which will reduce the number of unsold shoes at the end of the season. It was found out which models of shoes will be chosen by consumers with one or another psycho-type.

Keywords: leather and textile materials, footwear market, marketing research.

INTRODUCTION

Modern market relations require constant updating of the product offer, so first of all the urgent problem of production and release of new goods of modern designs and materials is relevant (Leshchyshyn *et al*., 2020; Slavinska *et al*., 2021). The range of a modern competitive shoe store should be represented by a variety of models, their designs, a diverse palette of colors and textures of classic and modern materials that will meet the requirements of the most demanding consumers (Anderson and Golden, 1987; Hu and Cheng, 2022; Slavinska, 2018).

It is logical that the range of products in the store should be formed in such a way as to satisfy the maximum number of requests, as each consumer – buyer has their own specific requirements and preferences, influenced by his natural psycho-type, temperament, lifestyle, field of activity, security level, etc. (Boeree, 2016).

The article considers the state of the domestic footwear market and presents the results of marketing research of consumer preferences taking into account the human psycho-type during the formation of the range of women's shoes from different materials, and clarifies how its range meets the needs of the population. The possibility of using different materials for shoe production is predicted for Kachorovska shoe store, Kyiv (Ukraine) and with the support of the brand during 2020-2021.

https://doi.org/10.24264/icams-2022.V.2

METHODOLOGY

Preliminary Research of Initial Data for Marketing Research and Processing of Results

The trade range is formed under the influence of the industry, as the capabilities of the manufacturer determine the composition of the offer. However, in a market economy, trade has a direct impact on the industrial assortment (Phelps, 2021). The trade is involved in market research, determination of purchasing power, in meetings of the artistic council. The trade makes proposals for optimizing and improving the assortment, focusing on demand, approving or rejecting certain models (Brauning, 2018).

Basic factor that affects the formation range products are consumer preferences. Classically, scientists study and evaluate the following criteria: price, material, product comfort, strength, lightness, design, color, and so on. Trade networks conduct active and regular work on their study. This is an important component of the marketing activities of any trading enterprise (Babych and Kernesh, 2019).

In practice, in most cases, the range of shoes presented in the store has a certain number of unsold products that remain in stock at the end of the season and not finding a consumer. According to previous studies, this figure reaches about 10-30%. According to preliminary studies, this figure reaches about 10-30%. Therefore, when forming the assortment of a particular brand, it is important to take into account not only fashion trends, but also the type, color spectrum and texture of the material, the shape of the toe and heel, as well as such factors as the psychotype and temperament of the buyer, which will reduce the number of unsold shoes at the end of the season.

In this paper we analyze the choice of footwear models according to the psychotype of a person. This will allow to form assortment, which will reduce the number of unsold shoes at the end of the season.

RESULTS AND DISCUSSION

Methods of Conducting Research

The Analysis of the Choice of Shoe Models of the Corresponding Human Psycho-Type is Compared

A person is born into society, has his own consciousness, communicates and interacts with other people and becomes a person. The fact that a person belongs to the human race is fixed in the concept of the individual. According to theoretical and analytical research, it was found that 55% of information transmitted by humans is perceived through visual signals – through its appearance; 38% of information is perceived through vocal signals – because of how a person uses his voice in communication (his tone, pronunciation, timbre, etc.) and only 7% of information perceived through verbal signals – through what a person says.

Thus, we can conclude that the largest percentage (38%) of people make their choices through external perception of the world in all its aspects.

The choice of shoes is clearly influenced by the psychological type, namely the type of human temperament. Classically, scientists have identified four main psychological types – sanguine, phlegmatic, choleric, melancholic.

https://doi.org/10.24264/icams-2022.V.2

Each of the well-known human psycho-types affects what choice the buyer will make. The practical application of this classification in marketing is quite complex. But still, having received information about a particular person, you can assess his temperament and the range of customers of the brand by this criterion, which will most successfully form a range of products and understand how to work with each customer.

To achieve a positive result in the research and work of a commercial enterprise should immediately take the initiative and offer the customer a certain model of choosing the appropriate product, for example, let the person make a choice independently and without haste, or push the buyer to the final choice by giving advice on the model. The type of temperament determines how quickly the customer will make a purchase and whether he will make it at all, what he will focus on when choosing it and more. All these factors also depend on a person's temperament.

In order for the results obtained during the marketing research to be considered reliable and to be applied to all people with significant variables, the sample must meet the requirements of representativeness (Garkavenko, 2002). The quantitative characteristic of the sample is its size, the people who participated in the research. (Kuleshova, 2021). The minimum number of respondents, on the basis of opinions and data of which it is possible to draw scientific conclusions – 20-30 people. But, of course, for this work, this is not enough. The number of respondents is calculated according to the well-known methodology according to formula (1):

$$n \geq \frac{\delta^2 z_{\frac{\alpha}{2}}^2}{d^2} \quad (1)$$

where, δ^2 is the variance of the population;
$z_{\frac{\alpha}{2}}$ - point of standard normal distribution;
d- trust integral.

Most often α= 0.06, then

$$z_{\frac{\alpha}{2}} = (1.96 * \delta)^{2/2} (d^2) \quad (2)$$

We need a probability of 0.95 to be in the range of the average $d \pm 0.02$. It is known that the amplitude of the visible value is 0.3, then $\delta = 0.3/3 = 0.1$. Based on the data obtained, we can calculate the optimal number of respondents.

$$n \geq \frac{(1.96*0.1)^2}{0.02^2} = 96 \quad (3)$$

So, after the calculations we get the required number of respondents, which is equal to 96 people.

Result

Research was held in the store of the trade brand "Kashorovska", Kyiv (Ukraine) for one month communication with customers. A total of 100 people were interviewed.

By analyzing the sales of the store for this period, the quantitative ratio of buyers was determined according to the psychotype of the person, the type of his temperament and the actual purchase in the researched period. Sociological research was conducted by various methods: experiment, observation, interview method, questionnaire.

Figure 1 shows the results of the study, namely the percentage of temperament types among buyers.

https://doi.org/10.24264/icams-2022.V.2

Figure 1. Percentage of temperament types among consumers

The results showed that there were the most sanguine people – 35%. These people are very energetic, passionate about ideas, easily make choices and know what they want. Phlegmatics who make informed decisions must think carefully about everything and cholerics – extremely inflammatory people who do not like to wait and are ready to do anything to get what they want, turned out to be equal, i.e., 25%. But melancholics – vulnerable, very unsure of their choice – 15%.

In the process of research and processing the results, the correlation between personality psychotype, preferences and temperament was determined. That is, the style of clothing, shoe design, color and texture of the material of things depends on the psychotype of a person. With the help of psychotype it is possible to determine almost all preferences of a person.

Based on the research, experimental scientists formed the assortment of shoes of this store. Footwear options of different designs and styles were selected for each of the psychotypes of a person and presented on separate shelves for the information of the client. Models were taken from the range of the "Kachorovska" store.

So, we can say that undoubtedly each person is unique and their clothes are just as different. It is impossible to develop one universal model of shoes or other product to suit a person with any psycho-type. Therefore, the most important thing is the competent formation and presentation of the range of shoes, in order to fully meet the needs of potential buyers with their own characteristics and psycho-type.

The results of the research correlate with the percentage of sales of finished goods (in the conditions of shoe store "Kachorovska", assortment 2020-2021) (Fig. 2).

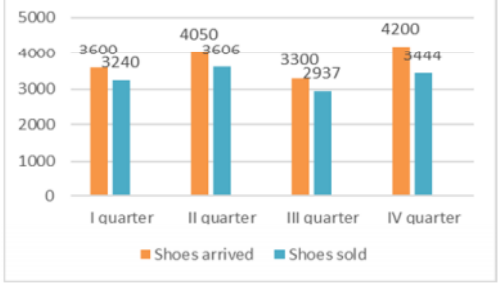

Figure 2. Analysis of the received goods and their sales for the quarter

Data are given quarterly:

- first quarter (January, February, March) – 3600 pairs of shoes were received, 3240 pairs were sold, the rest 360 pairs (10%);

https://doi.org/10.24264/icams-2022.V.2

- second quarter (April, May, June) – 4050 pairs of shoes were received, 3606 pairs were sold, the remaining 444 pairs (11%);
- the third quarter (July, August, September) – 3300 pairs of shoes arrived, 2937 pairs were sold, the remaining 363 pairs (11%);
- in the fourth quarter (October, November, December) – 4200 pairs of shoes arrived, 3444 pairs were sold, the rest of the pairs (18%);

Therefore, we can conclude that the percentage of sales of finished goods is within acceptable limits, as the balance in the warehouse averages 12.5% for the quarter. This means that assortment of the store in the process of scientific and practical research formed and placed on the shelves correctly, the shoe models developed for it meet the needs of people with different psychotypes and preferences. During the study, scientists have developed another interesting idea on the subject of the study, namely the consumer's reaction to a new product or information.

It is known that everyone has their own reaction to new information or the appearance of a new product on the market. The following groups of consumers are classically distinguished: "innovators" – consumers who risked trying a novelty; "Adepts" – followers who make the product fashionable and famous; "Progressives" – people who provide mass sales at the stage of product growth; "Skeptics" – are connected to demand at the stage of saturation; "Conservatives" – show demand when the product becomes "traditional".

After analyzing the range of footwear stores "Kachorovska" and the success of certain models, a diagram was formed, which shows the statistics of quantitative ratio of which shows the statistics of the quantitative correlation of the psychotype of buyers on specific cycles of the "life" of the product.

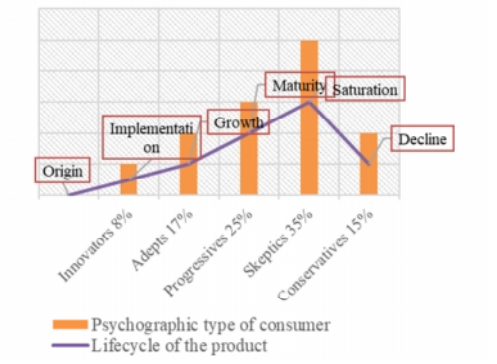

Figure 3. Product life cycle and groups of its consumers

Thus, each product has its own life cycle, which includes the following stages: origin, implementation, growth, maturity, saturation, decline. Each of these cycles has a certain group of consumers mentioned above. The diagram (Fig. 3) shows that some of the respondents will buy a new product at the implementation stage – its "innovators", "adepts" will buy the product in the active phase of its growth. These are people who follow trends and tell others about them. "Progressives" are buying in mass order that has crossed the line of maturity, that is, goods that are already familiar on store shelves and in the minds of consumers. "Skeptics" will be active at the saturation stage, and "conservatives" at the recession. From this, we can conclude that the range in the store should be constantly updated, it should be flexible to the needs of potential customers.

https://doi.org/10.24264/icams-2022.V.2

CONCLUSIONS

In this paper, a comparative analysis was made of the choice of shoe models according to the appropriate human psycho-type for the formation of the range, which will reduce the number of unsold shoes at the end of the season. It was found out which models of shoes will be chosen by consumers with one psycho-type or another. The modern assortment of footwear depending on a psycho-type of the person is formed. Specific constructions, colors, features of models for each psycho-type are given.

The reaction of consumers to the appearance of a new product, in this case – shoes, is analyzed.

The life cycle of a product and the consumer's reaction to it, which is active in one or another of its cycles, are compared. It is predicted in what quantity it will be appropriate to release a novelty of the season and place it on the store shelves for successful implementation.

Marketing research was conducted with the help of respondents (new customers and regular customers) of the shoe store brand "Kachorovska", Kyiv (Ukraine), which helped to properly form the range of women's shoes according to the psycho-type and temperament of the buyer. These data helped to create a system that allows you to properly and efficiently shape the range of shoes and thus fully satisfy the buyer and achieve the desired percentage of sales.

REFERENCES

Anderson, W.T. and Golden, L.L. (1987), "Lifestyle and Psychographics: A Critical Review and Recommendation", in T. Kinnear (ed.), *Advances in Consumer Research*, Ann Arbor, Michigan, Association for Consumer Research, XI, pp. 405-411.

Babych, A. and Kernesh, V. (2019), "Development of the Range of Women's Shoes Taking into Account Consumer Preferences" (in Ukrainian), *Bulletin of KhNU. Technical Sciences*, 1, pp. 77-81, https://doi.org/10.31891/2307-5732-2019-269-1-77-81.

Boeree, C.G. (2016), *Personality Theory: A Biosocial Approach*, Psychology Department, Shippensburg University, Accessed May 7. (http://webspace.ship.edu/cgboer/pttemp.html).

Brauning, M., Frick, J.E., Melnikov, J., Lubben, J., Keck, A. and Tchouboun, C. (2018), "Smart Solutions to Improve Wearing Comfort", *Journal of Fashion Technology & Textile Engineering*, 0(4), p. 2, https://doi.org/10.4172/2329-9568.S4-011.

Garkavenko, S. (2002), *Marketing* (in Ukrainian), Textbook, Libra, Kyiv, pp. 705.

Hu, M. and Cheng, Y. (2022), "Towards an Emotional Design of Apparel for Medical Professionals", *J Textile EngFashionTechnol*, 8(1), pp. 24-25, https://doi.org/10.15406/jteft.2022.08.00296.

Kuleshova, S. (2021), "Improvement of Methodology of Differentials" (in Ukrainian), *Fibers and Textiles*, 28(1), http://vat.ft.tul.cz/2021/1/VaT_2021_1_6.pdf.

Leshchyshyn, M., Garkavenko, S. and Babich, A. (2020), "Studying the Similarities of Deformation Properties of Leather Materials in the Process of Creating a Model of Shoes", *Proceedings of the 8th International Conference on Advanced Materials and Systems – ICAMS 2020*, pp. 83–88, https://doi.org/10.24264/icams-2020.I.10.

Phelps, N. (2021), "Ready-to-wear Dolce & Gabbana", VOGUE magazine, available at: https://www.vogue.com/fashion-shows/fall-2021-ready-to-wear/dolce-gabbana.

Slavinska, A., Syrotenko, O., Mytsa, V. and Dombrovska, O. (2021), "Evaluation of Color Harmony on the Scale of Psychological Perception in Families Look Clothes" (in Ukrainian), *Fibers and Textiles*, 28(3), pp. 82-93, available at: http://vat.ft.tul.cz/Archive/VaT_2021_3.html.

Slavinska, A., Zakharkevich, O., Kuleshova, S. and Syrotenko, O. (2018), "Development of a Technology of Interactive Design of Garments Using Add-ons of Virtual Mannequins", *Eastern-European Journal of Enterprise Technologies*, Engineering Technological System 6(1) (96), pp. 28-39, https://doi.org/10.15587/1729-4061.2018.148984.

USE OF CREATIVE METHODS AND UNTYPICAL MATERIALS IN THE DESIGN OF FASHION INDUSTRY PRODUCTS

MARYNA LESHCHYSHYN, ANTONINA BABYCH, VICTORIA KERNESH, POLINA BILOUS

Kyiv National University of Technologies and Design, Ukraine, marfiichuk@gmail.com, basienka@ukr.net, kievfoot@ukr.net, polbil@ukr.net

The article is to highlight and substantiate the results of scientific practical research, to prove in a theoretical and practical way the possibility of using upcycling technologies and non-typical used materials for the manufacture of modern designer functional and decorative and decorative (interior) products for the production of products of this segment, increasing the demand for products of Ukrainian designers. Innovative types of materials, manufacturing technologies and decoration of products of the fashion industry have been studied and analyzed. The question of the possibility of using used non-typical materials in the creation of modern collections of products of the fashion industry has been investigated. It was determined that the fashion industry in Ukraine is developing and being updated. This creative experiment made it possible to create an innovative niche for the designer's vision of the world of fashion and aesthetics, which leads to creative experiments, the introduction of innovative materials and technology into the process of manufacturing products. Such creative experiments are necessary to emphasize the peculiarity and individuality of the designer, as well as to reflect his innovation and style. A sketch project of eco-style products has been developed. A collection of interior products for decorating rooms made of paper vines has been produced. A collection of women's clothing decorated with accessories and shoes in an eco-style was developed and produced from used non-typical materials for this segment of products.

Keywords: material, design, upcycling technology.

FORMULATION OF THE PROBLEM

According to the definition of one of the famous design theorists, S. Khan-Magomedov (1995), design is «...a sphere of creativity related to socio-functional and aesthetic problems of the formation of the subject-spatial environment...; one of the important areas of style formation, which has a growing influence on general form-forming processes and historical concepts» (Khan-Magomedov, 1995). The basis of the profession of a designer of any profession is the problem of forming a creative personality, a unique style and worldview. It is these factors that condition and shape the spectrum of creative approaches to the study of specific issues of form formation and the practical use of methodological approaches and concepts regarding the search for a creative idea, the development of a creative source, and the solution of the given task according to the principle «from idea to finished product» (Vasilyeva, 2011).

Paper is usually used to make models of future products. With the help of a sheet of paper, the design features of the product are reproduced down to the smallest details and forms, and the technology of modular or node-based binding of parts or form elements to each other is developed into a product (Babich and Vasylieva, 2021; Bozhko, 1991).

Paper of various thicknesses and textures is a fertile material for creativity. With its help, it is easy to form and reproduce the external contour of a three-dimensional body, which in turn forms the potential of the structural elements of the product. With the help of paper models, you can achieve the desired fantasy or realistic shape, structure and functionality of the future product, by reproducing and working out in practice all possible variants of the system of folding and unfolding of the paper plane. Therefore, combinatorics and transformation of paper, in particular layout, is a visual method of creating a three-dimensional shape of a product. The world of product design of the

https://doi.org/10.24264/icams-2022.V.3

fashion industry, as well as fashion itself, is not yet sufficiently studied, diverse, unique, constantly new and innovative. Therefore, the task of this study is the analysis of non-typical materials, innovative manufacturing and decoration technologies for the purpose of their application in the design and manufacture of fashion industry products of various purposes and assortment.

ANALYSIS OF THE RECENT STUDIES

Theoretical and analytical studies of questions and problems of form formation and the use of innovations in the design of products of the fashion industry from the time of Ancient Egypt to the present day is an interesting and relevant topic that is still insufficiently studied and covered in the scientific literature (Elam, 2014).

The question of creating a form and its transformation into products of the fashion industry is based both on the analysis of research in periodical and scientific information sources, and on modern research of historical prototypes and modern developments in the design of products in the subject area.

The history of the development of products as a whole is part of the general history of culture and humanity and its material aspect. Research of this heritage as a whole, concretized in products can become a foundation for innovative future developments (Chuprina, 2011).

The analysis of previous theoretical studies of the use of innovations in the design of products in the fashion industry allowed the authors of this study to analyze and systematize the main areas of application of innovations in the design and technology of products, the use of materials, decoration of products and their elements, and allowed to obtain fundamentally new aesthetic and functional properties of materials and products, which opens up new opportunities for the development of the fashion industry.

The purpose of the work is the research and use of creative upcycling technologies and used non-typical materials for the production of modern designer functional and decorative and producing ornamental (interior) products.

PRESENTING MAIN MATERIAL

Due to the rapid change in living standards, the transformation of society and the transition to a new level of doing business, namely the production of goods and the provision of online services, as well as the struggle for the preservation of the eco system and the Earth as a whole, due to the rapid development of new technologies in the 21st century, more and more innovative design solutions, non-typical materials and technologies are appearing for the creation and manufacture of fashion industry products. Of course, these are not everyday things in use, but individual specimens that have a short podium or exhibition «life», but can take an honorable place in a museum, as a work of art and an example of the flight of designer's imagination.

Innovative proprietary technologies and non-standard vision of the designer make it possible not only to use various new and used materials but also to produce a product of the form and purpose that the designer intended (Torebaev and Myrkhalykov, 2014; Guseva *et al*., 2016).

They can be both functional and interior. The more unique and unusual the shape and material of the product, the more chances that this particular product will be competitive in society.

https://doi.org/10.24264/icams-2022.V.3

For any person of different eras, it is of great importance to create a comfortable and aesthetic space around oneself, to surround oneself with beautiful things, to decorate clothes, shoes, accessories and one's own home with interesting decorative elements, etc (Shcherban *et al*., 2018). One of the elements that helps a person turn bold ideas into reality and at the same time be on the «wave» of fashion is the use of classic and creative non-typical materials for the manufacture of products, taking into account the color and texture of the surface and elements of the product decoration.

All the conducted theoretical and analytical studies by direction led to the need to conduct experimental studies with the aim of studying the features and requirements for specific classical and non-typical materials at the stage of product design development and technological stages of materials preparation for the production of a certain fashionable product of the fashion industry, with the aim of making a modern ecological and a competitive product (Angelova *et al*., 2017).

In the process of research, it was found that almost any material, new or used, can be used in this industry, the main thing is to know how and in what way to work with it correctly. Since the issues of environmental protection and waste reduction are urgent issues, it was decided to move in this direction and explore the possibility of using used materials as the main ones for creating modern design products.

Today, products made of paper vines are popular (Fig. 1), so paper is the basis of paper vines. Designers of various branches actively use this material to create masterpieces of their time (Babich *et al*., 2020).

Figure 1. Visualization of design ideas of fashion industry products from different materials

Origami is a classic method of working with paper to create product forms. The purpose of this art is to create products by using a pattern of geometric folds. We, teachers, try to use this technique as part of a scientific circle for students studying in the specialty 182 – Technologies of light industry, the educational program «Fashion Industry» in practice for the development of creative potential, technical skills of working with form and material, and an aesthetic view (Babich *et al*., 2021). Such classes give a young person the opportunity to transfer their ideas and dreams to paper and later to any other material and create a perfect, functional and aesthetically attractive product or collection of products from the fashion industry and bring them closer to the concept of industrial design.

After researching this issue, it was found that modern people use gadgets every day to obtain information, but there are still a sufficient number of people in the world who

https://doi.org/10.24264/icams-2022.V.3

use newspapers and magazines to obtain certain information, which they simply throw away after reading. Having analyzed the amount of printing products thrown away by consumers every day, we became convinced of the need to use these materials to create modern design products in an eco-style from them without spending money and prove the feasibility of this project. For this, a group of researchers collected a certain number of discarded newspapers, developed a design project, sketches, selected interesting technologies for the manufacture of products, and began work on their creation.

At the design stage, the developers decided that the products would be both interior and functional. Therefore, the following technological approaches were used:

- - weaving products from paper vines (making baskets, toys, New Year's decorations, shoes);
- - technology of modular assembly of product elements (making a dress);
- - paper origami (making accessories).

The visualization of the design ideas of the talented student Polina Bilous is presented in the form of sketches and finished products made in various techniques, but from the same material, namely from recycled materials – used newspapers (Fig. 2-5).

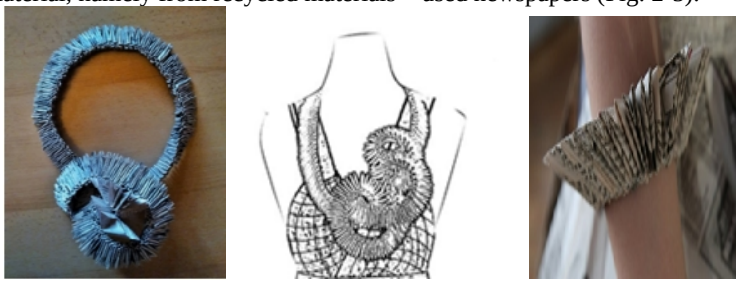

a) b) c)

Figure 2. Visualization of the design idea of the manufacture of accessories using the «origami» technique (the author's collection of «origami» by student Bilous P. was presented at an international competition «Chestnut Constellation», Kyiv): b) – sketches; a), c) – finished product (necklace, armband)

a) b)

Figure 3. Visualization of the design idea of shoe manufacturing: a) – sketches; b) – finished product

This technology for making competitive paper products can be implemented in the conditions of any creative fashion laboratory without re-equipment. The process does not require additional resources, investments and equipment. The economic feasibility of this

https://doi.org/10.24264/icams-2022.V.3

development consists in reducing the amount of waste and making exclusive interior and functional design products from them with their further implementation, as well as catwalk collections of products and accessories. At the moment, product samples have been produced, which take part in the international contests «Chestnut Constellation» and «Cave Chestnuts» (Ukraine, Kyiv). We are expanding scientific and creative horizons, and the presented collections of eco-style products will spread across the planet, finding their fans.

This project can be interesting as a way to create your own business for people with disabilities. Interior and collectible products have consumer demand and can be sold through online stores or design boutiques of decor and exclusive collectibles.

a) b) c)

Figure 4. Visualization of the finished set of products, the design of the idea of women's clothing on the model (the author's collection «Breath» of student Bilous P. was presented at an international competition «Cave Chestnuts – 2021», Kyiv): a – visualization of the costume on the model; b – sketches; c – finished product.

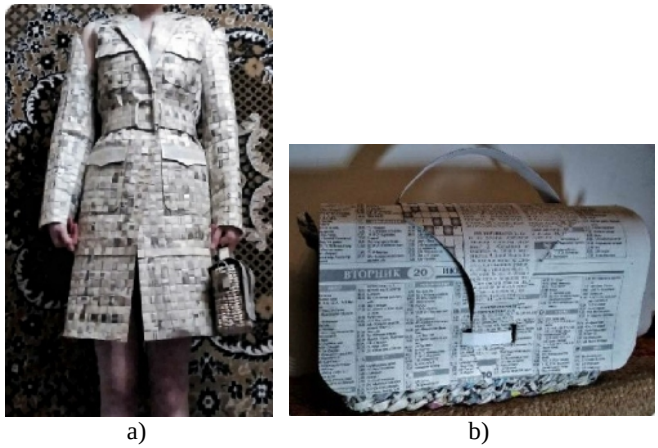

a) b)

Figure 5. Visualization of the finished set of products, the design idea of the female image on the model (author's collection «Emancipe», student Bilous P. prepared for participation in an international competition «Cave Chestnuts – 2022», Kyiv): a) – visualization of a coat and a bag on a model; b) – accessories (handbags)

https://doi.org/10.24264/icams-2022.V.3

CONCLUSIONS

The article researches and analyzes innovative types of materials, manufacturing technologies and decoration of products of the fashion industry. The question of the possibility of using used materials in the creation of modern collections of products of the fashion industry has been investigated. The issue of eco-design in products of the fashion industry has been theoretically studied and analyzed.

Collections of catwalk products in eco-style (clothes, shoes, accessories) and samples of interior products made of paper vines were developed and produced. The feasibility of this development has been proven theoretically.

The possibility of integrating innovations in the manufacture and decoration of products was demonstrated on the example of the student author's works of Bilous Polina under the guidance of experienced scientists-designers of the department of KTVSH (KNUTD). We consider this scientific project to be relevant in our time, because due to the use of innovative approaches and the embodiment of bold thoughts in catwalk collections, it contributes to the development and design thinking of a student, a young designer-beginner, the development of new constructive techniques by designers, the creation of modern technologies in the fashion industry, it provides an opportunity to diversify artistic and constructive-technological solution and expressiveness of the product.

REFERENCES

Angelova, Y., Mežinska, S., Lazov, L. (2017), "Innovative Laser Technology in Textile Industry: Marking and Engraving", *Proceedings of the 11th International Scientific and Practical Conference*, Vol. III, pp. 15–21, https://doi.org/10.17770/etr2017vol3.2610.

Babich, A.I. *et al*. (2020), "Development of a Collection of Eco-style Women's Shoes from Second-Hand Items", *Bulletin of the Khmelnytskyi National University*, № 3 (285): Series «Technical Sciences», pp. 198-203, Khmelnytskyi.

Babich, A.I., Kernesh, V., Belous, P. (2021), "Innovations in the Design of Products of the Fashion Industry, Non-typical Materials and Technologies for Their Manufacture", *Bulletin of the Khmelnytskyi National University*, № 6 (303): Series «Technical Sciences», pp. 229-235, Khmelnytskyi, https://doi.org/10.31891/2307-5732-2021-303-6-229-234.

Babich, A.I. and Vasylieva, N.S. (2021), "Forming an Assortment of Women's Bags with Elements of Transformation Based on Marketing Research", *Fashion Industry*, № 3, pp. 36-47, Kyiv.

Bozhko, Y.G. (1991), "Architectonics and Combinatorics of Form Formation: учеб. For Arts and Industry Universities and Architects Faculty" [text], Higher School, pp. 244, Kyiv.

Chuprina, N.V. (2011), "Combinatorial Shaping in Clothing: Primary Elements and Methods of Their", Collection «Technology and design», № 1, pp. 1-7, Kyiv.

Elam, K., (2014), *Geometry of Design. Proportions and Composition* [text], p. 108, St. Petersburg.

Guseva, M.A., Andreeva, E., Penrosova, I. (2016), "Innovative Finishing Technologies in the Traditional Assortment of Fur Products" [Electronic resource], Universum: Technical Sciences: Electronic, № 7 (28).

Khan-Magomedov, S. (1995), *Pioneers of Soviet Design*, Galart, p. 423, Moscow.

Shcherban, L.O. *et al*. (2018), "Innovative Technologies of Modern Clothing Design" [Electronic resource], *Technologies and Design*, № 1 (26), available at: http://nbuv.gov.ua/UJRN/td_2018_1_2.

Torebaev, B.P. and Myrkhalykov, Zh.U. (2014), "Innovative Technologies in the Design of Textiles and Clothing", *Innovative Technologies in Textile and Light Industry: Materials of Reports of the International Scientific and Technical Conference* (November 26–27, 2014, UO «VGTU»), T. 2: Design and Production of Clothes and Shoes, pp. 236–237, Vitebsk.

Vasilyeva, T.S. (2011), "Influence of New Technologies on Shape Formation in Clothing Design", Abstract of the dissertation. To apply for a candidate's degree of art criticism 17.00.06, «Technical Aesthetics and Design», p. 38, Moscow.

https://doi.org/10.24264/icams-2022.V.3

CASE STUDY – BASEMENT OF THE NATIONAL MUSEUM OF COTROCENI

LUCREȚIA MIU[1], IOANA LIDIA ILEA[2], RODICA ROXANA CONSTANTINESCU[1], MADALINA IGNAT[1], NICOLAE CATRINA[3], MARCEL IONESCU[4], DOINA CREANGĂ[5], EMANUEL VĂCĂLIE[1]

[1]*The National Research & Development Institute for Textiles and Leather - Leather and Footwear Research Institute Division, Bucharest, Romania, rodica.roxana@yahoo.com*

[2]*Cotroceni National Museum, 1 Geniului Blvd., Bucharest, Romania, ioana.ilea@muzeulcotroceni.ro*

[3]*SC RESTAURO CONCEPT S.R.L., Romania*

[4]*SC EUROPLASTIC S.R.L., Romania*

[5]*Bucovina National Museum, Romania*

The work presents a series of aspects related to the degree of biodeterioration of some heritage objects made of inorganic substrates (brick), and the identification of fungi and bacteria with a damaging action on historical materials. Inorganic substrates represented by dust particles from walls and bricks were studied. Fired clay bricks can be severely affected by various macroscopic forms of degradation, as a consequence of chemical, physical-mechanical and biological degradation processes as a result of exposure to aggressive environmental agents. The samples studied (they were collected in compliance with conservation-restoration norms) are part of the "Small Cellar" of the Cotroceni Palace, one of the few spaces where the walls of the old foundation built by Șerban Cantacuzino between 1679-1681, are still preserved. By monitoring the microclimate parameters of the "small cellar" space, it was concluded that there is a greater variation of the relative humidity from 40% to 63%, but also of the temperature from 16℃ to 22℃, fluctuations due to the change of seasons. The samples taken, developed on the culture medium and isolated were analyzed from the point of view of microbiota, and the identified fungi mainly belong to the genera *Mucor* sp., *Alternaria* sp., *Rhizopus* sp., *Fusarium* sp. and *Penicillium* sp. Three different treatments, Clic, Q and Top Crete, were tested and applied on the wall by brushing. After 7 days, samples were collected and tested regarding microbial loading and the results are a proof of the treatment efficiency. The samples were further monitored from a microbiological point of view, but also from the point of view of the appearance given to the bricks after treatment (color change, brick texture, organoleptic properties, etc.).

Keywords: brick, biodeterioration, fungi and bacteria

INTRODUCTION

Heritage goods of an inorganic nature (stone, brick, marble, concrete, etc.) are subject to attack by autotrophic microorganisms (chemosynthesizing and even photosynthesizing). Humidity is a particularly important factor in the biodegradation process, on the one hand, and in the conservation of heritage assets, on the other hand (Johansson *et al*., 2020). When we talk about humidity, we refer to the relative humidity of the air, but also to the humidity of the substrate; the latter depends a lot on the hygroscopicity of the materials, which is why water content varies. Relative humidity is always associated with temperature (Balksten *et al*., 2021), these physical factors are particularly important in understanding biodegradation processes.

Bacteria and fungi spread in nature through spores; they resist the action of extreme environmental factors thanks to special resistance structures; under certain conditions they can enter a state of anabiosis (having minimized metabolic processes). Bacteria and fungi spores are transported by air currents along with various impurities of an inorganic or organic nature (dead particulate organic substances).

https://doi.org/10.24264/icams-2022.V.4

Determination of mycobiota diversity: in order to determine mycobiota diversity, the samples taken and isolated were analyzed macroscopically and microscopically to identify specific characteristics. The presence of fungi on inorganic substrates is determined by microclimate conditions.

SHORT DESCRIPTION OF THE SPACE

The space where the tests were carried out is part of the Cotroceni Ensemble, a historical monument of category A, (according to LMI List – Cotroceni Palace – Presidential Administration LMI Code: B-II-a-A-19152), being known as the "Small Cellar", actually one of the few spaces where the walls of the old foundation of Șerban Cantacuzino are still preserved, built between 1679-1681 under the careful supervision of the ruler and entrusted for execution to his brother, Mihai Cantacuzino. This included the Orthodox rite church, the princely houses, the abbot's houses, the monks' cells and other annexes surrounded by an enclosure whose walls gave the whole the appearance of a real fortress. As a result of some calamities such as: fires and earthquakes, damages caused by the establishment of armies in the immediate vicinity or the transformations that occurred according to the taste of the rulers who lived in Cotroceni, the monumental complex has undergone radical changes and a major expansion over time. The descriptions from the chronicles made by foreign travelers, the information from the documents of the Cotroceni monastery and above all, the discoveries of a more recent date caused by the extensive restoration works carried out after the earthquake of 1977, allowed the recomposition of the major data of the Cotroceni architectural ensemble. The area that now houses the Cotroceni National Museum includes two groups of medieval spaces, located on the ground floor and basement, which have maintained their original constructive integrity: the kitchen, the dining room, the cells, the cellars of the princely houses and this cellar which probably belonged to the abbey (Ciho *et al*., 1993). The "small" cellar is located on the north side towards the large kitchen and has an area of 92 m^2. It consists of bays covered with semi-cylindrical vaults with three transverse arches. The walls facing the inner court have four niches above which are as many windows finished in broken arches, unlike those on the opposite side, which end in arches. The entrance to the cellar is through a smaller room, located at a higher level and whose ceiling is semi-cylindrical with broken arches (Ipate *et al*., 2011).

Currently, the "small cellar" houses elements from the lapidary of the Cotroceni National Museum, and it is also here that they want to lay the foundations of a documentation center for decorative arts. Being a space located below ground level and probably due to the concurrence of several factors such as: the age of the preserved elements of the old load-bearing masonry building made of brick with mortar and the fluctuations of humidity and temperature between seasons, degradations have appeared, somewhat specific to these types of rooms. The main types of damage noticed by visual examination (Balksten *et al*., 2021) consist of multiple areas and surfaces with chromatic changes consisting of white and gray spots, efflorescence, exfoliation of the layer covering the brick, degradation of this layer and of the brick itself to pulverization, probably due to the capillarity phenomenon, to atmospheric humidity or even to a potential biological attack; degradations of a physical nature: spalling, separation of layers from the surface, erosion and some mechanical damage at the plinth level.

https://doi.org/10.24264/icams-2022.V.4

Pre-industrial fired clay bricks were manufactured using a manual technology, involving variable firing temperatures and therefore a great heterogeneity of the final material (Franzoni *et al*., 2013). In particular, ancient fired clay bricks are characterized by variable open porosity, ranging from a few percent (for over-fired pieces) to about 45–50 %. Such high porosity makes bricks vulnerable to the same physical-mechanical degradation processes that affect natural stone, such as freeze-thaw cycles, crystallization of soluble salts (efflorescence and sub-efflorescence) and biological growth, mainly due to the presence of moisture in pores and salts.

Although there is a permanent interest for constant monitoring of microclimate parameters and two DH9 dehumidifiers are used, fluctuations in temperature and relative humidity between seasons are noted. Following the recordings made with a TROTEC BC05 thermohygrometer, we observe for the month of February this year an average temperature of 21.3°C and relative humidity of 40.1%, in April an average temperature of 16°C and RH of 50.6%, and in July an average temperature of 22.4°C and an average RH of 63.4%.

EXPERIMENTAL PART

Materials and Methods

1. Preliminary findings regarding the affected areas for sampling (Figure 1):
   - Whitish dust
   - Spots of different colors
   - Brown-black dots of various small sizes, very dense
   - Cracks with material separation

 a

https://doi.org/10.24264/icams-2022.V.4


b
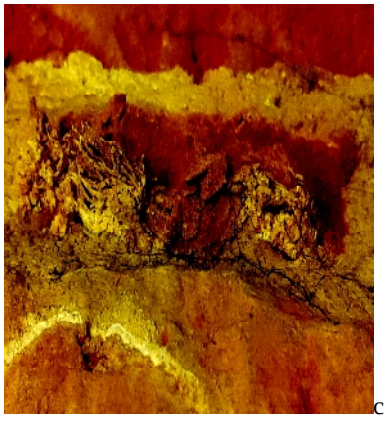
c

Figure 1. The small cellar - The Cotroceni Ensemble (a), deterioration details (b, c)

2. Working methods for determining the microbial load

Sampling method: the fingerprint method, used especially for collecting samples from heritage objects of high value. Another method used is that of sampling from different media. The samples obtained from the museum objects are small in size and were taken in compliance with the norms and principles of conservation (Franzoni *et al*., 2013; Vučetić *et al*., 2014).

The culture medium used was Sabouraud dextrose agar, and the plates were incubated for 5-7 days at temperatures of 20-25°C. In order to determine the diversity of the mycobiota, the samples taken and isolated were analyzed macroscopically and microscopically to identify specific characters.

RESULTS AND DISCUSSIONS

In the case of all types of substrates, a considerable fungal load was found, expressed in the number of colonies developed on the culture medium after sampling (Table 1).

Table 1. Microbiological characterisation

Macroscopic images	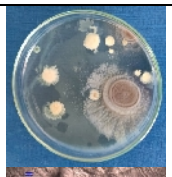	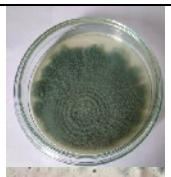	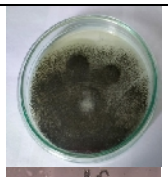	
Microscopic images Steromicroscop Leica, x50	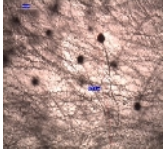		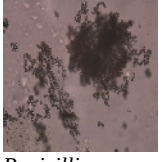	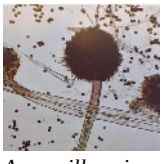
Description	*Mucor* sp. *Alternaria* sp.	*Aspergillus fumigatus*	*Penicillium* sp. *Aspergillus niger*	*Aspergillus niger*

https://doi.org/10.24264/icams-2022.V.4

The presence of fungi on inorganic supports is determined by the microclimate conditions. The identified fungi mainly belong to the genera *Mucor* sp., *Alternaria* sp., *Rhizopus* sp., *Fusarium* sp., *Penicillium* sp. Among the frequently encountered genera, *Alternaria* stands out, which is considered a cosmopolitan genus. The species of the genera *Fusarium* and *Penicillium* can develop in the presence of a water content of 6-10% of the substrate up to the relative humidity of 62-65%. The presence of fungi increases the retention capacity of dust particles, associating with the substrate and providing new nutrient resources for fungi.

Three different treatments were tested and applied on the wall by brushing (Table 2).

Table 2. Characterisation in terms of treatments applied

No.	Treatments		
	CLIC Sodium dichloroisocyanurate	Q Solution based on ammonium salts	Top Crete A+B Composition based on polyurethanes
1. Images of treatment application on the brick			
2. Images of Petri plates after 5-7 days from treatment application	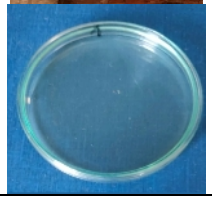	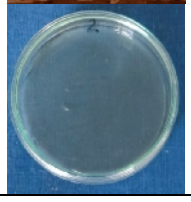	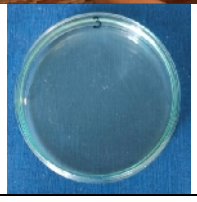

After 7 days, samples were collected and tested regarding microbial loading and the results are a prove of the treatment efficiency. Petri plates images shows no growth of microorganisms.

CONCLUSION

Application of the methodologies proposed in our study for the evaluation of cultural heritage concrete wall is a useful tool for obtaining analytical results that reflect the composition of the entire object.

The results show the isolation and identification of microorganisms involved in the biodeterioration of the concrete wall.

The treatments were monitored at 7 days, 21 days and 1 month and will be under observation for 6 months, 1 year, 2 years, etc., to check the biological effectiveness and the changes that may occur on the treated bricks. Depending on the results obtained, the optimal treatments will be selected or their optimization will be carried out.

https://doi.org/10.24264/icams-2022.V.4

Acknowledgement

This work was supported by a grant of the Romanian Ministry of Research, Innovation and Digitization, UEFISCDI, project number PN-III-P3- 3.5-EUK-2019-0196) / no. 253 of 10/08/2021.

REFERENCES

Balksten, K. and Strandberg-de Bruijn, P. (2021), "Understanding Deterioration due to Salt and Ice Crystallization in Scandinavian Massive Brick Masonry", *Heritage*, 4, 349–370, https://doi.org/10.3390/heritage4010022.

Ciho, B., Constantin, M., Fotescu, D., Lupu, G., Opriș, I., Orășanu, A.M., Pupeza, M. and Vlădescu, N. (1993), *The Cotroceni National Museum* (in Romanian), Redacția Publicațiilor pentru Străinătate, Bucharest, pp. 22-23.

Franzoni, E., Pigino, B., Leemann, A. and Lura, P. (2013), "Use of TEOS for Fired-Clay Bricks Consolidation", *Materials and Structures*, 47, 1175-1184, https://doi.org/10.1617/s11527-013-0120-7.

Ipate, M. (2011), "The Cotroceni Palace, Foundation of the Ruler Șerban Cantacuzino", in *National History Colloquium, History of Decorative and Conservation-Restoration Art*, Cotroceni National Museum, Bucharest, p. 56.

Johansson, P. and Wahlgren P. (2020), "Deterioration in Brick Buildings: Hygrothermal Performance and Measures to Save Them", *E3S Web of Conferences*, 172, 23005, https://doi.org/10.1051/e3sconf/202017223005.

Vučetić, S.B., Rudić, O.Lj., Markov, S.L., Bera, O.J., Vidaković, A.M., Skapin, A.S. and Ranogajec, G.J. (2014), "Antifungal Efficiency Assessment of the TiO_2 Coating on Façade Paints", *Environmental Science and Pollution Research*, 21, 11228-11237, https://doi.org/10.1007/s11356-014-3066-6.

MATERIALS FOR SURFACE DESIGN AND FINISHING FOR CONTEMPORARY FOOTWEAR – PART 1

OLGA NICULESCU, ELENA BADEA, ILARIA QUARATESI,
RODICA ROXANA CONSTANTINESCU, DANA GURAU

The National Research & Development Institute for Textiles and Leather - Leather and Footwear Research Institute Division, 93 Ion Minulescu, Bucharest, Romania, email: icpi@icpi.ro

The leather industry creates a product that is both natural and long lasting. Leather is unique in its ability to combine beauty, comfort and practicality. Finishing, the last operation in natural leather processing, determines the appearance and value of the finished product, and has the purpose of embellishment, providing lustre and pleasant feel, covering flaws and forming a surface layer that protects leather during wear while improving resistance to external factors. The quality of the pigment pastes used in the composition of the leather surface finishing films influences some of the physical-mechanical, technological and aesthetic properties of the finished products. The materials for finishing – pigment pastes with aesthetic effect – were obtained based on dioxide-titanium, metal pigment-aluminum, polymeric binder, lauryl alcohol ethoxylated with 7 moles of ethylene oxide, waxes and plasticizers and were characterized by physical-chemical, microscopical, spectral and rheological analyses. Pigment pastes with metallic effect were used in combination with film forming acrylic and polyurethane polymers, with high resistance to light and aging for finishing natural leathers, with applications in creative industries (modern footwear).

Keywords: natural leather, pigment pastes, surface design, creative industries

INTRODUCTION

The leather industry creates a product that is both natural and long lasting. Leather is unique in its ability to combine beauty, comfort and practicality. Well-made leather lasts a long time and unlike most man-made or synthetic materials it gets better with age, acquiring a depth of patina and wear pattern that is individual to the user. Investing in quality leather products is investing for the future.

Finishing, the last operation in natural leather processing, determines the appearance and value of finished product, and has the purpose of embellishment, providing lustre and pleasant feel, covering flaws and forming a surface layer that protects leather during wear while improving resistance to external factors (Lange, 1982; Heidemann, 1994). Pigments used in leather finishing must have certain characteristics, among which the most important are: fastness to light, resistance to weathering and high temperatures, high coating power, high dispersion degree, compatibility with the other components of coating dyes (Chiriţă and Chiriţă, 1999).

In leather finishing operations there are restrictions regarding the use of heavy metals, ethoxylated alkylphenols, formaldehyde and other toxic crosslinking agents in pigment pastes (ETAD, 2004; SG, 2006; Directive 2010/75/EU).

Ecological and Toxicological Association of Dyes and Organic Pigment Manufactures (ETAD) has set limits for heavy metal content in water-soluble dyes (for copper the permissible limit is 250 ppm). SG, "The Test Mark for Low Pollutant Leather Products", includes the limits for heavy metal content in leather products (for copper the permissible limit is 60.0 ppm). Environmental and toxicity concerns have led to new alternatives for finishing ancillary industry (Niculescu *et al*., 2015a; Niculescu *et al*., 2015b; Niculescu and Manta, 2019).

In the fashion industry the added value is only reflected by an efficient surface design, but the Surface Design is not just a type of finish, it is an art-science act that, if

https://doi.org/10.24264/icams-2022.V.5

well-known and coordinated, can be spectacular and sustainable at the same time (Pop *et al*., 2019).

Pigments are organic or inorganic chemical compounds which constitute the dye base for coatings. In order to obtain special finishing effects, when preparing pigment pastes, certain filling substances can be used (graphite, metallic aluminum powders for silver effects, or copper alloys for golden effects) (US Patent, 2005; EP Patent, 2014; Niculescu, 2022). Finishes with special effects are applied to leather to improve the organoleptic and aesthetic properties, related to fashion, such as: metallic, bicolor, antique, printed, pressed, waxed, etc.

Recipes are proposed to obtain stable pastes with aqueous dispersion medium using the components: dioxide-titanium white, acrylic resin as dispersion medium for pigments, light and ageing resistant vegetable oils as plasticizers (poppy seed oil), natural and artificial wax emulsions (beeswax, lanolin and stearin, the last obtained by splitting of natural fats), completely biodegradable non-ionic emulsifier – lauryl alcohol ethoxylated with 7 moles of ethylene oxide – as dispersing agent, metal pigment-aluminum for silver effects, and bronze powder for golden effects. Pigment pastes were used in combination with film forming polymers (acrylic and polyurethane) with resistance to light and aging for finishing natural leather for shoes (especially for women), with applications in creative industries.

EXPERIMENTAL

Materials

- Metal Pigment-Aluminum for silver effect (Messerini SRL, Italy).
- Bronze Powder-Rich Gold for golden effect (Messerini SRL, Italy).
- Dioxide-titanium white (Europlastic SRL, Bucharest).
- Acrylic binder Bindex Brillant (Pebeo, France), homogenous emulsion, dry substance – 30,24 %, density – 1.965 g/cm^3, pH – 6.5, Hoppler viscosity – 4.000 cP.
- Poppy oil (Pebeo, France), total fatty matters – 99%, Ford cup viscosity Φ 6 – 23 s, saponification index – 290 mg KOH/g, acidity index – 3 mg KOH/g, iodine index – 138g 100/g oil.
- Castor oil (SC Happynatura SRL, Bucharest), total fats – 64%, Ford cup viscosity Φ 6 – 57 s, saponification index – 14 mg KOH/g, acidity index– 9 mg KOH/g, iodine index – 92g 100/g oil.
- Nonionic emulsifier – lauryl alcohol ethoxylated with 7 mols ethylene oxide (SC Elton Corporation SA, Bucharest), density at 40°C – 0.950 g/cm^3, pH (10%) solution – 7-8.
- Wax emulsion AGE 7 (ICPI), dry substance – 12%, pH (10% solution) – 7.0.
- Pigment pastes (PPS with silver effect and PPG with golden effect), viscous and homogenous fluid, dry substance – 30-35%, pH (10% solution) – 7.0-8.0, ash – 25-30%.
- Finishing auxiliaries from Triderma, Germany (Triderma, 2020).

Methods

Attenuated Total Reflectance Fourier transform infrared spectroscopy (ATR-FTIR) measurements were run with a Jasco instrument (model 4200), in the following conditions: wavenumber range – 600-4000 cm^{-1}; data pitch – 0.964233 cm^{-1}; data points – 3610: aperture setting – 7.1 mm; scanning speed – 2 mm/s; number of scans – 30; resolution – 4 cm^{-1}.

https://doi.org/10.24264/icams-2022.V.5

Optical microscopy images were captured using a Leica stereomicroscope S8AP0 model with optic fiber cold light source, L2, with three levels of intensity, and magnification 20X and 100X.

Rheological behaviour was determined using Haake VT 550 rotational viscometer, equipped with MV1 sensor system for average viscosities and RheoWin Thermo Fischer software.

RESULTS AND DISCUSSION

Obtaining Pigment Pastes

The pigment pastes with special effect based on dioxide-titanium white and metal pigment-aluminum, for silver effect (PPS), or bronze powder, for golden effect (PPG), were obtained by means of the following operations:

- mixing powder pigment with vegetable oil emulsion (poppy seed oil) and non-ionic emulsifier;
  - 15-20% dioxide-titanium white, 10% metal pigment-aluminum or 10% bronze powder, 8-10% vegetable oil emulsified with 0.8-1.0% non-ionic emulsifier – polyehtoxylated lauryl alcohol (reported to the amount of oil);
- mixing the intermediate product with the acrylic binder (Bindex Acrylic), AGE 7 wax emulsion (made from beeswax, lanolin and triethanolamine monostearate), lauryl alcohol ethoxylate with 7 moles of ethylene oxide and water;
- 35-40% acrylic resin in which the pigment is dispersed, 1-2% wax emulsion, 8-10% fully biodegradable non-ionic emulsifier and water;
- The disperse system is subjected to mechanical stirring (60-80 rpm), at 25-30°C, for 3-4 h.

The composition of new pigment pastes is given in Table 1.

Table 1. The composition of new pigment pastes (PPS, PPG and M1, M2)

New pigment paste composition	Quantity (%) - PPS	Quantity (%) - PPG	Quantity (%) - M1	Quantity (%) - M2
Dioxide-titanium white	15-20	15-20	15-20	15-20
Metal pigment-aluminum	10	-	10	-
Bronze powder	-	10	-	10
Polyacrylic binder	35-40	35-40	35-40	35-40
Ethoxylated lauric alcohol	8-10	8-10	8-10	8-10
Poppy oil	8-10	8-10	-	-
Castor oil	-	-	8-10	8-10
Wax emulsion	1-2	1-2	1-2	1-2
Water	8-23	8-23	8-23	8-23

Obtaining the Finishing Film on Glass Plate

Finishing compositions were prepared containing: 100 g/L pigment pastes (PPS or PPG); 30 g/L wax emulsion (AGE 7); 300 g/L acrylic binder (AC87); 570 g/L water. With these dispersions, finishing films were obtained by deposition on glass plate and air drying.

Characterization of Pigment Pastes by Physical-Chemical Analyses

Physical-chemical characteristics are presented in Table 2.

https://doi.org/10.24264/icams-2022.V.5

Table 2. Physical-chemical characteristics of pigment pastes

Characteristics/ samples	Pigment paste (PPS)	Pigment paste (PPG)
Dry substance, %	32.48-34.65	31.88-34.16
pH 10% solution	7.0-8.0	7.0-8.0
Ash, %	25.67-27.45	27.35-29.24

The pigment pastes (PPS, PPG) are viscous and homogeneous fluids and dry substance content indicates that they are concentrated pastes.

Analysis of Pigment Pastes by Optical Microscopy

Table 3 illustrates optical images of metal pigment-aluminum and bronze powder.

Table 3. Optical images at 40X and 100X of the particle sizes of pigment powders (µm)

Particles of metal pigment-aluminum (40X)	Particle sizes of metal pigment-aluminum (100X): 9.0; 25.3; 32.7	Particles of bronze powder (40X)	Particle sizes of bronze powder 100X): 8.9; 17.2; 40.1; 42.8
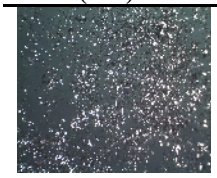	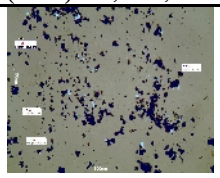	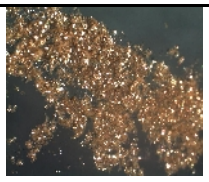	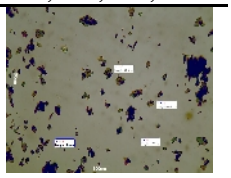

Images indicate an acircular geometry of particles, with agglomerate sizes ranging between 8.9 and 42.8 µm for the initial powder.

Characterization of Pigment Pastes by FT-IR

The new pigment pastes, dried on the glass plate, were analyzed by ATR-FTIR and spectra are shown in Figure 1.

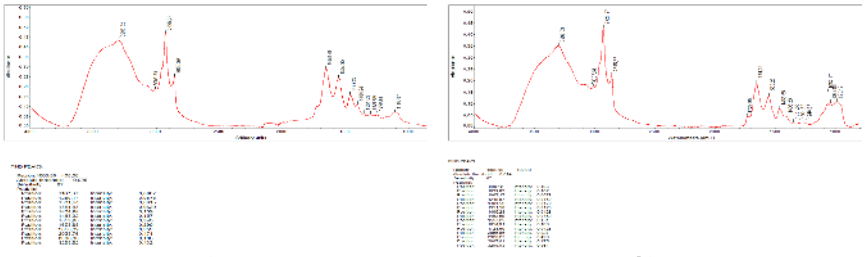

a) b)

Figure 1. ATR-FTIR spectra for pigment pastes PPS (a) and PPG (b)

The spectra of films obtained from the pigment pastes show characteristic bands of acrylic polymers: between 2925 and 2855, 1552 and 1463 cm^{-1} assigned to asymmetric and symmetric stretching and deformation vibrations of CH_3 and CH_2 groups, an intense

https://doi.org/10.24264/icams-2022.V.5

band at ≈ 1653 cm^{-1} typical for acrylates (the stretch of the ester carbonyl groups) and 1200-1000 cm^{-1} assigned to ether groups.

Rheological Behaviour of Pigment Pastes

The data of the rheological measurements are presented in Table 4.

Table 4. Rheological data for pigment paste PPS

$\dot{\gamma}$, s^{-1}	α	τ, mPa	η, mPa.s	ln η	ln $\dot{\gamma}$
16.2	1150	13110	809.2593	6.696119	2.785011
27	1650	18810	696.6667	6.546307	3.295837
48.6	2550	29070	598.1481	6.393838	3.883624
81	3700	42180	520.7407	6.255252	4.394449
145.8	5850	66690	457.4074	6.125574	4.982236
243	8700	99180	408.1481	6.01163	5.493061

Rheograms obtained for pigment pastes PPS are shown in Figure 2. The representation of the shear stress-shear rate curve for this paste (Fig. 2.a.) leads to the rheogram in Fig. 2.b., which shows a slightly pseudoplastic behavior. The PPS pigment paste does not exhibit time-dependent rheological behavior. The apparent viscosity decreases with increasing shear rates, suddenly between 16 and 49 s^{-1} and much slower for higher shear rates (Fig.2.b.). Linearization of the data from Fig.2.b. leads to the following equation of the line obtained by linear regression (Schramm, 2000):

$\ln \eta^* = 7.38253 - 0.25233 \ln \dot{\gamma}$, with a coefficient of r = 0.9986 (1)

A viscosity value η_0 of 1607 mPa.s or 1.607 Pa.s results from the equation of the straight line (Fig. 2.c.).

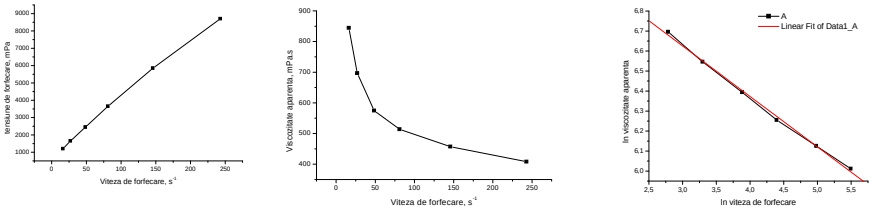

a) b) c)

Figure 2. Rheograms obtained for pigment paste PPS

Pigment paste PPS has a slightly pseudoplastic behaviour, therefore, under the action of shear stress, it decreases its viscosity.

CONCLUSIONS

• Pigment pastes are concentrated pastes with pH of 1/10 solution of 7.0-8.0, with good coating power.

https://doi.org/10.24264/icams-2022.V.5

• The spectra of films obtained from the pigment pastes show characteristic bands of acrylic polymers.

• Pigment pastes have a slightly pseudoplastic behaviour (under the action of shear stress, their viscosity decreases).

• The composition for natural leathers with special finishing effects, contains ecological components (titanium dioxide, acrylic resin, wax emulsion, vegetable oil and biodegradable non-ionic emulsifier, metal pigment-aluminum for silver effect or bronze powder for golden effect) and can be used for the surface finishing of natural leathers (white and pastel), in the composition of film-forming aqueous dispersions applied on the surface of natural leather for shoes (especially for women), to improve the organoleptic and aesthetic properties (related to fashion).

Acknowledgements

This research was funded by the Romanian Ministry of Research and Digitalization, CCCDI - UEFISCDI, PNCDI III - Program 1 – Development of the national RD system, Subprogram 1.2-Institutional Performance-RDI excellence funding projects, Contract no. 4PFE/2022 and Contract no. E!254/2021 (BIOSAFE LEATHER).

REFERENCES

Chiriţă, Gh. and Chiriţă, M. (1999), *Chemistry and Technology of Leather* (in Romanian), vol. I and II, Gh. Asachi Press, Iaşi.

Heidemann, E. (1994), *Fundamentals of Leather Manufacturing*, Eduard Roether KG Druckerei und Verlag, Darmstadt.

Lange, J. (1982), "Leather Finishing", *Leather library vol. V*, Umschau, Frankfurt.

Moldovan, Z. (2001), *Instrumental Analysis Methods*, University of Bucharest Press.

Niculescu, O. (2022), "Ecological Finishing Composition of Natural Leather", Patent Application RO A/100350/2022.

Niculescu, O., Leca, M., Moldovan, Z., Chelaru, C. and Gurău, D. (2015a), "Obtaining and Characterizing of an Ecologic Wax Emulsion for Finishing Natural Leathers and Furs", Revista de Chimie (Bucharest), 66(8), 1173-1176.

Niculescu, O., Leca, M., Staicu, T., Moldovan, Z., Chelaru, C. and Berechet, D.M. (2015b), "Obtaining and Characterizing of Some Ecologic Pigment Pastes for Finishing Natural Leathers and Furs", *Revista de Chimie* (Bucharest), 66(9), 1278-1281.

Niculescu, O., Manta, A. (2019), "Inorganic Pigment Pastes for Natural Leather Finishing", Patent RO A/00533/2019.

Pop, M., Gaidau, C., Niculescu, O. and Foiasi, T. (2019), "Ecology of Matter and the Surface Design in the Leather Fashion Industry", *Journal of Textile Science & Fashion Technology (JTSFT)*, 4(1), https://doi.org/10.33552/JTSFT.2019.04.000577.

Schramm, G. (2000), *A Practical Approach to Rheology and Rheometry*, 2nd ed., Gebrueder HAAKE GmbH, Karlsruhe.

Triderma (2020), *Leather Finishing Auxiliaries*, Germany.

*** (2004), Ecological and Toxicological Association of Dyes and Organic Pigment Manufactures (ETAD).

*** (2005), Patent US 0065257/2005.

*** (2006), SG, "The Test Mark for Low Pollutant Leather Products".

*** (2010), Directive 2010/75/EU of the European Parliament and of the Council of 24 November 2010 on industrial emissions (integrated pollution prevention and control).

*** (2014), Patent EP 2300541 B1/2014.

https://doi.org/10.24264/icams-2022.V.5

MATERIALS FOR SURFACE DESIGN AND FINISHING FOR CONTEMPORARY FOOTWEAR – PART 2

OLGA NICULESCU, ELENA BADEA, ILARIA QUARATESI,
RODICA ROXANA CONSTANTINESCU, DANA GURAU

The National Research & Development Institute for Textiles and Leather - Leather and Footwear Research Institute Division, 93 Ion Minulescu, Bucharest, Romania, email: icpi@icpi.ro

Leather has a natural beauty that, unlike many materials, improves with age, and has long been a component of luxury goods such as footwear, leather goods and clothing. It is a natural and durable material, unmatched by any synthetic product, in terms of hygienic and protective properties. Thanks to the skills of leather producers, who take the same basic raw material, natural leathers are processed through different technological processes and transformed into finished leathers for various clothing items with high-performance properties. Finishing is achieved through a series of technologies, using materials that provide the finished leather with the desired aesthetic characteristics related to fashion, colors and special effects (pearl, two-tone, antique, printed, glossy, matte, waxed, etc.). Hand-painted natural leather shoes are also in fashion, to give a personal touch to a luxury item. The work presents surface finishing technologies of ecological natural leathers (tanned without metals), using pigment pastes with a metallic effect, in combination with acrylic and polyurethane polymers, with resistance to light and aging. White and pastel finished leathers with silver and gold effect can be used in creative industries for artistic and luxury footwear (especially for women).

Keywords: natural leather, pigment pastes, surface design, creative industries

INTRODUCTION

Leather is fashionable in all colours while maintaining outstanding technical performance. The current ecological standards impose strict regulations in all processes technological and social, so that the carbon footprint is as small as possible (ETAD, 2004; SG, 2006; Directive 2010/75/EU).

In the field of eco-design, ethical-fashion, green product, etc., the theme of sustainability is not just a trend but a constant research topic under all aspects of the human-product-technology-consumption-environment relationship, developing the circular economy, based on four pillars: environment, economy, social and culture (Burdujan and Kral, 2015).

The global sustainability of products represents the coexistence of scientific, technical and cultural sustainability parameters, which, in the case of leather, through its ecological structure, involves modern finishing technologies and the eco concept of surface design (Pop and Horatau, 2019). In the fashion industry the added value is only reflected by an efficient surface design, but the Surface Design is not just a type of finish, it is an art-science act that, if well-known and coordinated, can be spectacular and sustainable at the same time (Pop *et al*., 2019).

Leather is finished (by spraying or using ecological finishing machines with rollers) using dispersed systems which contain: pigments, binders, waxes, preservatives, plasticizers, thickening agents, fillers, odorizing substances, penetrators, solvents etc. Environmental and toxicity concerns have led to new alternatives for finishing ancillary industry (Niculescu *et al*., 2015; Niculescu and Manta, 2019; Niculescu, 2022).

Finishes with special effects are applied to leather to improve the organoleptic and aesthetic properties, related to fashion, such as: metallic, bicolor, antique, waxed, etc.

The paper presents the dry leather finishing technologies using ecological materials (pigment pastes with a metallic effect) that provide the desired aesthetic characteristics for shoes. The bovine leathers were tanned (without metals) with syntans based on phenolsulfonic acids and aromatic oxysulfones and finished with ecological materials.

https://doi.org/10.24264/icams-2022.V.6

(Triderma, 2020). White and pastel finished leathers with special effect finish (silver and golden effect) can be used in creative industries for artistic and luxury footwear (especially for women).

EXPERIMENTAL

Materials

The nappa bovine leathers, tanned with syntans based on phenolsulphonic acids and aromatic oxysulfones and wet finished by retanning, fatliquoring (1.0-1.2 mm thick, white) (INCDTP – Division ICPI Bucharest, Romania).

Pigment pastes with silver effect (marked PPS), viscous and homogenous fluid, dry substance – 32-35%, pH (10% solution) – 7.0-8.0, ash – 25-8% (INCDTP – Division ICPI Bucharest, Romania).

Pigment pastes with golden effect (marked PPG), viscous and homogenous fluid, dry substance – 31-35%, pH (10% solution) – 7.0-8.0, ash – 27-29% (INCDTP – Division ICPI Bucharest, Romania).

Roda-Cryl 87 (Triderma, Germany), acrylic binder for ground coat, dry substance – 34.50%, pH (10% solution) – 6.0, Ford cup viscosity Φ4 – 14, density – 1.025 g/cm^3;

Roda-Pur Wx 1418 (Triderma, Germany) polyurethane binder for ground coat: dry substance – 19-21%, pH (10% solution) – 7.5-9.5.

Roda Wax MONO (Triderma, Germany), wax emulsion for ground coat: dry substance – 36.87%, pH (10% solution) – 4.2, Ford cup viscosity Φ4 – 12, kinematic viscosity, cSt – 8.97, density – 0.957 g/cm^3.

Roda feel KTA 950 (Triderma, Germany), aqueous wax emulsion for handle: dry substance – 12%, pH (10% solution) – 5.5.

Roda-Pur 5011 (Triderma, Germany), polyurethane dispersion (marked PU5011), dry substance – 40%, pH (10% solution) – 5.5, Ford cup viscosity Φ4 – 7, density – 1.053 g/cm^3.

Roda lacquer 93 (Triderma, Germany), nitrocellulose emulsion (marked LAC93), dry substance –15%, pH (10% solution) – 5.5, Ford cup viscosity Φ4 – 125, flash point – 82°C.

Methods

Physical-mechanical characteristics of finished leather assortments were determined according to the following standards: dry and wet abrasion (1-5 ranking) – SR EN ISO 11640:2002; resistance to repeated bending, number of flexions – SR EN ISO 5402:2012.

Finished leathers were artificially aged and tested according to ISO 17228/2015 standard, using Xenotest Apolo.

Optical microscopy images were captured using a Leica stereomicroscope S8AP0 model with optic fiber cold light source, L2, with three levels of intensity, and magnification 20X.

Elaboration of Dry Finishing Technologies for Natural Leathers for Shoes

Dry finishing technologies (application by spraying) have been developed for bovine hides into natural grain nappa, with silver and golden effect. The framework technology for dry finishing of bovine hides into natural grain nappa, with new pigment pastes, with silver and golden effect, is presented in Tables 1 and 2. Application of the final dressing was performed in two variants: P – polyurethane – Roda pur 5011 and N – nitrocellulose – Roda lac 93 (Triderma, 2020).

https://doi.org/10.24264/icams-2022.V.6

Table 1. Framework technology for dry finishing of bovine hides into natural grain nappa with silver effect (white and pastel)

Operation	Dispersion composition/application method
Applying dispersion I (basecoat)	100-120 g/L pigment paste (PPS) 2-5 g/L pigment paste (red, yellow, blue)* 150 g/L aqueous acrylic dispersion (Roda-cryl 87) 150 g/L aqueous polyurethane dispersion (Roda-pur 1418) 30 g/L aqueous wax emulsion (Roda wax MONO) 545-568 g/L water Application by spraying (2 passes dispersion I)
Intermediate pressing	In hydraulic press with the mirror or fog plate, parameters: - temperature – 50-60°C; pressure – 50-100 atm.
Applying dispersion I	By spraying (4-5 passes dispersion I)
Applying final dressing (fixing)	Emulsion/dispersion with the following composition: 700 g/L aqueous polyurethane dispersion (Roda pur 5011) or 700 g/L aqueous nitrocellulose emulsion (Roda-lac 93) 20 g/L aqueous wax emulsion (Roda feel KTA 950) 280 g/L water Application by spraying (2 passes final dressing)
Final pressing	In hydraulic press with the mirror plate, parameters: - temperature – 80-100°C; pressure – 50-100 atm.

* For finishing leathers in pastel colors with a silver effect, 2-5 g/L red, yellow or blue pigment pastes (Triderma SRL) were added in combination with the silver white pigment (PPS).

Table 2. Framework technology for dry finishing of bovine hides into natural grain nappa with golden effect

Operation	Dispersion composition/application method
Applying dispersion I (basecoat)	100-120 g/L pigment paste (PPG) 150 g/L aqueous acrylic dispersion (Roda-cryl 87) 150 g/L aqueous polyurethane dispersion (Roda-pur 1418) 30 g/L aqueous wax emulsion (Roda wax MONO) 550-570 g/L water Application by spraying (2 passes dispersion I)
Intermediate pressing	In hydraulic press with the mirror or fog plate, parameters: - temperature – 50-60°C; pressure – 50-100 atm.
Applying dispersion I	By spraying (4-5 passes dispersion I)
Applying final dressing (fixing)	Emulsion/dispersion with the following composition: 700 g/L aqueous polyurethane dispersion (Roda pur 5011) or 700 g/L aqueous nitrocellulose emulsion (Roda-lac 93) 20 g/L aqueous wax emulsion (Roda feel KTA 950) 280 g/L water Application by spraying (2 passes final dressing)
Final pressing	In hydraulic press with the mirror plate, parameters: - temperature – 80-100°C; pressure – 50-100 atm.

Testing Artificially Aged Finished Leather

The characteristics of finished natural grain nappa leather assortments aged with artificial light (Xenotest) for 7 days were determined.

The samples were marked:

https://doi.org/10.24264/icams-2022.V.6

- PPS-P (metal pigment-aluminum, poppy oil/ fixing with polyurethane dispersion);
- PPS-N (metal pigment-aluminum, poppy oil/ fixing with nitrocellulose emulsion);
- M1-P (metal pigment-aluminum, castor oil/ fixing with polyurethane dispersion);
- M1-N (metal pigment-aluminum, castor oil/ fixing with nitrocellulose emulsion);
- PPG-P (bronze powder, poppy oil/ fixing with polyurethane dispersion);
- PPG-N (bronze powder, poppy oil/ fixing with nitrocellulose emulsion);
- M2-P (bronze powder, castor oil/ fixing with polyurethane dispersion);
- M2-N (bronze powder, castor oil/ fixing with nitrocellulose emulsion).

RESULTS AND DISCUSSION

Characterization of Finished Leathers by Mechanical Methods

Physical-mechanical characteristics (resistance to dry/wet friction, resistance to repeated bending) and fastness to light (of leathers aged with artificial light-Xenotest, for 7 days) are shown in Table 3.

Table 3. Physical-mechanical characteristics of bovine hides into natural grain nappa

Samples	Resistance to dry friction (mark)	Resistance to wet friction (mark)	Resistance to repeated bending, number	Fastness to light after artificial ageing (1-8 ranking)
PPS-P	5/5	4/5	200.000	8
PPS-N	5/5	4/5	200.000	7-8
M1-P	5/4-5	4/4	190.000	7-8
M1-N	5/4	4/4	180.000	7
PPG-P	5/5	4/5	200.000	8
PPG-N	5/4-5	4/5	190.000	7-8
M2-P	5/4-5	4/3	180.000	7-8
M2-N	5/4	4/3	170.000	7
Standard	SR EN ISO 11640:2002	SR EN ISO 11640:2002	SR EN ISO 5402:2012	SR EN ISO 105-B02:2003

Leather samples (nappa) finished using prepared pigment pastes, according to the technologies presented in Tables 1 and 2, are within the limits specified in standards (ST 1619:1994), for natural leathers for shoes (min. 5/3 mark for resistance to dry friction, min. 4/2 mark for resistance to wet friction, min. 150.000 number for resistance to repeated bending).

Leather finished using the prepared pigment pastes (PPS and PPG) and polyurethane binder (final dressing) have higher marks for fastness to light after artificial ageing (8 on a scale of 1 to 8), and leather finished with nitrocellulose dressing have the mark 7 or between 7 and 8. Poppy seed oil, used as plasticizer, improves resistance to yellowing of coating films.

Analysis of Leathers Finished with New Pigment Pastes by Optical Microscopy

Table 4 illustrates optical images of leathers finished with pigment pastes with silver effect (PPS) and with golden effect (PPG). The resulting shades can be used to finish leather for footwear in a modern style.

https://doi.org/10.24264/icams-2022.V.6

Table 4. Optical images at 20X of the leathers finished with pigment pastes

Leather finished with pigment paste with silver effect (PPS)	Leather finished with pigment paste with golden effect (PPG)
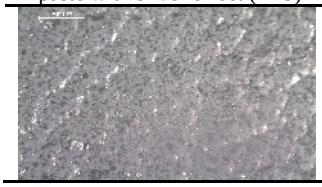	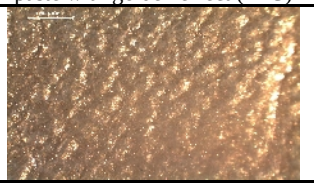

Macroscopic Images of Finished Leather for Creative Industries

Macroscopic images of leathers finished for creative industries are presented in Figures 1 (a-e), 2 and 3.

a)

b)

c)

d)

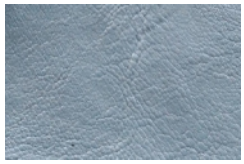

e)

Figure 1. Leathers finished with pigment pastes with silver (a) and golden (b) effect; leathers finished in pastel colors with pigment pastes (with silver and golden effect) (c-e)

Figure 2. Hand painted leather with pigment pastes (with silver and golden effect)

https://doi.org/10.24264/icams-2022.V.6

Figure 3. Leathers for artistic and luxury footwear

CONCLUSIONS

- Leather finished with pigment paste with silver and golden effect can be used for modern footwear.
- The highest resistance to light after aging under the influence of artificial light was found for leather finished with polyurethane dressing in comparison with leather finished with nitrocellulose dressing. Poppy seed oil, used as plasticizer, improves resistance to yellowing of coating films.
- The finishing composition can be used for the surface finishing of natural leather (white and pastel) for shoes (especially for women), to improve the organoleptic and aesthetic properties (related to fashion).
- Leather with silver and golden effect finish can be used in creative industries for artistic and luxury shoes (hand-painted natural leather shoes).

Acknowledgements

This research was funded by the Romanian Ministry of Research and Digitalization, CCCDI - UEFISCDI, PNCDI III - Program 1 – Development of the national RD system, Subprogram 1.2-Institutional Performance-RDI excellence funding projects, Contract no. 4PFE/ 2022 and Contract no. E!254/2021 (BIOSAFE LEATHER).

REFERENCES

Burdujan, J. and Kral, I. (2015), *The Framework for Sustainable Leather Manufacture*, United Nations Industrial Development Organization.

Niculescu, O. (2022), "Ecological Finishing Composition of Natural Leather", Patent Application RO A/100350/2022.

Niculescu, O. and Manta, A. (2019), "Inorganic Pigment Pastes for Natural Leather Finishing", Patent RO A/00533/2019.

Niculescu, O., Moldovan, Z., Leca, M., Chelaru, C., Alexandrescu, L. and Aboul-Enein, H.Y. (2015), "Characteristics of Natural Leather Finished with Some Ecofriendly Mixtures of Polymeric Aqueous Dispersions", Journal of Polymer Engineering, 35(6), 463-470, https://doi.org/10.1515/polyeng-2014-0286.

Pop, M. and Horatau, D. (2019), "Cultural Sustainability and Archetype in Creative Textile Design", *The Fourteenth International Conference on the Arts in Society*, Portugal, 19-21.

Pop, M., Gaidau, C., Niculescu, O. and Foiasi, T. (2019), "Ecology of Matter and the Surface Design in the Leather Fashion Industry", *Journal of Textile Science & Fashion Technology (JTSFT)*, 4(1), https://doi.org/10.33552/JTSFT.2019.04.000577.

Triderma (2020), *Leather Finishing Auxiliaries*, Germany.

*** (2004), Ecological and Toxicological Association of Dyes and Organic Pigment Manufactures (ETAD).

*** (2006), SG, "The Test Mark for Low Pollutant Leather Products".

*** (2010), Directive 2010/75/EU of the European Parliament and of the Council of 24 November 2010 on Industrial Emissions (Integrated Pollution Prevention and Control).

https://doi.org/10.24264/icams-2022.V.6

ECO-PRINTING LEATHER QUALITY IN DIFFERENT MORDANT METHODS

WEHANDAKA PANCAPALAGA[1*], JAMROJI[2], TUTIK SULISTYOWATI[3], RIRIN HARINNI[4], RINI PEBRI UTARI[5], MUHAMMAD KHOIRUL FUDDIN[6], RINALDY ACHMAD ROBERTH FATHONI[7], ENDANG SRI HARTATI[1], ASMAH HIDAYATI[1]

[1]*Animal Science Department*, [2]*Communication Science Department*, [3]*Sociology Department*, [4]*Public Health Department*, [5]*Civil Engineering Department*, [6]*Development Economics Department*, [7]*Management Business Department – University of Muhammadiyah Malang, St. Tlogomas 246 Malang, 65151, Indonesia, pancapalaga1966@gmail.com*

The leather coloring technique using the eco-printing method is carried out by transferring the colors and motifs of plants on the leather material by direct contact. This process requires mordant to maximize the color. The use of mordant is done in three ways, namely mordant is done at the beginning (pre-mordanting), mordant is done simultaneously (meta-mordanting), and mordant is done at the end (post-mordanting). This study aims to determine the quality of eco-printing leather with the implementation of different mordant methods. The research materials were 16 pieces of sheep's crust leather. The research treatment was using various mordant methods, namely pre-mordanting, meta-mordanting, and post-mordanting. Colorfastness, tensile strength, elongation, tear strength, flexibility, and fracture resistance were among the eco-printing leather qualities evaluated. The research was carried out in an experimental setting using a completely randomized design. To conclude, the best mordant method was carried out at the beginning of the eco-printing process on leather media (pre-mordanting), where the quality of eco-printing leather obtained of 5.44 ± 0.968 mm, crack resistance (distance) of 8.78 ± 0.97 mm, the tensile strength of 1743.64 ± 45.26 N/cm^2, leather elongation of 55.15 ± 10.26 %, tear strength of 268.24±132.49 N/cm, sewing strength of 1247.12 ± 649.91 N/cm, colorfastness of wet rubbing rated 4 (good), and dry rub of 4 (good).

Keywords: quality, eco-printing leather, crust leather

INTRODUCTION

Leather goods products are generally colored with synthetic materials. The advantages of synthetic coloring provide an attractive appearance, more varied colors, and is easy to work with. However, the use of synthetic dyes is not environmentally friendly because the waste from synthetic dyes can be dangerous, since some dyes can be degraded into carcinogenic and toxic compounds (Berhanu and Ratnapandian, 2017).

Therefore, the use of natural dyes for leather is increasingly in demand, for natural dyes have the advantage that they do not cause damage to the environment and do not have side effects on health. Furthermore, natural dyes are easier to find. Several studies of natural coloring on leather have been conducted using Henna leaf extract (*Lawsonia inermis*) (Musa *et al*., 2008), *Acacia catechu* extract (Pant and Gahlot, 2012), *Bixa orellana* seed extract (Selvi *et al*., 2016), *Tagetes erecta* L. flower extract (Marigold) (Pervaiz, 2017), and plant extract of *Osyris quadripartita* (Teklay and Kechi, 2017).

One of the natural colorings of leather can be done with the eco-printing method. This method is a natural coloring process that is different from what is commonly done by the community, because in addition to transferring color, it also produces natural forms that exist in plants (leaves and flowers), on the leather. The eco-printing method is used to decorate the surface of the skin with various shapes and colors (coloring) produced from natural materials (Izmal, 2016). Currently, eco-printing is widely used in textiles such as cotton, a combination of cotton and polyester, and a combination of cotton and Tencel (Izmal, 2016). Another study also compared the use of eco-printing on wool, silk, cotton, and flax (Rekabya *et al*., 2009).

https://doi.org/10.24264/icams-2022.V.7

A study on eco-printing on leather media is still limited compared to cloth media. Ristiani and Isnaini (2019) reported that eco-printing can be done on sheep leather material, by steaming at a medium temperature of 80°C resulting in good average color rubbing resistance with a score of 4 and 4-5. Meanwhile, according to Pancapalaga *et al*. (2021), the use of aluminum potassium sulfate in the natural coloring of leather using the eco-printing will increase wet rubbing resistance, sweat resistance, and washing resistance and will not to reduce the color intensity of eco-printed leathers. Besides the type of mordant that determines the quality of the leather color, the eco-printing is also the mordant method.

Therefore, further study on the mordant methods needs to be done. Generally, there are three mordant methods used, pre-mordant (mordant at the beginning), meta mordant (mordant simultaneously), and post-mordant (mordant at the end). This study aims to determine the quality of eco-printed leathers by implementing different mordant methods and also to determine which mordant methods produce the best quality of eco-printed leathers.

EXPERIMENTAL

Materials

The main research material used was 16 pieces of sheep crust leathers. The crust materials were obtained from leather craftsmen in Yogyakarta. The mordant material was $Al_2(SO_4)_3$, while the natural dyes were obtained from castor bean leaves and mangrove bark.

Methods

The instruments used in this study included analytical scales, stainless steel knives, basins, measuring cups, pencils, scissors, thermometers, buckets, shoes, plastic, ropes, stoves, pans, and thermometers. It also had a crock meter to test wet and dry rubbing resistance. A universal testing machine was used for the tensile strength test. A strength tester was used for the elongation and tear strength of the leather. Softness tester 300 equipment was used to measure skin softness and lastometer was used to measure leather crack resistance.

Implementation of Eco-Printing Method Coloring

The eco-printed leather process used the method proposed by Pancapalaga *et al*. (2021). The crust leathers were soaked in water for 6 hours until the color became bluish. Then, the crust leathers were soaked at the beginning (T1) with a solution of mordant (aluminum potassium sulphate) with a ratio between water and mordant of 1: 1 for 12 hours. Meanwhile, leathers of the T2 treatment were soaked at the beginning and the end (meta-mordant). After soaking, the crust leathers were dried. After a bit dry, the crust leathers were spread out on the floor that had been given a plastic base. The surface of the crust leathers was given red (*Jatropha gossypiifolia)* leaves and covered with a cloth that had been colored naturally with mangrove trunk extracts (*Rhizophora mucronata*). Then, the leathers were rolled on a pipe and tied with a cloth, and steamed for 1 hour. After cooling, the leather bond was opened and the crust was soaked (post-mordant or T3) for 12 hours. Finally, the leathers were dried at room temperature followed by laboratory testing to determine the quality of the eco-printed leathers.

https://doi.org/10.24264/icams-2022.V.7

Testing

The leather softness test was carried out according to ISO 17235 (2015). The eco-printing leather crack strength test was carried out according to ISO 3379 (2015). Tensile strength and leather elongation tests were carried out according to SNI. 06-1795-1990. The tear strength test was carried out based on SNI 06-1794-1990. The sewing strength test was carried out following SNI 06-1117-1989. The color fastness test due to dry and wet rubbing was carried out according to ISO 20433 (2012).

Data Analysis

The data of elasticity, crack resistance, tensile strength, elongation, tear strength, and sewing strength obtained were analyzed using ANOVA to determine the differences between each treatment. If the treatment has a significant effect, then Duncan's test was conducted as a follow-up. meanwhile, the color fastness to wet and dry rubbing was measured by assessing the color difference with the grayscale and rating it with marks from 1 to 5. The standard used was the standard issued by the International Standard Organization (ISO 20433:2012). The wet/dry rub fastness data obtained were tabulated and analyzed by the Kruskal Wallis test. To investigate the difference between treatments, it was continued by using the Mann-Whitney test.

RESULTS AND DISCUSSION

The leather color was transferred by direct contact of plant leaves and bark extract and steaming, with different mordant methods. The results of the influence of eco-printing processed leathers on physical and fastness resistances are presented below.

Table 1. The physical and fastness characteristics of eco-printed leathers

Mordant method	Softness (mm)	Crack resistance (distance) (mm)	Tensile strength (N/cm^2)	Elongation (%)	Tear strength (N/cm)	Sewing strength (N/cm)	Rubbing fastness	
							wet	dry
Pre-	5.44± 0.96[b]	8.78± 0.97[a]	1743.64± 745.26[a]	55.15± 10.26[a]	268.24± 132.49[b]	1247.12± 249.91[a]	4	4
Meta-	4.22± 0.33[a]	8.76 ±0.57[a]	1493.10± 603.98[a]	59.64± 10.99[a]	204.70± 55.10[ab]	895.26± 148.96[b]	3/4	3
Post-	4.30± 0.15[a]	7.67 ±0.56[a]	1137.65± 321.69[a]	57.89± 10.44[a]	144.48± 28.82[a]	862.45± 157.70[b]	3/4	3

Description: The notation followed by a different letter in one column indicates a significant difference ($P<0.05$).

Eco-Printed Leather Softness

Table 1 presents that the mordant method had a significant effect ($P<0.05$) on the eco-printing leather elasticity score. The highest eco-printing leather elasticity score produced by the mordant method was carried out by pre-mordant of 5.44 ± 0.96 mm while the lowest eco-printing leather elasticity was carried out by the meta-mordant method of 4.22 ± 0.33 mm. The high elasticity score in the pre-mordant method is because the leather soaked with the mordant before the dyeing process might provide an opportunity for the mordant to bind to the leather proteins. Thus, when the dye is applied, there is a maximum bond between the natural dye and the leather creating more elastic properties on the

https://doi.org/10.24264/icams-2022.V.7

leather. According to Abu (2016), the pre-mordant process aims to increase the absorption of natural dyes on the media and produce good elasticity and color sharpness.

Eco-Printed Leather Crack Resistance

In contrast to eco-printing leather elasticity presented in Table 1, the mordant methods show no significant effect ($P>0.05$) on crack resistance (distance) for mordant methods did not change the leather skin structure and caused the skin density remains. Hasan *et al*. (2014) argue that the elasticity of tanned leather was influenced by water content, fat, fiber structure, and leather thickness. However, the data in Table 1 indicate that the highest eco-printing leather crack resistance value was produced by the pre-mordant of 8.78 ± 0.97 mm, while the lowest was produced by the post-mordant of 7.67 ± 0.56 mm. Mustakim *et al.* (2007) added that crack resistance of the leather is closely related to changes in the structure of leather collagen, changes in the structure of collagen bonds in the leather might cause the strength of the leather to increase. Thus, leather is not easy to crack due to the gelatinization process of leather fibers.

Tensile Strength and Elongation of Eco-Printed Leather

Similar to the crack resistance, the mordant method also showed no significant effect ($P>0.05$) on the tensile strength and elongation of the eco-printing leather due to the meta-mordant did not change the chemical composition of eco-printing leather. It indicates that the collagen fibers and the webbing corners are still intact during the immersion process with the mordant. In other words, the leather structure, especially the corium of the leather has been perfectly bonded during the tanning process. According to Triatmojo (2014), leather with high tensile strength generally has low elongation, while those with low tensile strength have high elongation.

This is evident in the tensile strength and elongation values of the eco-printing leather produced. The highest tensile strength value of the eco-printing leather produced by the pre-mordant method of 1743.64 ± 745.26 N/cm^2, while the lowest was by the post-mordant method of 1137.65 ± 321.69 N/cm^2. On the other hand, the lowest elongation score was in the pre-mordant method of 55.15 ± 10.26 (%), while the highest elongation was in the meta-mordant method of 59.64 ± 10.99 (%).

Eco-Printed Leather Tear Strength

The use of different mordant methods had a significant effect ($P<0.05$) on the tear strength of the eco-printing leather. The highest eco-printing leather tear strength score was found in the pre-mordant method treatment of 268.24 ± 132.49 N/cm. The high tear strength value was due to the perfect absorption of natural color into the leather's collagen fiber cavities, thereby making the leather's ability to withstand tearing loads better. However, at the post-mordant method, the value of the tear strength of the eco-printing leather decreased. This is presumably because the absorption of color by the leather has reached the maximum absorption limit. Hence, it causes a decrease in the value of the tear strength. Prabhu and Bhut (2012) suggest that the pre-mordant method with aluminum potassium sulphate showed the lowest color that came out after washing, indicating a very good complexing of aluminum with natural dyestuffs. It is also said that the basic chemical bond between natural dyes and mordant, of them, is the covalent bond between the hydroxyl oxygen and the Al^{3+} ions.

https://doi.org/10.24264/icams-2022.V.7

Eco-Printed Leather Sewing Strength

In terms of the tear strength, the use of different mordant methods had a significant effect ($P<0.05$) on the sewing strength of eco-printing leather. This is probably due to the mordant method starting with the immersion of *aluminum potassium sulfate* causing an increase in acidity in the eco-printing leather. This increase in acidity changes the structure of the collagen protein in the eco-printed leather. Triatmojo (2014) stated that the factors that influence the sewing strength are the thickness of the leather, the content, and density of collagen protein, the angle of the braid of the collagen fibers, and the thickness of the corium. Moreover, the value of sewing strength is directly proportional to the tensile strength and tear strength, if the tensile strength and the tear strength are high, the sewing strength is also high.

Eco-Printed Leather Color to Wet and Dry Rubbing

Table 1 presents the mordant methods that affect the value of wet and dry rubbing resistance. The value of eco-printing leather color fastness due to wet and dry rubbing on average gave a score of 4 (good) compared to the meta- and post-mordant methods. The pre-mordant method has the highest value because it was carried out at the beginning with aluminum potassium sulfate Sulfate has the opportunity to bind to the skin tissue more perfectly. Thus, the value of colorfastness due to wet rubbing and dry rubbing is increasing, indicating that it does not fade easily. Mordant is a chemical substance that forms chemical bonds with natural dyes. The chemical bond between the mordant and the natural dye is formed first by soaking the leather first with the mordant and then dyeing it. This might help the absorption and fixation of natural dyes and also prevent color by rubbing. The color fading is assessed by light fastness tests as well as improve fastness (Boahin *et al*., 2011).

Figure 1. Eco-printed leather results with different mordant methods

Figure 1 visualizes the results of P1 and P3 colors clearer than P2. This indicates that the mordant method might affect the brightness of the color on the surface of the eco-printing leather. According to Ahmad and Hidayati (2018), the mordanting process functions as a color enhancer and changes natural dyes according to the type of metal as a binder. The surface of the leather is impregnated with mordant, then during the coloring process reacts with the mordant, forming a chemical bond and sticking firmly to the leather.

CONCLUSION

The best mordant method to be carried out is the pre-mordant method done at the beginning of the eco-printing process (before coloring) on leather material, with the

https://doi.org/10.24264/icams-2022.V.7

quality of the eco-printing leather obtained of 5.44 ± 0.968 mm for softness, crack resistance (distance) of 8.78 ± 0.97 mm, the tensile strength of 1743.64 ± 45.26 N/cm^2, elongation of 55.15 ± 10.26 %, tear strength of 144.48 ± 28.82 N/cm, sewing strength of 1247.12 ± 649.91 N/cm, wet rub colorfastness of 4 (good), and dry rub of 4 (good).

The light fastness of eco-printed leathers will be evaluated in the next stage of the research and A method for textile dyeing was proved to be applicable for leather also and can be useful for the creative industry.

Acknowledgment

Acknowledgments are addressed to the Ministry of Education and Culture which has funded this research and the Directorate of Research and Community Service (DPPM) of the Universitas Muhammadiyah Malang through the 2021 Higher Education Leading Applied Research Scheme (PTUPT), with contract number 313/E4.1/AK.04.PT/2021.

REFERENCES

Abu, A.K. (2016), "Pewarnaan Tumbuhan Alami Kain Sutera Dengan Menggunakan Fiksator Tawas, Tunjung Dan Kapur Tohor", *Jurnal Scientific Pinisi*, 2(2), 86-91.

Ahmad, A.F. and Hidayati, N. (2018), "Pengaruh jenis mordan dan proses mordanting terhadap kekuatan dan efektifitas warna padapewarnaan kain katun menggunakan zat warna daun jambu biji Australia", *Indonesia Journal of Halal*, 12(1), 1-5, https://doi.org/10.14710/halal.v1i2.4422.

Berhanu, T. and Ratnapandian, S. (2017), "Extraction and Optimization of Natural Dye from Hambo Hambo (Cassia singueana) Plant Used for Coloration of Tanned Leather Materials", *Advances in Materials Science and Engineering*, 1(7), 1-5, https://doi.org/10.1155/2017/7516409.

Boahin, J.O.B., Agyem, A. and Peligah, Y.S. (2011), "Exploring the Use of Suede Dye on Leather", *Journal of Science and Technology (Ghana)*, 31(2), 68–73, https://doi.org/10.4314/just.v31i2.69395.

Izmal, O.E. (2016), "Patterns from Nature: Contact Printing", *Journal of the Textile Association*, 77(2), 81-91, https://issuu.com/textileasociationindia/docs/e-journal_-_jul-aug__16.

ISO 3379 (2015), Specifies a Test Method for the Determination of Distension and Strength of the Leather Grain or Finished Surface.

ISO 20433 (2012), Leather - Tests for Colour Fastness - Colour Fastness to Cracking.

Musa, A.E., Madhan, B., Madhulatha, W., Raghava Rao, J. Gasmelseed, G.A. and Sadulla, S. (2008), "Coloring of Leather Using Henna - Natural Alternative Material for Dyeing", *Journal of the American Leather Chemists Association*, 104(5), 183-190.

Mustakim (2007), "Tingkat Penggunaan Bahan Samak Chrome Pada Kulit Kelinci", *Jurnal Ilmu dan Teknologi Hasil Ternak*, 2(2), 14-27.

Pancapalaga, W., Suyatno and Malik, A. (2021), "Crust Leather Quality with Eco-Printing Dyeing Method", *Indian Journal of Science and Technology*, 14(1), 71-75, https://doi.org/10.17485/IJST/v14i1.1982.

Pant, S. and Gahlot, M. (2012), "Dyeing of Leather with Natural Dyes Extracted from *Acacia catechu*", *Asian Dyer*, 2(9), 54-59.

Pervaiz, S., Mughal, T.A., Zafar Khan, F., Sikandar Hayat, F., Aslam, A. and Faheem Shah, S. (2017), "Environmental Friendly Leather Dyeing Using *Tagetes erecta* L. (Marigold) Waste Flowers", *International Journal of Biosciences*, 2017(10), 382-390, https://doi.org/10.12692/ijb/10.1.382-390.

Prabhu, K.H. and Bhute, A.S. (2012), "Plant Based Natural Dyes and Mordants: A Review", *Journal of Natural Product and Plant Resources*, 2(6), 649-664.

Rekabya, M., Salemb, A.A. and Nassara, S.H. (2009), "Eco-Friendly Printing of Natural Fabrics Using Natural Dyes from Alkanet and Rhubarb", *Journal of the Textile Institute*, 100(6), 486–495, https://doi.org/10.1080/00405000801962177.

Ristiani, S. and Isnaini (2019), "Eksplorasi teknik eco-printing pada media kulit", *Prosiding Seminar Nasional Industri Kerajinan Dan Batik*, 1(1), B-5.

Selvi, A.T., Aravindhan, R., Madhana, B. and Raoc, J.R. (2013), "Studies on the Application of Natural Dye Extract from *Bixa orellana* Seeds for Dyeing and Finishing of Leather", *Industrial Crops and Products*, (43), 84–86, https://doi.org/10.1016/j.indcrop.2012.07.015.

Teklay, N. and Kechi, A. (2018), "Optimization of Leather Dyeing using Natural Dye Extract", *International Journal of Scientific Engineering and Research*, 2(6), 136-141.

Triatmojo, S. and Abidin, M.Z. (2014), *Penyamakan Kulit Ramah Lingkungan*, Gadjah Mada University Press, Yogyakarta, Cetakan pertama.

Wirawan, B. (2019), "Teknik Pewarnaan Alam Eco Print Daun Ubi Dengan Penggunaan Fiksator Kapur, Tawas, Dan Tunjung", *Jurnal Litbang Kota Pekalongan*, 17(2), 1-5, https://doi.org/10.54911/litbang.v17i0.101.

OVERVIEW ON THE NEW GENERATION OF EXTRACTION TECHNIQUE: FABRIC SOLID-PHASE EXTRACTION

ELENA-CORNELIA TANASESCU[1,2], MIHAELA-CRISTINA LITE[1,2], ELENA PERDUM[1], LUCIA OANA SECĂREANU[1], OVIDIU IORDACHE[1], IRINA-MARIANA SANDULACHE[1], LUCIAN GABRIEL RADU[2]

[1]*The National Research & Development Institute for Textiles and Leather, Lucretiu Patrascanu, 16, 030508 Bucharest, Romania, email office@incdtp.ro*

[2]*Politehnica University of Bucharest, 1-7 Gheorghe Polizu Street, 011061, Bucharest, Romania, email secretariat@chimie.upb.ro*

Fabric phase sorptive extraction (FPSE) is a new-generation of sample preparation technique that effectively combines representative characteristics of solid-phase microextraction – SPME (equilibrium-based extraction) and solid phase extraction – SPE (exhaustive extraction). FPSE was introduced in 2014 by Kabir A. and Furon K.G. FPSE utilizes a fabric substrate (natural or synthetic such as cotton or polyester) that is chemically coated with a hybrid sorbent (organic-inorganic sol-gel). The entire assembly (fabric substrate coated with the sol-gel polymer) results in a fast and sensitive micro-extraction device. The FPSE development process can be described in 3 main steps: (1) Preparation of the fabric substrate for sol-gel coating, (2) preparation of the sol-solution for coating the substrate, and (3) formation of sol-gel coatings on the fabric substrate. Using this technique can be ensured a faster, cleaner, and with a high concentration of analyte solution. FPSE is a method that can be easily modified and used in different types of applications. For this reason, FPSE is increasingly used in the scientific community dealing with sample pretreatment. By using this technique, promising results have been obtained both for the extraction and determination of certain analytes from environmental samples, as well as from other types of samples, with complex matrices (food and biological samples). This study aims to summarize the existing data on FPSE and to briefly present this innovative method.

Keywords: FPSE, fabric, microextraction

FABRIC PHASE SOLID EXTRACTION DESCRIPTION

Sample preparation is a very important and inevitable step in the chemical analysis workflow since it can easily influence the obtained results. Most of the analytical samples cannot be analyzed directly with an injection into the analytical instrument. Sample preparation may involve a series of steps that can include dissolution, extraction, reaction with some chemical species, filtering, dilution, or many other techniques, and it is considered to be the most time-consuming part of the whole analysis.

Lately, low-cost, fast, and environmentally friendly procedures became necessary in order to improve quality of life and protect the environment. Hence, scientists aim toward developing new analytical methodologies compliant with the principles of green analytical chemistry (GAC) (Armenta *et al*., 2015).

Different types of sorbent-based sorptive microextraction methods are used in analytical laboratories, such as: solid-phase microextraction (SPME) (Belardi and Pawliszyn, 1989; Arthur and Pawliszyn, 1990), stir bar sorptive extraction (SBSE) (Baltussen *et al*., 1999; David and Sandra, 2007), microextraction by packed sorbents (MEPS) (Abdel-Rehim, 2004) and solvent-based sorptive microextraction techniques e.g., single-drop microextraction (SDME) (Jeannot and Cantwell, 1996; Jeannot and Cantwell, 1997), dispersive liquid-liquid microextraction (DLLME) (Rezaee *et al*., 2006) and hollow-fiber microextraction (HF-LPME) (Pedersen-Bjergaard and Rasmussen, 1999; Shen and Lee, 2002).

https://doi.org/10.24264/icams-2022.V.8

Fabric phase sorptive extraction (FPSE), is a new type of microextraction, developed by Kabir and Furton (Kabir and Furon, 2014). It utilizes sol-gel coating technology developed by Chong and co-workers (Chong *et al*., 1997) in order to create an inherently porous hybrid inorganic-organic sorbent material that is chemically bonded to the flexible and permeable substrate matrix, usually a fabric material.

The FPSE combines two extraction modes (SPME and SPE) into a single microextraction device. The procedure is based on the direct contact of the FPSE with the sample. Due to the created contact, the analytes are transferred onto the surface of FPSE, similarly to the direct-immersion SPME (equilibrium extraction mode). The extraction process may be facilitated by magnetic stirring, sonication etc. (Silva, 2017; Samanidou and Kabir, 2015).

The main steps of FPSE are presented in Figure 1.

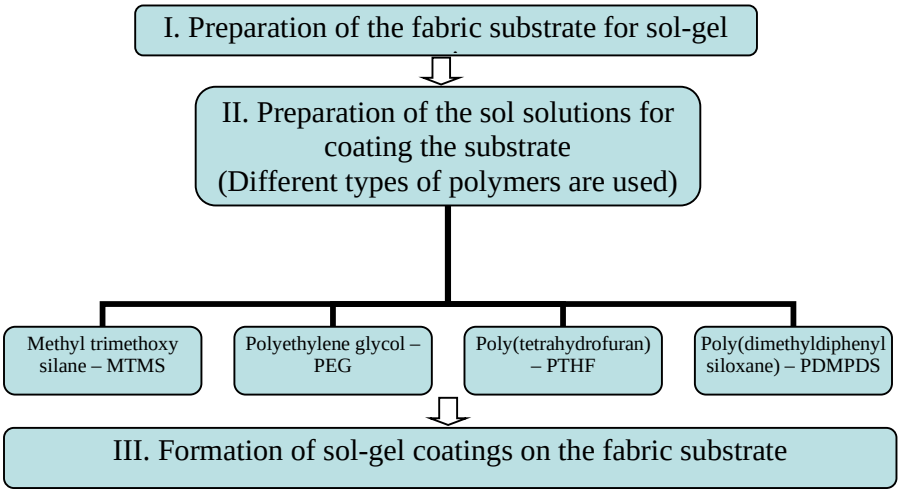

Figure 1. Main steps of FPSE

Currently, FPSE is considered to be the only microextraction technique that analyzes the substrate surface chemistry of the fabric to accomplish the overall selectivity and extraction efficiency of an FPSE membrane. Moreover, FPSE is the only microextraction technique that offers the possibility to use a complete range of sorbent chemistries such as polar, medium polar, nonpolar, cation exchanger, anion exchanger, mixed mode, zwitterionic, as well as zwitterionic mixed-mode sorbents (Kabir and Samanidou, 2021). It is important to note that all the before-mentioned sorbents can be coated on 100% cotton cellulose (hydrophilic), on fiberglass (neutral), or ~~on~~ polyester (hydrophobic) substrates.

Method development of fabric phase sorptive extraction is simple and straightforward. One of the big advantages is that FPSE does not require any sample pre-treatment process to reduce or minimize matrix interferents such as filtration or centrifugation (or any other type of pre-treatment process), and the FPSE membrane can be used directly with the sample, regardless of its complexity.

The extraction time is one of the most important factors that influence the extraction efficiency of an FPSE membrane. Generally, extraction efficiency is assessed between 0

https://doi.org/10.24264/icams-2022.V.8

and 60 min. The optimum time necessary for the desorption of the extracted analytes have been assessed in the range between 0 and 10 min.

Sample volume is another parameter in FPSE and depends on the availability and nature of the sample. The sample volume is directly proportional to the FPSE surface: for a smaller sample volume, a smaller FPSE membrane size can be used.

Table 1 presents the preparation of sol–gel sorbent coated FPSE membrane.

Table 1. Preparation of sol–gel sorbent coated FPSE membrane (adapted after Kabir and Samanidou, 2021)

Preparing the fabric substrate for sol-gel coating (Kabir *et al*., 2017; Kumar *et al*., 2014)	Preparing the sol-solution for coating the substrate (Kabir *et al*., 2013)	Formation of sol-gel coatings on the fabric substrate: Dip coating technology	Aging, thermal conditioning and cleaning	Cutting the FPSE membrane (Kabir and Samanidou, 2021)
Nonpolar analytes – polyester fabric	Sol-gel precursors: inorganic/organic modified	Coating the pretreated fabric with the sol-solution, typically 12h at room temperature	Conditioning under helium gas flow, typically for 24h at 50°C	Volume of sample<5mL – 1 cm diameter FPSE membrane
Medium-polar analytes – hydrophilic fabric: 100% cotton cellulose	Inorganic/organic active polymer	Drying the coated FPSE membrane in air, typically for 1h.	Cleaning the FPSE membrane.	5mL<Volume of sample<20 mL – 2.5cm x 2.0 cm size of FPSE membrane
Clean and activate the fabric surface	Compatible solvent system Acid catalyst and water			

FPSE technique extraction principle is analogous with solid phase microextraction (SPME), stir bar sorptive extraction (SBSE) and thin film microextraction (TFME) meaning direct immersion extraction.

The mass of the analyte extracted with FPSE (n), is proportional with the following parameters (Kabir and Samanidou, 2021):

- the coatings on the chosen substrate surface and the sample matrix (K_{es})
- the volume of the extracting phase (V_e)
- the volume of the sample (V_s)
- the initial concentration of the analyte (C_o)

The formula that can be used to express the mass of the extracted analyte is:

$$n = \frac{K_{es} V_e V_s C_o}{K_{es} V_e + V_s} \quad (1)$$

If the Sample volume if too large in comparison with the extracted sorbent volume (Ve<<Vs), the above equation can be expressed as:

$$n = K_{es} V_e V_s C_o \quad (2)$$

The extraction efficiency is influence by two factors: thermodynamic and kinetic factors (Lucena, 2012).

https://doi.org/10.24264/icams-2022.V.8

Many research groups have adopted this innovative sample preparation approach and have developed new analytical strategies with application in all analytical fields.

According to a review published by Kabir and Samanidou (2021), 66 papers have been published since 2014 to 2020 with an increased trend of publishing these works. In Table 2, some of the FPSE technique applications are presented.

Table 2. Applications of the FPSE Technique (Adapted after Zilfidou *et al*., 2018)

Type of technique	Fabric substrate	Sol-Gel coating	Sample	Reference
FPSE-HPLC-UV	Cellulose	PEG	Tap-Pond-Reclaimed Water Substituted phenols	Kabir *et al*., 2017
FPSE-HPLC-FLD	Cellulose	PTHF	Ground-River-Drinking, WWTP, Hospital wastewater Estrogens	Kumar *et al*., 2014
FPSE-HS-GC-MS	Fiber glass	PDMDPS	Environmental air Sexual pheromone	Alcudia-León *et al*., 2017
FPSE-HPLC-UV	Cellulose	PTHF	Industrial-Ground water, Borcher-Oakay alloy Heavy metal ions	Heena Kaur *et al*., 2017
FDSE-FI-FAAS	Polyester	PDMDPS	River-Coastal-Ditch water Toxic metals	Anthemidis *et al*., 2016
DFPSE-LC-MS/MS	Cellulose	PEG	River water, Effluent/influent wastewater Pharmaceuticals Personal care products	Lakade *et al*., 2016
Stir-FPSE-UPLCDAD	Cellulose	PEG	River-Stream water Herbicides	Roldán-Pijuán *et al*., 2015
SE/GC-MS	Cellulose	CW / PTHF / PDMS	Vegetable samples organophosphorus pesticides	Kaur *et al*., 2019

CONCLUSION

The ability to use the same FPSE membrane in SPME or SPE modes is a unique concept that allows the extraction to be performed while maintaining the performance characteristics of the extraction, such as robustness, specificity and efficiency.

FPSE can be successfully used with any chromatographic techniques, such as liquid and gas chromatography coupled with various detectors depending on the needs of the analysis. This new generation technique found applications in the analysis of drugs, pharmaceuticals, and other chemical compounds that are mainly found in environmental samples as well as in food samples and biological fluids.

https://doi.org/10.24264/icams-2022.V.8

Acknowledgment

This work was supported by the Ministry of Research and Innovation within Program 1 - Development of the national RD system, Subprogram 1.2 - Institutional Performance - RDI excellence funding projects, contract no. 4PFE/2021.

REFERENCES

Abdel-Rehim, M. (2004), "New Trend in Sample Preparation: On-line Microextraction in Packed Syringe for Liquid and Gas Chromatography Applications: Determination of Local Anaesthetics in Human Plasma Using Gas Chromatography-Mass Spectrometry", *Journal of Chromatography B*, 801, 317-321, https://doi.org/10.1016/j.jchromb.2003.11.042.

Alcudia-León, M.C., Lucena, R., Cárdenas, S., Valcárcel, M., Kabir, A. and Furton, K.G. (2017), "Integrated Sampling and Analysis Unit for the Determination of Sexual Pheromones in Environmental Air Using Fabric Phase Sorptive Extraction and Headspace-Gas Chromatography-Mass Spectrometry", *Journal of Chromatography A*, 1488, 17–25, https://doi.org/10.1016/j.chroma.2017.01.077.

Anthemidis, A., Kazantzi, V., Samanidou, V., Kabir, A. and Furton, K.G. (2016), "An Automated Flow Injection System for Metal Determination by Flame Atomic Absorption Spectrometry Involving On-line Fabric Disk Sorptive Extraction Technique", *Talanta*, 156–157, 64–70, https://doi.org/10.1016/j.talanta.2016.05.012.

Armenta, S., Garrigues, S., and de la Guardia, M. (2015), "The Role of Green Extraction Techniques in Green Analytical Chemistry", *Trends in Analytical Chemistry*, 71, 2–8, https://doi.org/10.1016/j.trac.2014.12.011.

Arthur, C.L. and Pawliszyn, J. (1990), "Solid Phase Microextraction with Thermal Desorption Using Fused Silica Optical Fibers", *Analytical Chemistry*, 62, 2145-2148, https://doi.org/10.1021/ac00218a019.

Baltussen, E., Sandra, P., David, F. and Cramers, C. (1999), "Stir Bar Sorptive Extraction (SBSE), a Novel Extraction Technique for Aqueous Samples: Theory and Principles", *Journal of Microcolumn Separations*, 11, 737-747, https://doi.org/10.1002/(SICI)1520-667X(1999)11:10<737::AID-MCS7>3.0.CO;2-4

Belardi, R.P. and Pawliszyn, J. (1989), "The Application of Chemically Modified Fused Silica Capillary Columns", *Water Pollution Research Journal of Canada*, 24, 179-191, https://doi.org/10.2166/wqrj.1989.010.

Chong, S.L., Wang, D., Hayes, J.D., Wilhite, B.W. and Malik, A. (1997), "Sol-Gel Coating Technology for the Preparation of Solid-Phase Microextraction Fibers of Enhanced Thermal Stability", *Analytical Chemistry*, 69, 3889-3898, https://doi.org/10.1021/ac9703360.

David, F. and Sandra, P.J. (2007), "Stir Bar Sorptive Extraction for Trace Analysis", *Journal of Chromatography A*, 1152, 54-69, https://doi.org/10.1016/j.chroma.2007.01.032.

Heena Kaur, R., Rani, S., Malik, A.K., Kabir, A. and Furton, K.G. (2017), "Determination of Cobalt (II), Nickel (II) and Palladium (II) Ions via Fabric Phase Sorptive Extraction in Combination with High-Performance Liquid Chromatography-UV Detection", *Separation Science and Technology*, 52, 81–90, https://doi.org/10.1080/01496395.2016.1232273.

Jeannot, M.A. and Cantwell, F.F. (1996), "Solvent Microextraction into a Single Drop", *Analytical Chemistry*, 68, 2236-2240, https://doi.org/10.1021/ac960042z.

Jeannot, M.A. and Cantwell, F.F. (1997), "Mass Transfer Characteristics of Solvent Extraction into a Single Drop at the Tip of a Syringe Needle", *Analytical Chemistry*, 69, 235-239, https://doi.org/10.1021/ac960814r.

Kabir, A., Furton, K.G. and Malik, A. (2013), "Innovations in Sol–Gel Microextraction Phases for Solvent-Free Sample Preparation in Analytical Chemistry", *Trends in Analytical Chemistry*, 45, 197–218, https://doi.org/10.1016/j.trac.2012.11.014.

Kabir, A. and Furon, K.G. (2014), US Patent Application No. 14.216,121.

Kabir, A., Mesa, R., Jurmain, J. and Furton, K.G. (2017), "Fabric Phase Sorptive Extraction Explained", *Separations*, 4, 21, https://doi.org/10.3390/separations4020021.

https://doi.org/10.24264/icams-2022.V.8

Kabir, A. and Samanidou, V. (2021), "Fabric Phase Sorptive Extraction: A Paradigm Shift Approach, Analytical and Bioanalytical Sample Preparation", *Molecules*, 26, 865, https://doi.org/10.3390/molecules26040865.

Kaur, R., Kaur, R., Rani, S., Malik, A.K., Kabir, A. and Furton K.G. (2019), "Application of Fabric Phase Sorptive Extraction with Gas Chromatography and Mass Spectrometry for the Determination of Organophosphorus Pesticides in Selected Vegetable Samples", *Journal of Separation Science*, 42, 862–870, https://doi.org/10.1002/jssc.201800854.

Kumar, R., Gaurav, H., Malik, A.K., Kabir, A. and Furton, K.G. (2014), "Efficient Analysis of Selected Estrogens Using Fabric Phase Sorptive Extraction and High Performance Liquid Chromatography-Fluorescence Detection", *Journal of Chromatography A*, 1359, 16–25, https://doi.org/10.1016/j.chroma.2014.07.013.

Lakade, S.S., Borrull, F., Furton, K.G., Kabir, A., Marcé, R.M. and Fontanals, N. (2016), "Dynamic Fabric Phase Sorptive Extraction for a Group of Pharmaceuticals and Personal Care Products from Environmental Waters", *Journal of Chromatography A*, 1456, 19–26, https://doi.org/10.1016/j.chroma.2016.05.097.

Lucena, R. (2012), "Extraction and Stirring Integrated Techniques: Examples and Recent Advances", *Analytical and Bioanalytical Chemistry*, 403, 2213-2223, https://doi.org/10.1007/s00216-012-5826-9.

Pedersen-Bjergaard, S. and Rasmussen, K.E. (1999), "Liquid-Liquid-Liquid Microextraction for Sample Preparation of Biological Fluids Prior to Capillary Electrophoresis", *Analytical Chemistry*, 71, 2650-2656, https://doi.org/10.1021/ac990055.

Rezaee, M., Assadi, Y., Hosseini, M., Agnee, E., Ahmadi, F. and Berijani, S. (2006), "Determination of Organic Compounds in Water Using Dispersive Liquid–Liquid Micro-Extraction", *Journal of Chromatography A*, 1116, 1-9, https://doi.org/10.1016/j.chroma.2006.03.007.

Roldán-Pijuán, M., Lucena, R., Cárdenas, S., Valcárcel, M., Kabir, A. and Furton, K.G. (2015), "Stir Fabric Phase Sorptive Extraction for the Determination of Triazine Herbicides in Environmental Waters by Liquid Chromatography", *Journal of Chromatography A*, 1376, 35–45, https://doi.org/10.1016/j.chroma.2014.12.027.

Samanidou, V.F. and Kabir, A., (2015), "Fabric Phase Sorptive Extraction in Pharmaceutical Analysis", *Pharmaceutica Analytica Acta*, 6, 6–8, https://doi.org/10.4172/2153-2435.1000e177.

Shen, G. and Lee, H.K. (2002), "Hollow Fiber-Protected Liquid-Phase Microextraction of Triazine Herbicides", *Analytical Chemistry*, 74(2002), 648-654, https://doi.org/10.1021/ac010561o.

Silva, F., Universidade, S., Fluminense, F. and Semaan, F.S. (2017), "Sample Preparation in Food Analysis: Practices, Problems and Future Outlook", *Thermal Techniques and Their Applications*, pp. 23–53, ISBN 978-1-53612-282-4.

Zilfidou, E., Kabir, A., Furton, K.G. and Samanidou, V. (2018), "Fabric Phase Sorptive Extraction: Current State of the Art and Future Perspectives", *Separations*, 5, 40, https://doi.org/10.3390/separations5030040.

https://doi.org/10.24264/icams-2022.V.8

VI.

EDUCATION AND DIGITALIZATION

SMART TEXTILES DIGITALIZATION USING CREATIVE METHODS

RALUCA MARIA AILENI, CRISTINA STROE

The National Research & Development Institute for Textiles and Leather, Lucretiu Patrascanu 16, Bucharest, Romania, raluca.aileni@incdtp.ro, cristina.stroe@incdtp.ro

This paper presents several aspects concerning the digitalization implementation using creative learning and teaching methods in the Erasmus+ DigiTEX project framework. The DigiTex project developed an e-learning platform for the course and end-users management. The students and teachers accessed the platform after enrolling, which allows an association of the end-users with the universities. The database associated with the e-learning platform contains information about students, teachers, course categories and contains. In the framework of the DigiTEX Erasmus+ project, the e-learning platform Moodle DigiTEX was used during the Intensive Study Program in Athens, Greece (2022) and will be used in multiplier events by all partners.

Keywords: textile, digitalization, courses, e-learning.

INTRODUCTION

The e-learning tools and methods are very attractive for students not only in the context of the pandemic crisis (Huang *et al*., 2013; Zabolotniaia *et al*., 2020; Petrisor, 2021; Pastore *et al*., 2021), helping to increase motivation (Oproiu, 2015; Radulescu *et al*., 2022; Islam *et al*., 2022; Blaga *et al*., 2019), understanding lesson by individual study and avoiding the inconvenient of distance. Some studies show that for EFL Master students, e-learning courses can have a negative impact (Benadla and Hadji, 2021; Babalola *et al*., 2022).

In addition, a challenge in e-learning tools is to select the best tools, considering the system quality and facilities (Makruf *et al*., 2022).

In the context of the Intensive programs for higher education learners C1 - Creative methods for co-design/co-development of medical, protective, sensorial and smart textiles, the DigiTex consortium and students involved had the opportunity to test the e-learning Digitex Moodle platform and use it for individual study of the courses.

DIGITEX PLATFORM

In the project, Erasmus+ DigiTEX, a course management system (CMS) was used to create the e-learning DigiTEX Moodle platform (e-digitex.eu/moodle). This platform was customized for learning management to host learning materials (courses, videos, quizzes, grades, groups) necessary for learning and multiplier events. The end-users (students, trainers, professors) can easily connect to the DigiTEX Moodle platform using the section outputs from www.e-digitex.eu (Figure 1).

https://doi.org/10.24264/icams-2022.VI.1

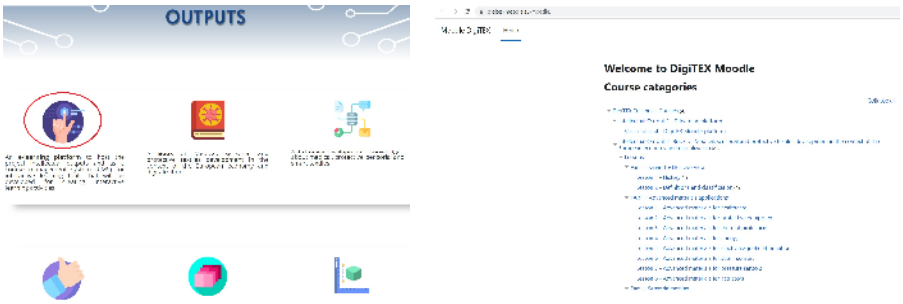

a.Moodle platform access from e-digitex.eu/outputs

b. DigiTex Moodle platform

Figure 1. DigiTex Moodle platform

The user login ensures the safety and privacy of sensitive personal data. The website administrator can enroll the users, and a password is generated automatically; the user is notified instantly. In this case, the user can change the password and is notified by email to access the link, which is valid for 30 minutes (Figure 2).

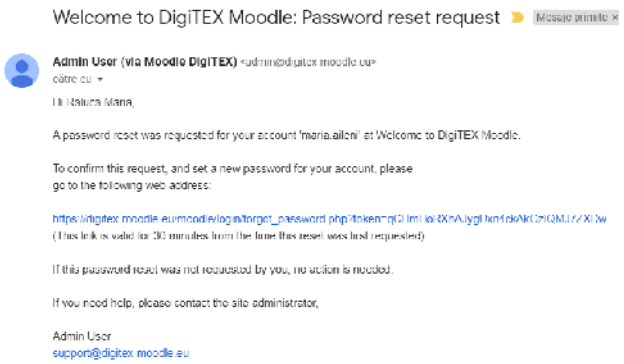

Figure 2. Password reset request

The platform integrates a database to manage the knowledge necessary for intellectual activities, learning, and teaching events. The information was adequately structured in a database for learning teaching activities in courses organized by categories.

The DigiTEX database developed contains several tables:

➔mdl_course_categories (Figure 3);
➔mdl_course (Figure 4);
➔mdl_enroll_student (Figure 5);
➔mdl_enroll_teacher (Figure 6).

https://doi.org/10.24264/icams-2022.VI.1

#	Name	Type	Collation	Attributes	Null	Default	Comments	Extra	Action
1	id	bigint			No	None		AUTO_INCREMENT	Change Drop More
2	name	varchar(255)	utf8_unicode_ci		No				Change Drop More
3	idnumber	varchar(100)	utf8_unicode_ci		Yes	NULL			Change Drop More
4	description	longtext	utf8_unicode_ci		Yes				Change Drop More
5	descriptionformat	tinyint			No	0			Change Drop More
6	parent	bigint			No	0			Change Drop More
7	sortorder	bigint			No	0			Change Drop More
8	coursecount	bigint			No	0			Change Drop More
9	visible	tinyint(1)			No	1			Change Drop More
10	visibleold	tinyint(1)			No	1			Change Drop More
11	timemodified	bigint			No	0			Change Drop More
12	depth	bigint			No	0			Change Drop More
13	path	varchar(255)	utf8_unicode_ci		No				Change Drop More
14	theme	varchar(50)	utf8_unicode_ci		Yes	NULL			Change Drop More

Figure 3. Table mdl_course_categories – DigiTex Moodle

#	Name	Type	Collation	Attributes	Null	Default	Comments	Extra	Action
1	id	bigint			No	None		AUTO_INCREMENT	Change Drop More
2	category	bigint			No	0			Change Drop More
3	sortorder	bigint			No	0			Change Drop More
4	fullname	varchar(254)	utf8_unicode_ci		No				Change Drop More
5	shortname	varchar(255)	utf8_unicode_ci		No				Change Drop More
6	idnumber	varchar(100)	utf8_unicode_ci		No				Change Drop More
7	summary	longtext	utf8_unicode_ci		Yes				Change Drop More
8	summaryformat	tinyint			No	0			Change Drop More
9	format	varchar(21)	utf8_unicode_ci		No	topics			Change Drop More
10	showgrades	tinyint			No	1			Change Drop More
11	newsitems	mediumint			No	1			Change Drop More

Figure 4. Table mdl_course – DigiTex Moodle

#	Name	Type	Collation	Attributes	Null	Default	Comments	Extra	Action
1	ID	bigint			No	None			Change Drop More
2	Enroll	varchar(20)	utf8mb4_unicode_ci		No	None			Change Drop More
3	Identification Code	int			No	None			Change Drop More
4	Name	char(40)	utf8mb4_unicode_ci		No	None			Change Drop More
5	Password	varchar(20)	utf8mb4_unicode_ci		No	None			Change Drop More
6	CourseID	bigint			No	None			Change Drop More
7	University	varchar(40)	utf8mb4_unicode_ci		No	None			Change Drop More

Figure 5. Table mdl_enroll_student – DigiTex Moodle

#	Name	Type	Collation	Attributes	Null	Default	Comments	Extra	Action
1	ID	bigint			No	None		AUTO_INCREMENT	Change Drop More
2	Enroll	bigint			No	None			Change Drop More
3	University	varchar(40)	utf8mb4_unicode_ci		No	None			Change Drop More
4	Name	char(40)	utf8mb4_unicode_ci		No	None			Change Drop More
5	ID Course	bigint			No	None			Change Drop More
6	Username	varchar(20)	utf8mb4_unicode_ci		No	None			Change Drop More
7	Password	varchar(20)	utf8mb4_unicode_ci		No	None			Change Drop More

Figure 6. Table mdl_enroll_teacher – DigiTex Moodle

https://doi.org/10.24264/icams-2022.VI.1

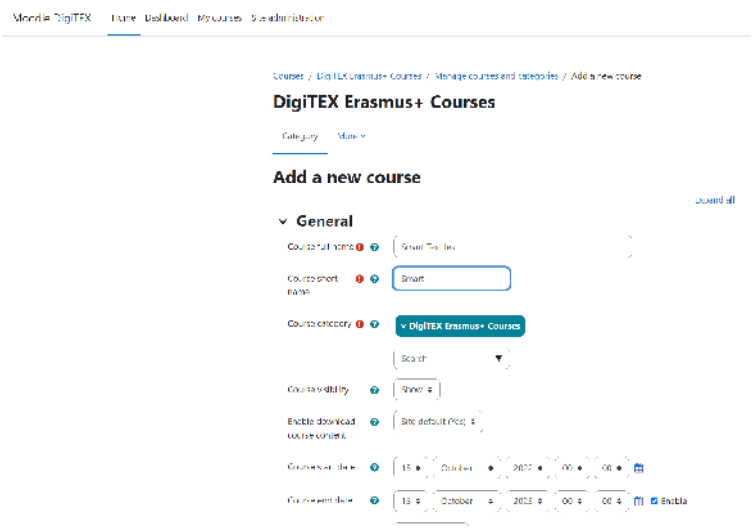

Figure 7. Teacher account – creating new courses

The platform developed allows login for 3 types of users (administrator, teacher (Figure 7) and student), each with different permission rights. The administrator can add courses can enroll/remove students and teachers from a specific course. The teacher can create courses (Figure 7), and the user students can see enrolled courses (figure 8).

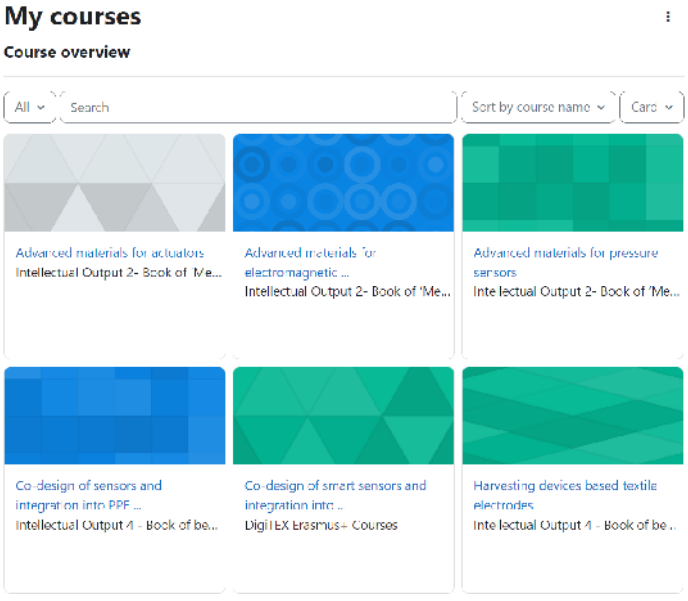

Figure 8. Student account – course overview

https://doi.org/10.24264/icams-2022.VI.1

In the framework of the DigiTex project, the INCDTP integrated into DigiTex Moodle platform six-course modules (Advanced materials for pressure sensors, Advanced materials for actuators, Co-design of smart sensors and integration into medical devices, Advanced materials for electromagnetic attenuation, Harvesting devices based textile electrodes, Co-design of sensors and integration into PPE products for fire and water protection).

CONCLUSIONS

In the intensive programmes for higher education learners C1 - Creative methods for co-design/co-development of medical, protective, sensorial and smart textiles, the students appreciated that this tool is very attractive, friendly and valuable for interactive and individual learning using creative methods. However, online learning cannot replace classical learning methods but can provide new added value. In the framework of the DigiTex Erasmus+ project, two intellectual outputs having course results have been integrated into the Digitex e-learning platform.

Acknowledgment

The research presented in this paper was prepared within INCDTP. Funds that support this work are from the Erasmus+ programme of the European Union, Project DigiTEX "Textile digitalization based on digital education and innovative e-Tools," agreement no. 2020-1-RO01-KA226-HE-095335.

This publication reflects the views only of the author, and the Commission cannot be held responsible for any use which may be made of the information contained therein.

REFERENCES

Babalola, E.O., Otunla, F.L. and Omolafe, E.V. (2022), "Undergraduates' Level of Acceptance and Utilization of Moodle Platform for Learning during Covid-19 Pandemic", *Indonesian Journal of Multidiciplinary Research*, 3(1), 31-40.

Benadla, D. and Hadji, M. (2021), "EFL Students Affective Attitudes towards Distance E-Learning Based on Moodle Platform during the Covid-19 Pandemic: Perspectives from Dr. MoulayTahar University of Saida, Algeria", *Arab World English Journal (AWEJ)*, Special Issue on Covid-19 Challenges, 55-67, https://doi.org/10.31235/osf.io/4xepz.

Blaga, M., Rădulescu, I.R., Van Langenhove, L., Stjepanovič, Z., Dias, A. and Dufkova, P. (2019), "Smart Education for Smart Textiles", *19th World Textile Conference on Textiles at the Crossroads*, Autex, https://doi.org/10.35530/TT.2019.38.

Huang, C.C., Wang, Y.M., Wu, T.W. and Wang, P.A. (2013), "An Empirical Analysis of the Antecedents and Performance Consequences of Using the Moodle Platform," *International Journal of Information and Education Technology*, 3(2), p.217, https://doi.org/10.7763/IJIET.2013.V3.267.

Islam, M.K., Sarker, M.F.H. and Islam, M.S. (2022), "Promoting Student-Centred Blended Learning in Higher Education: A Model", *E-Learning and Digital Media*, 19(1), 36-54, https://doi.org/10.1177/20427530211027721.

Makruf, I., Rifa'i, A.A. and Triana, Y. (2022), "Moodle-Based Online Learning Management in Higher Education", *International Journal of Instruction*, 15(1), 135-152, https://doi.org/10.29333/iji.2022.1518a.

Oproiu, G.C. (2015), "A Study about Using e-learning Platform (Moodle) in University Teaching Process", *Procedia-Social and Behavioral Sciences*, 180, 426-432, https://doi.org/10.1016/j.sbspro.2015.02.140.

Pastore, C., Kyosev, Y., Fassihi, A.A. and Flax, B. (2021), "Textile Education during the 2020 Pandemic: Experiences in US, South Africa and Germany", *Communications in Development and Assembling of Textile Products*, 2(1), 18-33, https://doi.org/10.25367/cdatp.2021.2.p18-33.

Petrişor, R.M. and Petrişor, S.M. (2021), "Digital Permanences in the Contemporary Educational Space. The Moodle Elearning Platform", *Land Forces Academy Review*, 26(1), 45-48, https://doi.org/10.2478/raft-2021-0007.

Radulescu, I.R., Dinis, A., Malengier, B., Cupar, A., Blaga, M. and Polansky, R. (2022), "E-learning Course of Software for Textile Design".

Zabolotniaia, M., Cheng, Z., Dorozhkin, E. and Lyzhin, A. (2020), "Use of the LMS Moodle for an Effective Implementation of an Innovative Policy in Higher Educational Institutions," *International Journal of Emerging Technologies in Learning (iJET)*, 15(13), 172-189, https://doi.org/10.3991/ijet.v15i13.14945.

https://doi.org/10.24264/icams-2022.VI.1

ANALYSIS OF THE LEARNING REQUIREMENTS OF LESS ADVANTAGED GROUPS ON THE ROMANIAN LEVEL

MARIAN CATALIN GROSU[1], ION RAZVAN RADULESCU[1], EMILIA VISILEANU[1], IRINA IONESCU[2], MANUELA AVADANEI[2], SABINA OLARU[1], XIANYI ZENG[3], SHEILA ODHIAMBO[4], ALEXANDRA CARDOSO[5], ANDREJA RUDOLF[6]

[1] *The National Research & Development Institute for Textiles and Leather, 16, Lucretiu Patrascanu, Sector 3, 030508.Bucharest, Romania, catalin.grosu@incdtp.ro; razvan.radulescu@incdtp.ro; e.visileanu@incdtp.ro*

[2] *Faculty of Industrial Design and Business Management, 29, Prof. Dr. Doc. Dimitrie Mangeron, 700050, Iasi, Romania, iirina@tex.tuiasi.ro; mavad@tex.tuiasi.ro*

[3] *The National School of Textile Arts and Industries- Ensait, Roubaix Cedex 1, France, xianyi.zeng@ensait.fr*

[4] *Hogeschool Gent - HOGENT, Geraard de Duivelstraat 5, 9000 Gent, Belgium, sheillatienoodhiambo@gmail.com*

[5] *CITEVE, Rua Fernando Mesquita, Vila Nova de Famalicão PORTUGAL acardoso@citeve.pt*

[6] *Faculty of Mechanical Engineering, University of Maribor, Smetanova ulica 17, 2000 Maribor, Slovenia andreja.rudolf@um,si*

The paper provides an analysis of the learning requirements of less advantaged groups on the national level, as a task in the framework of Digital Fashion Erasmus+ project. The first part of the analysis focused on the various groups of students from the "Gheorghe Asachi" Technical University of Iaşi with special physical and social situations, who benefited from online courses, in the pandemic context. The second part of the analysis focused on nine textile companies that respond to a questionnaire of INCDTP regarding the facilities offered for less advantaged groups of workers. Persons with minor impairments and of other nationalities are supported and integrated into textile enterprises. Depending on the type of difficulty, including the emergency due to the pandemic, various support actions were provided by the textile and clothing enterprises. The educational materials of Erasmus+ DigitalFashion will be conceived in six European languages. Students and professionals in the field of textiles and clothing may benefit from multilingual educational materials, identification of technical terms, and a multicultural environment.

Keywords: online training, disadvantaged groups, textile industry.

INTRODUCTION

Learning has positive benefits for individuals, communities, society, and the wider economy. Individuals face a range of situational, institutional, and dispositional barriers as they navigate learning opportunities (Pennacchia *et al*., 2018). The most disadvantaged learners were more likely to describe the cumulative effect of multiple barriers to learning. The disadvantaged groups include persons with disabilities and health conditions, such as the visually impaired, hearing impaired, mobility impaired; single parents; ethnic minorities, migrants, as well as persons of other nationalities, who have difficulties adapting to the workplace (Johansson and Höjer, 2012). The pandemic left a mark on the whole world and generated a dramatic need for change and adaptation in any field (Kecojevic *et al*., 2020). The shift from face-to-face to online teaching represented a big challenge for education institutions, and it's hard work to find solutions to continuing the courses (El-Soussi, 2022). People with a special social situation were disadvantaged in this period, more than in the pre-pandemic period (Raccanello *et al*., 2022). Advances in computer-based education are seen as an effective way of remedying this situation by providing assistance and compensation for

https://doi.org/10.24264/icams-2022.VI.2

learners with specific needs (Cinquin *et al*., 2019). Online training offers a lot of benefits, such as flexible learning hours, distance learning, and multimedia support. In the last years, the design of e-learning environments was improved, to support students' emotional well-being and performance (Mayer, 2020). The paper presents the situation of the less advantaged group (students and workers) involved in the textile & clothing field and aims to evidence the need for training for people with disabilities, to support them with adequate instruments, including online training, as the objective of DigitalFashion Erasmus + European project.

DIGITAL FASHION ERASMUS + PROJECT

The International Erasmus + Digital Fashion project aims to open the pathways for organizing Collaborative Online International Learning within partner institutions, other higher educational institutions, and industrial enterprises of common expertise and is addressed to higher education institution (HEI) students and young professionals, both in the textile field. Among them, special attention is given to people from disadvantaged groups, including those with disabilities. The project will create a collaborative international online teaching platform (COIL) that offers advantages to distance learning, facilitating the access of disadvantaged learners across national borders. The proposed training platform is a software system with non-discriminatory interfaces for users, which promotes equal opportunities and eliminates language barriers, being translated into six languages (English, French, Portuguese, Slovenian, Romanian, and Dutch). The platform that will be created within the project will contain a series of specific elements in a synergic way, as follows: *3D human, 3D garments, fabric, and fashion databases; Fashion and garment-making rules; Basic search engine; Online learning module (methods, process, content, and cases); Testing and evaluation; Websites of the project and partners institutions; User interface;*

In this regard, the "Gheorghe Asachi" Technical University of Iași (TUIASI) has analyzed the situation of less advantaged groups of students within the university. The National Research & Development Institute of Textiles and Leather (INCDTP) has analyzed the situation of the less advantaged groups among the employees of the textile industry, by questioning nine Textile & Clothing enterprises in this regard. In comparison, the situation from partner countries Portugal and Slovenia regarding the less advantaged group of textile students and workers is presented.

THE CONDITIONS OF STUDY FOR LESS ADVANTAGED GROUPS OF STUDENTS AND WORKERS

In TUIASI, there are enrolled 13000 (bachelor's, master and doctoral studies) students regardless of their race, religion, nationality, or state of health. Anyway, in the admittance process, future students are asked for a medical exam sheet. The family doctor or the TUIASI doctor just confirms that the candidate can follow the studies. These do not exclude the admission of less advantaged people. The Faculty of Industrial Design and Business Management (DIMA) has about 1000 students.

In TUIASI, 6 different types of less advantaged groups were identified and estimated as percentages, in Table 1.

https://doi.org/10.24264/icams-2022.VI.2

Table 1. The less advantaged groups at TUIASI

From abroad	Different ethnicity	Learning foreign languages
~ 5% (increasing year by year)	~1% Romany ethnicity	64 specializations learning in a foreign language
With special conditions	With impairments	With socio-economic problems
~ 5% of mothers/fathers	~ 1% - with speech and movement impairments	200 places for rural areas (2020/2021 academic year)

At the University of Maribor, there are comparative data in the last 3 years, of the students from the less advantaged group, presented in Table 2. From their total, in 2022, people with visual, hearing, and movement impairments represent 6.03%, up 41.5% compared to 2020. People with special status (parents, top athletes, recognized artists, long-term ill) represent 2022 93.96% of the total, a slight decrease of almost 1% compared to 2020. At the Faculty of Mechanical Engineering from University of Maribor, students with impairments represent ~11% in 2022, a decrease of almost 50% compared to 2020. People with special status represent almost 89% in 2022, an increase of 10% compared to 2020.

Table 2. The less advantaged groups at University of Maribor

Impairments (hearing, visual, movement)			Special status (mother/father, top athletes, recognized artists, long-term ill)		
2019/2020	2020/2021	2021/2022	2019/2020	2020/2021	2021/2022
6	9	12	164	177	187

With 123 employees (54 researchers) INCDTP has single 2 persons with minor mobility impairments. According to internal rules, these persons received additional support of 15% of the salary.

CITEVE, Technological Centre for the Textile and Clothing Industries of Portugal has 147 employees and 3 are disabled which need integration measures in workplaces.

Support Measurements for the Persons from the Less Advantaged Group

While in TUIASI, the support measurements concentrate on persons from abroad, especially from the Republic of Moldavia and Ukraine, of those with different ethnicity (e.g. Romany), with socio-economical problems (from rural areas), in Portugal, the emphasis is to disseminate and promote good practices in the disability area and to promote the international mobility of disabled students/teachers within Europe through the Erasmus+ Programme. More, there are measures for adopting Inclusive Signage and ColorADD Project – facilitating/providing an interpretation of information through universal signs and legends.

The Slovenian Association of Disabled Students with 212 members identified, for the adaptation, during the online courses, to the needs of students with disabilities including: “spotlight” feature that allows fixing video images of people who are actively involved in the delivery of the event (e.g., lip reading of the lecturer) and sign language interpreter for the students with hearing impairments; larger size and different styles of font and contrast in the color of the background and letters for the students with visual impairments and dyslexia.

Due to the good connections to the textile&clothing industry, INCDTP proposed to describe the support and training measures for persons with impairments in T&C

https://doi.org/10.24264/icams-2022.VI.2

enterprises. A survey with 6 questions was collected from 9 T&C enterprises, including the situation of the R&D institute itself, to assess the support and training measures of less advantaged groups within the T&C industry.

The first question was related to the type of disabilities of the employees, integrated within the working teams. Two enterprises out of 8 responded they do not have in their working teams people with disabilities (Fig. 1). A total number of 2 organizations each reported visual, hearing, and psychic impairments, while three organizations reported mobility impairments. Other impairments are presented in Fig. 2.

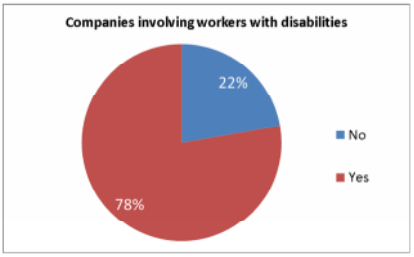

Figure 1. Companies involving workers with disabilities

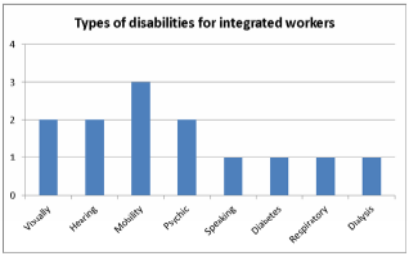

Figure 2. Types of disabilities for the integrated workers

As such, workers with minor disabilities are employed within the working teams of textile enterprises in 78% of the cases, with widespread types of impairments.

The second question was related to the support measures for workers with disabilities. The nine respondents pointed out some measures, presented in Fig 3. The following specific measures were also pointed out in Fig. 4.

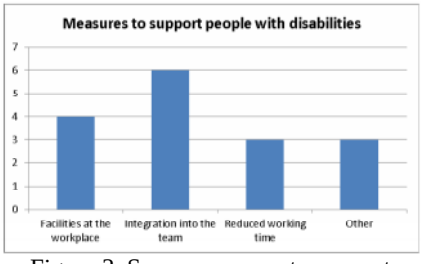

Figure 3. Some measures to support people with disabilities

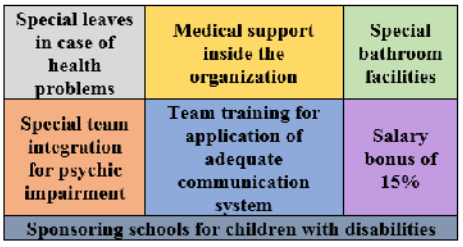

Figure 4. Specific measures to support workers with disabilities

Tax Reduction for Workers with Disabilities

In Romania, persons with disabilities are freed from paying income tax. Two enterprises have mentioned special measures in this regard: The first enterprise stated that customer loyalty is strengthened by communicating the support for workers with disabilities; the Second enterprise stated that workers with dialyzes benefit from the tax reduction.

Language Training and Support of Workers of Other Nationalities

Out of the nine respondents, six enterprises do not employ workers of other nationalities. Of the rest of the three enterprises, two enterprises (22%) organize training courses in the Romanian language for support and integration of the workers (Fig. 5).

https://doi.org/10.24264/icams-2022.VI.2

Other support measures for workers of other nationalities include logistics support, professional training courses, and consulting for integration (Fig. 6).

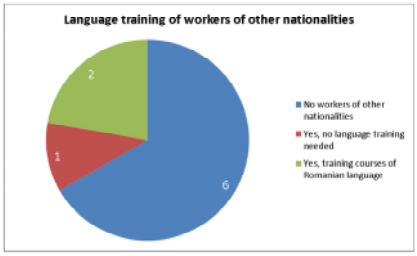

Figure 5. Language training of workers of other nationalities

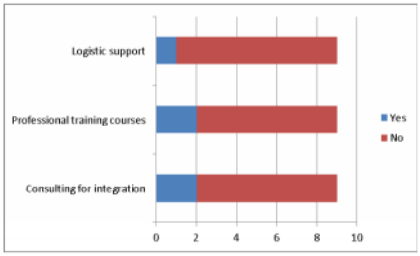

Figure 6. Other facilities for integration

Telework on the Romanian National Level and for T&C Enterprises

The second part of the survey analyses the measures taken by textile enterprises during the coronavirus pandemic.

According to a survey conducted by Genesis Property in February-March 2021, conducted on a total number of 1183 Internet users in Romania, 55% of the interviewed employees answered they are working either partially (17.3%) or exclusively (37.4%) from the location of the enterprise. 41% of the respondents have declared their office is safer, compared to the beginning of the pandemic, and are satisfied with the current work modality. Another 45% of the respondents reported their perception of the workplace within this context is neutral (Dobrescu, 2021).

The situation of telework in the T&C industry was assessed based on the survey conducted by INCDTP - Bucharest. The first question was related to the possibility of telework for the employees. Out of the nine respondents, only two textile & clothing enterprises and the research institute replied that partial telework was possible. Textiles being a manufacturing domain, where the employees have to work on machines, telework could be organized only in limited cases, with a focus on the administrative personnel of the enterprises (Fig. 7). The impossibility to organize telework for the manufacturing personnel was however accompanied by additional safety measures for the Coronavirus pandemic.

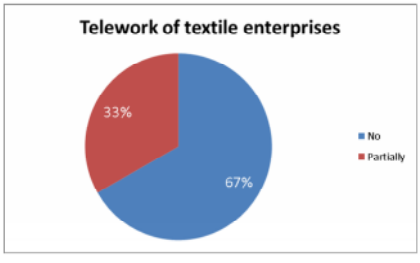

Figure 7. Telework of textile companies from Romania

INCDTP – Bucharest could also partially organize telework for researchers that worked on the analysis and interpretation of experimental data and research studies. However, the technicians had to be present at the workplace, to work with the testing equipment within the laboratories.

https://doi.org/10.24264/icams-2022.VI.2

Additional Safety Measures for the Coronavirus Pandemic

All of the nine interviewed textile and clothing enterprises provided additional safety measures for workers, such as masks and disinfectants, while three of them ensured a larger physical distance by reorganizing the workplace. Some of the other additional safety measures were: Providing medical leaves; Providing drugs; Free COVID-19 testing; Frequent disinfection of workplaces; Different time schedules; Doubling the transport capacity to the workplace.

CONCLUSIONS

The situation of disadvantaged groups of students and workers in textiles was is differently approached in the consortium countries of the Digital fashion Erasmus + project. In Romania, the two major education and training players, DIMA and INCDTP support less advantaged groups of students, especially those from abroad and with socio-economic problems. In Portugal and Slovenia, the emphasis is to disseminate and promote good practices in the disability area and to promote international mobilities and various technics to facilitate the interpretation of information through universal signs and legends.

Online training may provide support for both advantaged and disadvantaged groups of students and workers in the textile field. The disadvantaged groups of persons need special requirements and assistive technologies of online training. The training instruments provided by the DigitalFashion project are accessible for students and employees in textiles with minor impairments too. Students and workers with mobility impairment, which was reported as the most frequent impairment, may benefit from distance learning and flexible learning hours. Students and workers from abroad may benefit from the multilingual educational materials of DigitalFashion too. The virtual educational instruments envisaged by DigitalFashion will integrate less advantaged groups of persons through education and training into the textile community and the world of work.

REFERENCES

Cinquin, P.A., Guitton, P. and Sauzéon, H. (2019), "Online e-learning and Cognitive Disabilities: A Systematic Review", *Computers and Education*, 130, 152–167, https://doi.org/10.1016/j.compedu.2018.12.004.

Dobrescu, E.M. (2021), "Telework: Comparative Study" (in Romanian), *Geopolitica între realitate și emoții, între istorie și mit*, available at: https://corneliupivariu.com/telemunca-studiu-comparativ.

El-Soussi, A. (2022), "The Shift from Face-to-Face to Online Teaching Due to COVID-19: Its Impact on Higher Education Faculty's Professional Identity", *International Journal of Educational Research Open*, 3, 100139, https://doi.org/10.1016/j.ijedro.2022.100139.

Johansson, H. and Höjer, I. (2012), "Education for Disadvantaged Groups – Structural and Individual Challenges", *Children and Youth Services Review*, 34(6), 1135-1142, https://doi.org/10.1016/j.childyouth.2012.01.042.

Kecojevic, A., Basch, C.H., Sullivan, M. and Davi, N.K. (2020), "The Impact of the COVID-19 Epidemic on Mental Health of Undergraduate Students in New Jersey, Crosssectional Study", *PLoS One*, 15(9), e0239696, https://doi.org/10.1371/journal.pone.0239696.

Pennacchia, J., Jones, E. and Aldrigde, F. (2018), "Barriers to Learning for Disadvantaged Groups, Report of Qualitative Findings", Department for Education, Publishing: Social Science in Government.

Raccanello, D., Balbontín-Alvarado, R., da Silva Bezerra, D., Burro, R., Cheraghi, M., Dobrowolska, B., Fagbamigbe, A.F., Faris, M.E., França, T., González-Fernández, B., Hall, R., Inasius, F., Kar, S.K., Keržič, D., Lazányi, K., Lazăr, F., Machin-Mastromatteo, J.D., Marôco, J., Marques, B.P., Mejía-Rodríguez, O., Méndez Prado, S.M., Mishra, A., Mollica, C., Navarro Jiménez, S.G., Obadić, A., Mamun-ur-Rashid, M., Ravšelj, D., Tatalović Vorkapić, S., Tomaževič, N., Uleanya, C., Umek, L., Vicentini, G., Yorulmaz, Ö., Zamfir, A.-M. and Aristovnik, A. (2022), "Higher Education Students' Achievement Emotions and Their Antecedents in e-learning amid COVID-19 Pandemic: A Multi-Country Survey", *Learning and Instruction*, 80, 101629, https://doi.org/10.1016/j.learninstruc.2022.101629.

IMPACT OF INTENSIVE STUDY PROGRAMS ON HIGHER EDUCATION STUDENTS IN THE FIELD OF DESIGN AND MODELLING OF TEXTILE MATERIALS

ION RAZVAN RADULESCU[1], EMILIA VISILEANU[1], RAZVAN SCARLAT[1], MARIAN CATALIN GROSU[1], ANA DIAS[2], BENNY MALENGIER[3], ZORAN STJEPANOVIC[4], MIRELA BLAGA[5], RADEK POLANSKY[6]

[1] *The National Research & Development Institute for Textiles and Leather, L. Patrascanu 16, 030508 Bucharest, Romania, razvan.radulescu@incdtp.ro, e.visileanu@incdtp.ro, razvan.scarlat@incdtp.ro, catalin.grosu@incdtp.ro*

[2] *TecMinho, Interface of the University of Minho, Campus de Azurém, 4800-058, Guimaraes, Portugal, anadias@tecminho.uminho.pt*

[3] *Ghent University, Faculty of Engineering and Architecture, MATCH, Zwijnaarde 70A, 9000, Ghent, Belgium, benny.malengier@ugent.be*

[4] *University of Maribor, Faculty of Mechanical Engineering, Smetanova ulica 17, 2000 Maribor, Slovenia, zoran.stjepanovic@um.si*

[5] *Technical University IASI, Faculty DIMA, Str. D. Mangeron 29, 700050 Iasi, Romania, mirela.blaga@tex.tuasi.ro*

[6] *University West Bohemia, Faculty of Electrical Engineering, Univerzitní 2795/26, 301 00 Pilsen, Czech Republic, rpolansk@fel.zcu.cz*

The knowledge of software for design and modelling of textiles offers a competitive advantage within the world of work for young textile creatives. The Erasmus+ project OptimTex – "Software tools for textile creatives" has created a large set of educational materials and the corresponding e-learning resources in this competitive domain. Six educational modules, one Moodle e-learning platform with courses in six national languages, one e-learning instrument for quick access to the content and one glossary of terms were implemented during the two-year's project 2020-2022 (www.optimtex.eu). Two Intensive Study Programs (ISPs) of five days were already organized by the project's partners: one virtual ISP with the host Technical University of Iasi and one mobility ISP with the host University of Maribor. A total number of 27 students and 15 lecturers participated in the first ISP and a total number of 17 students and 12 lecturers participated in the second ISP. The six modules for Design and Modelling of woven structures, knitted structures, virtual prototyping of clothing, embroidered e-textiles, design of experiments, and TechTransfer had a high impact on the students. The impact was measured by feedback questionnaires and the interest in e-learning resources by the number of accesses (www.advan2tex.eu/portal/). This paper presents the impact of the educational materials on Higher Education students in relation to the envisaged objectives of the project.

Keywords: intensive study, textile design, modelling, virtual prototyping.

INTRODUCTION

The modelling of the digital future of Europe is our way to a better life and a big step to "green transition" and "climatic neutrality until 2050" (European Parliament, 2021).

While digitization represents the transition from analogue data to digital formats, and digitization is the way to use digitized information in current activity, digital transformation represents a significant pillar of development and implies the creation of completely new business concepts taking advantage of digitization (Webactiv, 2020). In the actual era, this concept is continuing wide spreading in every technical and technological domain. More, the concept is a common instrument in every daily life.

The use of digital tools in all sectors of activity is growing exponentially (Díaz Redondo *et al*., 2021). It is also the case in the textile industry, where many types of textile design software have been created to make the work of the textile industry easier

https://doi.org/10.24264/icams-2022.VI.3

and faster (Avadanei *et al*., 2020). Several textile design software is available as work and control tools, fast and efficient for both students and employees, ranging from design and graphic tools to business administration and quality control tools.

Educational systems have to adapt to the latest IT development, as beyond traditional education, the virtual education provides excellent opportunities for both teaching and learning (Rusu *et al*., 2018). The e-learning and micro-learning instruments are effective at achieving good outcomes, and the advantages they offer are especially great, compared to traditional instruments (Andron and Kifor, 2021). Research shows that on average, students retain between 25-60% more through online learning than they do in traditional classroom settings. Other studies show that, because it is self-paced, e-learning leads to increased student satisfaction and reduced stress. Today's learners want bite-sized information fast and on demand. And research suggests that this kind of microlearning makes learning 17 % more effective.

By implementing its objectives: preparing new educational materials on up-to-date textile design software applications; improving the employability of textile creatives within industry & research using adequate tools; fostering digital skills uptake by implementing e-learning instruments and creating educational synergies by enabling student mobility, the Erasmus+ project "Software tools for textile creatives - OptimTex" promotes the use of digital resources in the learning process (Radulescu *et al*., 2022). In this regard, the two intensive study programs (ISPs): one virtual ISP with the host Technical University of Iasi and one mobility ISP with the host University of Maribor were special exploitation activities accomplished within the second year of the project 2022, based on the educational materials conceived in the first year of the project 2021.

INTENSIVE STUDY PROGRAMS (ISP)

The organization of the ISPs with educational purpose is a major task within the implementation of the project's objectives, having as benefit the creation of inter-disciplinary and multi-cultural synergies between partner universities' expertise. Within these ISPs, the 6 modules (Figure 1) were presented interactively. The modules are available as e-learning courses on the Moodle platform (www.advan2tex.eu/portal/), in all the national languages of the project (CZ, DU, EN, PT, RO, SI).

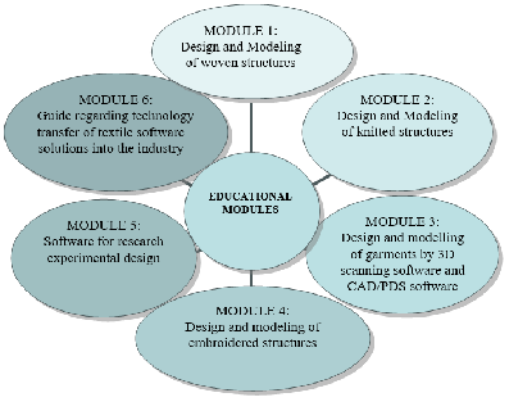

Figure 1. The 6 modules for design of e-textiles

https://doi.org/10.24264/icams-2022.VI.3

All the project partners have participated in the development of the ISPs. The main data of the already organized two ISPs every five days are presented in Table 1:

Table 1. Main information about the two ISPs

ISP	1st ISP – 21-25.03.2022	2nd ISP – 30.05 – 03.06.2022
Coordinator	The National Research & Development Institute for Textiles and Leather (INCDTP)	
Host	"Gheorghe Asachi" Technical University of Iasi (TUIASI)	University of Maribor (UM) University West Bohemia (UWB)
Presence	Virtual – Webex meetings (pandemic context)	With mobility of students and lecturers
Participants	27 students and 15 lecturers	17 students and 12 lecturers
Study modules	Design software for weaving; Design software for knitting; Design software for virtual prototyping of clothing; Design software for embroidery; Design software for experimental design of e-textiles;	
Main focus	Design and modelling of knitted structures - TUIASI	Design software for virtual prototyping of clothing – UM Design software for embroidery - UWB
Virtual platform	Project website www.optimtex.eu TAB E-learning (Moodle)	
E-learning instrument	Project website www.optimtex.eu TAB Instrument (JavaScript)	
Glossary of terms	Project website www.optimtex.eu TAB Glossary (PHP / MySQL)	
Q&A and Forum	yes	yes
Certificates	yes	yes

RESULTS

Beneficiary students of ISPs participated in completing an online feedback questionnaire. The content of the questionnaire includes 9 topics, which reflected the level of accessibility and diversity of the modules, the degree of matching of the course with each student's field of study, practical training with software in textile design, contribution to personal development, duration and structure of the course, course support materials, organization and logistics of the course, evaluation of the lecturers/teachers and the e-learning interaction.

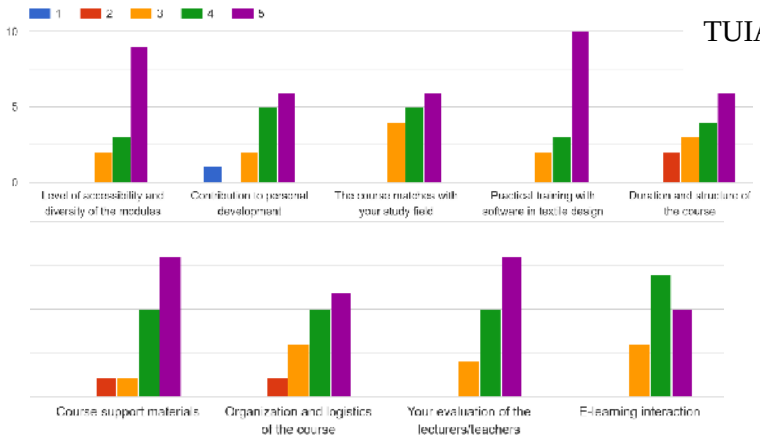

TUIASI

Figure 2. The level of appreciation regarding the organization of the course, by scores from 1 to 5 – ISP TUIASI

https://doi.org/10.24264/icams-2022.VI.3

The level of perception and satisfaction throughout the duration of the 1st ISP with host TUIASI are presented in Figure 2 (organization of the course) and Figure 3 (modules).

In the second section of the questionnaire, that means evaluation of lecturers and practical work of the modules, the students ranked the 6 studied modules according to their level of appreciation with scores from 1 to 6.

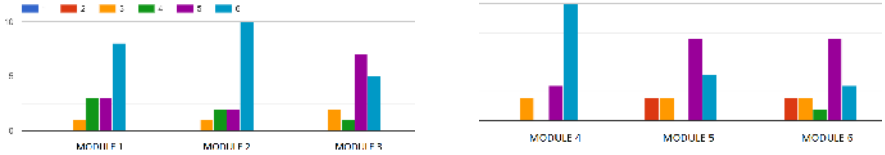

Figure 3. Ranking, by the respondents, lecturers and practical work of the modules, from the point of view of the degree of appreciation – ISP TUIASI

At section one of the questionnaire, the level of satisfaction regarding the organization of the 1st ISP courses was very high, the scores of 4-5 representing about 86% of the received responses. Special good impact was achieved at level of the accessibility of the course and practical training, as well as course support materials and support of lecturers. Less impact was related to personal development and matching with the study field, an aspect to be improved. Regarding e-learning interaction, the trainees had three weeks to study on Moodle the modules of the course, after the ISP course week. One reason the e-learning indicator was less evaluated is the completion of the questionnaire just at the end of the first ISP course week.

18 users, 16 new users, 28 pages views and a bounce rate of 70% were achieved on Moodle LMS, according to Google Analytics access monitoring during the four weeks of course. At section two of the questionnaire, the most appreciated module was the Knitting module, due to the practical work and the possibility to access the computer software of the Knitting LAB at TUIASI via TeamViewer. Second and third place was the weaving and embroidery module, also for the good showcasing of design software. During practical work with knitting, there was possible to manufacture the OptimTex flag on the knitted sample (Figure 4).

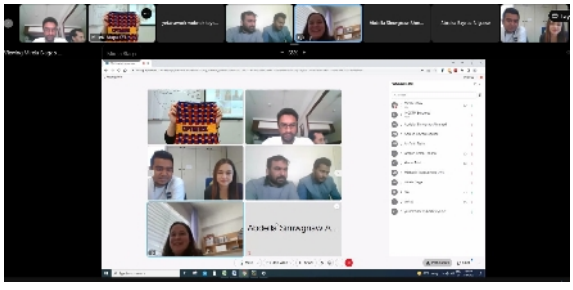

Figure 4. Print screen of the virtual course with the OptimTex flag

11 trainees had responded at the survey of the second ISP with host University of Maribor (Figures 5-6). A great impact was achieved with organization and logistics as well as with the support of the lecturers. Less impact was achieved with the course

https://doi.org/10.24264/icams-2022.VI.3

support materials and the matching with the domain of activity, however with a predominant score of 4, which means very satisfied.

Google Analytics presented similar interest regarding Moodle e-learning. The e-learning instrument and the Glossary of terms was accessed by 45 users during first ISP and by 38 users during the second ISP. Section two of the questionnaire shows best scores for the modules of Embroidery and Virtual Prototyping, due to the extensive and very successful practical work. The students had the possibility to design in Inkscape / Inkstich the leaking sensor and to embed some electrical components on the electric circuit of the fabric (Figure 7). They had also the possibility to experience 3D scanning of the own body and virtual prototyping software.

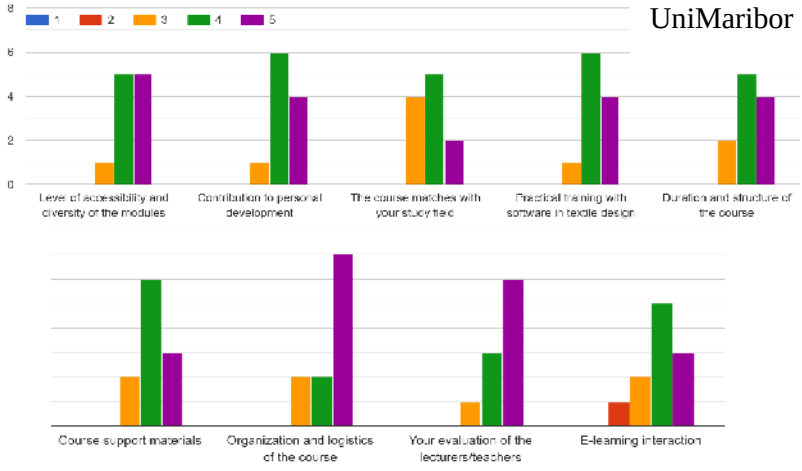

Figure 5. The level of appreciation regarding the organization of the course, by scores from 1 to 5 – ISP UniMaribor

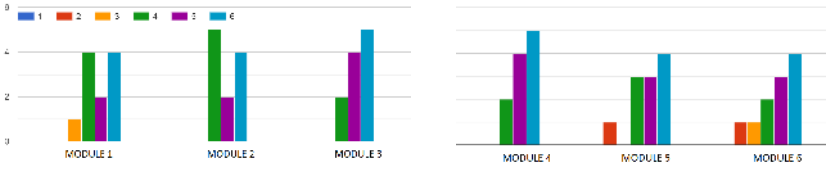

Figure 6. Ranking, by the respondents, of the modules studied, from the point of view of the degree of appreciation – ISP UniMaribor

All students of the ISP UniMaribor received certificates of attendance. The overall impact of the course was especially high and this was also reflected by the interviews registered on the OptimTex Youtube channel at: https://www.youtube.com/channel/UCMOSSavcYoiX2ygrIKx7gGg. The Youtube channel may be accessed via the optimtex.eu website TAB Multimedia.

https://doi.org/10.24264/icams-2022.VI.3

Figure 7. Practical work with embroidery of e-textiles at ISP UniMaribor

CONCLUSIONS

The educational materials of Erasmus+ OptimTex project are available in e-learning format on the Moodle platform and on the project's website. Knowledge in software for design of textiles was taught for Higher Education students within two ISP courses. Feed-back questionnaires revealed a high interest of the participants and a good organization of the courses. A third ISP will be organized in October 2022 at Ghent University.

Acknowledgement

This project was funded with support of the European Commission, Erasmus+ KA2 project "Software tools for textile creatives-OptimTex", grant agreement number 2020-1-RO01-KA203-079823. The publication of the scientific paper is funded by the Ministry of Research, Innovation and Digitization within Program 1 – Development of the national R&D system, Subprogram 1.2 – Institutional Performance – RDI excellence funding projects, Contract no. 4 PFE/2021.

REFERENCES

Andron, D. and Kifor, S. (2021), *Digital Technologies in the Didactic Activity* (in Romanian), "Lucian Blaga" University Press, Sibiu, ISBN 978-606-12-1854-7.

Avadanei, M., Olaru, S., Ionescu, I., Ursache, M., Ciobanu, L., Alexa, L., Luca, A., Olmos, M., Aslanidis, T., Belakova, D. and Silva, C. (2020), "ICT New Tools for a Sustainable Textile and Clothing Industry", *Industria Textila*, 71(5), pp. 504-512, https://doi.org/10.35530/IT.071.05.1811.

Díaz Redondo, R.P., Caeiro Rodríguez, M., López Escobar, J. and Fernández Vilas, A. (2021), "Integrating Micro-learning Content in Traditional e-learning Platforms", *Multimedia Tools and Applications*, 80, pp. 3121–3151, https://doi.org/10.1007/s11042-020-09523-z.

European Parliament (2021), "Digital Transformation: Importance, Advantages and EU Policies" (in Romanian), https://www.europarl.europa.eu/news/ro/headlines/society/20210414STO02010/transformarea-digitala-importanta-avantaje-si-politici-ue.

Radulescu, I.R. *et al*. (2022), "E-learning Course of Software for Textile Design", *International Conferences e-Society 2022 and Mobile Learning 2022*, pp. 258-259.

Rusu, B. and Tudose, M.B. (2018), "Qualitative Study to Identify Key Factors Affecting Student Perception towards the Use of e-learning in a Technical University", *ELSE-2018 – Book of abstracts*, Publisher: "Carol I" National Defence University Publishing House, Bucharest, p. 126.

Webactiv (2020), Digitization, digitalization and digital transformation, https://webactiv.ro/digitizare-digitalizare-si-transformare-digitala/

https://doi.org/10.24264/icams-2022.VI.3

WORKSHOP

MUSEION IoT-based system for understanding and controlling the environmental quality in museums

UNDERSTANDING AND CONTROLLING THE ENVIRONMENTAL QUALITY IN MUSEUMS THROUGH IoT: AN INTERNATIONAL RESEARCH AND PRACTICE COLLABORATION TO SUPPORT MUSEUMS IN THE IMPLEMENTATION OF CLIMATE ACTION

ELENA BADEA[1,2*], CRISTINA CARSOTE[1,3], CRISTINA BALACEANU[4], OANA ORZA[4], SABINA BOSOC[4], ROBERT STRECHE[4], GEORGE SUCIU[4], ZÓRA BARTA[5], VALÉRIA TÁLAI[5], ZSOLT VINICZAY[5]

[1] *National Research and Development Institute for Textile and Leather - Research Institute for Leather and Footwear (INCDTP-ICPI), ARCH Lab, Ion Minulescu Str. 93, Bucharest, Romania*

[2] *Department of Chemistry, Faculty of Sciences, University of Craiova, Calea Bucuresti Str. 107 I, Craiova, Romania*

[3] *National Museum of Romanian History, Calea Victoriei Str. 12, Bucharest, Romania*

[4] *S.C. BEIA Cercetare S.R.L., Peroni Str. 14-16, Bucharest, Romania*

[5] *SEACON Europe LTD, H-8000, 14, Móricz Zs utca, Székesfehérvár, Hungary*

MUSEION project aims at developing an integrated IoT based platform for the sustainable management of environmental control and adaptation to climate change of museum collections. The MUSEION solution will thus provide the optimization of resources such costs, energy, staff workload, while contributing to carbon footprint reduction. This solution is a replicable IoT-based system, which will solve the problems of real objects in real conditions (sustainable environmental control and adaptation to climate change). It will consider the main components of the museum system that influence its optimal climate (i.e, museum itself, artworks and visitors) and will continuously monitor and allow visualization of environmental and air quality markers. The monitoring reports will be elaborated by a software designed to real-time calculate the overall Indoor Air Quality (IAQ) Index. The main advantage provided by the MUSEION system consist in the simultaneous monitoring and evaluation of the environment quality and its impact on various artefacts in various conservation condition.

Keywords: IoT, environmental control, museum collections.

MONITORING INDOOR ENVIRONMENTAL QUALITY IN MUSEUMS

According to UNESCO, the current estimated total number of museums worldwide is around 104,000, with more than 60% in Europe and North America. More than 11,000 museums are located in Eastern Europe. For example, by 2019 there was a total of 791 museums and public collections in Romania, while 662 museums operated in Hungary in 2020, according to Statista (https://www.statista.com/). The survey made within the European project Memori (https://memori.nilu.no/) on indoor air quality management in European museums found that the majority of the institutions have not measured airborne pollutants and do not know the damages related to poor environmental quality conditions. Moreover, there are a number of other factors that need to be monitored indoor in public buildings such as museums and libraries. In addition to the effects on health and well-being of the staff and visitors, there is the costly and considerable damage on cultural objects that museum and library own and have to keep in functional conditions as long as possible.

Outdoor pollution and indoor pollution combined with climate change effects create an environment increasingly harmful for museum and library collections. Climate change affects global temperature and precipitation patterns, thus influencing the intensity and, in some cases, the frequency of extreme environmental events, such as forest fires, hurricanes, heat waves, floods, droughts, and storms. The expected impact

https://doi.org/10.24264/icams-2022.W.1

of climate change on built heritage is well-documented but one should also consider the changing indoor conditions (Leissner *et al*., 2015). Additionally, each material, depending on its preservation conditions, reacts differently to environmental parameters. Hence, due to the number of parameters and variables, and the synergy of their action, the control of indoor environment is a more complex problem than ever considered and needs a complex approach. It is therefore of vital importance to understand which pollutants and in what conditions cause negative effects to design effective monitoring systems enabling for preservation management supported and informed by knowledge resources.

To date, continuous measurement of climate and air quality parameters is not listed among those technologies conventionally used for preventive conservation in museums. Climate change and growing (mass) tourism are expected to strongly impact the preservation conditions of cultural heritage in the next decades, while a decrease in economic resources for heritage conservation is expected (Colette, 2007). To protect our heritage from these new conditions, adequate mitigation actions are required.

MUSEION Solution for Continuous Measurement and Understanding Climate and Air Quality Impact on Museum Objects

In this context, MUSEION aims at developing a digital platform for continuous environmental and AQ control as a smart decision support tool (Figure 1). The MUSEION platform will collect data from indoor sensors and transfer them for storage in the cloud through an IoT gateway. The real-time data will be further processed and visualized. An in-house developed software will calculate the index of air quality (IAQ) for all types of materials/artefacts enabling the conversion of environmental measurements into valuable judgements that support the analysis of the preservation conditions and identify the hazards that are endangering an artefact / a collection. IAQ index will assist museum professionals to implement suitable mitigation actions.

A pilot study for designing and optimizing the platform was selected, namely the Memorial houses “Fanny & Liviu Rebreanu” and “Ion Minulescu & Claudia Millian” owned by the National Museum of Romanian Literature. The collections in the two apartments, which occupy the entire second floor of a building from the interwar period, include literary documents, letters, manuscripts, unpublished photographs and an impressive collection of paintings and sculptures. The building is located in a central area of Bucharest, very trafficked.

MUSEION Architecture

Due to the extensive use of wireless sensor networks in all aspects of daily life, the project team tested different configurations for these networks’ types in scenarios that include a sensor-based system used for monitoring air quality, weather conditions and environmental factors. The system is powered by solar panels and it can operate independently. The system architecture (Figure 2) is composed of two monitoring stations (Figure 3): the one placed outdoor monitors temperature, relative humidity, pressure, carbon dioxide, nitrogen dioxide, sulphur dioxide, while the indoor station monitors brightness, temperature, relative humidity, volatile organic compounds, ozone, ammonia, hydrogen sulfide, vibrations and dust particles. The information is gathered wirelessly in a Gateway and sent via MQTT to a Broker. Once the data is received by the Broker, it is stored in the InfluxDB a database created to store information for continuous parameter analysis.

https://doi.org/10.24264/icams-2022.W.1

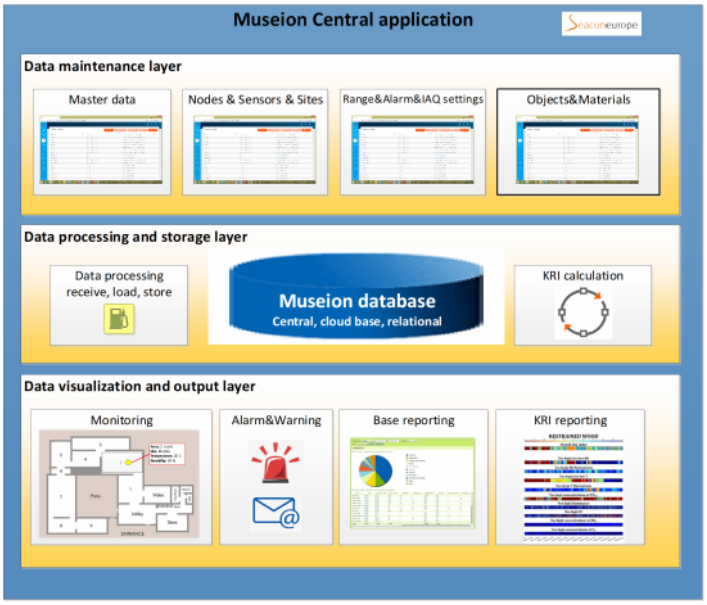

Figure 1. MUSEION system concept

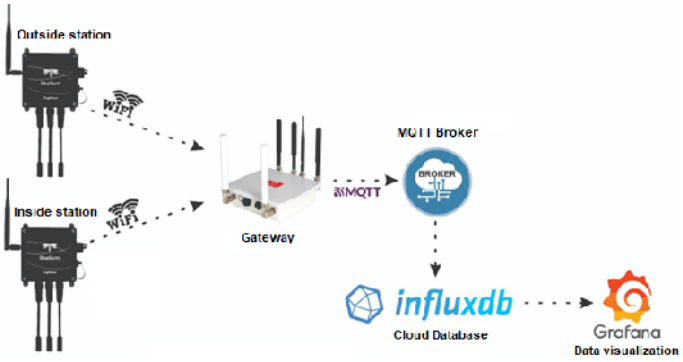

Figure 2. Architecture of the system

The monitored parameters saved in Grafana Cloud can be directly analysed with the use of charts, tables, and graphs using Grafana, an open-source web data visualization tool, which allows for the representation of the parameters. A dashboard especially designed for MUSEION project is illustrated in Figure 4. In this platform, thresholds for each parameter may also be established. In order to reduce the environmental risk to artefacts, museum caretakers are immediately informed when undesired situations occur, for example, when nominal values exceed the accepted values.

https://doi.org/10.24264/icams-2022.W.1

Figure 3a. Outdoor station installed on the balcony

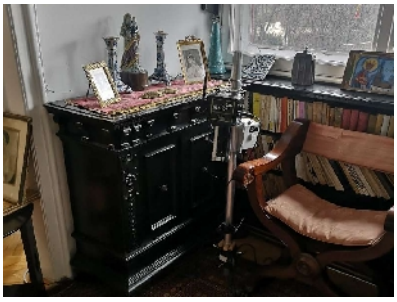

Figure 3b. Indoor station installed in one of the apartment's rooms

Figure 4. Example of Grafana dashboard

Data Analysis and Visualization

The software application that supports the analysis and visualization of IAQ index (Anaf *et al.*, 2018) using real measurement data is currently under development. It consists of database, web client user interface and communication, and data processing subsystem with complex functionality:

- Gather, store and process data; area description (facility and premises, measurement points also on the blueprint);
- Object and material description (including location and sensitivity against environmental parameters (from very low to very high-sensitivity) including photo; sensor network description (with measured characteristics) (Figure 5);
- Calculation parameter data storage (categories, intervals, risk levels); sensor network data reception and storage (near real time approx. 20 minutes);
- Key Risk Indicator (KRI) (Anaf *et al.*, 2018) calculation which is multi-step algorithm giving a number between 0 and 1 (0 = no damage, 0.05 = negligible damage, 0.25 = low damage, 0.5 = moderate damage, 0.75 = high damage, 1 = extremely high damage) that indicate the risk level each monitored material/object based on its material and conservation condition.

https://doi.org/10.24264/icams-2022.W.1

The calculation level is KRI factors, area / material / object/ sensitivity/ hour, the lowest level could be aggregated on higher level (day, season, facility etc.)

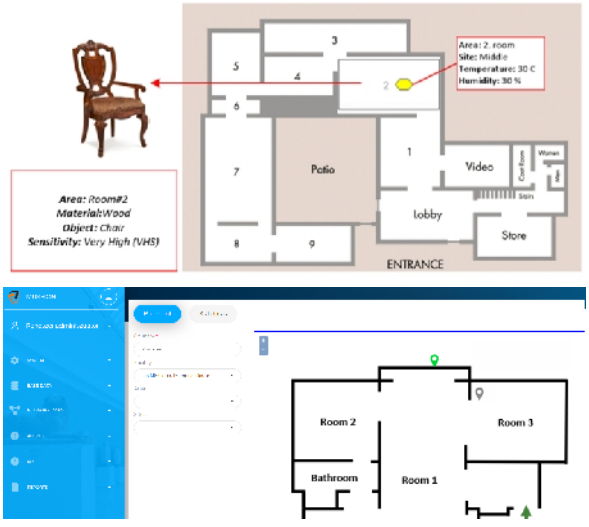

Figure 5. Example of location, object and material description

Data visualization includes (reporting examples are illustrated in Figures 6, 7):

- Dashboard with facility blueprint and last measures. By clicking on the measurement point, users can view the last received measurements and then backward values for certain intervals.
- Sensor measurement reports, which show the incoming measured data in different groupings, filters and display methods.
- KRI result reports showing the incoming measured data in different groupings, filters with coloring using different display methods.

FINAL REMARKS

For the MUSEION pilot study the continuous real-time indoor environmental quality monitoring is fundamental for an active management strategy. The collections are kept and exhibited in apartments in which the environmental quality conditions were mainly intended for human health and comfort. These conditions may be different from what is required to protect artefacts. Moreover, different artefacts (i.e., paper, textile, paintings and photographs) require different environmental conditions. Museion system is therefore essential to understand the dynamics of the different air quality factors and climate parameters and how to control them to achieve safe environment conditions while providing a healthy and safe facility for employees and visitors.

A workshop has been organized within the ICAMS 2022 Conference with various museum professionals and numerous stakeholders, potential users of Museion system, to get feedback and optimize the performance of the actual system.

https://doi.org/10.24264/icams-2022.W.1

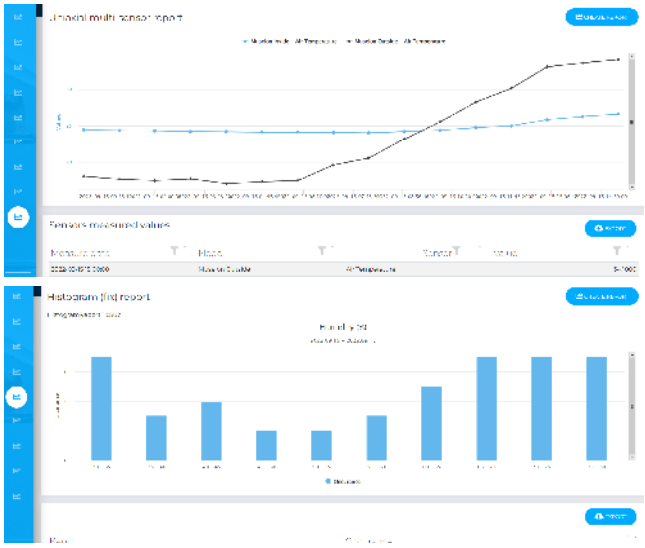

Figure 6. Monitoring reports

KRI group/KRI factors	Maximum / rank_value				Minimum / measured_value	Maximum / measured_value
	1-Low	2-Medium	3-High	4-Very high		
1-Temperature	1	1	1	1	7,76	34,1
01-Too high temperature	0,05	0,25	0,5	0,75	7,9	30,37
02-Too low temperature	0,05	0,25	0,5	0,75	7,9	30,37
03-Too large temperature fluctuation	1	1	1	1	7,76	34,1
2-Humidity	1	1	1	1	24,83	99,16
04-Too high humidity	1	1	1	1	27,15	98,37
05-Too low humidity	0,5	0,75	0,75	1	27,15	98,37
06-Too large humidity fluctuation	1	1	1	1	24,83	99,16
3-Radiation	0,05	1	1	1	0	16304
07-Too high illuminance	0,05	1	1	1	0,48	11470
08-Too high light fluctuation	0	1	1	1	0	16304
4-Air pollution	0,25	0,25	1	1	0	9,26
09-Too much sulfur dioxide - SO2	0,05	0,05	0,25	0,5	0	0,11
10-Too much sulfur dioxide fluctuation	0	0	0	0	0	0,11
11-Too much nitrogen dioxide - NO2	0,05	0,25	0,05	0,05	0,16	0,38
12-Too much nitrogen dioxide fluctuation	0	0	0	0	0,12	0,42
13-Too much ozone - O3	0,05	0,05	0,05	0,05	0	0
14-Too much ozone fluctuation	0	0	0	0	0	0
15-Too much carbon dioxide - CO2	0,05	0,05	0,05	0,05	0,08	0,81
16-Too much carbon dioxide fluctuation	0	0	0	0	0,06	0,93
17-Too much hidrogen sulfide - H2S	0,25	0,25	0,5	0,75	0,27	0,4
18-Too much hidrogen sulfide fluctuation	0	0	1	1	0,26	0,54
21-Too much dust particles PM2.5	0,05	0,25	0,75	0,5	0,14	8,67
22-Too much dust particles 2.5 fluctuation	0	0	0	0	0,02	9,28

Figure 7. KRI result report

REFERENCES

Anaf, W., Pernia, D.L. and Schalm, O. (2018), "Standardized Indoor Air Quality Assessments as a Tool to Prepare Heritage Guardians for Changing Preservation Conditions Due to Climate Change", *Geosciences*, 8(8), 276, https://doi.org/10.3390/geosciences8080276.

Colette, A. (2007), "Climate Change and World Heritage: Report on Predicting and Managing the Impacts of Climate Change on World Heritage and Strategy to Assist States Parties to Implement Appropriate Management Responses, UNESCO World Heritage Centre, http://unesdoc.unesco.org/images/0016/001600/160019m.pdf.

Leissner, J., Kilian, R., Kotova, L., Jacob, D., Mikolajewicz, U., Broström, T., Ashley-Smith, J., Schellen, H.L., Martens, M., van Schijndel, J., Antretter, F., Winkler, M., Bertolin, C., Camuffo, D., Simeunovic, G. and Vyhlídal, T. (2015), "Climate for Culture: Assessing the Impact of Climate Change on the Future Indoor Climate in Historic Buildings Using Simulations", *Heritage Science*, 3, 38, https://doi.org/10.1186/s40494-015-0067-9.

https://doi.org/10.24264/icams-2022.W.1

INDEX OF AUTHORS

E

F

G

H

I

J

K

L

M

N

O

P

Q

R

S

T

U

V

W

Y

Z

PARTNERS:

LEATHER ENGINEERING DEPARTMENT EGE UNIVERSITY, TURKEY

MUSTAFA KEMAL UNIVERSITY, TURKEY

CHINA LEATHER & FOOTWEAR RESEARCH INSTITUTE Co. Ltd., CHINA

"POLITEHNICA" UNIVERSITY BUCHAREST, ROMANIA

"GH. ASACHI" TECHNICAL UNIVERSITY OF IASI, ROMANIA

BUCHAREST ACADEMY OF ECONOMIC STUDIES, ROMANIA

ITA TEXCONF ROMANIAN ENTITY WITHIN INNOVATION & LEATHER TECHNOLOGICAL TRANSFER

CONFEDERATION OF NATIONAL ASSOCIATIONS OF TANNERS AND DRESSERS OF THE EUROPEAN COMMUNITY

SFERA FACTOR THE ROMANIAN LEATHER MANUFACTURERS ORGANIZATION

ISSN: 2068-0783